frontiers | Research Topics

Community series in targeting signalling pathways in inflammatory diseases, volume II

Edited by
Uzma Saqib, Mirza S. Baig, Syed Faisal and Suraj P. Parihar

Published in
Frontiers in Immunology

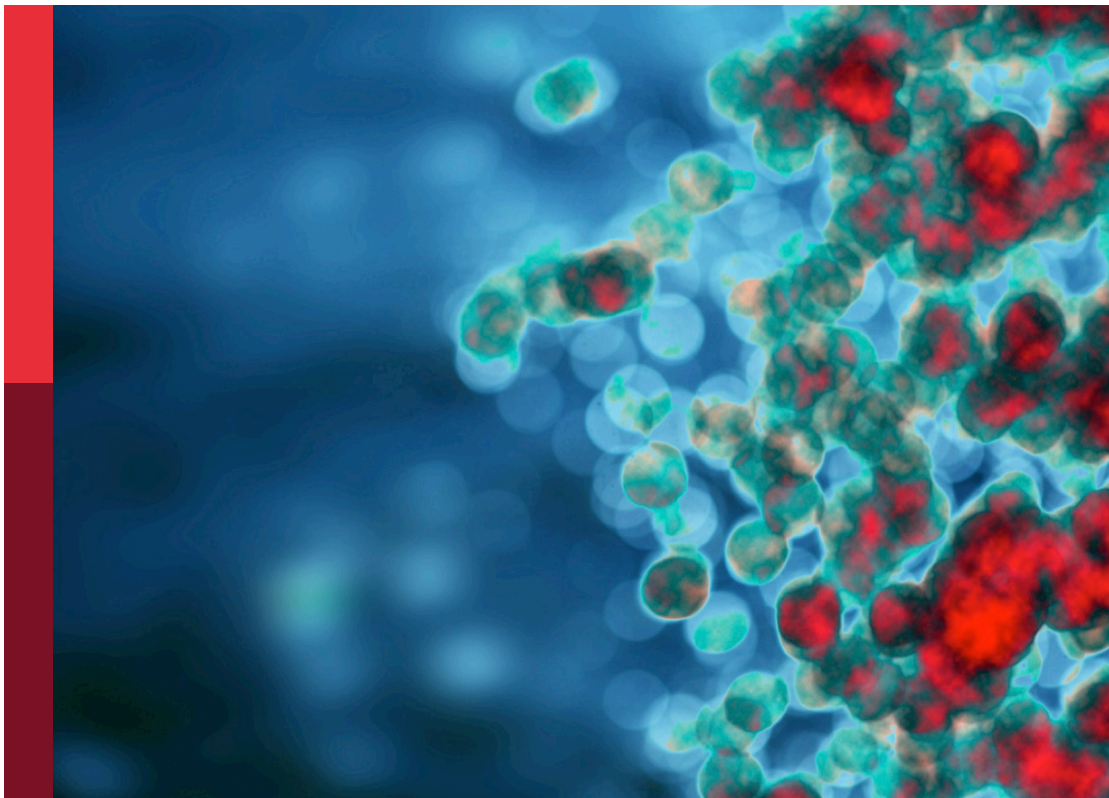

ISSN 1664-8714
ISBN 978-2-8325-6596-4
DOI 10.3389/978-2-8325-6596-4

Generative AI statement
Any alternative text (Alt text) provided alongside figures in the articles in this ebook has been generated by Frontiers with the support of artificial intelligence and reasonable efforts have been made to ensure accuracy, including review by the authors wherever possible. If you identify any issues, please contact us.

About Frontiers

Frontiers is more than just an open access publisher of scholarly articles: it is a pioneering approach to the world of academia, radically improving the way scholarly research is managed. The grand vision of Frontiers is a world where all people have an equal opportunity to seek, share and generate knowledge. Frontiers provides immediate and permanent online open access to all its publications, but this alone is not enough to realize our grand goals.

Frontiers journal series

The Frontiers journal series is a multi-tier and interdisciplinary set of open-access, online journals, promising a paradigm shift from the current review, selection and dissemination processes in academic publishing. All Frontiers journals are driven by researchers for researchers; therefore, they constitute a service to the scholarly community. At the same time, the *Frontiers journal series* operates on a revolutionary invention, the tiered publishing system, initially addressing specific communities of scholars, and gradually climbing up to broader public understanding, thus serving the interests of the lay society, too.

Dedication to quality

Each Frontiers article is a landmark of the highest quality, thanks to genuinely collaborative interactions between authors and review editors, who include some of the world's best academicians. Research must be certified by peers before entering a stream of knowledge that may eventually reach the public - and shape society; therefore, Frontiers only applies the most rigorous and unbiased reviews. Frontiers revolutionizes research publishing by freely delivering the most outstanding research, evaluated with no bias from both the academic and social point of view. By applying the most advanced information technologies, Frontiers is catapulting scholarly publishing into a new generation.

What are Frontiers Research Topics?

Frontiers Research Topics are very popular trademarks of the *Frontiers journals series*: they are collections of at least ten articles, all centered on a particular subject. With their unique mix of varied contributions from Original Research to Review Articles, Frontiers Research Topics unify the most influential researchers, the latest key findings and historical advances in a hot research area.

Find out more on how to host your own Frontiers Research Topic or contribute to one as an author by contacting the Frontiers editorial office: frontiersin.org/about/contact

Community series in targeting signalling pathways in inflammatory diseases, volume II

Topic editors

Uzma Saqib — Indian Institute of Technology Indore, India
Mirza S. Baig — Indian Institute of Technology Indore, India
Syed Faisal — National Institute of Animal Biotechnology (NIAB), India
Suraj P. Parihar — University of Cape Town, South Africa

Citation

Saqib, U., Baig, M. S., Faisal, S., Parihar, S. P., eds. (2025). *Community series in targeting signalling pathways in inflammatory diseases, volume II*. Lausanne: Frontiers Media SA. doi: 10.3389/978-2-8325-6596-4

Table of contents

frontiers | Frontiers in Immunology

TYPE Editorial
PUBLISHED 27 June 2025
DOI 10.3389/fimmu.2025.1639004

OPEN ACCESS

EDITED AND REVIEWED BY
Pietro Ghezzi,
Brighton and Sussex Medical School,
United Kingdom

*CORRESPONDENCE
Mirza S. Baig
msb.iit@iiti.ac.in
Uzma Saqib
uzmas2024@gmail.com

†These authors have contributed equally to this work

RECEIVED 01 June 2025
ACCEPTED 17 June 2025
PUBLISHED 27 June 2025

CITATION
Baig MS, Siddiqi F, Atre R, Parihar SP, Faisal S and Saqib U (2025) Editorial: Community series in targeting signalling pathways in inflammatory diseases, volume II. *Front. Immunol.* 16:1639004. doi: 10.3389/fimmu.2025.1639004

Editorial: Community series in targeting signalling pathways in inflammatory diseases, volume II

Mirza S. Baig[1*†], Faaiza Siddiqi[1†], Rajat Atre[1†], Suraj P. Parihar[2], Syed Faisal[3] and Uzma Saqib[4*]

[1]Department of Biosciences and Biomedical Engineering (BSBE), Indian Institute of Technology Indore (IITI), Indore, India, [2]Division of Medical Microbiology, Faculty of Health Sciences, University of Cape Town, Cape Town, South Africa, [3]National Institute of Animal Biotechnology (NIAB), Hyderabad, India, [4]School of Life Sciences, Devi Ahilya Vishwavidyalaya (DAVV), Indore, India

KEYWORDS

inflammation, macrophages, cytokines, anti-inflammatory drugs, TIRAP (TIR domain-containing adaptor protein), small-molecule inhibitors, peptide inhibitors

Editorial on the Research Topic
Community series in targeting signalling pathways in inflammatory diseases, volume II

The Toll-interleukin-1 Receptor (TIR) domain-containing adaptor protein (TIRAP) is a critical intracellular facilitator in immune surveillance that coordinates different signaling pathways. Its utility as a bridging entity, and its versatility in binding with diverse components of Toll-like Receptor (TLR) pathway, has been the subject of several investigations (1). During signal transmission, TIRAP undergoes distinct binding mechanisms and conformational changes leading to differential binding with various intracellular mediators thereby contributing to diverse effects in immunological responses. Among its notable interactions, TIRAP engages with proteins such as MyD88, TRAF6, and IRAK-2, facilitating downstream activation of NF-κB and AP-1 (2). Hence, a convoluted mesh of protein-protein interactions forms the foundation of TIRAP signaling, which is regulated through its TIR domain (2) (Figure 1A).

Signaling pathways governed by TIR-domain containing proteins have emerged as a key target for the development of anti-inflammatory therapeutic strategies (3). Dimerization is a central phenomenon required for the functionality of most TIR domains, that span over 200 amino acids and harbor a 14 residues BB loop motif. TIR-mediated signaling mainly relies on the function of the conserved BB loop responsible for signal complex assembly and stabilization (4). TIRAP is a 221 amino acid long protein, which is structured into two main domains namely an N-terminal phosphatidylinositol 4,5-bisphosphate (PIP2) binding domain (PBD) and a C-terminal Toll/interleukin-1 receptor (TIR) domain. TIRAP's positioning is mediated by Phosphatidylinositol 4-Phosphate 5-Kinase α (PIP5Kα), which generates PIP2, a crucial lipid that serves as a docking site for TIRAP (5, 6). TIRAP's TIR domain displays structural differences in contrast to the canonic TIR domains. It comprises an extended AB loop that links αA and αB that are developed due to the absence of αB helix classically situated between βB and βC strands (3). These

10.3389/fimmu.2025.1639004

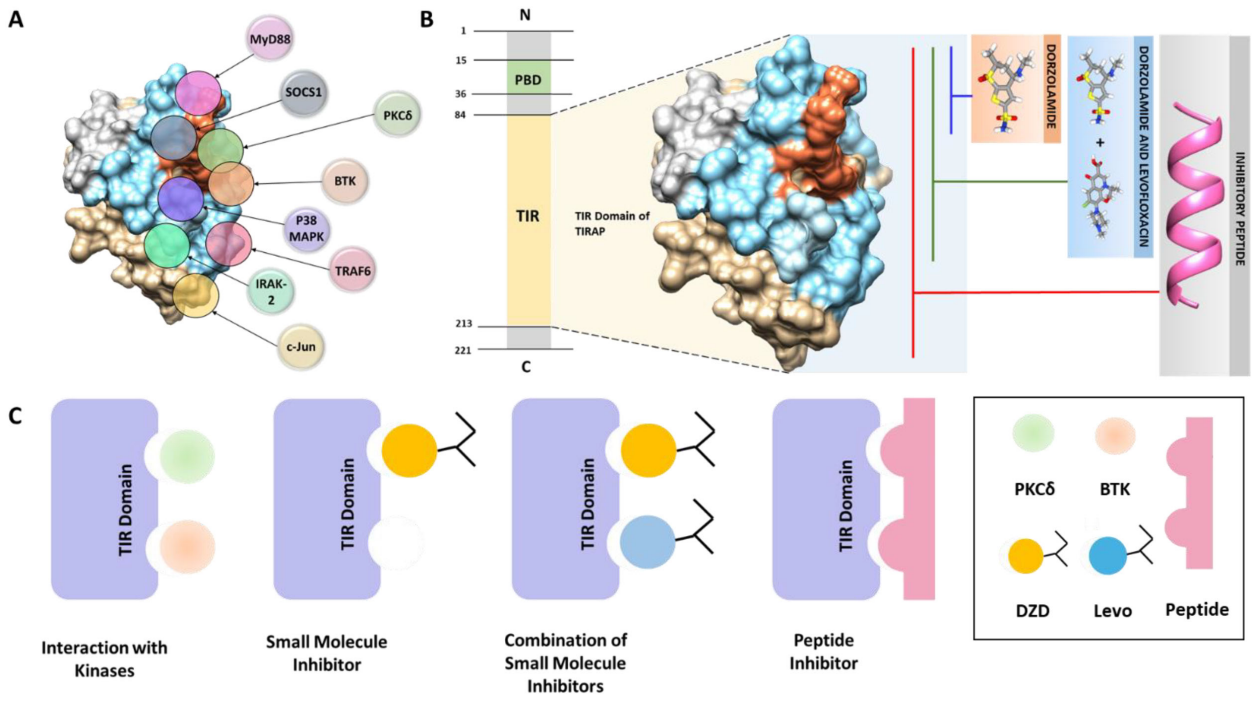

FIGURE 1
(A) Interaction of the TIR domain of TIRAP with various proteins involved in TLR-mediated signaling. **(B)** Strategies for inhibiting the TIR domain of TIRAP, including small molecules, combination therapies, and peptide-based approaches. **(C)** Diagrammatic representation showing inhibition of TIR domain interactions between TIRAP and BTK or PKCδ through targeted small molecules, combination treatments, or peptides.

unique structural characteristics of TIRAP have significant implications for immune signaling, as they influence its interactions with other signaling molecules. Consequently, strategies that target and modulate TIRAP-mediated signaling pathways hold promise for the treatment of diseases associated with dysregulated TIR-driven inflammatory responses (3, 7). For example, aberrant TIRAP signaling has been implicated in the pathogenesis of rheumatoid arthritis, where it contributes to destructive inflammation by promoting cytokine production and immune cell activation within affected joints (9).

Mechanistically, TIRAP is known to be activated via a post-translation modification i.e. phosphorylation by kinases namely BTK and PKCδ. Expanding TIR domain targeting through small molecules binding key residues, dual-molecule strategies, or peptide inhibitors spanning the domain, can enhance TIRAP inhibition and disrupt inflammatory signaling (Figure 1B). Previously, Rajpoot et al. explored the TIRAP-PKCδ axis and successfully repurposed an FDA approved compound, Dorzolamide (DZD), targeting the interface residues of PKCδ on TIRAP thereby dampening the downstream inflammatory signaling (8). Though DZD attenuated the PKCδ mediated TIRAP activation, BTK-mediated phosphorylation remains an area to explore.

Recently, Baig et al. proposed a combination therapeutic approach for TIRAP-mediated chronic inflammatory septic condition. They addressed two unique aspects of sepsis progression—the destruction of bacteria and the restoration of damaged organs through homeostasis by developing a novel combination of the broad-spectrum antibiotic Levofloxacin and the repurposed anti-inflammatory medication Dorzolamide (LeDoz) (10). Unlike individual drugs that target a single kinase binding site, we discovered that Levofloxacin and DZD interacted with a section inside the binding groove (19 residues) on the TIRAP TIR domain essential for its interaction with not only PKCδ but also with BTK, which are responsible for its activation (10).

Various such alternative modalities have been investigated to silence TIRAP signaling. In one study, molecular-docking and dynamics simulations predicted that the plant alkaloid Narciclasine binds with high affinity to the TIRAP TIR domain as well as other LPS–TLR4-pathway proteins, stabilizing the complexes and thereby suppressing pro-inflammatory signaling (11). In another investigation, Phycocyanin treatment up-regulated miR-3150a-3p, miR-6883-3p and miR-627-5p, which led to depleted TIRAP transcripts and reduced cellular proliferation, thereby establishing a post-transcriptional checkpoint on adaptor availability (12). Interestingly, one study demonstrated that synthetic decoy peptides derived from the TIRAP TIR domain competitively interrupted TIRAP–MyD88 recruitment, abolishing downstream NF-κB activation and highlighting the value of peptide-based blockade of adaptor–adaptor contacts (13). Collectively, these observations indicate that small molecules and miRNA inducers curtail TIRAP through binding or expression control, whereas peptide modalities can

potentially better dismantle the protein-interaction surfaces essential for signal propagation. Based on these insights, a therapeutic peptide has been proposed which targets the entire binding pocket in the TIR domain, dampening TIRAP homo-dimerization required for its functionality. THPdb (Therapeutic Peptides and Proteins Database) was screened against the TIRAP TIR domain, identifying a top candidate peptide. Following it's optimization, the peptide exhibited strong binding to TIRAP, interacting with residues 152–193, including the dimerization pocket. Additionally, its binding outside conventional pockets induced structural conformational changes, enhancing its inhibitory effect on TIRAP.

These findings highlight the potential of targeting this domain of TIRAP using small molecules, dual-molecule strategies, or peptide inhibitors as promising approaches to inhibit TIRAP function and disrupt downstream inflammatory signaling pathways. (Figure 1C). These strategies could pave the way for novel treatments for chronic inflammatory diseases, providing both structural insights and targeted interventions.

Author contributions

MB: Conceptualization, Data curation, Formal analysis, Funding acquisition, Investigation, Methodology, Project administration, Resources, Software, Supervision, Validation, Visualization, Writing – original draft, Writing – review & editing. FS: Formal analysis, Investigation, Methodology, Writing – original draft. RA: Formal analysis, Investigation, Methodology, Writing – original draft. SP: Formal analysis, Investigation, Methodology, Writing – original draft. SF: Formal analysis, Investigation, Methodology, Writing – original draft. US: Formal analysis, Investigation, Methodology, Writing – original draft.

Conflict of interest

The authors declare that the research was conducted in the absence of any commercial or financial relationships that could be construed as a potential conflict of interest.

The author(s) declared that they were an editorial board member of Frontiers, at the time of submission. This had no impact on the peer review process and the final decision.

Generative AI statement

The author(s) declare that no Generative AI was used in the creation of this manuscript.

Publisher's note

References

1. Fitzgerald KA, Palsson-McDermott EM, Bowie AG, Jefferies CA, Mansell AS, Brady G, et al. Mal (MyD88-adapter-like) is required for Toll-like receptor-4 signal transduction. *Nature*. (2001) 413:78–83. doi: 10.1038/35092578

2. Rajpoot S, Wary KK, Ibbott R, Liu D, Saqib U, Thurston TLM, et al. TIRAP in the mechanism of inflammation. *Front Immunol*. (2021) 12:697588. doi: 10.3389/fimmu.2021.697588

3. Saqib U, Baig M. Identifying the inhibition of TIR proteins involved in TLR signalling as an anti-inflammatory strategy. *SAR QSAR Environ Res*. (2018) 29:295–318. doi: 10.1080/1062936X.2018.1431308

4. Gay NJ, Gangloff M. Structure and function of toll receptors and their ligands. *Annu Rev Biochem*. (2007) 76:141–65. doi: 10.1146/annurev.biochem.76.060305.151318

5. Nguyen TTN, Kim YM, Kim TD, Le OTT, Kim JJ, Kang HC, et al. Phosphatidylinositol 4-Phosphate 5-Kinase α facilitates toll-like receptor 4-mediated microglial inflammation through regulation of the toll/interleukin-1 receptor domain-containing adaptor protein (TIRAP) location. *J Biol Chem*. (2013) 288:5645–59. doi: 10.1074/jbc.M112.410126

6. Bernard NJ, O'Neill LA. Mal, more than a bridge to MyD88. *IUBMB Life*. (2013) 65:777–86. doi: 10.1002/iub.1201

7. Atre R, Obukhov AG, Majmudar CY, Nair K, White FA, Sharma R, et al. Dorzolamide intermediates with potential anti-inflammatory activity. *Eur J Pharmacol*. (2025) 987:177160. doi: 10.1016/j.ejphar.2024.177160

8. Rajpoot S, Kumar A, Gaponenko V, Thurston TLM, Mehta D, Faisal SM, et al. Dorzolamide suppresses PKCδ -TIRAP-p38 MAPK signaling axis to dampen the inflammatory response. *Future Med Chem*. (2023) 15:533–54. doi: 10.4155/fmc-2022-0260

9. Sacre SM, Andreakos E, Kiriakidis S, Amjadi P, Lundberg A, Giddins G, et al. The toll-like receptor adaptor proteins myD88 and Mal/TIRAP contribute to the inflammatory and destructive processes in a human model of rheumatoid arthritis. *Am J Pathol*. (2007) 170:518–25. doi: 10.2353/ajpath.2007.060657

10. Baig MS, Rajat A, Rahul S. A composition for sepsis and method thereof. (2023).

11. Kingsley MK, Rao GK, Bhat BV. Effectiveness of narciclasine in suppressing the inflammatory response in sepsis: molecular docking and in silico studies. *Bioinform Biol Insights*. (2024) 18:1–18. doi: 10.1177/11779322241233436

12. Hao S, Li F, Li S, Li Q, Liu Y, Yang Q, et al. miR-3150a-3p, miR-6883-3p and miR-627-5p participate in the phycocyanin-mediated growth diminishment of A549 cells, via regulating a common target toll/interleukin 1 receptor domain-containing adaptor protein. *J Funct Foods*. (2022) 91. doi: 10.1016/j.jff.2022.105011

13. Couture LA, Piao W, Ru LW, Vogel SN, Toshchakov VY. Targeting toll-like receptor (TLR) signaling by toll/interleukin-1 receptor (TIR) domain-containing adapter protein/MyD88 adapter-like (TIRAP/Mal)-derived decoy peptides. *J Biol Chem*. (2012) 287:24641–8. doi: 10.1074/jbc.M112.360925

frontiers | Frontiers in Immunology

TYPE Original Research
PUBLISHED 04 March 2024
DOI 10.3389/fimmu.2024.1363947

OPEN ACCESS

EDITED BY
Suraj P. Parihar,
University of Cape Town, South Africa

REVIEWED BY
Makram Essafi,
Pasteur Institute of Tunis, Tunisia
Jehan J. El-Jawhari,
Nottingham Trent University, United Kingdom

*CORRESPONDENCE
Mehdi Shakibaei
mehdi.shakibaei@med.uni-muenchen.de

RECEIVED 31 December 2023
ACCEPTED 12 February 2024
PUBLISHED 04 March 2024

CITATION
Brockmueller A, Buhrmann C, Shayan P and Shakibaei M (2024) Calebin A modulates inflammatory and autophagy signals for the prevention and treatment of osteoarthritis. *Front. Immunol.* 15:1363947. doi: 10.3389/fimmu.2024.1363947

Calebin A modulates inflammatory and autophagy signals for the prevention and treatment of osteoarthritis

Aranka Brockmueller [1], Constanze Buhrmann [2], Parviz Shayan [3] and Mehdi Shakibaei [1]*

[1]Musculoskeletal Research Group and Tumor Biology, Faculty of Medicine, Institute of Anatomy, Chair of Vegetative Anatomy, Ludwig-Maximilians-University Munich, Munich, Germany, [2]Institute of Anatomy and Cell Biology, Faculty of Medicine, University of Augsburg, Augsburg, Germany, [3]Department of Parasitology, Faculty of Veterinary Medicine, University of Tehran, Tehran, Iran

Introduction: Osteoarthritis (OA) is associated with excessive cartilage degradation, inflammation, and decreased autophagy. Insufficient efficacy of conventional monotherapies and poor tissue regeneration due to side effects are just some of the unresolved issues. Our previous research has shown that Calebin A (CA), a component of turmeric (*Curcuma longa*), has pronounced anti-inflammatory and anti-oxidative effects by modulating various cell signaling pathways. Whether CA protects chondrocytes from degradation and apoptosis in the OA environment (EN), particularly *via* the autophagy signaling pathway, is however completely unclear.

Methods: To study the anti-degradative and anti-apoptotic effects of CA in an inflamed joint, an *in vitro* model of OA-EN was created and treated with antisense oligonucleotides targeting NF-κB (ASO-NF-κB), and IκB kinase (IKK) inhibitor (BMS-345541) or the autophagy inhibitor 3-methyladenine (3-MA) and/or CA to affect chondrocyte proliferation, degradation, apoptosis, and autophagy. The mechanisms underlying the CA effects were investigated by MTT assays, immunofluorescence, transmission electron microscopy, and Western blot analysis in a 3D-OA high-density culture model.

Results: In contrast to OA-EN or TNF-α-EN, a treatment with CA protects chondrocytes from stress-induced defects by inhibiting apoptosis, matrix degradation, and signaling pathways associated with inflammation (NF-κB, MMP9) or autophagy-repression (mTOR/PI3K/Akt), while promoting the expression of matrix compounds (collagen II, cartilage specific proteoglycans), transcription factor Sox9, and autophagy-associated proteins (Beclin-1, LC3). However, the preventive properties of CA in OA-EN could be partially abrogated by the autophagy inhibitor 3-MA.

Discussion: The present results reveal for the first time that CA is able to ameliorate the progression of OA by modulating autophagy pathway, inhibiting inflammation and apoptosis in chondrocytes, suggesting that CA may be a novel therapeutic compound for OA.

KEYWORDS

Calebin A, chondrocytes, osteoarthritis environment, inflammation, autophagy, 3D-culture

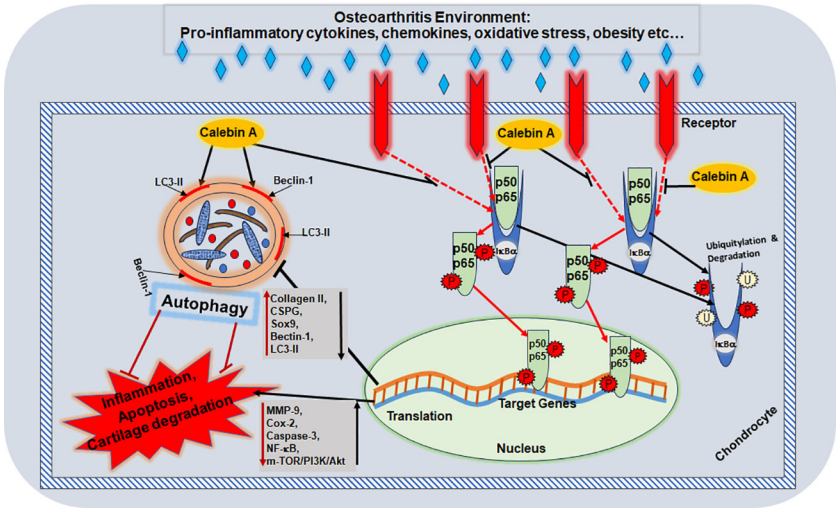

GRAPHICAL ABSTRACT

1 Introduction

Osteoarthritis (OA) represents the most common joint disease worldwide that affects an average of 18% of adults whereby the prevalence expands with increasing age and from 65 years onwards approximately half of the women and one-third of the men suffer from it (1). A degenerative, chronically progressive cartilage damage, accompanied by pain and functional limitations in the course, is the main issue of the disease, which may occur in any joint. Four stages are distinguished radiologically according to Kellgren–Lawrence classification from doubtful (I) to severe (IV) (2), and clinically, there are different courses such as silent, activated, or deformed. While a silent stage brings about minor problems for the patient, an activated stage results in metabolic abnormalities in articular cartilage, associated with inflammation, calcification, and destruction (3). Moreover, at the deformed stage, the articular cartilage has already disappeared in places, generating bone and tendon changes leading to joint deformities (4).

Based on the causes that trigger OA, there are primary forms by genetic predisposition as well as advanced age and secondary forms by joint dysplasia, overload, obesity, alcoholism, or metabolic disorders (5), all of which generate inflammatory events. *In vitro* and *in vivo* studies validated the cytokine, tumor necrosis factor (TNF)-α, as multifunctional key player in the pathophysiology of joint diseases such as OA, since its promotion of numerous further cytokines and enzymes activates an almost unstoppable pro-inflammatory cycle (6). Especially for the osteoarthritic synovial microenvironment, a TNF-α-forced induction of the main pro-inflammatory transcription factor, nuclear factor kappa-light-chain-enhancer of activated B-cells (NF-κB) is known (7). Persistent inflammation can quickly escalate to apoptosis in the naturally bradytrophic cartilage tissue due to its low maintenance capacity, and early defense mechanisms are necessary to stabilize cartilage homeostasis.

A crucial process here is autophagy, which breaks down dysfunctional and thus cartilage-damaging cell organelles or proteins. As part of the autophagy, joint cartilage cells activate a health-preserving and regenerative option by reducing inflammation and preventing apoptosis (8, 9). Thereby, both foreign substances and cell components to be degraded, such as discarded organelles, are taken up by autophagy and then referred to as the autophagosome. As a next step, for the purpose of

Abbreviations: 3-MA, 3-methyladenine; Akt, protein kinase B; ASO, antisense oligonucleotides; ASO-NF-κB, antisense oligonucleotides targeting NF-κB; CA, Calebin A; Coll II, collagen type II; CSPG, chondroitin sulfate proteoglycan; DAPI, 4′,6-diamidin-2-phenylindol; DMSO, dimethyl-sulfoxide; EN, environment; ECM, extracellular matrix; FBS, fetal bovine serum; HD, high density; IKK, IκB kinase; LC3, microtubule-associated protein 1A/1B-light chain 3; MMP, matrix metalloproteinase; mTOR, mammalian target of rapamycin; NF-κB, nuclear factor kappa-light-chain-enhancer of activated B-cells; OA, osteoarthritis; OA-EN, osteoarthritis environment; OD, optical density; PCH, primary canine chondrocytes; PI3K, phosphoinositide 3-kinase; SO, sense oligonucleotides; Sox9, SRY-box transcription factor 9; TEM, transmission electron microscopy; TNF, tumor necrosis factor; TNF-α-EN, TNF-α stimulated environment.

dismantling, the autophagosome fuses with lysosomes and thus forms autolysosomes (10). These activities of autophagic processes are regulated by chondrocyte's metabolism sensor, mammalian target of rapamycin' (mTOR) (11) with linked mTOR/PI3K/Akt signaling cascade (12), and determined by a high expression of corresponding Beclin-1 and LC3-II markers in differentiated cartilage cells (9). If this protective mechanism takes effect too late or not sufficiently, apoptosis as an irreversible initiation of cell death with the consequence of OA that requires treatment results. Non-pharmacological, pharmacological, or surgical approaches are available as OA-therapeutic possibilities offering more or less satisfactory results (5). Therefore due to their lack of side effects, a supportive co-treatment with phytopharmaceuticals such as the proven grape-derived resveratrol (13, 14) or curcumin from *Curcuma longa* (13, 15) gains importance.

Calebin A (CA), another little-known but highly effective polyphenolic ingredient of *Curcuma longa*, was first isolated approximately 20 years ago (16). The cornerstone for researching its medical potential was laid by demonstrating its safe use in animal experiments, where a study on Wistar rats was carried out without any sign of toxicity despite administration of 20, 50, or 100 mg CA/kg/body weight for 3 months (17). Contrarily, an extensive health-protecting effect of this natural compound gradually crystallizes (18), and after the first demonstration of CA's neuroprotective (16) and metabolism-modulating (19) action, a broad-based cancer-inhibiting effect was also proven. For example, the phytopharmacon suppresses growth and proliferation of gastric (20) or colorectal cancer (21, 22) cells. The inhibition of inflammatory cascades involving NF-κB and the associated interruption of disease intensification are considered to be the central mechanism of action here (22, 23).

Research into CA's influence on the musculoskeletal system is just beginning, and at least there are first findings of CA-induced bone stabilization through downregulation of RANKL signaling suppressing osteoclastogenesis (24). Tendons close to the joint could also benefit preventively or therapeutically from a CA-associated inhibition of inflammatory NF-κB cascade as recently demonstrated by 3D *in vitro* investigations (25). To summarize, to the best of our knowledge, the effectiveness of CA has not been previously studied in relation to OA and certainly not the associated chondroprotective autophagy processes.

Considering the above, the aim of these studies was to determine whether CA could be able to modulate both inflammatory and autophagic processes in chondrocytes that are exposed to an osteoarthritis environment (OA-EN). Therefore, all experiments were performed in multicellular 3D-culture models *in vitro* simulating a lifelike inflamed joint situation.

2 Materials and methods

2.1 Antibodies and chemical substances

As part of our experiments, the following antibodies were used: Beclin-1 (#3738) and LC3-II (#4108) from Cell Signaling Technology (Danvers, MA, USA); NF-κB (#MAB5078), MMP-9 (#MAB911), and caspase-3 (#AF835) from R&D Systems (Heidelberg, Germany); Sox9 (#TA802387) from OriGene Technologies (Herford, Germany); β-actin (#A4700), collagen type II (#AB761), and CSPG (#MAB5384-I) from Sigma-Aldrich (Taufkirchen, Germany); PI3K (#ab154598), Akt (#ab38449), and mTOR (#ab109268) from Abcam (Berlin, Germany); secondary immunofluorescence antibodies from Dianova (Hamburg, Germany); and secondary Western blot antibodies from EMD Millipore (Schwalbach, Germany). Furthermore, TNF-α was from R&D Systems (Heidelberg, Germany), 3-methyladenine (3-MA) from VWR International (Ismaning, Germany), and Epon from Plano (Marburg, Germany). BMS-345541, Fluoromount, DAPI, and MTT reagent were from Sigma-Aldrich (Taufkirchen, Germany). CA from Sabinsa Corporation (East Windsor, NJ, USA) was prepared as 5,000 μM stock in dimethyl-sulfoxide (DMSO) solution. The experimental concentrations were further diluted in cell culture medium without exceeding a DMSO concentration of 0.1%.

2.2 Origin and cultivation of the cells

Primary canine chondrocytes (PCHs) were isolated from cartilage samples obtained intraoperatively during joint procedures. Both the permission of the ethical committee of Ludwig-Maximilians-Universität (Munich, Germany) and the agreement of fully informed dog owner had preceded this. Fibroblasts (MRC-5) were obtained from the European Collection of Cell Cultures (Salisbury, UK), and T-lymphocytes (Jurkat) were purchased at Leibniz Institute (Braunschweig, Germany). PCH and MRC-5 grew as monolayer, while Jurkat were non-adherent cells. All cell lines were cultured in T175 cell culture flasks at 37°C and 5% CO_2 until 70% confluency in cell culture medium containing 10% fetal bovine serum (FBS). Then, they were washed in cell culture medium containing 3% FBS (serum-starved) three times and used for experiments, all of which were done in serum-starved cell culture medium.

Dulbecco's medium/Ham's F-12 from Seromed (Munich, Germany) was enriched with 3% or 10% FBS and further supplemented with glutamine, penicillin/streptomycin, ascorbic acid, essential amino acids (1% each), and 0.5% amphotericin B.

2.3 Transient transfection

PCH were transiently transfected with antisense/sense (ASO/SO) oligonucleotides (phosphorothioate-specific) from Eurofins MWG Operon (Ebersberg, Germany). The incubation ratio was 0.5 μM ASO/SO with 10 μl/ml Lipofectin from Invitrogen (Karlsruhe, Germany). Specifically, 5′-gGAGATGCGCA CTGTCCCTGGTC-3′ (ASO) corresponded to p65/NF-κB mRNA subunit, and 5′-gACCAGGGACAGTGCGCATCTC-3′ (SO) served as control substance, as described in the past (26).

2.4 Osteoarthritis environment

To simulate an osteoarthritic joint situation *in vitro*, we constructed a multicellular OA-EN in 3D (Figure 1). In this

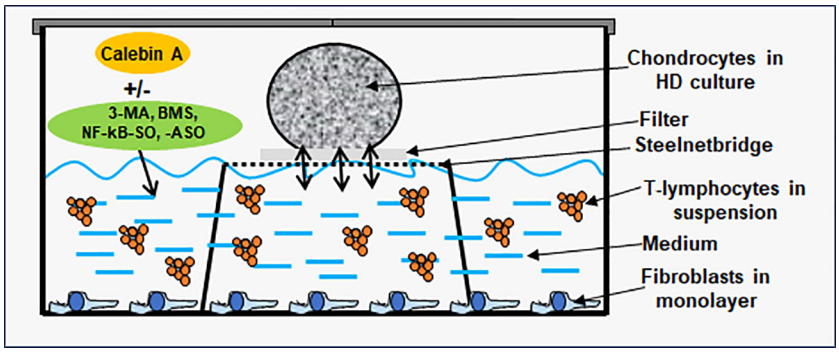

FIGURE 1
Osteoarthritis (OA) high-density (HD) environment (EN) culture model. The OA-EN was installed in well plates, where each well was equipped with a steelnet bridge and an overlying filter. Fibroblasts grew as monolayer on the bottom of the well and T-lymphocytes floated in the cell culture medium. This cell culture medium was filled up to the medium/air interface and enriched with additives such as Calebin A, 3-methyladenine (3-MA), BMS-345541 or NF-κB-SO/ASO. Chondrocytes were applied as HD culture on each filter.

context, three types of cells were combined, with PCH represented the cartilage tissue of the articular surface, MRC-5 fibroblasts represented an intact connective tissue, and Jurkat T-lymphocytes ensured the OA-associated inflammatory reaction. Therefore, PCH were cultivated as high density (HD) or coverglass culture in well plates. Additionally, fibroblasts (0.01 Mio./ml medium) were grown as monolayer on the bottom of the well plates, and Jurkat T-cells (0.01 Mio./ml medium) floated in cell culture medium suspension. The effectiveness of Jurkat cells to promote a pro-inflammatory intercellular cross-talk has been provided by a TNF-α-stimulated control (TNF-α-EN), based on previous comparisons with similar cytokines (27). The OA-EN was used in two cultivation variants for the present experiments.

2.4.1 High-density culture

HD cultures were established in well plates containing a small steelnet bridge with a filter placed on top it as shown in Figure 1 and as already used and described in detail (28, 29). The cell culture medium was filled up to the height of the filter. To start an experiment, PCH were passaged and centrifuged three times in order to obtain a liquid-free pellet. Afterwards, colonies of 2 Mio. PCH were applied to each filter (Figure 1) using a pipette, incubated with different treatments, and the pellets grown at the medium/air interface were evaluated. When the effect of an OA-EN was examined, a fibroblast monolayer was seeded on the bottom, and the cell culture medium was enriched with T-lymphocytes as previously described.

2.4.2 Coverglass culture

For coverglass cultures, PCH (5,000 cells/coverglass) were seeded on small, round coverglasses as published in the past (15). After 24 h, the coverglasses were placed on small stellnet bridges in well plates. To initiate an OA-EN, fibroblasts were grown on the bottom and T-lymphocytes floated in suspension with cell culture medium as described before. The treatments were added for 4 h, and then, the coverglasses were fixed with methanol before they were frozen at −20°C.

2.5 Immunofluorescence

For immunofluorescence investigation, PCH on coverglass cultures were processed as described earlier (15). After defrosting, the PCH on coverglasses were washed with Triton solution (0.5%) and bovine serum albumin (1%) in Hank's salt solution and incubated overnight with a primary antibody (1:80 diluted) at 4°C in a humidity chamber. One day later, the coverglasses were incubated with a secondary antibody (rhodamine-coupled, 1:100 diluted) for 2 h and stained with DAPI for 15 min to distinguish between viable and apoptotic PCH. Lastly, an embedding in Fluoromount and evaluation with a DM2000 microscope from Leica (Wetzlar, Germany) was carried out. Thereby, 400–500 PCH from 15 microscopic areas were counted and evaluated.

2.6 MTT assay

To compare the effect of various treatments on the viability of PCH, a MTT assay was chosen. Therefore, PCH were HD cultured, and after 3 days, the cell pellet was detached from the filter and washed in Hank's salt solution for three times to ensure that only PCH were evaluated. Next, the PCH-pellet was dissolved in sodium citrate solution (55 mM) and centrifuged and resuspended in MTT medium (with 3% FBS, without phenol red/vitamin C). Then, as explained earlier (15, 30), 100 µl of this suspension and 10 µl of MTT solution were pipetted into each well of a 96-well plate. After 3 h, the reaction was stopped by addition of 100 µl MTT solubilization solution each, and the optical density (OD) at 550 nm was evaluated with an ELISA reader from Bio-Rad (Munich, Germany).

2.7 Transmission electron microscopy

Ultrastructural analysis was carried out by transmission electron microscopy (TEM) as described before (22, 30). In short, PCH were grown in HD cultures, and the cell pellet was removed from the filter after 3 days. The cells were washed for three times in Hank's salt solution to rule out contaminations with other cell types. Thereafter, a fixation in osmium tetroxide for 2 h, an alcohol-induced dehydration, and an embedding in Epon were done. The resulting grids were cut with an Ultracut E from Reichert-Jung (Darmstadt, Germany) and uranyl-acetate/lead-citrate contrasted before evaluated by a TEM 10 microscope from Zeiss (Jena, Germany). To quantify the number of apoptotic cells, 250 cells from 20 different microscopic areas were counted.

2.8 Western blot

To generate Western blot samples, PCH were cultured as HD cultures, and after 7–10 days, the cell pellets were removed. Ensuring pure PCH samples, the cells were washed in Hank's salt solution for three times. The following procedure was as previously described (15, 22). First, the cells were treated with lysis buffer and centrifuged at 4°C and 10,000 rpm for 30 min. Then, their supernatants were frozen (−80°C) overnight and prepared with an Interchim Protein Quantification Kit (Montlucon Cedex, France) and 2-mercaptoethanol the next day. SDS-PAGE Western blottings were carried out with a BIO-RAD transblot apparatus (Munich, Germany). Therefore, sample-stocked nitrocellulose membranes from Fisher Scientific (Schwerte, Germany) were incubated in blocking buffer for 2 h, then incubated in primary antibodies (1:10,000 diluted) overnight, and finally incubated in secondary antibodies (1:10,000 diluted) for 1.5 h. For densitometric evaluation, QUANTITY ONE program from BIO-RAD (Munich, Germany) was used.

2.9 Statistics

All experiments including their evaluations were carried out three times, and the data presented in the figures represent their average results. In this relation, all data were evaluated by Student's t-test and *post-hoc* ANOVA with SPSS software from IBM (Ehningen, Germany). After determination of percentage effects and 95% confidence intervals, p-values <0.05 were considered as statistically significant.

3 Results

In this study, we designed a multicellular pro-inflammatory high-density and *vivo*-mimicking osteoarthritic environment (OA-EN) to investigate the effect of CA focused on inflammation and autophagy signaling on the suppression of OA-EN cross-talk (Figure 1).

3.1 Calebin A, similar to a specific IKK inhibitor or a specific ASO against NF-κB, suppresses the downregulation of chondrocyte viability triggered by OA-EN, but not in the presence of an autophagy-inhibitor, as shown by the MTT assay

Given the established anti-inflammatory effect of the phytopharmaceutical across diseases, PCH were cultured in 3D-HD settings as basal control, in a pro-inflammatory (TNF-α-EN or OA-EN) or in an autophagy-inhibited (3-MA) microenvironment and observed with or without the addition of CA. Furthermore, the role of inflammation in OA-EN was measured by blocking NF-κB using transient transfection (NF-κB-ASO) or specific IKK inhibitor (BMS-345541). The viability of chondrocytes exposed to these different conditions was then assessed and statistically compared using the MTT assay (Figure 2).

First, it became apparent that a CA treatment (5 μM) in an inflammation-free medium increased the number of viable PCH by more than half compared to the untreated, basal control, but this was abrogated after suppression of autophagy. After treatment of the basal control with 10 mM 3-MA, only 38% of viable PCH were measured. The contrast were even greater in the CA-treated basal control, where only 10% of viable chondrocytes was detectable through the addition of 3-MA (Figure 2).

In the next step, an inflammatory environment was created using the pro-inflammatory cytokine TNF-α. In this TNF-α-EN, 47% fewer PCH survived the treatment period than in the basal control. However, an addition of 5 μM CA to the TNF-α-EN resulted in more than a doubling of the number of viable cells. Here, too, the inhibition of autophagy had a significant effect, as the addition of 3-MA (10 mM) resulted in the survival of 51% of the PCH compared to the TNF-α control. In the CA-treated TNF-α-EN, even only 11% of the chondrocytes remained viable in the autophagy-downregulated situation (Figure 2). Subsequently, the OA-EN containing fibroblasts and T-lymphocytes was established for viability determination as described in *Material and methods*. Probably due to its strong inflammatory effect, 60% fewer cells remained viable in the OA-EN than in the basal control. Interestingly, a CA supplementation led to a concentration-dependent enhancement of PCH viability. While a treatment with 1 μM CA resulted in an increase of 27%, a dose of 5 μM CA led to almost a tripling of viability. At long last, an enrichment of OA-EN with 10 μM CA still slightly exceeded this (Figure 2), so that we determined 5 μM CA as the optimal experimental concentration.

In order to include the self-repair capacity, chondrocytes in the OA-EN were furthermore treated with 10 mM 3-MA, acting as an autophagy inhibitor. The inhibition of autophagy resulted in a significant loss of 40% PCH viability compared to OA-EN control, and a CA supplementation failed to prevent this (Figure 2). This became visible by a detailed examination of the CA-treated OA-EN because after the addition of 3-MA, only 9% viable PCH were found in comparison to the 3-MA-free CA-OA-EN.

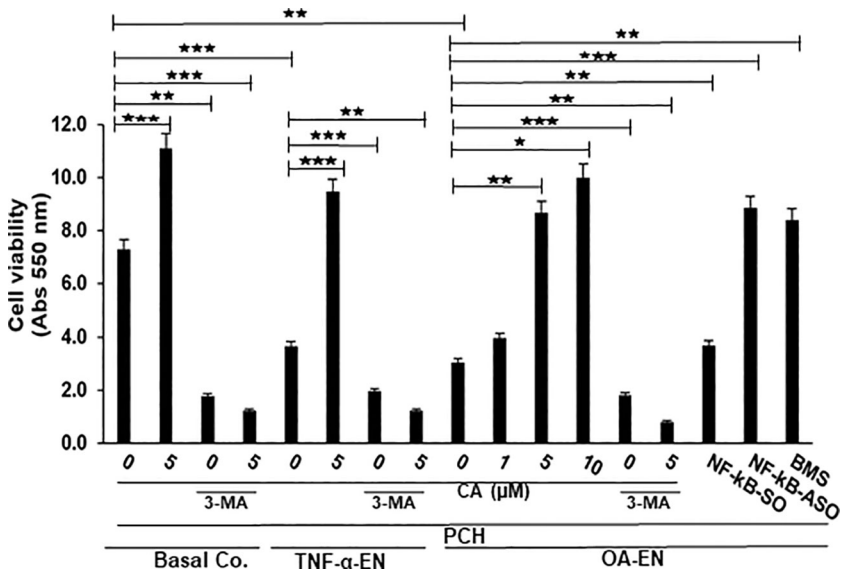

FIGURE 2
Impact of Calebin A (CA) on inflammation-triggered chondrocytes (PCH). PCH were high-density cultured as inflammation-free basal control (Basal Co.), TNF-α environment (TNF-α-EN), or osteoarthritis environment (OA-EN) and treated without additives or with supplementation of 1 μM, 5 μM, or 10 μM CA; 10 mM 3-methyladenine (3-MA); 0.5 μM NF-κB-SO/ASO; or 5 μM BMS-345541 as demonstrated on the x-axis. MTT measuring at 550 nm optical density represented PCH cell viability as shown on the y-axis. The values were given as mean ± SD, n = 3. *$p < 0.05$; **$p < 0.01$; ***$p < 0.001$ were classified as statistically significant.

Finally, the role of inflammation in OA development was illuminated. When the OA-EN was treated with the transfection control substance NF-κB-SO (0.5 μM), the PCH viability was comparable to the OA-EN control. However, when the main inflammatory transcription factor NF-κB was eliminated by transient transfection with NF-κB-ASO (0.5μM), the number of viable cells more than doubled, and this was confirmed by NF-κB blocking with the specific inhibitor BMS-345541 (Figure 2).

All considered, inflammatory processes and the associated downregulation of autophagy limited PCH viability, while a CA treatment was able to reverse these processes and thus promote the PCH viability. These results indicate that inhibition of inflammation and concomitant promotion of autophagy may be one of the key mechanisms of CA as anti-OA agent.

3.2 Calebin A promoted OA-EN-inhibited autophagic protein expression and protected chondrocytes from apoptosis, but not in the presence of an autophagy-inhibitor, as shown by immunofluorescence

As a bradytrophic tissue, articular cartilage relies on self-repair mechanisms. Autophagic processes are particularly important in this respect, and for this reason, the next step was to investigate whether CA influences this early alert system in OA. Therefore, PCH were grown in coverglass cultures without or with OA-EN and treated without or with CA and/or 3-MA. Afterwards, the immunocytochemical localization of autophagy marker Beclin-1 (Figure 3, upper row) and the viability-indicating DAPI staining (Figure 3, middle row) were evaluated by immunofluorescence microscopy, both individually and as a merge view (Figure 3, lower row).

In the inflammation-free basal control, PCH showed a moderate but even Beclin-1 labeling with strong-adhesion pseudopodia and marginally detectable apoptosis. The apoptosis rate remained low when CA was added to the basal control, but the autophagy-indicating labeling changed, as numerous strongly marked punctate autophagic vesicles were now manifested here (Figure 3).

An initiation of the multicellular OA-EN led to a significantly different result, as hardly any stabilizing pseudopodia were visible. In addition, 40% of apoptotic PCH were found, representing cell death, which was particularly outstanding in the merge view. Interestingly, a CA supplementation of OA-EN led to an 80% suppression of this apoptosis, the rate of which almost reached the initial value of the basal control. Moreover, numerous strongly Beclin-1 marked vesicles and a distinct pseudopodia-rich autophagic phenotype become obvious. In order to ensure that the observed CA-induced effects aimed on PCH autophagy, these self-protection processes were switched off using the autophagy-blocker 3-MA, with the result of a very high apoptosis rate (80%) and a non-significant effect of CA treatment (Figure 3).

Overall, these results show that inflammatory processes in PCH limit autophagy activity, leading to a predominance of apoptosis. However, CA treatment reduces inflammation, promotes autophagy, and suppresses apoptosis, resulting in a PCH-promoting equilibrium under OA conditions.

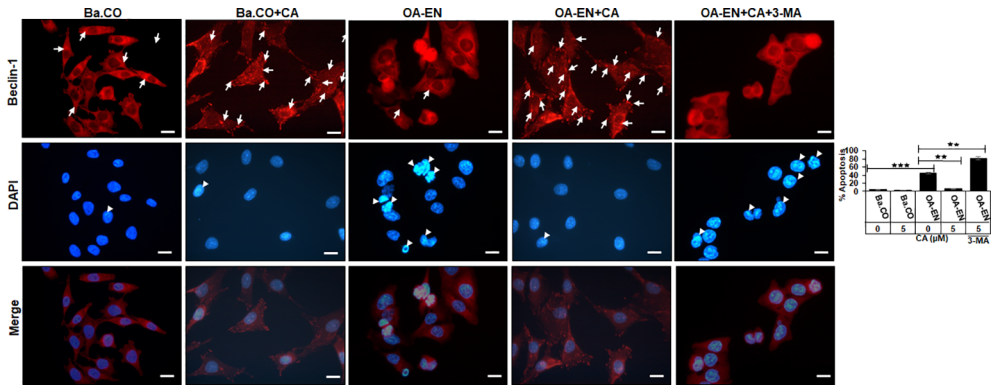

FIGURE 3
Impact of Calebin A (CA) on immunocytochemical localization of Beclin-1 in chondrocytes (PCH). PCH were incubated as basal control (Ba.CO) or osteoarthritis environment (OA-EN) as coverglass cultures and left treatment free or treated with 5 µM CA with or without 10 mM 3-methyladenine (3-MA). Immunofluorescence investigation was carried out after labeling with anti-Beclin-1 antibody (upper row, red), staining with DAPI (middle row, blue), and their merging (lower row, red and blue). A scale bar corresponds to 30 µm. The statistic chart includes x-axis (treatments) and y-axis (apoptosis rate in %). The values were given as mean ± SD, n = 3. $^{**}p < 0.01$, $^{***}p < 0.001$ were classified as statistically significant.

3.3 Calebin A abolishes OA-EN-induced apoptosis, degradation of chondrocytes and promotes autophagosomes, as shown by transmission electron microscopy

To assess the suspected interplay of autophagy and apoptosis in detail at the ultrastructural level, HD-PCH cultures were maintained without (basal control) or with (TNF-α-EN/OA-EN) inflammatory conditions and with/without the addition of CA. The evaluation of chondrocyte's ultrastructure was then carried out by TEM (Figure 4).

The observation of the basal control revealed intact PCH with a smooth surface embedded in a well-organized extracellular matrix (ECM), few autophagic vesicles, and rare apoptosis (Figure 4A). With a constant low cell death rate, an addition of 5 µM CA to the basal control led to a marked formation of stable, pseudopodia-rich PCH containing numerous autophagosomes and autolysosomes (Figure 4B). In contrast, the PCH in TNF-α-EN were deformed due to inflammation and had an extraordinarily high number of 78% of cells with mitochondrial changes or even apoptotic bodies (Figure 4C). Interestingly, the PCH morphology significantly changed through a 5 µM CA supplementation to the TNF-α-EN, as apoptosis rate was drastically reduced to 13%, and the cells resumed their vesicle and pseudopodia-rich shape with a marked augmentation in the number of autophagosomes and autolysosomes (Figure 4D).

A similar sight of destroyed PCH as in treatment-free TNF-α-EN was also to be seen in treatment-free OA-EN. Here, the cells lost their stable form, and more than 80% of them were mitochondrially changed or apoptotic (Figure 4E). An addition of CA to the OA-EN affected concentration dependence, as while the apoptosis rate persisted at 65% during treatment of 1 µM CA, it was reduced considerably to 14% by 5 µM CA. Now, the morphology corresponded to the basal control treated with 5 µM CA and the TNF-α-EN treated with the same concentration (Figures 4F-H). Therefore, and because a higher dosage of 10 µM CA clearly resulted in higher autophagosome and autolysosome formation than the basal control, 5 µM CA was confirmed as the optimal concentration for our PCH studies. Altogether, the inflammatory environment prevented autophagy and simultaneously induced apoptosis in chondrocytes and a degradation of the ECM. The natural polyphenol CA was able to modulate the interplay of autophagy and apoptosis and stabilized chondrocytes and ECM synthesis by at least promoting autophagy and suppressing inflammation, mitochondrial changes, and apoptosis.

3.4 Calebin A maintains the functionality of chondrocytes and protects them from pathological processes in OA-EN, but not in the presence of an autophagy inhibitor

After noticing large possibilities of CA for autophagy modulation, we wanted to clarify these detailed effects on molecular processes in chondrocytes. Therefore, PCH were HD cultivated as basal control or in OA-EN, where OA-EN was carried out as control or treated with 5 µM CA, 10 mM 3-MA, or a combination of both and the subsequent evaluation occurred by Western blotting.

First, an indication of the PCH viability was provided by examination of their essential ECM components collagen type II (Coll II) and chondroitin sulfate proteoglycan (CSPG). Compared to basal control, both parameters decreased due to the cultivation of the chondrocytes in OA-EN. However, an addition of CA led to a significant increase in Coll II and CSPG, so that their expression was not only higher than in treatment-free OA-EN but also significantly stronger than in the basal control. Interestingly, an inhibition of autophagic pathways by 3-MA ensured low levels of Coll II and CSPG, and this was not reversible by CA supplementation (Figure 5A). Furthermore, the chondrogenic transcription factor Sox9 was very impressively influenced in the same way because its solid expression found in the basal control was massively downregulated by OA-EN-induced inflammation. A treatment of PCH with CA interrupted this tendency and upregulated Sox9 at a

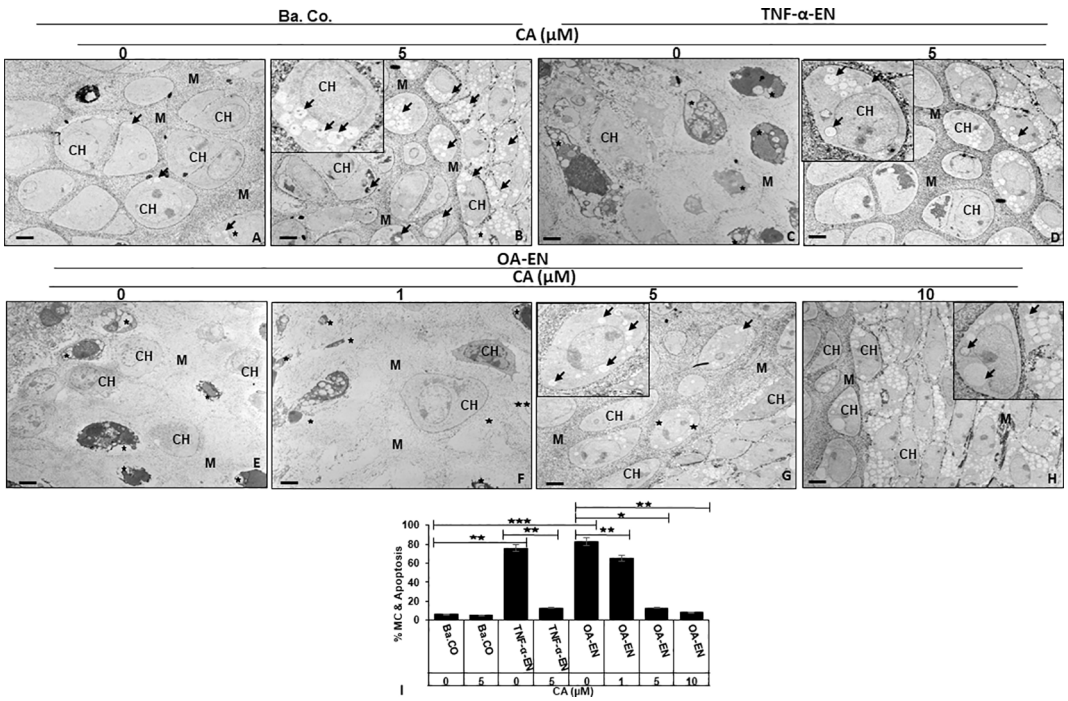

FIGURE 4
Impact of Calebin A (CA) on chondrocyte (PCH) ultrastructure focusing autophagy-apoptosis interplay. PCH were high density (HD) cultured without inflammation (basal control, Ba.Co., **A, B**), in TNF-α environment (TNF-α-EN, **C, D**), or in osteoarthritis environment (OA-EN, **E–H**). The cultures were left treatment-free or treated with 1, 5, or 10μM CA and thereafter investigated by transmission electron microscope (TEM). Marking: CH, chondrocyte; M, matrix; arrow, autophagic vesicle/autophagosome/autolysosome; star, mitochondrial changes/apoptosis. Magnification: **(A–H)** ×5,000; scale bar = 1 μM. Insets: ×15,000. The statistic diagram **(I)** shows different treatments (x-axis) and the rate of mitochondrial changes (MC) and apoptosis in % (y-axis). The values were given as mean ± SD (n = 3). *$p < 0.05$, **$p < 0.01$, ***$p < 0.001$ were classified as statistically significant.

value exceeding that of the basal control. Also for this parameter, a suppression of autophagy *via* 3-MA addition leads to a decline in expression, which could not be reversed by CA (Figure 5A).

Next, inflammation marker p-NF-κB-p65, cell-degradation-associated MMP-9, and apoptosis indicator cleaved-caspase-3, representing possible pathological signaling processes in chondrocytes, were considered in a differentiated manner. As expected, the expression of phosphorylated and thereby activated inflammatory p-NF-κB-p65 was significantly expanded by OA-EN in contrast to the basal control. A CA treatment of OA-EN suppressed this inflammation markedly, confirming CA's extensive anti-inflammatory impact, whereas the addition of autophagy-hampering 3-MA entailed an increase in p-NF-κB-p65 that was not annullable by CA (Figure 5B). In line with this, the inflammation-accompanying degradation and degradation-resulting apoptosis also reproduced this dynamic tendency. Both parameters were significantly forced in OA-EN and downregulated due to CA supplementation, but not in the presence of 3-MA (Figure 5B).

All in all, these findings summarize a physiology-restricting and pathology-promoting influence of the osteoarthritic environment but confirm CA's PCH-supporting possibilities, which are noticeable, among other things, through the modulation of ECM components, integral transcription factors, inflammatory cascades, and the induction of cell degradation and apoptosis.

3.5 Calebin A disrupts the impaired expression of autophagy-specific markers and autophagy-inhibitory signaling pathways regulated by OA-EN in chondrocytes, but not in the presence of an autophagy inhibitor

To finally confirm the results described, the Western blot evaluation was profoundly investigated. For this reason, the samples explained in the previous subchapter were immunoblotted with antibodies against autophagy-related marker proteins and signaling molecules associated with autophagy pathways in chondrocytes (Figure 6).

Concerning this matter, the known autophagic benchmarks Beclin-1 and LC3-II were found to be clearly expressed in PCH from basal control and comparatively downregulated in the OA-EN. Then, very interesting and never shown before, a CA supplementation of PCH lead to a significant upregulation of both autophagy parameters despite OA-EN. In the following, PCH treated with the autophagy-inhibitor 3-MA showed a marginal expression of both, Beclin-1 and LC3-II, regardless of whether CA has been added to OA-EN or not. These findings confirmed the specificity of 3-MA as an anti-autophagy protein on the one hand and demonstrated the dependence of CA's effect on intact autophagy mechanisms in PCH on the other hand (Figure 6A).

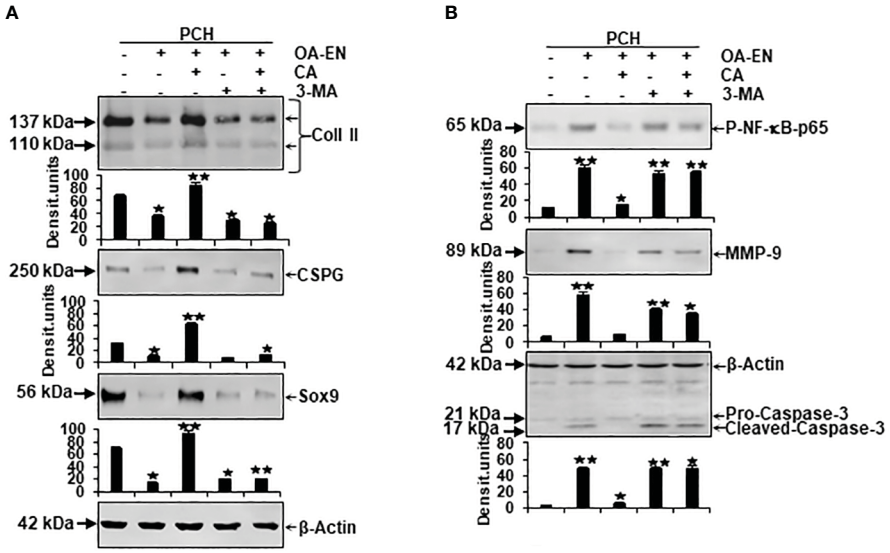

FIGURE 5
Impact of Calebin A (CA) on the physiological and pathological protein expression in chondrocytes (PCH). x-axis: PCH from high density (HD) cultures grew as basal control or in osteoarthritis environment (OA-EN) without treatment or with an addition of 5 µM CA, 10 mM 3-MA, or both combined. y-axis: Western blotting was evaluated taking densitometric units into account with, related to OA-EN control, *p<0.05 and **p<0.01 (n = 3). **(A)** The protein expression of extracellular matrix (ECM; collagen type II, CSPG) and chondrocyte-specific transcription factor (Sox9) was investigated. **(B)** Then, the levels of inflammation (p-NF-κB-p65), cell degradation (MMP-9), and apoptosis (cleaved-caspase-3) were examined. (A+B) β-actin was used as housekeeping control.

At long last, the investigation of mTOR, PI3K, and Akt proteins completed the experiments, as their axis is known to be induced by inflammatory processes and to prevent autophagy in chondrocytes as a consequence thereof. All three proteins were found in small quantities in the basal control but, as expected, highly concentrated in PCH after OA-EN cultivation. This overexpression of mTOR, PI3K, and Akt could be mitigated by CA addition to the inflamed chondrocytes. However, if the PCH were treated with 3-MA, the chondrocytes lacked a physiological counterpart and the inflammatory processes dominated, which was reflected in an increased level of the mTOR/PI3K/Akt cascade and could not be reversed by CA (Figure 6B).

In summary, these Western blot evaluations confirm the inflammation promotion and autophagy suppression of OA-EN but underline the importance of autophagy signaling pathways in CA's physiology-regulating effects in chondrocytes.

4 Discussion

OA is a widespread disease in society as a whole (1), which leads to progressive, irreversible, and only symptomatically treatable limitations in the everyday lives of affected people (5). It would therefore be important from both an economic and a patient perspective to reduce or at least limit the OA-induced joint damages. Against this background of a great need for the further development of preventive or therapeutic strategies, complementary treatment options involving natural phytopharmaceuticals such as grape-ingredient resveratrol (13, 14) or turmeric-derived curcumin (15, 31) are discussed. As CA, a fairly novel turmeric component, shows more and more a wide-ranging potential against divers health issues (18, 23), we wanted to examine its suitability in this respect. Therefore, multicellular culture models were established, and CA's influences on OA-EN (Figure 1) stressed chondrocytes were observed with a special focus on autophagic self-repair processes. On this occasion, the present investigations revealed following key facts: OA-EN (I) promotes inflammation, degradation, and apoptosis in PCH and (II) reduces viability and autophagy in PCH. However, CA (III) represses inflammation, pathological tendencies, and apoptosis in PCH and, in parallel, (IV) strengthens chondrocyte's ECM, viability, physiological processes, (V) enhances their autophagic self-repair capacities, and (VI) exerts its chondroprotective abilities largely *via* regulation of autophagy.

After the implementation of OA-EN, we found that this multicellular setting had comparable effects to the TNF-α-EN on cell viability (Figure 2) and ultrastructure (Figure 4) and that an addition of CA had very similar effects in both environments. This was based on the background knowledge that the cytokine TNF-α has been known for many years as a pro-inflammatory product of T-lymphocytes and monocytes (32). As a result, it has a significant share in spreading harmful inflammation in various tissues including cartilage, where TNF-α destroys the organization of chondrocyte's matrix (15, 33), and serves as a relevant target for natural substances. In sum, these observations pointed out the inflammatory characteristics of OA-EN confirming earlier *in vitro* results from analogical co-culture models (27, 34) and the clinical situation of inflamed OA joints (35). As a result of the chronic inflammation, OA patients develop dysfunctional, degraded, and thus apoptotic chondrocytes (36), which, interestingly, we were able to simulate with our OA-EN culture (Figures 4, 5). Moreover,

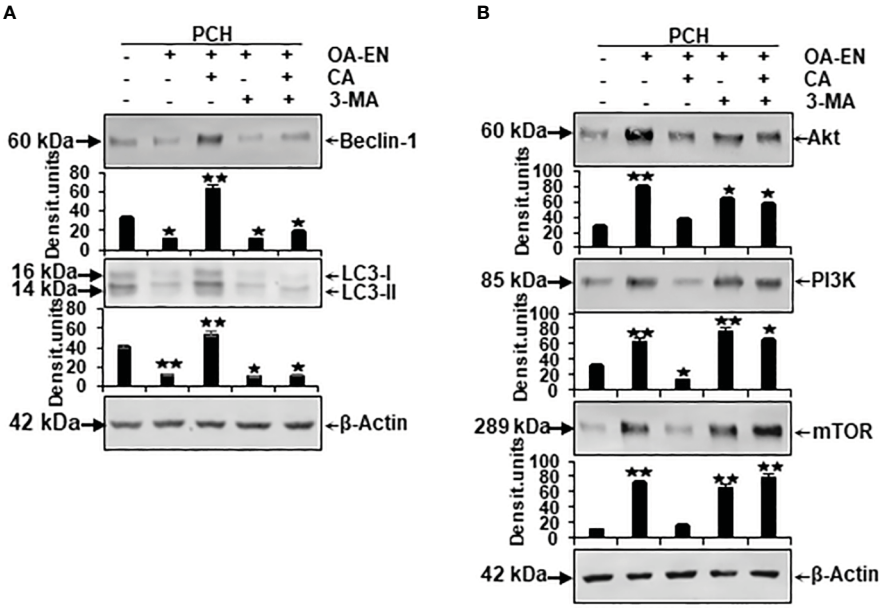

FIGURE 6
Impact of Calebin A (CA) on the expression of autophagy-specific markers and autophagy-associated signaling pathways in chondrocytes (PCH). x-axis: high-density (HD) cultured PCH were treated as basal control or in osteoarthritis environment (OA-EN) without supplementation or with of 5 μM CA, 10 mM 3-MA, or a combination thereof. y-axis: densitometric units of Western blots were evaluated with *p<0.05 and **p<0.01, (n = 3) compared to OA-EN control. The protein expression of autophagy-specific parameters (**A**, Beclin-1, LC3-II) and signaling pathways (**B**, Akt, PI3K, mTOR) was demonstrated, and β-actin **(A, B)** served as housekeeping control.

beyond this clinically known scenario, the present findings demonstrated a clear inflammation-associated limitation of autophagic self-repair processes in chondrocytes (Figures 3, 6). Altogether, joint inflammations result in massively destructive properties that needs to be interrupted.

Based on the observed pathological effects of OA-EN on PCH, the next step was to specifically investigate the influence of the natural polyphenol CA on these cells. In this context, chondrocytes grown without an inflammatory environment (basal control) were left untreated or supplemented with CA, and a comparison with each other showed not only a non-toxicity of CA toward chondrocytes but, on the contrary, a viability promotion (Figure 2), autophagy support (Figures 3, 4), and even apoptosis repression (Figures 3, 4) turned out. These properties are obvious similar to a known chondrocyte stabilization by the structurally related turmeric component curcumin of which, by long-term research, a regulation of inflammatory, autophagic, and apoptotic signaling pathways were identified (15, 37). Interestingly, CA maintained its valuable anti-degenerative (MMP-9) and anti-apoptotic (caspase-3) features despite an initiation of OA-EN resulting in a significant anti-inflammatory (NF-κB) capacity (Figures 4, 5B). A comparative and confirmatory prevention of inflammation of the phytotherapeutic in other constellations, for example, in the tumor microenvironment of cancer cells (22, 23, 38) or tumor-associated bone loss (24), underlines its modulatory potential to restore cell homeostasis and promote the natural physiology of healthy tissue.

A further important balancing mechanism for cartilage tissue is the perpetuation of an intact ECM, which consists of collagen, elastins, and proteoglycans (39), and, due to its high water binding, has both a protective and nutritional function (40). As an advantage, our results pointed to CA's support of Coll II, CSPG, and thus ECM synthesis and the expression of cartilage-specific transcription factor Sox9 (Figure 5A), suggesting a holistic, broad-based positive influence on PCH despite an OA-promoting environment.

When considering CA's modulation of chondrocyte signaling, we noticed the regulation of autophagy as a crucial interface between physiology and pathology. Autophagy represents an evolutionarily conserved intracellular homeostatic mechanism, ensuring the survival of cells such as chondrocytes by initiating the disposal of damaged cell organelles, microorganisms, and from which new energy is derived (41). These self-repair processes are particularly important against the development or spread of OA-induced joint alterations (42). The modulation of mTOR/Akt/PI3K pathway thereby acts as a key regulator related to autophagic processes in chondrocytes, and in recent studies, phytochemicals demonstrated their potential for influencing this signaling. Curcumin, for example, is able to avert cytokine-stimulated cartilage degradation by inhibiting mTOR/Akt/PI3K signals and accompanying promotion of collagen production and suppression of MMP expression (43). Moreover, isorhynchophylline, used in traditional Chinese medicine, impedes osteoarticular and chondrogenic inflammation by the upregulation of autophagic Beclin-1 and LC3-II proteins and a simultaneous downregulation of the mTOR/Akt/PI3K signaling

pathway (44). Consistent with these findings, our results showed a clear CA-related promotion of autophagosomes, autolysosomes (Figure 4), and autophagy-specific molecular markers (Beclin-1, LC3-II), and an undoubted suppression of mTOR/Akt/PI3K pathway (Figure 6) in PCH with an assumed increase in their self-repair and thus OA-defense capacity. Moreover, a much more far-reaching fact was revealed: all the cartilage-promoting effects described so far could only be observed to a very weak extent in the presence of the autophagy-inhibitor 3-MA (Figures 2, 3, 5), which seems to make the modulation of autophagic processes a central mechanism of CA's holistic chondroprotection. These insights gained into the influence of CA on chondrocytes are completely new, as to the best of our knowledge, this has never been studied before. It remains undisputed that this research work offers a very first basis, which would have to be deepened by further detailed projects. In order to be able to assess the transferability of the *in vitro* results to processes in human joints, the tolerability and bioavailability of CA must first be clarified. In this respect, a non-toxicity observed even at high doses in experiments with rats (17) appears to be motivating. The bioavailability of curcumin could serve as an indication here, which, for many years, was considered to be low, but can now be significantly increased through special purification and new formulations that lead to improved intestinal absorption (45). Overall, the credibility of our new results was strengthened not only by repeated experiments but also by other phytotherapeutics with noticeable anti-OA properties, for example, extracted from *Luzula sylvatica* (46), *Olea europaea* (40), *Uncaria rhynchophylla* (44), *Boswellia serrata*, *Curcuma longa*, or *Tamarindus indica* (47). Therefore, an establishment of plant-based supplements for OA prevention or co-therapy could represent an approach worth pursuing. Finally, it cannot be ruled out that the phytotherapeutic agent CA could close a treatment gap, since the multicellular cross-talk, which has been successfully modulated in the present results, is currently considered to have hidden therapeutic potential (48), especially with regard to the regenerative and OA-averting ability of cartilage.

5 Conclusion

Contemplating an increasing human life expectancy and growing OA prevalences, the need for cost-effective, abundant, and well-tolerated therapeutic options remains undisputed. Within the present study, the natural polyphenol CA demonstrated for the first time a significant upregulation of autophagosomes, autolysosomes, Beclin-1, LC3-II, Coll II, CSPG, and Sox9, and simultaneous downregulation of NF-κB, MMP-9, caspase-3, and mTOR/PI3K/Akt pathway in chondrocytes. Thereby, the control of autophagic signals crystallized as one of the key mechanisms in its multitarging, anti-inflammatory, anti-degrading, and apoptosis-preventing effects in PCH. All summarized, CA seems to be a suitable co-therapeutic agent for the prevention or treatment of OA and more in-depth research in this area, especially on a clinical level, in the future would be welcome.

Data availability statement

The raw data supporting the conclusions of this article will be made available by the authors, without undue reservation.

Author contributions

AB: Investigation, Methodology, Validation, Visualization, Writing – original draft, Writing – review & editing. CB: Investigation, Methodology, Writing – review & editing. PS: Writing – review & editing. MS: Conceptualization, Data curation, Supervision, Visualization, Writing – original draft, Writing – review & editing.

Funding

The author(s) declare that no financial support was received for the research, authorship, and/or publication of this article.

Acknowledgments

The authors are grateful to Sabinsa Corporation (East Windsor, NJ, USA) for the generous gift of Calebin A and to Andreas Eimannsberger for his continuous technical service.

Conflict of interest

The authors declare that the research was conducted in the absence of any commercial or financial relationships that could be construed as a potential conflict of interest.

The author(s) declared that they were an editorial board member of Frontiers, at the time of submission. This had no impact on the peer review process and the final decision.

Publisher's note

References

1. Fuchs J, Scheidt-Nave C, Kuhnert R. 12-month prevalence of osteoporosis in Germany. *J Health Monitoring*. (2017) 2:57–61. doi: 10.17886/RKI-GBE-2017-067

2. Kellgren JH, Lawrence J. Radiological assessment of osteo-arthrosis. *Ann rheumatic diseases*. (1957) 16:494. doi: 10.1136/ard.16.4.494

3. Huskisson EC, Dieppe PA, Tucker AK, Cannell LB. Another look at osteoarthritis. *Ann Rheum Dis*. (1979) 38:423–8. doi: 10.1136/ard.38.5.423

4. Hildebrandt G, Kamprad F-H. Degenerative Joint Disease Activated Osteoarthrosis Deformans: Hip, Knee, Shoulder and Other Joints. In: *Radiotherapy for Non-Malignant Disorders* Springer: Berlin, Heidelberg (2008). p. 317–32.

5. Taruc-Uy RL, Lynch SA. Diagnosis and treatment of osteoarthritis. *Prim Care*. (2013) 40:821–36, vii. doi: 10.1016/j.pop.2013.08.003

6. Frondoza CG, Sohrabi A, Polotsky A, Phan PV, Hungerford DS, Lindmark L. An in vitro screening assay for inhibitors of proinflammatory mediators in herbal extracts using human synoviocyte cultures. *In Vitro Cell Dev Biol Anim*. (2004) 40:95–101. doi: 10.1290/1543-706X(2004)0402.0.CO;2

7. Cheleschi S, Tenti S, Lorenzini S, Seccafico I, Barbagli S, Frati E, et al. Synovial Fluid Regulates the Gene Expression of a Pattern of microRNA via the NF-κB Pathway: An In Vitro Study on Human Osteoarthritic Chondrocytes. *Int J Mol Sci*. (2022) 23:8334. doi: 10.3390/ijms23158334

8. Ramos YFM, Mobasheri A. MicroRNAs and regulation of autophagy in chondrocytes. *Methods Mol Biol*. (2021) 2245:179–94. doi: 10.1007/978-1-0716-1119-7_13

9. Vesela B, Svandova E, Ramesova A, Kratochvilova A, Tucker AS, Matalova E. Caspase inhibition affects the expression of autophagy-related molecules in chondrocytes. *Cartilage*. (2021) 13:956s–68s. doi: 10.1177/1947603520938444

10. Settembre C, Arteaga-Solis E, Ballabio A, Karsenty G. Self-eating in skeletal development: implications for lysosomal storage disorders. *Autophagy*. (2009) 5:228–9. doi: 10.4161/auto.5.2.7390

11. Srinivas V, Bohensky J, Shapiro IM. Autophagy: a new phase in the maturation of growth plate chondrocytes is regulated by HIF, mTOR and AMP kinase. *Cells tissues organs*. (2009) 189:88–92. doi: 10.1159/000151428

12. Chen J, Crawford R, Xiao Y. Vertical inhibition of the PI3K/Akt/mTOR pathway for the treatment of osteoarthritis. *J Cell Biochem*. (2013) 114:245–9. doi: 10.1002/jcb.24362

13. Shakibaei M, John T, Seifarth C, Mobasheri A. Resveratrol inhibits IL-1 beta-induced stimulation of caspase-3 and cleavage of PARP in human articular chondrocytes in vitro. *Ann N Y Acad Sci*. (2007) 1095:554–63. doi: 10.1196/annals.1397.060

14. Yuce P, Hosgor H, Rencber SF, Yazir Y. Effects of intra-articular resveratrol injections on cartilage destruction and synovial inflammation in experimental temporomandibular joint osteoarthritis. *J Oral Maxillofac Surg*. (2021) 79:344.e1–.e12. doi: 10.1016/j.joms.2020.09.015

15. Buhrmann C, Brockmueller A, Mueller AL, Shayan P, Shakibaei M. Curcumin attenuates environment-derived osteoarthritis by sox9/NF-kB signaling axis. *Int J Mol Sci*. (2021) 22:7645. doi: 10.3390/ijms22147645

16. Park SY, Kim DS. Discovery of natural products from Curcuma longa that protect cells from beta-amyloid insult: a drug discovery effort against Alzheimer's disease. *J Nat Prod*. (2002) 65:1227–31. doi: 10.1021/np010039x

17. Majeed M, Nagabhushanam K, Natarajan S, Bani S, Pandey A, Karri SK. Investigation of repeated dose (90 day) oral toxicity, reproductive/developmental toxicity and mutagenic potential of 'Calebin A'. *Toxicol Rep*. (2015) 2:580–9. doi: 10.1016/j.toxrep.2015.03.009

18. Brockmueller A, Mueller AL, Kunnumakkara AB, Aggarwal BB, Shakibaei M. Multifunctionality of Calebin A in inflammation, chronic diseases and cancer. *Front Oncol*. (2022) 12:962066. doi: 10.3389/fonc.2022.962066

19. Lai CS, Liao SN, Tsai ML, Kalyanam N, Majeed M, Majeed A, et al. Calebin-A inhibits adipogenesis and hepatic steatosis in high-fat diet-induced obesity via activation of AMPK signaling. *Mol Nutr Food Res*. (2015) 59:1883–95. doi: 10.1002/mnfr.201400809

20. Li Y, Li S, Han Y, Liu J, Zhang J, Li F, et al. Calebin-A induces apoptosis and modulates MAPK family activity in drug resistant human gastric cancer cells. *Eur J Pharmacol*. (2008) 591:252–8. doi: 10.1016/j.ejphar.2008.06.065

21. Buhrmann C, Brockmueller A, Harsha C, Kunnumakkara AB, Kubatka P, Aggarwal BB, et al. Evidence That Tumor Microenvironment Initiates Epithelial-To-Mesenchymal Transition and Calebin A can Suppress it in Colorectal Cancer Cells. *Front Pharmacol*. (2021) 12:699842. doi: 10.3389/fphar.2021.699842

22. Brockmueller A, Girisa S, Motallebi M, Kunnumakkara AB, Shakibaei M. Calebin A targets the HIF-1α/NF-κB pathway to suppress colorectal cancer cell migration. *Front Pharmacol*. (2023) 14:1203436. doi: 10.3389/fphar.2023.1203436

23. Tyagi AK, Prasad S, Majeed M, Aggarwal BB. Calebin A, a novel component of turmeric, suppresses NF-κB regulated cell survival and inflammatory gene products leading to inhibition of cell growth and chemosensitization. *Phytomedicine*. (2017) 34:171–81. doi: 10.1016/j.phymed.2017.08.021

24. Tyagi AK, Prasad S, Majeed M, Aggarwal BB. Calebin A downregulates osteoclastogenesis through suppression of RANKL signalling. *Arch Biochem Biophys*. (2016) 593:80–9. doi: 10.1016/j.abb.2016.02.013

25. Mueller AL, Brockmueller A, Kunnumakkara AB, Shakibaei M. Calebin A, a compound of turmeric, down-regulates inflammation in tenocytes by NF-κB/scleraxis signaling. *Int J Mol Sci*. (2022) 23:1695. doi: 10.3390/ijms23031695

26. Buhrmann C, Shayan P, Aggarwal BB, Shakibaei M. Evidence that TNF-β (lymphotoxin α) can activate the inflammatory environment in human chondrocytes. *Arthritis Res Ther*. (2013) 15:R202. doi: 10.1186/ar4393

27. Buhrmann C, Popper B, Aggarwal BB, Shakibaei M. Resveratrol downregulates inflammatory pathway activated by lymphotoxin α (TNF-β) in articular chondrocytes: Comparison with TNF-α. *PloS One*. (2017) 12:e0186993. doi: 10.1371/journal.pone.0186993

28. Seifarth C, Csaki C, Shakibaei M. Anabolic actions of IGF-I and TGF-beta1 on Interleukin-1beta-treated human articular chondrocytes: evaluation in two and three dimensional cultures. *Histol histopathol*. (2009) 24:1245–62. doi: 10.14670/HH-24.1245

29. Shakibaei M, Abou-Rebyeh H, Merker HJ. Integrins in ageing cartilage tissue in vitro. *Histol histopathol*. (1993) 8:715–23. doi: 10.14670/HH-24.1245

30. Brockmueller A, Buhrmann C, Shayan P, Shakibaei M. Resveratrol induces apoptosis by modulating the reciprocal crosstalk between p53 and Sirt-1 in the CRC tumor microenvironment. *Front Immunol*. (2023) 14:1225530. doi: 10.3389/fimmu.2023.1225530

31. Shakibaei M, John T, Schulze-Tanzil G, Lehmann I, Mobasheri A. Suppression of NF-kappaB activation by curcumin leads to inhibition of expression of cyclo-oxygenase-2 and matrix metalloproteinase-9 in human articular chondrocytes: Implications for the treatment of osteoarthritis. *Biochem Pharmacol*. (2007) 73:1434–45. doi: 10.1016/j.bcp.2007.01.005

32. Desch CE, Dobrina A, Aggarwal BB, Harlan JM. Tumor necrosis factor-alpha exhibits greater proinflammatory activity than lymphotoxin in vitro. *Blood*. (1990) 75:2030–4. doi: 10.1182/blood.V75.10.2030.bloodjournal75102030

33. Séguin CA, Bernier SM. TNFalpha suppresses link protein and type II collagen expression in chondrocytes: Role of MEK1/2 and NF-kappaB signaling pathways. *J Cell Physiol*. (2003) 197:356–69. doi: 10.1002/jcp.10371

34. Samavedi S, Diaz-Rodriguez P, Erndt-Marino JD, Hahn MS. A three-dimensional chondrocyte-macrophage coculture system to probe inflammation in experimental osteoarthritis. *Tissue Eng Part A*. (2017) 23:101–14. doi: 10.1089/ten.tea.2016.0007

35. Goudarzi R, Thomas P, Ryan S. Joint dysfunctionality alleviation along with systemic inflammation reduction following arthrocen treatment in patients with knee osteoarthritis: A randomized double-blind placebo-controlled clinical trial. *Medicina (Kaunas Lithuania)*. (2022) 58:228. doi: 10.3390/medicina58020228

36. Vassão PG, de Souza ACF, da Silveira Campos RM, Garcia LA, Tucci HT, Renno ACM. Effects of photobiomodulation and a physical exercise program on the expression of inflammatory and cartilage degradation biomarkers and functional capacity in women with knee osteoarthritis: a randomized blinded study. *Adv Rheumatol (London England)*. (2021) 61:62. doi: 10.1186/s42358-021-00220-5

37. Chen T, Zhou R, Chen Y, Fu W, Wei X, Ma G, et al. Curcumin ameliorates IL-1β-induced apoptosis by activating autophagy and inhibiting the NF-κB signaling pathway in rat primary articular chondrocytes. *Cell Biol Int*. (2021) 45:976–88. doi: 10.1002/cbin.11541

38. Buhrmann C, Kunnumakkara AB, Kumar A, Samec M, Kubatka P, Aggarwal BB, et al. Multitargeting effects of calebin A on Malignancy of CRC cells in multicellular tumor microenvironment. *Front Oncol*. (2021) 11:650603. doi: 10.3389/fonc.2021.650603

39. Childs RD, Nakao H, Isogai N, Murthy A, Landis WJ. An analytical study of neocartilage from microtia and otoplasty surgical remnants: A possible application for BMP7 in microtia development and regeneration. *PloS One*. (2020) 15:e0234650. doi: 10.1371/journal.pone.0234650

40. Varela-Eirín M, Carpintero-Fernández P, Sánchez-Temprano A, Varela-Vázquez A, Paíno CL, Casado-Díaz A, et al. Senolytic activity of small molecular polyphenols from olive restores chondrocyte redifferentiation and promotes a pro-regenerative environment in osteoarthritis. *Aging*. (2020) 12:15882–905. doi: 10.18632/aging.v12i16

41. Hale AN, Ledbetter DJ, Gawriluk TR, Rucker EB3rd. Autophagy: regulation and role in development. *Autophagy*. (2013) 9:951–72. doi: 10.4161/auto.24273

42. Caramés B, Taniguchi N, Otsuki S, Blanco FJ, Lotz M. Autophagy is a protective mechanism in normal cartilage, and its aging-related loss is linked with cell death and osteoarthritis. *Arthritis rheumatism*. (2010) 62:791–801. doi: 10.1002/art.27305

43. Han G, Zhang Y, Li H. The combination treatment of curcumin and probucol protects chondrocytes from TNF-α Induced inflammation by enhancing autophagy and reducing apoptosis via the PI3K-akt-mTOR pathway. *Oxid Med Cell longevity*. (2021) 2021:5558066. doi: 10.1155/2021/5558066

44. Jiang J, Li J, Xiong C, Zhou X, Liu T. Isorhynchophylline alleviates cartilage degeneration in osteoarthritis by activating autophagy of chondrocytes. *J orthopaedic Surg Res*. (2023) 18:154. doi: 10.1186/s13018-023-03645-4

45. Kothaplly S, Alukapally S, Nagula N, Maddela R. Superior bioavailability of a novel curcumin formulation in healthy humans under fasting conditions. *Adv Ther*. (2022) 39:2128–38. doi: 10.1007/s12325-022-02081-w

46. Cholet J, Decombat C, Delort L, Gainche M, Berry A, Ogeron C, et al. Potential anti-inflammatory and chondroprotective effect of luzula sylvatica. *Int J Mol Sci*. (2022) 24:127. doi: 10.3390/ijms24010127

47. Prasad N, Vinay V, Srivastava A. Efficacy of a proprietary combination of Tamarindus indica seeds and Curcuma longa rhizome extracts in osteoarthritis: a clinical investigation. *Food Nutr Res*. (2023) 20:67. doi: 10.29219/fnr.v67.9268

48. Brose TZ, Kubosch EJ, Schmal H, Stoddart MJ, Armiento AR. Crosstalk between mesenchymal stromal cells and chondrocytes: the hidden therapeutic potential for cartilage regeneration. *Stem Cell Rev Rep*. (2021) 17:1647–65. doi: 10.1007/s12015-021-10170-6

frontiers | Frontiers in Immunology

TYPE Original Research
PUBLISHED 27 March 2024
DOI 10.3389/fimmu.2024.1368516

OPEN ACCESS

EDITED BY
Uzma Saqib,
Indian Institute of Technology Indore, India

REVIEWED BY
Bisheng Zhou,
University of Illinois Chicago, United States
Didier Communi,
Université libre de Bruxelles, Belgium

*CORRESPONDENCE
Tong Li
litong3zx@sina.com
Wenqing Gao
gaowenqing0906@126.com

†These authors have contributed equally to this work

RECEIVED 10 January 2024
ACCEPTED 11 March 2024
PUBLISHED 27 March 2024

CITATION
Zheng Y, Wang Y, Qi B, Lang Y, Zhang Z, Ma J, Lou M, Liang X, Chang Y, Zhao Q, Gao W and Li T (2024) IL6/adiponectin/HMGB1 feedback loop mediates adipocyte and macrophage crosstalk and M2 polarization after myocardial infarction. *Front. Immunol.* 15:1368516. doi: 10.3389/fimmu.2024.1368516

IL6/adiponectin/HMGB1 feedback loop mediates adipocyte and macrophage crosstalk and M2 polarization after myocardial infarction

Yue Zheng[1,2,3†], Yuchao Wang[1,2,3†], Bingcai Qi[2,3,4†], Yuheng Lang[2,3,5†], Zhibin Zhang[1,2,3], Jie Ma[6], Minming Lou[6], Xiaoyu Liang[2,3,5], Yun Chang[2,3,5], Qiang Zhao[7], Wenqing Gao[1,2,3,5*] and Tong Li[1,2,3,4,5*]

[1]School of Medicine, Nankai University, Tianjin, China, [2]Department of Heart Center, The Third Central Hospital of Tianjin, Nankai University Affiliated Third Center Hospital, Tianjin, China, [3]Department of Heart Center, Tianjin Key Laboratory of Extracorporeal Life Support for Critical Diseases, Tianjin, China, [4]The Third Central Clinical College of Tianjin Medical University, Tianjin, China, [5]Department of Heart Center, Tianjin Extracorporeal Membrane Oxygenation (ECMO) Treatment and Training Base, Tianjin, China, [6]Department of Heart Center, Tianjin Kang Ting Biological Engineering Group CO. LTD, Tianjin, China, [7]State Key Laboratory of Medicinal Chemical Biology, Key Laboratory of Bioactive Materials (Ministry of Education), Frontiers Science Center for Cell Responses, College of Life Sciences, Nankai University, Tianjin, China

Background: Differences in border zone contribute to different outcomes post-infarction, such as left ventricular aneurysm (LVA) and myocardial infarction (MI). LVA usually forms within 24 h of the onset of MI and may cause heart rupture; however, LVA surgery is best performed 3 months after MI. Few studies have investigated the LVA model, the differences in border zones between LVA and MI, and the mechanism in the border zone.

Methods: The LVA, MI, and SHAM mouse models were used. Echocardiography, Masson's trichrome staining, and immunofluorescence staining were performed, and RNA sequencing of the border zone was conducted. The adipocyte-conditioned medium-treated hypoxic macrophage cell line and LVA and MI mouse models were employed to determine the effects of the hub gene, adiponectin (*ADPN*), on macrophages. Quantitative polymerase chain reaction (qPCR), Western blot analysis, transmission electron microscopy, and chromatin immunoprecipitation (ChIP) assays were conducted to elucidate the mechanism in the border zone. Human subepicardial adipose tissue and blood samples were collected to validate the effects of ADPN.

Results: A novel, simple, consistent, and low-cost LVA mouse model was constructed. LVA caused a greater reduction in contractile functions than MI owing to reduced wall thickness and edema in the border zone. ADPN impeded cardiac edema and promoted lymphangiogenesis by increasing macrophage infiltration post-infarction. Adipocyte-derived ADPN promoted M2 polarization and sustained mitochondrial quality via the ADPN/AdipoR2/HMGB1 axis. Mechanistically, ADPN impeded macrophage HMGB1 inflammation and decreased interleukin-6 (IL6) and HMGB1 secretion. The secretion of IL6 and

HMGB1 increased ADPN expression via STAT3 and the co-transcription factor, YAP, in adipocytes. Based on ChIP and Dual-Glo luciferase experiments, STAT3 promoted ADPN transcription by binding to its promoter in adipocytes. *In vivo*, ADPN promoted lymphangiogenesis and decreased myocardial injury after MI. These phenotypes were rescued by macrophage depletion or HMGB1 knockdown in macrophages. Supplying adipocytes overexpressing STAT3 decreased collagen disposition, increased lymphangiogenesis, and impaired myocardial injury. However, these effects were rescued after HMGB1 knockdown in macrophages. Overall, the IL6/ADPN/HMGB1 axis was validated using human subepicardial tissue and blood samples. This axis could serve as an independent factor in overweight MI patients who need coronary artery bypass grafting (CABG) treatment.

Conclusion: The IL6/ADPN/HMGB1 loop between adipocytes and macrophages in the border zone contributes to different clinical outcomes post-infarction. Thus, targeting the IL6/ADPN/HMGB1 loop may be a novel therapeutic approach for cardiac lymphatic regulation and reduction of cell senescence post-infarction.

KEYWORDS

myocardial infarction, adiponectin, macrophage, IL6, lymph-angiogenesis, LNP-MertK

1 Introduction

Coronary artery disease (CAD) is currently responsible for one in every seven all-cause-related deaths (1). Myocardial injury induced by myocardial infarction (MI) or ischemia/reperfusion (I/R), including percutaneous coronary intervention (PCI), can result in a lower left ventricular ejection fraction (LVEF) and induce life-threatening symptoms, such as severe thrombosis, malignant arrhythmia, and cardiac rupture (2, 3).

Left ventricular aneurysm (LVA), one of the most severe MI complications, usually results in a significantly lower LVEF and can induce life-threatening symptoms, such as malignant arrhythmia and cardiac rupture (4). If a paradoxical movement occurs in an apical aneurysm, heart functions, including LVEF and arrhythmia, are exacerbated (5). Acute ventricular aneurysms usually form within 24 h after the onset of MI and may induce heart rupture; however, LVA surgery is best performed 3 months after MI because the incidence of surgical death is higher within 3 months and waiting enables improved ventricular wall myocardial function and scar formation of the infarcted myocardium (4, 5). Border zone differences contribute to different outcomes post-infarction owing to the stretch force resulting from unstable hemodynamic homeostasis, such as LVA and MI (5). Few studies have focused on the effects of border zones on LVA formation and MI progression. Therefore, the LVA model and efficient treatments to prevent LVA formation should be urgently evaluated.

Adipose tissue regulates granulopoiesis and cardiac functions post-infarction (6, 7). The adipokine, adiponectin, inhibits LPS-induced HMGB1 release in RAW264.7 macrophages (8) and regulates FXR agonism-mediated cardioprotection against post-infarction remodeling and dysfunction (9). Re-activation of the epicardium resulted in cardiac remodeling after myocardial injury via paracrine secretion. Adipose tissues in the epicardium and sub-epicardium also increased *de novo* vessel formation in the peri-infarct zone near the epicardium or the "epicardial border zone," which may be a novel therapeutic approach for cardiac lymphatic regulation (10, 11).

In the present study, we constructed a simple, consistent, and low-cost LVA mouse model. Differences in the border zone between the MI and LVA groups were investigated, and RNA sequencing of the border zone from the LVA, MI, and SHAM groups was performed. Finally, the effects of the hub gene, adiponectin (ADPN), were explored in cell lines and mouse models.

2 Methods

2.1 Cell source and processing

The HL-1, 3T3-L1, and RAW264.7 cell lines were purchased from the Chinese Academy of Medical Sciences and were cultured in Dulbecco's modified Eagle's medium (DMEM) containing 10% (v/v) fetal bovine serum (FBS) in a 37°C, 5% CO_2 incubator before the experiment.

Adipocyte differentiation was induced as previously described (12). The cells were cultured in 6-well plates (5×10^5 cells per well) and transfected. The expression of ADPN or STAT3 in adipocytes was knocked down using 9 μL of lipo2000 (11668-019, Invitrogen), 50 nM of the appropriate siRNA 3 μL [siADPN pool (mmu-ADPN-1, mmu-ADPN-2, and mmu-ADPN-3; RIBIBIO, China) or siSTAT3 pool (mmu-STAT3-1, mmu-STAT3-2, and mmu-STAT3-3; RIBIBIO, China)], and 250 μL of OptiMEM (31985-070, Gibco) per well. STAT3 was overexpressed in adipocytes using lipo2000, STAT3 plasmid (RIBIBIO, China), and OptiMEM. Non-sense sequences were used as negative controls (210011, Ubigene).

RAW 264.7 macrophages with HMGB1 knockdown were obtained using adenovirus (m-HMGB1-shRNA-GFP-Puro from 293T cells, 6.57×10^8 TU/mL, MOI:100, 7.6 L, Genechem, Shanghai). Cells were cultured in 6-well plates (5×10^5 cells per well), transfected using shRNA HMBG1 (MOI = 10), and screened using puromycin (2 μg/mL, Genechem, Shanghai) to obtain the infected RAW 264.7 macrophages.

RAW 264.7 macrophages were maintained in high-glucose DMEM (Gibco, USA) containing 10% fetal bovine serum (AusgeneX, Australia) and 1% penicillin/streptomycin (Solarbio, China) at 37°C under normal (5% CO_2 and 95% air) or hypoxia (5% CO_2, 94% N_2, and 1% O_2) conditions. To determine the effects of adipocyte-derived ADPN on macrophages, the cells were cultured in the conditioned medium (CM) from siNC or siADPN adipocytes. To determine the macrophage receptor that binds adipocyte-derived ADPN, macrophage receptor-binding antibodies, including AdipoR1 (ab126611), AdipoR2 (ab77612), aVb3 (EMD Millipore, MAB1876-Z), and aVb5 (EMD Millipore, MAB1961), were added to siNC CM, which was then administered to macrophages.

2.2 Animals

Adult C57Bl/6J male mice (young: 7–8 weeks old, weight 22–25 g; aged: 20–22 weeks old, weight approximately 35 g) were purchased from Charles River (Beijing, China). Adult experimental Axin2 knockout (KO) mice (background: C57Bl/6J) were fed and propagated at Nankai University. PCR genotyping of Axin2 KO and WT mice was performed using primers 5′-AGTCCATCTTCATTCCGCCTAGC-3′ and 5′-TGGTAATG CTGCAGTGGCTTG-3′ for the wild type, and primers 5′-AGTC CATCTTCATTCCGCCTAGC-3′ and 5′-AAGCTGCGTCG GATACTTGCGA-3′ for the Axin2 mutant.

Mice were maintained in a specific pathogen-free environment with free access to food and water and a 12 h/12 h light–dark cycle. The study protocol was approved by the Ethics Committee of Nankai University (approval no. 2022-SYDWLL-000486).

2.3 Mouse model and treatment

Mice were anesthetized via inhalation of isoflurane (1.5%–2%, MSS-3, England). LVA and MI mouse models were established by ligating the left anterior descending (LAD) artery. MI was induced in adult male mice according to previous studies (10), whereas LVA was induced in adult male mice according to previous studies, with a slight modification. Briefly, the heart in the LVA group was ligated at the LAD at the same level as the heart in the MI group; however, the suture was snipped day 5 after the operation. The LVA model was considered to be successfully established based on the paradoxical movement of the left ventricle. The sham-operated animals underwent the same procedure as the MI and LVA model animals but did not undergo coronary artery ligation.

To determine the effects of ADPN on the formation and progression of LVA, ADPN [ip., 5 ng/(g·day), bs0471P, Bioss] was administered from day 1 to day 14, day 1 to day 3, day 1 to day 7, day 3 to day 14, and day 7 to day 14 after LAD ligation. To elucidate the effects of ADPN and HMGB1 on the crosstalk between adipocytes and macrophages, ADPN, clodronate liposomes, and AAV-shHMGB1 were applied in MI and LVA mouse models. Clodronate liposomes (iv., 0.1 mL/25 g, Yeasen) were used to eliminate bone marrow-derived macrophages. AAV-shHMGB1 was administered as a pre-treatment day 14 before the operation to impede HMGB1 expression in macrophages. To determine the effects of the STAT3/ADPN/HMGB1 axis on the crosstalk between adipocytes and macrophages, adipocytes overexpressing STAT3, siSTAT3 adipocytes, and AAV-shHMGB1 were used in the MI and LVA mouse models.

To reduce pain in the animal experiments, the animals were killed via cervical dislocation after isoflurane anesthesia (5%, MSS-3, England).

2.4 LVA model validation

To validate the successful construction of the LVA model, hearts were collected on day 28 after the operation, and a regular agarose (agarose G-10, Blowest, 162135) intra-chamber cast was used to recapture the inner chamber spatial structure and the bulging shape of the LVA. To screen the time window of LVA model formation, computed tomography (CT, Nanoscan, Mediso, width: approximately 1,929, center: approximately −35) was applied to perform *in vivo* imaging of mouse cardiopulmonary parts and validate the success of LVA model development at different time points (days 1, 3, 7, and 30 after model construction). Based on paradoxical movement, intrachamber casts, and CT, the LVA mouse model was validated.

2.5 Echocardiographic examination

Cardiac function was evaluated using a Vevo® 2100 system equipped with a 30-MHz transducer (FUJIFILM VisualSonics, Inc. Toronto, Canada). Heart function was measured using the two-dimensional parasternal long axis. Left ventricular internal dimensions in diastole (LVID,d), systole (LVID,s), left ventricular ejection fraction (LVEF, %), and fractional shortening (LVFS, %) were measured using M-mode.

2.6 Histology analysis

After mice were killed, heart samples were collected, fixed in 4% paraformaldehyde overnight, and embedded in paraffin or OCT (6

μm). Hematoxylin and eosin (HE) staining (G1120, Solarbio, China) and Masson's staining (G1340, Solarbio, China) were performed to detect anatomical morphology changes and collagen deposition. The average infarct size was obtained by calculating the average length of the circumference in the infarct and normal areas. The infarcted area was determined by calculating the average area in the infarct portion and total area (13). The related wall thickness of the border zone was also determined, and the three were measured using the ImageJ software.

For immunofluorescent analysis, the tissue slides were incubated with the following primary antibodies: rabbit anti-Cx43 (1:200, ab11370), anti-LYVE1 (1:200, ab218535), anti-ZO-1 (1:200, ab61357), mouse anti-CD68 (1:200, ab31630), rabbit anti-HMGB1 (1:200, ab79823), mouse anti-ADPN (1:200, ab22554), mouse anti-cTNT (1:200, ab8295), and rabbit anti-Ki67 (1:200, ab16667) at 4°C overnight, followed by the secondary antibodies, Alexa Fluor 488- and Alexa Fluor 594-conjugated second antibody (Abcam, 1:200). The nuclei were stained with 4′,6-diamidino-2-phenylindole (DAPI; Southern Biotech, USA). At least three different heart sections were obtained from each mouse and more than six random images of the at-risk areas were obtained from each section. Images were captured using a fluorescence microscope (ECLIPSE TS2R, Nikon, Japan).

2.7 Cytokine and chemokine measurements

For the protein chip, blood samples were collected and centrifuged for 10 min at 3,000 rpm. The concentrations of cytokine and chemokine were measured using an antibody-coated microsphere-based multiplex cytokine immunoassay that can quantify seven cytokines contemporaneously using 25 μL of mouse serum (MTH17MAG-47k MILLIPLEX MAP Mouse Cytokine/Chemokine Magnetic Bead Panel, MERCK Millipore Corporation, Germany). The following cytokines were measured: GM-CSF, IFN-γ, IL-1β, IL-6, IL-10, IL-22, and TNF-α. All samples, standards, and quality controls were assayed according to the manufacturers' instructions. The samples were incubated overnight at 4°C and washed using a magnetic plate washer. The plates were read using a multiplex plate reader and its accompanying software (Luminex x-MAP Technology, MILLIPLEX). All cytokine and chemokine concentrations are expressed in pg/mL.

To investigate myocardial injury on days 3 and 7 after construction of the mouse model, the left ventricular heart samples from different groups were collected and the mouse ADPN ELISA kit (ab226900), mouse CKMB ELISA kit (JL12422, Jianglaibio, China), and LDH ELISA kit (JL20162, Jianglaibio, China) were used to measure the levels of the corresponding proteins. The concentrations of cytokines secreted by macrophages were measured using the mouse IL6 ELISA kit (ab222503), mouse HMGB1 ELISA kit (JL13702, Jianglaibio, China), and mouse C1qTNF9 ELISA kit (CSB-E16713h, Cusabio, China). The human IL6 ELISA kit (CSB-E04638h, Cusabio, China), human HMGB1 ELISA kit (CSB-E08223h, Cusabio, China), and human ADPN ELISA kit (CSB-E07270h, Cusabio, China) were utilized to determine protein expression in sub-epicardial adipose tissues. Optical density (OD) was measured using a microplate reader (VICTOR Nivo Multimode Microplate Reader, PerkinElmer). All cytokine concentrations are expressed in pg/mL.

2.8 RNA-sequencing of the border zone area

The border zones of the LVA and MI heart samples, and the same area of heart samples from the SHAM group were dissected (n = 5 per group). Total RNA was extracted using a TRIzol reagent kit (Invitrogen, Carlsbad, CA, USA). RNA quality was assessed using an Agilent 2100 Bioanalyzer (Agilent Technologies, Palo Alto, CA, USA) and checked via RNase-free agarose gel electrophoresis. After total RNA extraction, eukaryotic mRNA was enriched using oligo (dT) beads, whereas prokaryotic mRNA was enriched by removing rRNA using the Ribo-Zero™ Magnetic Kit (Epicenter, Madison, WI, USA). The enriched mRNA was fragmented into short fragments using fragmentation buffer, reverse transcribed into cDNA with random primers, purified using the QiaQuick PCR extraction kit (Qiagen, Venlo, The Netherlands), end-repaired, extended with a poly(A) tail, and ligated to Illumina sequencing adapters. The ligation products were size-selected by agarose gel electrophoresis, amplified via PCR, and sequenced using Illumina HiSeq2500 (Gene Denovo Biotechnology Co., Guangzhou, China).

The differentially expressed genes (DEGs) were assessed using the "limma" package. Genes with log2|fold change|>1 and $p < 0.05$ were considered DEGs. GO/KEGG pathway analyses were performed using the "clusterProfiler" package in R (14, 15). Statistical significance was set at $p < 0.05$ for the enrichment analyses.

To investigate the hub genes, DEGs between the MI and LVA groups were uploaded to STRING (version 11) to construct a protein–protein interaction (PPI) network (16). The results of STRING analysis were imported into Cytoscape v.3.7.1, and hub genes were investigated using the Cytoscape plug-in, MCODE (17). A significant PPI was identified by a combined score >0.4.

Single-cell sequencing data for hub DEGs were obtained from the Single Cell Portal (https://singlecell.broadinstitute.org/). Single-cell sequencing data of the human heart from a single-cell portal were used to explore the expression of ADPN, AdipoR1, and AdipoR2 (SCP498) (18).

2.9 qPCR analysis

The mRNA of heart samples in the border zone or cells was extracted, and qRT-PCR was performed. Total RNA was collected using TRIzol and reverse transcribed. The amplified cDNA samples were then mixed using TB Green® Premix Ex Taq™ II (TaKaRa, RR820). B-actin was used as an internal reference; the $2^{-\Delta\Delta Ct}$ method was used for the calculation. The primer details are listed in Supplementary Table 1.

2.10 Flow cytometry

To determine the effects of different treatments on macrophage M2 polarization, samples were blocked with anti-Rh Fc receptor binding (Invitrogen, 2296579); stained with CD206 (CD206-FITC, Invitrogen 141704) and Edu (Edu-AF594, Invitrogen 2420611) (cell sample), CD206 and CD86 (CD86-PE/Cyanine7, Invitrogen, 105014) (heart sample), or CD206 and F4/80 (F4/80-PE, Invitrogen 157304) (heart sample); and evaluated using a flow cytometer (Cytometer, USA). Following staining for MertK (MertK-PE/Cyanine7, Invitrogen, 2555774), flow cytometry was performed to determine the effect of LNP-MertK on macrophages. Nystatin, a decreasing endocytic reagent, was used to reverse the above effects (MCE 1400-61-9). Data were analyzed using FlowJo 10.6.2 (BD Biosciences).

2.11 Western blot

Proteins were extracted using RIPA buffer (CWBIO, China). The protein concentration was measured using a BCA assay kit. The samples were mixed with SDS-PAGE loading buffer, electrophoresed via SDS-PAGE, and transferred onto Millipore or GE PVDF membranes. The PVDF membranes were blocked with 5% skim milk for 1 h and incubated with primary followed by secondary antibodies (all 1:5,000, Affinity, China). The membranes were then bound to ECL and analyzed using an image system software (Protein Simple, USA).

The following primary antibodies were employed: anti-p65 (1:1,000, CST #6959), anti-p-p65 (1:1,000, ab194726), anti-LC3 (1:2,000, ab192890), anti-ADPN (1:1,000, ab22554), anti-HMGB1 (1:1,000, ab79823), anti-GPX4 (1:1,000, ab125066), anti-P62 (1:1,000, ab109012), anti-YAP (1:1,000, CST#8418S), anti-STAT3 (1:1,000, ab109085), and anti-β-actin (1:5,000, Sigma).

2.12 Transmission electron microscope

A transmission electron microscope (TEM) was used to examine the ultrastructure of macrophages. Briefly, cells and heart samples were fixed with glutaraldehyde and osmic acid (Solarbio, China), and then cut into ultrathin sections with a thickness of 50–70 nm using an ultrathin microtome. Ultrathin sections were stained with 2% uranyl acetate and lead citrate. The mitochondria and lysosomes were observed using a TEM (HT7800, HITACHI).

2.13 Oxidative stress levels

Raw264.7 cells were cultured under normal oxygen or hypoxic conditions for 8 h. Oxidative stress levels were measured by detecting reactive oxygen species (ROS; S0033; Beyotime, China), according to the manufacturer's instructions. The fluorescence signal was recorded using 520- and 590-nm lasers and detected using a fluorescence microscope (ECLIPSE TS2R; Nikon, Japan).

2.14 Autophagy measurement

Raw264.7 cells were cultured in normal oxygen or hypoxic conditions for 8 h with or without treatment. Autophagy was determined using the MDC method (C3018S, Beyotime, China). The fluorescence signal was recorded using a 355-nm laser and detected using a fluorescence microscope (ECLIPSE TS2R, Nikon, Japan).

2.15 Oil O staining

To analyze lipid deposition in adipocytes, Oil O staining (G1262, Solarbio, China) was performed for the different groups. To analyze lipid deposition in the human subepicardial layer, modified Oil O staining (G1261, Solarbio, China) was performed. Images were captured using a light microscope (ECLIPSE E100; Nikon, Tokyo, Japan).

2.16 Chromatin immunoprecipitation assay

Macrophages or adipocytes were fixed with formaldehyde at room temperature for 10 min, washed with PBS, and collected. The cells were then placed in an ultrasonic water bath (60 W, SCIENTZ-48, SCIENTZ, China). The long-stranded DNA of the gene was broken into 200- to 1,000-bp DNA fragments and centrifuged at 16,000 × *g* for 15 min at room temperature to obtain the supernatant. A total of 20 μL of supernatant was employed as the input. The c-Jun (ab32137, 2.5-5 μg/10^6 cells) and STAT3 (ab76315, 2.5-5 μg/10^6 cells) antibodies and their corresponding IgG antibodies (A7016; Beyotime, China) were added to the remaining supernatant, which was incubated overnight at 4°C. Magnetic beads were then added for 2 h at room temperature (CST #9005). After centrifugation at 16,000 × *g* for 2 min at 4°C, the precipitate was eluted stepwise with a low-salt buffer solution, high-salt buffer solution, and NaCl solution to remove chromatin. EDTA, Tris-HCl, and protease were added to the sample, which was then incubated at 65°C for 1 h. Finally, the phenol-chloroform method was used to extract the 50-μL purified product for PCR detection. The primer details are outlined in Supplementary Table 2.

2.17 Dual-Glo luciferase experiment

The ADPN promoter [bp −1k/+120 relative to the transcriptional start site (TSS)] was cloned into the luciferase reporter gene vector, pGL3-Basic (Promega). Four 5′-truncated sequences of the ADPN promoter in the luciferase reporter gene vector were transfected into adipocytes from different treatment groups. The Dual-Glo luciferase experiment was carried out 48 h after transfection following the protocol provided by the manufacturer. The OD values

weremeasured using a microplate reader (VICTOR Nivo Multimode Microplate Reader, PerkinElmer). The intensity was calculated by dividing the luciferase value by the renilla value (Promega E2920).

2.18 LNP and LNP-MertK construction

Lipid nanoparticle (LNP) and LNP containing MertK (LNP-MertK) were constructed as previously described (19). LNP was administered via the iv route. Of note, LNP can specifically bind to bone marrow-derived macrophages (CD68+). LNP-MertK was used to increase MertK expression and macrophage phagocytosis to eliminate unwanted materials in cardiomyocytes and the microenvironment. Nystatin, which decreases endocytic reagent, was administered via the ip route and used to rescue the effects of LNP-MertK after MI.

2.19 Patient enrollment and human sample analysis

To further validate the effects of the IL6/STAT3/ADPN/HMGB1 axis, blood samples were collected from patients after admission, and sub-epicardial samples were collected from patients that underwent coronary artery bypass grafting (CABG). The following inclusion criteria were employed: (1) diagnosed with CAD; (2) normal BMI (BMI ≤ 24 kg/m^2), overweight (24 < BMI < 28 kg/m^2), or obese (BMI ≥ 28 kg/m^2); and (3) patients with complete medical information and laboratory examinations. The following exclusion criteria were employed: (1) history of nephropathy, especially DM; (2) history of hepatopathy; (3) history of diabetic oculopathy; (4) history of tumors; (5) cardiac arrest or ECPR; (6) MODS or irreversible brain damage; (7) surgery within 6 months of this study; (8) aortic insufficiency or aortic dissection; and (9) uncontrolled bleeding. The protocols were approved by Tianjin Third Central Hospital.

Univariate and multivariate logistic regression analyses were performed to assess the correlation between patients with CAD in different BMI groups and the expression levels of ADPN, IL6, and HMGB1. Receiver operating characteristic (ROC) analysis and joint ROC analysis were performed to investigate the diagnostic value of ADPN, IL6, and HMGB1 in patients with CAD in the different BMI groups.

2.20 Statistical analysis

Data are presented as mean ± SD, median (Q1–Q3), or frequency (percentage). Statistical analyses were performed using SPSS 23.0. The Shapiro–Wilk normality test, Welch's *t*-test (two groups), and one- or two-way ANOVA with Bonferroni post-hoc analyses were used for comparisons between different groups. Multiple comparison *p*-values less than 0.05 were considered to indicate statistical significance. Randomization and blinding strategies were used whenever possible.

3 Results

3.1 Changes in the border zone are critical in LVA formation

The LVA mouse model was successfully constructed and validated using an agarose intrachamber cast and CT (Supplementary Figure 1). CT was also performed to screen the time window of LVA formation. Bulging was found to appear before day 7 and then progressively enlarge on day 30. Based on CT, the volume of the bulging left ventricular free wall in the LVA group occupied almost 1/3 of all left ventricles on day 30 after the operation. Furthermore, left ventricular paradoxical movement appeared.

Left ventricular functions in the LVA and MI groups were impaired at 1 and 4 weeks after operation compared to those in the SHAM group. LVEF and LVFS in the LVA group were remarkably reduced compared to those in the MI and SHAM groups (Figures 1A, B). Masson's staining and hematoxylin and eosin staining were performed to assess LVA formation (Supplementary Figures 2A, B). The infarcted area significantly decreased, while the infarcted size did not significantly change on day 28 compared to that on day 7 in the LVA group (Supplementary Figures 2D, E). The wall thickness of the border zone decreased during this process in the LVA group (Figure 1C). The infarcted area was significantly larger while the infarct size was significantly lower on day 7 in the LVA group than in the MI group. Immunofluorescent staining for cTNT was observed in the border zone, suggesting that the number of injured cardiomyocytes decreased during LVA formation (Supplementary Figure 2C; Figure 1D).

Immunoregulation after cardiac injury is critical for heart recovery. Hearts in the LVA group were associated with a "global" activation of pro-inflammatory and anti-inflammatory cytokines (Supplementary Figure 3). In the pro-inflammatory phase (<3 days), IL-1b expression was elevated in the LVA and MI groups. Besides the decrease in IL-1β and peak IL-6 at 3 days, other cytokines peaked at 5 days. On day 7 after the operation, the expression of all cytokines was higher in the LVA group than in the MI group, indicating that immunoregulation of the infarcted area and border zone in the LVA heart was more remarkable than that in the MI heart.

Finally, 65 mice were used in the survival study. The mortality rate of LVA mice was higher than that of MI mice. To avoid the influence of the surgical procedure time, we recorded the time but found no significant difference between the two groups (Supplementary Figure 4). Taken together, these results indicate that the LVA model was successfully constructed. Many more differences were found in the border zone between the two groups, which may play a critical role in LVA formation and MI progression.

3.2 ADPN expression is associated with wall thickness in the border zone in LVA and MI mice

To explore the difference between the LVA and MI border zones, we performed RNA-seq of the border zone in the three groups on day 7 after the operation. A total of 1,340 upregulated

10.3389/fimmu.2024.1368516

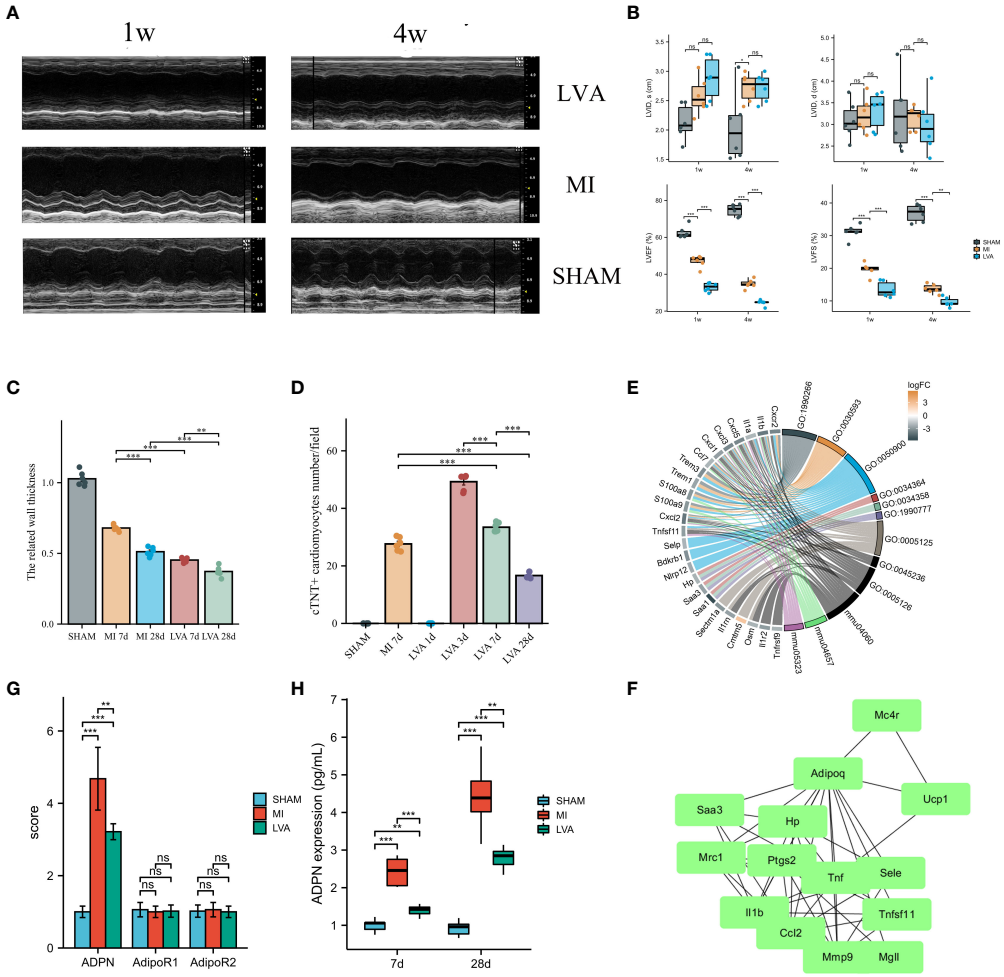

FIGURE 1
ADPN expression was associated with the wall thickness in the border zone and LVA formation. **(A, B)** LVA and MI decreased heart function. The representative echocardiographic images **(A)** and quantitative analysis **(B)** of LVA, MI and SHAM mice heart samples at 1 week and 4 weeks after the operation. LVID, d, left ventricular internal diameter at end-diastole; LVID, s, left ventricular internal diameter at end-systole; LVEF (%), left ventricle ejection fraction; LVFS (%), left ventricle fractional shortening (n = 6 per group). **(C)** The wall thickness in the border zone of SHAM, MI (7 days and 28 days) and LVA (7 days and 28 days) heart samples. **(D)** Immunofluorescent staining of aSMA demonstrated the injury cardiomyocytes in the border zone of SHAM, MI (7 days) and LVA (1 day, 3 days, 7 days, and 28 days) heart samples. **(E)** The chord diagram of the relationship between DEGs and enriched pathways after RNA-sequencing analysis. **(F)** PPI analysis showed the inflammation module of DEGs in the border zone between LVA, MI, and SHAM at 7 days after model construction (n = 3 per group). ADPN, adiponectin. **(G)** The qPCR analysis of ADPN, AdipoR1, and AdipoR2 among three groups. AdipoR1 and AdipoR2, the two receptors of ADPN. **(H)** ADPN expression in the border zone at 7 days and 28 days after operation among three groups using ELISA. $^{**}p < 0.01$; $^{***}p < 0.001$; ns, not significant.

and 971 downregulated DEGs were identified between the LVA and MI border zones. Further enrichment analysis was performed, which mainly revealed cytokine–cytokine receptor interactions, granulocyte chemotaxis, and chemokine activity (Figure 1E; Supplementary Table 3). PPI network analysis was performed, and a module comprising TNF, IL1b, ADPN, UCP1, and CCL2 was obtained (Figure 1F). Quantitative polymerase chain reaction (qPCR) analysis and ELISA were performed to determine ADPN expression. The mRNA and protein levels of ADPN were lower in the LVA group than in the MI group. No significant difference in mRNA levels was found between the two ADPN receptors, suggesting that ADPN expression may be associated with the related wall thickness of the border zone and contribute to LVA formation and MI progression (Figures 1G, H).

3.3 ADPN impedes cardiac edema and promotes cardiac lymphangiogenesis post-infarction

To explore the effects of ADPN on the related wall thickness of the border zone and LVA formation, an echocardiogram was recorded and the LVEF was measured. Compared to the LVEF in LVA mice administered PBS, the LVEF in mice administered ADPN increased from day 1 to day 7 while that in mice administered ADPN decreased after day 7 (Figures 2A–E; Supplementary Table 4). When this mechanism was further explored, ADPN supplementation decreased cardiac edema and impeded the progression of subepicardial edema in LVA mice within day 7 after the operation (Figures 2F, G). Cardiac

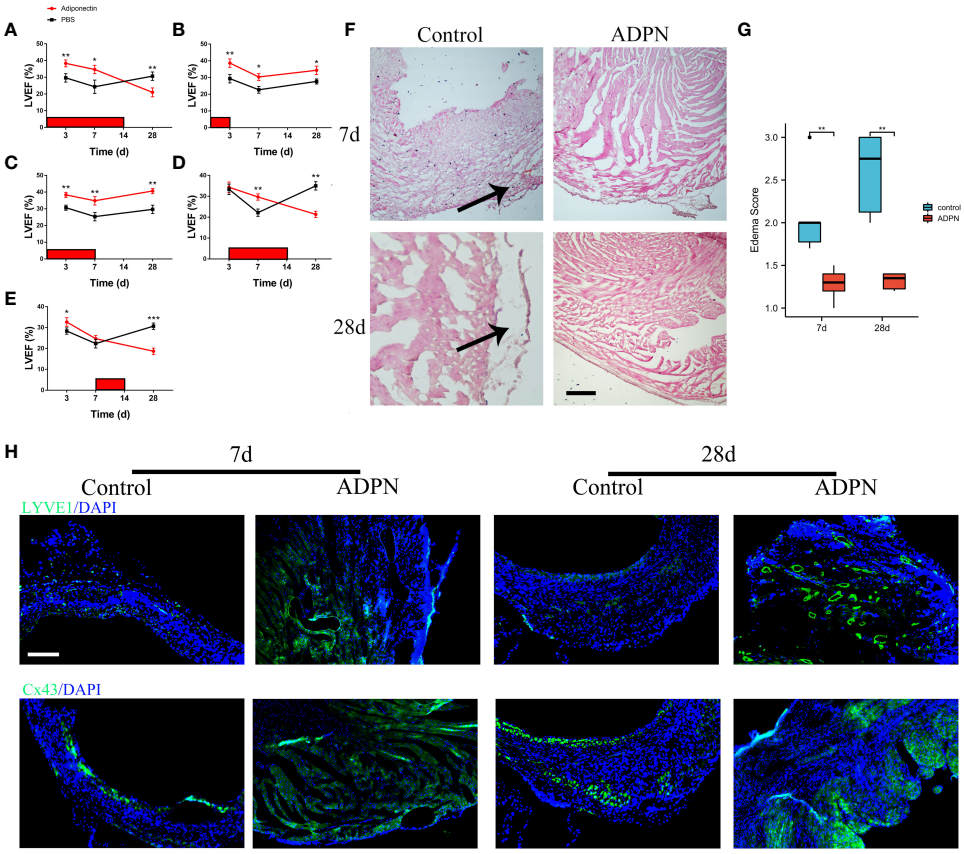

FIGURE 2
ADPN impeded edema and promoted lymphangiogenesis within 7 days after the operation. **(A–E)** Effect of ADPN treatment on cardiac functions during LVA formation. 5 ng/(g·day) ADPN was injected i.p. from day 1 to 14 **(A)**, day 1 to 3 **(B)**, day 1 to 7 **(C)**, day 3 to 14 **(D)**, and day 7 to 14 **(E)** after LAD ligation. LVEF (%) was evaluated by echocardiography. (n = 8 per group) **(F, G)** The representative images **(F)** and quantity analysis **(G)** of the HE staining at 7 days and 28 days in the border zone of the LVA group treated with ADPN or PBS from day 1 to 7 after operation. Scale bar, 500 μm. Arrow, cardiac edema. **(H)** The representative immunofluorescence images of LYVE1 and Cx43 cells in the LVA group treated with ADPN or PBS from day 1 to 7 after operation. Scale bar, 500 μm. *p < 0.05; **p < 0.01; ***p < 0.001.

lymphatic growth and Cx43 expression in the border zone of ADPN-treated mice were higher than those in age-matched PBS-treated mice on day 28 after the operation (Figure 2H).

To determine the effects of ADPN on cardiac lymphangiogenesis and LYVE1+ macrophages in the border zone, ADPN and the Cx43 agonist and inhibitor, verapamil and Gap19, were administered to the LVA mouse model; verapamil and Gap19 were used to regulate Cx43 expression in the border zone. The LVA border zone in the verapamil group exhibited increased Cx43- and Cx43-associated macrophage infiltration (Supplementary Figure 5A). LYVE1+ macrophages and lymphatic capillaries increased in the border zone following treatment with ADPN +verapamil compared to treatment with ADPN alone; these levels were restored using Gap19 (Supplementary Figures 5C, D).

According to a previous report, ADPN decreases Axin2 expression (20). To explore the effects of ADPN on Cx43 and Cx43-associated macrophage infiltration, Axin2 KO mice were used. The overexpression of Wnt canonical signaling rescued the effects of Cx43 expression and Cx43-associated macrophage infiltration (Supplementary Figure 5B). LYVE1+ macrophages and lymphatic capillaries were also rescued in the border zone of Axin2 KO mice (Supplementary Figures 5E, F). Co-staining of ZO-1 and Cx43 was higher in the ADPN-treated LVA group than in the non-treated LVA group (Supplementary Figure 5G).

Taken together, these results indicate that ADPN expression levels differed after coronary occlusion, leading to a significant difference in the number of lymphangiogenesis and infiltrated LYVE1+ macrophages, inducing different statuses of the border zone and different mouse models, such as MI and LVA (Supplementary Figure 5H).

3.4 Adipocyte-derived ADPN promotes macrophage M2a polarization and decreases inflammatory cytokine secretion via the ADPN/AdipoR2/HMGB1 axis

Single-cell sequencing revealed that ADPN was mainly secreted by adipocytes, and the two receptors were expressed in almost all cardiac cells (Figure 3A). Therefore, cell–cell crosstalk may occur after MI. To explore the effects of ADPN on macrophages, ADPN expression was knocked down in adipocytes, and RAW264.7

macrophages were cultured with siNC or siADPN adipocyte-conditioned medium (Figure 3B). The siNC adipocyte-conditioned medium promoted macrophage M2 polarization based on polarization-related mRNAs and CD206 and Edu staining via flow cytometry. This effect was decreased by treatment with siADPN adipocyte-conditioned medium (Figures 3C, D). HMGB1 expression increased while p-p65 expression decreased in normoxic and hypoxic macrophages treated with ADPN (Figure 3E).

Based on previous reports, endogenous HMGB1 mediates ferroptosis and autophagy (21). HMGB1 was found to be knocked down in hypoxic macrophages (Supplementary Figure 6A). ROS levels in the hypoxic HMGB1 knockdown macrophage group were markedly higher than those in the hypoxic and normal oxygen macrophage groups (Supplementary Figure 6B). Autophagy was increased using the MDC method. Furthermore, LC3B/A expression increased in the hypoxia macrophage group compared to that in the normal oxygen macrophage group. This change was rescued in the hypoxia HMGB1 knockdown macrophage group (Supplementary Figures 6C, D). The expression of the ferroptosis marker, GPX4, increased in the hypoxia HMGB1 knockdown macrophage group (Supplementary Figure 6D). Macrophage HMGB1 knockdown decreased IL-1β and TNF-α, and increased IL-6, Arg1, IL-10, and Mrc1 expression under the hypoxia condition, indicating macrophage M2a polarization (Supplementary Figure 6E).

To determine the effects of adipocyte-derived ADPN on HMGB1 and HMGB1-mediated pathways in macrophages, HMGB1 knockdown or control macrophages were treated with ADPN. HMGB1 knockdown rescued the effects of ADPN on HMGB1-mediated p65 and decreased autophagy (Figure 3F). After treatment with CM and the AdipoR2 receptor antibody, HMGB1 expression decreased and p65 expression increased, suggesting that the ADPN/AdipoR2/HMGB1/p65 axis regulates immune responses in macrophages (Figure 3G). The effects of ADPN and HMGB1 on macrophage mitochondria were also investigated. Based on the results, ADPN decreased megamitochondria engulfing lysosome and promoted migrasome formation in hypoxic macrophages. The phenotypes were also rescued by HMGB1 knockdown in macrophages (Figures 3H, I). siNC adipocyte-conditioned medium impeded IL6, HMGB1, and C1qTNF9 secretion from macrophages, whereas the effect was reversed by treatment with siADPN adipocyte-conditioned medium (Figure 3J).

The effects of the ADPN/HMGB1 axis on macrophages and MI progression were validated *in vivo* using an MI mouse model. Compared to the heart sections in the MI group, the fibrotic area decreased after treatment with ADPN; this phenotype was rescued by macrophage depletion (liposome group) or HMGB1 knockdown in macrophages (Figure 4A). The same trend was observed for the other effects of ADPN. Treatment with ADPN promoted lymphangiogenesis and increased the number of ki67+ cTNT+ cardiomyocytes after MI. However, these phenotypes were rescued by macrophage depletion or HMGB1 knockdown (Figures 4B, C). ADPN was found to promote M2a polarization. After macrophage HMGB1 knockdown, M2a polarization transformed into M2b polarization on days 3 and 7 post-infarction (Figure 4D). Treatment with ADPN also decreased LDH and CKMB expression on days 3 and 7 after surgery. These phenotypes were rescued by macrophage depletion or HMGB1 knockdown in macrophages (Figure 4E).

Taken together, these results highlight the effects of the ADPN/HMGB1 axis on the regulation of macrophage polarization and cardiac injury in cardiac stress and MI mouse models.

3.5 IL6 and HMGB1 promotes ADPN expression in adipocytes via STAT3 and the co-transcription factor, YAP

We investigated the transcriptional regulation of ADPN in adipocytes. IL6 promoted STAT3 expression in adipocytes, and IL6+HMGB1 promoted a higher expression of STAT3 and YAP in adipocytes (Figure 5A). Immunofluorescent staining with STAT3 and nuclear plasma separation experiments revealed that STAT3 translocation to the nucleus increased in hypoxic adipocytes pre-treated with IL6 and markedly increased in adipocytes pre-treated with IL6+HMGB1 (Figures 5B, C). ADPN expression was elevated in hypoxic adipocytes pre-treated with IL6 and markedly increased in adipocytes pre-treated with IL6+HMGB1. Lipid deposition was found to decrease in the IL6 and IL6+HMGB1 hypoxic adipocyte groups (Figures 5D, E). ChIP analysis and luciferase reporter gene experiments revealed that STAT3 promoted ADPN transcription by binding to the ADPN promoter (Figures 5F–H).

To validate the effects of the IL6/STAT3/ADPN axis on MI progression and LVA formation, adipocytes overexpressing STAT3, siSTAT3 adipocytes (as a negative control), and AAV-HMGB1 were administered to the MI and LVA mouse models. Supplying adipocytes overexpressing STAT3 decreased collagen disposition, increased lymphangiogenesis, and impaired myocardial injury (LDH and CKMB ELISA results, and immunofluorescent images with Ki67 and cTNT). However, these effects were rescued after HMGB1 knockdown in macrophages (Figure 6). Supplying adipocytes overexpressing STAT3 to the LVA mouse model increased the related wall thickness and decreased LDH and CKMB at 7 days after the operation (Supplementary Figure 7). Overall, adipocyte-derived STAT3 impedes MI and LVA progression via HMGB1 in macrophages.

3.6 Targeting MertK improves heart functions after MI

Due to the aging-related reduction in MertK expression and macrophage phagocytosis, we constructed and used LNP-MertK to increase macrophage MertK expression and phagocytosis. Thereafter, we determined whether LNP-MertK can exhibit a synergistic effect with ADPN on MI progression. First, we analyzed the homing of senescent macrophages to the bone marrow. The homing of senescent macrophages was found to increase in aged mice. These macrophages may decrease the immune response, promote cardiac adverse remodeling, and

10.3389/fimmu.2024.1368516

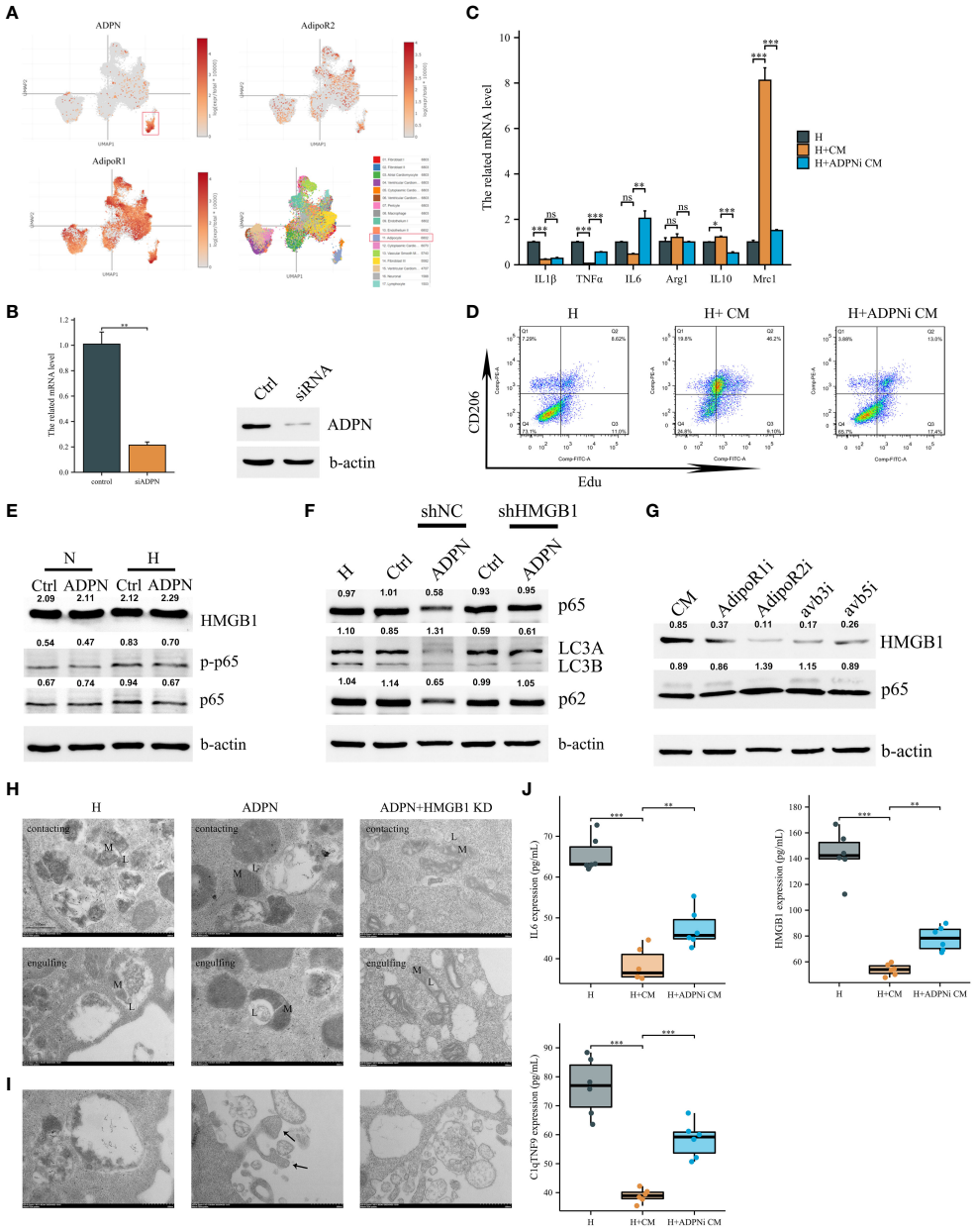

FIGURE 3
Adipocyte-derived ADPN promoted macrophage M2a polarization and decreased inflammatory cytokine secretion via the ADPN/AdipoR2/HMGB1 axis. **(A)** Single-cell sequencing analysis demonstrated that ADPN was mainly expressed in adipocytes in the subepicardial layer while the two ADPN receptors were expressed in almost cells in heart. **(B)** The ADPN knockdown efficiency in adipocytes using qPCR and WB analysis. **(C)** The polarization-related mRNA levels in hypoxic macrophages were measured using qPCR analysis when treated with the conditional medium of ADPN knockdown or control adipocytes. CM, conditional medium. **(D)** Flow cytometry of CD206 and Edu staining to determine the M2 polarization in hypoxic macrophage when treated with the conditional medium of ADPN knockdown or control adipocytes. **(E)** WB analysis demonstrated HMGB1 and inflammatory response in normoxic and hypoxic macrophages when treated with ADPN or control. **(F)** After HMGB1 knockdown, ADPN effects on inflammatory response and autophagy were rescued in hypoxic macrophages. **(G)** WB analysis showed that HMGB1 and inflammatory response in hypoxic macrophages when treated with the conditional medium of adipocytes and binding with macrophage AdipoR1, AdipoR2, avb3, and avb5 using the antibodies. **(H)** HMGB1 knockdown or control RAW264.7 macrophages were exposed to hypoxia with ADPN treatment, then were fixed by high-pressure freezing and analyzed by TEM. Mitochondria–lysosome contacts (contacting) and megamitochondria engulfing lysosome (engulfing) were shown in different groups. L, lysosome, or lysosome-related organelle; M, mitochondrion. **(I)** The unfit materials ejection from macrophages using TEM. Arrow, migrasomes. Scale bar, 500 nm. **(J)** The IL6, HMGB1, and C1qTNF9 expressions secreted by hypoxic macrophages when treated with the conditional medium of ADPN knockdown or control adipocytes. ADPNi, ADPN knockdown in adipocytes. *$p < 0.05$; **$p < 0.01$; ***$p < 0.001$; ns, not significant.

induce LVA formation (Supplementary Figure 8A). Echocardiography revealed that LVEF and LVFS in the LNP-MertK group were higher than those in the MI and LNP groups (Supplementary Figure 9A). Masson's trichrome staining also revealed a smaller infarcted area and more surviving cardiomyocytes in the LNP-MertK group (Supplementary Figure 9B). Transwell analysis revealed that the phagocytosis of LNP-MertK-treated macrophages was increased and rescued by

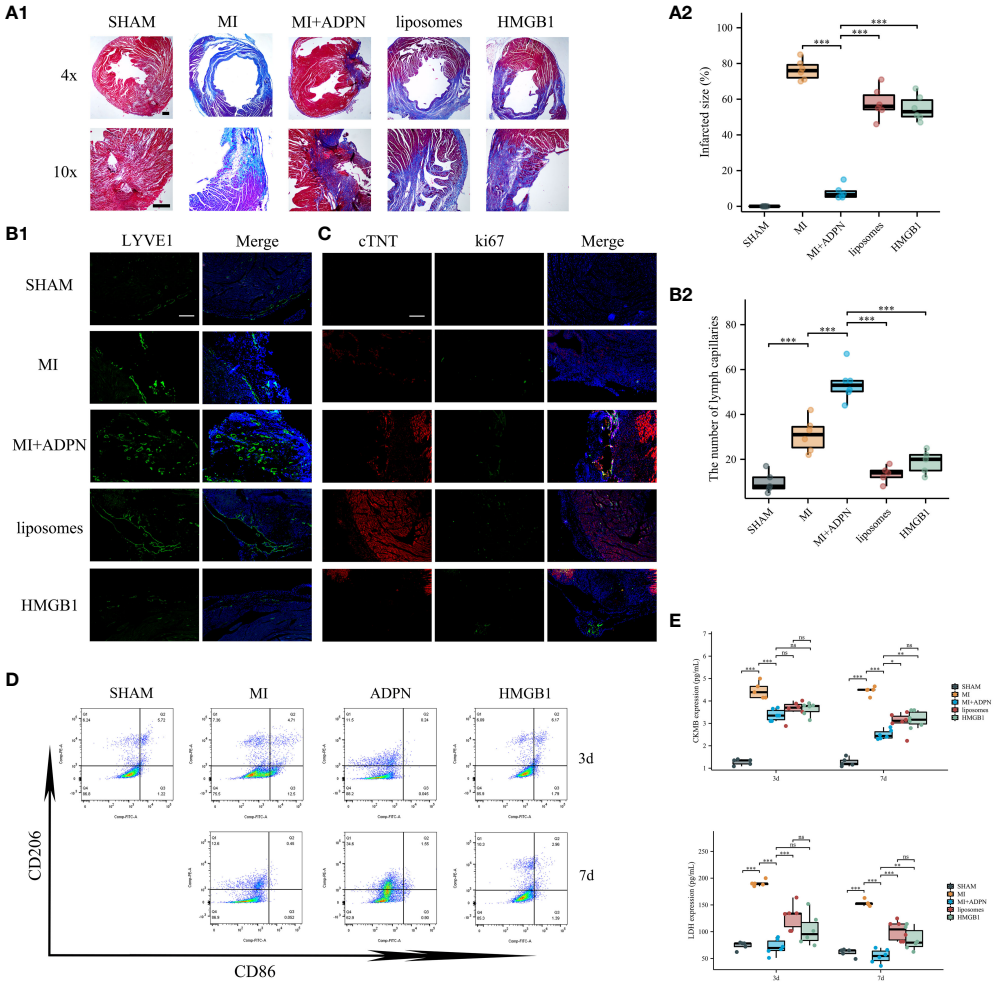

FIGURE 4
ADPN impeded MI progression via macrophage HMGB1. **(A)** The fibrosis representative images (A1) and quantitative analysis (A2) of heart sections using Masson's staining in SHAM, MI, MI+ADPN, MI+ADPN+liposomes administration and MI+ADPN+ HMGB1 knockdown in macrophages groups. AAV-shHMGB1 was utilized to knock down HMGB1 in macrophages. **(B)** The immunofluorescent images with LYVE1 (B1) and quantitative analysis (B2) in different groups. **(C)** The immunofluorescent images with Ki67 and cTNT in different groups. cTNT, injured cardiomyocyte marker. **(D)** Flow cytometry of CD206 and CD86 staining to determine the M2a and M2b polarization in hypoxic macrophage in an MI mouse model when treated with ADPN or ADPN+AAV-shHMGB1. **(E)** The border zone CKMB expression (up) and LDH expression (down) at 3 days and 7 days after operation in different groups using ELISA. Liposomes, MI+ADPN+clodronate liposomes administration group; HMGB1, MI+ADPN+HMGB1 knockdown in macrophages. Scale bar, 500 μm. $*p < 0.05$; $**p < 0.01$; $***p < 0.001$; ns, not significant.

nystatin. Macrophage phagocytosis decreased to zero upon treatment with nystatin (Supplementary Figure 9C). Based on flow cytometry, LNP-MertK promoted macrophage phagocytosis in the more myocardial adverse mitochondria (Supplementary Figure 9D). LNP-MertK also promoted M1 polarization at day 3 and M2 polarization at day 7 after operation (Supplementary Figures 8E, 7B). ADPN enhanced the effects of LNP-MertK on M2 polarization at day 7 after the operation (Supplementary Figure 8B). Both LNP-MertK and LNP decreased CKMB and LDH expression; however, LNP-MertK expression decreased further after MI (Supplementary Figure 9F). LNP-MertK and ADPN increased the abundance of the LYVE1+ MertK+ macrophages compared with LNP-MertK alone (Supplementary Figure 9G). LNP-MertK also increased VEGF-C expression on days 3 and 7 after MI (Supplementary Figure 9H). Overall, targeting MertK increased macrophage phagocytosis and M2 polarization, and impeded macrophage senescence, thereby improving heart function after MI.

3.7 IL6/ADPN/HMGB1 axis contributes to the diagnosis and prognosis of aging patients with CABG

To validate the effects of IL6, HMGB1, and ADPN in humans, human subepicardial and blood samples were collected based on the inclusion and exclusion criteria. Patients with obesity and CAD can be divided into two groups based on the lipid deposition of sub-epicardial adipocytes analyzed by oil O staining. Lipid deposition was negatively correlated with ADPN immunofluorescence staining in sub-epicardial adipocytes (Figures 7A, B). The high mRNA and protein levels of ADPN were confirmed using qPCR and ELISA

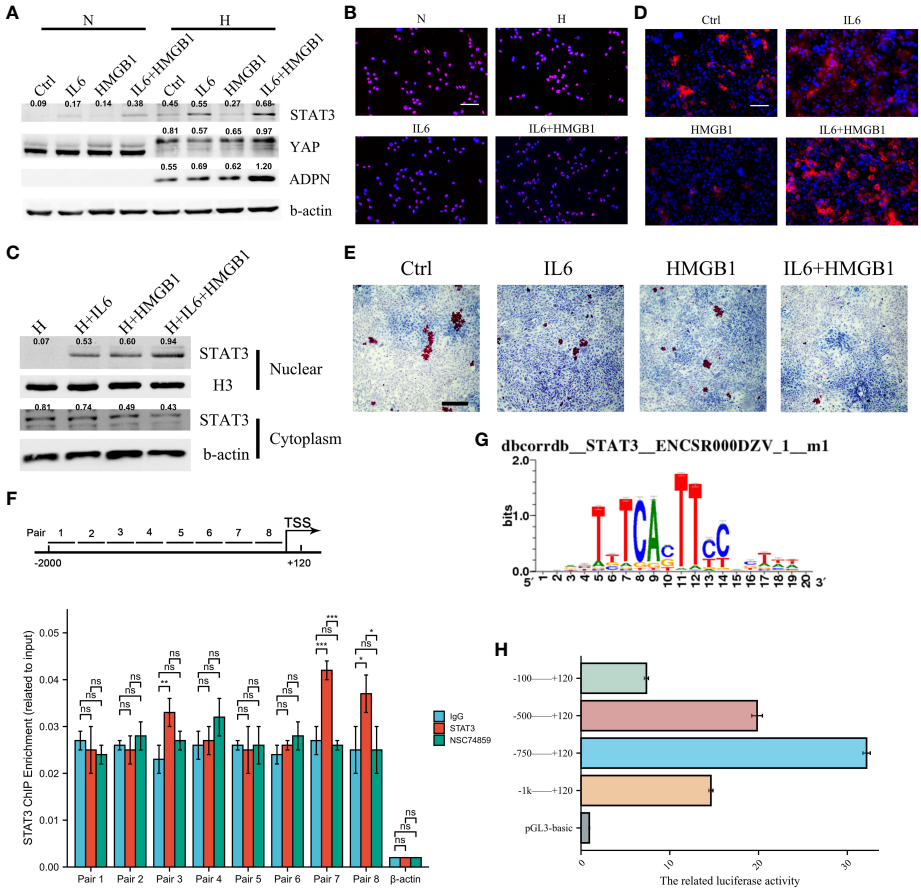

FIGURE 5
IL6 and HMGB1 promoted ADPN expression in adipocytes via STAT3 and co-transcriptional factor YAP. **(A)** STAT3, YAP, and ADPN expressions were determined in normoxic and hypoxic adipocytes pre-treated with control, IL6, HMGB1, or both. **(B)** Immunofluorescent staining was used to show STAT3 distribution in hypoxic adipocytes pre-treated with control, IL6, HMGB1, or both. Scale bar, 100 μm. **(C)** Nuclear plasma separation experiment demonstrated STAT3 distribution in hypoxic adipocytes pre-treated with control, IL6, HMGB1, or both. **(D)** Immunofluorescent staining with ADPN in hypoxic adipocytes pre-treated with control, IL6, HMGB1, or both. Scale bar, 100 μm. **(E)** Oil O staining was used in hypoxic adipocytes pre-treated with control, IL6, HMGB1, or both. Scale bar, 500 μm. **(F)** ChIP analysis demonstrated that STAT3 promoted ADPN transcription. NSC74859 was used in adipocytes to inhibit STAT3 expression, which was as a negative control. **(G)** The motif of STAT3 and ADPN promoter. **(H)** Luciferase reporter gene experiment was used to validate whether STAT3 promoted ADPN transcription. *$p < 0.05$; ***$p < 0.001$; ns, not significant.

(Figures 7C, D). However, the levels of secreted IL6 and HMGB1 were found to be downregulated using ELISA (Figures 7E, F).

The expression levels of IL6, HMGB1, and ADPN in human blood samples were determined using ELISA. The baseline characteristics of young, middle-aged, and aged patients with CABG are shown in Supplementary Table 5. Systolic pressure, albumin, and ADPN were positively correlated with aging in patients with CABG, while IL6 and HMGB1 were negatively correlated with aging (Supplementary Table 5). According to univariate and multivariate logistic analyses, TG, albumin, and ADPN/(IL6*HMGB1) are independent factors in young, middle, and aging patients with CABG, highlighting the clinical value of the IL6/ADPN/HMGB1 axis in aging patients with CABG (Figures 7G, H; Supplementary Table 6).

Overall, the IL6/ADPN/HMGB1 axis was found to be differentially expressed in human subepicardial tissue and blood samples. Moreover, the independent factors for aging patients with CABG led to MI progression, LVA formation, and heterogeneity among patients with CAD (Figure 8).

4 Discussion

LVA is a severe complication of MI. The clinical manifestations of ventricular remodeling include LV expansion and a reduction in cardiac systolic and diastolic functions (22). In this study, we constructed an LVA mouse model to determine the mechanism of LVA formation and the differences in the border zone between LVA and MI hearts. RNA sequencing and further experiments revealed that the hub gene, ADPN, was involved in the crosstalk between adipocytes and macrophages after MI, LVA, and cardiac stress in a mouse model. Thus, ADPN could be a potential target to block LVA formation and MI progression, especially in patients with CAD and obesity or type 2 diabetes.

Cardiac remodeling after MI relies on a balance between debris removal and scar formation (23), and hemodynamic homeostasis during LVA formation. In this study, the stretch force near the plication site increased, inducing the angle of the border zone at 4 weeks after the operation, which may be due to unstable hemodynamic homeostasis, including turbulent flow in the left

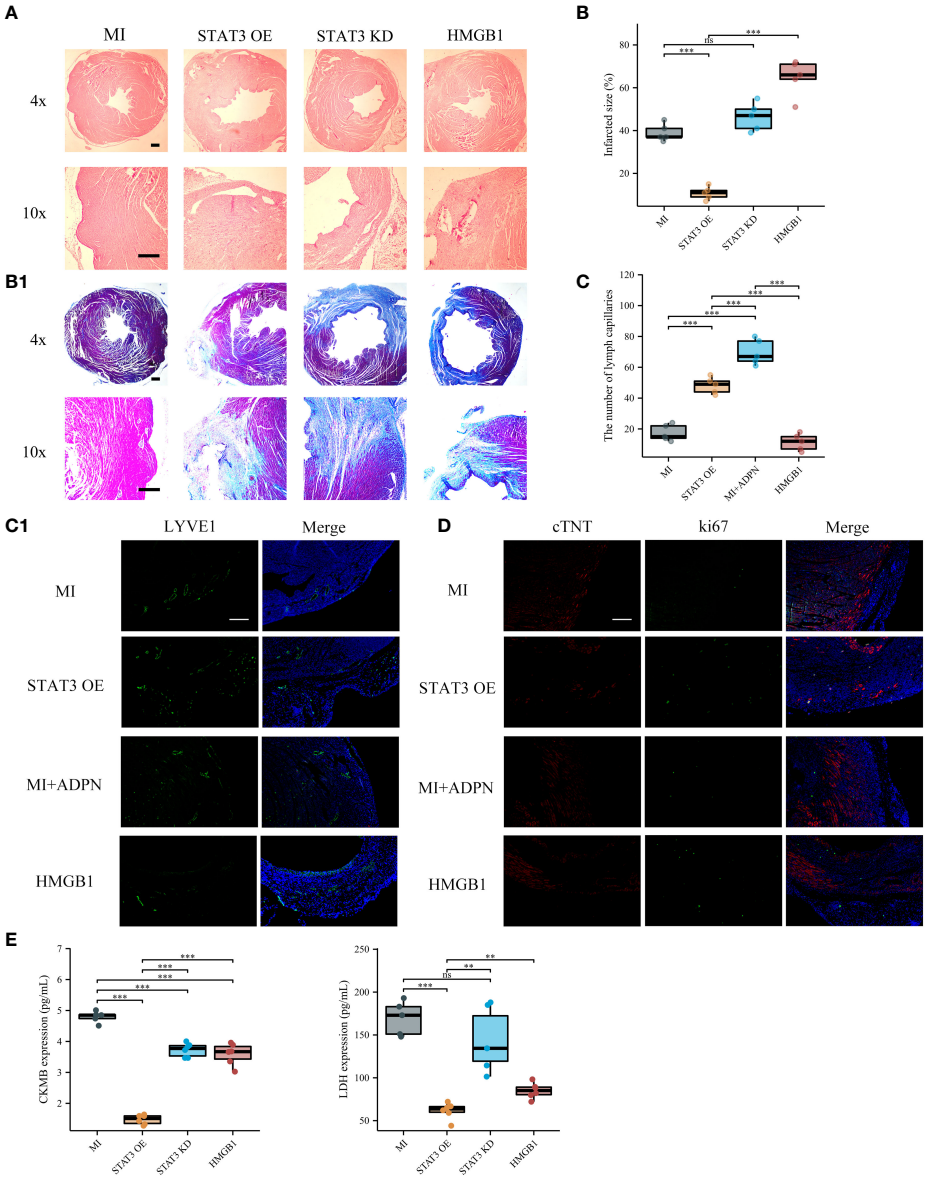

FIGURE 6
Supplying STAT3 overexpressed adipocytes increased lymphangiogenesis after MI via macrophage HMGB1. **(A)** The HE representative images of heart sections in MI, MI+STAT3 overexpressed adipocytes, MI+STAT3 knockdown adipocytes, and MI+STAT3 overexpressed adipocytes+HMGB1 knockdown macrophage groups. AAV-shHMGB1 was utilized to knock down HMGB1 in macrophages. **(B)** The fibrosis representative images (B1) and quantitative analysis (B2) of heart sections using Masson's staining in MI, MI+STAT3 overexpressed adipocytes, MI+STAT3 knockdown adipocytes, and MI+STAT3 overexpressed adipocytes+HMGB1 knockdown macrophage groups. **(C)** The immunofluorescent images with LYVE1 (C1) and quantitative analysis (C2) in MI, MI+STAT3 overexpressed adipocytes, MI+ADPN treatment, and MI+STAT3 overexpressed adipocytes+HMGB1 knockdown macrophage groups. MI+ADPN treatment as the positive control. **(D)** The immunofluorescent images with Ki67 and cTNT in MI, MI +STAT3 overexpressed adipocytes, MI+ADPN treatment, and MI+STAT3 overexpressed adipocytes+HMGB1 knockdown macrophage groups. MI +ADPN treatment as the positive control. cTNT, injured cardiomyocyte marker. **(E)** The border zone CKMB expression (up) and LDH expression (down) at 7 days after operation in different groups using ELISA. HMGB1, MI+STAT3 overexpressed adipocytes+HMGB1 knockdown macrophage group. Scale bar, 500 μm. $^{**}p < 0.01$; $^{***}p < 0.001$; ns, not significant.

ventricle. The instable hemodynamic homeostasis led to the related poor stress resistance in the border zone and LVA formation, which was consistent with the results of Jackson et al. (24) and Ratcliffe et al. (25). These investigators found that the stretch force toward the border zone contributed to its extension, called the "diluted" border zone.

The "diluted" border zone was correlated with LVA formation due to the imbalance between border zone stress and left ventricular hemodynamic instability. Cytokine levels were determined to analyze the immunoregulatory mechanism in LVA formation. LVA was suggested to induce more remarkable inflammatory reactions than MI. After RNA sequencing and validation, ADPN was associated with border zone thickness and LVA formation. ADPN impeded cardiac edema and promoted cardiac lymphangiogenesis post-infarction. Trauma induced myocardial ischemia/reperfusion injury by increasing apoptosis, enlarging

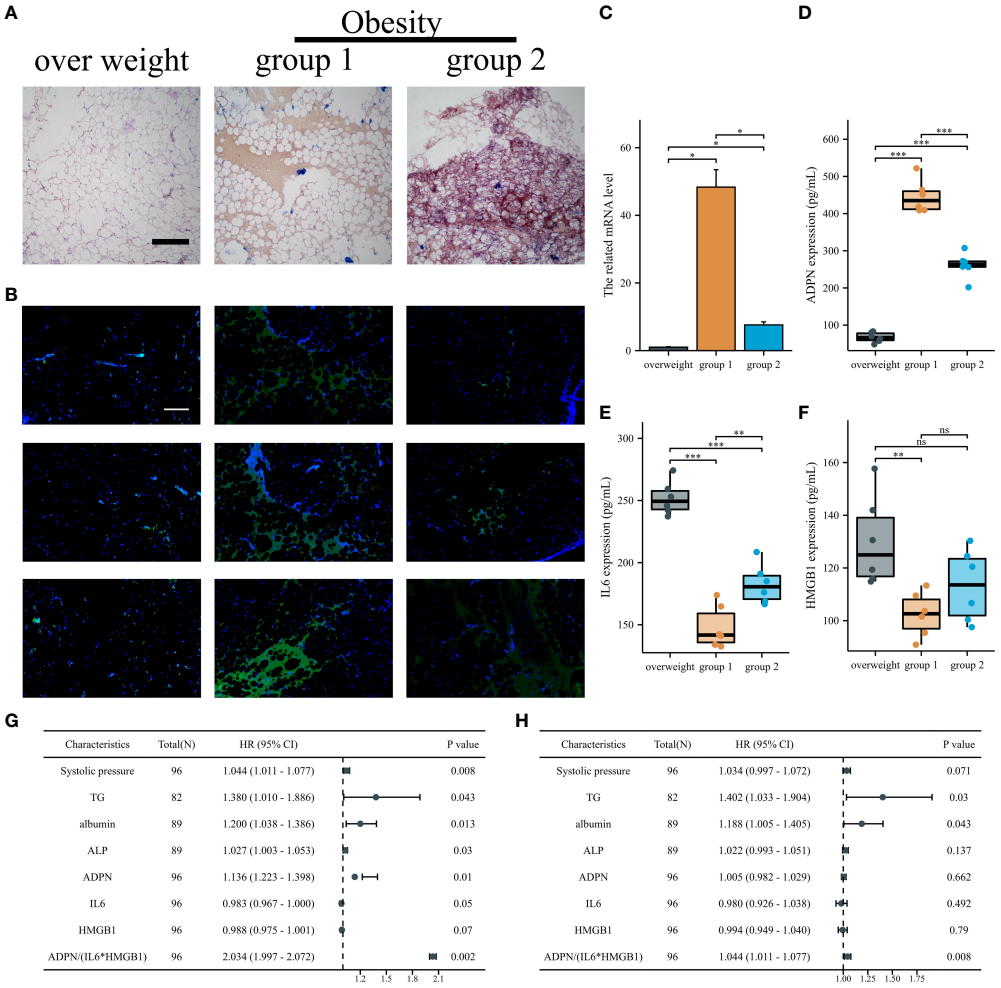

FIGURE 7
IL6/ADPN/HMGB1 axis contributed to the diagnosis and prognosis of CABG patients. **(A)** Oil O staining demonstrated the lipid deposition of sub-epicardial adipocytes in patients with overweight and obesity. Scale bar, 500 μm. **(B)** Immunofluorescent staining with ADPN in sub-epicardial adipocytes in patients with overweight and obesity. Scale bar, 500 μm. **(C)** The ADPN mRNA level was measured using qPCR in sub-epicardial adipocytes in patients with overweight and obesity. **(D–F)** ADPN **(D)**, IL6 **(E)**, and HMGB1 **(F)** expressions of human sub-epicardial samples in patients with overweight and obesity were determined using ELISA. **(G, H)** Univariate **(G)** and multivariate logistic regression analysis **(H)** of young, middle, and aged CABG patients. *$p < 0.05$; **$p < 0.01$; ***$p < 0.001$; ns, not significant.

infarct size, and decreasing cardiac function. Plasma adiponectin concentrations decreased after traumatic injury. Both etanercept and exogenous adiponectin supplementation (3 days post-trauma or 10 min before reperfusion) markedly inhibited oxidative/nitrative stress and ischemia/reperfusion injury in WT mice, whereas adiponectin supplementation substantially attenuated post-traumatic ischemia/reperfusion injury in adiponectin-knockout mice (26). As ADPN has the same domain as TNFa, TNF-α antagonism was found to ameliorate myocardial ischemia-reperfusion injury in mice by upregulating adiponectin (27). The cardioprotective effects of TNF-α neutralization are partially due to the upregulation of ADPN based on a comparison of ADPN knockout mice with WT mice (26, 27).

The resolution of cardiac edema is bimodal, with peaks appearing within 3 h and day 7 after MI (28). Therefore, LVA was induced in adult male mice according to previous protocols, with slight modifications. In this study, the heart in the LVA group was ligated at the LAD and the same level as the heart in the MI group; however, the suture was snipped on day 5 after the operation. At day 5 post-infarction, cardiac edema and inflammation increased. After snipping of the suture, left ventricular hemodynamic instability and the stress of the border zone increased; thus, left ventricular paradoxical movement appeared and LVA formation occurred.

The left ventricle in the LVA group was characterized by systolic dyskinesia and paradoxical bulging, whereas that in the MI group was only characterized by systolic dyskinesia. In this study, ADPN expression levels differed after coronary occlusion, leading to a significant difference in the lymphangiogenesis number and infiltration of LYVE1+ macrophages, thereby inducing different mouse models, such as MI and LVA. Mice administered ADPN had more cardiac lymphatic growth in the border zone than age-

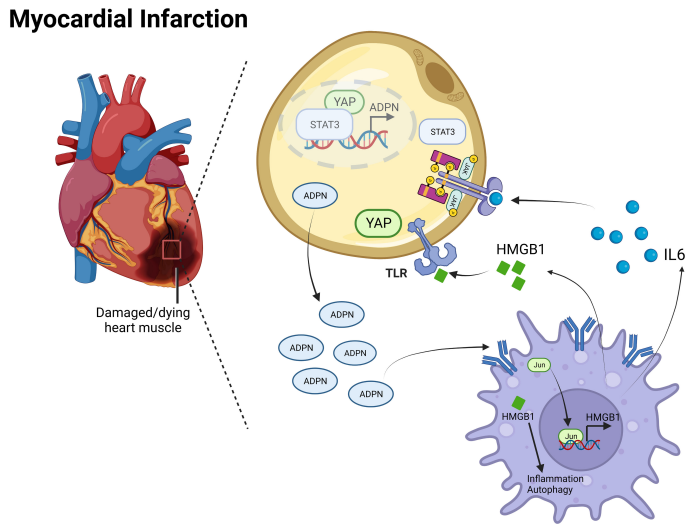

FIGURE 8
Mechanism diagram of the IL6/ADPN/HMGB1 axis on crosstalk between adipocytes and macrophages after MI. ADPN regulated HMGB1 expression and HMGB1-mediated inflammatory response and autophagy in macrophages via AdipoR2/c-Jun. Moreover, ADPN impeded HMGB1and IL6 secretion in hypoxic macrophages, especially in aged hypoxic macrophages. IL6 triggered STAT3 and HMGB1 promoted YAP translocate to nuclear, which raised ADPN expression through binding to ADPN promoter. Therefore, the IL6/ADPN/HMGB1 axis contributed to macrophage phagocytosis, senescence, inflammatory response, and autophagy, which led to MI progression, LVA formation, and CAD patients' heterogeneity.

matched PBS-administered mice on day 28 after the operation, with improved heart function dependent on the administration time, which may be partly due to the expression or localization of Cx43 and macrophage status and abundance. The relationship between Cx43 and cardiac lymphatic growth is consistent with that reported in a previous study (29). Previous studies revealed that Cx37, Cx47, and Cx43 are the main connexin proteins that affect the developing lymphatic tissue (30). Mutations in these genes can lead to lymphatic disorders in mice and humans (31–33). In this study, Cx43 was expressed in the cardiac lymphatic vasculature during LVA formation following treatment with ADPN. Mouse models revealed that Cx43 expression affects not only lymphangiogenesis but also the maintenance of lymphatic function via LYVE1+ macrophages, which further strengthens our findings that ADPN affects Cx43+ LYVE1+ macrophages. Further studies are needed to fully elucidate how ADPN and connexins regulate these vessels, which may provide a therapeutic avenue to impede MI progression and LVA formation.

Cx43 dephosphorylation results in arrhythmia and cardiomyocyte apoptosis after cardiac ischemia/reperfusion (34). Macrophages facilitate electrical conduction in the heart via Cx43 expression (35). The decrease in oxygen in the cell lowers the pH and induces Cx43 degradation, resulting in MI-related complications, including arrhythmia (34, 36). To determine the effects of Cx43 on the injured myocardium following treatment with ADPN, verapamil and Gap19 were used. Verapamil was first used to treat hypertension and arrhythmias via the L-type calcium channels (37). However, verapamil indirectly affected Cx43 localization and stabilization (29, 38). During LVA formation, ADPN and verapamil synergistically enhanced LYVE1+ macrophages and lymphatic capillaries in the border zone (almost in the epicardial layer) via Cx43. Axin2 KO mice were used. Consistent activation of the Wnt/β-catenin signaling pathway was observed in adult mice (39), which also demonstrated the effects of Cx43 on LYVE1+ macrophages and lymphatic capillaries.

In this study, adipocyte-derived ADPN promoted macrophage M2a polarization and decreased inflammatory cytokine secretion via the ADPN/AdipoR2/HMGB1 axis; MMP and autophagy were lower in hypoxic HMGB1 knockdown macrophages than in non-knockdown macrophages, suggesting that HMGB1 is a key target of mitochondrial, autophagy, and inflammatory regulation. Hypoxia-reprogramed megamitochondrion contacted and engulfed lysosome to mediate mitochondrial self-digestion (40), which was consistent with the TEM results of the ADPN and ADPN+HMGB1 knockdown groups. According to Bushra et al., ADPN suppressed ROS production and apoptosis, and improved migration and barrier functions in hyperglycemic cells under 30 mM glucose conditions. Bioinformatics analysis revealed that the signaling pathways of integrin, HMGB1, STAT3, NFkB, and p38-AMPK were mainly involved in the actions of ADPN (41), which were consistent with our findings. ADPN promotes VEGF-C-dependent lymphangiogenesis through the AMPK/p38 signaling pathway (42, 43), which is consistent with the effects of ADPN on hypoxic macrophages.

ADPN decreased IL6, HMGB1, and C1qTNF9 secretion from macrophages, which may also be a senescence-associated secretory phenotype (SASP) (44). Macrophage senescence can partly explain the differences in immune responses after MI and the heterogeneity in the prognosis of patients with CAD. C1qTNF9 also regulates the fate of implanted mesenchymal stem cells to protect against MI injury (45, 46).

Macrophages are involved in all CAD stages. CD169+ macrophage or its "eat me" receptor Mertk deficiency impaired myocardial mitochondria elimination and cardiomyocyte-related hypoxic senescence in the early infarction period; therefore, ventricular functions decreased, and metabolic alterations appeared (47). MertK+ TREM2^{high} and MertK+ LYVE1+ macrophages negatively regulate inflammation and resolve lipid mediators related to the M2c anti-inflammatory effects (48). In addition, loss of CCR2^{-} macrophages led to the accumulation of the extracellular matrix component, hyaluronic acid (HA), which was needed to be cleared; this process required sensing by the HA receptor, LYVE-1 (49).

MI- or I/R-induced myocardial injury generates stress-induced senescent cells (SISCs), which play a critical role in the pathophysiology of adverse cardiac remodeling and heart failure by secreting proinflammatory molecules and matrix-degrading proteases (50). The removal of SISCs decreased inflammatory cytokines and normal cell death via macrophage efferocytosis. Abundant high-molecular-mass hyaluronic acid (HMM-HA) contributes to the longevity of the longest-lived rodents. HMM-HA also reduces inflammation during aging through several pathways, including a direct immunoregulatory effect on immune cells and protection from oxidative stress. LYVE1 on the cell membrane responds to HMM-HA in the matrix, alleviates senescence, and increases macrophage efferocytosis under stress (51). Therefore, LYVE1 may be a therapeutic target for the treatment of macrophage and cardiomyocyte senescence, and may improve the prognosis of patients with CAD. In our previous study, a CCR2 inhibitor was found to increase the ratio of CCR2^{-} macrophages, thereby strengthening the effects of adiponectin against myocardial injury after infarction (12). In this study, LNP-MertK was used to improve macrophage phagocytosis and heart function after MI by decreasing senescence. *In vivo*, transiently engineered CAR T-cell therapy delivered mRNA through LNP injection to reprogram T cells to recognize cardiac fibroblasts, thereby restoring heart function (52). We investigated whether this method could be used to treat macrophages after MI. Treatment with LNP-MertK increased the efficiency of endocytosis of the mitochondria and other unfit materials. Thus, LNP-MertK can be used to treat myocardial ischemia and/or reperfusion injury and increase the survival of cardiomyocytes to help outlive the early infarction period and decrease patient recurrent events. The effects of macrophage phagocytosis and senescence alleviation after LNP-MertK mRNA vaccine-like administration may be determined by evaluating migrasomes from macrophages (53, 54). Patients undergoing acute MI would survive longer if such treatment could be used in the early infarction period, which should be further investigated.

The crosstalk between adipocytes and macrophages is critical for disease progression. Adipocyte-derived lactate is a signaling metabolite that potentiates adipose macrophage inflammation by targeting PHD2 (55). Of note, intercellular mitochondrial transfer between adipocytes and macrophages is impaired in obesity (56). Macrophages limit the release of adipocyte mitochondria into the blood and cardiomyocytes; these effects are rescued during aging (57). In this study, IL6 and HMGB1 promoted ADPN expression in adipocytes via STAT3 and the co-transcription factor, YAP. The YAP/TEAD1 complex is a default repressor of the cardiac HMGB1/Toll-Like Receptor (TLR) axis (58) and may be a potential target for regulating the crosstalk between adipocytes and macrophages after MI. In this study, patients with CAD and obesity were divided into two groups based on lipid deposition and ADPN expression in the sub-epicardial adipocytes. The IL6/ADPN/HMGB1 axis was differentially expressed in human subepicardial tissue and blood samples, and was an independent factor in patients with CAD, which may partly explain the obesity paradox in patients that are overweight or obese, particularly among those who develop symptomatic CAD. However, BMI and other parameters of body composition are not consistent with the CAD risk factors for adverse short-term outcomes (59, 60). After treatment with high-thermogenic beige adipocytes (HBACs)-condition medium, the expression levels of antioxidant and anti-apoptotic genes were upregulated in H9c2 cardiomyocytes via NRF2 activation. Furthermore, HBAC-conditioned medium significantly attenuated ischemic rat heart tissue injury via NRF2 activation (61). Therefore, highly thermogenic beige adipocytes exert beneficial effects on cardiac injury by modulating NRF2 and are promising therapeutic agents for MI. The various modes of fat grafts after transplantation highlight the importance of macrophage-mediated ECM remodeling in graft preservation after fat grafting (62). This study may help preserve the retention rate of fat grafts.

This study had some limitations. First, more evidence and clearer explanations, especially regarding hemodynamic instability and border-zone stress, are needed for LVA formation. Second, intercellular mitochondrial transfer between adipocytes and macrophages, and mitochondrial and lipid droplet interactions, still need to be clearly elucidated in epicardial adipocyte ADPN-conditional knockout mice. Third, other leukocyte populations were not included. The effects of other target genes in RNA-seq analysis on Tregs or other leukocyte populations must be investigated using adipocyte-conditioned medium and conditional knockout mice. Finally, large sample sizes were not employed, and follow-up of the cohort was not conducted. The effects of the IL6/ADPN/HMGB1 axis must be examined in a large double-blind follow-up multicenter cohort.

5 Conclusion

Overall, ADPN impedes cardiac edema and promotes cardiac lymphangiogenesis by regulating Cx43. The IL6/STAT3/ADPN/HMGB1 axis contributes to the regulation of macrophage M2a polarization and sustained mitochondrial quality via crosstalk between adipocytes and macrophages in a mouse model. These findings were validated using human samples.

Data availability statement

The datasets presented in this study can be found in online repositories. The names of the repository/repositories and accession number(s) can be found below: PRJNA1064646 (SRA).

Ethics statement

This study was approved by the Ethics Committee of Tianjin Third Central Hospital. The studies were conducted in accordance with the local legislation and institutional requirements. The participants provided their written informed consent to participate in this study. This study was approved by the Ethics Committee of Nankai University (no. 2022-SYDWLL-000486). The study was conducted in accordance with the local legislation and institutional requirements.

Author contributions

YZ: Writing – review & editing, Writing – original draft, Visualization, Methodology, Investigation, Data curation, Conceptualization. YW: Writing – review & editing, Investigation, Data curation. BQ: Writing – review & editing, Methodology, Investigation, Data curation. YL: Writing – review & editing, Resources, Methodology. ZZ: Writing – review & editing, Investigation. JM: Writing – review & editing, Validation, Resources. ML: Writing – review & editing, Validation, Resources. XL: Writing – review & editing, Visualization. YC: Writing – review & editing, Visualization. QZ: Writing – review & editing, Supervision. WG: Writing – review & editing, Supervision, Resources, Funding acquisition, Data curation. TL: Writing – review & editing, Supervision, Resources, Funding acquisition, Data curation.

Funding

The author(s) declare financial support was received for the research, authorship, and/or publication of this article. This work was sponsored by the Tianjin Key Medical Discipline (Specialty) Construction Project (TJYXZDXK-035A), the Tianjin Biomedical Industry Chain Innovation Project (21ZXSYSY00030), the Tianjin Health Research Project (TJWJ2022XK026), the Tianjin Health Research Project (TJWJ2022MS020), the Tianjin "Project + Team" Key Training Special Project (XC202040), the Tianjin "131" Innovative Talent Team Project (201939), the Key Project of Tianjin Natural Science Foundation (21JCZDJC00240), the Tianjin Municipal Health and Health Committee Science and Technology Project (ZD20001), the Tianjin Health Committee Traditional Chinese Medicine and Integrated Traditional Chinese and Western Medicine Project (2021139), the Tianjin Science and Technology Project (21JCYBJC01250), the Tianjin Science and Technology Project (21JCYBJC01590), the Natural Science Foundation of Tianjin Science and Technology Bureau (21JCQNJC01460), the Tianjin Health Research Project (TJWJ2023XK018), and the Tianjin Health Research Project (TJ WJ2023QN046).

Acknowledgments

We would like to express our gratitude to Dr. Yu for presenting Axin2 KO mice and all those who helped us during the writing of this manuscript. Thanks to all the peer reviewers for their opinions and suggestions.

Conflict of interest

Authors JM and ML are employed by Tianjin Kang Ting Biological Engineering Group CO. LTD.

The remaining authors declare that the research was conducted in the absence of any commercial or financial relationships that could be construed as a potential conflict of interest.

Publisher's note

Supplementary material

The Supplementary Material for this article can be found online at: https://www.frontiersin.org/articles/10.3389/fimmu.2024.1368516/full#supplementary-material

SUPPLEMENTARY FIGURE 1
A simple, consistent, and low-cost LVA mice model construction. **(A)** Ligation site of heart organ in left coronary artery descending branch. **(B)** Intra-chamber cast and optical image of LVA (left) and MI (right), illustrating an outward bulge in the free wall of the left ventricle. **(C)** Optical LVA formation of mice heart: end-diastole (left) and end-systole (right) ligated at 4-4.5mm from its coronary origin. **(D)** Pattern picture of heart movement in LVA formation. **(E, F)** Coronal **(E)** and sagittal **(F)** position of computed tomography of LVA formation. SHAM and MI were 7d capture after model construction (n=6 per group). LVA formation was labeled with rectangle.

SUPPLEMENTARY FIGURE 2
LVA formation process. **(A)** Masson's staining of representative images showed the LVA forming process in the total scenery (up, 25x) and the border regions (down, 100x) at 1d, 3d, 7d and 28d after operation. The SHAM and MI images at 7d after operation were as negative and positive control, respectively. Scale bar, 500μm and 100μm. **(B)** HE staining at border zone of representative images at the same d. Scale bar, 100μm. **(C)** Representative images of heart sections at border zone stained for cTNT (red) at the same day. Scale bar, 25μm. **(D–F)** Comparison of infarction area **(D)** and infarction size **(E)** in border zone compared to SHAM group. ** $P<0.01$, *** $P<0.001$, **** $P<0.0001$.

SUPPLEMENTARY FIGURE 3
Activation of pro-inflammatory and anti-inflammatory during LVA formation and progression. **(A)** The standard curve of the cytokine and chemokine

measurements: IFN-ur GM-CSF, IL-1SF IL-6, IL-10, IL-22 and TNF22 **(B)** The concentrations of the cytokine and chemokine measurements: GM-CSF, IFNCS IL-1SF IL-6, IL-10, IL-22 and TNF2 among the three groups at 1d, 3d, 5d, 7d and 28d after operation (n=5 per group). LVA vs. MI: * P<0.05; ** P<0.01; *** P<0.001; **** P<0.0001.

SUPPLEMENTARY FIGURE 4
The survival rate among 3 groups. **(A)** The survival rate of LVA, MI and SHAM (n=25, 25 and 20, respectively). **(B)** Operation time of LVA, MI and SHAM (n=12 per group).

SUPPLEMENTARY FIGURE 5
ADPN regulated LYVE1+ macrophages and lymph-angiogenesis via Cx43 and Wnt canonical signaling. **(A)** The representative immunofluorescence images of Cx43 expression and Cx43 associated macrophages in the LVA mice treated with ADPN, verapamil and/or Gap19 from day 1 to 7. **(B)** The representative immunofluorescence images of Cx43 expression and Cx43 associated macrophages in WT or Axin2 KO LVA mice treated with ADPN and Gap19 from day 1 to 7, demonstrating that consistent activation of Wnt canonical signaling rescued the effects of downregulated Cx43 expression on Cx43 associated macrophages infiltration. **(C, D)** The representative immunofluorescence images **(C)** and quantity analysis **(D)** of LYVE1+ macrophages and lymph-angiogenesis in the LVA mice treated with ADPN, verapamil and/or Gap19 from day 1 to 7. **(E, F)** The representative immunofluorescence images **(E)** and quantity analysis **(F)** of LYVE1+ macrophages and lymph-angiogenesis in WT or Axin2 KO LVA mice treated with ADPN and Gap19 from day 1 to 7, demonstrating that consistent activation of Wnt canonical signaling rescued the effects of downregulated Cx43 expression. **(G)** The representative immunofluorescence images of Cx43 and ZO-1 expression and localization in the LVA mice treated with ADPN or control from day 1 to 7. **(H)** The mechanism diagram of MI and LVA formation. The ADPN expression level differed after coronary occlusion, leading to the significant difference of lymph-angiogenesis number and infiltrated LYVE1+ macrophages, thus inducing different mice model, such as MI and LVA formation. Scale bar, 500μm. * P<0.05; ** P<0.01; *** P<0.001; ns, not significant. Arrow, LYVE1+ macrophages. Scale bar, 500μm.

SUPPLEMENTARY FIGURE 6
HMGB1 knockdown led to mitochondrial quality control, autophagy reduction and M2b polarization in hypoxic macrophages. **(A)** qPCR and WB analysis demonstrated the HMGB1 knockdown efficiency in hypoxic macrophages. **(B)** ROS measurement in normal oxygen, hypoxia and HMGB1 knockdown Raw264.7. **(C)** Autophagy measurement in normal oxygen, hypoxia and HMGB1 knockdown Raw264.7 using MDC method. **(D)** The represented WB images of GPX4 and LC3 protein expression in normal oxygen, hypoxia and HMGB1 knockdown Raw264.7. **(E)** The related mRNA levels of IL1b, TNFa, IL6, Arg1, IL10 and Mrc1 in N, H and HMGB1 KD group. KD, knockdown; N, normal oxygen Raw264.7; H, hypoxia Raw264.7; HMGB1 KD, hypoxia HMGB1 knockdown Raw264.7. Scale bar, 100μm. *P<0.05; **P<0.01; ***P<0.001.

SUPPLEMENTARY FIGURE 7
Supplying STAT3 overexpressed adipocytes decreased injury after LVA formation. **(A)** The HE representative images of heart sections in LVA and LVA+STAT3 overexpressed adipocytes groups. **(B)** The related wall thickness of border zone in LVA and LVA+STAT3 overexpressed adipocytes groups. **(C)** The border zone CKMB expression and LDH expression at 7d after operation in LVA and LVA+STAT3 overexpressed adipocytes groups using ELISA. Scale bar, 500μm. ***P<0.001.

SUPPLEMENTARY FIGURE 8
Aged macrophages hided in bone marrow. **(A)** The immunofluorescent images with b-gal and CD68 in bone marrow in young and aged MI mice. **(B)** Flow cytometry of F4/80 and CD206 staining to determine the macrophage M2 polarization in border zone of aged MI mice when treated LNP-MertK or LNP-MertK+ADPN at 7d after operation.

SUPPLEMENTARY FIGURE 9
Targeting MertK improved the heart functions after MI. **(A)** The representative echocardiogram image and quantity analysis, including LVEF and LVFS, in the SHAM, MI, MI+LNP and MI+LNP-MertK groups. **(B)** The representative images of Masson's staining in the MI and MI+LNP-MertK groups. Scale bar, 500um. **(C)** HL-1 cardiomyocytes were pretreated with JC-1 and hypoxia 4h. Green labeled represented bad mitochondrial function. After that, transwell analysis was applied to cardiomyocytes (up) and macrophages, LNP treated macrophages or LNP-MertK treated macrophages (down). Nystatin was utilized to rescue the effects of LNP-MertK. Scale bar, 100um. **(D)** MitoTracker® Red was used to pretreat hypoxic cardiomyocytes and transwell analysis and flow cytometry were used to analyze the protective effects of LNP-MertK on myocardial mitochondrial. **(E)** The macrophage polarization in four groups at 3d (up) and 7d (down) after operation. **(F)** The CKMB expression (up) and LDH expression (down) at 3d and 7d after MI using ELISA. **(G)** Flow cytometry of LYVE1 and MertK staining to determine the abundance of infiltrated phagocytic macrophages when treated with LNP-MertK or LNP-MertK+ADPN. **(H)** VEGFC expression was determined using ELISA at 3d and 7d after operation in the SHAM, MI, MI+LNP and MI+LNP-MertK groups. * P<0.05; **P<0.01; ***P<0.001; ns, not significant.

References

1. Naghavi M, Abajobir AA, Abbafati C, Abbas KM, Abd-Allah F, Abera SF, et al. Global, regional, and national age-sex specific mortality for 264 causes of death, 1980–2016: a systematic analysis for the Global Burden of Disease Study 2016. *Lancet*. (2017) 390:1151–210. doi: 10.1016/S0140-6736(17)32152-9

2. Chang J, Liu X, Sun Y. Mortality due to acutemyocardial infarction in China from 1987 to 2014: Secular trends and ageperiod-cohort effects. *Int J Cardiol*. (2017) 227:229–38. doi: 10.1016/j.ijcard.2016.11.130

3. You J, Wang X, Wu J, Gao L, Wang X, Du P, et al. Predictors and prognosis of left ventricular thrombus in post-myocardial infarction patients with left ventricular dysfunction after percutaneous coronary intervention. *J Thorac Dis*. (2018) 10:4912–22. doi: 10.21037/jtd

4. Sherrid MV, Bernard S, Tripathi N, Patel Y, Modi V, Axel L, et al. Apical aneurysms and mid-left ventricular obstruction in hypertrophic cardiomyopathy. *JACC Cardiovasc Imaging*. (2023) 16:591–605. doi: 10.1016/j.jcmg.2022.11.013

5. Ruzza A, Czer LSC, Arabia F, Vespignani R, Esmailian F, Cheng W, et al. Left ventricular reconstruction for postinfarction left ventricular aneurysm: review of surgical techniques. *Tex Heart Inst J*. (2017) 44:326–35. doi: 10.14503/THIJ-16-6068

6. Michael H, Mariaelvy B, Donato S, Remco TAM, Jean-Yves S, Irene N, et al. Pericardial adipose tissue regulates granulopoiesis, fibrosis, and cardiac function after myocardial infarction. *Circulation*. (2018) 137:948–60. doi: 10.1161/CIRCULATIONAHA.117.028833

7. Lu G, Dina X, Jing L, Wayne BL, Theodore AC, Bernard L, et al. Small extracellular microvesicles mediated pathological communications between dysfunctional adipocytes and cardiomyocytes as a novel mechanism exacerbating ischemia/reperfusion injury in diabetic mice. *Circulation*. (2020) 141:968–83. doi: 10.1161/CIRCULATIONAHA.119.042640

8. Elfeky M, Kaede R, Okamatsu-Ogura Y, Kimura K. Adiponectin inhibits LPS-induced HMGB1 release through an AMP kinase and heme oxygenase-1-dependent pathway in RAW 264 macrophage cells. *Mediators Inflamm.*. (2016) 2016:5701959. doi: 10.1155/2016/5701959

9. Xia Y, Zhang F, Zhao S, Li Y, Chen X, Gao E, et al. Adiponectin determines farnesoid X receptor agonism-mediated cardioprotection against post-infarction remodelling and dysfunction. *Cardiovasc Res*. (2018) 114:1335–49. doi: 10.1093/cvr/cvy093

10. Zhou B, Honor LB, He H, Ma Q, Oh JH, Butterfield C, et al. Adult mouse epicardium modulates myocardial injury by secreting paracrine factors. *J Clin Invest*. (2011) 121:1894–904. doi: 10.1172/JCI45529

11. Sun QN, Wang YF, Guo ZK. Reconstitution of myocardial lymphatic vessels after acute infarction of rat heart. *Lymphology*. (2012) 45:80–6.

12. Zheng Y, Gao W, Qi B, Zhang R, Ning M, Hu X, et al. CCR2 inhibitor strengthens the adiponectin effects against myocardial injury after infarction. *FASEB J*. (2023) 37:e23039. doi: 10.1096/fj.202300281RR

13. Takagawa J, Zhang Y, Wong ML, Sievers RE, Kapasi NK, Wang Y, et al. Myocardial infarct size measurement in the mouse chronic infarction model:

comparison of area- and length-based approaches. *J Appl Physiol (1985)*. (2007) 102:2104–11. doi: 10.1152/japplphysiol.00033.2007

14. Ashburner M, Ball CA, Blake JA, Botstein D, Butler H, Cherry JM, et al. Gene ontology: tool for the unification of biology. *Gene Ontol Consortium Nat Genet*. (2000) 25:25–9. doi: 10.1038/75556

15. Kanehisa M, Goto S. KEGG: kyoto encyclopedia of genes and genomes. *Nucleic Acids Res*. (2000) 28:27–30. doi: 10.1093/nar/28.1.27

16. Szklarczyk D, Gable AL, Lyon D, Junge A, Wyder S, Huerta-Cepas J, et al. STRING v11: protein-protein association networks with increased coverage, supporting functional discovery in genome-wide experimental datasets. *Nucleic Acids Res*. (2019) 47:D607–13. doi: 10.1093/nar/gky1131

17. Shannon P, Markiel A, Ozier O, Baliga NS, Wang JT, Ramage D, et al. Cytoscape: a software environment for integrated models of biomolecular interaction networks. *Genome Res*. (2003) 13:2498–504. doi: 10.1101/gr.1239303

18. Tucker NR, Chaffin M, Fleming SJ, Hall AW, Parsons VA, Bedi KC Jr, et al. Transcriptional and cellular diversity of the human heart. *Circulation*. (2020) 142:466–82. doi: 10.1161/CIRCULATIONAHA.119.045401

19. Gonçalves C, Ramalho MJ, Silva R, Silva V, Marques-Oliveira R, Silva AC, et al. Lipid nanoparticles containing mixtures of antioxidants to improve skin care and cancer prevention. *Pharmaceutics*. (2021) 13:2042. doi: 10.3390/pharmaceutics13122042

20. Nicu C, Jackson J, Shahmalak A, Pople J, Ansell D, Paus R. Adiponectin negatively regulates pigmentation, Wnt/β-catenin and HGF/c-Met signalling within human scalp hair follicles ex vivo. *Arch Dermatol Res*. (2023) 315:603–12. doi: 10.1007/s00403-021-02291-2

21. Li Y, Chen Y, Yang T, Chang K, Deng N, Zhao W, et al. Targeting circulating high mobility group box-1 and histones by extracorporeal blood purification as an immunomodulation strategy against critical illnesses. *Crit Care*. (2023) 27:77. doi: 10.1186/s13054-023-04382-0

22. Parikh NI, Gona P, Larson MG, Fox CS, Benjamin EJ, Murabito JM, et al. Long-term trends in myocardial infarction incidence and case fatality in the National Heart, Lung, and Blood Institute's Framingham Heart study. *Circulation*. (2009) 119:1203–10. doi: 10.1161/CIRCULATIONAHA.108.825364

23. Yan X, Zhang H, Fan Q, Hu J, Tao R, Chen Q, et al. Dectin-2 deficiency modulates th1 differentiation and improves wound healing after myocardial infarction. *Circ Res*. (2017) 120:1116–29. doi: 10.1161/CIRCRESAHA.116.310260

24. Jackson BM, Gorman JH III, Moainie SL, Guy TS, Narula N, Narula J, et al. Extension of borderzone myocardium in postinfarction dilated cardiomyopathy. *J Am Col Cardiol*. (2002) 40:1160–7. doi: 10.1016/S0735-1097(02)02121-6

25. Ratcliffe MB. Non-ischemic infarct extension: A new type of infarct enlargement and a potential therapeutic target. *J Am Col Cardiol*. (2002) 40:1168–71. doi: 10.1016/S0735-1097(02)02113-7

26. Liu S, Yin T, Wei X, Yi W, Qu Y, Liu Y, et al. Downregulation of adiponectin induced by tumor necrosis factor α is involved in the aggravation of posttraumatic myocardial ischemia/reperfusion injury. *Crit Care Med*. (2011) 39:1935–43. doi: 10.1097/CCM.0b013e31821b85db

27. Gao C, Liu Y, Yu Q, Yang Q, Li B, Sun L, et al. TNF-α antagonism ameliorates myocardial ischemia-reperfusion injury in mice by upregulating adiponectin. *Am J Physiol Heart Circ Physiol*. (2015) 308:H1583–1591. doi: 10.1152/ajpheart.00346.2014

28. Fernandez-Jimenez R, Sanchez-Gonzalez J, Aguero J, Garcia-Prieto J, Lopez-Martin GJ, Garcia-Ruiz JM, et al. Myocardial edema after ischemia/reperfusion is not stable and follows a bimodal pattern: imaging and histological tissue characterization. *J Am Coll Cardiol*. (2015) 65:315–23. doi: 10.1016/j.jacc.2014.11.004

29. Trincot CE, Xu W, Zhang H, Kulikauskas MR, Caranasos TG, Jensen BC, et al. Adrenomedullin induces cardiac lymphangiogenesis after myocardial infarction and regulates cardiac edema *via* connexin 43. *Circ Res*. (2019) 124:101–13. doi: 10.1161/CIRCRESAHA.118.313835

30. Munger SJ, Geng X, Srinivasan RS, Witte MH, Paul DL, Simon AM. Segregated Foxc2, NFATc1 and Connexin expression at normal developing venous valves, and Connexin-specific differences in the valve phenotypes of Cx37, Cx43, and Cx47 knockout mice. *Dev Biol*. (2016) 412:173–90. doi: 10.1016/j.ydbio.2016.02.033

31. Kanady JD, Dellinger MT, Munger SJ, Witte MH, Simon AM. Connexin37 and Connexin43 deficiencies in mice disrupt lymphatic valve development and result in lymphatic disorders including lymphedema and chylothorax. *Dev Biol*. (2011) 354:253–66. doi: 10.1016/j.ydbio.2011.04.004

32. Munger SJ, Davis MJ, Simon AM. Defective lymphatic valve development and chylothorax in mice with a lymphatic-specific deletion of Connexin43. *Dev Biol*. (2017) 421:204–18. doi: 10.1016/j.ydbio.2016.11.017

33. Ferrell RE, Baty CJ, Kimak MA, Karlsson JM, Lawrence EC, Franke-Snyder M, et al. GJC2 missense mutations cause human lymphedema. *Am J Hum Genet*. (2010) 86:943–8. doi: 10.1016/j.ajhg.2010.04.010

34. Jingyi X, Xinxin Y, Yutong Y, Min C, Lulin W, Zhongshan G, et al. Connexin 43 dephosphorylation contributes to arrhythmias and cardiomyocyte apoptosis in ischemia/reperfusion hearts. *Basic Res Cardiol*. (2019) 114(5):40. doi: 10.1007/s00395-019-0748-8

35. Maarten H, Sebastian C, Ling X, Aguirre AD, King KR, Hanley A, et al. Macrophages facilitate electrical conduction in the heart. *Cell*. (2017) 169:510–522.e20. doi: 10.1016/j.cell.2017.03.050

36. Kieken F, Mutsaers N, Dolmatova E, Virgil K, Wit AL, Kellezi A, et al. Structural and molecular mechanisms of gap junction remodeling in epicardial border zone myocytes following myocardial infarction. *Circ Res*. (2009) 104:1103–12. doi: 10.1161/CIRCRESAHA.108.190454

37. Curtis MJ, Walker MJ. The mechanism of action of the optical enantiomers of verapamil against ischaemia-induced arrhythmias in the conscious rat. *Br J Pharmacol*. (1986) 89:137–47. doi: 10.1111/j.1476-5381.1986.tb11129.x

38. Zhou P, Zhang SM, Wang QL, Wu Q, Chen M, Pei JM. Anti-arrhythmic effect of verapamil is accompanied by preservation of cx43 protein in rat heart. *PloS One*. (2013) 8:e7156710. doi: 10.1371/journal.pone.0071567

39. Yan Y, Tang D, Chen M, Huang J, Xie R, Jonason JH, et al. Axin2 controls bone remodeling through the beta-catenin-BMP signaling pathway in adult mice. *J Cell Sci*. (2009) 122:3566–78. doi: 10.1242/jcs.051904

40. Hao T, Yu J, Wu Z, Jiang J, Gong L, Wang B, et al. Hypoxia-reprogramed megamitochondrion contacts and engulfs lysosome to mediate mitochondrial self-digestion. *Nat Commun*. (2023) 14:4105. doi: 10.1038/s41467-023-39811-9

41. Bushra S, Al-Sadeq DW, Bari R, Sahara A, Fadel A, Rizk N. Adiponectin ameliorates hyperglycemia-induced retinal endothelial dysfunction, highlighting pathways, regulators, and networks. *J Inflamm Res*. (2022) 15:3135–66. doi: 10.2147/JIR.S358594

42. Huang CY, Chang AC, Chen HT, Wang SW, Lo YS, Tang CH. Adiponectin promotes VEGF-C-dependent lymphangiogenesis by inhibiting miR-27b through a CaMKII/AMPK/p38 signaling pathway in human chondrosarcoma cells. *Clin Sci (Lond)*. (2016) 130:1523–33. doi: 10.1042/CS20160117

43. Wang Y, Liang B, Lau WB, Du Y, Guo R, Yan Z, et al. Restoring diabetes-induced autophagic flux arrest in ischemic/reperfused heart by ADIPOR (adiponectin receptor) activation involves both AMPK-dependent and AMPK-independent signaling. *Autophagy*. (2017) 13:1855–69. doi: 10.1080/15548627.2017.1358848

44. Di Micco R, Krizhanovsky V, Baker D, d'Adda di Fagagna F. Cellular senescence in ageing: from mechanisms to therapeutic opportunities. *Nat Rev Mol Cell Biol*. (2021) 22:75–95. doi: 10.1038/s41580-020-00314-w

45. Yan W, Guo Y, Tao L, Lau WB, Gan L, Yan Z, et al. C1q/tumor necrosis factor-related protein-9 regulates the fate of implanted mesenchymal stem cells and mobilizes their protective effects against ischemic heart injury *via* multiple novel signaling pathways. *Circulation*. (2017) 136:2162–77. doi: 10.1161/CIRCULATIONAHA.117.029557

46. Liu D, Gu G, Gan L, Yan W, Zhang Z, Yao P, et al. Identification of a CTRP9 C-Terminal polypeptide capable of enhancing bone-derived mesenchymal stem cell cardioprotection through promoting angiogenic exosome production. *Redox Biol*. (2021) 41:101929. doi: 10.1016/j.redox.2021.101929

47. Nicolás-Ávila JA, Lechuga-Vieco AV, Esteban-Martínez L, Sánchez-Díaz M, Díaz-García E, Santiago DJ, et al. A network of macrophages supports mitochondrial homeostasis in the heart. *Cell*. (2020) 183:94–109.e23. doi: 10.1016/j.cell.2020.08.031

48. Alivernini S, MacDonald L, Elmesmari A, Finlay S, Tolusso B, Gigante MR, et al. Distinct synovial tissue macrophage subsets regulate inflammation and remission in rheumatoid arthritis. *Nat Med*. (2020) 26:1295–306. doi: 10.1038/s41591-020-0939-8

49. Voisin B, Nadella V, Doebel T, Goel S, Sakamoto K, Ayush O, et al. Macrophage-mediated extracellular matrix remodeling controls host Staphylococcus aureus susceptibility in the skin. *Immunity*. (2023) 56:1561–1577.e9. doi: 10.1016/j.immuni.2023.06.006

50. Lee JR, Park BW, Park JH, Lim S, Kwon SP, Hwang JW, et al. Local delivery of a senolytic drug in ischemia and reperfusion-injured heart attenuates cardiac remodeling and restores impaired cardiac function. *Acta Biomater*. (2021) 135:520–33. doi: 10.1016/j.actbio.2021.08.028

51. Zhang Z, Tian X, Lu JY, Boit K, Ablaeva J, Zakusilo FT, et al. Increased hyaluronan by naked mole-rat Has2 improves healthspan in mice. *Nature*. (2023) 621:196–205. doi: 10.1038/s41586-023-06463-0

52. Rurik JG, Tombácz I, Yadegari A, Méndez Fernández PO, Shewale SV, Li L, et al. CAR T cells produced in vivo to treat cardiac injury. *Science*. (2022) 375:91–6. doi: 10.1126/science.abm0594

53. Jiao H, Jiang D, Hu X, Du W, Ji L, Yang Y, et al. Mitocytosis, a migrasome-mediated mitochondrial quality-control process. *Cell*. (2021) 184:2896–2910.e13. doi: 10.1016/j.cell.2021.04.027

54. Zheng Y, Lang Y, Qi B, Li T. TSPAN4 and migrasomes in atherosclerosis regression correlated to myocardial infarction and pan-cancer progression. *Cell Adh Migr*. (2023) 17:14–9. doi: 10.1080/19336918.2022.2155337

55. Feng T, Zhao X, Gu P, Yang W, Wang C, Guo Q, et al. Adipocyte-derived lactate is a signalling metabolite that potentiates adipose macrophage inflammation *via* targeting PHD2. *Nat Commun*. (2022) 13:5208. doi: 10.1038/s41467-022-32871-3

56. Brestoff JR, Wilen CB, Moley JR, Li Y, Zou W, Malvin NP, et al. Intercellular mitochondria transfer to macrophages regulates white adipose tissue homeostasis and is impaired in obesity. *Cell Metab*. (2021) 33:270–282.e8. doi: 10.1016/j.cmet.2020.11.008

57. Borcherding N, Jia W, Giwa R, Field RL, Moley JR, Kopecky BJ, et al. Dietary lipids inhibit mitochondria transfer to macrophages to divert adipocyte-derived mitochondria into the blood. *Cell Metab*. (2022) 34:1499–1513.e8. doi: 10.1016/j.cmet.2022.08.010

58. Gao Y, Sun Y, Ercan-Sencicek AG, King JS, Akerberg BN, Ma Q, et al. YAP/TEAD1 complex is a default repressor of cardiac toll-like receptor genes. *Int J Mol Sci*. (2021) 22:6649. doi: 10.3390/ijms22136649

59. Julia R. How the U.S. Low-Fat Diet Recommendations of 1977 Contributed to the Declining Health of Americans. Honors Scholar Theses. (2016). p. 490.

60. Powell-Wiley TM, Poirier P, Burke LE, Després JP, Gordon-Larsen P, Lavie CJ, et al. Obesity and cardiovascular disease: A scientific statement from the american heart association. *Circulation*. (2021) 143:e984–e1010. doi: 10.1161/CIR.0000000000000973

61. Moon H, Choi JW, Song BW, Kim IK, Lim S, Lee S, et al. Brite adipocyte FGF21 attenuates cardiac ischemia/reperfusion injury in rat hearts by modulating NRF2. *Cells*. (2022) 11:567. doi: 10.3390/cells11030567

62. Zhang X, Jin X, Li Y, Xu M, Yao Y, Liu K, et al. Macrophage-mediated extracellular matrix remodeling after fat grafting in nude mice. *FASEB J*. (2022) 36:e22550. doi: 10.1096/fj.202200037R

frontiers | Frontiers in Immunology

TYPE Original Research
PUBLISHED 22 April 2024
DOI 10.3389/fimmu.2024.1344098

OPEN ACCESS

EDITED BY
Mirza S. Baig,
Indian Institute of Technology Indore, India

REVIEWED BY
Vicente Escamilla-Rivera,
University of Arizona, United States
Manlin Qi,
Jilin University, China
Lin Wang,
Peking University, China

*CORRESPONDENCE
Jie Liu
18661801995@163.com
Xue Li
lixue@qdu.edu.cn

RECEIVED 25 November 2023
ACCEPTED 25 March 2024
PUBLISHED 22 April 2024

CITATION
Li Y, Xia X, Niu Z, Wang K, Liu J and Li X (2024) $_{h}CeO_2$@ $Cu_{5.4}O$ nanoparticle alleviates inflammatory responses by regulating the CTSB–NLRP3 signaling pathway. *Front. Immunol.* 15:1344098. doi: 10.3389/fimmu.2024.1344098

$_{h}CeO_2$@ $Cu_{5.4}O$ nanoparticle alleviates inflammatory responses by regulating the CTSB–NLRP3 signaling pathway

Ying Li[1,2], Xiaomin Xia[1,2], Zhaojun Niu[1,2], Ke Wang[1,2], Jie Liu[1,2]* and Xue Li[1,2]*

[1]Department of Stomatology, The Affiliated Hospital of Qingdao University, Qingdao University, Qingdao, China, [2]School of Stomatology, Qingdao University, Qingdao, China

Inflammatory responses, especially chronic inflammation, are closely associated with many systemic diseases. There are many ways to treat and alleviate inflammation, but how to solve this problem at the molecular level has always been a hot topic in research. The use of nanoparticles (NPs) as anti-inflammatory agents is a potential treatment method. We synthesized new hollow cerium oxide nanomaterials ($_{h}CeO_2$ NPs) doped with different concentrations of $Cu_{5.4}O$ NPs [the molar ratio of Cu/(Ce + Cu) was 50%, 67%, and 83%, respectively], characterized their surface morphology and physicochemical properties, and screened the safe concentration of $_{h}CeO_2$@$Cu_{5.4}O$ using the CCK8 method. Macrophages were cultured, and *P.g*-lipopolysaccharide-stimulated was used as a model of inflammation and co-cultured with $_{h}CeO_2$@$Cu_{5.4}O$ NPs. We then observe the effect of the transcription levels of CTSB, NLRP3, caspase-1, ASC, IL-18, and IL-1β by PCR and detect its effect on the expression level of CTSB protein by Western blot. The levels of IL-18 and IL-1β in the cell supernatant were measured by enzyme-linked immunosorbent assay. Our results indicated that $_{h}CeO_2$@$Cu_{5.4}O$ NPs could reduce the production of reactive oxygen species and inhibit CTSB and NLRP3 to alleviate the damage caused by the inflammatory response to cells. More importantly, $_{h}CeO_2$@$Cu_{5.4}O$ NPs showed stronger anti-inflammatory effects as $Cu_{5.4}O$ NP doping increased. Therefore, the development of the novel nanomaterial $_{h}CeO_2$@$Cu_{5.4}O$ NPs provides a possible new approach for the treatment of inflammatory diseases.

KEYWORDS

cerium oxide nanoparticles, copper-based nanoparticles, CTSB, NLRP3, anti-inflammation

1 Introduction

Inflammation is the immune response that occurs when biological tissues are stimulated, which can be caused by infection or tissue damage. Inflammation can clear pathogens and promote tissue healing (1). However, the inflammatory response is sometimes the main cause of tissue damage—for example, if the stimulating factor persists and the inflammation does not subside, the infiltration of various inflammatory cells and the accumulation of inflammatory factors could alter the structure and function of normal tissues (2). Many studies have shown that inflammation is associated with many systemic diseases such as atherosclerosis (3), cancer (4), and diabetes (5). The complexity and unpredictability of inflammation make the treatment of inflammatory diseases a major challenge.

In recent years, nanotechnology has been developing rapidly, and nanoparticles are widely used in various fields, including in the monitoring and treatment of inflammatory diseases. There have been many reports in the literature that nanoparticles have anti-inflammatory properties and that they have better cell penetration than conventional drugs, resulting in better efficacy and durability in therapy (6–9). Therefore, nanomaterial-based drugs or drug carriers are proved to be a potential candidate for modulating inflammation (10–12).

There are increasing reports on the ability of nano-enzymes to treat different inflammatory diseases. It is worth mentioning that due to their unique valence state structure, cerium oxide nanoparticles (CeO_2 NPs) have been found to possess various enzyme mimetic activities, thereby scavenging reactive oxygen species (ROS), including superoxide dismutase (SOD), catalase (CAT), oxidase-like activities, etc. (13) Cerium is a class of rare earth elements in the oxides of which trivalent (Ce^{3+}) and tetravalent (Ce^{4+}) states coexist. Due to this property, many studies have been conducted to evaluate the efficacy of CeO_2 NPs in various inflammatory disease—for example, CeO_2 NPs alleviated hypoxia-induced oxidative stress and inflammation in the lungs of mice (14). In another study, CeO_2 NPs ameliorated inflammation in a model of periodontitis by reducing ROS production and inhibiting MAPK- NF-κB signaling (15).

$Cu_{5.4}O$ NPs is a new type of nano-enzymes synthesized in recent years. The ratio of Cu NPs to Cu_2O NPs is 3.4 by controlling the temperature and the ratio of materials required for the synthesis, so it is named as $Cu_{5.4}O$ NPs. It has attracted attention because of its highly efficient catalytic performance and ultra-small particle size (16, 17). Copper, one of the essential trace elements for human growth and development, plays a key role in many cellular physiological processes (18). Cu NPs have excellent catalytic properties and can scavenge H_2O_2 and $O_2^{\bullet-}$ but not •OH, whereas Cu_2O NPs can react with both H_2O_2 and •OH. Therefore, it is speculated that $Cu_{5.4}O$ may have spectroscopic mimetic enzyme catalytic properties and antioxidant activity, which has been confirmed in previous studies: $Cu_{5.4}O$ NPs have a high scavenging efficiency against H_2O_2 (80%), $O_2^{\bullet-}$ (50%), and •OH (80%) at a lower concentration (150–200 ng/mL) (16). Therefore, both CeO_2 NPs and $Cu_{5.4}O$ NPs can be used as potential anti-inflammatory agents.

Pyroptosis is a recently discovered new type of programmed cell death that has the dual effect of protecting cells from endogenous and exogenous dangers and causing pathological inflammation (19). The classical activation pathway of pyroptosis is triggered by NLRP3 inflammasome. When it is stimulated by pathogen-associated molecular patterns or danger-associated molecular patterns, it could activate caspase-1, which could cause the release of proinflammatory factors such as IL-18 and IL-1β. Much of the literature suggested that the NLRP3 inflammasome is associated with various inflammatory diseases—for example, it is well known that LDL is a key factor in the formation of atherosclerosis, and it has been shown that phagocytosis of LDL induces the secretion of IL-1β through the activation of the NLRP3 inflammasome, which plays an important role in the development of atherosclerosis (20). Cathepsin B (CTSB) is a class of cysteine protein hydrolases found in lysosomes that primarily function as protein degraders and are involved in apoptosis (21). Recently, it has been found that CTSB is also involved in the pathological processes of many inflammatory diseases—for example, CTSB was significantly upregulated in coxsackievirus B3-induced myocarditis tissues, and CTSB knockout mice exhibited less inflammatory cell infiltration (22). It has also been found that CTSB expression was higher in the intestinal macrophages of mice with inflammatory bowel disease than in normal controls, and when CSTB was inhibited, only mild inflammation was shown in tissue sections (23).

In summary, CeO_2 NPs and $Cu_{5.4}O$ NPs as nano-enzymes all have excellent antioxidant properties; they eliminate ROS in the inflammatory region and can be used as potential anti-inflammatory agents. In the study of the mechanism of inflammatory diseases, both CTSB and NLRP3 inflammasome have a promoting effect on inflammation. Therefore, we constructed a new nano-system, hollow cerium dioxide loaded with copper oxide ($_hCeO_2@Cu_{5.4}O$ NPs), and investigated whether its anti-inflammatory effects on macrophages could be mediated through the CTSB–NLRP3 signaling pathway (Scheme 1). The specific experiments include the following: (1) development of novel $_hCeO_2$ doped with different Cu/(Ce + Cu) molar ratios of 50%, 67%, and 83% and characterization of their physical and chemical properties using transmission electron microscopy (TEM), X-ray diffraction (XRD), and X-ray photoelectron spectroscopy (XPS). Determination of enzyme mimetic activity using antioxidant kit; (2) evaluation of the biosafety of $_hCeO_2@Cu_{5.4}O$ NPs by CCK8, live and dead cell staining, and hemolysis assay; and (3) evaluation of the inhibitory effect of $_hCeO_2@Cu_{5.4}O$ NPs on the secretion of inflammatory factors and its effect on the CTSB–NLRP3 pathway by RT-qPCR and Western blot methods. The experimental results showed that $_hCeO_2@Cu_{5.4}O$ NPs have good biocompatibility and broad-spectrum enzyme mimetic activity and are able to inhibit the CTSB–NLRP3 signal pathway in multiple ways. Therefore, this study could provide a feasible approach for the treatment of inflammatory diseases.

10.3389/fimmu.2024.1344098

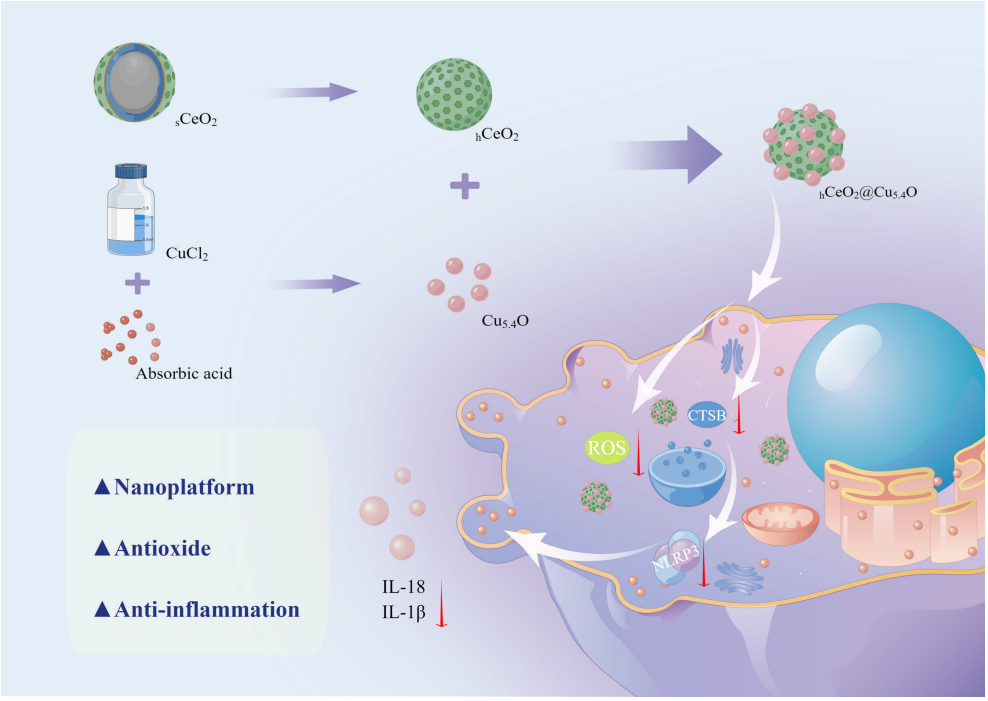

SCHEME 1
Schematic diagram of the synthesis process of $_hCeO_2$@$Cu_{5.4}O$ NPs and the mechanism of its anti-inflammatory effect. (By Figdraw).

2 Materials and methods

2.1 Materials and reagents

Polyvinylpyrrolidone (PVP) was purchased from Ourchem (Shanghai, China). Tetraethoxysilane (TEOS) and cerium (III) nitrate hexahydrate [$Ce(NO_3)_3{\cdot}6H_2O$] were obtained from Macklin (Shanghai, China). Hexamethylenetetramine (HMTA), sodium hydroxide (NaOH), and copper (II) chloride dihydrate ($CuCl_2{\cdot}2H_2O$) were purchased from Hushi (Shanghai, China). L-Ascorbic acid was purchased from Amethyst (Beijing, China). Cell Counting Kit-8 and CA-074Me were obtained from Dalian Meilun. AM/PI Double Staining Kit was purchased from Beyotime Biotechnology (Shanghai, China). ABclonal (Wuhan, China) supplied ABScript III RT Master Mix and SYBR Green Fast qPCR Mix. CathepsinB Rabbit mAb was purchased from Cell Signaling Technology (Boston, MA, USA). Beta-actin polyclonal antibody and goat anti-rabbit IgG were purchased from Elabscience Biotechnology Co., Ltd. (Wuhan, China). Reagent-grade water was obtained from ultra-pure water system (Ulupure, Chengdu, China) in all experiments. All other reagents were of analytical grade without further purification.

2.1.1 Preparation of hollow CeO2 ($_hCeO2$) NPs

The synthesis of hollow CeO_2 ($_hCeO_2$) NPs was referred to a previous literature (24). In brief, 30 mL of absolute ethanol, 5 mL of 4 mol/L ammonia solution, and 4 mL of deionized water were put into an oil bath and mixed. When the above-mentioned solution was heated to 60°C, the mixture of 5 mL TEOS and 20 mL of absolute ethanol was slowly dripped into the mixture. The mixture was stirred at 60°C for 4 h. After cooling to room temperature, the mixture was washed three times with ethanol and dried under vacuum at 60°C to obtain silica (SiO_2) NPs.

Then, 0.1 g silica and 1 g PVP were added to 40 mL of deionized water. When the oil bath was heated to 75°C, 5 mL of 0.5 mmol cerium nitrate and 5 mL of 0.5 mmol HMTA were added in turn. The mixture was stirred at 95°C for 2 h, washed and centrifuged three times after cooling, and dried to obtain SiO_2@CeO_2 core–shell ($_sCeO_2$) NP precursors.

The $_sCeO_2$ NP precursors were heated to 600°C at 5°C/min for 2 h, and then heating was naturally dropped to room temperature to obtain $_sCeO_2$ NPs.

Next, 0.1 g $_sCeO_2$NPs was dispersed in 40 mL of 2 mol/L sodium hydroxide and stirred for 24 h, centrifuged, washed three times with ethanol, and dried to obtain $_hCeO_2$ NPs.

2.1.2 Preparation of $Cu_{5.4}O$ NP solution

The synthesis of $Cu_{5.4}O$ NPs was modified a little based on the previous literature (16). In detail, 10 mM $CuCl_2{\cdot}2H_2O$ was dissolved in 50 mL deionized water and stirred at 80°C in an oil bath for 10 min, and then 50 mL of 100 mM L-Ascorbic acid was added slowly to the above-mentioned solution. When the temperature of the solution is reduced to normal temperature, adjust the pH of the solution to 8 to 9 with 1 M NaOH solution and then stir for 12 h at 80°C. The large aggregates are then removed by centrifugation to obtain $Cu_{5.4}O$ NPs.

2.1.3 Preparation of $_hCeO_2$@$Cu_{5.4}O$ NPs

Different masses of $_hCeO_2$ NPs were weighed and added to $Cu_{5.4}O$ NPs solution so that the molar ratio of Ce/Cu is 0.2:1, 0.5:1, and 1:1, respectively. They were referred to as $_hCeO_2$@83%$Cu_{5.4}O$, $_hCeO_2$@67%$Cu_{5.4}O$, and $_hCeO_2$@50%$Cu_{5.4}O$. After stirring for 24 h, the precipitate obtained after centrifugation and drying is $_hCeO_2$@$Cu_{5.4}O$ NPs. Nanoparticles were obtained after washing three times using ethanol to remove impurities and then drying.

2.2 Dispersion and sterilization of nanoparticles

A total of 1 mg nanoparticles was weighed and exposed to UV light for 30 min, then dispersed in 10 mL of complete medium containing 10% FBS, stirred for 1 h at room temperature, and then diluted and stirred for another 24 h for subsequent experiments. The content of endotoxin in all dispersions was less than 0.5 EU/mL ($_hCeO_2$@83%$Cu_{5.4}O$ NPs: 0.453 EU/mL, $_hCeO_2$@67%$Cu_{5.4}O$ NPs: 0.444 EU/mL, and $_hCeO_2$@50%$Cu_{5.4}O$ NPs: 0.463 EU/mL) using the Chromogenic LAL Endotoxin Assay Kit (Beyotime, Shanghai). Dynamic light scattering (DLS) was carried out in suspensions using the zeta potentiometer (Zetasizer Nano ZS, England). The hydrated particle size and zeta potential of the nanoparticles were then calculated.

2.3 Characterization

The surface morphology of the nanoparticles was observed using transmission electron microscopy (HT7700, Japan), and particle size analysis of electron microscopy images of $Cu_{5.4}O$ NPs was performed using ImageJ. Elemental analysis of nanomaterials was carried out by X-ray diffraction (Xtalab Synergy, Netherlands) and comparison with standard mapping.

Analysis of the surface chemical composition and elemental valence of nanomaterials were determined by X-ray photoelectron spectroscopy (Smart Lab 3KW, Japan).

2.4 SOD, CAT, and T-AOC enzyme mimic activity

To evaluate the antioxidant properties of $_hCeO_2$@$Cu_{5.4}O$ NPs, we measured its superoxide dismutase (SOD), catalase (CAT), and total antioxidant (T-AOC) capacity using an enzyme calibrator (Elx800, Bio Tek, United States). The SOD, CAT, and T-AOC enzyme mimic activities of $_hCeO_2$@$Cu_{5.4}O$ NPs were measured by using SOD assay kit (Solebo, China), CAT assay kit (Solebo, China), and T-AOC assay kit (Solebo, China), respectively.

SOD is an enzyme found widely in plants, animals, and cells and catalyzes the disproportionation of superoxide anions to produce H_2O_2 and O_2. The superoxide anion produced during metabolism reduces azotetrazolium to methyl salts, and SOD scavenges the superoxide anion, thereby reducing the formation of methyl salts and thus affecting its absorbance at 560 nm. The reagents were mixed thoroughly according to the instructions and divided into test group, control group, and two blank groups. A total of 18 µL 10 mg/L $_hCeO_2$@$Cu_{5.4}O$ NPs was added to the test group and the control group, and after 30 min of immersion in 37°C water bath, the absorbance value was measured at 560 nm, which was recorded as A test, A control, A blank 1, and A blank 2, respectively. The inhibition rate and SOD activity were calculated from the above-mentioned values.

CAT is an enzyme that mainly scavenges H_2O_2, and the absorbance value at 240 nm of the reaction solution changes when H_2O_2 is decomposed, thus calculating the CAT activity. Specifically, the CAT detection working solution was bathed at 37°C for 10 min, and 1 mL of the above-mentioned liquid was added to 35 µL of 10 mg/L $_hCeO_2$@$Cu_{5.4}O$ NPs. After mixing, the absorbance value at 240 nm was measured immediately, and then the absorbance value after 1 min was measured, and the CAT activity was calculated according to the absorbance value.

The total antioxidant level of the nanoparticles was determined. The total antioxidant capacity of the samples was calculated by measuring the amount of Fe^{3+}-TPTZ reduced to Fe^{2+}-TPTZ in an acidic environment. Furthermore, 6 µL 10 mg/L $_hCeO_2$@$Cu_{5.4}O$ NPs was mixed with 180 µL working solution and 18 µL distilled water, and the 593-nm absorbance value was measured after reacting at room temperature for 10 min. The 593-nm absorbance value was measured after the working solution without nanoparticles was mixed with distilled water for 10 min and substituted into the formula to determine the total antioxidant capacity.

2.5 Determination of intracellular ROS

The ROS assay kit (Beyotime, Shanghai) was used to measure the ROS in cells treated with lipopolysaccharide (LPS) and nanoparticles. In short, RAW 264.7 cells were seeded into six-well plates at 3×10^4 cells per well and divided into six groups: the first group was the blank control group. The second group was treated with *P.g*-LPS (1 µg/mL) for 3 h to establish an *in vitro* inflammation model. The third group was pretreated with cathepsin B inhibitor (CA-074Me) for 2 h and then treated with LPS for 3 h as a positive control group. Four to six groups were treated with *P.g*-LPS followed by the addition of safe concentrations (10 mg/L) of the three groups of drugs for 24 h. The medium containing nanoparticles was then replaced with serum-free medium supplemented with 10 uM DCFH-DA and incubated at 37°C for 30 min. The cells were washed three times with serum-free medium and placed under an inverted fluorescence microscope for observation.

2.6 Cell culture

Mouse leukemia cells of monocyte macrophage (RAW264.7) were purchased from American Type Culture Collection (ATCC, Manassas, VA, USA) and cultured in Dulbecco's modified Eagle's medium (DMEM) with 10% fetal bovine serum (FBS). The L929 cell line was purchased from ScienCell (SanDiego, CA, USA) and

cultured in DMEM with 10% FBS, 10,000 U/mL penicillin, and 10 mg/mL streptomycin. All cell lines were cultured at 37°C in an incubator with 5% CO_2. The cells were passaged when the cell density reached 80%–90%.

2.7 Cytotoxicity assay

2.7.1 Cytocompatibility test

The cytotoxicity of the nanoparticles was evaluated by using Cell Counting Kit-8 (Shanghai St Er), and the safe concentration was screened for subsequent experiments. L929 cells were seeded into 96-well plates at 5×10^3 cells per well. After cell adhesion, different concentrations (10, 20, 30, 40, and 50 mg/L) of nanoparticles were added to the culture for 24, 48, and 72 h. The medium-containing nanoparticles were removed and washed three times with PBS. Then, 10% CCK8 reagent was added, and the cells were incubated in an incubator at 37°C for 0.5–3 h in the dark. The absorbance at 450 nm was then determined using a microplate reader (Bio-Tek, Winooski, VT, USA). Five parallel wells were set up for each group, and the experiment was repeated three times.

After treatment of the nanoparticles, the cells were washed three times with PBS and incubated with calcian-AM and PI for 30 min before being observed under a fluorescence inverted microscope.

2.7.2 Hemolysis test

For the hemolysis assay, fresh blood was collected from mice and added with anticoagulant and saline to test the hemolytic potential of nanoparticles. Blood diluted with distilled water was used as a positive control, and blood diluted with saline was used as a negative control. The cells were incubated at 37°C for 4 h and centrifuged at 2,500 RPM for 10 min, the supernatant was removed, and the absorbance at 545 nm was recorded using a microplate reader. Hemolysis rates were calculated according to the following formula:

$$\text{Hemolysis rate} = (OD_{exper} - OD_{negative})/(OD_{positive} - OD_{negative})$$

where OD_{exper}, $OD_{negative}$, and $OD_{positive}$ represent the measured absorbance of the nanoparticle sample, negative control, and positive control, respectively.

2.7.3 Cytocompatibility test with LPS and $_hCeO_2$@$Cu_{5.4}O$ co-treatment

To assess the toxicity of the combined treatment with LPS and nanoparticles (10 mg/L), CCK8 was used to evaluate the cytotoxicity. RAW cells were seeded into 96-well plates at a density of 5×10^3 cells per well. After cell adhesion, LPS was added to treat the cells for 3 h, and then the cells were treated with the medium containing 10 mg/L nanoparticles for 24/48/72 h. After removal of the medium, the cells were washed three times with PBS, and the cells were added with 10% CCK8 reagent and incubated at 37°C in the dark for 0.5–3 h. The absorbance at 450 nm was measured using a microplate reader. To assess the effect of nanoparticles on absorbance at 450 nm, 100 uL of 10 mg/L $_hCeO_2$@83%$Cu_{5.4}O$, $_hCeO_2$@67%$Cu_{5.4}O$, and $_hCeO_2$@50%$Cu_{5.4}O$ was added to a 96-well plate. CCK8 reagent was added to a concentration of 10% and incubated at 37°C in the dark for 0.5–3 hours. The absorbance at 450 nm was measured using a microplate reader. Five parallel wells were set up for each group, and the experiment was repeated three times.

2.8 Uptake and intracellular localization of $_hCeO_2$@$Cu_{5.4}O$ NPs

After 24 h of treatment with $_hCeO_2$@$Cu_{5.4}O$ NPs, RAW264.7 cells were washed three times with PBS, and cell precipitates were collected. These were fixed with 2.5% glutaraldehyde at 4°C for 24 h, washed three times with PBS, and then fixed with 1% osmic acid for 1 to 2 h. Finally, the samples were dehydrated with gradient concentrations of ethanol and propanol and were treated overnight with an embedded agent. The sections were then double-stained with lead citrate–uranyl acetate, and the slices were imaged using Hitachi HT-7800.

2.9 Real-time PCR

Cells were grouped and treated as in Section 2.5. Then, the expressions of NLRP3 pathway-relative factors, TNF-α and TGF-β, were measured using quantitative real-time PCR. We also determined gene expression in cells treated with LPS and nanoparticles for 12 h as well as nanoparticles alone for 24 h.

The total RNA of RAW264.7 was extracted by using RNA-Easy (Vazyme). RNA was reverse-transcribed into cDNA using a reverse transcription kit (ABScript III RT Master Mix for qPCR with gDNA Remover, ABclomal). RT-qPCR was performed using Universal

TABLE 1 Primer sequences used in this study.

Gene	Forward sequence (5′ to 3′)	Reverse sequence (5′ to 3′)
β-Actin	CATCCGTAAAGACCTCTA GCCAAC	ATGGAGCCACCGATCCACA
IL-1β	TCCAGGATGAGGACATGA GCAC	GAACGTCACACACCAGCAG GTTA
IL-18	TGGCTGCCATGTCAGAA GACT	CCAGGTCTCCATTTTCTTC AGGT
CTSB	CTTCCCATGTCGGCAAT CAG	GTGTAGTTGAGACCGGT GGA
NLRP3	CCTGACCCAAACCCACC AGT	TTCTTTCGGATGAGGCTGC TTA
ASC	AGAGACATGGGCTTACAG GAGC	CCACAAAGTGTCCTGTTCT GGC
Caspase-1	TGCCGTGGAGAGAAACAA GGA	TGGTGTTGAAGAGCAGAAA GCA
TNF-α	ACTCCAGGCGGTGCCTA TGT	GTGAGGGTCTGGGCCATA GAA
TGF-β	CTTCAGCCTCCACAGAGAA GAACT	TGTGTCCAGGCTCCAAAT ATAG

SYBR Green Mix (ABclomal), cDNA, and primers under the following conditions: 95°C for 5 s and 60°C for 30 s with 40 cycles. β-Actin was an internal control of genes. Data results were analyzed with $2^{-\Delta\Delta Ct}$. The primer sequences were as shown in Table 1.

2.10 Western blot assay

The cells were grouped and treated as in Section 2.5. After 24 h of treatment with nanoparticles, total proteins were extracted using RIPA buffer (Elabscience Biotechnology Co., Ltd.). The proteins were separated using 10% gel (Epizyme, shanghai) and then transferred to PVDF membranes (Solarbio, Beijing). After blocking with fast blocking western (Solarbio, Beijing) for 10 min at room temperature, PVDF membranes were incubated with primary antibodies (CST, 1:1,000) overnight at 4°C. β-Actin (Elabscience, 1:1,000) was used as an internal reference. The membranes were then incubated with the secondary antibody HRP goat anti-rabbit IgG (Elabscience, 1:5,000) for 1 h. Finally, each group of proteins was detected using electrochemiluminescent ECL reagents. The protein bands were quantified using Image software.

2.11 Immunofluorescence

RAW264.7 was seeded on the coverslips of a 24-well plate at a density of 5×10^4 cells per well, treated as described above, washed three times with PBS, and then post-fixed with 4% paraformaldehyde (Elabscience, Wuhan) for 15 min, followed by permeabilization with 0.2% Triton X-100 for 15 min and blocking with 10% blocking serum (Solarbio, Beijing) for 60 min. Anti-CTSB primary antibody (CST, 1:500) was applied to the cells and left overnight at 4°C. The cells were then treated in the dark with secondary antibody FITC conjugated goat anti-rabbit IgG (Elabscience, 1:100) for 1 h. Finally, DAPI staining solution (Solarbio, Beijing) was added for 10 min at room temperature. Subsequently, the DAPI staining solution was removed, and the cells were washed with PBS, blocked, and observed using an inverted fluorescent microscope.

2.12 Enzyme-linked immunosorbent assay

After completion of the cell treatment, the cell supernatant fluid was collected. IL-18 and IL-1β content, respectively, in cell supernatant fluid were determined using an enzyme-linked immunosorbent assay (ELISA) kit (Reed Biotech, Wuhan) according to the manufacturer's instructions.

2.13 Statistical analysis

All experiments were repeated three times, and data were analyzed using one-way ANOVA and Tukey's multiple-comparison test in GraphPad software, with a single asterisk indicating significant differences between data ($p< 0.05$) and two and more asterisks indicating a strong difference between data ($p< 0.01$). The data in the graphs represent mean ± standard deviation.

3 Results and discussion

3.1 Characterization

From the transmission electron microscopy (TEM) images and particle size analysis (Figures 1A, B), it can be seen that the synthesized $Cu_{5.4}O$ NPs were homogeneously dispersed and morphologically uniform in solution, mostly between 3 and 5 nm in diameter. As shown in Figures 1C, D, the oxidation state of copper was studied by X-ray diffraction (XRD) pattern and X-ray photoelectron spectroscopy (XPS). The dominant peaks $2\theta = 43.3°$, 50.4°, and 74.2° correspond to (111), (200), and (220) in the copper lattice structure, and the other peaks 2θ = 29.6°, 36.4°, 42.3°, and 61.3° correspond to (110) (111), (200), and (220) in the copper oxide lattice structure, respectively. The XPS spectrum of the $Cu_{5.4}O$ NPs in Figure 1D also suggested that $Cu_{5.4}O$ NP was a mixture of Cu NPs and Cu_2O NPs, and the ratio of Cu to Cu_2O can be calculated to be approximately 3.4 based on the peak area and mass fraction of both. All of the above-mentioned data were consistent with previous reports in the literature (16, 24).

The TEM images of $_hCeO_2$ and $_hCeO_2$@$Cu_{5.4}O$ NPs are shown in Figures 2A–D. In Figure 2A, it can be seen that $_hCeO_2$ has an obvious hollow structure and a rough surface with a diameter of approximately 80–100 nm. Figures 2B–D were $_hCeO_2$@83%$Cu_{5.4}O$ NPs, $_hCeO_2$@67%$Cu_{5.4}O$ NPs, and $_hCeO_2$@50%$Cu_{5.4}O$ NPs, respectively. Figures 2B–D showed that $_hCeO_2$ doped with $Cu_{5.4}O$ NPs does not change the hollow form of $_hCeO_2$, and there were scattered $Cu_{5.4}O$ NPs around $_hCeO_2$. According to DLS data (Figure 2E), the average particle size of $_hCeO_2$@83%$Cu_{5.4}O$ NPs is approximately 140.3 nm, the zeta potential of $_hCeO_2$@83%$Cu_{5.4}O$ NPs, $_hCeO_2$@67%$Cu_{5.4}O$ NPs, and $_hCeO_2$@50%$Cu_{5.4}O$ NPs is -6.08, -6.21, and -5.59 mV, respectively (Figure 2F). The zeta potential is closely related to the stability of the dispersion. In general, the greater the absolute value of the zeta potential, the better the stability of the dispersion (25). As shown in Figure 2G, the XRD test of the synthesized $_hCeO_2$ NPs was consistent with the typical cerium spectra (JSPDS-34-0394), confirming its cubic fluorite structure. It is noteworthy that the XRD tests of three other samples doped with different proportions of $Cu_{5.4}O$ NPs were also consistent with $_hCeO_2$ NPs, which indicated that $Cu_{5.4}O$ NPs was in a highly dispersed or doped state into the $_hCeO_2$ NPs lattice or the yield of $Cu_{5.4}O$ NPs in the mixed product of both is relatively low. As shown in Figure 2H, the elemental valence states of $_hCeO_2$ NPs were analyzed, and the peaks at 885.0 and 903.5 eV in the XPS test belong to Ce^{3+}, the peaks at 882.1, 888.1, 898.5, 900.9, 906.4, and 916.4 eV were in Ce^{4+}, and the coexistence of the two indicates that it has peroxidase-mimicking activity and superoxide dismutase mimetic activity potential. In addition, after quantitative calculations, the percentage of Ce^{3+} in $_hCeO_2$ was 27.64%, and the percentages of Ce^{3+} in $_hCeO_2$@50%$Cu_{5.4}O$ NPs, $_hCeO_2$@67%

10.3389/fimmu.2024.1344098

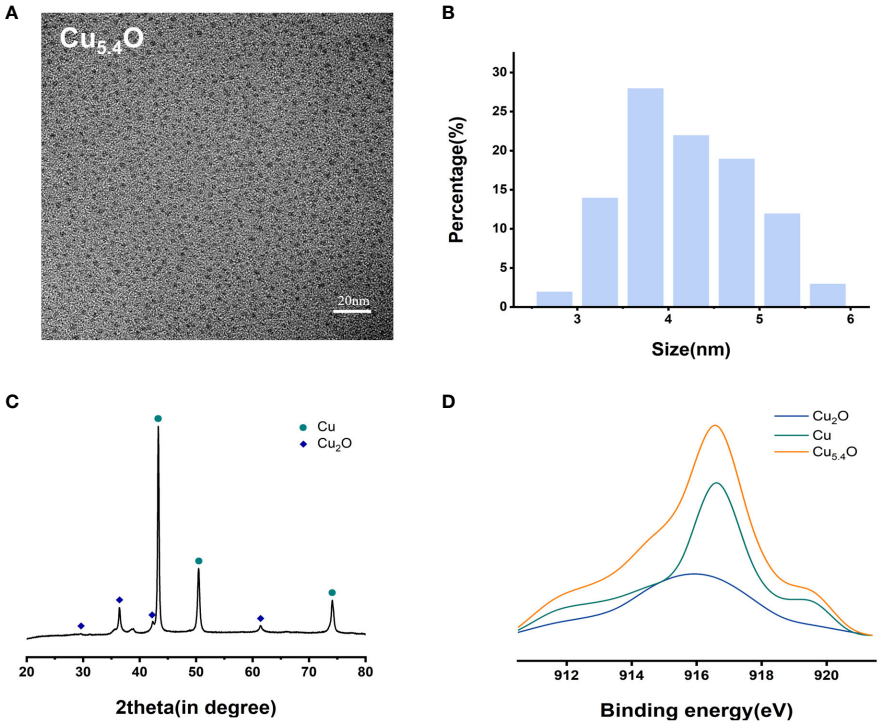

FIGURE 1
Characterization of $Cu_{5.4}O$ nanoparticles. **(A)** TEM images. **(B)** Particle size distribution. **(C)** XRD analysis. **(D)** XAES spectra.

$Cu_{5.4}O$ NPs, and $_hCeO_2$@83%$Cu_{5.4}O$ NPs were 31.68%, 35.17%, and 36.95%, respectively. The content of Ce^{3+} showed an increasing tendency with the increase of $Cu_{5.4}O$ NP incorporation.

ROS play an important role in the development of inflammation by inducing oxidative stress. It has been documented that ROS activates NF-κB signaling and NF-κB, as an upstream signaling molecule, stimulates histone TB release and NLRP3 inflammasome activation and promotes the aggregation of inflammatory cells and the expression of inflammatory factors (26, 27). Therefore, scavenging ROS is crucial for inflammatory diseases, and nanomaterials with enzyme-mimicking activity have excelled in the field of scavenging ROS in recent years. Therefore, various enzymatic activities and total antioxidant properties of the nanoparticles were further investigated.

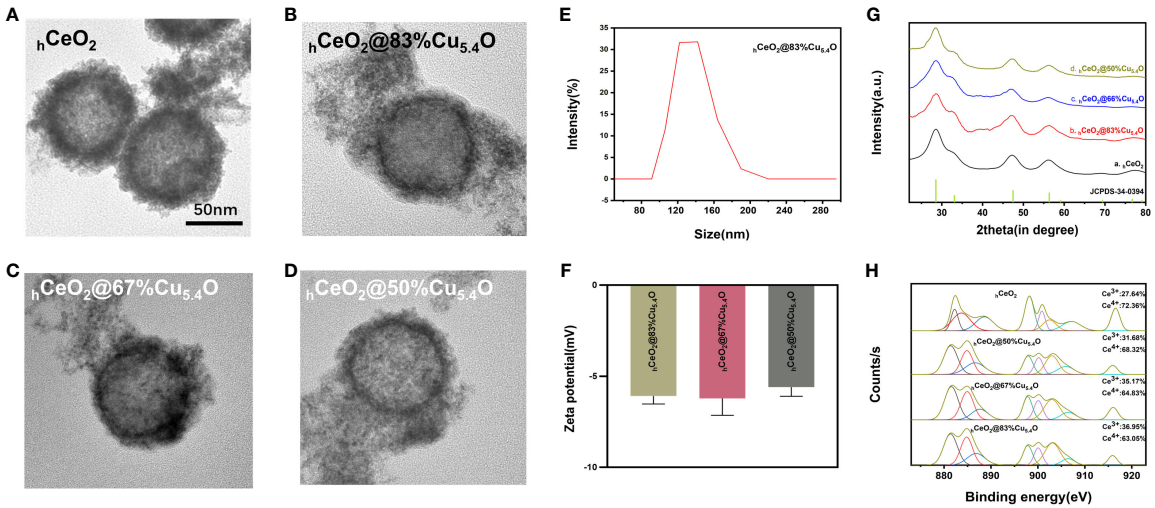

FIGURE 2
Characterization of $_hCeO_2$ and $_hCeO_2$@$Cu_{5.4}O$ nanoparticles (NPs). **(A)** TEM image of $_hCeO_2$ NPs. **(B)** TEM image of $_hCeO_2$@83%$Cu_{5.4}O$ NPs. **(C)** TEM image of $_hCeO_2$@67%$Cu_{5.4}O$ NPs. **(D)** TEM image of $_hCeO_2$@50%$Cu_{5.4}O$ NPs. **(E)** Particle size distribution of $_hCeO_2$@83%$Cu_{5.4}O$ NPs. **(F)** Zeta potential analysis of $_hCeO_2$@$Cu_{5.4}O$ NPs. **(G)** XRD analysis of $_hCeO_2$@$Cu_{5.4}O$ NPs. **(H)** XPS analysis of $_hCeO_2$@$Cu_{5.4}O$ NPs.

CeO_2 NPs have attracted much attention as a nano-enzyme, which has good biocompatibility and a variety of enzyme mimetic activities (28). The antioxidation property of CeO_2 NPs is mainly related to the coexistence of two valence states (Ce^{3+}/Ce^{4+}) on cerium surface and mainly depends on the proportion of valence states (29). Superoxide dismutase (SOD), an enzyme capable of scavenging superoxide anion, is considered as a ROS detoxification enzyme because it can convert superoxide anion to H_2O_2 with low oxidation efficiency (30). The SOD enzymatic pseudo-activity of CeO_2 NPs is achieved by the valence state conversion of Ce^{3+} (reduced state) and Ce^{4+} (oxidized state). The superoxide anion oxidizes Ce^{3+} to Ce^{4+}, and the superoxide anion is reduced to H_2O_2. CAT enzyme mimetic activity is accomplished by the reaction of Ce^{4+} with H_2O_2 and its decomposition to H_2O and O_2, which protects cells from H_2O_2 damage while Ce^{4+} is converted to Ce^{3+} (31). This ability to switch between two oxidation states, Ce^{3+} and Ce^{4+}, endows CeO_2 NPs with regenerative properties.

There have been many studies utilizing Ce^{3+}/Ce^{4+} interconversion on the surface of CeO_2 NPs to scavenge ROS for the treatment of arthritis and inflammatory bowel disease (32–34). It has been suggested that the mechanism of CeO_2 NP antioxidant is related to the presence of Ce^{3+}, which makes the oxygen vacancies come out (35). It was reported that as the particle size of CeO_2 NPs decreases, the Ce^{3+} on its surface gradually increases and its antioxidant effect is enhanced (35). Another research found that cerium dioxide nanocubes (0.17 μg/mL) containing a higher amount of Ce^{3+} (63%) were more effective in the ROS scavenging efficiency in HUVEC than that of CeO_2 NPs (2.0 μg/mL) with a lower percentage of Ce^{3+} (49%) than on the surface (36). Thus, the higher the Ce^{3+}/Ce^{4+} on the CeO_2 NP surface, the higher the concentration of defects and oxygen vacancies in the lattice with higher superoxide dismutase mimetic activity, and the better it is able to cope with oxidative stress and inflammatory diseases. As shown in Figure 2H, the doping of $Cu_{5.4}O$ NPs increased the Ce^{3+} content of $_hCeO_2$@$Cu_{5.4}O$ NPs. When the Cu/(Ce+Cu) molar ratio was 83%, the Ce^{3+} content of $_hCeO_2$@$Cu_{5.4}O$ NPs was 36.95%, which was an increase of 9.31% compared with that of $_hCeO_2$ NPs, which was more favorable for the scavenging of ROS, leading to better treatment of inflammatory diseases.

Cu, as a trace element in the human body, participates in many enzymatic reactions and brings a large surface area to volume ratio due to its small size, which leads to the appearance of surface effects (37). As for the antioxidant properties of $Cu_{5.4}O$ NPs, a study conducted XPS tests before and after its treatment with H_2O_2 and showed that the two peaks corresponding to Cu^+ and Cu^0, Cu 2p2/3 and Cu2p1/2 were not shifted, and a few new peaks appeared. Therefore, it is speculated that the ROS scavenging performance of Cu is mainly attributed to its inherent multi-enzyme mimetic properties (16). In one study, $Cu_{5.4}O$ NPs were found to protect cells from 250 μM H_2O_2 at a very low concentration (25 ng/mL), and the mRNA levels of antioxidant genes were all significantly increased in the kidneys of $Cu_{5.4}O$ NP-treated mice. The phosphorylation of NF-κB and IκB was significantly reduced. The expression of NF-κB signaling pathway downstream inflammatory factor expression was also decreased, suggesting that $Cu_{5.4}O$ NPs could protect renal tissues from oxidative stress by reducing the production of pro-inflammatory factors (16). It has also been shown that $Cu_{5.4}O$ NPs were combined with hydrogels to investigate their effects on wound healing, and the results indicated that $Cu_{5.4}O$@Hep-PEG inhibited the expression of pro-inflammatory factors, scavenging of ROS, and promoting wound healing. In addition, $Cu_{5.4}O$@Hep-PEG also promoted cellular cell proliferation as well as angiogenesis due to the presence of $Cu_{5.4}O$ NPs (38).

In this study, as shown in Figure 3A, the SOD performance decreases with the reduction of $Cu_{5.4}O$ NP doping, so we speculated that the SOD activity of $Cu_{5.4}O$ NPs plays a major role in the composite particles, Alternatively, when the amount of doped Cu is less, the less Ce^{4+} is reduced to Ce^{3+}. In Figures 3B, C, the three groups of different proportions of nanoparticles showed great CAT and total antioxidant properties, with the best CAT and total antioxidant properties at a molar ratio of (Cu/Ce+Cu) of 67%. Simple $_hCeO_2$ and $Cu_{5.4}O$ NPs showed good enzymatic activity, and Cu^+ was easy to react with Ce^{4+} to generate Ce^{3+} and Cu^{2+} after $Cu_{5.4}O$ NP doping. From the discussion above, it can be seen that when the ratio of Ce^{3+}/Ce^{4+} is large, CeO_2 NPs showed better SOD mimics activity. Therefore, when the molar ratio of Cu/(Ce+Cu) was 83%, the nanoparticles exhibited the most excellent SOD-mimicking activity, which is more conducive to scavenging ROS, eliminating oxidative stress, and treating inflammatory diseases.

3.2 $_hCeO_2$@$Cu_{5.4}O$ NPs protect RAW264.7 cells from ROS damage

ROS are inevitable by-products of cellular metabolism, including superoxide anion ($O_2^{\bullet-}$), hydroxyl radical ($^{\bullet}OH$), hydrogen peroxide (H_2O_2), etc., but endogenous ROS are extremely susceptible to interact with biomolecules and cause intracellular oxidative stress and DNA damage (39, 40). Oxidative stress, in general, can trigger inflammation, and excessive inflammation can, in turn, cause oxidative stress, inducing damage to cellular and tissue structure and function (41). In addition, it has been shown that ROS promotes the disruption of lysosomal membrane integrity and lysosomal membrane permeabilization (LMP) by initiating phospholipase A2 and activating lysosomal Ca^{2+} channels to allow the leakage of intra-lysosomal enzymes such as CTSB into the cytoplasm (42). Furthermore, ROS activates NF-κB signaling, and NF-κB, as an upstream signaling molecule, stimulates histone TB release and NLRP3 inflammasome activation and promotes the aggregation of inflammatory cells and the expression of inflammatory factors (26, 27). In summary, ROS plays an important role in the development of inflammation by inducing oxidative stress, increasing lysosomal membrane permeability to promote CTSB release, and activating NLRP3 inflammasomes, thereby promoting inflammation. Therefore, scavenging ROS is crucial for inflammatory diseases, and nanomaterials with enzyme-mimicking activity have excelled in the field of scavenging ROS in recent years.

In this study, we determined ROS scavenging due to the antioxidant properties of $_hCeO_2$@$Cu_{5.4}O$. As shown in

10.3389/fimmu.2024.1344098

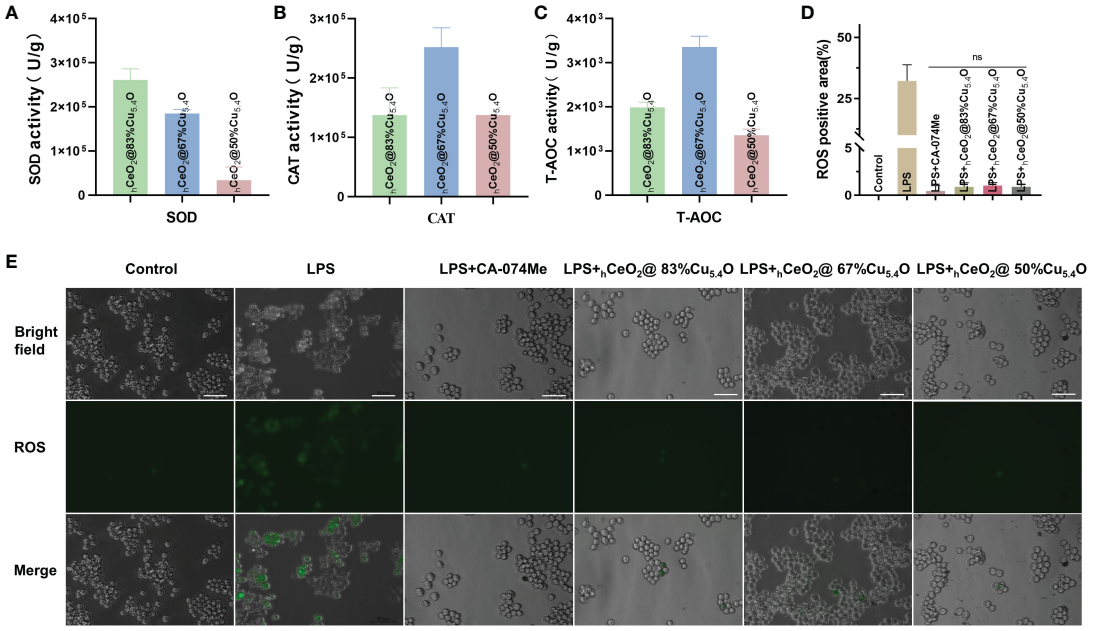

FIGURE 3
Ability of $_{h}CeO_{h}$@Cu5.4O nanoparticles (NPs) to scavenge reactive oxygen species (ROS). **(A)** SOD enzymatic activities of $_{h}CeO_{h}$@Cu5.4O NPs. **(B)** CAT enzymatic activities of $_{h}CeO_{h}$@Cu5.4O NPs. **(C)** T-AOC enzymatic activities of $_{h}CeO_{h}$@Cu5.4ONPs. **(D, E)** Intracellular ROS levels in RAW 264.7 cells treated with lipopolysaccharide (LPS) alone and the combined application of 10 mg/L $_{h}CeO_{h}$@Cu5.4ONPs. Scale bar: 50 mm. (n=3; ns: no significance.)

Figures 3D, E, the ROS levels were confirmed by using inverted fluorescence microscopy, and the results showed that the fluorescence intensity of cells treated with nanoparticles was reduced, and there was no significant statistical difference between the cells treated with the three groups of nanoparticles and the CA-074Me-treated group. We thus demonstrated that nanoparticles are able to scavenge ROS *in vitro*.

3.3 Biosafety assessment

Studies have shown that nanoparticles, especially metal-based nanoparticles, may cause a variety of adverse reactions in cells, such as oxidative stress and cell death (43). As a novel nanomaterial, biosafety evaluation is essential for biomedical applications. Previous studies have shown that hollow cerium dioxide has no significant cytotoxicity at concentrations ranging from 0 to 200 mg/L (24). However, studies on the toxicity of $Cu_{5.4}O$ NPs are limited, with articles stating no significant cytotoxicity at 600 ng/mL (38).

In this experiment, cytocompatibility and blood compatibility were used to analyze the biocompatibility of nanoparticles. In the CCK8 assay, L929 was used to evaluate the cytocompatibility of the nanoparticle. Figures 4A–C were the results of the CCK8 experiment with the molar ratio of (Cu/Ce+Cu) of 83%, 67%, and 50%, respectively. It can be seen that, with the decrease of $Cu_{5.4}O$ NPs, the activity of cells treated with nanoparticles increases gradually, which indicated that the toxicity of nanoparticles was mainly attributed to the doped $Cu_{5.4}O$ NPs. In addition, in each group, the cytotoxicity of 0–50 mg/L nanoparticles was tested. The results showed that all three groups of nanoparticles showed excellent cytocompatibility within 24 h, and no significant difference was observed. However, at 48 and 72 h, significant cytotoxicity was observed when the concentration was higher than 10 mg/L, and the cytotoxicity increased with the increase of the concentration. Similar results were obtained with live or dead staining (Figure 4E). With respect to blood compatibility, the hemolysis results (Figure 4D) showed good blood compatibility of the nanoparticles. In conclusion, our synthesized nanoparticles showed excellent biocompatibility at 10 mg/L, and a safe concentration of 10 mg/L was used for all three proportions of drugs in subsequent experiments.

However, it has been reported that nanoparticles may interfere with the results of conventional toxicity measurement through different mechanisms (44–46), such as the absorption and scattering of light at a certain wavelength by nanoparticles or the reaction with substrates to interfere with the absorbance value. In order to exclude the possible interference of nanoparticles on the assay, firstly, we removed the medium containing nanoparticles and cleaned it with PBS before the assay. Secondly, considering the interference of nanoparticles entering the cells, we tested the effect of nanoparticles on the absorbance value of the CCK8 reagent (Figure 5A). The results showed that there was no difference in absorbance compared with the CCK8 reagent without nanoparticles.

In the subsequent experiments, LPS and $_{h}CeO_{2}$@$Cu_{5.4}O$ NPs were used to treat the RAW 264.7 cells, so we also conducted a toxicity test for LPS and $_{h}CeO_{2}$@$Cu_{5.4}O$ NP co-treatment. The results are shown in Figures 5B–D. The cell viability was increased

10.3389/fimmu.2024.1344098

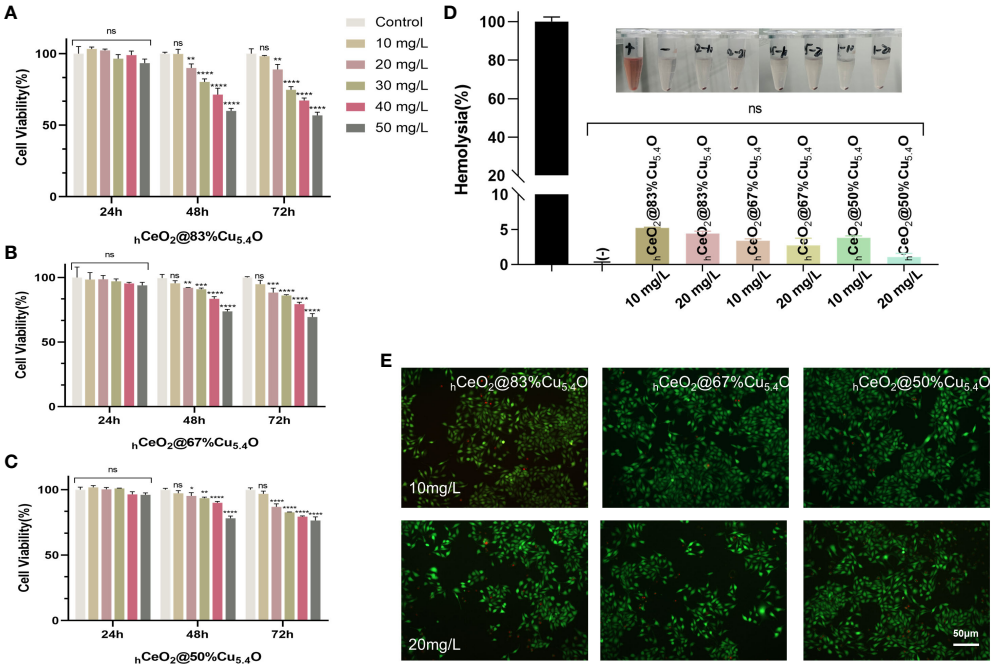

FIGURE 4
Biocompatibility of $_hCeO_2$@$Cu_{5.4}O$ nanoparticles (NPs). **(A–C)** The 24, 48-, and 72-h cytocompatibility of $_hCeO_2$@$Cu_{5.4}O$ NPs with the molar ratio of Cu/(Ce+Cu) was 83%, 67%, and 50%, respectively. **(D)** Blood compatibility of $_hCeO_2$@$Cu_{5.4}O$ NPs. (+) and (-) represent positive and negative controls, respectively. **(E)** Live/dead fluorescence staining images of fibroblasts treated with nanoparticles for 24 and 48 h. Data represent mean ± SD (n = 5; ns: no significance; * represents significant differences. *P< 0.05, **P < 0.005, ***P < 0.0005, ****P < 0.0001).

after 1-ug/mL LPS treatment, which was consistent with the previous literature (47), but there was no significant statistical difference. There was no significant change in cell viability after adding 10 mg/L nanoparticles compared with the LPS group. The toxicity of nanoparticles depends on many factors, including their chemical composition, size, and surface properties. It has been reported that the toxicity of metal nanoparticles is mainly derived from the metal ions released from them, and exceeding a certain concentration of metal ions may increase the production of intracellular ROS and the occurrence of cytotoxicity (48, 49). However, in this study, the nanoparticle concentration of 10 mg/L was not toxic to RAW 264.7 at 24, 48, or 72 h.

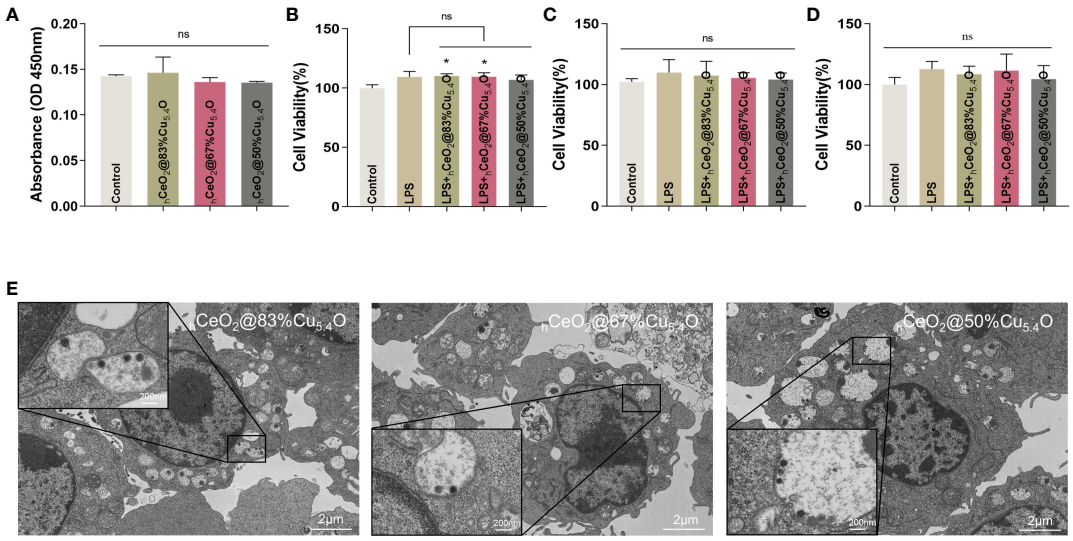

FIGURE 5
Biocompatibility of $_hCeO_2$@$Cu_{5.4}O$ nanoparticles (NPs) treated with lipopolysaccharide (LPS). **(A)** Absorbance values of the culture medium containing $_hCeO_2$@$Cu_{5.4}O$ NPs added with CCK8 reagent at 450 nm. **(B–D)** Cell viability of RAW264.7 cells treated with LPS and $_hCeO_2$@$Cu_{5.4}O$ NPs for 24, 48, and 72 h. **(E)** Bio-TEM images of $_hCeO_2$@$Cu_{5.4}O$ NP cellular uptake. (n=3; ns: no significance; *p<0.05.)

3.4 Uptake of $_{h}CeO_2@Cu_{5.4}O$ NPs in RAW264.7 macrophages

Immune cells are the first barrier for nanoparticles to penetrate into cells (50). It is necessary to study the uptake of nanoparticles by macrophages, which is essential for nanoparticles to exert their effects and potentially induce a toxic response. Studies have reported the presence of nanoparticles in the endosome after a 3-h incubation period with cells, forming relatively large and dense aggregates (50). Furthermore, nanoparticles were detectable in the cytoplasm after 24 h (51). Some research suggested that nanoparticles continue to degrade within the cells over time (52).

In our study, we took TEM images of cells treated with nanoparticles for 24 h. As shown in Figure 5E, the nucleus and the cytoplasm were clearly visible in the image, and the nanoparticles can be observed in the cytoplasm. The cell membrane folds and fuses to internalize the nanoparticles, and vesicles that internalize nanoparticles, as well as vesicles that internalize particle aggregates, can also be observed in the cytoplasm. This could also indicate that, at the concentration of 10 mg/L, $_{h}CeO_2@Cu_{5.4}O$ NPs can enter the cells and provide evidence for the intracellular anti-inflammatory effect. However, some studies have shown that with the increase of nanoparticle concentration, the number and volume of intracellular vesicles increase, which may hinder the function of other organelles and eventually lead to cell death (53). In this study, combined with the screening of the safe concentration of $_{h}CeO_2@Cu_{5.4}O$ NPs in the previous 24-, 48-, and 72-h CCK8 experiment, the follow-up anti-inflammatory study could be carried out on the premise that the concentration of 10 mg/L was relatively able to ensure the cell activity.

3.5 $_{h}CeO_2@Cu_{5.4}O$ NPs reduce NRLP3 inflammasome activation and inflammatory factor expression by reducing CTSB release

3.5.1 Reduced protein expression of CTSB in RAW264.7

The inflammatory cascade initiated by LPS via the toll-like receptor 4/CD14 receptor complex (TLR4) plays a crucial role in LPS-stimulated inflammatory responses. TLR4 recognizes and binds LPS, recruiting and activating the downstream molecule NF-κB, which enters the nucleus and induces the transcription of NLPR3, IL-18, and IL-1β, leading to the release of pro-inflammatory mediators as well as inflammation generation and development (1, 54). Inflammation is a defensive response that protects the host from harmful stimuli of endogenous and exogenous origin. On the other hand, infiltration of inflammatory cells and accumulation of inflammatory factors disrupt the structure and function of normal tissues and promote the development of a variety of inflammatory disorders (1, 55). The NLRP3 inflammatory vesicle plays an important role in the activation of caspase-1 and the subsequent release of inflammatory factors. In a mouse model of periodontitis, researchers found that the knockdown of NLRP3 prevented IL-1β release and inhibited osteoclast differentiation, implying that inflammasome may be closely related to the pathological process of periodontitis (56). There are also many studies showing that NLRP3 is also capable of inducing different aseptic inflammatory disorders, more so than atherosclerosis, lung inflammation due to mechanical distraction, and drug-induced hepatitis (57–59). CTSB, as a class of proteases, is mainly found in lysosomes. However, under certain specific circumstances, lysosomal membrane permeability is enhanced and CTSB is released, thus participating in many pathological mechanisms, especially playing an important role in the development of inflammatory diseases. CTSB has been proposed to promote NLRP3 activation and inflammatory factor production. It has been shown that the expression of CTSB, NLRP3, IL-18, and IL-1β was upregulated in PA-induced inflammation, while the above-mentioned molecules are not significantly different from control after the addition of CTSB inhibitors (60). Therefore, CTSB may regulate IL-18\IL-1β secretion by regulating the NLRP3 inflammasome. In another study, it was found that CTSB/NLRP3 expression was increased in cerulein-induced pancreatitis, and the addition of CA-074Me not only inhibited CTSB activity but also downregulated NLRP3, ASC, and caspase-1 expression. The levels of IL-18 and IL-1β were also significantly reduced in the CA-074Me addition group compared with the control group (61).

In this study, we investigated the expression and interrelationships of CTSB, NLRP3, ASC, and caspase-1 in mouse macrophages in order to understand the possible molecular mechanism of nanoparticles in the inflammatory pathway. The RNA expression of each component of the CTSB–NLRP3 pathway and inflammatory factors IL-18 and IL-1β was evaluated. Our results suggested that LPS-induced cellular inflammation was associated with the CTSB–NLRP3 pathway and that $_{h}CeO_2@Cu_{5.4}O$ NPs can alleviate the inflammatory response by inhibiting this signaling pathway.

We used the group of LPS-stimulated cells with inflammatory response as a positive control group. Figure 6A shows the Western blot bands and quantitative analysis plots, respectively. We found that LPS stimulation significantly increased the CTSB protein levels, which were significantly reduced after nanomaterial treatment, and the most significant protein reduction was observed when the molar ratio Cu/(Ce+Cu) was 83% ($_{h}CeO_2@83\%Cu_{5.4}O$). The localization of CTSB in mouse macrophages was also examined (Figure 6B). DAPI was used to show the nucleus marked as blue fluorescence, while CTSB is marked as green fluorescence. The fluorescence images showed an increase in CTSB after LPS stimulation and a decrease in CTSB after nanoparticle treatment. Therefore, we hypothesized that nanoparticles improved the inflammatory response induced by LPS stimulation by reducing the release of CTSB and that $_{h}CeO_2@83\%Cu_{5.4}O$ inhibited the release of CTSB best.

3.5.2 Inhibiting the CTSB–NLRP3 signaling pathway in LPS-stimulated inflammation model

The specific mechanism of NLRP3 inflammasome activation is still unclear, and the widely accepted model is the double signal model. First, the above-mentioned LPS or other microbial molecules stimulate as the first signal, upregulating the expression

10.3389/fimmu.2024.1344098

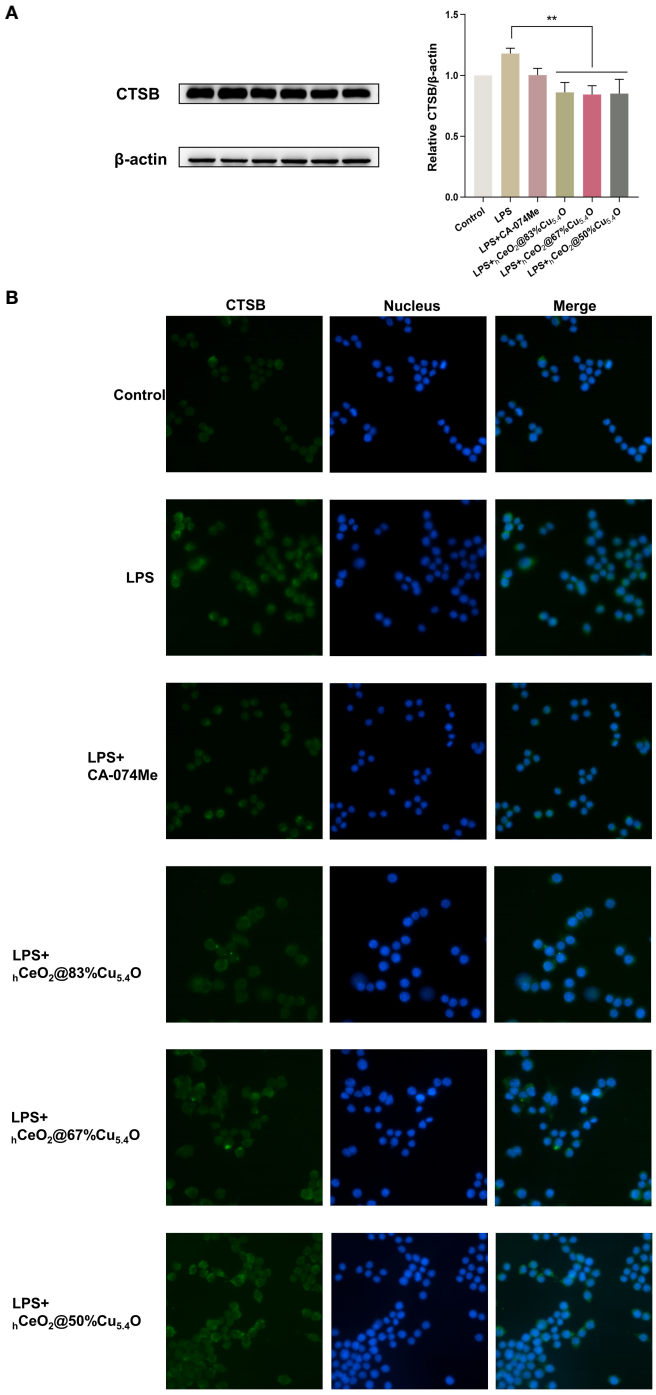

FIGURE 6
$_{h}CeO_{2}$@ $Cu_{5.4}O$ nanoparticles (NPs) reduce lipopolysaccharide (LPS)-induced CTSB release in RAW264.7 cells. **(A)** Western blot analysis of CTSB protein expression upon RAW264.7 cells treated with 1 μg/mL LPS and $_{h}CeO_{2}$@$Cu_{5.4}O$ NPs for 24 h. Data are presented as mean ± SD from three independent experiments. *n* = 3; * represents significant differences. ***P*< 0.005. **(B)** CTSB immunofluorescent staining.

of NLRP3 and IL-1β through the transcription factor NF-κB. Signal two can be provided by many stimuli, including ATP, ROS, oxidized mtDNA, K^+ efflux, lysosomal rupture, CTSB, etc. Among them, CTSB is a lysosomal enzyme that is widely expressed in mammalian cells and is a marker of lysosome-specific damage (62). When the integrity of the lysosomal membrane is disrupted, lysosomal enzymes such as CTSB leak into the cytoplasm, leading to a series of cellular homeostasis imbalances, pathological processes, and cell apoptosis. Studies have found that in microglial cells, CTSB can chronically activate the NF-κB signaling pathway by degrading IκBα (63); and other studies have found that chemical inhibitors of tissue protease B, such as CA-074Me, can inhibit NLRP3 activation, leading to the conclusion that CTSB can affect NLRP3 in different ways, including

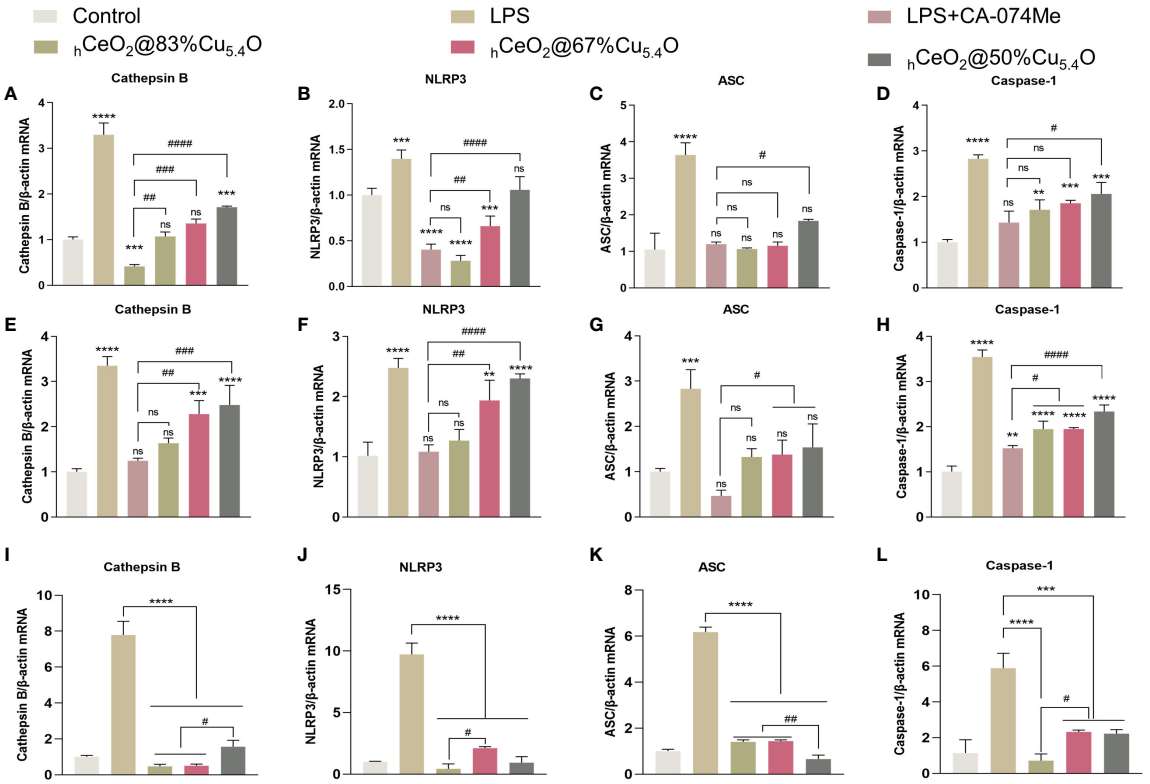

FIGURE 7
Inhibiting the CTSB–NLRP3 signaling pathway in a lipopolysaccharide (LPS)-stimulated inflammation model. **(A–D)** mRNA expression of IL-18, IL-1b, CTSB, NLRP3, ASC, and caspase-1 in RAW264.7 cells treated with LPS and $_{h}CeO_2$@$Cu_{5.4}O$ nanoparticles (NPs) for 24 h. **(E–H)** mRNA expression of IL-18, IL-1β, CTSB, NLRP3, ASC, and caspase-1 in RAW264.7 cells treated with LPS and $_{h}CeO_2$@$Cu_{5.4}O$ NPs for 12 h. **(I–L)** mRNA expression of CTSB, NLRP3, ASC, and caspase-1 in RAW264.7 cells treated only with $_{h}CeO_2$@$Cu_{5.4}O$ NPs for 24 h.(n = 3; ns: no significance; * and # represent significant differences. **P < 0.005, ***P < 0.0005, ****P < 0.0001, $^{\#}P < 0.05$, $^{\#\#}P < 0.005$, $^{\#\#\#}P < 0.0005$, and $^{\#\#\#\#}P < 0.0001$).

inhibiting the activation of NF-κB, reducing the expression of NLRP3 genes, and inhibiting the activation of NLRP3 (64, 65).

As shown in Figures 7A–D, NLRP3, ASC and caspase-1 expression increased after LPS treatment and decreased after the addition of CA-074Me, indicating that the reduction of CTSB reduced the expression of NLRP3 inflammasome. The addition of nanomaterials also reduced the NLRP3 inflammasome components, indicating that nanomaterials reduce the expression of NLRP3 inflammasome by inhibiting CTSB and reduce the release of inflammatory factors, thereby reducing the inflammatory response. Moreover, when the Ce/Cu ratio was 0.2 ($_{h}CeO_2$@83% $Cu_{5.4}O$), the effect on inflammation was the best, and with the decrease of Cu doping, the inhibitory effect on inflammation was weakened. In addition, Figures 7E–H show the gene expression of cells treated with LPS and nanoparticles for 12 h. The results show that the anti-inflammatory effect of cells treated with LPS and nanoparticles for 12 h is about the same as that of cells treated for 24 h, but the anti-inflammatory effect is not as good as that treated with LPS for 24 h. As shown in Figures 7I–L, to further understand the effect of nanoparticles on the CTSB–NLRP3 signaling pathway, we treated cells with nanoparticles only for 24 h and that $_{h}CeO_2$@ $Cu_{5.4}O$ showed an obvious inhibitory effect to NLRP3 inflammasome-related factor gene expression. From the above-mentioned experiments, $_{h}CeO_2$@83%$Cu_{5.4}O$ NPs had the best effect.

We believe the possible reasons for this phenomenon were as follows: (1) Cu in $Cu_{5.4}O$ NPs could reduce Ce^{4+} to Ce^{3+}. The more $Cu_{5.4}O$ NPs doped, the more Ce^{3+} is reduced, which exerts better SOD activity and reduces inflammation. (2) The anti-inflammatory effect of $Cu_{5.4}O$ NPs: Their ultra-small size and more active site exposure give them ultra-high antioxidant capacity. The particle size of $Cu_{5.4}O$ NPs was mostly 3–5 nm, which belongs to ultra-small nanoparticles. It has been reported that it can enter the mitochondrial permeability transition pore, thus maintaining the normal function of the mitochondria and alleviating oxidative stress. It can also enter the cells to play a role through phagocytosis (16). Thus, the increase in $Cu_{5.4}O$ NPs increases its antioxidant and anti-inflammatory effects.

In general, LPS can stimulate macrophages to M1 polarization, recruit inflammatory cells, secrete inflammatory factors, and facilitate the clearance of pathogens. M2 macrophages play an important role in resolving inflammation and tissue repair (66). We also tested the effect of $_{h}CeO_2$@$Cu_{5.4}O$ NPs on the gene expression of TNF-α and TGF-β, and as shown in Figures 8B, C, $_{h}CeO_2$@$Cu_{5.4}O$ NPs were able to reduce the expression of TNF-α and increase the expression of TGF-β, further suggesting that

10.3389/fimmu.2024.1344098

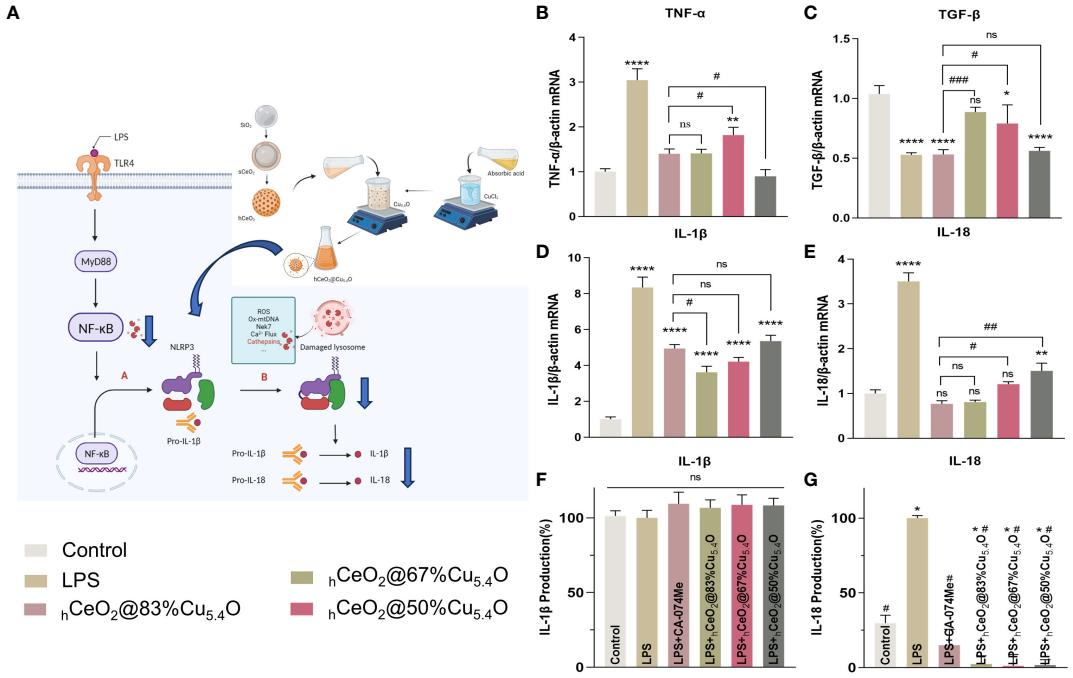

FIGURE 8
Secretion of IL-18 and IL-1β pro-inflammatory cytokines. **(A)** Schematic representation of $_{h}CeO_2@Cu_{5.4}O$ nanoparticles (NPs) on the CTSB–NLRP3 signaling pathway. **(B, C)** mRNA expression of TNF-a and TGF-β in RAW264.7 cells treated with $_{h}CeO_2@Cu_{5.4}O$ NPs for 24 h. **(D, E)** mRNA expression of IL-18 and IL-1β in RAW264.7 cells treated with $_{h}CeO_2@Cu_{5.4}O$ NPs for 24 h. **(F, G)** Effects of $_{h}CeO_2@Cu_{5.4}O$ NPs on the secretion of IL-18 and IL-1β in LPS-induced RAW264.7 cell supernatant. (n = 3; ns: no significance; * and # represent significant differences. *P < 0.05, **P < 0.005, ****P < 0.0001, $^{\#}P < 0.05$, $^{\#\#}P < 0.005$, $^{\#\#\#}P < 0.0005$).

$_{h}CeO_2@Cu_{5.4}O$ NPs may alleviate inflammation by promoting macrophage polarization to M2 type.

3.5.3 The secretion of IL-18 and IL-1β pro-inflammatory cytokines

After activation of NLRP3 inflammasome, pro-IL-18 and pro-IL-1β could be cleaved into mature IL-18 and IL-1β (Figures 8A) (67). As shown in Figures 8D, E, the mRNA expression levels of the inflammatory factors IL-18 and IL-1β were increased in the LPS-treated group, while their expression was decreased by the addition of CA-074Me. These results indicated that CTSB is involved in LPS-induced inflammatory response. The expression levels of all CTSB, IL-18, and IL-1β decreased after adding $_{h}CeO_2@Cu_{5.4}O$, indicating that $_{h}CeO_2@Cu_{5.4}O$ may alleviate inflammatory response by inhibiting CTSB.

To evaluate the effect of nanoparticles on the secretion of IL-18 and IL-1β in the culture supernatant of macrophages, the levels of IL-18 and IL-1β in the culture supernatant of RAW 264.7 macrophages were analyzed. As shown in Figures 8F, G, IL-18 production was significantly increased in the LPS group compared with the control group. Compared with the LPS group, the groups treated with different $_{h}CeO_2@Cu_{5.4}O$ showed a significant reduction in IL-18 level. However, there was no significant difference in the IL-1β levels among the groups. It has been documented that IL-1β production is dependent on ASC that is not expressed in RAW264.7 (68, 69). Studies have shown that some pro-IL-1β is released into the culture medium after RAW264.7 is stimulated, and most pro-IL-1β is retained in the cells. When co-stimulated with other stimuli, pro-IL-1β and IL-1β are released from the cells together (69). However, other studies have shown that the expression of IL-1β in the supernatant of RAW264.7 cells treated with LPS increased (70, 71). In the future, we need to combine LPS- and NLRP3-specific agonists to further explore the inhibitory effect on IL-1β.

4 Conclusion

In this study, a novel $_{h}CeO_2@Cu_{5.4}O$ NPs was prepared by doping different amounts of $Cu_{5.4}O$ NPs into $hCeO_2$ NPs. $_{h}CeO_2@Cu_{5.4}O$ NPs has good biocompatibility and excellent ROS scavenging ability. $_{h}CeO_2$ @ $Cu_{5.4}O$ NPs was demonstrated to attenuate the inflammatory response by scavenging ROS, reducing the release of CTSB, and inhibiting the activation of the NLPR3 inflammasome. $_{h}CeO_2@Cu_{5.4}O$ NPs could alleviate the inflammatory responses by regulating the CTSB–NLRP3 signaling pathway, where the $_{h}CeO_2@83\%Cu_{5.4}O$ NPs had the strongest antioxidant and anti-inflammatory effects. This study provides a new idea for nanoparticles to attenuate LPS-induced inflammatory response.

Data availability statement

The original contributions presented in the study are included in the article/supplementary material. Further inquiries can be directed to the corresponding authors.

Ethics statement

Ethical approval was not required for the studies on animals in accordance with the local legislation and institutional requirements because only commercially available established cell lines were used.

Author contributions

YL: Writing – original draft. XX: Writing – review & editing. ZN: Writing – review & editing. KW: Writing – review & editing. JL: Writing – review & editing. XL: Writing – review & editing.

Funding

The author(s) declare financial support was received for the research, authorship, and/or publication of this article. This work was supported by China Postdoctoral Science Foundation (2023M732676), Shandong Provincial Natural Science Foundation Youth Project (ZR2021QH251), and Clinical Medicine +X Research Project of Affiliated Hospital of Qingdao University (QDFY+X2021055).

Conflict of interest

The authors declare that the research was conducted in the absence of any commercial or financial relationships that could be construed as a potential conflict of interest.

Publisher's note

All claims expressed in this article are solely those of the authors and do not necessarily represent those of their affiliated organizations, or those of the publisher, the editors and the reviewers. Any product that may be evaluated in this article, or claim that may be made by its manufacturer, is not guaranteed or endorsed by the publisher.

References

1. Afsar UA. An overview of inflammation:mechanism and consequences. *Front Biol.* (2011) 6:274–81. doi: 10.1007/s11515-011-1123-9

2. Nathan C, Ding AH. Nonresolving inflammation. *Cell.* (2010) 140:871–82. doi: 10.1016/j.cell.2010.02.029

3. Weber C, Hristov M. Atherogenesis and inflammation. *Hamostaseologie.* (2015) 35:99. doi: 10.1055/s-0037-1619816

4. Singh N, Baby D, Rajguru JP, Patil PB, Thakkannavar SS, Pujari VB. Inflammation and cancer. *Ann Afr Med.* (2019) 18:121–6. doi: 10.4103/aam.aam_56_18

5. Xie W, Du L. Diabetes is an inflammatory disease: evidence from traditional Chinese medicines. *Diabetes Obes Metab.* (2011) 13(4):289–301. doi: 10.1111/j.1463-1326.2010.01336.x

6. Algarni A, Fayomi A, Al Garalleh H, Afandi A, Brindhadevi K, Pugazhendhi A. Nanofabrication synthesis and its role in antibacterial, anti-inflammatory, and anticoagulant activities of AgNPs synthesized by Mangifera indica bark extract. *Environ Res.* (2023) 231:115983. doi: 10.1016/j.envres.2023.115983

7. Uchiyama MK, Deda DK, Rodrigues SFD, Drewes CC, Bolonheis SM, Kiyohara PK, et al. *In vivo* and *in vitro* toxicity and anti-inflammatory properties of gold nanoparticle bioconjugates to the vascular system. *Toxicological Sci.* (2014) 142:497–507. doi: 10.1093/toxsci/kfu202

8. Agarwal H, Nakara A, Shanmugam VK. Anti-inflammatory mechanism of various metal and metal oxide nanoparticles synthesized using plant extracts: A review. *Biomedicine Pharmacotherapy.* (2019) 109:2561–72. doi: 10.1016/j.biopha.2018.11.116

9. Tripathi P, Tripathi P, Kashyap L, Singh V. The role of nitric oxide in inflammatory reactions. *FEMS Immunol Med Microbiol.* (2007) 51:443–52. doi: 10.1111/j.1574-695X.2007.00329.x

10. Agrawal G, Aswath S, Laha A, Ramakrishna S. Electrospun nanofiber-based drug carrier to manage inflammation. *Adv Wound Care (New Rochelle).* (2023) 12:529–43. doi: 10.1089/wound.2022.0043

11. Luo W, Bai L, Zhang J, Li Z, Liu Y, Tang X, et al. Polysaccharides-based nanocarriers enhance the anti-inflammatory effect of curcumin. *Carbohydr polymers.* (2023) 311:120718. doi: 10.1016/j.carbpol.2023.120718

12. Qi M, Ren X, Li W, Sun Y, Sun X, Li C, et al. NIR responsive nitric oxide nanogenerator for enhanced biofilm eradication and inflammation immunotherapy against periodontal diseases. *Nano Today.* (2022) 43:101447. doi: 10.1016/j.nantod.2022.101447

13. Sadidi H, Hooshmand S, Ahmadabadi A, Javad Hoseini S, Baino F, Vatanpour M, et al. Cerium oxide nanoparticles (Nanoceria): hopes in soft tissue engineering. *Molecules.* (2020) 25(19):4559. doi: 10.3390/molecules25194559

14. Arya A, Sethy NK, Singh SK, Das M, Bhargava K. Cerium oxide nanoparticles protect rodent lungs from hypobaric hypoxia-induced oxidative stress and inflammation. *Int J Nanomedicine.* (2013) 8:4507–19. doi: 10.2147/IJN

15. Yu Y, Zhao S, Gu D, Zhu B, Liu H, Wu W, et al. Cerium oxide nanozyme attenuates periodontal bone destruction by inhibiting the ROS-NFκB pathway. *Nanoscale.* (2022) 14:2628–37. doi: 10.1039/D1NR06043K

16. Liu TF, Xiao BW, Xiang F, Tan JL, Chen Z, Zhang XR, et al. Ultrasmall copper-based nanoparticles for reactive oxygen species scavenging and alleviation of inflammation related diseases. *Nat Commun.* (2020) 11(1):2788. doi: 10.1038/s41467-020-16544-7

17. Xiong J, Wang Y, Xue Q, Wu X. Synthesis of highly stable dispersions of nanosized copper particles using L-ascorbic acid. *Green Chem.* (2011) 13:900–4. doi: 10.1039/c0gc00772b

18. Ingle AP, Paralikar P, Shende S, Gupta I, Biswas JK, da Silva Martins LH, et al. Copper in medicine: Perspectives and toxicity. In: Rai M, Ingle AP, Medici S, eds. *Biomedical Applications of Metals.* Cham: Springer International Publishing (2018). pp. 95–112. doi: 10.1007/978-3-319-74814-6_4

19. Bergsbaken T, Fink SL, Cookson BT. Pyroptosis: host cell death and inflammation. *Nat Rev Microbiol.* (2009) 7:99–109. doi: 10.1038/nrmicro2070

20. Jiang Y, Wang M, Huang K, Zhang Z, Shao N, Zhang Y, et al. Oxidized low-density lipoprotein induces secretion of interleukin-1β by macrophages via reactive oxygen species-dependent NLRP3 inflammasome activation. *Biochem Biophys Res Commun.* (2012) 425:121–6. doi: 10.1016/j.bbrc.2012.07.011

21. Man SM, Kanneganti T-D. Regulation of lysosomal dynamics and autophagy by CTSB/cathepsin B. *Autophagy.* (2016) 12:2504–5. doi: 10.1080/15548627.2016.1239679

22. Wang Y, Jia L, Shen J, Wang Y, Fu Z, S-a Su, et al. Cathepsin B aggravates coxsackievirus B3-induced myocarditis through activating the inflammasome and promoting pyroptosis. *Plos Pathogens.* (2018) 14(1):e1006872. doi: 10.1371/journal.ppat.1006872

23. Menzel K, Hausmann M, Obermeier F, Schreiter K, Dunger N, Bataille F, et al. Cathepsins B, L and D in inflammatory bowel disease macrophages and potential therapeutic effects of cathepsin inhibition *in vivo*. *Clin Exp Immunol.* (2006) 146:169–80. doi: 10.1111/j.1365-2249.2006.03188.x

24. Ma X, Cheng Y, Jian H, Feng Y, Chang Y, Zheng R, et al. Hollow, rough, and nitric oxide-releasing cerium oxide nanoparticles for promoting multiple stages of wound healing. *Advanced healthcare materials.* (2019) 8:e1900256. doi: 10.1002/adhm.201900256

25. Li F, Li J, Song X, Sun T, Mi L, Liu J, et al. Alginate/Gelatin hydrogel scaffold containing nCeO2 as a potential osteogenic nanomaterial for bone tissue engineering. *Int J Nanomedicine.* (2022) 17:6561–78. doi: 10.2147/IJN.S388942

26. Michael JM, Liu Z. Crosstalk of reactive oxygen species and NF-KB signaling. *Cell Res.* (2011) 21:103–15. doi: 10.1038/cr.2010.178

27. Codolo G, Plotegher N, Pozzobon T, Brucale M, Tessari I, Bubacco L, et al. Triggering of inflammasome by aggregated alpha-synuclein, an inflammatory response in synucleinopathies. *PloS One.* (2013) 8(1):e55375. doi: 10.1371/journal.pone.0055375

28. Liu X, Wu J, Liu Q, Lin A, Li S, Zhang Y, et al. Synthesis-temperature-regulated multi-enzyme-mimicking activities of ceria nanozymes. *J Materials Chem B*. (2021) 9:7238–45. doi: 10.1039/D1TB00964H

29. Dong HJ, Zhang C, Fan YY, Zhang W, Gu N, Zhang Y. Nanozyme and their ROS regulation effect in cells. *Prog Biochem Biophysics*. (2018) 45:105–17. doi: 10.16476/j.pibb.2017.0460

30. Yasui K, Baba A. Therapeutic potential of superoxide dismutase (SOD) for resolution of inflammation. *Inflammation Res*. (2006) 55:359–63. doi: 10.1007/s00011-006-5195-y

31. Celardo I, Pedersen JZ, Traversa E, Ghibelli L. Pharmacological potential of cerium oxide nanoparticles. *Nanoscale*. (2011) 3:1411–20. doi: 10.1039/c0nr00875c

32. Zeng F, Shi YH, Wu CN, Liang JM, Zhong QX, Briley K, et al. A drug-free nanozyme for mitigating oxidative stress and inflammatory bowel disease. *J Nanobiotechnology*. (2022) 20(1):107. doi: 10.1186/s12951-022-01319-7

33. Li MY, Liu J, Shi L, Zhou C, Zou MZ, Fu D, et al. Gold nanoparticles-embedded ceria with enhanced antioxidant activities for treating inflammatory bowel disease. *Bioact Mater*. (2023) 25:95–106. doi: 10.1016/j.bioactmat.2023.01.015

34. Kim J, Kim HY, Song SY, Go SH, Sohn HS, Baik S, et al. Synergistic oxygen generation and reactive oxygen species scavenging by manganese Ferrite/Ceria co-decorated nanoparticles for rheumatoid arthritis treatment. *ACS Nano*. (2019) 13:3206–17. doi: 10.1021/acsnano.8b08785

35. Shlapa Y, Solopan S, Sarnatskaya V, Siposova K, Garcarova I, Veltruska K, et al. Cerium dioxide nanoparticles synthesized via precipitation at constant pH: Synthesis, physical-chemical and antioxidant properties. *Colloids Surfaces B: Biointerfaces*. (2022) 220:112960. doi: 10.1016/j.colsurfb.2022.112960

36. Gupta A, Das S, Neal CJ, Seal S. Controlling the surface chemistry of cerium oxide nanoparticles for biological applications. *J Materials Chem B*. (2016) 4:3195–202. doi: 10.1039/C6TB00396F

37. Qiao XJ, Arsalan M, Ma X, Wang YH, Yang SY, Wang Y, et al. A hybrid of ultrathin metal-organic framework sheet and ultrasmall copper nanoparticles for detection of hydrogen peroxide with enhanced activity. *Anal Bioanal Chem*. (2021) 413:839–51. doi: 10.1007/s00216-020-03038-0

38. Peng Y, He DF, Ge X, Lu YF, Chai YH, Zhang YX, et al. Construction of heparin-based hydrogel incorporated with Cu5.4O ultrasmall nanozymes for wound healing and inflammation inhibition. *Bioact Mater*. (2021) 6:3109–24. doi: 10.1016/j.bioactmat.2021.02.006

39. Gough DR, Cotter TG. Hydrogen peroxide: a Jekyll and Hyde signalling molecule. *Cell Death Dis*. (2011) 2(10):e213. doi: 10.1038/cddis.2011.96

40. Bryan N, Ahswin H, Smart N, Bayon Y, Wohlert S, Hunt JA. Reactive oxygen species (ROS) - a family of fate deciding molecules pivotal in constructive inflammation and wound healing. *Eur Cells Materials*. (2012) 24:249–65. doi: 10.22203/eCM

41. Rimessi A, Previati M, Nigro F, Wieckowskic MR, Pinton P. Mitochondrial reactive oxygen species and inflammation: Molecular mechanisms, diseases and promising therapies. *Int J Biochem Cell Biol*. (2016) 81:281–93. doi: 10.1016/j.biocel.2016.06.015

42. Kavcic N, Pegan K, Turk B. Lysosomes in programmed cell death pathways: from initiators to amplifiers. *Biol Chem*. (2017) 398:289–301. doi: 10.1515/hsz-2016-0252

43. Valodkar M, Rathore PS, Jadeja RN, Thounaojam M, Devkar RV, Thakore S. Cytotoxicity evaluation and antimicrobial studies of starch capped water soluble copper nanoparticles. *J Hazard Mater*. (2012) 201:244–9. doi: 10.1016/j.jhazmat.2011.11.077

44. Andraos C, Yu IJ, Gulumian M. Interference: A much-neglected aspect in high-throughput screening of nanoparticles. *Int J Toxicol*. (2020) 39:397–421. doi: 10.1177/1091581820938335

45. Guadagnini R, Kenzaoui BH, Walker L, Pojana G, Magdolenova Z, Bilanicova D, et al. Toxicity screenings of nanomaterials: challenges due to interference with assay processes and components of classic *in vitro* tests. *Nanotoxicology*. (2015) 9:13–24. doi: 10.3109/17435390.2013.829590

46. Drasler B, Sayre P, Steinhaeuser KG, Petri-Fink A, Rothen-Rutishauser B. *In vitro* approaches to assess the hazard of nanomaterials (vol 8, pg 99, 2017). *Nanoimpact*. (2018) 9:51–1. doi: 10.1016/j.impact.2017.10.002

47. Yin Q, Jiang D, Li L, Yang Y, Wu P, Luo Y, et al. LPS promotes vascular smooth muscle cells proliferation through the TLR4/Rac1/Akt signalling pathway. *Cell Physiol Biochem*. (2017) 44:2189–200. doi: 10.1159/000486024

48. Horie M, Tabei Y. Role of oxidative stress in nanoparticles toxicity. *Free Radical Res*. (2021) 55:331–42. doi: 10.1080/10715762.2020.1859108

49. Chang Y-N, Zhang M, Xia L, Zhang J, Xing G. The toxic effects and mechanisms of CuO and ZnO nanoparticles. *Materials*. (2012) 5:2850–71. doi: 10.3390/ma5122850

50. Mi X-J, Xu XY, Choi HS, Kim H, Cho IH, Yi T-H, et al. The immune-enhancing properties of hwanglyeonhaedok-tang-mediated biosynthesized gold nanoparticles in macrophages and splenocytes. *Int J Nanomedicine*. (2022) 17:477–94. doi: 10.2147/IJN.S338334

51. Lee JK, Sayers BC, Chun K-S, Lao H-C, Shipley-Phillips JK, Bonner JC, et al. Multi-walled carbon nanotubes induce COX-2 and iNOS expression via MAP Kinase-dependent and -independent mechanisms in mouse RAW264.7 macrophages. *Particle Fibre Toxicol*. (2012) 9(1):14. doi: 10.1186/1743-8977-9-14

52. Zhang L, Xiao S, Kang X, Sun T, Zhou C, Xu Z, et al. Metabolic conversion and removal of manganese ferrite nanoparticles in RAW264.7 cells and induced alteration of metal transporter gene expression. *Int J Nanomedicine*. (2021) 16:1709–24. doi: 10.2147/IJN.S289707

53. Hashimoto M, Toshima H, Yonezawa T, Kawai K, Narushima T, Kaga M, et al. Responses of RAW264.7 macrophages to water-dispersible gold and silver nanoparticles stabilized by metal-carbon σ-bonds. *J BioMed Mater Res A*. (2014) 102:1838–49. doi: 10.1002/jbm.a.34854

54. Liu C, Yao Q, Hu TT, Cai ZL, Xie QW, Zhao JH, et al. Cathepsin B deteriorates diabetic cardiomyopathy induced by streptozotocin via promoting NLRP3-mediated pyroptosis. *Mol Therapy-Nucleic Acids*. (2022) 30:198–207. doi: 10.1016/j.omtn.2022.09.019

55. Rubartelli A, Lotze MT, Latz E, Manfredi AJ. Mechanisms of sterile inflammation. *Front Immunol*. (2013) 4:398. doi: 10.3389/fimmu.2013.00398

56. Chen Y, Yang Q, Lv C, Chen Y, Zhao W, Li W, et al. NLRP3 regulates alveolar bone loss in ligature-induced periodontitis by promoting osteoclastic differentiation. *Cell Proliferation*. (2021) 54(2):e12973. doi: 10.1111/cpr.12973

57. Chen GY, Nuñez G. Sterile inflammation: sensing and reacting to damage. *Nat Rev Immunol*. (2010) 10(12):826–37. doi: 10.1038/nri2873

58. Duewell P, Kono H, Rayner KJ, Sirois CM, Vladimer G, Bauernfeind FG, et al. NLRP3 inflammasomes are required for atherogenesis and activated by cholesterol crystals. *Nature*. (2010) 464:1357–U1357. doi: 10.1038/nature08938

59. Imaeda AB, Watanabe A, Sohail MA, Mahmood S, Mohamadnejad M, Sutterwala FS, et al. Acetaminophen-induced hepatotoxicity in mice is dependent on Tlr9 and the Nalp3 inflammasome. *J Clin Invest*. (2009) 119:305–14. doi: 10.1172/JCI35958

60. Tang Y, Cao G, Min X, Wang T, Sun S, Du X, et al. Cathepsin B inhibition ameliorates the non-alcoholic steatohepatitis through suppressing caspase-1 activation. *J Physiol Biochem*. (2018) 74:503–10. doi: 10.1007/s13105-018-0644-y

61. Wang J, Wang L, Zhang X, Xu Y, Chen L, Zhang W, et al. Cathepsin B aggravates acute pancreatitis by activating the NLRP3 inflammasome and promoting the caspase-1-induced pyroptosis. *Int Immunopharmacol*. (2021) 94:107496. doi: 10.1016/j.intimp.2021.107496

62. Lunov O, Uzhytchak M, Smolková B, Lunova M, Jirsa M, Dempsey NM, et al. Remote actuation of apoptosis in liver cancer cells via magneto-mechanical modulation of iron oxide nanoparticles. *Cancers (Basel)*. (2019) 11(12):1873. doi: 10.3390/cancers11121873

63. Ni JJ, Wu Z, Peterts C, Yamamoto K, Qing H, Nakanishi H. The critical role of proteolytic relay through cathepsins B and E in the phenotypic change of microglia/macrophage. *J Neurosci*. (2015) 35:12488–501. doi: 10.1523/JNEUROSCI.1599-15.2015

64. He Y, Hara H, Núñez G. Mechanism and regulation of NLRP3 inflammasome activation. *Trends Biochem Sci*. (2016) 41:1012–21. doi: 10.1016/j.tibs.2016.09.002

65. Kelley N, Jeltema D, Duan Y, He Y. The NLRP3 inflammasome: an overview of mechanisms of activation and regulation. *Int JMol Sci*. (2019) 20(13):3328. doi: 10.3390/ijms20133328

66. Jeganathan S, Fiorino C, Naik U, Sun HS, Harrison RE. Modulation of osteoclastogenesis with macrophage M1-and M2-inducing stimuli. *PloS One*. (2014) 9(8):e104498. doi: 10.1371/journal.pone.0104498

67. Swanson KV, Deng M, Ting JPY. The NLRP3 inflammasome: molecular activation and regulation to therapeutics. *Nat Rev Immunol*. (2019) 19:477–89. doi: 10.1038/s41577-019-0165-0

68. Pelegrin P, Barroso-Gutierrez C, Surprenant A. P2X7 Receptor differentially couples to distinct release pathways for IL-1β in mouse macrophage. *J Immunol*. (2008) 180:7147–57. doi: 10.4049/jimmunol.180.11.7147

69. Hirano S, Zhou Q, Furuyama A, Kanno S. Differential regulation of IL-1β and IL-6 release in murine macrophages. *Inflammation*. (2017) 40:1933–43. doi: 10.1007/s10753-017-0634-1

70. Xiang P, Chen T, Mou Y, Wu H, Xie P, Lu G, et al. NZ suppresses TLR4/NF-κB signalings and NLRP3 inflammasome activation in LPS-induced RAW264.7 macrophages. *Inflammation Res*. (2015) 64:799–808. doi: 10.1007/s00011-015-0863-4

71. Xie Q, Shen W-W, Zhong J, Huang C, Zhang L, Li J. Lipopolysaccharide/adenosine triphosphate induces IL-1β and IL-18 secretion through the NLRP3 inflammasome in RAW264.7 murine macrophage cells. *Int J Mol Med*. (2014) 34:341–9. doi: 10.3892/ijmm.2014.1755

frontiers | Frontiers in Immunology

TYPE Review
PUBLISHED 02 May 2024
DOI 10.3389/fimmu.2024.1383503

OPEN ACCESS

EDITED BY
Uzma Saqib,
Indian Institute of Technology Indore, India

REVIEWED BY
Matthias Clauss,
Indiana University Bloomington, United States
Stephen Ray Reeves,
University of Washington, United States

*CORRESPONDENCE
Yanmei Wang
6418372@qq.com
Chengshi He
hcs6512@126.com
Zhongyu Han
hzyczy1997@163.com
Xiaohong Zhang
2653099978@qq.com

†These authors have contributed equally to this work

RECEIVED 07 February 2024
ACCEPTED 16 April 2024
PUBLISHED 02 May 2024

CITATION
Wang Y, Huang X, Luo G, Xu Y, Deng X, Lin Y, Wang Z, Zhou S, Wang S, Chen H, Tao T, He L, Yang L, Yang L, Chen Y, Jin Z, He C, Han Z and Zhang X (2024) The aging lung: microenvironment, mechanisms, and diseases.
Front. Immunol. 15:1383503.
doi: 10.3389/fimmu.2024.1383503

The aging lung: microenvironment, mechanisms, and diseases

Yanmei Wang[1,2*†], Xuewen Huang[1†], Guofeng Luo[1], Yunying Xu[1], Xiqian Deng[1], Yumeng Lin[3], Zhanzhan Wang[4], Shuwei Zhou[5], Siyu Wang[6], Haoran Chen[1], Tao Tao[2], Lei He[2], Luchuan Yang[2], Li Yang[2], Yutong Chen[7], Zi Jin[8], Chengshi He[9*], Zhongyu Han[1*] and Xiaohong Zhang[10*]

[1]School of Medical and Life Sciences, Chengdu University of Traditional Chinese Medicine, Chengdu, China, [2]Institute of Traditional Chinese Medicine of Sichuan Academy of Chinese Medicine Sciences (Sichuan Second Hospital of T.C.M), Chengdu, China, [3]Eye School of Chengdu University of Traditional Chinese Medicine, Chengdu, China, [4]Department of Respiratory and Critical Care Medicine, The First People's Hospital of Lianyungang, Lianyungang, China, [5]Jiangsu Key Laboratory of Molecular and Functional Imaging, Department of Radiology, Zhongda Hospital, School of Medicine, Southeast University, Nanjing, China, [6]Department of Gastroenterology, The First Hospital of Hunan University of Chinese Medicine, Changsha, China, [7]The Second Clinical Medical College, Zhejiang Chinese Medical University, Hangzhou, China, [8]Department of Anesthesiology and Pain Rehabilitation, Shanghai YangZhi Rehabilitation Hospital (Shanghai Sunshine Rehabilitation Center), School of Medicine, Tongji University, Shanghai, China, [9]Department of Respiratory ,Hospital of Chengdu University of Traditional Chinese Medicine, Chengdu, China, [10]Department of Emergency Medicine Center, Sichuan Province People's Hospital University of Electronic Science and Technology of China, Chengdu, China

With the development of global social economy and the deepening of the aging population, diseases related to aging have received increasing attention. The pathogenesis of many respiratory diseases remains unclear, and lung aging is an independent risk factor for respiratory diseases. The aging mechanism of the lung may be involved in the occurrence and development of respiratory diseases. Aging-induced immune, oxidative stress, inflammation, and telomere changes can directly induce and promote the occurrence and development of lung aging. Meanwhile, the occurrence of lung aging also further aggravates the immune stress and inflammatory response of respiratory diseases; the two mutually affect each other and promote the development of respiratory diseases. Explaining the mechanism and treatment direction of these respiratory diseases from the perspective of lung aging will be a new idea and research field. This review summarizes the changes in pulmonary microenvironment, metabolic mechanisms, and the progression of respiratory diseases associated with aging.

KEYWORDS

aging, immunity microenvironment, mechanism, lung diseases, therapy

Introduction

Aging is the gradual decline of physiological functions, characterized by signs like dry skin, wrinkles, and memory loss. Over the last two centuries, life expectancy in developed countries has doubled (1, 2). By 2050, it is expected that those over 65 will make up approximately 20% of the global population (3). Since 1939, caloric restriction in mice has been shown to extend lifespan (4). New research finds that targeting specific loci or altering metabolic pathways can delay the aging process (5).

Cellular senescence, a hallmark of aging, is the irreversible cessation of cell division, often marked by DNA damage, inflammatory secretions, and metabolic changes. It occurs during both development and adulthood, contributing to aging organ degeneration (6). However, the exact relationship between cellular senescence and aging, and how the former influences the latter, remains unclear.

The lung, crucial for gas exchange and sensitive to external stimuli, is highly susceptible to aging. It matures by age 10–12, reaching peak function at 20 in women and 25 in men (7). Aging degrades lung barrier integrity and pathogen resistance while increasing immune sensitivity, thus heightening disease risk and mortality from conditions like lung cancer and inflammation. Understanding how aging affects lung health and exacerbates pathological damage is a critical research area.

In this manuscript, we review the research progress on the role of pulmonary aging in the pathogenesis of respiratory diseases, including the mechanism and response pathway of how various cells in the pulmonary microenvironment cope with the molecular level of aging. We believe that this manuscript will help readers to further understand age-related respiratory diseases and can also provide new ideas for the study of the pathogenesis and clinical treatment of various respiratory diseases.

Morphology, respiratory indices, and function changes in the aging lung

Morphology changes

"Senile lung" describes lung aging, marked by alveolar and duct expansion, and basement membrane thickening, leading to decreased lung elasticity and increased compliance (2, 8).

Aging leads to terminal air space enlargement, increased alveolar duct and terminal bronchiole size, and a reduction in alveolar area and number. For instance, the total alveolar area decreases from 70 m^2 in individuals aged 30–39 to approximately 60 m^2 in those 70–79 years old, dropping approximately 2.5 m^2 every decade (8, 9). Additionally, aging increases lung collagen content and thickens the alveolar basement membrane (10). These anatomical changes result in several physiological alterations: reduced elastic recoil, increased lung compliance, diminished oxygen diffusion capacity, early airway collapse, intrapulmonary gas retention, and decreased expiratory flowrate. These changes can obstruct small airways, potentially leading to chronic obstructive pulmonary disease (COPD) in the elderly (11). Furthermore, smoking exacerbates COPD risk and progression in this age group, intertwining with aging to accelerate the disease's severity.

Respiratory indices changes

After birth, total lung capacity (TLC) increases, but in the elderly, inspiratory muscle strength, thoracic compliance, and lung elastic recoil decrease, leading to lower TLC, tidal volume (TV), inspiratory reserve volume (IRV), and expiratory reserve volume (ERV) compared to young adults.

Vital capacity (VC), the maximum air volume exhaled after forced inspiration, decreases with age, approximately 200 ml every decade starting from age 20, from approximately 3,500 ml in men and 2,500 ml in women at age 30, to 75% of that by age 70 due to increased thoracic rigidity and decreased lung recoil and respiratory muscle strength.

Functional residual capacity (FRC), the gas volume remaining in the lungs after a quiet expiration, increases with age, leading to alveolar distension and increased respiratory muscle load. This results in a 20% increase in energy expenditure for respiration in 60-year-olds compared to 20-year-olds (12). Aging also enlarges alveoli and alters supportive structures, reducing lung elasticity and causing premature small airway closure during expiration, thus increasing FRC (12, 13).

The spirometric index FEV1/FVC, crucial for diagnosing COPD, shows that FEV1 and FVC peak at 27 years in men and 20 in women, then decline, with FEV1 decreasing faster after 65 years of age (14).

In addition, as respiratory indicators reflecting small airway ventilation function, expiratory flowrates (V25–75, Vmax25, Vmax75) decrease with age, indicating small airway function decline. Closed volume (CV)/VC and closed capacity (CC)/TLC ratios increase with age due to earlier small airway closure in the elderly during expiration.

Function changes

Lung functionality peaks between ages 18 and 25 and remains stable until approximately 35 years old, after which it gradually declines (15). This decline is attributed to reduced respiratory muscle strength and chest wall function in older adults, leading to decreased ventilation capacity. In general, with increasing age, TV may slightly decrease. This is mainly due to the slight decrease in lung capacity, increased stiffness of lung tissue, and potential decline in respiratory muscle function as individuals age, all of which can impact TV. On the other hand, research has shown that TV can be increased through training, depending on individual lifestyle and physiological conditions (16).

From age 35, lung function decreases even in healthy individuals, with stiffer blood vessel walls and reduced elasticity impacting blood supply to alveoli and gas exchange (17–21). Aging also reduces alveolar surface area and capillary density, affecting lung ventilation function, all leading to ventilation/perfusion ratio

imbalance and lower arterial oxygen partial pressure (PaO_2) in the elderly (16). In older lungs, there is a diminished response to hypoxemia and hypercapnia and less recognition of bronchoconstriction (22). The aging lung's response to hypoxemia and hypercapnia, measured by oral occlusion pressure, shows a 50% and 60% decrease, respectively, in the elderly compared to young adults, indicating a reduced ability to integrate sensory information and generate appropriate neural responses (21).

Microenvironment of aging lung

For air-breathing animals, the lung is a vital organ of the respiratory system. Mammals and other structurally complex animals have two lungs, located on the left and right sides of the chest cavity near the spine and heart. The primary function of the lungs is to facilitate gas exchange, transporting oxygen from the air into the bloodstream and removing carbon dioxide from the blood into the atmosphere. As a functionally important and structurally complex organ, the aging lung harbors various types of cells, including resident cells and immune cells within the lung microenvironment. Previous research has utilized light microscopy and electron microscopy to observe the immune reactions and cellular morphology of lung tissue, defining resident cells in the lung (23). Advanced techniques such as single-cell sequencing and immunohistochemistry have expanded our understanding, revealing over 40 distinct cell types in human lungs. However, the effects of aging on lung cell composition and function remain partially understood. Age alone is a risk factor for lung diseases, with cellular aging contributing to different pathological outcomes. This knowledge opens new avenues for investigating chronic respiratory disease mechanisms by examining the aging lung's unique structures and the biological impact of aging on different cell types.

Lung parenchymal cells

"Lung parenchymal cells" refers to the cells that make up the functional tissue of the lungs. Comprising a multitude of minute alveoli with thin walls, it constitutes an immense surface area (24). These cells include various types, such as alveolar epithelial cells, bronchial epithelial cells, and endothelial cells. These cells each have their own functions; alveolar epithelial cells, for example, play a crucial role in gas exchange by lining the inner surface of the alveoli, where oxygen is taken up and carbon dioxide is released (25).

Airway epithelial cells

Airways are divided into respiratory and conducting zones by terminal bronchioles. They secrete mucins and fluids, lined with respiratory cells and ciliated pseudostratified epithelium. Epithelial cells form polarized junctional complexes with claudins for protection (26). Ciliated cells are predominant, supported by club, serous, neuroendocrine, and goblet cells. Subepithelial basal cells serve as progenitors for airway epithelium regeneration (27). In the airways, submucosal glands secrete mucins (like MUC2 and MUC5B) and fluids and can release defense proteins upon stimulation (27, 28). Mucus, a high molecular weight glycoprotein, facilitates pathogen clearance and plays a role in maintaining homeostasis in the airway (29).

Aging can induce alterations in the function and structure of tracheal epithelial cells, characterized by diminished proliferative capacity, elevated apoptosis, and decreased metabolic activity. These modifications will impair tracheal epithelial cell function, consequently impacting the normal physiological function of the trachea.

Alveolar epithelial cell

Alveolar epithelial cells (AECs), including squamous AEC1s and cuboidal AEC2s, are crucial for gas exchange. AEC1s cover approximately 95% of the respiratory membrane, while AEC2s, also progenitor cells for AEC1s, contribute to repair and innate immunity by releasing surfactants (30).

Experimental studies comparing young (2–3-months-old) and aged (26-months-old) rats revealed a decrease in alveolar epithelial cell (AEC) proliferation and surfactant protein levels in older rats, alongside an increase in apoptosis rate. Furthermore, an electron microscopy of aged lungs showed significant degenerative changes in AEC2s, with shorter telomere mice displaying cellular senescence markers like inflammation and immune responses (31). This senescence leads to prolonged oxidative stress and inflammation, impairing gas exchange across the alveolar membrane (32). Additionally, single-cell transcriptional analysis indicated an upregulation of MHC class I on aged AEC2s, highlighting aging's impact on immune responses (33).

Endothelial cell

Endothelial cells line the inner walls of blood vessels, forming a single layer crucial for maintaining vascular health through tight junctions and adhesion molecules like vascular endothelial cadherin (34, 35). They regulate blood vessel tone, permeability, and inflammation, playing a key role in vasodilation via nitric oxide (NO) production (36). Aging impairs these functions, leading to decreased NO synthesis and disrupted vascular relaxation, affecting molecules such as ICAM-1 and PAI-1 that are involved in inflammation and thrombosis, thereby increasing the risk of atherosclerosis and respiratory diseases (37). While insights are mainly from rodent studies, more research is needed to fully understand these mechanisms.

Airway smooth muscle

Airway smooth muscle (ASM) plays a pivotal role in airway size regulation, utilizing adhesion molecules like E-cadherin and

VCAM1 for stability and inflammation prevention (38). It interacts with extracellular matrix components via integrins to modulate contractility (39). Desmin, a cytoskeletal protein, is vital for cell shape, intracellular transport, and organelle organization, with its expression decreasing in aged lungs, potentially reducing airway contractility (40, 41). Conversely, the expression of alpha-smooth muscle actin and vimentin might increase in the distal airways of elderly lungs, indicating possibly enhanced peripheral airway contractility (41). These findings highlight complex age-related alterations in ASM function that warrant further investigation.

Pulmonary progenitor cells

Pulmonary progenitor cells, vital for lung development and repair, differentiate into cell types like alveolar and capillary endothelial cells. Found in alveolar and airway regions, AT2 cells are key alveolar progenitors, transforming into AT1 cells for gas exchange upon stimulation (42). Research reveals two AT2 subtypes: surfactant producing and AT1 differentiating (43). Airway basal progenitor cells ensure lung stability and repair, generating various lung cells post-damage (44, 45). Interstitial progenitor cells, or fibroblasts, contribute to alveolar remodeling. Aging decreases stem cell numbers and repair efficiency, leading to diseases like emphysema and pulmonary fibrosis (46). The effect of aging on lung stem cells and remodeling needs further exploration. Understanding how aging impacts airway function is vital for improving elderly health.

Interstitial region of the lung

The lung interstitium, situated between lung parenchyma, consists of connective tissue, lymphatics, nerve fibers, and blood vessels, crucial for structure, nutrition, and gas exchange support. It encompasses the central and peripheral fibrous systems and septal tissue, essential for maintaining alveolar-capillary gas exchange integrity.

Fibroblasts are an important component of the interstitial region, generating extracellular matrix (ECM) components like collagen fibers, and matrix metalloproteinases (MMPs) play a key role in tissue integrity. Aging fibroblasts are implicated in lung remodeling and respiratory diseases (47). To understand the changes in fibroblasts under the influence of aging, several research groups have shown altered ECM protein expression, as evidenced by proteomics and microarray studies (48). Additionally, single-cell RNA sequencing indicates decreased collagen XIV and decorin in aged fibroblasts, affecting the lung tissue's integrity and elasticity (49). Researchers have utilized methods like microarray, liquid chromatography-mass spectrometry, and atomic force microscopy to study the ECM in the lung and its relation to aging (49–52). They identified at least 32 age-related proteins in the lung's ECM, whose changes disrupt its biomechanical balance, leading to aging-related damage in lung tissues.

The pulmonary microenvironment represents a complex ecosystem, wherein each component plays a pivotal role in the aging process. When exploring the impact of the pulmonary microenvironment on health, an unavoidable question emerges: does cellular senescence constitute the core driving force behind pulmonary aging? This question is thought-provoking, as it is closely related to the decline in lung function and the onset and progression of pulmonary diseases. Cellular senescence is a multifactorial-driven process, involving alterations in gene expression. In the lungs, this process may be accelerated by factors such as environmental pollutants, smoking, and chronic inflammation. Therefore, understanding how cellular senescence affects the pulmonary microenvironment, and how to intervene in this process to decelerate pulmonary aging, has become a focal point of current research.

Immunity and inflammation in aging lung

Aging significantly impacts pulmonary immunity by affecting immune cells in the lungs. Alveolar macrophages (AMs), crucial for innate immunity, show altered cytokine secretion and reduced phagocytosis abilities with age, leading to slower immune responses (53, 54). Other immune cells also experience quantitative and functional declines, affecting monocyte production and T- and B-cell receptor expression, ultimately compromising lymphocyte function (55). Research suggests that the aging phenotype of circulating monocytes is influenced by the pulmonary microenvironment, highlighting the role of the aging microenvironment in immune function changes (56). Immune senescence in the elderly increases susceptibility to infections and lung diseases, emphasizing the importance of understanding age-related changes for improving respiratory disease outcomes in older individuals.

Innate immunity

Innate immunity, our first line of non-specific defense present from birth, includes barriers like skin and internal components such as phagocytes (e.g., neutrophils, macrophages) and natural killer cells. These elements identify and fight off pathogens, triggering inflammation for pathogen removal and tissue healing. However, aging can weaken these immune cells, disturbing the balance of inflammatory responses in the lungs. This imbalance exacerbates outcomes in elderly patients with inflammatory lung conditions. This section delves into the primary innate immune cells in the lungs and how aging affects their functionality.

Alveolar macrophages

AMs, part of the mononuclear-phagocyte system, are long-lived and numerous, playing critical roles in pulmonary immunity by collaborating with bronchial perivascular interstitial macrophages (IMs) and pulmonary epithelial cells (57). They clear debris and toxic particles, produce anti-inflammatory factors like IL-4 and IL-10, and are key in tissue damage control and initiating inflammatory responses (58, 59). Additionally, AMs recognize stimuli through PRRs, activating signaling pathways and cytokine release (e.g.,

TNF-α, IL-6) from epithelial cells, thus recruiting immune cells and promoting inflammation. Impaired AM function can lead to chronic inflammation or fibrosis due to the accumulation of activated AMs and excessive immune cell recruitment.

With aging, the decline in AM number and functionality impairs pulmonary innate immunity, increasing susceptibility to chronic inflammatory lung diseases in the elderly (60). Aged AMs exhibit weakened phagocytosis and pathogen clearance, reduced lipid breakdown, and increased lipoprotein deposition in alveoli (60–62). Moreover, aged macrophages produce fewer chemokines and cytokines, weakening the innate immune response (63). Age-related changes in cell communication and PRRs expression heighten vulnerability to infections (64). Elevated reactive oxygen species (ROS) levels with age further diminish AM function (65, 66). Consequently, reduced AM efficacy leads to heightened lung inflammation and tissue damage in the elderly.

Dendritic cells

Dendritic cells (DCs) are located in the alveoli, alveolar septa, and lung lymphatic tissues (67). They play a key role in antigen presentation and immune regulation. Despite similar morphologies between young and aged DCs, upon encountering foreign antigens, DCs utilize their dendritic projections to capture and internalize these antigens. Following internalization, antigens are processed and presented on the DC surface as antigen–protein complexes via MHC molecules. Stimulated by PRRs, DCs produce cytokines like TNF-α and IL-6, and mature DCs migrate to pulmonary lymph nodes to present antigen information to T cells, facilitating their differentiation into effector or memory T cells. This antigen presentation process is vital for immune response regulation.

In summary, DCs play a vital role in lung immune responses, but their number and function decline with age, leading to reduced antigen capture and processing abilities (68, 69). Therefore, these changes contribute to raise the risk of respiratory diseases potentially.

Innate lymphocytes

Innate lymphocytes, categorized into ILC1, ILC2, ILC3, and NK cells, are pivotal in immune defense. NK cells, part of Group 1 with ILC1, are notable for their capacity to eliminate tumor and infected cells by detecting changes like the absence of MHC-I molecules on the cell surface and by secreting cytotoxins (e.g., perforin) and cytokines (IFN-γ and TNF-α) (70). Their decline with age increases the risk of lung diseases in the elderly by impairing immune functions (71). ILC2 cells, through IL4 and IL5 secretion, target extracellular pathogens and allergens, while ILC3 cells, producing IL17 and IL22, aid in lymph node development. Collectively, ILCs are crucial in pulmonary health and innate immune system regulation.

Neutrophils

Neutrophils, comprising 50%–70% of white blood cells, are essential for the immune response, rapidly migrating to infection sites via chemotaxis and utilizing lysosomal enzymes to digest pathogens and debris, thus preventing infection spread (72). They also recruit additional immune cells by releasing inflammatory mediators. However, aging leads to decreased bone marrow production and reduced neutrophil counts, alongside diminished antioxidant capacity and increased ROS production, impairing phagocytosis and heightening infection risks (73–75). Studies indicate an age-related increase in neutrophils within bronchoalveolar lavage fluid (BAL) and imbalances in injury models (75, 76). Therefore, we can conclude that aging and injury prolong neutrophil recruitment times, causing accumulation in lung tissue and exacerbating pulmonary diseases and inflammation (76–78).

Adaptive immunity

Adaptive immunity combats foreign pathogens through specificity, memory, cell dependence, and clone selectivity. It targets specific pathogens via receptors on B and T cells. Memory allows for a rapid response upon re-exposure to the same pathogen, facilitated by long-lasting immune cells generated after initial contact. Clone selectivity, through diverse B- and T-cell clones, ensures effective, enduring protection against various pathogens.

Bronchus-associated lymphoid tissue (BALT) is a lymphoid tissue present beneath the respiratory mucosal layer, including lymph nodes, lymphoid follicles, and diffuse lymphoid tissue, playing a role in immune surveillance and defense, thereby protecting the respiratory system from infection and disease.

T lymphocytes

T lymphocytes, critical for cell-mediated immunity, originate as precursor cells in the bone marrow and mature into naive T cells in the thymus, expressing CD4+ or CD8+ for antigen recognition. In the elderly, naive T-cell production and TCR diversity decline due to miR181a deficiency and increased dual-specific phosphatase (DUSP)6 activity (79). These cells, upon antigen exposure and cytokine activation (e.g., IL-2, IL-4), differentiate into effector and memory T cells, with effector cells being either helper T cells (Th) releasing cytokines to modulate immune responses or cytotoxic T cells (CTL) that eliminate infected or cancerous cells through perforin and granzyme B. CD4+ T cells diversify into Th1, Th2, and Th17 based on cytokine profile, while Th17 and Treg cells share a precursor requiring TGF-β for differentiation (80). Aging impacts T-cell quantity and functionality, manifesting as reduced CD8+ T-cell proliferation, increased apoptosis susceptibility in CD4+ cells due to elevated CD39 expression, and diminished pathogen clearance, leading to compromised pulmonary immunity (81). This contributes to immune senescence, characterized by a delayed response to new antigens and inefficient immune memory formation.

B lymphocytes

B-cell development initiates in the bone marrow from hematopoietic stem cells, requiring BCR ligand binding for progression. Immature B cells evolve through T1 and T2 transitional stages. Driven by CXCL13 and CXCR5, they migrate

to the spleen, becoming T1B cells and further mature into T2B cells (82). These T2B cells differentiate into either follicular or marginal zone cells based on receptor signals (83). Naive B cells, which have not encountered antigens, include all spleen-resident B cells. Upon injury and inflammation, B cells activate, producing plasma cells that secrete antibodies, including immunoglobulins (Ig) and complement, and memory B cells for sustained immune memory against antigens, which protects the human body (84). Age affects B-cell development, particularly from naive to mature stages, with elderly mice showing increased inhibitory TFR cell expansion, fewer initial and immature B cells, and reduced antibody specificity and affinity, raising the risk of lung diseases in the elderly (85, 86).

Although there have been many studies on age-related changes in innate and adaptive immunity, the question of how immune impairment leads to lung diseases and increases mortality risk still remains. The combination of individual genetics and environmental changes still brings us many unknowns and challenges. To solve this problem, multi-omics methods have been used to longitudinally describe individual immune systems, which has also facilitated the development of "immune aging" scores that better describe an individual's immune state than their actual age (87). This study and others have emphasized an important concept that actual age is not a reliable indicator of biological age.

Senescence mechanism related to pulmonary disease

Aging can lead to a decrease in the number and functional defects of lung stem cells, and pulmonary remodeling. One of the morphological characteristics of senescent lungs is the decrease in bronchioles and increased pulmonary alveolar diameter. Previous text has detailed the physiological functions and morphological changes in aging lungs. At the molecular and cellular levels, several aging mechanisms have been proposed by López-Otín et al., including cellular senescence, mitochondrial dysfunction, immunosenescence, and homeostatic disruption, which act on the pulmonary epithelium, impairing its repair function, resulting in loss of "fidelity", and manifesting in related pathological findings such as fibrosis and airway wall remodeling. These have been demonstrated in diseases such as COPD, idiopathic pulmonary fibrosis (IPF), and acute respiratory distress syndrome (ARDS) (88–91). It should be noted that although cell senescence is related to disease, it is also a normal life activity of the normal lung tissue to maintain homeostasis (92, 93). Next, we will explore how these aging mechanisms causally contribute to pulmonary diseases and identify potential therapeutic targets.

Aging and cell senescence

Aging leads to declines in body function, with notable impacts on lung elasticity and function due to increased stiffness and tissue composition changes (94). At the cellular level, aging is characterized by reduced cell function, cell cycle arrest (mediated by proteins like Cdkn2a and Cdkn1a), or increased apoptosis, connecting subcellular damage such as protein homeostasis disruption and mitochondrial damage to organ aging (95). Specifically, in lungs, aging impairs AEC2 cells, crucial for organ function, by hindering the differentiation of pulmonary epithelial progenitor cells, weakening defense and immune clearance, for example, via HLA-E inhibition (96). The risk of respiratory diseases increases with senescent cell accumulation, with older mice showing more severe lung damage and slower recovery than younger ones (97–99). Senescent cells, although non-replicating, release the senescence-associated secretory phenotype (SASP)—a cocktail of cytokines, growth factors, and enzymes—which plays roles in wound healing, immune response, and aged cell clearance (100). These factors can activate surface receptors like TNFR and ILR, triggering intracellular signaling pathways and activating NF-κB to regulate inflammation and the cell cycle through NEMO, dependent on ATM phosphorylation (101).

Cellular activities significantly depend on age, making the study of cell aging vital for disease understanding and prevention. Despite considerable progress in cell aging research, its mechanisms remain complex and variable, necessitating further in-depth exploration.

Mitochondrial dysfunction

As cells age, mitochondria experience increased volume, loss of cristae, and inner membrane damage (102–104). Aging disrupts protein homeostasis in mitochondria, damages mitochondrial DNA (mtDNA), and leads to the formation of superoxide-generating electron transport chains (105–107). These changes activate inflammatory pathways like NF-κB, causing inflammation and impairing mitochondria's ability to manage energy metabolism and cell death regulation. This mitochondrial dysfunction is linked to diseases such as IPF, COPD, and severe asthma, with increased damaged mtDNA found in lung tissues of these patients (102, 108–111). Simultaneously, studies indicate that mitochondrial dysfunction contributes to aging, suggesting a cyclical relationship (65, 66).

Inflammation and aging

Inflammation has progressed to a chronic state due to lifestyle and biological factors in aging, involving the accumulation of "metabolic waste" triggering inflammation. Misfolded proteins and cell debris activate immune responses by binding to PRRs. Chronic stimuli in aging lungs cause sustained inflammation, leading to tissue damage and an imbalance between pro- and anti-inflammatory actions. Neutrophils release factors like IL, TNF-α, and IFN, increasing systemic pro-inflammatory cytokines and oxidative stress (112). Targeting TNF-α in mice can speed up aging and inflammation. While some inflammation is crucial for fighting pathogens, an excess can damage lung tissue and lead to diseases. Neutrophils release NETs, which have both antibacterial

benefits and immune-regulating effects, but excessive production can worsen COPD (73).

It has been found that the intestinal microbiota of elderly people also undergoes certain changes with the body's inflammatory response (113). Ecological imbalance in the elderly, marked by a shift from anti-inflammatory to pro-inflammatory microbial products in the gut, contributes to inflammation. Additionally, aging lung and adipose cells release SASP, further intensifying inflammation and its associated damage, linking adipose tissue dysfunction with systemic inflammation and aging (114).

Immunosenescence

Immunosenescence leads to a slow yet prolonged immune response, especially in aging T and B cells, lowering resistance to infections and cancer. Aging diminishes AT2 cells' renewal and differentiation, weakening immune functions. Aged lungs have fewer effective macrophages in phagocytosis, chemotaxis, and antigen presentation. Single-cell sequencing shows that in IPF patients, aged macrophages come from circulating monocytes, not from lung progenitor cells (115). Puchta et al. found that the senescent phenotype of monocytes in elderly mice is linked to the aging bone marrow microenvironment rather than being intrinsic to the cells (55). Adaptive immunity is also compromised in the elderly, with reduced lymphocyte activation, humoral responses, and lower counts of naive T cells and receptors. The balance between Th17 cells, which promote autoimmunity and inflammation, and Treg cells, which suppress these responses and maintain immune homeostasis, is disrupted (80).

Immune aging contributes to age-related lung diseases, reducing resistance to infections, changing throat microbiota, and increasing harmful bacteria. These factors, combined with lower respiratory function, difficulty swallowing, and poor vocal cord coordination, raise pneumonia risk by allowing bacteria into the lower respiratory tract. In severe asthma, COPD, and IPF, macrophage activity and T-cell activation are decreased due to less phagocytosis and lower T-cell CD28+ expression, resulting in immune function decline (116–122).

Autophagy

Autophagy, critical for cellular cleanup and turnover in lung cells, involves forming autophagosomes to degrade unwanted components, a process regulated by autophagy-related genes (ATGs) and microtubule-associated proteins (e.g., MAP1LC3B) (123). Key regulators, including transcription factor EB (TFEB), transcription factor A (TFAM), and mammalian target of rapamycin (mTOR), influence this pathway. Aging activates mTOR, leading to increased cell proliferation and reduced autophagy (124).

Autophagy's disruption, particularly with aging, is linked to lung diseases like fibrosis, COPD, PAH, and cancer. Studies indicate that older mice and IPF patients show more significant declines in autophagy and related inflammation markers. The process where epithelial cells transform and migrate, known as EMT, is key in fibrosis. PINK1, a kinase in mitochondria, is crucial for mitophagy and mitochondrial health, impacting lung function (102, 108). The PINK1-PARK2 pathway, crucial for mitophagy, when impaired, increases the risk of pulmonary fibrosis and hastens cell aging. Mitophagy, vital for lung function due to high energy needs, is disrupted in this pathway, worsening conditions like COPD by enhancing cell damage and aging. Targeting autophagy with treatments like mTOR inhibitors, including rapamycin and everolimus, offers new strategies for managing diseases, notably cancer (102, 108, 125).

Nutrition sensing and metabolism

Nutrient-sensing pathways in lung tissues change with aging, impacting metabolism. AEC2 cells adjust metabolism based on nutrient and energy levels, responding to stress or hypoxia. Disruption of regulatory pathways (HIF2a, AMPK, and mTOR) with aging impairs nutrient sensing (126). Nutrient-sensing pathways in lung tissues change with aging, impacting metabolism. AEC2 cells adjust metabolism based on nutrient and energy levels, responding to stress or hypoxia. Disruption of regulatory pathways (HIF2a, AMPK, and mTOR) with aging impairs nutrient sensing (127–129). Similar changes are also observed in COPD and severe asthma (130–132). Enhanced insulin-IGF-1-mTORC1 signaling also accelerates the aging process, being the major accelerator of aging (4, 133). Targeting nutrition-related pathways, such as inhibiting the insulin-IGF-1-mTORC1 axis, has shown potential in extending lifespan (6).

Self-DNA

Self-DNA, released from the nucleus or mitochondria due to cell senescence or damage, acts as a DAMP, triggering autocrine and paracrine inflammatory responses through PRR activation, potentially causing tissue damage and inflammatory diseases (134). Elevated free DNA levels in IPF, COPD, and severe asthma patients' blood and sputum indicate self-DNA's role in age-related lung conditions (135). Additionally, neutrophil aggregation and heightened NET production in response to stimuli like IL-8 are noted in COPD and severe asthma (136–138). mtDNA, a key self-DNA source, is particularly effective in inducing lung damage/inflammation. Studies have shown that a link exists between increased systemic inflammation and higher free DNA levels in the bloodstream (139–141).

Oxidative stress

Oxidative stress occurs when cells produce excess reactive oxygen species (ROS), overwhelming antioxidant defenses and causing cellular damage. ROS, including superoxide ions and hydrogen peroxide, are normal metabolic byproducts essential for signaling and defense mechanisms. However, their imbalance can

lead to oxidative damage, contributing to lung diseases. Theories linking ROS accumulation with aging, such as the free radical aging theory and mitochondrial aging theory, emphasize the impact of ROS on age-related changes (142, 143). Elevated ROS levels have been associated with respiratory conditions like pulmonary fibrosis and lung cancer (144).

Oxidative stress negatively affects lung diseases like pulmonary hypertension, COPD, and fibrotic lung disease, with the antioxidant NAC known for counteracting free radical-induced mutagenesis (145). This dual nature highlights the importance of a balanced approach in using antioxidants for lung tissue rejuvenation, acknowledging both their potential benefits and risks in promoting tumorigenesis. Given its significant role in lung health, understanding oxidative stress in lung aging is crucial for unraveling the mechanisms behind lung diseases and maintaining lung health.

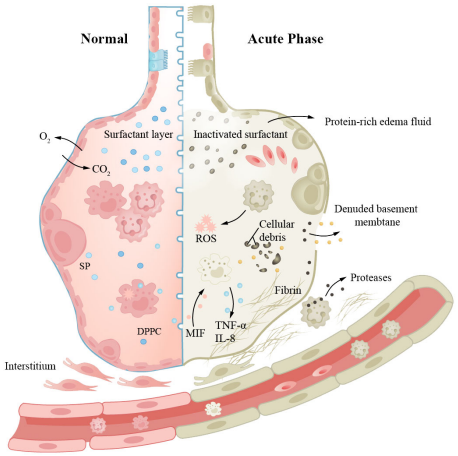

FIGURE 1
Aging increases the risk of ARDS, and epithelial cell senescence may be a key factor. The left side represents "normal", while the right side represents "acute injury". Aging leads to an increased probability of infection, immune dysregulation, and pathological manifestations such as damaged alveolar-capillary barrier, inactivation of surfactant, and formation of intra-alveolar hyaline membranes, resulting in pulmonary edema and inflammatory manifestations. Prolonged disease duration can also lead to pulmonary fibrosis.

Age-related pulmonary disease

ARDS

ARDS is a severe and urgent form of lung injury that typically occurs after severe trauma, severe infection, or surgery. The pathological findings include injured alveolar capillary barriers, decreased surfactant, formation of hyaline membranes within alveoli, and alveolar collapse, leading to pulmonary edema, inflammatory manifestations, and respiratory distress with hypoxemia (146, 147). In the acute phase, rapid coagulation and overactive inflammation response result in excessive inflammatory response and lung damage and dysfunction. The ability of the body to repair damaged tissues and restore lung function depends on the severity and duration of the disease. Otherwise, excessive fibrosis will lead to pulmonary fibrosis (146).

Studies have shown that aging increases the risk of ARDS; epithelial cell senescence may be crucial (91, 148). AEC2s senescence, reduced pulmonary stem cell storage, and impaired normal repair may lead to ARDS. In ARDS patients, senescence results in more severe illness and poorer prognosis. In addition, some biological processes associated with ARDS, such as infection, inflammation, and oxidative stress, are also related to aging mechanisms (Figure 1). For ARDS patients, mechanical ventilation is usually required to maintain respiration and oxygenation. Ventilation strategies and positive end-expiratory pressure (PEEP) levels need to be chosen according to patient conditions. Severe infection is a high-risk pathogenic factor for ARDS, and it is also a common complication and cause of death following non-infectious ARDS. Aging increases the likelihood of infection, exacerbates immune and inflammatory disorders, and is closely associated with mortality in ARDS patients. Severe SARS-CoV-2 infection may involve long-term pulmonary fibrosis after ARDS; the degree of fibrosis is associated with mortality (149, 150). Antibiotic treatment should be started as early as possible, using broad-spectrum antibiotics and providing sufficient dosage and course. The role of glucocorticoids in ARDS treatment is still controversial, but they are effective in anti-inflammatory and pulmonary fibrosis remission. For ARDS patients, mechanical ventilation is typically required to maintain respiration and oxygenation. The ventilation strategy and PEEP level need to be selected according to the patient's condition. Prone positioning has been shown to improve gas exchange and respiratory mechanics in ARDS patients (151), but it must be performed with caution to avoid damaging vascular catheters and endotracheal tubes. Studies have shown that ARDS patients usually have lower Health-Related Quality of Lif (HRQoL) scores, and some patients may experience long-term mental health problems, such as anxiety and depression, which will further affect their quality of life. Research on how to enhance patient symptoms and prognosis is ongoing.

COPD

COPD is a common chronic inflammatory lung disease in the elderly. Clinical research indicates that one-fifth of all hospitalized patients aged 75 and older have COPD, highlighting the age-dependent nature of the disease. It is characterized by cough and exertional breathlessness, with irreversible damage to pulmonary function. Smoking, air pollution, and occupational exposure are contributing factors, with smoking being the most important. Patients have long-term inflammation in their small tracts, eventually leading to tissue fibrosis and AWR. We find that in normal aging lungs, the tissue is also in a state of chronic inflammation, similar to the pathological state of COPD patients (152). Airway stem cell (such as club cell) senescence leads to decreased renewal and differentiation functions, resulting in AWR. Age-related changes in respiratory structure and function increase the susceptibility of the elderly to COPD (153–157). Scientists also

propose whether the disease triggers change in the baseline level of normal aging lungs (152). Studies have found that there are numerous aging epithelial cells and fibroblasts in patient tissue sections. Fibroblasts isolated from diseased lungs show senescent phenotype and abnormal repair capacity (158). Monocytes derived from circulating blood play a crucial role in pulmonary fibrosis (159), where macrophage phagocytosis activity is decreased, through the action of CXC chemokine subfamily members, interacting with relevant receptors on CTL and monocytes; secretion of corresponding cytokines leads to damage of alveolar epithelial cells (Figure 2). The pro-inflammatory cytokines (IL-6 and TNF-α) and MMPs produced by these macrophages are associated with disease severity. Basal cells, as progenitor cells of the airway, have their self-renewal and differentiation abilities impaired after disease onset, leading to delayed wound healing and even abnormal healing (160, 161). Clinical control experiments show that COPD patients secrete more SASP and the secretion increases with age (162). Scientists detected excessive ROS in patient lung tissues and BAL, accompanied by reduced mitochondrial respiration and corresponding increased levels of damaged mtDNA (163). Cilia are cell organs on the surface of airway epithelial cells that can clear mucus and bacteria from the respiratory tract through regular movements. Decreased ciliary clearance function is also an important cause of airway inflammation and infection in COPD patients. Studies have found that the ciliary clearance function in COPD patients is significantly lower than that in healthy individuals, which may lead to bacterial retention and proliferation in the respiratory tract, thereby causing infection and inflammation.

Aging is an independent risk factor for COPD, and various stimuli that promote aging pathways deserve our attention and discussion. Smoke contains a large number of harmful chemicals, such as tar, carbon monoxide, and nicotine, which cause oxidative stress in lung cells, generate free radicals, damage cell DNA, shorten telomeres, and accelerate cell aging. It also triggers inflammation, leading to cell and tissue damage, and ultimately reduces lung elasticity and fibrosis. Emphysema is a chronic lung disease characterized by the destruction of alveolar walls and excessive inflation of alveoli. Smokers are more susceptible to it than non-smokers. Klotho is a b-glucuronidase that has been found to be deficient in the early stage, which may contribute to lung tissue damage and inflammation (164). In smokers, Klotho levels are further reduced, making the lung tissue more sensitive (165).

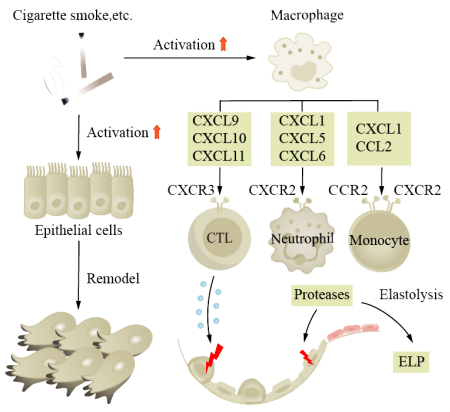

FIGURE 2
Aging increases the susceptibility to COPD and promotes its progression. Smoking is a major risk factor for the disease, causing long-term inflammation of the small airways, ultimately leading to tissue fibrosis and airway wall remodeling. In aged lungs, the function of airway progenitor cells decreases, resulting in chronic inflammation. Macrophages, under the influence of chemokine CXC subfamily, damage alveolar epithelial cells. ELP, exogenous lipoid pneumonia.

AECOPD, or the acute exacerbation of COPD, refers to a persistent deterioration beyond the daily situation in a short period of time, 80% of which is caused by bacteria. It is characterized by shortness of breath, increased sputum production, and purulence (11, 166). Common diagnostic methods include bacterial culture and PCR detection. Antibiotics are the mainstay of treatment, and the choice of antibiotics should be based on the pathogen. Traditional Chinese medicine, such as Yupingfeng, is also effective in treating COPD, especially for patients with severe cough and sputum situation (167, 168). Acute exacerbations put COPD patients at risk of pulmonary failure, severe damage to pulmonary function, and decreased quality of life.

IPF

IPF is the most common type of fibrotic interstitial lung disease (ILDs), which will be focused on here. IPF is a progressive interstitial lung disease characterized by progressive breathlessness, coughing, and chest pain. The lung tissue alternates between injury and repair, eventually leading to the formation of large amounts of fibrotic tissue and even scars, reducing pulmonary elasticity and impairing gas exchange function (169). The etiology and pathogenesis of IPF are complex. The specific cause is still unclear; it has been found that adult mouse AEC2s senescence leads to pulmonary fibrosis, which is similar to humans, and fibrosis is associated with p21/p53 and TGF-β. Researchers found that mice exhibited reduced pulmonary fibrosis after treating selective anti-aging AEC2s (170). Currently, there is research evidence indicating that pulmonary fibrosis is associated with high glycolytic behavior. Inflammatory response is a crucial step in initiating lung tissue remodeling, as inflammatory cells release inflammatory cytokines, chemokines, and enzymes that damage alveolar walls and surrounding tissues. Fibroblasts are activated and secrete collagen, elastin, and extracellular matrix components such as proteoglycans, which continue to produce and deposit in damaged areas, eventually forming fibrotic scar tissue. The TGF-β/Smad signaling pathway is considered a key regulatory factor for pulmonary fibrosis (171). TGF-β binds to cell surface receptors, activating the Smad signaling pathway and promoting fibroblast proliferation and collagen synthesis and ECM remodeling. The Wnt/β-catenin signaling pathway also plays a role in the pathogenesis of IPF. Wnt proteins bind to cell surface receptors, leading to the accumulation of β-catenin in the cell nucleus, activating downstream genes and causing pulmonary fibrosis (172). The TNF-α/NF-κB signaling pathway is a classic pathway. In this

pathway, TNF-α binds to cell surface receptors, activating the NF-κB (nuclear factor-κB) signaling pathway, leading to inflammation and fibrosis (Figure 3). Furthermore, patients with pulmonary fibrosis may exhibit mtDNA damage, manifesting premature aging symptoms and inflammatory responses (163).

The repair capacity of aged lungs decreases, and the repair process does not end with the removal of fibroblasts, but rather produces a continuous fibrotic response, which is associated with a positive feedback of fibroblast apoptosis inhibition. This positive feedback refers to the ability of fibroblasts to produce signals that inhibit their own apoptosis, thus reducing or preventing their own death (173, 174). In some chronic inflammatory lung diseases, fibroblasts can produce various growth factors and cytokines, such as TGF-β, epidermal growth factor (EGF), and IL-6, which promote fibroblast proliferation and migration and inhibit their apoptosis. Clinical studies have shown that those who survive acute diseases are often affected by long-term lung damage and reduced HRQoL. IPF patients usually show earlier aging-related physiological changes than healthy individuals. Moreover, researchers have found that aging-related genes (SIRT1, SIRT2, and FOXO3) and proteins (β-galactosidase) may play a role in the pathogenesis of IPF. Although the connection between age and IPF is established, the interplay between other contributing factors and age remains unknown. Further investigation is required to elucidate the specific signaling pathways and molecular interactions involved in the regulation of these processes. Genetic factors also contribute to the disease; mutations can make individuals more susceptible to pulmonary fibrosis. Environmental factors, such as smoking and occupational exposure, may also affect the incidence of IPF.

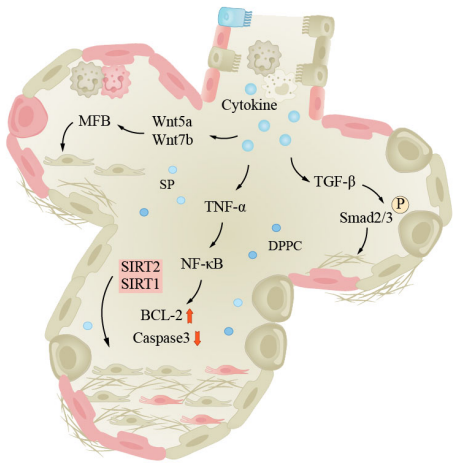

FIGURE 3
Lung fibrosis under the influence of aging. The pathogenesis of IPF is complex, inflammation is an important process in pulmonary tissue remodeling, and aging is a significant factor in inducing infection. The pathways shown in the figure are important pathways for inflammation-induced pulmonary fibrosis. Smad, Smad protein; TGF-β, transforming growth factor-beta; TNF-α, tumor necrosis factor-α; Wnt/β-catenin, wingless/β-catenin pathway; NF-κB, nuclear factor-κB.

Pneumonia

Pneumonia is a pulmonary inflammation caused by bacteria, viruses, fungi, or parasites. The common pathogenic bacteria of bacterial pneumonia are pneumococcal bacteria, which are the most common cause of community-acquired pneumonia (CAP) in the elderly, mainly affecting the pulmonary parenchyma (175). The main pathogenic viruses of viral pneumonia are influenza viruses and coronaviruses, mainly affecting the pulmonary interstitium. The main symptoms of pneumonia include coughing, fever, shortness of breath, and chest pain. According to World Health Organization data, CAP is the most common type of pneumonia; the mortality rate of pneumonia is approximately 12% in developing countries and approximately 9% in developed countries (176). Generally, the mortality rate of ordinary pneumonia is low, while severe pneumonia and infection with viruses such as COVID-19 have higher mortality rates. Age is a risk factor that increases the elderly's susceptibility to pneumonia. The elderly have weakened lungs in clearing pathogens, with impaired ciliated epithelium clearance in the airways and swallowing clearance mechanisms, increasing the risk of pneumonia, excessive bacterial adhesion and accumulation in the lungs can easily lead to community-acquired pneumonia (37, 175, 177–180). With increasing age, the body's immune regulatory function decreases, and the risk of pulmonary infection increases. In elderly chronic pulmonary inflammation, TNF-α can induce epithelial cells to express more TNF receptors and enhance the inflammatory response. In addition, oxidative stress can also lead to the upregulation of epithelial cell surface receptors, such as peroxisome proliferator-activated receptor (PPAR). At the same time, the lung function decline in the aging process and damage to mitochondria can lead to telomere damage and increased SASP through the NF-κB pathway, triggering a series of subsequent reactions, increasing the risk of pneumonia (Figure 4). The main treatment methods for pneumonia are anti-infection and symptomatic treatment. When the disease is critical, broad-spectrum antibiotics should be used first to cover all possible pathogenic microorganisms as much as possible.

Asthma

Asthma is a common chronic inflammatory disease of the airways that can occur at any age. The main characteristics of the disease are hyperreactivity of the airways and airway obstruction. Stimuli such as allergens and cold air trigger excessive reactions in the body's various cytokines and receptors, leading to airway spasm and contraction, and patients experience symptoms such as wheezing, shortness of breath, and coughing. Long-term asthma patients may see an increase in the number of ASM cells, goblet cells, and mucus glands, leading to AWR (39, 181). Although asthma can occur in all age groups, the inflammation and clinical manifestations of asthma in older adults are different from those in younger adults. Studies have shown that severe asthma phenotypes

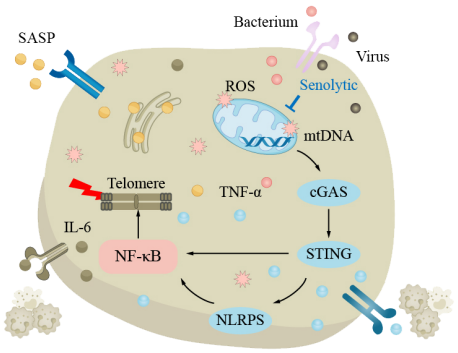

FIGURE 4
The clearance mechanism of the lungs in the elderly is impaired, which increases the susceptibility to pneumonia. In the elderly lungs, excessive bacteria accumulate in the lungs, making pneumonia more likely to occur. The decline in lung function with aging is attributed to elevated levels of reactive oxygen species (ROS) and impaired mitochondrial function, resulting in telomere damage and upregulation of senescence-associated secretory phenotype (SASP) via the NF-κB pathway, triggering a series of subsequent reactions that increase the risk of pneumonia.

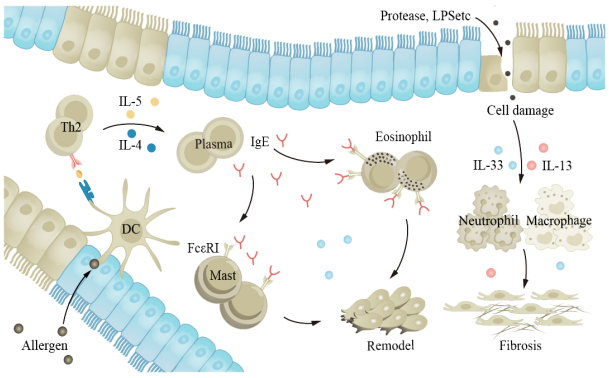

FIGURE 5
The aging lung is more susceptible to allergens and irritants, exacerbating asthma. Allergens and proteases stimulate the airway epithelium, leading to interactions between various cytokines and receptors within the body, promoting inflammation and causing airway constriction. EGF and FGF play a role in the process of airway remodeling in asthma. FGF, fibroblast growth factor; EGF, epidermal growth factor.

are more common in older adults (182). Older adults have decreased pulmonary immune capacity, making them more sensitive to allergens and stimuli and therefore more susceptible to exacerbation of asthma (15, 60, 62, 64, 183). Th2 secrete IL-4, IL-5, and other cytokines, inducing the production of immunoglobulin E (IgE) and promoting inflammation. IgE is an important antibody in asthma; its main function is to bind to the FcεRI receptor on the surface of mast cells and eosinophils, leading to cell activation and the release of inflammatory mediators (Figure 5). Cholinergic M receptors and histamine H1 receptors are also present in ASM cells and mast cells, and activation leads to ASM contraction. The exact cause of AWR is not clear, but it is known that EGF and fibroblast growth factor (FGF) play a role in asthma AWR.

Lung cancer

Cancer is a disease characterized by abnormal proliferation and differentiation of cells, usually caused by gene mutations and expression disorders. Age and genetics can increase the risk of developing cancer. The latest statistical data from the National Cancer Center shows that approximately 4.06 million new cases of malignant tumors are diagnosed in China each year, with lung cancer having the highest incidence and mortality rates among malignant tumors, far exceeding those of colorectal cancer, liver cancer, gastric cancer, and breast cancer (184). Lung cancer is also one of the high-incidence and high-mortality malignant tumors globally, with a 5-year relative overall survival rate of approximately 22% (185). It can be divided into squamous cell carcinoma, adenocarcinoma, large-cell carcinoma, and non-small cell lung cancer (NSCLC), which accounts for approximately 80%–85% of all lung cancers. The occurrence and development of NSCLC are closely related to the expression of cancer driver factor, which include gene mutations, amplification, and abnormal expression. Ultra-deep sequencing of normal human skin and esophageal tissue shows that high levels of somatic mutations exist in normal human tissues (186, 187). These mutations are related to skin squamous cell carcinoma and age-related mutations, suggesting that age-dependent microenvironmental changes in the lung play a key role in the progression of lung cancer.

Currently, known oncogenic drivers include epidermal growth factor receptor (EGFR), anaplastic lymphoma kinase (ALK), ROS proto-oncogene 1 (ROS1), B-Raf proto-oncogene (BRAF), and human epidermal growth factor receptor 2 (HER2). The expression of these oncogenic drivers varies in different subgroups of non-small-cell lung cancer patients. Research has found an interesting phenomenon: in lung cancer patients under 50 years old, there is a higher proportion of lung cancer with targetable genomic changes, such as EGFR mutations, ALK or ROS1 fusions, or ERBB2 insertions. In older lung cancer patients, the proportion of other oncogenic drivers, such as KRAS mutations, BRAF V600E, and MET exon 14 skipping, is higher (62, 188). Therefore, we can target different oncogenic drivers and choose corresponding targeted therapy drugs to inhibit their activity, to achieve the purpose of treating NSCLC. With age, DNA damage and mutations in the human body may increase, increasing the risk of cancer (189). At the same time, some genetic mutations related to cancer may also be associated with aging. Genetic factors also play a promoting role in the occurrence of cancer, but it needs to be emphasized that cancer is not inherited directly, but the susceptibility to cancer is inherited, not the cancer itself. Approximately one-eight of cancers are related to genetic gene mutations, while more are influenced by diet, environment, and lifestyle habits. The immune system in elderly lung cancer patients plays an important role in the development of the disease. The body can recognize and eliminate abnormal cells through immune surveillance; effector B cells produce antibodies to clear cancer

cells, but at the same time, they can also cause inflammatory reactions, exacerbating the condition. Inflammatory cells can secrete some cytokines and chemokines, such as TNF-α, IL-1, and IL-8. These factors can attract more immune cells to the inflammatory site, promoting the growth and spread of the tumor. Meanwhile, inflammatory cells can also damage the DNA of lung cancer cells by releasing free radicals, thereby promoting the malignant transformation of lung cancer cells.

Lung cancer treatment consists of medical and surgical therapies. Chemotherapy, targeted therapy, and immunotherapy are currently common approaches. Immunological checkpoint inhibitors (ICIs) are a type of immunotherapy drug that enhances the immune system's response by inhibiting checkpoint receptor molecules on immune cells (such as cytotoxic T cells) (Figure 6). Examples of targeted PD-1 pathway drugs include pembrolizumab and atezolizumab. Recent studies have shown that the balance of PD-1 expression between effector T cells (Teff) and Treg in the tumor microenvironment can predict the response to PD-1 cancer immunotherapy (63). When the PD-1 on effector T cells binds to PD-L1 on tumor cells, the activity of Teff is inhibited, reducing the ability to attack tumor cells. However, when the PD-1 on Treg binds to PD-L1 on tumor cells, it can enhance the function of regulatory T cells, further suppressing the immune response (190). Although the efficacy of immunotherapy drugs has been reported to decrease, there are currently limited numbers of elderly patients in prospective clinical trials, and we cannot yet draw accurate conclusions (191, 192).

Sepsis

Sepsis is a severe systemic infection syndrome characterized by the growth and reproduction of pathogenic bacteria in a local area, continuous invasion of the bloodstream, and production of toxins. These toxins are then disseminated through the bloodstream, causing obvious toxic symptoms and significant damage to other organs and tissues. The most common source of infection in elderly patients with sepsis is the respiratory tract. The underlying cause is the imbalance between pro- and anti-inflammatory responses in the body. Severe sepsis and septic shock are more severe forms of this condition. Due to abnormal immune function, pre-existing diseases, and age factors, the incidence and mortality rates of severe sepsis and infectious shock increase in elderly patients (193, 194). The mortality rate for elderly patients is 50%–60% (194). Cytokine storm is an overwhelming immune response, characterized by a disproportionate production of cytokines, intensifying inflammatory reactions, and leading to systemic infections in elderly patients, which is a key feature in the pathogenesis of sepsis (195). In the course of disease progression, bacterial lipopolysaccharide is the main molecule that induces the production of cytokines. LPS passes through lipopolysaccharide-binding protein, lipopolysaccharide receptor CD14, and Toll-like receptors to activate antigen-presenting cells such as monocytes, macrophages, and DCs, which produce and release cytokines. In addition, exotoxins act as superantigens, bridging the MHC II class molecules expressed on antigen-presenting cells with the receptors on T lymphocytes, promoting the binding of co-stimulatory molecules CD28/CD86, and inducing the production and release of cytokines by macrophages and T lymphocytes (Figure 7). With age, the oxidative stress response increases, resulting in an increase in the generation of reactive oxygen species, especially in the aging pulmonary vasculature (196, 197). This leads to more severe clinical symptoms in elderly patients (194, 198). Severe sepsis and septic shock patients often require mechanical ventilation, which is independently associated with increased mortality in elderly patients (194, 198).

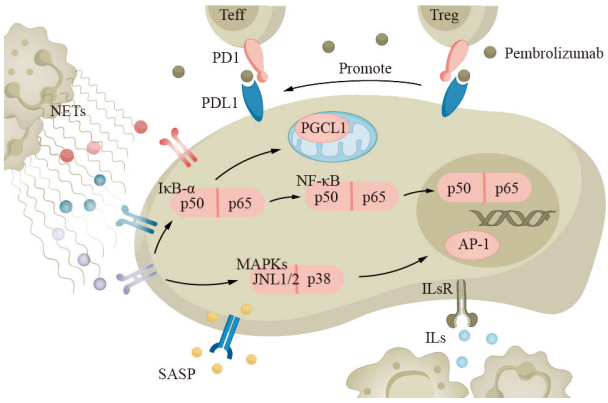

FIGURE 6
The immune system in elderly lung cancer patients plays an important role in the development of the disease. Neutrophils, macrophages, and other inflammatory cells secrete cytokines and chemokines, such as TNF-α and IL-1, which promote tumor growth and metastasis. Tumor cells can evade the immune system through the PD-1 pathway, inhibiting T-cell activity. Immune checkpoint inhibitors (ICIs) like pembrolizumab can suppress the PD-1 pathway and enhance immune response. ICIs, immune checkpoint inhibitors.

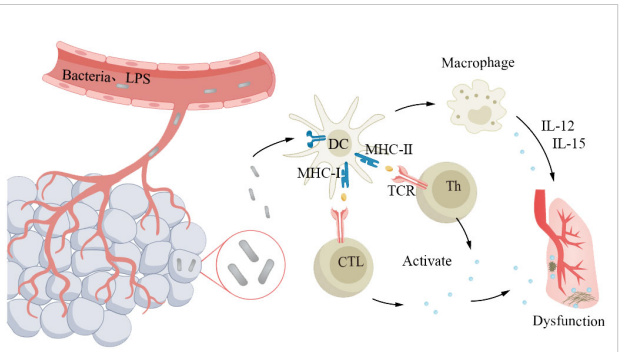

FIGURE 7
Older adults with abnormal immune function are more susceptible to severe sepsis. The pathogen proliferates locally and invades the bloodstream, leading to systemic symptoms and significant lung damage. Antigens primarily interact with the receptors on antigen-presenting cells expressing major histocompatibility complex molecules and T lymphocytes, triggering the release of cytokines from macrophages and T lymphocytes, resulting in pulmonary dysfunction. Elderly individuals experience a decline in immune function, which makes them susceptible to developing a cytokine storm, leading to exacerbated systemic infection.

Targeted aging therapy for respiratory diseases

The treatment options for age-related lung diseases are currently limited. Patients with ARDS are often refractory to treatment, and the efficacy of glucocorticoids (GCs) is generally moderate. The mechanism of action primarily involves the binding of the GC receptor (GR) to NF-κB in a process known as "transrepression" (199, 200). NF-κB serves as a central mediator of inflammation and aging, and it represents a potential therapeutic target for age-related lung diseases (201).

COPD or severe asthma patients may experience symptom relief following GC treatment (202). In patients with GC refractory obstructive airway diseases, the use of theophylline and phosphoinositide 3-kinase delta (PI3K-δ) inhibitors can be considered to reduce the acetylation of GR/histones and achieve therapeutic goals (203). Some novel biologic therapies, such as omalizumab and mepolizumab targeting specific pathways, have shown promise in treating severe asthma patients, although individual responses may vary. The ongoing "Targeting Aging with Metformin (TAME)" trial aims to evaluate the health effects of metformin in individuals aged 65–80, as it may reduce the risk of adverse outcomes in asthma and COPD patients.

Anti-aging drugs possess significant therapeutic potential in pulmonary diseases, particularly for IPF patients, through inducing apoptosis. Studies have shown that anti-aging drugs can effectively restore the physical function of IPF patients, often combining dasatinib and quercetin. Dasatinib is a selective tyrosine kinase inhibitor that is commonly believed to mitigate the degree of pulmonary fibrosis and improve patients' lung function and quality of life, whereas quercetin can inhibit inflammatory responses and fibrotic processes. The combination of both drugs has a synergistic effect, known as the Dasatinib–Quercetin (DQ) mixture. Another therapeutic approach called senomorphics works by intervening in specific mechanisms during the aging process rather than inducing cell apoptosis (204).

Targeted therapeutic strategies that activate DNA via PRRs can mitigate inflammatory responses in age-related pulmonary diseases. By inhaling recombinant DNaseI, high levels of extracellular DNA released by inflammatory cells after pulmonary infection can be degraded, thereby reducing inflammation (205, 206). H-151 is a potent STING inhibitor that achieves its therapeutic effect by inhibiting the cGAS-STING axis. Overall, DNaseI and H-151 exhibit potential therapeutic effects in pulmonary injury and disease models. However, further research is needed to demonstrate their efficacy and determine their potential impact in clinical applications.

Targeted therapy for lung cancer involves treatment strategies aimed at specific molecular targets within lung cancer cells. These targets can include aberrantly active proteins, mutated genes, or overexpressed receptors. By attacking these targets, tumor cells can be targeted more precisely while minimizing damage to normal cells. EGFR is a tyrosine kinase receptor whose aberrant activation or mutation is associated with the development and progression of certain NSCLC. Drugs targeting EGFR include Gefitinib and Erlotinib. ALK gene fusion is common in some NSCLC patients, and drugs targeting ALK include Crizotinib and Alectinib. These drugs inhibit the activity of ALK fusion proteins, blocking tumor cell proliferation. Additionally, previously mentioned PD-1 and PD-L1 immune checkpoint proteins help tumors evade immune attack by inhibiting immune responses in the tumor microenvironment. Targeted drugs include Pembrolizumab and Nivolumab.

We are all aware of the close association between the development of sepsis and the abnormal release of inflammatory mediators. Therefore, some research is exploring treatment approaches that target inflammatory mediators to suppress the inflammatory response. For example, anti-TNF drugs, anti-IL-1 drugs, etc. inhibit the production of inflammatory mediators, thereby reducing the inflammatory response and organ damage. It is also possible to target the modulation of the immune system, specifically by activating co-stimulatory signals in T cells, such as anti-CD28 antibodies, to enhance the immune system's responsiveness and control infection.

Given that pulmonary diseases can also accelerate aging, targeted therapy against aging mechanisms could provide broad clinical benefits, aiming to prevent pulmonary diseases and complement more specific medical interventions.

Conclusion

Lung aging is a complex process characterized by cumulative damage and repair changes in the pulmonary cell system. It is closely related to the microenvironment of the lung. Age-related intrinsic mechanisms, such as stem cell pool depletion, mitochondrial dysfunction, increased oxidative stress, and telomere shortening, disrupt the maintenance of pulmonary cell homeostasis. Normal lung aging is associated with various structural and functional changes in the respiratory tract, leading to declines in pulmonary function, lung remodeling, reduced regeneration, and increased susceptibility to pulmonary diseases.

The lung has multiple innate and adaptive defense systems to maintain homeostasis and respond to external stimuli. However, with aging, various cell types in the lung, such as AEC1s, AEC2s, fibroblasts, endothelial cells, and ASM cells, undergo compositional and functional changes, increasing the susceptibility of older adults to the development and progression of pulmonary diseases. Immune senescence exacerbates the production of oxygen-free radicals and increases the production of pro-inflammatory cytokines, making persistent lower respiratory inflammation a reason why older adults are more susceptible to toxic environments and accelerated lung function decline. The poor prognosis and recovery of pulmonary diseases are attributed to age-related changes in innate and adaptive immune responses. Genetic background and lifestyle further promote pulmonary age-related changes, increasing the incidence and

progression of airway diseases and susceptibility to infectious stimuli and toxins. Although research has revealed how the immune system of older adults is susceptible to bacterial and viral lung infections, the challenge lies in identifying which age-related molecular changes are targetable and which will have therapeutic benefits. Therefore, to prevent and treat pulmonary aging-related diseases, it is necessary to focus on the changes in the pulmonary microenvironment and take corresponding measures for intervention. In-depth study of lung aging mechanisms, exploration of age-related immune changes, and construction of prevention and immunomodulatory strategies are crucial for improving the prognosis of elderly patients.

Author contributions

YW: Writing – original draft. XH: Writing – original draft. GL: Writing – original draft. YX: Writing – original draft. XD: Writing – original draft. YL: Writing – original draft. ZW: Writing – original draft. SZ: Writing – original draft. SW: Writing – original draft. HC: Writing – original draft. TT: Writing – original draft. LH: Writing – original draft. LCY: Writing – original draft. LY: Writing – original draft. YC: Writing – original draft. ZJ: Writing – original draft. CH: Writing – review & editing. ZH: Writing – review & editing, Writing – original draft, Supervision, Conceptualization. XZ: Writing – review & editing.

Funding

The author(s) declare financial support was received for the research, authorship, and/or publication of this article. The work was supported by Sichuan Cadre Health Research Project Sichuan Ganyan 2022-1001 and 2023-1001, Sichuan Provincial Department of Science and Technology Scientific Research Project 2022JDZH0027, and Sichuan Provincial Department of Science and Technology Provincial Scientific Research Institute Basic Scientific Research Project 2023JDKY0028.

Conflict of interest

The authors declare that the research was conducted in the absence of any commercial or financial relationships that could be construed as a potential conflict of interest.

Publisher's note

References

1. Oeppen J, Vaupel JW. Demography. Broken limits to life expectancy. *Science*. (2002) 296:1029–31. doi: 10.1126/science.1069675

2. Rappaport I, Mayer E. Emphysema and the senile lung. *J Am Geriatr Soc*. (1954) 2:581–91. doi: 10.1111/j.1532-5415.1954.tb01181.x

3. Dzau VJ, Inouye SK, Rowe JW, Finkelman E, Yamada T. Enabling healthful aging for all - the national academy of medicine grand challenge in healthy longevity. *N Engl J Med*. (2019) 381:1699–701. doi: 10.1056/NEJMp1912298

4. Campisi J, Kapahi P, Lithgow GJ, Melov S, Newman JC, Verdin E. From discoveries in ageing research to therapeutics for healthy ageing. *Nature*. (2019) 571:183–92. doi: 10.1038/s41586-019-1365-2

5. de Cabo R, Mattson MP. Effects of intermittent fasting on health, aging, and disease. *N Engl J Med*. (2019) 381:2541–51. doi: 10.1056/NEJMra1905136

6. López-Otín C, Blasco MA, Partridge L, Serrano M, Kroemer G. The hallmarks of aging. *Cell*. (2013) 153:1194–217. doi: 10.1016/j.cell.2013.05.039

7. Agusti A, Faner R. Lung function trajectories in health and disease. *Lancet Respir Med*. (2019) 7:358–64. doi: 10.1016/s2213-2600(18)30529-0

8. Stolk J, Putter H, Bakker EM, Shaker SB, Parr DG, Piitulainen E, et al. Progression parameters for emphysema: A clinical investigation. *Respir Med*. (2007) 101:1924–30. doi: 10.1016/j.rmed.2007.04.016

9. Aziz ZA, Wells AU, Desai SR, Ellis SM, Walker AE, MacDonald S, et al. Functional impairment in emphysema: contribution of airway abnormalities and distribution of parenchymal disease. *AJR Am J Roentgenol*. (2005) 185:1509–15. doi: 10.2214/ajr.04.1578

10. Mays PK, Bishop JE, Laurent GJ. Age-related changes in the proportion of types I and iii collagen. *Mech Ageing Dev*. (1988) 45:203–12. doi: 10.1016/0047-6374(88)90002-4

11. Sharma G, Hanania NA, Shim YM. The aging immune system and its relationship to the development of chronic obstructive pulmonary disease. *Proc Am Thorac Soc*. (2009) 6:573–80. doi: 10.1513/pats.200904-022RM

12. Janssens JP, Pache JC, Nicod LP. Physiological changes in respiratory function associated with ageing. *Eur Respir J*. (1999) 13:197–205. doi: 10.1034/j.1399-3003.1999.13a36.x

13. Kerstjens HA, Rijcken B, Schouten JP, Postma DS. Decline of fev1 by age and smoking status: facts, figures, and fallacies. *Thorax*. (1997) 52:820–7. doi: 10.1136/thx.52.9.820

14. Johnson BD, Reddan WG, Pegelow DF, Seow KC, Dempsey JA. Flow limitation and regulation of functional residual capacity during exercise in a physically active aging population. *Am Rev Respir Dis*. (1991) 143:960–7. doi: 10.1164/ajrccm/143.5_Pt_1.960

15. Sharma G, Goodwin J. Effect of aging on respiratory system physiology and immunology. *Clin Interv Aging*. (2006) 1:253–60. doi: 10.2147/ciia.2006.1.3.253

16. Crapo RO, Jensen RL, Hegewald M, Tashkin DP. Arterial blood gas reference values for sea level and an altitude of 1,400 meters. *Am J Respir Crit Care Med*. (1999) 160:1525–31. doi: 10.1164/ajrccm.160.5.9806006

17. Cardús J, Burgos F, Diaz O, Roca J, Barberà JA, Marrades RM, et al. Increase in pulmonary ventilation-perfusion inequality with age in healthy individuals. *Am J Respir Crit Care Med*. (1997) 156:648–53. doi: 10.1164/ajrccm.156.2.9606016

18. Emirgil C, Sobol BJ, Campodonico S, Herbert WH, Mechkati R. Pulmonary circulation in the aged. *J Appl Physiol*. (1967) 23:631–40. doi: 10.1152/jappl.1967.23.5.631

19. Kronenberg RS, Drage CW. Attenuation of the ventilatory and heart rate responses to hypoxia and hypercapnia with aging in normal men. *J Clin Invest*. (1973) 52:1812–9. doi: 10.1172/jci107363

20. Mackay EH, Banks J, Sykes B, Lee G. Structural basis for the changing physical properties of human pulmonary vessels with age. *Thorax*. (1978) 33:335–44. doi: 10.1136/thx.33.3.335

21. Peterson DD, Pack AI, Silage DA, Fishman AP. Effects of aging on ventilatory and occlusion pressure responses to hypoxia and hypercapnia. *Am Rev Respir Dis*. (1981) 124:387–91. doi: 10.1164/arrd.1981.124.4.387

22. Tack M, Altose MD, Cherniack NS. Effect of aging on the perception of resistive ventilatory loads. *Am Rev Respir Dis*. (1982) 126:463–7. doi: 10.1164/arrd.1982.126.3.463

23. Crapo JD, Barry BE, Gehr P, Bachofen M, Weibel ER. Cell number and cell characteristics of the normal human lung. *Am Rev Respir Dis*. (1982) 126:332–7. doi: 10.1164/arrd.1982.126.2.332

24. Suki B, Stamenović D, Hubmayr R. Lung parenchymal mechanics. *Compr Physiol*. (2011) 1:1317–51. doi: 10.1002/cphy.c100033

25. Bissonnette EY, Lauzon-Joset JF, Debley JS, Ziegler SF. Cross-talk between alveolar macrophages and lung epithelial cells is essential to maintain lung homeostasis. *Front Immunol*. (2020) 11:583042. doi: 10.3389/fimmu.2020.583042

26. Koval M. Claudin heterogeneity and control of lung tight junctions. *Annu Rev Physiol*. (2013) 75:551–67. doi: 10.1146/annurev-physiol-030212-183809

27. Rogers DF. Airway goblet cells: responsive and adaptable front-line defenders. *Eur Respir J*. (1994) 7:1690–706. doi: 10.1183/09031936.94.07091690

28. Choksi SP, Lauter G, Swoboda P, Roy S. Switching on cilia: transcriptional networks regulating ciliogenesis. *Development*. (2014) 141:1427–41. doi: 10.1242/dev.074666

29. Wu AM, Csako G, Herp A. Structure, biosynthesis, and function of salivary mucins. *Mol Cell Biochem*. (1994) 137:39–55. doi: 10.1007/bf00926038

30. Yee M, Gelein R, Mariani TJ, Lawrence BP, O'Reilly MA. The oxygen environment at birth specifies the population of alveolar epithelial stem cells in the adult lung. *Stem Cells*. (2016) 34:1396–406. doi: 10.1002/stem.2330

31. Cui H, Xie N, Banerjee S, Dey T, Liu RM, Antony VB, et al. Cd38 mediates lung fibrosis by promoting alveolar epithelial cell aging. *Am J Respir Crit Care Med*. (2022) 206:459–75. doi: 10.1164/rccm.202109-2151OC

32. Moliva JI, Rajaram MV, Sidiki S, Sasindran SJ, Guirado E, Pan XJ, et al. Molecular composition of the alveolar lining fluid in the aging lung. *Age (Dordr)*. (2014) 36:9633. doi: 10.1007/s11357-014-9633-4

33. Peters U, Papadopoulos T, Müller-Hermelink HK. Mhc class ii antigens on lung epithelial of human fetuses and neonates. Ontogeny and expression in lungs with histologic evidence of infection. *Lab Invest*. (1990) 63:38–43.

34. Langer HF, Chavakis T. Leukocyte-endothelial interactions in inflammation. *J Cell Mol Med*. (2009) 13:1211–20. doi: 10.1111/j.1582-4934.2009.00811.x

35. Petri B, Phillipson M, Kubes P. The physiology of leukocyte recruitment: an in vivo perspective. *J Immunol*. (2008) 180:6439–46. doi: 10.4049/jimmunol.180.10.6439

36. Shasby DM. Cell-cell adhesion in lung endothelium. *Am J Physiol Lung Cell Mol Physiol*. (2007) 292:L593–607. doi: 10.1152/ajplung.00386.2006

37. Jane-Wit D, Chun HJ. Mechanisms of dysfunction in senescent pulmonary endothelium. *J Gerontol A Biol Sci Med Sci*. (2012) 67:236–41. doi: 10.1093/gerona/glr248

38. Stephens NL. Airway smooth muscle. *Lung*. (2001) 179:333–73. doi: 10.1007/s004080000073

39. Damera G, Tliba O, Panettieri RA Jr. Airway smooth muscle as an immunomodulatory cell. *Pulm Pharmacol Ther*. (2009) 22:353–9. doi: 10.1016/j.pupt.2008.12.006

40. Singh SR, Kadioglu H, Patel K, Carrier L, Agnetti G. Is desmin propensity to aggregate part of its protective function? *Cells*. (2020) 9(2):491. doi: 10.3390/cells9020491

41. Yamamoto Y, Tanaka A, Kanamaru A, Tanaka S, Tsubone H, Atoji Y, et al. Morphology of aging lung in F344/N rat: alveolar size, connective tissue, and smooth muscle cell markers. *Anat Rec A Discovery Mol Cell Evol Biol*. (2003) 272:538–47. doi: 10.1002/ar.a.10172

42. Yu H, Lin Y, Zhong Y, Guo X, Lin Y, Yang S, et al. Impaired at2 to at1 cell transition in pm2.5-induced mouse model of chronic obstructive pulmonary disease. *Respir Res*. (2022) 23:70. doi: 10.1186/s12931-022-01996-w

43. Travaglini KJ, Nabhan AN, Penland L, Sinha R, Gillich A, Sit RV, et al. A molecular cell atlas of the human lung from single-cell rna sequencing. *Nature*. (2020) 587:619–25. doi: 10.1038/s41586-020-2922-4

44. Rock JR, Onaitis MW, Rawlins EL, Lu Y, Clark CP, Xue Y, et al. Basal cells as stem cells of the mouse trachea and human airway epithelium. *Proc Natl Acad Sci U.S.A*. (2009) 106:12771–5. doi: 10.1073/pnas.0906850106

45. Rock JR, Randell SH, Hogan BL. Airway basal stem cells: A perspective on their roles in epithelial homeostasis and remodeling. *Dis Model Mech*. (2010) 3:545–56. doi: 10.1242/dmm.006031

46. Kotton DN, Morrisey EE. Lung regeneration: mechanisms, applications and emerging stem cell populations. *Nat Med*. (2014) 20:822–32. doi: 10.1038/nm.3642

47. Yanai H, Shteinberg A, Porat Z, Budovsky A, Braiman A, Ziesche R, et al. Cellular senescence-like features of lung fibroblasts derived from idiopathic pulmonary fibrosis patients. *Aging (Albany NY)*. (2015) 7:664–72. doi: 10.18632/aging.100807

48. Yang KE, Kwon J, Rhim JH, Choi JS, Kim SI, Lee SH, et al. Differential expression of extracellular matrix proteins in senescent and young human fibroblasts: A comparative proteomics and microarray study. *Mol Cells*. (2011) 32:99–106. doi: 10.1007/s10059-011-0064-0

49. Angelidis I, Simon LM, Fernandez IE, Strunz M, Mayr CH, Greiffo FR, et al. An atlas of the aging lung mapped by single cell transcriptomics and deep tissue proteomics. *Nat Commun*. (2019) 10:963. doi: 10.1038/s41467-019-08831-9

50. Decaris ML, Gatmaitan M, FlorCruz S, Luo F, Li K, Holmes WE, et al. Proteomic analysis of altered extracellular matrix turnover in bleomycin-induced pulmonary fibrosis. *Mol Cell Proteomics*. (2014) 13:1741–52. doi: 10.1074/mcp.M113.037267

51. Schiller HB, Fernandez IE, Burgstaller G, Schaab C, Scheltema RA, Schwarzmayr T, et al. Time- and compartment-resolved proteome profiling of the extracellular niche in lung injury and repair. *Mol Syst Biol*. (2015) 11:819. doi: 10.15252/msb.20156123

52. Sicard D, Haak AJ, Choi KM, Craig AR, Fredenburgh LE, Tschumperlin DJ. Aging and anatomical variations in lung tissue stiffness. *Am J Physiol Lung Cell Mol Physiol*. (2018) 314:L946–l55. doi: 10.1152/ajplung.00415.2017

53. Boyd AR, Shivshankar P, Jiang S, Berton MT, Orihuela CJ. Age-related defects in tlr2 signaling diminish the cytokine response by alveolar macrophages during murine pneumococcal pneumonia. *Exp Gerontol*. (2012) 47:507–18. doi: 10.1016/j.exger.2012.04.004

54. Renshaw M, Rockwell J, Engleman C, Gewirtz A, Katz J, Sambhara S. Cutting edge: impaired toll-like receptor expression and function in aging. *J Immunol*. (2002) 169:4697–701. doi: 10.4049/jimmunol.169.9.4697

55. Puchta A, Naidoo A, Verschoor CP, Loukov D, Thevaranjan N, Mandur TS, et al. Tnf drives monocyte dysfunction with age and results in impaired anti-pneumococcal immunity. *PloS Pathog*. (2016) 12:e1005368. doi: 10.1371/journal.ppat.1005368

56. Duong L, Radley HG, Lee B, Dye DE, Pixley FJ, Grounds MD, et al. Macrophage function in the elderly and impact on injury repair and cancer. *Immun Ageing*. (2021) 18:4. doi: 10.1186/s12979-021-00215-2

57. Gibbings SL, Thomas SM, Atif SM, McCubbrey AL, Desch AN, Danhorn T, et al. Three unique interstitial macrophages in the murine lung at steady state. *Am J Respir Cell Mol Biol*. (2017) 57:66–76. doi: 10.1165/rcmb.2016-0361OC

58. Fiorentino DF, Zlotnik A, Mosmann TR, Howard M, O'Garra A. Il-10 inhibits cytokine production by activated macrophages. *J Immunol*. (1991) 147:3815–22. doi: 10.4049/jimmunol.147.11.3815

59. Mosser DM, Zhang X. Interleukin-10: new perspectives on an old cytokine. *Immunol Rev*. (2008) 226:205–18. doi: 10.1111/j.1600-065X.2008.00706.x

60. Wong CK, Smith CA, Sakamoto K, Kaminski N, Koff JL, Goldstein DR. Aging impairs alveolar macrophage phagocytosis and increases influenza-induced mortality in mice. *J Immunol*. (2017) 199:1060–8. doi: 10.4049/jimmunol.1700397

61. Hearps AC, Martin GE, Angelovich TA, Cheng WJ, Maisa A, Landay AL, et al. Aging is associated with chronic innate immune activation and dysregulation of monocyte phenotype and function. *Aging Cell*. (2012) 11:867–75. doi: 10.1111/j.1474-9726.2012.00851.x

62. Li Z, Jiao Y, Fan EK, Scott MJ, Li Y, Li S, et al. Aging-impaired filamentous actin polymerization signaling reduces alveolar macrophage phagocytosis of bacteria. *J Immunol*. (2017) 199:3176–86. doi: 10.4049/jimmunol.1700140

63. Metcalf TU, Cubas RA, Ghneim K, Cartwright MJ, Grevenynghe JV, Richner JM, et al. Global analyses revealed age-related alterations in innate immune responses after stimulation of pathogen recognition receptors. *Aging Cell*. (2015) 14:421–32. doi: 10.1111/acel.12320

64. Shaw AC, Panda A, Joshi SR, Qian F, Allore HG, Montgomery RR. Dysregulation of human toll-like receptor function in aging. *Ageing Res Rev*. (2011) 10:346–53. doi: 10.1016/j.arr.2010.10.007

65. Forrest JB. The effect of changes in lung volume on the size and shape of alveoli. *J Physiol*. (1970) 210:533–47. doi: 10.1113/jphysiol.1970.sp009225

66. Suzuki M, Betsuyaku T, Ito Y, Nagai K, Nasuhara Y, Kaga K, et al. Down-regulated nf-E2-related factor 2 in pulmonary macrophages of aged smokers and patients with chronic obstructive pulmonary disease. *Am J Respir Cell Mol Biol*. (2008) 39:673–82. doi: 10.1165/rcmb.2007-0424OC

67. GeurtsvanKessel CH, Lambrecht BN. Division of labor between dendritic cell subsets of the lung. *Mucosal Immunol*. (2008) 1:442–50. doi: 10.1038/mi.2008.39

68. Agrawal A, Agrawal S, Cao JN, Su H, Osann K, Gupta S. Altered innate immune functioning of dendritic cells in elderly humans: A role of phosphoinositide 3-kinase-signaling pathway. *J Immunol*. (2007) 178:6912–22. doi: 10.4049/jimmunol.178.11.6912

69. Agrawal A, Gupta S. Impact of aging on dendritic cell functions in humans. *Ageing Res Rev*. (2011) 10:336–45. doi: 10.1016/j.arr.2010.06.004

70. Spits H, Artis D, Colonna M, Diefenbach A, Di Santo JP, Eberl G, et al. Innate lymphoid cells–a proposal for uniform nomenclature. *Nat Rev Immunol*. (2013) 13:145–9. doi: 10.1038/nri3365

71. Nogusa S, Ritz BW, Kassim SH, Jennings SR, Gardner EM. Characterization of age-related changes in natural killer cells during primary influenza infection in mice. *Mech Ageing Dev*. (2008) 129:223–30. doi: 10.1016/j.mad.2008.01.003

72. Silva MT, Correia-Neves M. Neutrophils and macrophages: the main partners of phagocyte cell systems. *Front Immunol*. (2012) 3:174. doi: 10.3389/fimmu.2012.00174

73. Brinkmann V, Zychlinsky A. Beneficial suicide: why neutrophils die to make nets. *Nat Rev Microbiol*. (2007) 5:577–82. doi: 10.1038/nrmicro1710

74. Chen MM, Palmer JL, Plackett TP, Deburghgraeve CR, Kovacs EJ. Age-related differences in the neutrophil response to pulmonary pseudomonas infection. *Exp Gerontol*. (2014) 54:42–6. doi: 10.1016/j.exger.2013.12.010

75. Corberand J, Ngyen F, Laharrague P, Fontanilles AM, Gleyzes B, Gyrard E, et al. Polymorphonuclear functions and aging in humans. *J Am Geriatr Soc*. (1981) 29:391–7. doi: 10.1111/j.1532-5415.1981.tb02376.x

76. Nomellini V, Brubaker AL, Mahbub S, Palmer JL, Gomez CR, Kovacs EJ. Dysregulation of neutrophil cxcr2 and pulmonary endothelial icam-1 promotes age-related pulmonary inflammation. *Aging Dis*. (2012) 3:234–47.

77. Starr ME, Ueda J, Yamamoto S, Evers BM, Saito H. The effects of aging on pulmonary oxidative damage, protein nitration, and extracellular superoxide dismutase down-regulation during systemic inflammation. *Free Radic Biol Med*. (2011) 50:371–80. doi: 10.1016/j.freeradbiomed.2010.11.013

78. Zemans RL, Colgan SP, Downey GP. Transepithelial migration of neutrophils: mechanisms and implications for acute lung injury. *Am J Respir Cell Mol Biol*. (2009) 40:519–35. doi: 10.1165/rcmb.2008-0348TR

79. Griffith AV, Fallahi M, Venables T, Petrie HT. Persistent degenerative changes in thymic organ function revealed by an inducible model of organ regrowth. *Aging Cell*. (2012) 11:169–77. doi: 10.1111/j.1474-9726.2011.00773.x

80. Lee GR. The balance of th17 versus treg cells in autoimmunity. *Int J Mol Sci*. (2018) 19(3):730. doi: 10.3390/ijms19030730

81. Richner JM, Gmyrek GB, Govero J, Tu Y, van der Windt GJ, Metcalf TU, et al. Age-dependent cell trafficking defects in draining lymph nodes impair adaptive immunity and control of west nile virus infection. *PloS Pathog*. (2015) 11:e1005027. doi: 10.1371/journal.ppat.1005027

82. Pan Z, Zhu T, Liu Y, Zhang N. Role of the cxcl13/cxcr5 axis in autoimmune diseases. *Front Immunol*. (2022) 13:850998. doi: 10.3389/fimmu.2022.850998

83. Wang Y, Liu J, Burrows PD, Wang JY. B cell development and maturation. *Adv Exp Med Biol*. (2020) 1254:1–22. doi: 10.1007/978-981-15-3532-1_1

84. Allie SR, Bradley JE, Mudunuru U, Schultz MD, Graf BA, Lund FE, et al. The establishment of resident memory B cells in the lung requires local antigen encounter. *Nat Immunol*. (2019) 20:97–108. doi: 10.1038/s41590-018-0260-6

85. Holodick NE, Rothstein TL. B cells in the aging immune system: time to consider B-1 cells. *Ann N Y Acad Sci*. (2015) 1362:176–87. doi: 10.1111/nyas.12825

86. Sage PT, Tan CL, Freeman GJ, Haigis M, Sharpe AH. Defective tfh cell function and increased tfr cells contribute to defective antibody production in aging. *Cell Rep*. (2015) 12:163–71. doi: 10.1016/j.celrep.2015.06.015

87. Alpert A, Pickman Y, Leipold M, Rosenberg-Hasson Y, Ji X, Gaujoux R, et al. A clinically meaningful metric of immune age derived from high-dimensional longitudinal monitoring. *Nat Med*. (2019) 25:487–95. doi: 10.1038/s41591-019-0381-y

88. Hecker L. Mechanisms and consequences of oxidative stress in lung disease: therapeutic implications for an aging populace. *Am J Physiol Lung Cell Mol Physiol*. (2018) 314:L642–l53. doi: 10.1152/ajplung.00275.2017

89. Kovacs EJ, Boe DM, Boule LA, Curtis BJ. Inflammaging and the lung. *Clin Geriatr Med*. (2017) 33:459–71. doi: 10.1016/j.cger.2017.06.002

90. López-Otín C, Blasco MA, Partridge L, Serrano M, Kroemer G. Hallmarks of aging: an expanding universe. *Cell*. (2023) 186:243–78. doi: 10.1016/j.cell.2022.11.001

91. Murtha LA, Morten M, Schuliga MJ, Mabotuwana NS, Hardy SA, Waters DW, et al. The role of pathological aging in cardiac and pulmonary fibrosis. *Aging Dis*. (2019) 10:419–28. doi: 10.14336/ad.2018.0601

92. Storer M, Mas A, Robert-Moreno A, Pecoraro M, Ortells MC, Di Giacomo V, et al. Senescence is a developmental mechanism that contributes to embryonic growth and patterning. *Cell*. (2013) 155:1119–30. doi: 10.1016/j.cell.2013.10.041

93. Zhou Q, Yang L, Qu M, Wang Y, Chen P, Wang Y, et al. Role of senescent fibroblasts on alkali-induced corneal neovascularization. *J Cell Physiol*. (2012) 227:1148–56. doi: 10.1002/jcp.22835

94. Verbeken EK, Cauberghs M, Lauweryns JM, van de Woestijne KP. Anatomy of membranous bronchioles in normal, senile and emphysematous human lungs. *J Appl Physiol (1985)*. (1994) 77:1875–84. doi: 10.1152/jappl.1994.77.4.1875

95. Bhatia-Dey N, Kanherkar RR, Stair SE, Makarev EO, Csoka AB. Cellular senescence as the causal nexus of aging. *Front Genet*. (2016) 7:13. doi: 10.3389/fgene.2016.00013

96. Ventura MT, Casciaro M, Gangemi S, Buquicchio R. Immunosenescence in aging: between immune cells depletion and cytokines up-regulation. *Clin Mol Allergy*. (2017) 15:21. doi: 10.1186/s12948-017-0077-0

97. Hecker L, Logsdon NJ, Kurundkar D, Kurundkar A, Bernard K, Hock T, et al. Reversal of persistent fibrosis in aging by targeting nox4-nrf2 redox imbalance. *Sci Transl Med*. (2014) 6:231ra47. doi: 10.1126/scitranslmed.3008182

98. Huang WT, Akhter H, Jiang C, MacEwen M, Ding Q, Antony V, et al. Plasminogen activator inhibitor 1, fibroblast apoptosis resistance, and aging-related susceptibility to lung fibrosis. *Exp Gerontol*. (2015) 61:62–75. doi: 10.1016/j.exger.2014.11.018

99. Kling KM, Lopez-Rodriguez E, Pfarrer C, Mühlfeld C, Brandenberger C. Aging exacerbates acute lung injury-induced changes of the air-blood barrier, lung function, and inflammation in the mouse. *Am J Physiol Lung Cell Mol Physiol*. (2017) 312:L1–l12. doi: 10.1152/ajplung.00347.2016

100. Demaria M, Ohtani N, Youssef SA, Rodier F, Toussaint W, Mitchell JR, et al. An essential role for senescent cells in optimal wound healing through secretion of pdgf-aa. *Dev Cell*. (2014) 31:722–33. doi: 10.1016/j.devcel.2014.11.012

101. Salminen A, Kauppinen A, Kaarniranta K. Emerging role of nf-Kb signaling in the induction of senescence-associated secretory phenotype (Sasp). *Cell Signalling*. (2012) 24:835–45. doi: 10.1016/j.cellsig.2011.12.006

102. Mora AL, Bueno M, Rojas M. Mitochondria in the spotlight of aging and idiopathic pulmonary fibrosis. *J Clin Invest*. (2017) 127:405–14. doi: 10.1172/jci87440

103. Payne BA, Chinnery PF. Mitochondrial dysfunction in aging: much progress but many unresolved questions. *Biochim Biophys Acta*. (2015) 1847:1347–53. doi: 10.1016/j.bbabio.2015.05.022

104. Tocchi A, Quarles EK, Basisty N, Gitari L, Rabinovitch PS. Mitochondrial dysfunction in cardiac aging. *Biochim Biophys Acta*. (2015) 1847:1424–33. doi: 10.1016/j.bbabio.2015.07.009

105. Kim SJ, Cheresh P, Jablonski RP, Williams DB, Kamp DW. The role of mitochondrial DNA in mediating alveolar epithelial cell apoptosis and pulmonary fibrosis. *Int J Mol Sci*. (2015) 16:21486–519. doi: 10.3390/ijms160921486

106. Korolchuk VI, Miwa S, Carroll B, von Zglinicki T. Mitochondria in cell senescence: is mitophagy the weakest link? *EBioMedicine*. (2017) 21:7–13. doi: 10.1016/j.ebiom.2017.03.020

107. Lal A, Gomez E, Calloway C. Increased mitochondrial DNA deletions and copy number in transfusion-dependent thalassemia. *JCI Insight*. (2016) 1(12):e88150. doi: 10.1172/jci.insight.88150

108. Bueno M, Lai YC, Romero Y, Brands J, St Croix CM, Kamga C, et al. Pink1 deficiency impairs mitochondrial homeostasis and promotes lung fibrosis. *J Clin Invest*. (2015) 125:521–38. doi: 10.1172/jci74942

109. Ryter SW, Rosas IO, Owen CA, Martinez FJ, Choi ME, Lee CG, et al. Mitochondrial dysfunction as a pathogenic mediator of chronic obstructive pulmonary disease and idiopathic pulmonary fibrosis. *Ann Am Thorac Soc*. (2018) 15:S266–s72. doi: 10.1513/AnnalsATS.201808-585MG

110. Ryu C, Sun H, Gulati M, Herazo-Maya JD, Chen Y, Osafo-Addo A, et al. Extracellular mitochondrial DNA is generated by fibroblasts and predicts death in idiopathic pulmonary fibrosis. *Am J Respir Crit Care Med*. (2017) 196:1571–81. doi: 10.1164/rccm.201612-2480OC

111. Trian T, Benard G, Begueret H, Rossignol R, Girodet PO, Ghosh D, et al. Bronchial smooth muscle remodeling involves calcium-dependent enhanced mitochondrial biogenesis in asthma. *J Exp Med*. (2007) 204:3173–81. doi: 10.1084/jem.20070956

112. Franceschi C, Campisi J. Chronic inflammation (Inflammaging) and its potential contribution to age-associated diseases. *J Gerontol A Biol Sci Med Sci*. (2014) 69 Suppl 1:S4–9. doi: 10.1093/gerona/glu057

113. Oishi Y, Manabe I. Macrophages in age-related chronic inflammatory diseases. *NPJ Aging Mech Dis*. (2016) 2:16018. doi: 10.1038/npjamd.2016.18

114. Stout MB, Justice JN, Nicklas BJ, Kirkland JL. Physiological aging: links among adipose tissue dysfunction, diabetes, and frailty. *Physiol (Bethesda)*. (2017) 32:9–19. doi: 10.1152/physiol.00012.2016

115. Byrne AJ, Powell JE, O'Sullivan BJ, Ogger PP, Hoffland A, Cook J, et al. Dynamics of human monocytes and airway macrophages during healthy aging and after transplant. *J Exp Med*. (2020) 217(3):e20191236. doi: 10.1084/jem.20191236

116. Gilani SR, Vuga LJ, Lindell KO, Gibson KF, Xue J, Kaminski N, et al. Cd28 down-regulation on circulating cd4 T-cells is associated with poor prognoses of patients with idiopathic pulmonary fibrosis. *PloS One*. (2010) 5:e8959. doi: 10.1371/journal.pone.0008959

117. Hamzaoui A, Chaouch N, Graïri H, Ammar J, Hamzaoui K. Inflammatory process of cd8+ Cd28- T cells in induced sputum from asthmatic patients. *Mediators Inflammation*. (2005) 2005:160–6. doi: 10.1155/mi.2005.160

118. Hodge G, Jersmann H, Tran HB, Holmes M, Reynolds PN, Hodge S. Lymphocyte senescence in copd is associated with loss of glucocorticoid receptor expression by pro-inflammatory/cytotoxic lymphocytes. *Respir Res*. (2015) 16:2. doi: 10.1186/s12931-014-0161-7

119. Hodge G, Mukaro V, Reynolds PN, Hodge S. Role of increased cd8/cd28(Null) T cells and alternative co-stimulatory molecules in chronic obstructive pulmonary disease. *Clin Exp Immunol*. (2011) 166:94–102. doi: 10.1111/j.1365-2249.2011.04455.x

120. Allden SJ, Ogger PP, Ghai P, McErlean P, Hewitt R, Toshner R, et al. The transferrin receptor cd71 delineates functionally distinct airway macrophage subsets during idiopathic pulmonary fibrosis. *Am J Respir Crit Care Med*. (2019) 200:209–19. doi: 10.1164/rccm.201809-1775OC

121. Liang Z, Zhang Q, Thomas CM, Chana KK, Gibeon D, Barnes PJ, et al. Impaired macrophage phagocytosis of bacteria in severe asthma. *Respir Res*. (2014) 15:72. doi: 10.1186/1465-9921-15-72

122. Taylor AE, Finney-Hayward TK, Quint JK, Thomas CM, Tudhope SJ, Wedzicha JA, et al. Defective macrophage phagocytosis of bacteria in copd. *Eur Respir J*. (2010) 35:1039–47. doi: 10.1183/09031936.00036709

123. Martinez-Lopez N, Athonvarangkul D, Singh R. Autophagy and aging. *Adv Exp Med Biol*. (2015) 847:73–87. doi: 10.1007/978-1-4939-2404-2_3

124. He LQ, Lu JH, Yue ZY. Autophagy in ageing and ageing-associated diseases. *Acta Pharmacol Sin*. (2013) 34:605–11. doi: 10.1038/aps.2012.188

125. Patel AS, Song JW, Chu SG, Mizumura K, Osorio JC, Shi Y, et al. Epithelial cell mitochondrial dysfunction and pink1 are induced by transforming growth factor-beta1 in pulmonary fibrosis. *PloS One*. (2015) 10:e0121246. doi: 10.1371/journal.pone.0121246

126. Salminen A, Kaarniranta K, Kauppinen A. Age-related changes in ampk activation: role for ampk phosphatases and inhibitory phosphorylation by upstream signaling pathways. *Ageing Res Rev*. (2016) 28:15–26. doi: 10.1016/j.arr.2016.04.003

127. Kang YP, Lee SB, Lee JM, Kim HM, Hong JY, Lee WJ, et al. Metabolic profiling regarding pathogenesis of idiopathic pulmonary fibrosis. *J Proteome Res*. (2016) 15:1717–24. doi: 10.1021/acs.jproteome.6b00156

128. Kottmann RM, Kulkarni AA, Smolnycki KA, Lyda E, Dahanayake T, Salibi R, et al. Lactic acid is elevated in idiopathic pulmonary fibrosis and induces myofibroblast differentiation via ph-dependent activation of transforming growth factor-B;. *Am J Respir Crit Care Med*. (2012) 186:740–51. doi: 10.1164/rccm.201201-0084OC

129. Zhao YD, Yin L, Archer S, Lu C, Zhao G, Yao Y, et al. Metabolic heterogeneity of idiopathic pulmonary fibrosis: A metabolomic study. *BMJ Open Respir Res*. (2017) 4:e000183. doi: 10.1136/bmjresp-2017-000183

130. Ghosh N, Choudhury P, Kaushik SR, Arya R, Nanda R, Bhattacharyya P, et al. Metabolomic fingerprinting and systemic inflammatory profiling of asthma copd overlap (Aco). *Respir Res*. (2020) 21:126. doi: 10.1186/s12931-020-01390-4

131. Kelly RS, Dahlin A, McGeachie MJ, Qiu W, Sordillo J, Wan ES, et al. Asthma metabolomics and the potential for integrative omics in research and the clinic. *Chest*. (2017) 151:262–77. doi: 10.1016/j.chest.2016.10.008

132. Ran N, Pang Z, Gu Y, Pan H, Zuo X, Guan X, et al. An updated overview of metabolomic profile changes in chronic obstructive pulmonary disease. *Metabolites*. (2019) 9(6):111. doi: 10.3390/metabo9060111

133. Saxton RA, Sabatini DM. Mtor signaling in growth, metabolism, and disease. *Cell*. (2017) 168:960–76. doi: 10.1016/j.cell.2017.02.004

134. West AP, Shadel GS. Mitochondrial DNA in innate immune responses and inflammatory pathology. *Nat Rev Immunol*. (2017) 17:363–75. doi: 10.1038/nri.2017.21

135. Casoni GL, Ulivi P, Mercatali L, Chilosi M, Tomassetti S, Romagnoli M, et al. Increased levels of free circulating DNA in patients with idiopathic pulmonary fibrosis. *Int J Biol Markers*. (2010) 25:229–35. doi: 10.5301/JBM.2010.6115

136. Pedersen F, Marwitz S, Holz O, Kirsten A, Bahmer T, Waschki B, et al. Neutrophil extracellular trap formation and extracellular DNA in sputum of stable copd patients. *Respir Med*. (2015) 109:1360–2. doi: 10.1016/j.rmed.2015.08.008

137. Pham DL, Ban GY, Kim SH, Shin YS, Ye YM, Chwae YJ, et al. Neutrophil autophagy and extracellular DNA traps contribute to airway inflammation in severe asthma. *Clin Exp Allergy*. (2017) 47:57–70. doi: 10.1111/cea.12859

138. Wright TK, Gibson PG, Simpson JL, McDonald VM, Wood LG, Baines KJ. Neutrophil extracellular traps are associated with inflammation in chronic airway disease. *Respirology*. (2016) 21:467–75. doi: 10.1111/resp.12730

139. Jylhävä J, Jylhä M, Lehtimäki T, Hervonen A, Hurme M. Circulating cell-free DNA is associated with mortality and inflammatory markers in nonagenarians: the vitality 90+ Study. *Exp Gerontol*. (2012) 47:372–8. doi: 10.1016/j.exger.2012.02.011

140. Pinti M, Cevenini E, Nasi M, De Biasi S, Salvioli S, Monti D, et al. Circulating mitochondrial DNA increases with age and is a familiar trait: implications for "Inflamm-aging". *Eur J Immunol*. (2014) 44:1552–62. doi: 10.1002/eji.201343921

141. Teo YV, Capri M, Morsiani C, Pizza G, Faria AMC, Franceschi C, et al. Cell-free DNA as a biomarker of aging. *Aging Cell*. (2019) 18:e12890. doi: 10.1111/acel.12890

142. Harman D. Aging: A theory based on free radical and radiation chemistry. *J Gerontol*. (1956) 11:298–300. doi: 10.1093/geronj/11.3.298

143. Alexeyev MF. Is there more to aging than mitochondrial DNA and reactive oxygen species? *FEBS J*. (2009) 276:5768–87. doi: 10.1111/j.1742-4658.2009.07269.x

144. Liu X, Chen Z. The pathophysiological role of mitochondrial oxidative stress in lung diseases. *J Transl Med*. (2017) 15:207. doi: 10.1186/s12967-017-1306-5

145. Bjelakovic G, Nikolova D, Gluud LL, Simonetti RG, Gluud C. Mortality in randomized trials of antioxidant supplements for primary and secondary prevention: systematic review and meta-analysis. *Jama*. (2007) 297:842–57. doi: 10.1001/jama.297.8.842

146. Frenzel J, Gessner C, Sandvoss T, Hammerschmidt S, Schellenberger W, Sack U, et al. Outcome prediction in pneumonia induced ali/ards by clinical features and peptide patterns of balf determined by mass spectrometry. *PloS One*. (2011) 6:e25544. doi: 10.1371/journal.pone.0025544

147. Meduri GU, Eltorky MA. Understanding ards-associated fibroproliferation. *Intensive Care Med*. (2015) 41:517–20. doi: 10.1007/s00134-014-3613-0

148. Cheifetz IM. Year in review 2015: pediatric ards. *Respir Care*. (2016) 61:980–5. doi: 10.4187/respcare.05017

149. Bellani G, Laffey JG, Pham T, Fan E, Brochard L, Esteban A, et al. Epidemiology, patterns of care, and mortality for patients with acute respiratory distress syndrome in intensive care units in 50 countries. *Jama*. (2016) 315:788–800. doi: 10.1001/jama.2016.0291

150. Rocco PR, Dos Santos C, Pelosi P. Lung parenchyma remodeling in acute respiratory distress syndrome. *Minerva Anestesiol*. (2009) 75:730–40.

151. Sud S, Friedrich JO, Adhikari NK, Taccone P, Mancebo J, Polli F, et al. Effect of prone positioning during mechanical ventilation on mortality among patients with acute respiratory distress syndrome: A systematic review and meta-analysis. *Cmaj*. (2014) 186:E381–90. doi: 10.1503/cmaj.140081

152. Mercado N, Ito K, Barnes PJ. Accelerated ageing of the lung in copd: new concepts. *Thorax*. (2015) 70:482–9. doi: 10.1136/thoraxjnl-2014-206084

153. Babb TG, Rodarte JR. Mechanism of reduced maximal expiratory flow with aging. *J Appl Physiol (1985)*. (2000) 89:505–11. doi: 10.1152/jappl.2000.89.2.505

154. Quirk JD, Sukstanskii AL, Woods JC, Lutey BA, Conradi MS, Gierada DS, et al. Experimental evidence of age-related adaptive changes in human acinar airways. *J Appl Physiol (1985)*. (2016) 120:159–65. doi: 10.1152/japplphysiol.00541.2015

155. Turner JM, Mead J, Wohl ME. Elasticity of human lungs in relation to age. *J Appl Physiol*. (1968) 25:664–71. doi: 10.1152/jappl.1968.25.6.664

156. Verbeken EK, Cauberghs M, Mertens I, Clement J, Lauweryns JM, Van de Woestijne KP. The senile lung. Comparison with normal and emphysematous lungs. 2. Functional aspects. *Chest*. (1992) 101:800–9. doi: 10.1378/chest.101.3.800

157. Verbeken EK, Cauberghs M, Mertens I, Clement J, Lauweryns JM, Van de Woestijne KP. The senile lung. Comparison with normal and emphysematous lungs. 1. Structural aspects. *Chest*. (1992) 101:793–9. doi: 10.1378/chest.101.3.793

158. Comhair SA, Erzurum SC. Antioxidant responses to oxidant-mediated lung diseases. *Am J Physiol Lung Cell Mol Physiol*. (2002) 283:L246–55. doi: 10.1152/ajplung.00491.2001

159. Misharin AV, Morales-Nebreda L, Reyfman PA, Cuda CM, Walter JM, McQuattie-Pimentel AC, et al. Monocyte-derived alveolar macrophages drive lung fibrosis and persist in the lung over the life span. *J Exp Med*. (2017) 214:2387–404. doi: 10.1084/jem.20162152

160. Ghosh M, Miller YE, Nakachi I, Kwon JB, Barón AE, Brantley AE, et al. Exhaustion of airway basal progenitor cells in early and established chronic obstructive pulmonary disease. *Am J Respir Crit Care Med*. (2018) 197:885–96. doi: 10.1164/rccm.201704-0667OC

161. Zhou F, Onizawa S, Nagai A, Aoshiba K. Epithelial cell senescence impairs repair process and exacerbates inflammation after airway injury. *Respir Res*. (2011) 12:78. doi: 10.1186/1465-9921-12-78

162. Woldhuis RR, Heijink IH, van den Berge M, Timens W, Oliver BGG, de Vries M, et al. Copd-derived fibroblasts secrete higher levels of senescence-associated secretory phenotype proteins. *Thorax*. (2021) 76:508–11. doi: 10.1136/thoraxjnl-2020-215114

163. Jaeger VK, Lebrecht D, Nicholson AG, Wells A, Bhayani H, Gazdhar A, et al. Mitochondrial DNA mutations and respiratory chain dysfunction in idiopathic and connective tissue disease-related lung fibrosis. *Sci Rep*. (2019) 9:5500. doi: 10.1038/s41598-019-41933-4

164. Kuro-o M. Klotho as a regulator of oxidative stress and senescence. *Biol Chem*. (2008) 389:233–41. doi: 10.1515/bc.2008.028

165. Gao W, Yuan C, Zhang J, Li L, Yu L, Wiegman CH, et al. Klotho expression is reduced in copd airway epithelial cells: effects on inflammation and oxidant injury. *Clin Sci (Lond)*. (2015) 129:1011–23. doi: 10.1042/cs20150273

166. van Durme Y, Verhamme KMC, Stijnen T, van Rooij FJA, Van Pottelberge GR, Hofman A, et al. Prevalence, incidence, and lifetime risk for the development of copd in the elderly: the rotterdam study. *Chest*. (2009) 135:368–77. doi: 10.1378/chest.08-0684

167. Chen R, Zhan Y, Lin Z, Wu X, Zhou J, Yang Z, et al. Correction: effect of yupingfeng granules on clinical symptoms of stable copd: study protocol for a multicenter, double-blind, and randomized controlled trial. *BMC Complement Med Ther*. (2024) 24:77. doi: 10.1186/s12906-024-04369-6

168. Hu M, Ding P, Ma J, Yang N, Zheng J, Zhou N. Cost-effectiveness analysis of the tcm "Yupingfeng granules" in the treatment of acute exacerbations of copd based on a randomized clinical trial. *Int J Chron Obstruct Pulmon Dis*. (2022) 17:2369–79. doi: 10.2147/copd.S374782

169. Selman M, Thannickal VJ, Pardo A, Zisman DA, Martinez FJ, Lynch JP 3rd. Idiopathic pulmonary fibrosis: pathogenesis and therapeutic approaches. *Drugs*. (2004) 64:405–30. doi: 10.2165/00003495-200464040-00005

170. Yao C, Guan X, Carraro G, Parimon T, Liu X, Huang G, et al. Senescence of alveolar type 2 cells drives progressive pulmonary fibrosis. *Am J Respir Crit Care Med*. (2021) 203:707–17. doi: 10.1164/rccm.202004-1274OC

171. Inui N, Sakai S, Kitagawa M. Molecular pathogenesis of pulmonary fibrosis, with focus on pathways related to tgf-B and the ubiquitin-proteasome pathway. *Int J Mol Sci*. (2021) 22(11):6107. doi: 10.3390/ijms22116107

172. Li L, Lv S, Li X, Liu J. Wnt-induced secreted proteins-1 play an important role in paraquat-induced pulmonary fibrosis. *BMC Pharmacol Toxicol*. (2022) 23:21. doi: 10.1186/s40360-022-00560-y

173. Parker MW, Rossi D, Peterson M, Smith K, Sikström K, White ES, et al. Fibrotic extracellular matrix activates a profibrotic positive feedback loop. *J Clin Invest*. (2014) 124:1622–35. doi: 10.1172/jci71386

174. Thannickal VJ. Aging, antagonistic pleiotropy and fibrotic disease. *Int J Biochem Cell Biol*. (2010) 42:1398–400. doi: 10.1016/j.biocel.2010.05.010

175. Shivshankar P, Boyd AR, Le Saux CJ, Yeh IT, Orihuela CJ. Cellular senescence increases expression of bacterial ligands in the lungs and is positively correlated with increased susceptibility to pneumococcal pneumonia. *Aging Cell*. (2011) 10:798–806. doi: 10.1111/j.1474-9726.2011.00720.x

176. Barbagelata E, Cillóniz C, Dominedò C, Torres A, Nicolini A, Solidoro P. Gender differences in community-acquired pneumonia. *Minerva Med*. (2020) 111:153–65. doi: 10.23736/s0026-4806.20.06448-4

177. Incalzi RA, Maini CL, Fuso L, Giordano A, Carbonin PU, Galli G. Effects of aging on mucociliary clearance. *Compr Gerontol A*. (1989) 3 Suppl:65–8.

178. Proença de Oliveira-Maul J, Barbosa de Carvalho H, Goto DM, Maia RM, Fló C, Barnabé V, et al. Aging, diabetes, and hypertension are associated with decreased nasal mucociliary clearance. *Chest*. (2013) 143:1091–7. doi: 10.1378/chest.12-1183

179. Ho JC, Chan KN, Hu WH, Lam WK, Zheng L, Tipoe GL, et al. The effect of aging on nasal mucociliary clearance, beat frequency, and ultrastructure of respiratory cilia. *Am J Respir Crit Care Med*. (2001) 163:983–8. doi: 10.1164/ajrccm.163.4.9909121

180. Whitsett JA. Airway epithelial differentiation and mucociliary clearance. *Ann Am Thorac Soc*. (2018) 15:S143–s8. doi: 10.1513/AnnalsATS.201802-128AW

181. Prakash YS. Emerging concepts in smooth muscle contributions to airway structure and function: implications for health and disease. *Am J Physiol Lung Cell Mol Physiol*. (2016) 311:L1113–l40. doi: 10.1152/ajplung.00370.2016

182. Gillman A, Douglass JA. Asthma in the elderly. *Asia Pac Allergy*. (2012) 2:101–8. doi: 10.5415/apallergy.2012.2.2.101

183. Childs BG, Durik M, Baker DJ, van Deursen JM. Cellular senescence in aging and age-related disease: from mechanisms to therapy. *Nat Med*. (2015) 21:1424–35. doi: 10.1038/nm.4000

184. Sung H, Ferlay J, Siegel RL, Laversanne M, Soerjomataram I, Jemal A, et al. Global cancer statistics 2020: globocan estimates of incidence and mortality worldwide for 36 cancers in 185 countries. *CA Cancer J Clin*. (2021) 71:209–49. doi: 10.3322/caac.21660

185. Caetano MS, Hassane M, Van HT, Bugarin E, Cumpian AM, McDowell CL, et al. Sex specific function of epithelial stat3 signaling in pathogenesis of K-ras mutant lung cancer. *Nat Commun*. (2018) 9:4589. doi: 10.1038/s41467-018-07042-y

186. Martincorena I, Roshan A, Gerstung M, Ellis P, Van Loo P, McLaren S, et al. Tumor evolution. High burden and pervasive positive selection of somatic mutations in normal human skin. *Science*. (2015) 348:880–6. doi: 10.1126/science.aaa6806

187. Martincorena I, Fowler JC, Wabik A, Lawson ARJ, Abascal F, Hall MWJ, et al. Somatic mutant clones colonize the human esophagus with age. *Science*. (2018) 362:911–7. doi: 10.1126/science.aau3879

188. Sacher AG, Dahlberg SE, Heng J, Mach S, Jänne PA, Oxnard GR. Association between younger age and targetable genomic alterations and prognosis in non-small-cell lung cancer. *JAMA Oncol*. (2016) 2:313–20. doi: 10.1001/jamaoncol.2015.4482

189. Willis C, Fiander M, Tran D, Korytowsky B, Thomas JM, Calderon F, et al. Tumor mutational burden in lung cancer: A systematic literature review. *Oncotarget*. (2019) 10:6604–22. doi: 10.18632/oncotarget.27287

190. Kumagai S, Togashi Y, Kamada T, Sugiyama E, Nishinakamura H, Takeuchi Y, et al. The pd-1 expression balance between effector and regulatory T cells predicts the clinical efficacy of pd-1 blockade therapies. *Nat Immunol*. (2020) 21:1346–58. doi: 10.1038/s41590-020-0769-3

191. Elias R, Morales J, Rehman Y, Khurshid H. Immune checkpoint inhibitors in older adults. *Curr Oncol Rep*. (2016) 18:47. doi: 10.1007/s11912-016-0534-9

192. Whelehan S, Lynch O, Treacy N, Gleeson C, Oates A, O'Donovan A. Optimising clinical trial design in older cancer patients. *Geriatrics (Basel)*. (2018) 3 (3):34. doi: 10.3390/geriatrics3030034

193. Hodge S, Hodge G, Scicchitano R, Reynolds PN, Holmes M. Alveolar macrophages from subjects with chronic obstructive pulmonary disease are deficient in their ability to phagocytose apoptotic airway epithelial cells. *Immunol Cell Biol*. (2003) 81:289–96. doi: 10.1046/j.1440-1711.2003.t01-1-01170.x

194. Ely EW, Wheeler AP, Thompson BT, Ancukiewicz M, Steinberg KP, Bernard GR. Recovery rate and prognosis in older persons who develop acute lung injury and the acute respiratory distress syndrome. *Ann Intern Med*. (2002) 136:25–36. doi: 10.7326/0003-4819-136-1-200201010-00007

195. Bruunsgaard H, Skinhøj P, Qvist J, Pedersen BK. Elderly humans show prolonged in vivo inflammatory activity during pneumococcal infections. *J Infect Dis*. (1999) 180:551–4. doi: 10.1086/314873

196. Al-Shaer MH, Choueiri NE, Correia ML, Sinkey CA, Barenz TA, Haynes WG. Effects of aging and atherosclerosis on endothelial and vascular smooth muscle function in humans. *Int J Cardiol*. (2006) 109:201–6. doi: 10.1016/j.ijcard.2005.06.002

197. Cleaver JO, You D, Michaud DR, Pruneda FA, Juarez MM, Zhang J, et al. Lung epithelial cells are essential effectors of inducible resistance to pneumonia. *Mucosal Immunol*. (2014) 7:78–88. doi: 10.1038/mi.2013.26

198. Siner JM, Pisani MA. Mechanical ventilation and acute respiratory distress syndrome in older patients. *Clin Chest Med*. (2007) 28:783–91. doi: 10.1016/j.ccm.2007.08.008

199. Barnes PJ. Anti-inflammatory actions of glucocorticoids: molecular mechanisms. *Clin Sci (Lond)*. (1998) 94:557–72. doi: 10.1042/cs0940557

200. Kagoshima M, Ito K, Cosio B, Adcock IM. Glucocorticoid suppression of nuclear factor-kappa B: A role for histone modifications. *Biochem Soc Trans*. (2003) 31:60–5. doi: 10.1042/bst0310060

201. Ghosh S, May MJ, Kopp EB. Nf-kappa B and rel proteins: evolutionarily conserved mediators of immune responses. *Annu Rev Immunol*. (1998) 16:225–60. doi: 10.1146/annurev.immunol.16.1.225

202. Ambrosino N, Paggiaro P. The management of asthma and chronic obstructive pulmonary disease: current status and future perspectives. *Expert Rev Respir Med*. (2012) 6:117–27. doi: 10.1586/ers.12.2

203. Adcock IM, Ito K, Barnes PJ. Histone deacetylation: an important mechanism in inflammatory lung diseases. *Copd*. (2005) 2:445–55. doi: 10.1080/15412550500346683

204. Kim EC, Kim JR. Senotherapeutics: emerging strategy for healthy aging and age-related disease. *BMB Rep*. (2019) 52:47–55. doi: 10.5483/BMBRep.2019.52.1.293

205. Schuliga M, Read J, Blokland KEC, Waters DW, Burgess J, Prêle C, et al. Self DNA perpetuates ipf lung fibroblast senescence in a cgas-dependent manner. *Clin Sci (Lond)*. (2020) 134:889–905. doi: 10.1042/cs20191160

206. Benmerzoug S, Rose S, Bounab B, Gosset D, Duneau L, Chenuet P, et al. Sting-dependent sensing of self-DNA drives silica-induced lung inflammation. *Nat Commun*. (2018) 9:5226. doi: 10.1038/s41467-018-07425-1

frontiers | Frontiers in Immunology

TYPE Review
PUBLISHED 10 May 2024
DOI 10.3389/fimmu.2024.1398927

OPEN ACCESS

EDITED BY
Uzma Saqib,
Indian Institute of Technology Indore, India

REVIEWED BY
Reinhard Depping,
University of Lübeck, Germany
Samir Parekh,
Icahn School of Medicine at Mount Sinai, United States

*CORRESPONDENCE
Lin Chen
chenlinhx@med.uestc.edu.cn

†These authors have contributed equally to this work

RECEIVED 11 March 2024
ACCEPTED 25 April 2024
PUBLISHED 10 May 2024

CITATION
Li D, Fang H, Zhang R, Xie Q, Yang Y and Chen L (2024) Beyond oncology: Selinexor's journey into anti-inflammatory treatment and long-term management. *Front. Immunol.* 15:1398927. doi: 10.3389/fimmu.2024.1398927

Beyond oncology: Selinexor's journey into anti-inflammatory treatment and long-term management

Dan Li[1†], Hong Fang[2†], Rong Zhang[2], Qian Xie[2], Yang Yang[2] and Lin Chen[2,3*]

[1]Respiratory Medicine Department, Wuhou District People's Hospital, Chengdu, China, [2]Department of Pulmonary and Critical Care Medicine, Sichuan Provincial People's Hospital, School of Medicine, University of Electronic Science and Technology of China, Chengdu, China, [3]Department of Pulmonary and Critical Care Medicine, Mayo Clinic, MN, United States

Selinexor, a selective inhibitor of nuclear export (SINE), is gaining recognition beyond oncology for its potential in anti-inflammatory therapy. This review elucidates Selinexor's dual action, highlighting its anti-tumor efficacy in various cancers including hematologic malignancies and solid tumors, and its promising anti-inflammatory effects. In cancer treatment, Selinexor has demonstrated benefits as monotherapy and in combination with other therapeutics, particularly in drug-resistant cases. Its role in enhancing the effectiveness of bone marrow transplants has also been noted. Importantly, the drug's impact on key inflammatory pathways provides a new avenue for the management of conditions like sepsis, viral infections including COVID-19, and chronic inflammatory diseases such as Duchenne Muscular Dystrophy and Parkinson's Disease. The review emphasizes the criticality of managing Selinexor's side effects through diligent dose optimization and patient monitoring. Given the complexities of its broader applications, extensive research is called upon to validate Selinexor's long-term safety and effectiveness, with a keen focus on its integration into clinical practice for a diverse spectrum of disorders.

KEYWORDS

Selinexor, oncology, inflammatory diseases, nuclear export inhibition, therapeutic mechanisms

1 Introduction

Selinexor, also known as KPT-330, is an oral small molecule drug that Selectively Inhibits Nuclear Export (SINE). It specifically inhibits exportin 1 (XPO1), which exports various proteins (including tumor suppressor proteins and growth regulators) from the nucleus to the cytoplasm (1). By inhibiting XPO1, Selinexor effectively traps these proteins in the nucleus, leading to the reactivation of tumor suppressor functions and induction of apoptosis in cancer cells. Selinexor's mechanism of action distinguishes it from other

oncology therapies, making it a viable clinical option for treating various tumor types, such as multiple myeloma and diffuse large B-cell lymphoma (1). Additionally, Selinexor has shown potential therapeutic applications beyond its initial approval for hematological malignancies, including breast cancer (2), lung adenocarcinoma (3), and gastric cancer (4), by inducing cell cycle arrest and promoting apoptosis.

However, Selinexor has emerged as a pivotal agent in the treatment of certain oncologic conditions, particularly demonstrating efficacy in scenarios where traditional therapies have failed. It is important to recognize that Selinexor is not intended as a first-line treatment option, nor is it recommended for direct comparison with standard treatment modalities. Its utility is specifically recognized in the treatment of drug-resistant or treatment-refractory cases, offering a novel avenue for patients who have exhausted other therapeutic options. This distinct role underscores the importance of understanding Selinexor's unique mechanism of action, its therapeutic potential, and the need for precise patient selection criteria to optimize treatment outcomes.

But it is encouraging that Selinexor has demonstrated not only anti-tumor effects but also anti-inflammatory effects and protection against other inflammatory diseases, such as COVID-19 (5), sepsis (6), and Duchenne muscular dystrophy (DMD) (7). The applications of Selinexor will not be limited to oncology, and there may be broader areas that can be explored. The role of Selinexor will be explored in detail.

2 Selinexor in anti-cancer treatment

2.1 Selinexor in hematologic malignancies

Selinexor has shown effectiveness against blood cancers by inhibiting tumor growth and inducing the death of cancer cells, with a better safety profile for healthy cells compared to older treatments. Studies indicate its success as both a solo treatment and in combination with other therapies across various blood cancer types.

In significant research, the STORM trial investigated Selinexor in patients with advanced myeloma who had undergone numerous treatments, finding that approximately 26% experienced a reduction in cancer severity (8). The Boston trial examined the combination of Selinexor with bortezomib and dexamethasone in 402 patients, revealing that this regimen extended progression-free survival to nearly 14 months, offering notable benefits particularly to older individuals and those with renal issues (9).

The SADAL study evaluated Selinexor in individuals with advanced Large B-Cell Lymphoma after 2-5 prior treatments, reporting a 28% response rate and an average survival of 9 months with manageable side effects (10). An additional investigation into various Non-Hodgkin's Lymphomas (NHL) in 70 patients showed a 31% response rate, supporting Selinexor's role in treating relapsed or refractory cases (11).

Regarding other blood cancer types, a Phase I clinical trial combining Selinexor with chemotherapy for relapsed/refractory Acute Myeloid Leukemia (AML) reported a 70% overall response rate and a 50% complete remission rate (12). Another AML study with Selinexor, cytarabine, and idarubicin showed a 47.6% response rate and a median complete remission duration of 34 days, highlighting variable outcomes in such AML treatments (13). In chronic lymphocytic leukemia (CLL), Selinexor has been found to boost the effects of chemotherapeutic agents like Fludarabine and Bendamustine, or sustain the impact of PI3Kδ inhibitors, effectively overcoming resistance to single-agent therapies and preserving the drugs' ability to kill tumor cells (14).

2.2 Selinexor in non-hematologic malignancies

Selinexor is broadening its horizons from blood cancers to include treatments for solid tumors, showcasing its versatility in oncology. This expansion reflects an active pursuit to uncover its full potential beyond hematologic applications, emphasizing the necessity for comprehensive clinical evaluations across various cancer types.

For advanced and metastatic malignancies, Selinexor has demonstrated a promising safety and efficacy profile. A Phase 1 study underscored its tolerability in patients with a range of advanced cancers, suggesting a potential for broader applicability (15).

In the realm of soft tissue sarcoma (STS), Selinexor's combination with doxorubicin has yielded partial remission in 21% of patients, and stable disease in 63% (16, 17). This finding is significant, particularly for a diverse and rare cancer like STS, highlighting Selinexor's capacity to fill therapeutic gaps where targeted options are limited.

Gynecological cancers, too, have seen potential benefits from Selinexor, with a Phase I study indicating partial or complete remission in patients treated with a combination of Selinexor, paclitaxel, and carboplatin (18). This promising result opens up new avenues for treatment in ovarian and endometrial cancers.

Research has broadened Selinexor's application to encompass a variety of solid tumors, addressing complex cases such as salivary gland tumors, recurrent glioblastoma, metastatic triple-negative breast cancer, and castration-resistant prostate cancer (19–22). Although the outcomes of these studies vary, they collectively indicate potential clinical benefits of Selinexor across diverse solid tumors. Notably, the integration of Selinexor with radiotherapy has been shown to enhance apoptosis and reduce proliferation in colorectal cancer cell lines and xenograft tumor models, compared to either treatment alone. This synergistic effect has led to decreased tumor sizes and improved responses to radiation (23).

This exploration into non-hematologic malignancies with Selinexor represents a significant stride in cancer treatment, hinting at a versatile and effective option for a range of solid tumors. The ongoing challenge is to fine-tune treatment protocols and deepen understanding of its optimal use, particularly in combination therapies and specific patient demographics, to maximize Selinexor's therapeutic advantage.

2.3 Summary of Selinexor in anti-tumor treatment

Selinexor, typically not used as a standalone therapy in antitumor regimens, excels when combined with other

treatments, especially for blood cancers. This strategy offers renewed hope for patients who have exhausted other therapeutic options. The drug's ability to enhance the efficacy of combination therapy regimens is marked by its capacity to attenuate the harsh effects of chemotherapy and maintain cancer cell sensitivity to ongoing treatments (24–26). Moreover, the integration of Selinexor into treatment strategies not only improves outcomes for resistant cases but also aids in preparing patients for bone marrow or stem cell transplants. By reducing cancer burden pre-transplant, Selinexor increases the likelihood of successful chemotherapy preparatory regimens, broadening the eligibility for these life-extending procedures (27–29).

While Selinexor introduces significant therapeutic benefits, its administration is not without challenges. A primary concern is hematological toxicities such as thrombocytopenia, which affects approximately 54% of treated patients, necessitating close monitoring and potential dose adjustments to mitigate severe bleeding risks (30). Gastrointestinal side effects are prevalent, with nausea and vomiting reported frequently. These effects can substantially impact patient quality of life and adherence to the therapy regime. Effective management strategies often involve supportive care measures, including the use of antiemetics and dietary adjustments to help patients better tolerate treatment (30). Concerns about hepatotoxicity are underscored by instances of elevated ALT levels, signaling potential liver injury. Though relatively rare, regular monitoring of liver function is essential for detecting any hepatic injury early, allowing for timely medical intervention (30). Additionally, Selinexor treatment has been associated with a heightened risk of infections, particularly upper respiratory tract infections, observed in about 17.8% of patients in clinical trials. This necessitates rigorous monitoring and preemptive management strategies to mitigate the risk and manage any infections promptly (30).

The use of biomarkers plays a critical role in monitoring Selinexor's efficacy and managing resistance. Studies such as the BOSTON and STORM trials have uncovered a three-gene signature (WNT10A, DUSP1, and ETV7) that predicts Selinexor's efficacy in treating multiple myeloma, in terms of both depth and duration of response (31). ABCC4, or ATP-binding cassette subfamily C member 4, has emerged as a significant biomarker for Selinexor sensitivity in multiple myeloma, with varying expression levels correlating with the drug's effectiveness. This suggests ABCC4's potential as a novel indicator of drug response, highlighted by weighted gene co-expression network analysis demonstrating its predictive value (32). Further, CRISPR-Cas9 screening has identified ASB8 as a critical element enhancing Selinexor sensitivity in various cancer types through the modulation of XPO1 proteasomal degradation. Additionally, the TGFβ-SMAD4 pathway has been identified as a significant factor in resistance to multiple myeloma, suggesting its potential as a biomarker for predicting therapeutic outcomes and devising strategies to overcome resistance (33). Monitoring the activity or expression of XPO1 and NF-kB, which are directly tied to Selinexor's mechanism of action, can provide valuable insights into treatment effectiveness. These biomarkers are instrumental in adjusting therapeutic approaches to maximize patient benefits while minimizing adverse effects (34–36).

In summary, Selinexor's role in overcoming chemotherapy resistance and facilitating bone marrow transplants underscores its value in treating blood cancers. This approach could significantly improve the chances of a cure for some patients.

3 Introduction to Selinexor and inflammation

The rationale for exploring Selinexor's role in inflammatory pathways stems from its unique mechanism of action. By inhibiting XPO1, Selinexor effectively traps crucial regulatory proteins within the nucleus, thereby impeding their normal function in the cytoplasm. This action leads to the modulation of several cellular pathways involved in cell survival, inflammation, and immune responses. The nuclear retention of these proteins can result in the downregulation of pro-inflammatory cytokines and the modulation of other key components of inflammatory pathways.

This broad mechanism suggests a potential utility for Selinexor beyond oncology, targeting inflammatory and autoimmune diseases where dysregulation of cytokine signaling plays a significant role. The anti-inflammatory effects of Selinexor have been observed in various models of disease, providing a promising outlook for its application in treating chronic and acute inflammatory conditions.

3.1 Mechanism of action of Selinexor in inflammation

3.1.1 Focusing on proteins involved in inflammation

Selinexor targets several key pathways central to inflammation, notably the NF-κB and STAT3 signaling pathways. Under typical conditions, NF-κB is confined in the cytoplasm bound to IκB proteins. In response to inflammatory stimuli, IκB degrades, allowing NF-κB to enter the nucleus and activate genes that escalate the inflammatory response. Selinexor intervenes by stabilizing IκBα, thus hindering the nuclear translocation of NF-κB. This prevention reduces the transcription of pro-inflammatory cytokines and mediators, critical components that perpetuate inflammation. The suppression of these mediators is crucial for controlling inflammatory processes across various conditions (6).

Building on this mechanism, Selinexor also modulates the STAT3 signaling pathway, which plays a pivotal role in mediating inflammation. By retaining STAT3 in the nucleus, Selinexor limits its capability to activate downstream genes responsible for the inflammatory response. This containment reduces the overall inflammatory activity, providing therapeutic benefits especially in diseases where STAT3 is overly active (37).

Selinexor's influence on immune regulation is primarily achieved through its action on NF-κB and STAT3, critical transcription factors involved in immune cell activation. By retaining these factors in the nucleus, Selinexor prevents them from promoting the expression of genes that drive the inflammatory and immune responses. This results in a reduction

of immune cell activation and inflammatory signaling, making it beneficial for treating conditions with excessive immune activation (6).

3.1.2 Changes in cytokine profiles due to Selinexor treatment

Cytokines, small proteins crucial for cell signaling, play significant roles in the immune response during inflammation. Key cytokines like tumor necrosis factor-alpha (TNF-α), interleukins (IL-1β, IL-6), and interferons (IFNs) drive inflammatory responses, and their dysregulation can exacerbate disease severity and progression. Selinexor's ability to modulate cytokine production largely stems from its inhibition of nuclear export. By blocking the nuclear export of transcription factors such as NF-κB and STAT3, Selinexor prevents them from activating genes responsible for pro-inflammatory cytokine production. This suppression leads to a notable reduction in cytokine levels, directly impacting the inflammatory process (6).

Clinically, Selinexor's effect on cytokine levels has profound implications. It has been shown to significantly reduce concentrations of key pro-inflammatory cytokines, thereby alleviating symptoms and lessening disease severity. For instance, in diseases like rheumatoid arthritis or inflammatory bowel disease, where cytokine overproduction leads to tissue damage, Selinexor's ability to modulate cytokine production can prevent tissue damage and reduce symptoms (38).

Furthermore, by altering cytokine profiles, Selinexor offers a new therapeutic approach for conditions inadequately managed by existing medications. This includes diminishing chronic disease flare-ups, reducing reliance on steroids or other immunosuppressants, and potentially improving patient quality of life. Additionally, the altered localization of signaling molecules through Selinexor's action affects downstream signaling pathways essential for immune cell development and function, notably reducing the proliferation and differentiation of pro-inflammatory T cells crucial in autoimmune and inflammatory diseases.

3.1.3 Specific effects on T cells

Selinexor modulates T cell function primarily through the indirect effects of inhibiting nuclear export, which is crucial since T cells are central to both cell-mediated immunity and the modulation of other immune responses through cytokine production. By altering the localization and activity of key transcription factors such as NF-κB and STAT3, which are vital for T cell activation and proliferation, Selinexor prevents these factors from triggering the gene expression necessary for T cell responses. This retention within the nucleus significantly curtails the proliferation and activation of T cells, particularly those implicated in inflammatory responses (38).

Furthermore, T cells are prolific producers of cytokines like interleukin-2 (IL-2), interferon-gamma (IFN-γ), and tumor necrosis factor-alpha (TNF-α), which drive inflammation. By reducing the availability of transcription factors necessary for cytokine gene activation, Selinexor effectively diminishes cytokine production (39). This reduction is crucial for alleviating the inflammatory response, offering therapeutic benefits in diseases characterized by cytokine storms or persistent inflammation.

The suppression of inappropriate immune responses by Selinexor, especially in autoimmune diseases where T cells target self-antigens, alleviates symptoms associated with these conditions. By dampening T cell activation and reducing inflammatory cytokine levels, Selinexor aids in managing inflammatory diseases and contributes to maintaining immune homeostasis. These actions underscore Selinexor's potential to modulate the immune system in ways fundamentally different from traditional immunosuppressive or immunostimulatory therapies, providing a novel approach to treating conditions where immune regulation is beneficial, such as autoimmune disorders and chronic inflammation.

Furthermore, Selinexor's ability to prevent the creation of neutrophil extracellular traps (NETs) while maintaining neutrophil function provides strategic benefits in the treatment of illnesses defined by high NET activity (40). It affects cell death mechanisms, such as PANoptosis (pyroptosis, apoptosis, and necroptosis), by controlling the nuclear export of ADAR1-p150, highlighting its potential for treating cancer and inflammatory illnesses by modulating cell death pathways (41).

The therapeutic scope of Selinexor in anti-inflammatory therapy is complicated, encompassing nuclear output inhibition, cytokine production control, modulation of critical signaling pathways, and antiviral actions, as illustrated in Figure 1. These features make Selinexor and other SINE compounds intriguing candidates for the treatment of chronic inflammatory disorders and viral infections, paving the way for further study into their broad therapeutic applications.

3.2 Clinical implications of Selinexor's anti-inflammatory actions

3.2.1 Sepsis

Clinical studies have established Selinexor's efficacy in modulating key inflammatory pathways in sepsis. In animal models, treatment with Selinexor has been observed to significantly improve survival rates. Specifically, it reduces lung damage caused by lipopolysaccharide (LPS) and decreases the accumulation of inflammatory cells in the peritoneal area. These effects are linked to reduced levels of pro-inflammatory cytokines such as TNF-α, IL-6, and HMGB1 (6). Selinexor's mechanism of action in sepsis involves the inhibition of crucial inflammatory pathways, notably NF-kB and MAPK p38, which are integral to the inflammatory cascade in sepsis. This inhibition is significant as it directly affects the pathways that exacerbate sepsis, providing a targeted approach to reducing acute inflammatory reactions (6).

3.2.2 Antiviral applications

Selinexor and Verdinexor, members of the SINE chemical family, demonstrate potent antiviral properties by inhibiting the nuclear export of viral proteins crucial for assembly and replication.

10.3389/fimmu.2024.1398927

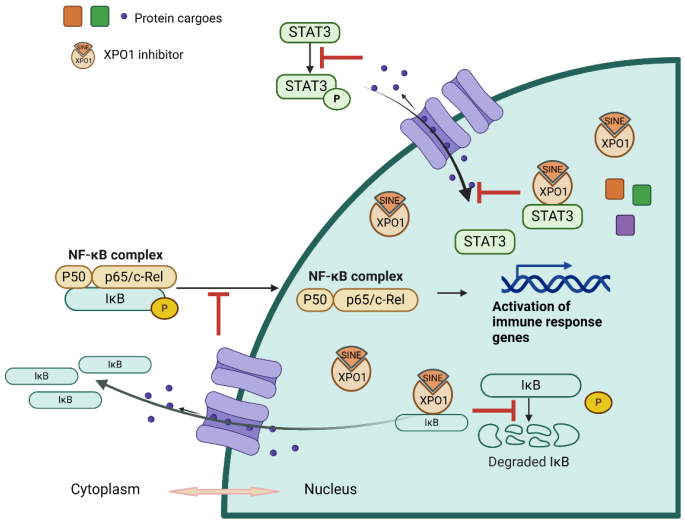

FIGURE 1
Illustration of Selinexor's Mechanism of Action in Modulating Inflammatory Pathways. This diagram depicts the mechanism of action of Selinexor in inhibiting inflammation. It shows the stabilization of IκBα, which prevents the translocation of NF-κB to the nucleus and the subsequent reduction in pro-inflammatory cytokine transcription. The image outlines Selinexor's effect on various components of the inflammatory pathway, highlighting its role in downregulating cytokine production and modulating immune responses.

In animal models, including ferrets in COVID-19 studies, Selinexor has effectively reduced viral loads and mitigated inflammatory damage, indicating its role in managing severe viral infections through immune modulation and cytokine storm reduction (37). Verdinexor disrupts the lifecycle of Respiratory Syncytial Virus (RSV) by sequestering RSV M proteins in the cell nucleus, inhibiting replication of both A and B strains. This action simultaneously enhances p53 activity and reduces XPO1 levels, offering a strategic advantage against RSV (42).

In the context of COVID-19, Selinexor blocks the nuclear export of essential viral proteins such as ORF3b, ORF9b, and the nucleocapsid N protein, crucial for SARS-CoV-2 replication. It also reduces the cell surface presence of the ACE-2 receptor, limiting viral entry. Furthermore, Selinexor modulates immune responses by controlling the release of inflammatory cytokines, potentially alleviating cytokine storms commonly associated with severe COVID-19 cases through the inhibition of NF-kB pathways and direct effects on STAT3 and IL-6 transcription (37). Conversely, research by Rahman et al. suggests that pretreatment with Selinexor may enhance coronavirus replication, including in SARS-CoV-2 and mouse hepatitis virus (MHV), illustrating the complex effects of Selinexor on viral replication and inflammation, and underscoring the necessity for precise administration timing (40, 43).

These findings reveal the dual potential of Selinexor and KPT-335 in combating viral infections, showcasing their ability to control viral growth and inflammation. Despite promising initial results, the complexities and some contradictory findings underscore the need for further research to fully understand their therapeutic potential beyond cancer treatment and to integrate them into broader therapeutic frameworks.

3.2.3 Chronic inflammatory diseases

Selinexor, along with other SINE compounds such as KPT-8602, exhibits potential in treating both acute and chronic inflammatory diseases, spanning conditions like Duchenne Muscular Dystrophy (DMD), Parkinson's Disease (PD), Calcific Aortic Valve Disease (CAVD), and pulmonary fibrosis. These compounds inhibit key inflammatory pathways, offering new therapeutic strategies across a spectrum of diseases.

In chronic conditions like DMD, Selinexor and KPT-8602 have shown promise by modulating inflammatory cytokines and pathways, improving muscle function, and slowing disease progression. Specifically, KPT-8602 not only enhances muscular architecture but also reduces serum levels of biomarkers associated with bone and muscle turnover, fostering conditions conducive to muscle healing and renewal (7). This dual approach targets both the structural damage and inflammatory underpinnings of DMD, making KPT-8602 a valuable therapeutic option. For PD, these compounds protect dopaminergic neurons by mitigating neuroinflammation, thereby potentially delaying the progression of the disease. The inhibition of critical pathways such as NF-kB and the NLRP3 inflammasome underscores their capacity to protect against neuronal degeneration, a hallmark of PD (44). In the realm of CAVD, Selinexor has demonstrated the ability to modulate inflammatory responses that contribute to pathological calcification, suggesting a role in managing diseases characterized by such calcifications (42). Recent insights into Selinexor's impact on pulmonary fibrosis reveal its effectiveness through the inhibition of the XPO1 protein, influencing GBP5/NLRP3 inflammasome signaling pathways crucial in the inflammatory responses associated with fibrosis. This action suggests that Selinexor could

be instrumental in treating conditions marked by widespread inflammation and fibrotic transformations (45).

Overall, the exploration of SINE compounds in treating benign diseases has garnered significant attention due to promising results that suggest a potential to control, if not decelerate, the progression of these conditions (42, 44). The broad applicability of SINE compounds in diverse inflammatory and autoimmune conditions supports continued research into their comprehensive anti-inflammatory effects across various diseases.

4 Limitations and future directions

As Selinexor's role in treating both cancerous and non-cancerous conditions continues to be explored, it is evident that while the drug offers promising results in managing inflammation, there are significant gaps and limitations in our understanding that necessitate further investigation. One primary concern is Selinexor's specificity as an XPO1 inhibitor, which influences a broad spectrum of proteins and can lead to unintended consequences, including severe side effects. This broad activity presents challenges, especially in chronic conditions where long-term treatment is required, as balancing efficacy and safety becomes critical (46, 47). The need for optimal dosing to achieve the desired anti-inflammatory effects without compromising safety is a significant hurdle, with higher doses potentially increasing the risk of adverse effects.

Additionally, while it is recognized that Selinexor modulates several key inflammatory pathways, the precise mechanisms by which it impacts specific conditions remain poorly understood. This incomplete mechanistic insight hampers the development of targeted therapies that could enhance Selinexor's efficacy while minimizing side effects.

Looking ahead, future research should focus on developing targeted delivery systems that can localize Selinexor's action to specific tissues or organs. This strategy would potentially reduce systemic side effects and enhance efficacy in localized inflammatory conditions, such as inflammatory bowel disease or rheumatoid arthritis. Exploring combination therapies that include Selinexor and other anti-inflammatory agents may also improve therapeutic effects and possibly reduce the necessary dosages, which could be tailored to specific pathways active in various inflammatory diseases.

Longitudinal studies are crucial for assessing the long-term effects and safety of Selinexor in chronic inflammation. Such studies would provide a more comprehensive understanding of its benefits and risks. Further research into identifying biomarkers that predict responses to Selinexor could improve patient selection and treatment monitoring, facilitating personalized treatment approaches that optimize therapeutic outcomes while minimizing adverse effects.

Moreover, expanding research to explore Selinexor's effects in non-cancerous inflammatory diseases could uncover additional therapeutic uses and provide new insights into its anti-inflammatory properties, potentially opening new avenues for treatment across a broader range of inflammatory disorders. This ongoing research and the development of new clinical strategies are essential for fully realizing the potential of Selinexor in the management of both malignant and benign diseases, ensuring that treatments are both effective and safe for long-term use.

5 Conclusion

Selinexor is distinguished by its unique nuclear inhibition, exhibiting extensive effects. By trapping tumor suppressor proteins within the cell nucleus, Selinexor induces apoptosis in cancer cells, proving effective against various types of tumors, including hematologic malignancies and solid tumors. This positions it as a key therapeutic approach in oncology, especially valuable in cases resistant to conventional treatments.

Similarly, Selinexor demonstrates robust anti-inflammatory action through its key mechanism of XPO1 inhibition, which suppresses the activity of regulatory factors such as NF-kB and STAT3. This action effectively modulates immune responses and inflammatory pathways, enhancing its utility in treating both acute and chronic inflammatory diseases such as sepsis, DMD, and PD. This dual functionality not only broadens its therapeutic applications beyond oncology but also highlights its potential to manage a diverse array of diseases.

However, the transition of Selinexor from an anti-cancer to an anti-inflammatory agent has unveiled both its versatility and the complexities associated with its broader applications. Ongoing research is crucial in further unraveling its full potential, aiming to harness its capabilities while addressing any associated risks more effectively. The extensive clinical trials and continuous research efforts are essential to ensure the long-term safety and efficacy of Selinexor, optimizing its use in clinical practice.

As research advances, Selinexor continues to stand out not only for its significant therapeutic implications but also as a paradigm shift in the management of complex disorders. Its ability to concurrently address oncological and inflammatory diseases underscores its potential as a versatile therapeutic tool. This highlights the importance of continued investigations into its mechanisms and therapeutic applications to fully realize and utilize its extensive benefits.

Author contributions

DL: Writing – original draft, Investigation. HF: Writing – original draft, Data curation. RZ: Writing – review & editing, Resources. QX: Writing – review & editing. YY: Writing – original draft. LC: Writing – review & editing, Supervision, Conceptualization.

Funding

The author(s) declare financial support was received for the research, authorship, and/or publication of this article. This work is

supported by Project of Sichuan Provincial Department of Science and Technology (2021YFS0373).

Acknowledgments

We express our sincere gratitude to Dr. Qingxiang Sun for his invaluable guidance and assistance throughout the research and preparation of this manuscript. His expertise in navigating complex literature and explaining intricate mechanisms has been essential to our work. Additionally, we acknowledge Bio-render for providing the tools necessary to illustrate mechanisms clearly and effectively. Special thanks to Shenzhen METSTR Technology Co., Ltd. for granting us access to cutting-edge literature, which significantly contributed to the depth and quality of this review.

Conflict of interest

The authors declare that the research was conducted in the absence of any commercial or financial relationships that could be construed as a potential conflict of interest.

Publisher's note

References

1. Walker JS, Garzon R, Lapalombella R. Selinexor for advanced hematologic Malignancies. *Leuk Lymphoma*. (2020) 61:2335–50. doi: 10.1080/10428194.2020.1775210

2. Martini S, Figini M, Croce A, Frigerio B, Pennati M, Gianni AM, et al. Selinexor sensitizes TRAIL-R2-positive TNBC cells to the activity of TRAIL-R2xCD3 bispecific antibody. *Cells*. (2020) 9:2231. doi: 10.3390/cells9102231

3. Rosen JC, Weiss J, Pham NA, Li Q, Martins-Filho SN, Wang Y, et al. Antitumor efficacy of XPO1 inhibitor Selinexor in KRAS-mutant lung adenocarcinoma patient-derived xenografts. *Transl Oncol*. (2021) 14:101179. doi: 10.1016/j.tranon.2021.101179

4. Subhash VV, Yeo MS, Wang L, Tan SH, Wong FY, Thuya WL, et al. Anti-tumor efficacy of Selinexor (KPT-330) in gastric cancer is dependent on nuclear accumulation of p53 tumor suppressor. *Sci Rep*. (2018) 8:12248. doi: 10.1038/s41598-018-30686-1

5. Lee JG, Huang W, Lee H, van de Leemput J, Kane MA, Han Z. Characterization of SARS-CoV-2 proteins reveals Orf6 pathogenicity, subcellular localization, host interactions and attenuation by Selinexor. *Cell Biosci*. (2021) 11:58. doi: 10.1186/s13578-021-00568-7

6. Wu M, Gui H, Feng Z, Xu H, Li G, Li M, et al. KPT-330, a potent and selective CRM1 inhibitor, exhibits anti-inflammation effects and protection against sepsis. *Biochem Biophys Res Commun*. (2018) 503:1773–9. doi: 10.1016/j.bbrc.2018.07.112

7. English KG, Reid AL, Samani A, Coulis GJF, Villalta SA, Walker CJ, et al. Next-generation SINE compound KPT-8602 ameliorates dystrophic pathology in zebrafish and mouse models of DMD. *Biomedicines*. (2022) 10:2400. doi: 10.3390/biomedicines10102400

8. Chari A, Vogl DT, Gavriatopoulou M, Nooka AK, Yee AJ, Huff CA, et al. Oral selinexor-dexamethasone for triple-class refractory multiple myeloma. *N Engl J Med*. (2019) 381:727–38. doi: 10.1056/NEJMoa1903455

9. Delimpasi S, Mateos MV, Auner HW, Gavriatopoulou M, Dimopoulos MA, Quach H, et al. Efficacy and tolerability of once-weekly selinexor, bortezomib, and dexamethasone in comparison with standard twice-weekly bortezomib and dexamethasone in previously treated multiple myeloma with renal impairment: Subgroup analysis from the BOSTON study. *Am J Hematol*. (2022) 97:E83–6. doi: 10.1002/ajh.26434

10. Ben-Barouch S, Kuruvilla J. Selinexor (KTP-330) - a selective inhibitor of nuclear export (SINE): anti-tumor activity in diffuse large B-cell lymphoma (DLBCL). *Expert Opin Investig Drugs*. (2020) 29:15–21. doi: 10.1080/13543784.2020.1706087

11. Ben Barouch S, Bhella S, Kridel R, Kukreti V, Prica A, Crump M, et al. Long-term follow up of relapsed/refractory non-Hodgkin lymphoma patients treated with single-agent selinexor - a retrospective, single center study. *Leuk Lymphoma*. (2022) 63:1879–86. doi: 10.1080/10428194.2022.2047674

12. Bhatnagar B, Zhao Q, Mims AS, Vasu S, Behbehani GK, Larkin K, et al. Phase 1 study of Selinexor in combination with salvage chemotherapy in adults with relapsed or refractory Acute myeloid leukemia. *Leuk Lymphoma*. (2023) 64:2091–100. doi: 10.1080/10428194.2023.2253480

13. Fiedler W, Chromik J, Amberg S, Kebenko M, Thol F, Schlipfenbacher V, et al. A Phase II study of selinexor plus cytarabine and idarubicin in patients with relapsed/refractory acute myeloid leukaemia. *Br J Haematol*. (2020) 190:e169–73. doi: 10.1111/bjh.16804

14. Alexander TB, Lacayo NJ, Choi JK, Ribeiro RC, Pui CH, Rubnitz JE. Phase I study of selinexor, a selective inhibitor of nuclear export, in combination with fludarabine and cytarabine, in pediatric relapsed or refractory acute leukemia. *J Clin Oncol*. (2016) 34:4094–101. doi: 10.1200/JCO.2016.67.5066

15. Ho J, Heong V, Peng Yong W, Soo R, Ean Chee C, Wong A, et al. A phase 1 study of the safety, pharmacokinetics and pharmacodynamics of escalating doses followed by dose expansion of the selective inhibitor of nuclear export (SINE) selinexor in Asian patients with advanced or metastatic Malignancies. *Ther Adv Med Oncol*. (2022) 14:17588359221087555. doi: 10.1177/17588359221087555

16. Lewin J, Malone E, Al-Ezzi E, Fasih S, Pedersen P, Accardi S, et al. A phase 1b trial of selinexor, a first-in-class selective inhibitor of nuclear export (SINE), in combination with doxorubicin in patients with advanced soft tissue sarcomas (STS). *Eur J Cancer*. (2021) 144:360–7. doi: 10.1016/j.ejca.2020.10.032

17. Gounder MM, Zer A, Tap WD, Salah S, Dickson MA, Gupta AA, et al. Phase IB study of selinexor, a first-in-class inhibitor of nuclear export, in patients with advanced refractory bone or soft tissue sarcoma. *J Clin Oncol*. (2016) 34:3166–74. doi: 10.1200/JCO.2016.67.6346

18. Rubinstein MM, Grisham RN, Cadoo K, Kyi C, Tew WP, Friedman CF, et al. A phase I open-label study of selinexor with paclitaxel and carboplatin in patients with advanced ovarian or endometrial cancers. *Gynecol Oncol*. (2021) 160:71–6. doi: 10.1016/j.ygyno.2020.10.019

19. Hernando-Calvo A, Malone E, Day D, Prawira A, Weinreb I, Yang SYC, et al. Selinexor for the treatment of recurrent or metastatic salivary gland tumors: Results from the GEMS-001 clinical trial. *Cancer Med*. (2023) 12:20299–310. doi: 10.1002/cam4.6589

20. Lassman AB, Wen PY, van den Bent MJ, Plotkin SR, Walenkamp AME, Green AL, et al. A phase II study of the efficacy and safety of oral selinexor in recurrent glioblastoma. *Clin Cancer Res*. (2022) 28:452–60. doi: 10.1158/1078-0432.CCR-21-2225

21. Shafique M, Ismail-Khan R, Extermann M, Sullivan D, Goodridge D, Boulware D, et al. A phase II trial of selinexor (KPT-330) for metastatic triple-negative breast cancer. *Oncologist*. (2019) 24:887–e416. doi: 10.1634/theoncologist.2019-0231

22. Wei XX, Siegel AP, Aggarwal R, Lin AM, Friedlander TW, Fong L, et al. A phase II trial of selinexor, an oral selective inhibitor of nuclear export compound, in Abiraterone- and/or enzalutamide-refractory metastatic castration-resistant prostate cancer. *Oncologist*. (2018) 23:656–e64. doi: 10.1634/theoncologist.2017-0624

23. von Fallois M, Depping R. Strahlensensibilität durch Inhibition von XPO1 in Zelllinien kolorektaler Karzinome gesteigert [Radiation response enhanced by inhibition of XPO1 in preclinical rectal cancer models]. *Strahlenther Onkol*. (2016) 192:961–2. doi: 10.1007/s00066-016-1060-2

24. Vogl DT, Dingli D, Cornell RF, Huff CA, Jagannath S, Bhutani D, et al. Selective inhibition of nuclear export with oral selinexor for treatment of relapsed or refractory multiple myeloma. *J Clin Oncol*. (2018) 36:859–66. doi: 10.1200/JCO.2017.75.5207

25. Chen C, Siegel D, Gutierrez M, Jacoby M, Hofmeister C, Gabrail N, et al. Safety and efficacy of selinexor in relapsed or refractory multiple myeloma and Waldenstrom macroglobulinemia. *Blood*. (2018) 131:855–63. doi: 10.1182/blood-2017-08-797886

26. Ranganathan P, Kashyap T, Yu X, Meng X, Lai TH, McNeil B, et al. XPO1 inhibition using selinexor synergizes with chemotherapy in acute myeloid leukemia by targeting DNA repair and restoring topoisomerase IIα to the nucleus. *Clin Cancer Res*. (2016) 22:6142–52. doi: 10.1158/1078-0432.CCR-15-2885

27. Wang AY, Weiner H, Green M, Chang H, Fulton N, Larson RA, et al. A phase I study of selinexor in combination with high-dose cytarabine and mitoxantrone for

remission induction in patients with acute myeloid leukemia. *J Hematol Oncol*. (2018) 11:4. doi: 10.1186/s13045-017-0550-8

28. Klement P, Fiedler W, Gabdoulline R, Dallmann LK, Wienecke CP, Schiller J, et al. Molecular response patterns in relapsed/refractory AML patients treated with selinexor and chemotherapy. *Ann Hematol*. (2023) 102:323–8. doi: 10.1007/s00277-022-05075-4

29. Martínez Sánchez MP, Megías-Vericat JE, Rodríguez-Veiga R, Vives S, Bergua JM, Torrent A, et al. A phase I trial of selinexor plus FLAG-Ida for the treatment of refractory/relapsed adult acute myeloid leukemia patients. *Ann Hematol*. (2021) 100:1497–508. doi: 10.1007/s00277-021-04542-8

30. Jagannath S, Delimpasi S, Grosicki S, Van Domelen DR, Bentur OS, Špička I, et al. Association of selinexor dose reductions with clinical outcomes in the BOSTON study. *Clin Lymphoma Myeloma Leuk*. (2023) 23:917–23. doi: 10.1016/j.clml.2023.08.018

31. Restrepo P, Bhalla S, Ghodke-Puranik Y, Aleman A, Leshchenko V, Melnekoff DT, et al. A three-gene signature predicts response to selinexor in multiple myeloma. *JCO Precis Oncol*. (2022) 6:e2200147. doi: 10.1200/PO.22.00147

32. Hu F, Chen XQ, Li XP, Lu YX, Chen SL, Wang DW, et al. Drug resistance biomarker ABCC4 of selinexor and immune feature in multiple myeloma. *Int Immunopharmacol*. (2022) 108:108722. doi: 10.1016/j.intimp.2022.108722

33. Kwanten B, Deconick T, Walker C, Wang F, Landesman Y, Daelemans D. E3 ubiquitin ligase ASB8 promotes selinexor-induced proteasomal degradation of XPO1. *BioMed Pharmacother*. (2023) 160:114305. doi: 10.1016/j.biopha.2023.114305

34. Schmidt J, Braggio E, Kortuem KM, Egan JB, Zhu YX, Xin CS, et al. Genome-wide studies in multiple myeloma identify XPO1/CRM1 as a critical target validated using the selective nuclear export inhibitor KPT-276. *Leukemia*. (2013) 27:2357–65. doi: 10.1038/leu.2013.172

35. Deng M, Zhang M, Xu-Monette ZY, Pham LV, Tzankov A, Visco C, et al. XPO1 expression worsens the prognosis of unfavorable DLBCL that can be effectively targeted by selinexor in the absence of mutant p53. *J Hematol Oncol*. (2020) 13:148. doi: 10.1186/s13045-020-00982-3

36. Vitale C, Griggio V, Todaro M, Riganti C, Jones R, Boccellato E, et al. Anti-tumor activity of selinexor in combination with antineoplastic agents in chronic lymphocytic leukemia. *Sci Rep*. (2023) 13:16950. doi: 10.1038/s41598-023-44039-0

37. Mostafa-Hedeab G, Al-Kuraishy HM, Al-Gareeb AI, Welson NN, El-Saber Batiha G, Conte-Junior CA. Selinexor and COVID-19: the neglected warden. *Front Pharmacol*. (2022) 13:884228. doi: 10.3389/fphar.2022.884228

38. Haines JD, Herbin O, de la Hera B, Vidaurre OG, Moy GA, Sun Q, et al. Nuclear export inhibitors avert progression in preclinical models of inflammatory demyelination. *Nat Neurosci*. (2015) 18:511–20. doi: 10.1038/nn.3953

39. Baron S, Rashal T, Vaisman D, Elhasid R, Shukrun R. Selinexor, a selective inhibitor of nuclear export, inhibits human neutrophil extracellular trap formation *in vitro*. *Front Pharmacol*. (2022) 13:1030991. doi: 10.3389/fphar.2022.1030991

40. Kashyap T, Murray J, Walker CJ, Chang H, Tamir S, Hou B, et al. Selinexor, a novel selective inhibitor of nuclear export, reduces SARS-CoV-2 infection and protects the respiratory system *in vivo*. *Antiviral Res*. (2021) 192:105115. doi: 10.1016/j.antiviral.2021.105115

41. Jorquera PA, Mathew C, Pickens J, Williams C, Luczo JM, Tamir S, et al. Verdinexor (KPT-335), a selective inhibitor of nuclear export, reduces respiratory syncytial virus replication *in vitro*. *J Virol*. (2019) 93:e01684–18. doi: 10.1128/JVI.01684-18

42. Dutta P, Kodigepalli KM, LaHaye S, Thompson JW, Rains S, Nagel C, et al. KPT-330 prevents aortic valve calcification via a novel C/EBPβ Signaling pathway. *Circ Res*. (2021) 128(9):1300–16. doi: 10.1161/CIRCRESAHA.120.318503

43. Rahman MM, Estifanos B, Glenn HL, Kibler K, Li Y, Jacobs B, et al. Nuclear export inhibitor Selinexor targeting XPO1 enhances coronavirus replication. *bioRxiv [Preprint]*. (2023) 13. doi: 10.1101/2023.02.09.527884

44. Liu S, Wang S, Gu R, Che N, Wang J, Cheng J, et al. The XPO1 inhibitor KPT-8602 ameliorates Parkinson's disease by inhibiting the NF-κB/NLRP3 pathway. *Front Pharmacol*. (2022) 13:847605. doi: 10.3389/fphar.2022.847605

45. Zhang J, Zhang Y, Chen Q, Qi Y, Zhang X. The XPO1 inhibitor selinexor ameliorates bleomycin-induced pulmonary fibrosis in mice via GBP5/NLRP3 inflammasome signaling. *Int Immunopharmacol*. (2024) 130:111734. doi: 10.1016/j.intimp.2024.111734

46. Crochiere M, Kashyap T, Kalid O, Shechter S, Klebanov B, Senapedis W, et al. Deciphering mechanisms of drug sensitivity and resistance to Selective Inhibitor of Nuclear Export (SINE) compounds. *BMC Cancer*. (2015) 15. doi: 10.1186/s12885-015-1790-z

47. Miyake T, Pradeep S, Bayraktar E, Stur E, Handley K, Wu S, et al. NRG1/ERBB3 pathway activation induces acquired resistance to XPO1 inhibitors. *Mol Cancer Ther*. (2020) 19:1727–35. doi: 10.1158/1535-7163.MCT-19-0977

10.3389/fimmu.2024.1398927

Glossary

.

SINE	Selectively Inhibits Nuclear Export
XPO1	Exportin 1
COVID-19	Coronavirus Disease 2019
DMD	Duchenne muscular dystrophy
DDR	DNA damage response
STORM	Selinexor Treatment with Refractory Myeloma
BOSTON	Bortezomib, Selinexor, and Dexamethasone in Patients with Multiple Myeloma
SADAL	Selinexor in patients with relapsed or refractory diffuse large B-cell lymphom
NHL	Non-Hodgkin's Lymphoma
AML	Acute Myeloid Leukemia
CLL	Chronic lymphocytic leukemia
STS	Soft Tissue Sarcoma
NK	Natural Killer
HLA-E	Human Leukocyte Antigen E
NF-kB	Nuclear Factor Kappa-Light-Chain-Enhancer of Activated B cells
IκBα	Inhibitor of NF-kB alpha
STAT3	Signal Transducer and Activator of Transcription 3
NETs	Neutrophil Extracellular Traps
ADAR1-p150	Adenosine Deaminase Acting on RNA 1, p150 isoform
LPS	lipopolysaccharide
RSV	respiratory syncytial virus
HMGB1	High Mobility Group Box 1
MHV	mouse hepatitis virus
FLAG-Ida	Fludarabine, Cytarabine, Granulocyte colony-stimulating factor (G-CSF), and Idarubicin
ALT	Alanine Transaminase
CRISPR-Cas9	Clustered Regularly Interspaced Short Palindromic Repeats" and "CRISPR associated protein 9
ASB8	Ankyrin Repeat and SOCS Box Containing 8
TGFβ-SMAD4	Transforming Growth Factor Beta-SMAD Family Member 4 Pathway
WNT10A	Wnt Family Member 10A
DUSP1	Dual Specificity Phosphatase 1
ETV7	ETS Variant Transcription Factor 7
ABCC4	ATP-binding cassette subfamily C member 4
WGCNA	weighted gene co-expression network analysis
NFATc1	Nuclear Factor of Activated T Cells 1
PD	Parkinson's Disease
NLRP3	NLR Family Pyrin Domain Containing 3
CAVD	calcific aortic valve disease

frontiers | Frontiers in Immunology

TYPE Original Research
PUBLISHED 13 May 2024
DOI 10.3389/fimmu.2024.1364161

OPEN ACCESS

EDITED BY
Syed Faisal,
National Institute of Animal Biotechnology (NIAB), India

REVIEWED BY
Olivia Favor McDonald,
Michigan State University, United States
Marco Orecchioni,
Augusta University, United States

*CORRESPONDENCE
Yiqing Li
qzg599@126.com
Lei Zhao
leizhao@hust.edu.cn
Yiping Dang
dangyipingewuhan@163.com

†These authors have contributed equally to this work

RECEIVED 01 January 2024
ACCEPTED 01 May 2024
PUBLISHED 13 May 2024

CITATION
Mao J, Chen Y, Zong Q, Liu C, Xie J, Wang Y, Fisher D, Hien NTT, Pronyuk K, Musabaev E, Li Y, Zhao L and Dang Y (2024) Corilagin alleviates atherosclerosis by inhibiting NLRP3 inflammasome activation via the Olfr2 signaling pathway *in vitro* and *in vivo*. *Front. Immunol.* 15:1364161. doi: 10.3389/fimmu.2024.1364161

Corilagin alleviates atherosclerosis by inhibiting NLRP3 inflammasome activation via the Olfr2 signaling pathway *in vitro* and *in vivo*

Jinqian Mao[1†], Yunfei Chen[1†], Qiushuo Zong[1], Cuiling Liu[2], Jiao Xie[2], Yujie Wang[1], David Fisher[3], Nguyen Thi Thu Hien[4], Khrystyna Pronyuk[5], Erkin Musabaev[6], Yiqing Li[1*], Lei Zhao[2*] and Yiping Dang[1*]

[1]Department of Vascular Surgery, Union Hospital, Tongji Medical College, Huazhong University of Science and Technology, Wuhan, China, [2]Department of Infectious Diseases, Union Hospital, Tongji Medical College, Huazhong University of Science and Technology, Wuhan, China, [3]Department of Medical Biosciences, Faculty of Natural Sciences, University of The Western Cape, Cape Town, South Africa, [4]Hai Phong University of Medicine and Pharmacy, Haiphong, Vietnam, [5]Department of Infectious Diseases, O.Bogomolets National Medical University, Kyiv, Ukraine, [6]Research Institute of Virology, Ministry of Health, Tashkent, Uzbekistan

Introduction: Atherosclerosis, a leading cause of global cardiovascular mortality, is characterized by chronic inflammation. Central to this process is the NOD-like receptor pyrin domain containing 3 (NLRP3) inflammasome, which significantly influences atherosclerotic progression. Recent research has identified that the olfactory receptor 2 (Olfr2) in vascular macrophages is instrumental in driving atherosclerosis through NLRP3- dependent IL-1 production.

Methods: To investigate the effects of Corilagin, noted for its anti-inflammatory attributes, on atherosclerotic development and the Olfr2 signaling pathway, our study employed an atherosclerosis model in ApoE$^{-/-}$ mice, fed a high-fat, high-cholesterol diet, alongside cellular models in Ana-1 cells and mouse bone marrow-derived macrophages, stimulated with lipopolysaccharides and oxidized low-density lipoprotein.

Results: The vivo and vitro experiments indicated that Corilagin could effectively reduce serum lipid levels, alleviate aortic pathological changes, and decrease intimal lipid deposition. Additionally, as results showed, Corilagin was able to cut down expressions of molecules associated with the Olfr2 signaling pathway.

Discussion: Our findings indicated that Corilagin effectively inhibited NLRP3 inflammasome activation, consequently diminishing inflammation, macrophage polarization, and pyroptosis in the mouse aorta and cellular models via the Olfr2 pathway. This suggests a novel therapeutic mechanism of Corilagin in the treatment of atherosclerosis.

KEYWORDS

atherosclerosis, inflammation, Olfr2, NLRP3 inflammasome, corilagin, therapeutic strategies

Introduction

Cardiovascular diseases, the leading cause of death globally, represent a severe health burden across both the high-income and developing nations (1–3). Atherosclerosis is the dominant risk factor for cardiovascular events including myocardial infarction, strokes, and peripheral arterial disease (4). Although various treatments exist for arteriosclerosis, including lipid-lowering and anti-platelet aggregation therapy, issues such as drug resistance, intolerance, and increased risk of sever bleeding events are prevalent (3, 5–7). Atherosclerosis is recognized as a chronic inflammatory condition characterized by the presence of immune cells in lesions, which produce a range of pro-inflammatory cytokines (8, 9). Macrophages, the pro-inflammatory cells, make significant contributions to the development of atherosclerosis (10). Normal and modified lipoproteins are accumulated in macrophages, promoting foam cell formation and activation of innate immune receptors likes NOD-like and Toll-like receptors (NLRs and TLRs) to exacerbate inflammation and plaque progression (11, 12).

The NOD-like receptor pyrin domain containing 3 (NLRP3) inflammasome, a complex of multimeric cytosolic proteins, is pivotal in atherosclerotic progression (2, 8, 13, 14). Additionally, dysregulation of TLRs is a crucial mechanism for inflammation and atherosclerosis, primarily due to their role in regulating the expression of key molecules (8, 15–17). The activation of the NLRP3 inflammasome in macrophages typically requires two distinct signals: priming and activation (2, 8, 18). During priming, TLRs or cytokine receptors, stimulated by damage-associated and pathogen-associated molecular patterns, transcriptionally upregulate NLRP3, pro-IL-18, and pro–IL-1β via NF-κB signaling, thus facilitates NLRP3-mediated inflammasome assembly (2, 8, 19–21). In the activation phase, factors such as phagolysosomal rupture, disrupted ion homeostasis, mitochondrial damage, or reactive oxygen species are identified as common triggers for NLRP3 activation (2, 22–24). Subsequently, NIMA-related kinase 7 (NEK7) interacts with NLRP3 to recruit pro-caspase-1 through the apoptosis-associated speck-like protein containing a caspase recruitment domain (ASC). Activated caspase-1 then converts pro-IL-1β and pro-IL-18 into their active forms, also triggering gasdermin D (GSDMD) production (2, 25–28). NLRP3 inflammasome activation could cause the overexpression of inflammatory factors involved in atherosclerosis progression (8, 29), the polarization of macrophages into M1 type that fosters tissue destruction and secretion of pro-inflammatory factors (30, 31), and the increasing expression of GSDMD resulting in pyroptosis to enhance vascular permeability and membrane damage (32–34). Recently, Orecchioni et al. have revealed that olfactory receptor 2 (Olfr2) interacts with TLR4 in vascular macrophages leading to NLRP3 inflammasomes activation via adenylate cyclase 3 (Adcy3) to drive atherosclerosis development, provides a new target for the prevention and treatment of atherosclerosis (35).

Corilagin, a polyphenolic monomer isolated from Phyllanthus urinaria, exhibits diverse pharmacological properties including antitumor, antioxidant, and anti-inflammatory effects (17, 36). It can ameliorate inflammatory lesions in macrophages by inhibiting NLRP3 inflammasome activation and pyroptosis (37, 38). Nonetheless, the specific impact of Corilagin on NLRP3 inflammasome activation in atherosclerosis necessitates further investigation. TLR4 can provide the priming signal of NLRP3 inflammasome activation via NF-κB pathway (12). Several researches have indicated Corilagin's potential in preventing and treating atherosclerosis (17, 39–42), and find Corilagin probably mitigate atherosclerosis by inhibiting the TLR4 signaling pathway (17, 40). However, its regulatory mechanisms remain unclear, necessitating further investigation into its anti-atherosclerotic efficacy. Consequently, we hypothesize that Corilagin can suppress the activation of NLRP3 inflammasome to alleviate atherosclerosis by disrupting the Olfr2 signaling pathway. This study aims to examine the potential effects and mechanisms of Corilagin on atherosclerosis through the Olfr2 pathway, employing treatments on Ana-1 cells, primary mouse bone marrow-derived macrophages (BMDMs), and atherosclerotic models in ApoE$^{-/-}$ mice.

Materials and methods

Reagents

Corilagin standard substance (SC9500, purity ≥ 98%) for cells and aspirin for animals (A8830, purity ≥ 98%) were purchased from Solarbio (Beijing, China). Corilagin for animal experimentation (N0272, purity 90% ~ 99%) was obtained from Hengcheng Zhiyuan Biotechnology (Sichuan, China). Aspirin for cells (B21505, purity ≥ 98%) was purchased from Yuanye Biotechnology (Shanghai, China). Oxidized low-density lipoprotein (Ox-LDL) was purchased from Yiyuan Biotechnology (YB-002, Guangzhou, China). Lipopolysaccharides (LPS, L8880) was purchased from Solarbio. Fetal bovine serum (FBS, 10099–141) and Roswell Park Memorial Institute (RPMI)-1640 were obtained from Gibco (New York, USA). Phosphate buffer saline (PBS) was obtained from Servicebio (G4202, Wuhan, China) and 4% paraformaldehyde (PFA) was purchased from Biosharp (BL520, Guangzhou, China).

Cell culture and infection

The Ana-1 cell line, a murine macrophage line Ana-1 cells, was obtained from the Type Culture Collection of the Chinese Academy of Sciences (Shanghai, China). Cells were cultured in RPMI-1640 medium containing 10% FBS and maintained at 37°C in a saturated humidity incubator with 5% CO2. The lentivirus of short hairpin (Sh)-Olfr2 (Sh-Olfr2), Olfr2-overexpression (Olfr2-OE), Sh-Control (Sh-Ctrl), and Control-OE (Ctrl-OE) were constructed by GeneChem (Shanghai, China). Ana-1 cells were planted into 6-well plates with a density of 1×10^5/well for 24h and then infected with lentivirus with a multiplicity of infection of 40 according to our previous experiment (17). The medium was replaced within 12h after infection and were cultured for an additional 72h. Then, 2μg/ml of puromycin (Sigma–Aldrich, St. Louis, MO, USA) was added to the complete medium to kill the wild-type cells for 2 weeks, and

the culture medium was changed every 2 days. The efficiency of infection was determined by quantitative real-time PCR (RT-qPCR). We cultured the remaining lentivirus-infected cells for further experimentations.

BMDMs generation

The femora and tibiae from C57BL/6J were flushed with 5ml ice cold RPMI-1640 medium to isolate mouse bone marrow. Bone marrow cells were filtered by a 70μm cell strainer (BS-70-XBS, Biosharp) and red blood cell lysis buffer (R1010, Solarbio) was utilized to lyse red blood cells. The remaining cells were cultured in RPMI-1640 medium supplemented with 20ng/ml of mouse recombinant macrophage-colony stimulating factor (315–02, Peprotech, NJ, USA) for 7 days. The culture medium was changed every 2 days to obtain BMDMs for further studies.

Cell stimulation and treatment

Ana-1 Cells or BMDMs were seeded at 6-well plates overnight. They were divided into 6 groups: the Control group, the Model group, the Aspirin group (Positive control group), the Corilagin (100μg/ml) group, the Corilagin (50μg/ml) group, and the Corilagin (25μg/ml) group. Except the Control group, the other groups were stimulated with LPS (1μg/ml) and Ox-LDL (100μg/ml) for 24h. Subsequently, the Aspirin group and the Corilagin (100, 50 and 25μg/ml) groups were treated with aspirin and different concentrations of Corilagin. In addition, the lentivirus-infected cells were grown on 6-well plates for 24h and divided into 8 groups: the Sh-Ctrl group, the Sh-Olfr2 group, the Sh-Ctrl +Corilagin (100μg/ml) group, the Sh-Olfr2+Corilagin (100μg/ml) group, the Ctrl-OE group, the Olfr2-OE group, the Ctrl-OE +Corilagin (100μg/ml) group, and the Olfr2-OE+Corilagin (100μg/ml) group. After all groups stimulating by LPS+Ox-LDL for 24h, the Sh-Ctrl+Corilagin group, the Sh-Olfr2+Corilagin group, the Ctrl-OE+Corilagin group, and the Olfr2-OE+Corilagin group were treated with Corilagin. After treating with Corilagin for 24h in our study, cell culture medium and cell lysates were gathered for subsequent experiments (Supplementary Figure 1).

Animal treatments and sample collection

All animal experimental protocols are approved by the Animal Care and Use Committee of Bainte Biotechnology (Wuhan, China) [[2023] IACUC number: 004]. ApoE$^{-/-}$ mice (male, 5 weeks, 18–24g) were provided by Bainte Biotechnology and exposed to a 12-h light/dark cycle in plenty of water and food. After a week of adaptive feeding, mice were randomly divided into 14 groups with six mice in each group: the Control group, the Model group, the Aspirin group, the Corilagin (40mg/kg) group, the Corilagin (20mg/kg) group, the Corilagin (10mg/kg) group, the Sh-Ctrl group, the Sh-Olfr2 group, the Sh-Ctrl+Corilagin group, the Sh-Olfr2+Corilagin group, the Ctrl-OE group, the Olfr2-OE group, the Ctrl-OE +Corilagin group, and the Olfr2-OE+Corilagin group. The Control group was fed a normal diet while other groups were fed a high fat and cholesterol diet (D12108C; HFK Bios) for 8 weeks. After feeding 8 weeks, the Sh-Ctrl group, the Sh-Olfr2 group, the Sh-Ctrl+Corilagin (40mg/kg) group, the Sh-Olfr2+Corilagin (40mg/kg) group, the Ctrl-OE group, the Olfr2-OE group, the Ctrl-OE+Corilagin (40mg/kg) group, and the Olfr2-OE+Corilagin (40mg/kg) group were injected lentivirus (4×10^7Tfu, 20μl) via tail vein. Simultaneously, the same amount of physiologic (0.9%) saline were gave in the Control group, the Model group, the Sh-Ctrl group, the Sh-Olfr2 group, the Ctrl-OE group and the Olfr2-OE group, and other groups were treated with aspirin or different concentrations of Corilagin through intragastric administration every 2 days for 2 weeks (Supplementary Figure 2). Finally, mice were sacrificed and perfused with PBS. Aortas were divided into two segments: the vessel closed to aortic root was reserved in 4% PFA for hematoxylin and eosin (HE), Oil Red O, and immunohistochemical (IHC) staining, whereas the other section was placed at -80°C for RT-qPCR and western blotting (WB) analysis. Blood samples were collected by removing mouse eyeballs. Serum was separated by centrifugation at 4°C (2500rpm, 15min) and stored at -80°C for serum lipids detection and Enzyme-Linked Immunosorbent Assay (ELISA) analysis.

Quantitative real-time PCR analysis

The mRNA expressions of Olfr2, iNOS, Adcy3, NLRP3, GSDMD, Caspase-1, Arg-1, NEK7, ASC, IL-1β, IL-18, and TNF-α were measured by RT-qPCR. Total RNA was isolated from Ana-1 cells, BMDMs, or aortas by Trizol reagent (R401–01, Vazyme, Nanjing, China). The isolated total RNA was reverse transcribed into complimentary (c)DNA via the HiScript II Q RT SuperMix (R223–01, Vazyme). The RT-qPCR was performed on StepOne^{TM} Plus device (Applied Biosystems, Foster City, CA, USA) following the protocol of HiScript II One Step RT-qPCR SYBR Green Kit (Q221–01, Vazyme). The $2^{-\Delta\Delta CT}$ method was used to analyze the relative mRNA expression normalized to the reference gene GAPDH. All primers were synthesized by TSINGKE (Wuhan, China). The primer sequences of genes were presented in Table 1.

Western blotting analysis

The protein expressions of iNOS (A3774, Abclonal), Adcy3 (19492–1-AP, Proteintech), NLRP3 (ab270449, Abcam), GSDMD (66387–1-Ig, Proteintech), Caspase-1 (22915–1-AP, Proteintech), Arg-1 (16001–1-AP, Proteintech), NEK7 (A19816, Abclonal), and ASC (67824, Cell Signaling Technology) were measured by WB. Total protein was isolated from Ana-1 cells, BMDMs, or aortas by RIPA lysis buffer and protease inhibitor (P0013B and P1005, Beyotime, Shanghai, China), and quantified according to the instructions of the BCA Protein Assay Kit (P0012, Beyotime). The protein samples were separated by 10% sodium dodecyl sulfate–polyacrylamide gel electrophoresis and transferred to polyvinylidene difluoride membranes. Membranes were blocked

TABLE 1 Primer sequences used in this study.

Primer	Forward	Reverse
Olfr2	CTTGCTGGCTTCATTGGTTCCG	CCATGACAGCAAGAAGGACACAC
Adcy3	CCAACTTTGCTGACTTCTACAC	TGTCCAGGAGAGAGTCAAAATC
NEK7	GCTGTCTGCTATATGAGATGGC	CCGAATAGTGATCTGACGGGAG
NLRP3	ATTACCCGCCCGAGAAAGG	TCGCAGCAAAGATCCACACAG
ASC	GCTACTATCTGGAGTCGTATGGC	GACCCTGGCAATGAGTGCTT
Caspase-1	CACAGCTCTGGAGATGGTGA	GGTCCCACATATTCCCTCCT
GSDMD	CCATCGGCCTTTGAGAAAGTG	ACACATGAATAACGGGGTTTCC
IL-1β	TTCAGGCAGGCAGTATCACTC	GAAGGTCCACGGGAAAGACAC
IL-18	GACTCTTGCGTCAACTTCAAGG	CAGGCTGTCTTTTGTCAACGA
Arg-1	CTCCAAGCCAAAGTCCTTAGAG	AGGAGCTGTCATTAGGGACATC
iNOS	CCCTTCAATGGTTGGTACATGG	ACATTGATCTCCGTGACAGCC
TNF-α	CAGGCGGTGCCTATGTCTC	CGATCACCCCGAAGTTCAGTAG
GAPDH	GAGCAAGGACACTGAGCAAGA	GCCCCTCCTGTTATTATGGGG

with 5% non-fat milk in Tris-buffered saline and Tween 20 (TBST) for 1h and incubated with primary antibodies at 4°C overnight. After washing thrice with TBST, membranes were incubated with horseradish peroxidase-conjugated secondary antibody (SA00001–1 and SA00001–2, Proteintech, Wuhan, China) for 1h at room temperature (RT). These membranes were exposed in a dark room via electrochemiluminescence reagent (BL520, Biosharp). Finally, the grayscale values were measured by ImageJ software to quantify the WB bands contracted with GAPDH (60004–1-Ig, Proteintech).

Serum lipids and inflammatory cytokines analysis

Triglyceride (TG), Total cholesterol (TC), high-density lipoprotein cholesterol (HDL-C), and low-density lipoprotein cholesterol (LDL-C) in the serum of mice were detected by an automatic biochemical analyzer (Shenzhen Leidu Life Sciences, China). The level of IL-1β, IL-18, and TNF-α in the mouse serum or cell supernatant was measured through ELISA Kits from Ruixin Biotechnology (Quanzhou, China).

Histological analysis

Sections were stained with HE to visualize pathological changes in the vascular tissue and Oil red O staining was applied for lipid plaques analysis. Images were captured by an electron microscope (Olympus, Tokyo, Japan) and analyzed by ImageJ software. Besides, Olfr2 expression in animal model was examined through IHC staining. The tissue sections were stained with Olfr2 antibody (1:500, OSR00025G, Thermo Fischer) followed by Goat Anti-Rabbit IgG (1:200, G1213, Servicebio, Wuhan, China). The sections were incubated with 3,3-diaminobenzidine and counterstained with hematoxylin. Finally, images were captured by an automatic scanning microscope (Zeiss, Germany) and analyzed via ImageJ software.

Flow cytometric analysis

Cluster of differentiation (CD) 86 and CD206 expressions were measured by flow cytometric (FC) analysis. Ana-1 cells or BMDMs treated as indicated above were incubated with Mouse Fc block™ solution (553141, BD Biosciences, San Jose, CA, USA) for 5min at 4°C. Then they were stained with fluorescein isothiocyanate anti-F4/80 antibody (123107, BioLegend, San Diego, CA, USA), phycoerythrin anti-cluster of CD 86 antibody (E-AB-F099D), and peridinin chlorophyll protein/Cyanine5.5 anti-CD11b antibody (E-AB-F1081J, Elabscience, Wuhan, China) for 30 min at 4°C. All cells were washed two times with cold PBS and incubated with BD Cytofix/Cytoperm™ Fixation and Permeabilization Solution (554722) for 30min at 4°C. In order to permeabilization, the fixed cells were washed two times and incubated in 1X BD Perm/Wash™ buffer (554723) for 15min at 4°C. The fixed/permeabilized cells were thoroughly suspended in 100μL of 1X BD Perm/Wash™ buffer and stained with allophycocyanin anti-CD206 antibody (141707, BioLegend) in the dark for 30min at RT. After washing twice with PBS, cell suspensions were analyzed on a BD FACSCalibur™ flow cytometer and calculated by FlowJo software (Treestar Inc).

Immunofluorescence analysis

The Olfr2 expression was performed by immunofluorescence (IF) analysis. Ana-1 cells or BMDMs were cultured on 14 mm round coverslips (BS-14-RC, Biosharp) in the 24-well plate (703001, Nest) and treated as described above. Cells were fixed with 4% PFA

for 10min at RT. After washed three times with cold PBS, samples were incubated with 5% BSA (G1208, Servicebio) for 10min at RT and maintained in Olfr2 antibody (1:500, Thermo Fischer) at 4°C overnight. Subsequently, cells were washed three times and stained with secondary antibody (1:200, GB25303, Servicebio) for 1h at RT. DAPI (G1012, Servicebio) was used to stain nuclei in the dark for 10min. After washed three times, coverslips were sealed with anti-fluorescence quenching reagent (G1401, Servicebio) on glass slides. Images were captured by Zeiss scanning microscope and analyzed via ImageJ software.

Statistical analysis

All statistical analyses were performed by using GraphPad Prism 9.0 software. Data were presented as the mean ± standard deviation (SD). Shapiro-Wilk test was performed to assess the normalcy, and $p > 0.05$ was defined as normally distributed. Brown-Forsythe test was performed to assess the equality of variances, and $p > 0.05$ was defined as equal variances. Student's t-test was performed to compare data between two groups and one-way analysis of variance (ANOVA) test was performed for multiple comparisons, and $p < 0.05$ was defined as statistically significant.

Result

Effects of corilagin on atherosclerosis *in vivo*

To investigate the impact of Corilagin on atherosclerotic lesion formation, we established an ApoE$^{-/-}$ mouse model for *in vivo* experiments. HE staining, as depicted in Figure 1A, demonstrated that the aorta intima in the Model group was notably deformed and thickened, with the formation of plaques predominantly composed of foam cells and fibrous tissue. In contrast with the Model or Aspirin group, the Corilagin (40mg/kg) group exhibited a reduction in intima thickness and foam cell numbers. In addition, the percentage of red lipid plaques in the Corilagin groups was lower than that in both the Model and Aspirin group (Figure 1A). Furthermore, serum lipid levels of TG, TC and LDL-C in the Corilagin (20 and 40mg/kg) groups were reduced, while HDL-C levels were elevated compared to both the Model and Aspirin group (Figure 1D). These results indicated that Corilagin effectively mitigates atherosclerotic lesions in this animal model.

Effects of corilagin on Olfr2 and downstream molecules *in vivo* and vitro

To explore the effect of Corilagin on Olfr2 expression, qRT-PCR, IHC and IF were performed to assess Olfr2 levels in aortic tissues and cellular models. Olfr2 expression was significantly reduced in the Corilagin (40mg/kg or 100μg/ml) group compared to both the Model and Aspirin group (Figures 1A, 1B, 2A, 2C, 3A, 3C). The reduction in Olfr2 expression in atherosclerotic mice and cellular models probably suggested a potential pathway through that Corilagin regulated atherosclerosis development. To elucidate the underlying molecular mechanisms of Corilagin's anti-atherosclerotic effects, we further analyzed downstream molecules associated with Olfr2 *in vivo* and vitro experiments. The mRNA and protein levels of Adcy3, NLRP3 inflammasome effectors (NLRP3, Caspase-1, NEK7 and ASC) and the cell pyroptosis-related molecule (GSDMD) were lower in the Corilagin (40mg/kg or 100μg/ml) group than in the Model group (Figures 1B, 1C, 2A, 2B, 3A, 3B). In the Corilagin (40mg/kg) group, both mRNA and protein levels of iNOS in mouse aortic tissues were significantly reduced compared to the Model group, as evidenced in Figures 1B, 1C. Conversely, Arg-1 levels demonstrated a reverse pattern, indicating an anti-inflammatory effect. Similarly, in cellular models, the Corilagin treatment (100μg/ml) led to a reduction in M1 macrophage polarization markers (iNOS and CD86), while markers associated with M2 macrophage polarization (Arg-1 and CD206) were elevated, compared to the Model group (Figures 2A, 2D, 3A, 3D). Additionally, inflammatory factors such as IL-1β, IL-18, and TNF-α measured via RT-qPCR and ELISA, showed reduced expression following Corilagin (40mg/kg or 100μg/ml) treatment when compared to the Model or Aspirin group (Figures 1B, 1E, 2A, 2E, 3A, 3E). Consequently, these results led us to hypothesize that Corilagin could suppress NLRP3 inflammasome activation and subsequent cytokine production, macrophage polarization, and cell pyroptosis by inhibiting the Olfr2 signaling pathway.

Effects of corilagin on atherosclerosis after downregulating Olfr2 *in vivo*

We specifically downregulated Olfr2 expression in the animal model to further demonstrate the mechanism behind Corilagin therapeutic effects. As depicted in Figures 4A, 4D, the Sh-Olfr2 group exhibited improvements in pathological changes, percentage of lipid deposition, and serum lipid levels of TG, TC and LDL-C compared to the Sh-Ctrl group. These data might illustrate that the attenuation of Olfr2 expression may contribute to prevent atherosclerotic lesions. Additionally, when Olfr2 expression was decreased, the therapeutic effects of Corilagin on pathological changes, lipid deposition percentages, and serum lipid levels were diminished (Figures 4A, 4D). These outcomes indicated Olfr2 might serve as a critical pathway for Corilagin's atherosclerosis prevention effects.

Effects of corilagin on Olfr2 and downstream molecules after downregulating Olfr2 *in vivo* and vitro

To validate our hypothesis that Corilagin could suppress NLRP3 inflammasome activation and subsequent cytokine production, macrophage polarization, and pyroptosis by inhibiting the Olfr2 signaling pathway, we investigated the changes of Olfr2 and downstream molecules expression after downregulating Olfr2. Compared to the Sh-Ctrl group, Olfr2

10.3389/fimmu.2024.1364161

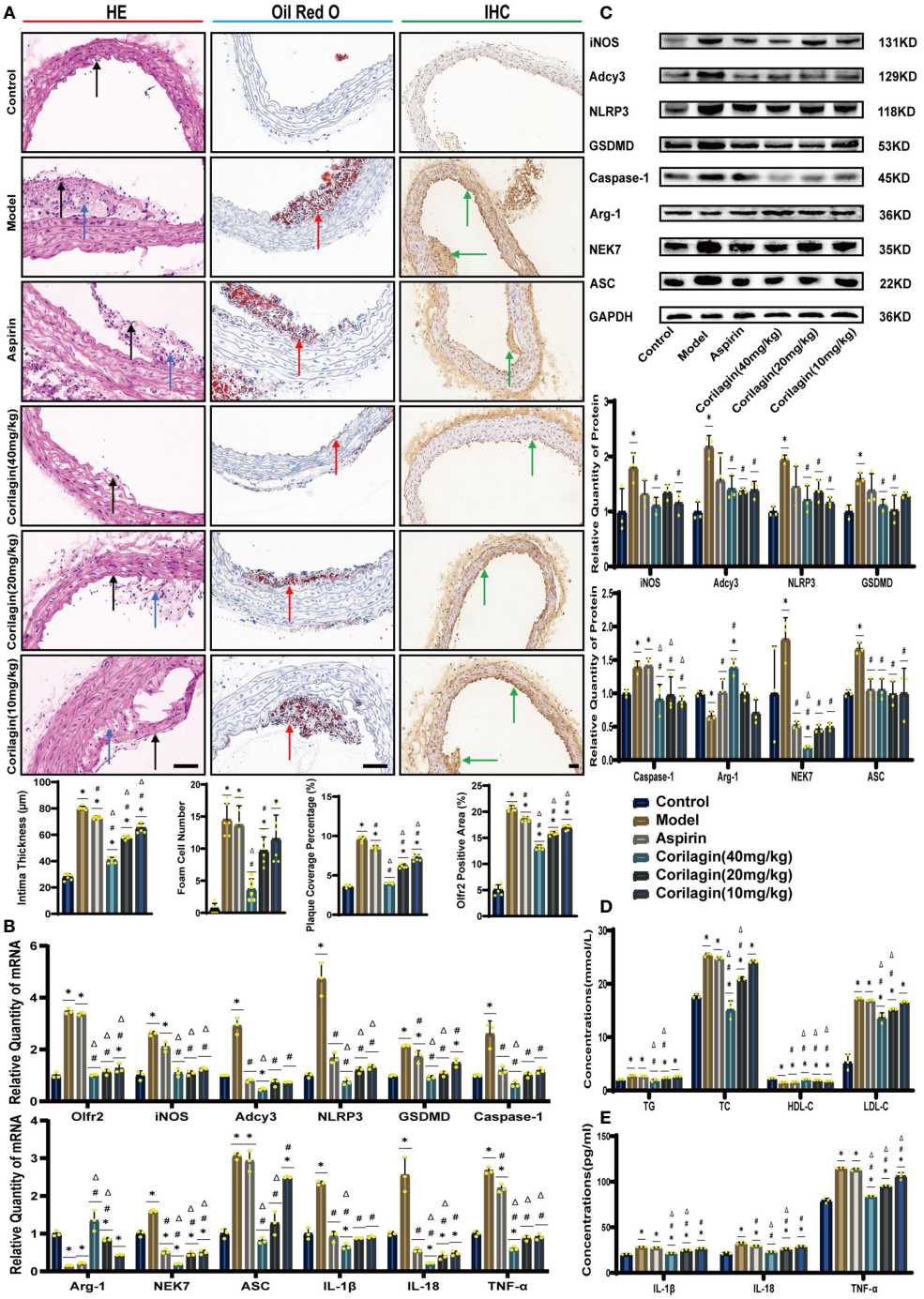

FIGURE 1
Effects of Corilagin on atherosclerosis and Olfr2 signal pathway *in vivo*. **(A)** Pathological changes, plaque coverage percentage, and Olfr2 expression in mouse aorta were visualized by HE, Oil red O, and IHC staining respectively and quantitative analyses of intima thickness and foam cell number based on HE, plaque coverage percentage based on Oil red O, and Olfr2 expression based on IHC. Black arrows indicated aorta intima and blue arrows indicated foam cell and fibrous tissue in HE. Yellow arrows indicated lipid plaque in Oil red O. Green arrows indicated the area of Olfr2 expression in IHC. $^{*}p < 0.05$ compared with the Control group, $^{\#}p < 0.05$ compared with the Model group, $^{\Delta}p < 0.05$ compared with the Aspirin group determined by one-way ANOVA test (n = 6). Data was presented as the mean ± SD. Scale bars, 50μm. **(B)** mRNA expression of Olfr2, Adcy3, NLRP3, Caspase-1, ASC, NEK7, GSDMD, IL-1β, IL-18, Arg-1, iNOS, and TNF-α in mouse aorta was measured by RT-qPCR. $^{*}p < 0.05$ compared with the Control group, $^{\#}p < 0.05$ compared with the Model group, $^{\Delta}p < 0.05$ compared with the Aspirin group determined by one-way ANOVA test (n = 3). Data was presented as the mean ± SD. **(C)** Protein expression of iNOS, Adcy3, NLRP3, GSDMD, Caspase-1, NEK7, Arg-1, and ASC in mouse aorta was measured by WB and quantitative analyses of protein level based on WB. $^{*}p < 0.05$ compared with the Control group, $^{\#}p < 0.05$ compared with the Model group, $^{\Delta}p < 0.05$ compared with the Aspirin group determined by one-way ANOVA test (n = 3). Data was presented as the mean ± SD. **(D)** Serum lipids of mice were detected by an automatic biochemical analyzer. $^{*}p < 0.05$ compared with the Control group, $^{\#}p < 0.05$ compared with the Model group, $^{\Delta}p < 0.05$ compared with the Aspirin group determined by one-way ANOVA test (n = 3). Data were presented as the mean ± SD. **(E)** IL-1β, IL-18, and TNF-α in the mouse serum were measured by ELISA. $^{*}p < 0.05$ compared with the Control group, $^{\#}p < 0.05$ compared with the Model group, $^{\Delta}p < 0.05$ compared with the Aspirin group determined by one-way ANOVA test (n = 3). Data was presented as the mean ± SD.

10.3389/fimmu.2024.1364161

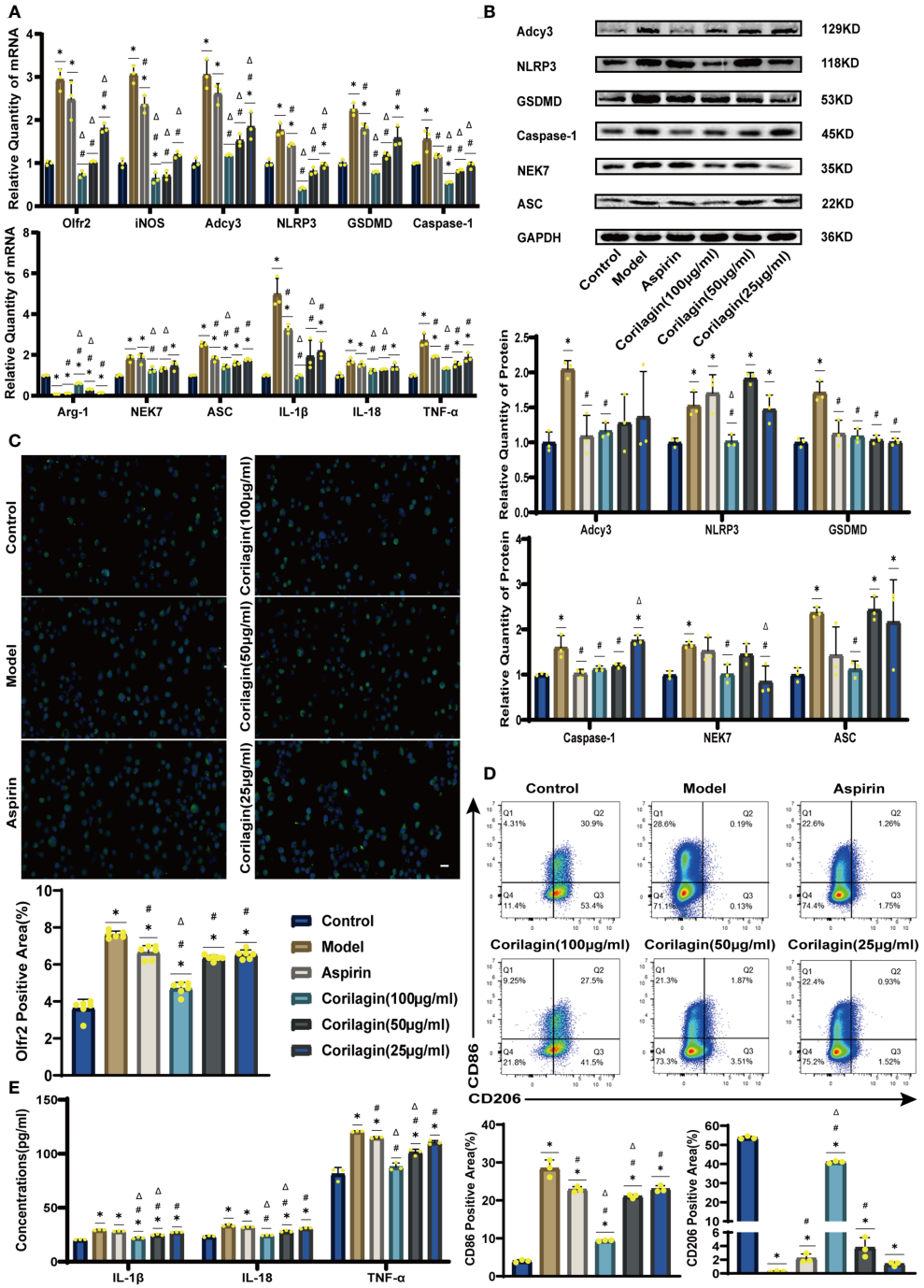

FIGURE 2
Effects of Corilagin on Olfr2 signal pathway in LPS+Ox-LDL-induced Ana-1 cells. **(A)** mRNA expression of Olfr2, Adcy3, NLRP3, Caspase-1, ASC, NEK7, GSDMD, IL-1β, IL-18, Arg-1, iNOS, and TNF-α in Ana-1 cells was measured by RT-qPCR. *$p < 0.05$ compared with the Control group, $^{\#}p < 0.05$ compared with the Model group, $^{\Delta}p < 0.05$ compared with the Aspirin group determined by one-way ANOVA test (n = 3). Data was presented as the mean ± SD. **(B)** Protein expression of Adcy3, NLRP3, GSDMD, Caspase-1, NEK7, and ASC in Ana-1 cells was measured by WB and quantitative analyses of protein level based on WB. *$p < 0.05$ compared with the Control group, $^{\#}p < 0.05$ compared with the Model group, $^{\Delta}p < 0.05$ compared with the Aspirin group determined by one-way ANOVA test (n = 3). Data was presented as the mean ± SD. **(C)** Olfr2 expression in Ana-1 cells was visualized by IF and quantitative analyses of Olfr2 level based on IF. *$p < 0.05$ compared with the Control group, $^{\#}p < 0.05$ compared with the Model group, $^{\Delta}p < 0.05$ compared with the Aspirin group determined by one-way ANOVA test (n = 6). Data was presented as the mean ± SD. Scale bars, 20μm. **(D)** CD86 and CD206 expression in Ana-1 cells were measured by FC and quantitative analyses of CD86 and CD206 level based on FC. *$p < 0.05$ compared with the Control group, $^{\#}p < 0.05$ compared with the Model group, $^{\Delta}p < 0.05$ compared with the Aspirin group determined by one-way ANOVA test (n = 3). Data was presented as the mean ± SD. **(E)** IL-1β, IL-18, and TNF-α in Ana-1 cell supernatant were measured by ELISA. *$p < 0.05$ compared with the Control group, $^{\#}p < 0.05$ compared with the Model group, $^{\Delta}p < 0.05$ compared with the Aspirin group determined by one-way ANOVA test (n = 3). Data was presented as the mean ± SD.

10.3389/fimmu.2024.1364161

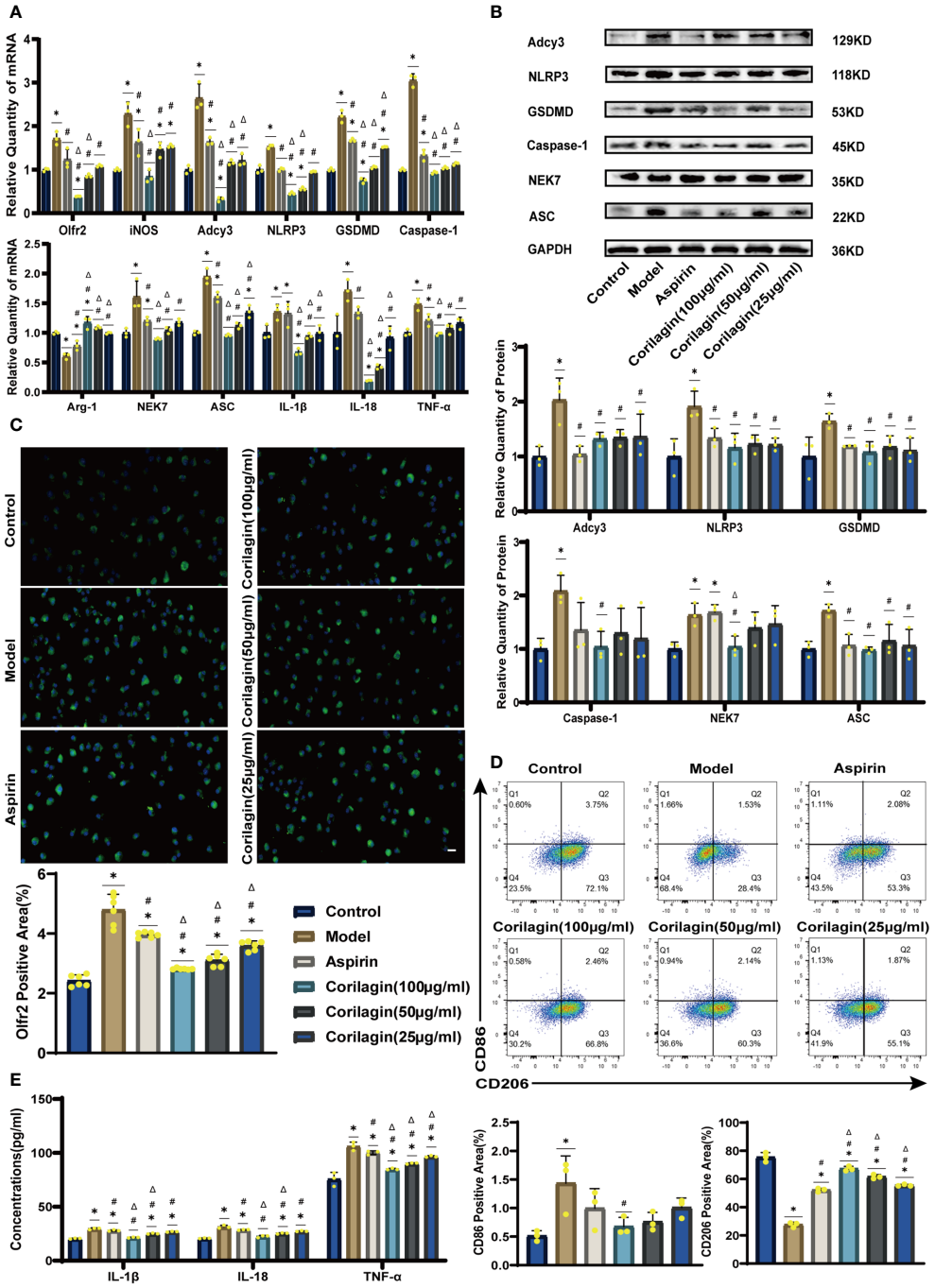

FIGURE 3
Effects of Corilagin on Olfr2 signal pathway in LPS+ox-LDL-induced primary mouse BMDMs. **(A)** mRNA expression of Olfr2, Adcy3, NLRP3, Caspase-1, ASC, NEK7, GSDMD, IL-1β, IL-18, Arg-1, iNOS, and TNF-α in primary mouse BMDMs was measured by RT-qPCR. *$p < 0.05$ compared with the Control group, $^{\#}p < 0.05$ compared with the Model group, $^{\Delta}p < 0.05$ compared with the Aspirin group determined by one-way ANOVA test (n = 3). Data was presented as the mean ± SD. **(B)** Protein expression of Adcy3, NLRP3, GSDMD, Caspase-1, NEK7, and ASC in primary mouse BMDMs was measured by WB and quantitative analyses of protein level based on WB. *$p < 0.05$ compared with the Control group, $^{\#}p < 0.05$ compared with the Model group, $^{\Delta}p < 0.05$ compared with the Aspirin group determined by one-way ANOVA test (n = 3). Data was presented as the mean ± SD. **(C)** Olfr2 expression in primary mouse BMDMs was visualized by IF and quantitative analyses of Olfr2 level based on IF. *$p < 0.05$ compared with the Control group, $^{\#}p < 0.05$ compared with the Model group, $^{\Delta}p < 0.05$ compared with the Aspirin group determined by one-way ANOVA test (n = 6). Data was presented as the mean ± SD. Scale bars, 20μm. **(D)** CD86 and CD206 expression in primary mouse BMDMs were measured by FC and quantitative analyses of CD86 and CD206 level based on FC. *$p < 0.05$ compared with the Control group, $^{\#}p < 0.05$ compared with the Model group, $^{\Delta}p < 0.05$ compared with the Aspirin group determined by one-way ANOVA test (n = 3). Data was presented as the mean ± SD. **(E)** IL-1β, IL-18, and TNF-α in primary mouse BMDMs cell supernatant were measured by ELISA. *$p < 0.05$ compared with the Control group, $^{\#}p < 0.05$ compared with the Model group, $^{\Delta}p < 0.05$ compared with the Aspirin group determined by one-way ANOVA test (n = 3). Data was presented as the mean ± SD.

10.3389/fimmu.2024.1364161

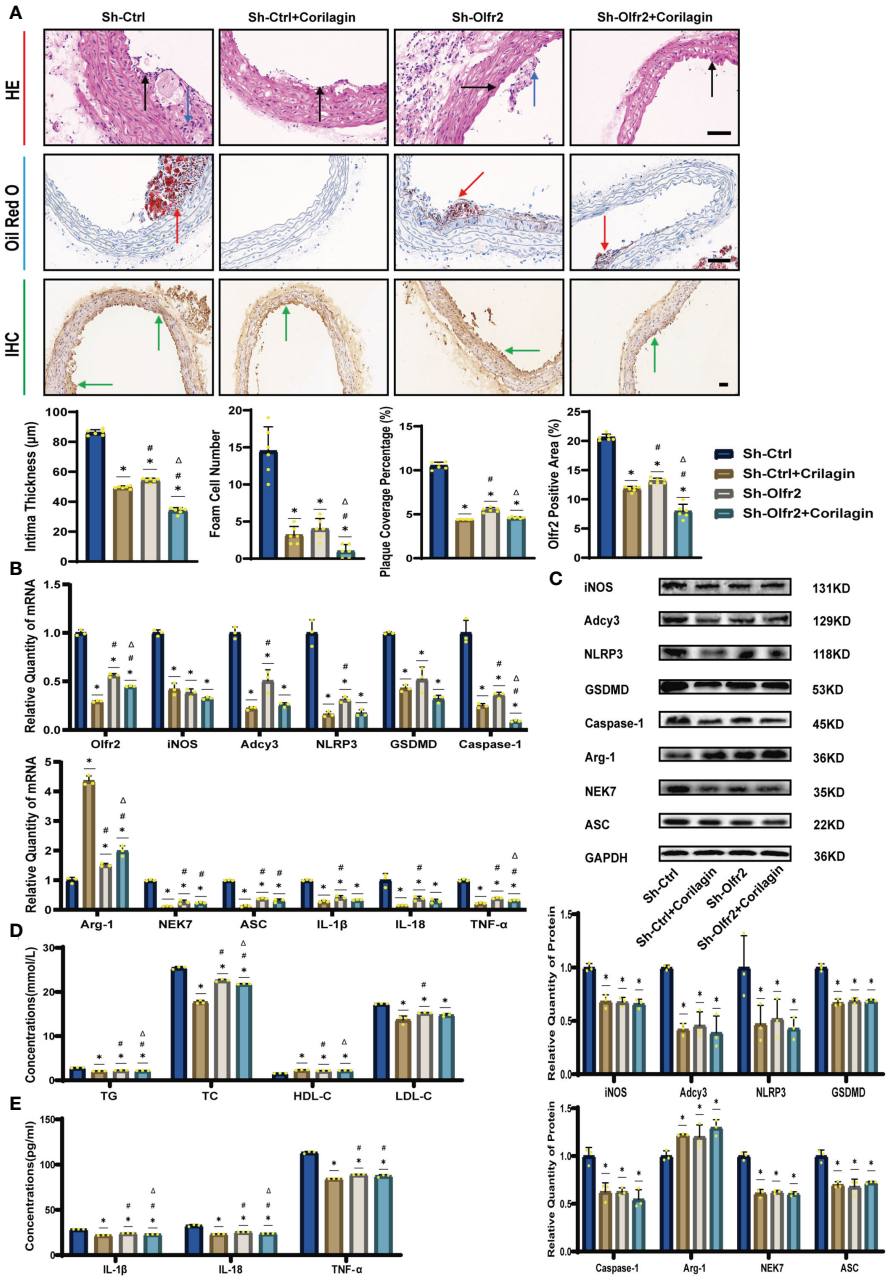

FIGURE 4
Effects of Corilagin on atherosclerosis and Olfr2 signal pathway after downregulating Olfr2 *in vivo*. **(A)** Pathological changes, plaque coverage percentage, and Olfr2 expression in mouse aorta were visualized by HE, Oil red O, and IHC staining respectively and quantitative analyses of intima thickness and foam cell number based on HE, plaque coverage percentage based on Oil red O, and Olfr2 expression based on IHC. Black arrows indicated aorta intima and blue arrows indicated foam cell and fibrous tissue in HE. Yellow arrows indicated lipid plaque in Oil red O. Green arrows indicated the area of Olfr2 expression in IHC. $^{*}p < 0.05$ compared with the Sh-Ctrl group determined by one-way ANOVA test (n = 6), $^{\#}p < 0.05$ compared with the Sh-Ctrl+Corilagin group determined by one-way ANOVA test (n = 6), $^{\Delta}p < 0.05$ compared with the Sh-Olfr2 group determined by Student's t-test (n = 6). Data was presented as the mean ± SD. Scale bars, 50μm. **(B)** mRNA expression of Olfr2, Adcy3, NLRP3, Caspase-1, ASC, NEK7, GSDMD, IL-1β, IL-18, Arg-1, iNOS, and TNF-α in mouse aorta was measured by RT-qPCR. $^{*}p < 0.05$ compared with the Sh-Ctrl group determined by one-way ANOVA test (n = 3), $^{\#}p < 0.05$ compared with the Sh-Ctrl+Corilagin group determined by one-way ANOVA test (n = 3), $^{\Delta}p < 0.05$ compared with the Sh-Olfr2 group determined by Student's t-test (n = 3). Data was presented as the mean ± SD. **(C)** Protein expression of iNOS, Adcy3, NLRP3, GSDMD, Caspase-1, NEK7, Arg-1, and ASC in mouse aorta was measured by WB and quantitative analyses of protein level based on WB. $^{*}p < 0.05$ compared with the Sh-Ctrl group determined by one-way ANOVA test (n = 3), $^{\#}p < 0.05$ compared with the Sh-Ctrl +Corilagin group determined by one-way ANOVA test (n = 3), $^{\Delta}p < 0.05$ compared with the Sh-Olfr2 group determined by Student's t-test (n = 3). Data was presented as the mean ± SD. **(D)** Serum lipids of mice were detected by an automatic biochemical analyzer. $^{*}p < 0.05$ compared with the Sh-Ctrl group determined by one-way ANOVA test (n = 3), $^{\#}p < 0.05$ compared with the Sh-Ctrl+Corilagin group determined by one-way ANOVA test (n = 3), $^{\Delta}p < 0.05$ compared with the Sh-Olfr2 group determined by Student's t-test (n = 3). Data was presented as the mean ± SD. **(E)** IL-1β, IL-18, and TNF-α in the mouse serum were measured by ELISA. $^{*}p < 0.05$ compared with the Sh-Ctrl group determined by one-way ANOVA test (n = 3), $^{\#}p < 0.05$ compared with the Sh-Ctrl+Corilagin group determined by one-way ANOVA test (n = 3), $^{\Delta}p < 0.05$ compared with the Sh-Olfr2 group determined by Student's t-test (n = 3). Data was presented as the mean ± SD.

mRNA levels in the Sh-Olfr2 group fell nearly 50% and 60% in the ApoE$^{-/-}$ mouse and Ana-1 cell models (Figures 4B, 4A). These results confirmed the effective inhibition of Olfr2 expression in this study. As illustrated in Figures 4A–C, 4E, 5A–5E, the reduction in Olfr2, iNOS, Adcy3, NLRP3, GSDMD, Caspase-1, NEK7, ASC, IL-1β, IL-18, TNF-α, and CD86 induced by Corilagin was less pronounced when Olfr2 expression was decreased. Therefore, we inferred that Corilagin could suppress NLRP3 inflammasome activation to prevent inflammatory cytokines secretion, markers of M1 macrophage polarization expression, and pyroptosis-related molecule production via inhibiting the Olfr2 signaling pathway.

Effects of corilagin on atherosclerosis by upregulating Olfr2 *in vivo*

To verify that Corilagin exerted anti-atherosclerotic effects via the Olfr2 signaling pathway, we conducted *in vivo* experiments involving the upregulation of Olfr2 to monitor changes in atherosclerotic conditions. As depicted in Figures 6A, 6D, the Olfr2-OE group exhibited more severe pathological changes, increased lipid deposition percentage, and elevated serum lipid levels of TG, TC and LDL-C compared to the Ctrl-OE group. These findings suggested that boosting Olfr2 levels could intensify atherosclerosis. Moreover, when Olfr2 expression was augmented, the therapeutic effects of Corilagin on reducing histological changes and lipid deposition were more pronounced (Figures 6A, 6D). These results indicated that Corilagin's influence on atherosclerosis was indeed associated with Olfr2 expression.

Effects of corilagin on Olfr2 and downstream molecules after upregulating Olfr2 *in vivo* and vitro

We augmented Olfr2 expression in ApoE$^{-/-}$ mice and Ana-1 cell models to further elucidate the molecular mechanisms of Corilagin anti-atherosclerotic effects. Compared to the Ctrl-OE group, the level of Olfr2 mRNA in the Olfr2-OE group increased by approximately 120% and 150% *in vivo* and vitro samples, respectively (Figure 6B, 7A). This elevation indicates a successful increase in Olfr2 expression following upregulation. Notably, with enhanced Olfr2 expression, Corilagin more effectively reduced the expression of molecules involved in the Olfr2 signaling pathway in the Olfr2-OE+Corilagin group (Figures 6A–6C, 6E, 7A–7E). This trend supported and potentially strengthened the conclusion illustrated in the second part of results, affirming the role of Corilagin in modulating the Olfr2 signaling pathway.

Discussion

Atherosclerosis and its associated complications represent significant sources of morbidity and mortality, making the development of effective therapies for both prevention and treatment crucial (1–4). Although a variety of pharmaceutical options are available for managing atherosclerotic disease, limitations persist, such as resistance or intolerance to statins (43) and increased bleeding risk associated with antiplatelet medications (44). Concurrently, Chinese herbal medicines are often regarded as complementary or alternative treatment for atherosclerosis (45).

Inflammation is a critical driver of atherosclerosis. Thus, targeting therapeutic interventions at inflammatory pathways is essential for improving atherosclerotic outcomes (2). Several signaling pathways implicated in the inflammatory response are associated with atherosclerosis, including the NLRP3 inflammasome, TLRs, proprotein convertase subtilisin/kexin type 9, Notch, and Wnt signaling pathways. Notably, the NLRP3 inflammasome pathway has emerged as a prominent target for atherosclerotic disease treatment (2, 8, 46). In conjunction with TLR4, Olfr2 expressed in mouse vascular macrophages can active NLRP3 inflammasome to promote the development of atherosclerosis (35). According to previous findings, Corilagin can inhibit NLRP3 inflammasome activation and pyroptosis in ischemia-reperfusion induced intestinal and lung injury (38), and ameliorate atherosclerosis by restraining the TLR4 signaling pathway (17, 40). Consequently, this study aims to explore whether Corilagin can influence atherosclerosis through the Olfr2 signaling pathway.

After administering Corilagin to ApoE$^{-/-}$ mice on a high-fat and cholesterol diet, we observed a reduction in serum lipid levels of TG, TC, and LDL-C, alongside alleviated pathological changes and lipid deposition. These results suggest a pronounced therapeutic effect of Corilagin on atherosclerosis. In both the mouse aorta and cellular models, expressions of the Olfr2 signaling pathway related molecules (Olfr2 and Adcy3) and NLRP3 inflammasome associated effectors (NLRP3, Caspase-1, NEK7 and ASC), were diminished following Corilagin treatment. Additionally, inflammatory factors (IL-1β, IL-18, and TNF-α), M1 macrophage polarization markers (iNOS and CD86), and the pyroptosis-related molecule (GSDMD), were also reduced. In conclusion, we hypothesized that Corilagin mitigated atherosclerotic development by suppressing NLRP3 inflammasome activation, thereby curtailing the expression of inflammatory cytokines, M1 macrophage polarization, and pyroptosis through the inhibition of the Olfr2 signaling pathway.

To further validate the effect of Corilagin, we modulated Olfr2 expression both in Ana-1 cells and in animal models, involving both upregulation and downregulation. According to Orecchioni et al., enhancing Olfr2 levels can intensify atherosclerosis, and genetic manipulation to reduce Olfr2 in mice has shown a significant decrease in atherosclerotic plaques (35). In our experiments that modulated Olfr2 expression both *in vitro* and *in vivo*, we observed analogous outcomes confirming that the Olfr2 signaling pathway indeed activated the NLRP3 inflammasome, exacerbating atherosclerosis development and progression. Upon downregulation of Olfr2, no substantial differences in LDL-C levels or pathological changes were noted regardless of Corilagin treatment, while lipid plaque percentages were reduced, and the expression levels of Olfr2, iNOS, Adcy3, NLRP3, GSDMD, Caspase-1, NEK7, ASC, IL-1β, IL-18, TNF-α, and CD86 were similar or decreased with Corilagin treatment. Conversely, when Olfr2

10.3389/fimmu.2024.1364161

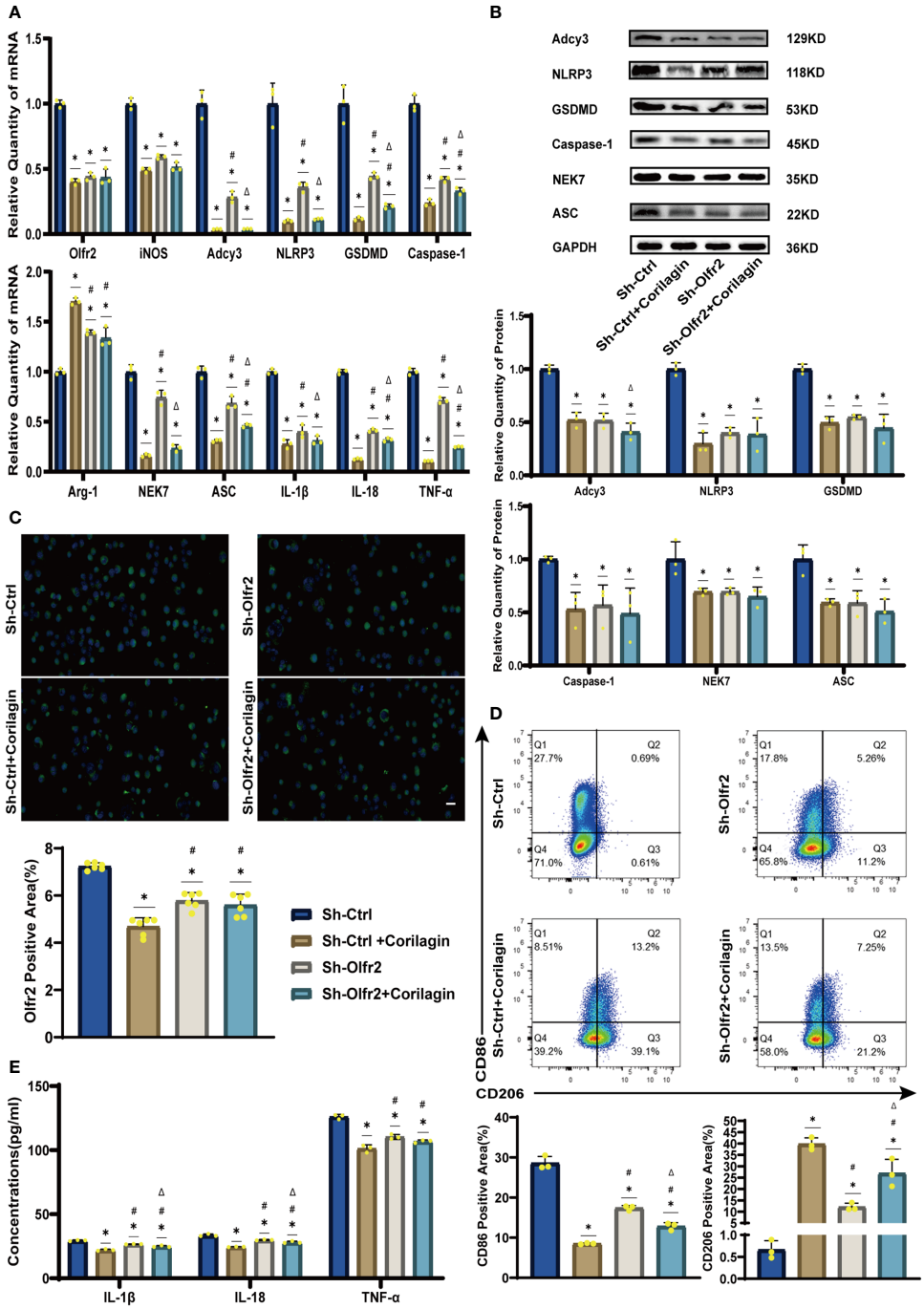

FIGURE 5
Effects of Corilagin on Olfr2 signal pathway after downregulating Olfr2 *in vitro*. **(A)** mRNA expression of Olfr2, Adcy3, NLRP3, Caspase-1, ASC, NEK7, GSDMD, IL-1β, IL-18, Arg-1, iNOS, and TNF-α in Ana-1 cells was measured by RT-qPCR. $^{*}p < 0.05$ compared with the Sh-Ctrl group determined by one-way ANOVA test (n = 3), $^{\#}p < 0.05$ compared with the Sh-Ctrl+Corilagin group determined by one-way ANOVA test (n = 3), $^{\Delta}p < 0.05$ compared with the Sh-Olfr2 group determined by Student's t-test (n = 3). Data was presented as the mean ± SD. **(B)** Protein expression of Adcy3, NLRP3, GSDMD, Caspase-1, NEK7, and ASC in Ana-1 cells was measured by WB and quantitative analyses of protein level based on WB. $^{*}p < 0.05$ compared with the Sh-Ctrl group determined by one-way ANOVA test (n = 3), $^{\#}p < 0.05$ compared with the Sh-Ctrl+Corilagin group determined by one-way ANOVA test (n = 3), $^{\Delta}p < 0.05$ compared with the Sh-Olfr2 group determined by Student's t-test (n = 3). Data was presented as the mean ± SD. **(C)** Olfr2 expression in Ana-1 cells was visualized by IF and quantitative analyses of Olfr2 level based on IF. $^{*}p < 0.05$ compared with the Sh-Ctrl group determined by one-way ANOVA test (n = 6), $^{\#}p < 0.05$ compared with the Sh-Ctrl+Corilagin group determined by one-way ANOVA test (n = 6), $^{\Delta}p < 0.05$ compared with the Sh-Olfr2 group determined by Student's t-test (n = 6). Data was presented as the mean ± SD. Scale bars, 20μm. **(D)** CD86 and CD206 expression in Ana-1 cells were measured by FC and quantitative analyses of CD86 and CD206 level based on FC. $^{*}p < 0.05$ compared with the Sh-Ctrl group determined by one-way ANOVA test (n = 3), $^{\#}p < 0.05$ compared with the Sh-Ctrl+Corilagin group determined by one-way ANOVA test (n = 3), $^{\Delta}p < 0.05$ compared with the Sh-Olfr2 group determined by Student's t-test (n = 3). Data was presented as the mean ± SD. **(E)** IL-1β, IL-18, and TNF-α in Ana-1 cell supernatant were measured by ELISA. $^{*}p < 0.05$ compared with the Sh-Ctrl group determined by one-way ANOVA test (n = 3), $^{\#}p < 0.05$ compared with the Sh-Ctrl+Corilagin group determined by one-way ANOVA test (n = 3), $^{\Delta}p < 0.05$ compared with the Sh-Olfr2 group determined by Student's t-test (n = 3). Data was presented as the mean ± SD.

10.3389/fimmu.2024.1364161

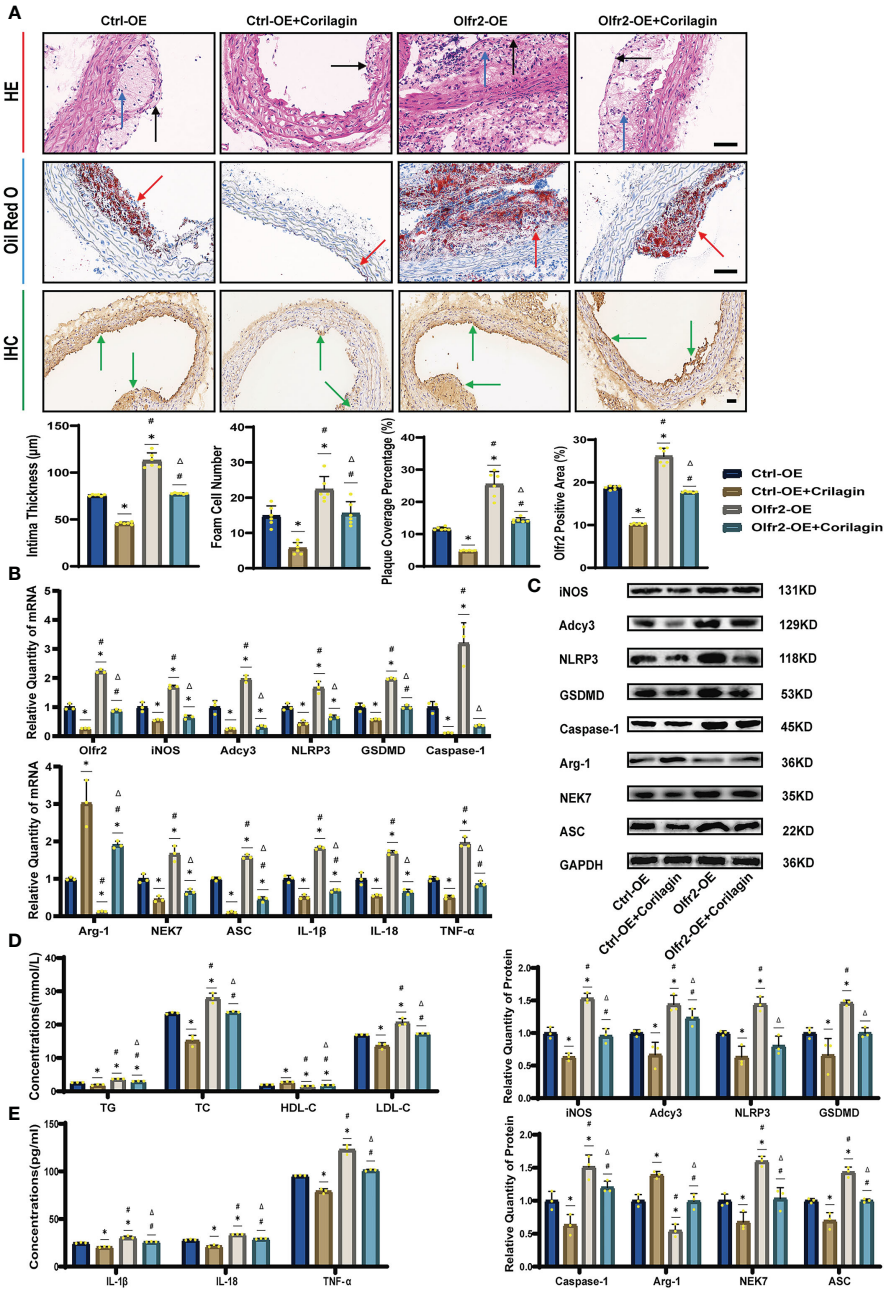

FIGURE 6
Effects of Corilagin on atherosclerosis and Olfr2 signal pathway after upregulating Olfr2 *in vivo*. **(A)** Pathological changes, plaque coverage percentage, and Olfr2 expression in mouse aorta were visualized by HE, Oil red O, and IHC staining respectively and quantitative analyses of intima thickness and foam cell number based on HE, plaque coverage percentage based on Oil red O, and Olfr2 expression based on IHC. Black arrows indicated aorta intima and blue arrows indicated foam cell and fibrous tissue in HE. Yellow arrows indicated lipid plaque in Oil red O. Green arrows indicated the area of Olfr2 expression in IHC. $^{*}p < 0.05$ compared with the Ctrl-OE group determined by one-way ANOVA test (n = 6), $^{\#}p < 0.05$ compared with the Ctrl-OE +Corilagin group determined by one-way ANOVA test (n = 6), $^{\Delta}p < 0.05$ compared with the Ctrl-Olfr2 group determined by Student's t test (n = 6). Data was presented as the mean ± SD. Scale bars, 50μm. **(B)** mRNA expression of Olfr2, Adcy3, NLRP3, Caspase-1, ASC, NEK7, GSDMD, IL-1β, IL-18, Arg-1, iNOS, and TNF-α in mouse aorta was measured by RT-qPCR. $^{*}p < 0.05$ compared with the Ctrl-OE group determined by one-way ANOVA test (n = 3), $^{\#}p < 0.05$ compared with the Ctrl-OE+Corilagin group determined by one-way ANOVA test (n = 3), $^{\Delta}p < 0.05$ compared with the Ctrl-Olfr2 group determined by Student's t test (n = 3). Data was presented as the mean ± SD. **(C)** Protein expression of iNOS, Adcy3, NLRP3, GSDMD, Caspase-1, NEK7, Arg-1, and ASC in mouse aorta was measured by WB and quantitative analyses of protein level based on WB. $^{*}p < 0.05$ compared with the Ctrl-OE group determined by one-way ANOVA test (n = 3), $^{\#}p < 0.05$ compared with the Ctrl-OE+Corilagin group determined by one-way ANOVA test (n = 3), $^{\Delta}p < 0.05$ compared with the Ctrl-Olfr2 group determined by Student's t test (n = 3). Data was presented as the mean ± SD. **(D)** Serum lipids of mice were detected by an automatic biochemical analyzer. WB and quantitative analyses of protein level based on WB. $^{*}p < 0.05$ compared with the Ctrl-OE group determined by one-way ANOVA test (n = 3), $^{\#}p < 0.05$ compared with the Ctrl-OE+Corilagin group determined by one-way ANOVA test (n = 3), $^{\Delta}p < 0.05$ compared with the Ctrl-Olfr2 group determined by Student's t test (n = 3). Data was presented as the mean ± SD. **(E)** IL-1β, IL-18, and TNF-α in the mouse serum were measured by ELISA. $^{*}p < 0.05$ compared with the Ctrl-OE group determined by one-way ANOVA test (n = 3), $^{\#}p < 0.05$ compared with the Ctrl-OE+Corilagin group determined by one-way ANOVA test (n = 3), $^{\Delta}p < 0.05$ compared with the Ctrl-Olfr2 group determined by Student's t test (n = 3). Data was presented as the mean ± SD.

10.3389/fimmu.2024.1364161

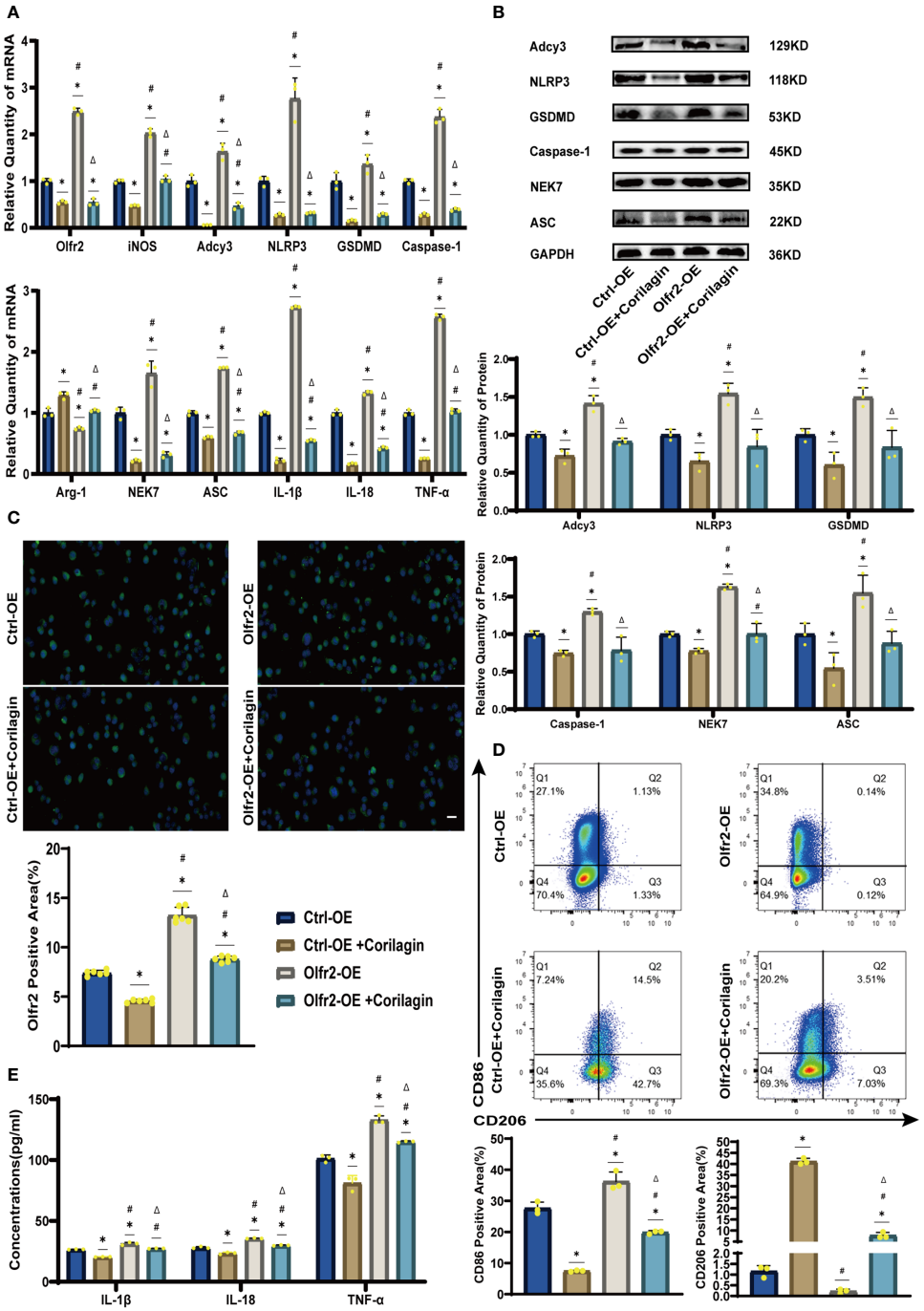

FIGURE 7
Effects of Corilagin on Olfr2 signal pathway after upregulating Olfr2 *in vitro* **(A)** mRNA expression of Olfr2, Adcy3, NLRP3, Caspase-1, ASC, NEK7, GSDMD, IL-1β, IL-18, Arg-1, iNOS, and TNF-α in Ana-1 cells was measured by RT-qPCR. $^{*}p < 0.05$ compared with the Ctrl-OE group determined by one-way ANOVA test (n = 3), $^{\#}p < 0.05$ compared with the Ctrl-OE+Corilagin group determined by one-way ANOVA test (n = 3), $^{\Delta}p < 0.05$ compared with the Ctrl-Olfr2 group determined by Student's t test (n = 3). Data was presented as the mean ± SD. **(B)** Protein expression of Adcy3, NLRP3, GSDMD, Caspase-1, NEK7, and ASC in Ana-1 cells was measured by WB and quantitative analyses of protein level based on WB. $^{*}p < 0.05$ compared with the Ctrl-OE group determined by one-way ANOVA test (n = 3), $^{\#}p < 0.05$ compared with the Ctrl-OE+Corilagin group determined by one-way ANOVA test (n = 3), $^{\Delta}p < 0.05$ compared with the Ctrl-Olfr2 group determined by Student's t test (n = 3). Data was presented as the mean ± SD. **(C)** Olfr2 expression in Ana-1 cells was visualized by IF and quantitative analyses of Olfr2 level based on IF. $^{*}p < 0.05$ compared with the Ctrl-OE group determined by one-way ANOVA test (n = 6), $^{\#}p < 0.05$ compared with the Ctrl-OE+Corilagin group determined by one-way ANOVA test (n = 6), $^{\Delta}p < 0.05$ compared with the Ctrl-Olfr2 group determined by Student's t test (n = 6). Data was presented as the mean ± SD. Scale bars, 20μm. **(D)** CD86 and CD206 expression in Ana-1 cells were measured by FC and quantitative analyses of CD86 and CD206 level based on FC. $^{*}p < 0.05$ compared with the Ctrl-OE group determined by one-way ANOVA test (n = 3), $^{\#}p < 0.05$ compared with the Ctrl-OE+Corilagin group determined by one-way ANOVA test (n = 3), $^{\Delta}p < 0.05$ compared with the Ctrl-Olfr2 group determined by Student's t test (n = 3). Data was presented as the mean ± SD. **(E)** IL-1β, IL-18, and TNF-α in Ana-1 cell supernatant were measured by ELISA. $^{*}p < 0.05$ compared with the Ctrl-OE group determined by one-way ANOVA test (n = 3), $^{\#}p < 0.05$ compared with the Ctrl-OE+Corilagin group determined by one-way ANOVA test (n = 3), $^{\Delta}p < 0.05$ compared with the Ctrl-Olfr2 group determined by Student's t test (n = 3). Data was presented as the mean ± SD.

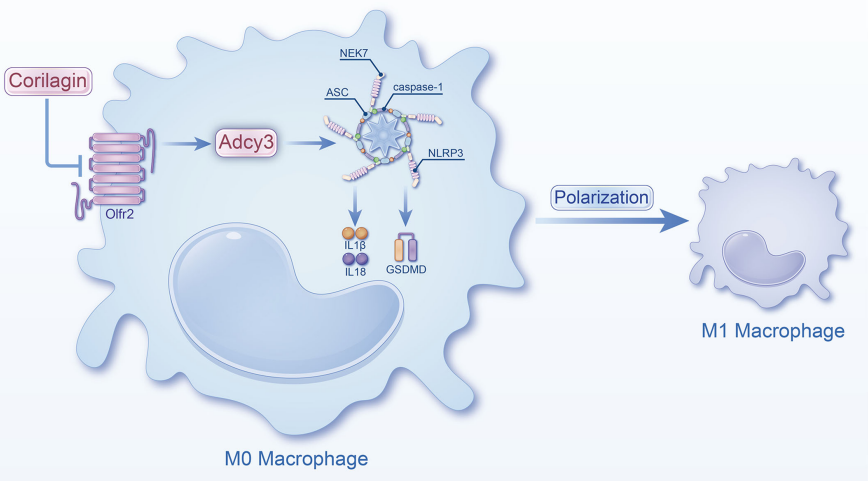

FIGURE 8
Schematic of the study. Corilagin can inhibit the Olfr2 and Adcy3 expression, then suppress NLRP3 inflammasome activation to prevent inflammatory cytokines expression, M1 macrophage polarization, and cell pyroptosis-related molecule expression.

expression was increased, the effects of Corilagin in mitigating atherosclerosis and suppressing the Olfr2 signaling pathway were enhanced. Consequently, our findings suggested the anti-atherosclerotic effects of Corilagin might be attributed to its interaction with the Olfr2 signaling pathway. Previous studies have shown that Corilagin can reduce serum lipid levels in atherosclerotic animal models (40, 41). Our study found a same trend and it might be related to the Olfr2 signaling pathway. Corilagin may directly or indirectly affect various lipid regulatory systems, to reduce lipid uptake and lipogenesis in cellular and animal experiments (47–49). Nevertheless, there is a limitation in our research that the mechanisms of Corilagin's effects on serum lipid levels in atherosclerosis, are warranting exploration remains. Additionally, future research should also consider the interaction between Olfr2 and NLRP3, and whether alternative molecular pathways or additional mechanisms within the Olfr2 pathway might contribute to Corilagin's atherosclerosis-mitigating effects.

In summary, Corilagin exhibited therapeutic effects in experimental atherosclerosis models, potentially through the inhibition of the Olfr2 signaling pathway (Figure 8). However, a notable limitation of our research was the lack of exploration into whether Corilagin might inhibit downstream molecules through alternative mechanisms.

Conclusions

Corilagin exerts the anti-atherosclerosis efficacy by inhibiting the Olfr2 signaling pathway *in vitro* and *in vivo*, leading to the suppression of NLRP3 inflammasome activation, reducing inflammatory cytokines expression, M1 macrophage polarization, and expression of pyroptosis-related molecule. This study highlights the promising strategy and significant potential of Corilagin as a treatment for atherosclerosis. Consequently, further investigations into the mechanisms of Corilagin are warranted to identify novel therapeutic approaches.

Data availability statement

The original contributions presented in the study are included in the article/Supplementary Material. Further inquiries can be directed to the corresponding authors.

Ethics statement

The animal study was approved by Institutional Animal Care and Use Committee of Bainte Biotechnology (Wuhan, China). The study was conducted in accordance with the local legislation and institutional requirements.

Author contributions

JM: Data curation, Methodology, Writing – original draft. YC: Data curation, Methodology, Writing – original draft. QZ: Investigation, Project administration, Writing – original draft. CL: Software, Writing – original draft. JX: Data curation, Writing – original draft. YW: Formal Analysis, Writing – original draft. DF: Conceptualization, Project administration, Writing – original draft. NH: Conceptualization, Project administration, Writing – original draft. KP: Conceptualization, Project administration, Writing – original draft. EM: Conceptualization, Project administration, Writing – original draft. YL: Conceptualization, Methodology, Project administration, Writing – review & editing. LZ: Conceptualization, Software, Supervision, Writing – review & editing. YD: Data curation, Writing – review & editing.

Funding

The author(s) declare financial support was received for the research, authorship, and/or publication of this article. This work is supported by the National Natural Science Foundation of China (81974530, 81600373, and 82100518) and the Hubei International Sciencific and Technological Cooperation Project (2022EHB039 and 2023EHA057).

Conflict of interest

The authors declare that the research was conducted in the absence of any commercial or financial relationships that could be construed as a potential conflict of interest.

Publisher's note

Supplementary material

The Supplementary Material for this article can be found online at: https://www.frontiersin.org/articles/10.3389/fimmu.2024.1364161/full#supplementary-material

References

1. Libby P. The changing landscape of atherosclerosis. *Nature* (2021) 592:524–33. doi: 10.1038/s41586–021-03392–8

2. Grebe A, Hoss F, Latz E. NLRP3 inflammasome and the IL-1 pathway in atherosclerosis. *Circ Res* (2018) 122:1722–40. doi: 10.1161/circresaha.118.311362

3. Bułdak Ł. Cardiovascular diseases-A focus on atherosclerosis, its prophylaxis, complications and recent advancements in therapies. *Int J Mol Sci* (2022) 23(9):4695. doi: 10.3390/ijms23094695

4. Frostegård J. Immunity, atherosclerosis and cardiovascular disease. *BMC Med* (2013) 11:117. doi: 10.1186/1741–7015-11–117

5. Libby P, Buring JE, Badimon L, Hansson GK, Deanfield J, Bittencourt MS, et al. Atherosclerosis. *Nat Rev Dis Primers* (2019) 5:56. doi: 10.1038/s41572-019-0106-z

6. Lankala CR, Yasir M, Ishak A, Mekhail M, Kalyankar P, Gupta K. Application of nanotechnology for diagnosis and drug delivery in atherosclerosis: A new horizon of treatment. *Curr Probl Cardiol* (2023) 48:101671. doi: 10.1016/j.cpcardiol.2023.101671

7. Xu S, Pelisek J, Jin ZG. Atherosclerosis is an epigenetic disease. *Trends Endocrinol Metab* (2018) 29:739–42. doi: 10.1016/j.tem.2018.04.007

8. Kong P, Cui ZY, Huang XF, Zhang DD, Guo RJ, Han M. Inflammation and atherosclerosis: signaling pathways and therapeutic intervention. *Signal Transduct Target Ther* (2022) 7:131. doi: 10.1038/s41392–022-00955–7

9. Ruparelia N, Choudhury R. Inflammation and atherosclerosis: what is on the horizon? *Heart* (2020) 106:80–5. doi: 10.1136/heartjnl-2018–314230

10. Barrett TJ. Macrophages in atherosclerosis regression. *Arterioscler Thromb Vasc Biol* (2020) 40:20–33. doi: 10.1161/atvbaha.119.312802

11. Bäck M, Yurdagul A Jr., Tabas I, Öörni K, Kovanen PT. Inflammation and its resolution in atherosclerosis: mediators and therapeutic opportunities. *Nat Rev Cardiol* (2019) 16:389–406. doi: 10.1038/s41569–019-0169–2

12. Zhang Q, Wang L, Wang S, Cheng H, Xu L, Pei G, et al. Signaling pathways and targeted therapy for myocardial infarction. *Signal Transduct Target Ther* (2022) 7:78. doi: 10.1038/s41392-022-00925-z

13. Sharma A, Choi JSY, Stefanovic N, Al-Sharea A, Simpson DS, Mukhamedova N, et al. Specific NLRP3 inhibition protects against diabetes-associated atherosclerosis. *Diabetes* (2021) 70:772–87. doi: 10.2337/db20–0357

14. Paramel Varghese G, Folkersen L, Strawbridge RJ, Halvorsen B, Yndestad A, Ranheim T, et al. NLRP3 inflammasome expression and activation in human atherosclerosis. *J Am Heart Assoc* (2016) 5:e003031. doi: 10.1161/jaha.115.003031

15. Lee JY, Hwang DH. The modulation of inflammatory gene expression by lipids: mediation through Toll-like receptors. *Mol Cells* (2006) 21:174–85. doi: 10.1016/S1016-8478(23)12877-9

16. Lee JY, Zhao L, Hwang DH. Modulation of pattern recognition receptor-mediated inflammation and risk of chronic diseases by dietary fatty acids. *Nutr Rev* (2010) 68:38–61. doi: 10.1111/nure.2010.68.issue-1

17. Li Y, Wang Y, Chen Y, Wang Y, Zhang S, Liu P, et al. Corilagin Ameliorates Atherosclerosis in Peripheral Artery Disease via the Toll-Like Receptor-4 Signaling Pathway *in vitro* and *in vivo*. *Front Immunol* (2020) 11:1611. doi: 10.3389/fimmu.2020.01611

18. Pellegrini C, Antonioli L, Lopez-Castejon G, Blandizzi C, Fornai M. Canonical and non-canonical activation of NLRP3 inflammasome at the crossroad between immune tolerance and intestinal inflammation. *Front Immunol* (2017) 8:36. doi: 10.3389/fimmu.2017.00036

19. Bauernfeind FG, Horvath G, Stutz A, Alnemri ES, MacDonald K, Speert D, et al. Cutting edge: NF-kappaB activating pattern recognition and cytokine receptors license NLRP3 inflammasome activation by regulating NLRP3 expression. *J Immunol* (2009) 183:787–91. doi: 10.4049/jimmunol.0901363

20. Christgen S, Kanneganti TD. Inflammasomes and the fine line between defense and disease. *Curr Opin Immunol* (2020) 62:39–44. doi: 10.1016/j.coi.2019.11.007

21. Christgen S, Place DE, Kanneganti TD. Toward targeting inflammasomes: insights into their regulation and activation. *Cell Res* (2020) 30:315–27. doi: 10.1038/s41422–020-0295–8

22. Zhou R, Yazdi AS, Menu P, Tschopp J. A role for mitochondria in NLRP3 inflammasome activation. *Nature* (2011) 469:221–5. doi: 10.1038/nature09663

23. Shimada K, Crother TR, Karlin J, Dagvadorj J, Chiba N, Chen S, et al. Oxidized mitochondrial DNA activates the NLRP3 inflammasome during apoptosis. *Immunity* (2012) 36:401–14. doi: 10.1016/j.immuni.2012.01.009

24. Iyer SS, He Q, Janczy JR, Elliott EI, Zhong Z, Olivier AK, et al. Mitochondrial cardiolipin is required for Nlrp3 inflammasome activation. *Immunity* (2013) 39:311–23. doi: 10.1016/j.immuni.2013.08.001

25. Sharma BR, Kanneganti TD. NLRP3 inflammasome in cancer and metabolic diseases. *Nat Immunol* (2021) 22:550–9. doi: 10.1038/s41590–021-00886–5

26. Liaqat A, Asad M, Shoukat F, Khan AU. A spotlight on the underlying activation mechanisms of the NLRP3 inflammasome and its role in atherosclerosis: A review. *Inflammation.* (2020) 43:2011–20. doi: 10.1007/s10753–020-01290–1

27. Koushki K, Shahbaz SK, Mashayekhi K, Sadeghi M, Zayeri ZD, Taba MY, et al. Anti-inflammatory action of statins in cardiovascular disease: the role of inflammasome and toll-like receptor pathways. *Clin Rev Allergy Immunol* (2021) 60:175–99. doi: 10.1007/s12016–020-08791–9

28. Jiang C, Xie S, Yang G, Wang N. Spotlight on NLRP3 inflammasome: role in pathogenesis and therapies of atherosclerosis. *J Inflammation Res* (2021) 14:7143–72. doi: 10.2147/jir.S344730

29. Martínez GJ, Celermajer DS, Patel S. The NLRP3 inflammasome and the emerging role of colchicine to inhibit atherosclerosis-associated inflammation. *Atherosclerosis.* (2018) 269:262–71. doi: 10.1016/j.atherosclerosis.2017.12.027

30. Yang S, Yuan HQ, Hao YM, Ren Z, Qu SL, Liu LS, et al. Macrophage polarization in atherosclerosis. *Clin Chim Acta* (2020) 501:142–6. doi: 10.1016/j.cca.2019.10.034

31. Hou P, Fang J, Liu Z, Shi Y, Agostini M, Bernassola F, et al. Macrophage polarization and metabolism in atherosclerosis. *Cell Death Dis* (2023) 14:691. doi: 10.1038/s41419-023-06206-z

32. Li M, Wang ZW, Fang LJ, Cheng SQ, Wang X, Liu NF. Programmed cell death in atherosclerosis and vascular calcification. *Cell Death Dis* (2022) 13:467. doi: 10.1038/s41419–022-04923–5

33. Puylaert P, Zurek M, Rayner KJ, De Meyer GRY, Martinet W. Regulated necrosis in atherosclerosis. *Arterioscler Thromb Vasc Biol* (2022) 42:1283–306. doi: 10.1161/atvbaha.122.318177

34. Zhaolin Z, Guohua L, Shiyuan W, Zuo W. Role of pyroptosis in cardiovascular disease. *Cell Prolif.* (2019) 52:e12563. doi: 10.1111/cpr.12563

35. Orecchioni M, Kobiyama K, Winkels H, Ghosheh Y, McArdle S, Mikulski Z, et al. Olfactory receptor 2 in vascular macrophages drives atherosclerosis by NLRP3-dependent IL-1 production. *Science* (2022) 375:214–21doi: 10.1126/science.abg3067

36. Yamada H, Nagao K, Dokei K, Kasai Y, Michihata N. Total synthesis of (-)-corilagin. *J Am Chem Soc* (2008) 130:7566–7. doi: 10.1021/ja803111z

37. Wu S, Liao J, Hu G, Yan L, Su X, Ye J, et al. Corilagin alleviates LPS-induced sepsis through inhibiting pyroptosis via targeting TIR domain of MyD88 and binding CARD of ASC in macrophages. *Biochem Pharmacol* (2023) 217:115806. doi: 10.1016/j.bcp.2023.115806

38. Li W, Yang K, Li B, Wang Y, Liu J, Chen D, et al. Corilagin alleviates intestinal ischemia/reperfusion-induced intestinal and lung injury in mice via inhibiting NLRP3 inflammasome activation and pyroptosis. *Front Pharmacol* (2022) 13:1060104. doi: 10.3389/fphar.2022.1060104

39. Tao Y, Zhang L, Yang R, Yang Y, Jin H, Zhang X, et al. Corilagin ameliorates atherosclerosis by regulating MMP-1, -2, and -9 expression *in vitro* and *in vivo*. *Eur J Pharmacol* (2021) 906:174200. doi: 10.1016/j.ejphar.2021.174200

40. Meng D, Deng X, Wu Y, Wu J, Zhang Y, Zhang J, et al. Corilagin ameliorates macrophages inflammation in atherosclerosis through TLR4-NFκB/MAPK pathway. *Heliyon* (2023) 9:e16960. doi: 10.1016/j.heliyon.2023.e16960

41. He B, Chen D, Zhang X, Yang R, Yang Y, Chen P, et al. Antiatherosclerotic effects of corilagin via suppression of the LOX-1/MyD88/NF-κB signaling pathway *in vivo* and *in vitro*. *J Nat Med* (2022) 76:389–401. doi: 10.1007/s11418-021-01594-y

42. Duan W, Yu Y, Zhang L. Antiatherogenic effects of phyllanthus emblica associated with corilagin and its analogue. *Yakugaku Zasshi* (2005) 125:587–91. doi: 10.1248/yakushi.125.587

43. Reiner Z. Resistance and intolerance to statins. *Nutr Metab Cardiovasc Dis* (2014) 24:1057–66. doi: 10.1016/j.numecd.2014.05.009

44. Gawaz M, Geisler T, Borst O. Current concepts and novel targets for antiplatelet therapy. *Nat Rev Cardiol* (2023) 20:583–99. doi: 10.1038/s41569–023-00854–6

45. Wang C, Niimi M, Watanabe T, Wang Y, Liang J, Fan J. Treatment of atherosclerosis by traditional Chinese medicine: Questions and quandaries. *Atherosclerosis.* (2018) 277:136–44. doi: 10.1016/j.atherosclerosis.2018.08.039

46. Weber C, Habenicht AJR, von Hundelshausen P. Novel mechanisms and therapeutic targets in atherosclerosis: inflammation and beyond. *Eur Heart J* (2023) 44:2672–81. doi: 10.1093/eurheartj/ehad304

47. Nandini HS, Naik PR. Action of corilagin on hyperglycemia, hyperlipidemia and oxidative stress in streptozotocin-induced diabetic rats. *Chem Biol Interact* (2019) 299:186–93. doi: 10.1016/j.cbi.2018.12.012

48. Jiang Y, Zhao L, Ma J, Yang Y, Zhang B, Xu J, et al. Preventive mechanisms of Chinese Tibetan medicine Triphala against nonalcoholic fatty liver disease. *Phytomedicine.* (2024) 123:155229. doi: 10.1016/j.phymed.2023.155229

49. Yang MH, Vasquez Y, Ali Z, Khan IA, Khan SI. Constituents from Terminalia species increase PPARα and PPARγ levels and stimulate glucose uptake without enhancing adipocyte differentiation. *J Ethnopharmacol* (2013) 149:490–8. doi: 10.1016/j.jep.2013.07.003

frontiers | Frontiers in Immunology

TYPE Review
PUBLISHED 04 June 2024
DOI 10.3389/fimmu.2024.1406538

OPEN ACCESS

EDITED BY
Uzma Saqib,
Indian Institute of Technology Indore, India

REVIEWED BY
Sutripta Sarkar,
Barrackpore Rastraguru Surendranath College, India
Zhongjian Chen,
Tongji University, China

*CORRESPONDENCE
Jin Ding
jhDingJin@zju.edu.cn
Yanping Chen
jhyanping_chen@163.com
Jianfeng Yang
yjf-1976@163.com

RECEIVED 25 March 2024
ACCEPTED 13 May 2024
PUBLISHED 04 June 2024

CITATION
Hu Y, Lu Y, Fang Y, Zhang Q, Zheng Z, Zheng X, Ye X, Chen Y, Ding J and Yang J (2024) Role of long non-coding RNA in inflammatory bowel disease.
Front. Immunol. 15:1406538.
doi: 10.3389/fimmu.2024.1406538

Role of long non-coding RNA in inflammatory bowel disease

Yufei Hu[1], Yifan Lu[1], Yi Fang[1], Qizhe Zhang[2], Zhuoqun Zheng[1], Xiaojuan Zheng[1], Xiaohua Ye[1], Yanping Chen[1*], Jin Ding[1*] and Jianfeng Yang[3*]

[1]Department of Gastroenterology, Affiliated Jinhua Hospital, Zhejiang University School of Medicine, Jinhua, Zhejiang, China, [2]Department of Geriatrics, Affiliated Jinhua Hospital, Zhejiang University School of Medicine, Jinhua, Zhejiang, China, [3]Department of Gastroenterology, Affiliated Hangzhou First People's Hospital, School of Medicine, Westlake University, Hangzhou, Zhejiang, China

Inflammatory bowel disease (IBD) is a group of recurrent chronic inflammatory diseases, including Crohn's disease (CD) and ulcerative colitis (UC). Although IBD has been extensively studied for decades, its cause and pathogenesis remain unclear. Existing research suggests that IBD may be the result of an interaction between genetic factors, environmental factors and the gut microbiome. IBD is closely related to non-coding RNAs (ncRNAs). NcRNAs are composed of microRNA(miRNA), long non-coding RNA(lnc RNA) and circular RNA(circ RNA). Compared with miRNA, the role of lnc RNA in IBD has been little studied. Lnc RNA is an RNA molecule that regulates gene expression and regulates a variety of molecular pathways involved in the pathbiology of IBD. Targeting IBD-associated lnc RNAs may promote personalized treatment of IBD and have therapeutic value for IBD patients. Therefore, this review summarized the effects of lnc RNA on the intestinal epithelial barrier, inflammatory response and immune homeostasis in IBD, and summarized the potential of lnc RNA as a biomarker of IBD and as a predictor of therapeutic response to IBD in the future.

KEYWORDS

inflammatory bowel disease, long non-coding RNA, intestinal barrier, immune homeostasis, biomarkers

1 Introduction

Inflammatory bowel disease (IBD) is a group of immune-mediated chronic, non-specific and recurrent inflammatory diseases, which can involve the whole digestive tract, mainly including Crohn's disease (CD) and ulcerative colitis (UC) (1). CD is characterized by affecting all layers of the intestinal wall in any part of the gastrointestinal tract in a discontinuous manner most commonly at the end of the terminal ileum or perianal region. The main symptoms are abdominal pain, weight loss, and varying degrees of diarrhea, often accompanied by complications such as stenosis, abscess, and fistula. In contrast, UC is characterized by inflammation that begins in the rectum and spreads proximally in a continuous manner, but the inflammation is limited to the mucosa and

submucosa of the gut. Diarrhea, mucopurulent bloody stool and tenesmus are typical symptoms of active UC. As the incidence of IBD continues to increase globally, this disease is receiving increasing attention (2). Currently, the commonly used drugs for the treatment of IBD include aminosalicylic acids, glucocorticoids, immunosuppressants and biological inhibitors, which are mainly aimed at inducing and maintaining remission. 5-aminosalicylic acid (5-ASA), an active ingredient of aminosalicylic acid drugs, can treat IBD by anti-inflammatory and antioxidant effects (3). In UC patients, 5-ASA can also prevent colon cancer by regulating immunity and correcting intestinal flora imbalance. The adverse reactions of 5-ASA containing sulphapyridine (SP) were great, so the new preparation mesalazine was developed for clinical use. Mesalazine has a good effect on mild to moderate UC, but the effect on CD is not uncertain. The ECCO guidelines published in 2020 clearly state that it is not recommended for the induction and maintenance of remission in CD (4). Glucocorticoids can inhibit the activation of pro-inflammatory genes by regulating the transcription of anti-inflammatory protein genes and induce the degradation of pro-inflammatory gene mRNA to achieve anti-inflammatory effect (5). In the treatment of IBD with steroids, we should not only pay attention to hormone-related adverse reactions, which are related to the dose, administration method and duration of drugs (6), but also pay attention to hormone resistance. Immunosuppressants reduce the body's immune response by inhibiting lymphocyte proliferation and activation. Because immunosuppressive agents need to be treated for a period of time to reach a stable plasma concentration, they are not suitable for the treatment of IBD in the acute phase. Studies have found that long-term use of immunosuppressants can increase the incidence of infection (7), which is an important factor leading to death in IBD patients. Biological agents can bind to specific targets and improve intestinal mucosal injury in IBD patients by blocking downstream inflammatory response and lymphocyte migration, thereby controlling symptoms and disease progression. At present, many biological agents have been used in the clinical stage for different pathways and targets. Common adverse reactions include infections, gastrointestinal reactions, allergies, headache and even severe infections, opportunistic infections and malignant tumors. Although the above drugs are effective at present, they have many limitations, because the etiology and pathogenesis of IBD are unclear. A growing body of evidence suggests that IBD may be the result of an interaction between genetic factors, environmental factors and the gut microbiome. Therefore, understanding its pathogenesis will help to explore better treatments.

RNA can be divided into messenger RNAs (mRNAs) that have the ability to encode proteins and non-coding RNAs (ncRNAs) that do not have the ability to encode proteins. Studies have found that only a small part of the 3 billion base pairs of the human genome has the ability to encode proteins, and the remaining about 98% of RNA is ncRNAs (8), including microrna (miRNA), small nucleolar RNA (snoRNA), long non-coding RNA (lncRNA), and circular RNA (circ RNA). NcRNAs play a key role in the regulation of some intracellular processes in prokaryotic and eukaryotic organisms. It involves the transcriptional and post-transcriptional levels of gene expression regulation, including mediating chromatin modification, regulating the activity of transcription factors, affecting the stability and processing and translation of mRNA, and regulating the function and localization of proteins. MiRNA, about 18–24 nucleotides in length, is post-transcriptional regulator that regulate post-transcriptional gene silencing to block translation by targeting the 3' -untranslated region (3'UTR) of specific mRNA (9). At present, we have conducted the most thorough research on miRNA, and found differences in miRNA expression in IBD. In addition, miRNA plays a pro-inflammatory or anti-inflammatory role in regulating the pathogenesis of IBD, such as dysautophagy, activation of necrosis factor-κ B (NF-κB), and increased permeability of intestinal epithelium (10).

In contrast to miRNA, the role of lnc RNA in IBD has been poorly studied. Lnc RNAs are more than 200 nucleotide RNA molecules that are structurally similar to miRNA and may have A cap-like structure and polyA tails. According to current findings, they exhibit different functional roles, including regulating protein coding through chromatin remodeling, regulating gene expression through transcription, post-transcription, or guiding chromatin modification complexes to bind to specific genomic sites (11), and regulating protein activity and stability. The role of lnc RNA in immune dysfunction and autoimmune diseases such as rheumatoid arthritis (12), osteoarthritis (13), asthma (14), and type 1 diabetes mellitus (15) has attracted more and more attention. Existing studies have shown that lnc RNA plays an important role in the pathophysiology of IBD (16). Qiao et al. found the first association between lnc RNA and IBD in 2013 (17). They found that patients with clinically active CD had significantly higher levels of lnc RNA DQ786243 expression in peripheral blood cells compared with healthy controls or with inactive disease (17). Another lncRNA associated with CD pathophysiology is NRON, which is a non-coding repressor of NFAT. The molecule is involved in the RNA-protein complex, which prevents nuclear translocation of NFAT to inhibit NFAT. Leucine-rich repeat kinase-2 (LLRK2), a putative CD susceptibility gene, is also part of an RNA-protein complex. Some researchers have proposed a molecular mechanism of CD severity by finding that LRRK2-deficient mice are more sensitive to DSS-induced colitis (18). Similarly, another lncRNA, BC012900, was found to be significantly up-regulated in active UC tissues and stimulated by cytokines and pathogens through known IBD molecular pathways such as Toll-like and NOD2 receptors (19).

In this review, we highlight the role of lnc RNA in regulating gene expression and influencing the pathogenesis of IBD, as well as their potential as biomarkers and predictors of therapeutic response in IBD. By summarizing the effects of lnc RNA on intestinal epithelial barrier, inflammatory response and immune homeostasis in inflammatory bowel disease, this paper emphasizes the importance of lnc RNA in individualized therapy and treatment of IBD patients.

2 Roles of lnc RNAs in IBD

2.1 LncRNAs and intestinal barrier dysregulation

Intestinal barrier is mainly composed of intestinal epithelial cells and tight junction proteins between epithelial cells (20), which

can block various harmful substances, such as intestinal microbiota, microbial products and antigens. Under normal circumstances, intestinal epithelial cells are constantly renewed to ensure the integrity of the intestinal epithelium. However, when hemorrhagic shock, acute pancreatitis, severe trauma and other conditions occur, the intestinal mucosa will appear ischemia or hypoxia, and the intestinal barrier will be damaged, causing the displacement of harmful substances and bacteria in the intestinal cavity, and even causing systemic inflammatory response syndrome or multiple organ dysfunction (21). Studies in patients with IBD have shown that the intestinal barrier function is disrupted regardless of whether the IBD disease is active or dormant. In addition, a decrease in compact connectin, increased apoptosis of epithelial cells, increased intestinal permeability, and disruption of intestinal barrier function were observed in patients with CD (22). Increased permeability of the intestinal epithelium was also observed during the inactive phase of the disease, suggesting a high probability of disease recurrence. In terms of intestinal barrier function, lnc RNAs can maintain intestinal homeostasis through various aspects, such as regulating intestinal epithelial regeneration and intestinal immunity (23, 24). At present, many studies have revealed the relationship between lnc RNAs and intestinal barrier in IBD, and further indicated the role of lncRNAs in IBD.

2.1.1 Lnc RNA H19

H19 is an imprinted gene located on human chromosome 11p15.5 (Figure 1) (25). Lnc RNA H19 is mainly expressed in the embryo, generally decreased at birth, and significantly increased in tumors (26). We found that H19 promotes epithelial-mesenchymal transformation, and its knockdown can inhibit the growth of multiple myeloma cells through the NF-κB pathway, suggesting that H19 may play a role in the development of inflammatory diseases (27). Zou et al. reported that overexpression of Lnc RNA H19 increased the abundance of miR-675p and decreased the expression of zonula occludin 1 (ZO-1) and E-cadherin (E-cad), thus destroying the integrity of the intestinal barrier (28). This process is blocked by ubiquitous RNA-binding protein HuR. In another study, miR-675p was identified as a regulator targeting the 3'-untranslated region (3'UTR) of VDR mRNA in ulcerative colitis patient tissues (29). H19 expression exhibited a negative correlation with vitamin D receptor (VDR) mRNA expression (29). In the above studies, we can speculate that Lnc RNA H19 increases the abundance of miR-675, which targets VDR mRNA, causes the decrease of ZO-1 and E-cad expression, and finally destroys the intestinal barrier. Based on the function of H19 as a competing endogenous RNA (ceRNA), another target of action for Lnc RNA H19 in the intestinal barrier was discovered (30, 31). Zhi et al. found that during acute intestinal ischemia, miR-874 promoted paracellular permeability by changing the level of TNF-α and TJ proteins through targeting the 3'UTR of aquaporin 3 (AQP3), causing disruption of intestinal barrier function (32). Su et al. verified that Lnc RNA H19, as a ceRNA, regulated the expression of AQP3 by competing with miR-874, causing intestinal barrier dysfunction (33).

2.1.2 PLnc RNA1

Prostate cancer-upregulated long noncoding RNA1 (PLnc RNA1), a newly discovered lncRNA transcript, also known as

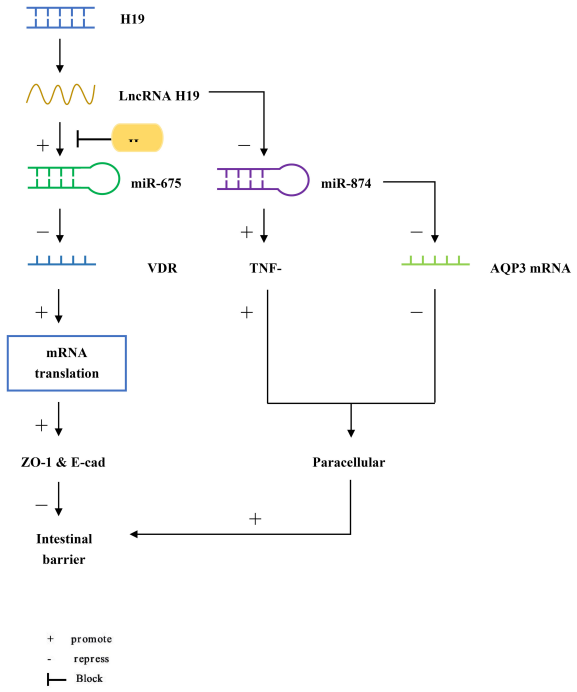

FIGURE 1
LncRNA H19 increases the abundance of miR-675, but it is blocked by HuR. miR-675 targets the 3'UTR of VDR mRNA to reduce the translation of ZO-1 and E-cad, causing intestinal barrier dysfunction. In addition, miR-874 targets the 3'UTR of AQP3 and increases the level of TNF-α, which enhances intestinal paracellular permeability and also causes intestinal barrier dysfunction.

CBR3 antisense RNA 1 (CBR3-AS1), located on chromosome 21q22.12, is upregulated in hepatocellular carcinoma (34), esophageal squamous cell carcinoma (35) and prostate cancer (Figure 2) (36). Overexpressed PLnc RNA1 has been reported to protect the intestinal epithelial barrier from damage by dextran sulfate sodium (DSS) (37). This is due to the fact that miR-34c binds to PLnc RNA1 and can directly target the 3'UTR of Myc-associated zinc-finger protein (MAZ), thereby regulating the expression of ZO-1 and occludin to regulate intestinal barrier function. In addition, the knockdown of PLnc RNA1 can reduce the expression of MAZ, and its effect can be reversed by down-regulating miR-34c, which indicates that PLnc RNA1 can also directly regulate the expression of MAZ (37).

2.1.3 Lnc RNA SPRY4-IT1

The SPROUTY4 intron transcript 1 (SPRY4-IT1) on chromosome 5q31.3 is transcribed from the SPRY4 gene (Figure 3) (38). Previous studies have shown that SPRY4-IT1 is essential for maintaining basal epithelial barrier function. Xiao et al. found in a study that lncRNA SPRY4-IT1 protected intestinal barrier function by stabilizing TJ mRNA and enhancing its translation (39). This study showed that by silencing SPRY4-IT1, the mRNA expression of TJ proteins ocgludin, claudin-1, claudin-3 and JAM-1 could be reduced, resulting in impaired intestinal barrier function (39). Conversely, increasing the level of SPRY4-IT1 increased the expression of TJ protein, which promoted the function of the

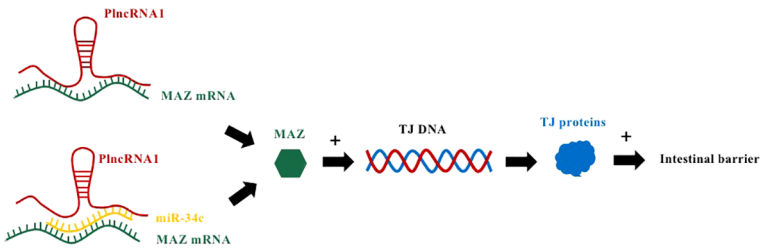

FIGURE 2
PlncRNA1 and miR-34c mediate IBD by affecting MAZ mRNA to regulate TJ proteins. PlncRNA1 directly interacts with MAZ mRNA and promotes the expression of MAZ. In addition, PlncRNA1 reduction affects the level of miR34c expressed by MAZ. MAZ interacts with the DNA sequences of the promoters of ZO-1, occludin, and claudin-5 to increase their expression.

intestinal barrier (39). SPRY4-IT1 directly interacts with TJ mRNA, and SPRY4-IT1 can also bind to RNA-binding protein HuR and then interact with TJ mRNA to increase the number of TJ protein and promote the function of intestinal barrier.

2.1.4 Lnc RNA uc.173

Lnc RNA uc.173 is a transcribed ultra-conservative (T-UCR) region transcript representing the homologous region of human, rat, and mouse genomes (Figure 4) (40). A study determined the expression of 21 T-UCR genes, including uc.173, in mouse intestinal mucosa from the whole genome profile analysis, and found that increasing the expression of Lnc RNA uc.173 gene could increase the growth of intestinal epithelial cells, while decreasing the expression level reduced the renewal of intestinal epithelial cells (IECs) (41). This is due to the fact that lncRNA uc.173 destroys the pri-miR-195 transcript and induces degradation of miR-195 to down-regulate the expression of miRNA195, thereby stimulating intestinal epithelial cell renewal. It was later found that the complementary sequence capable of interacting with Lnc RNA uc.173 was located in the central stem region of pri-miR-195 (upstream of the 3' terminal), indicating that this region can control the degradation of pri-miRNA. However, the relationship between miR-195 and IECs has not been clearly clarified so far.

2.1.5 Lnc RNA BC012900

At present, the study of BC012900 is not thorough. A recent study reported that some cytokines such as TNF-α can regulate the expression of UC-related lncRNAs such as BC012900 (42). They further demonstrated that overexpression of BC012900 can significantly inhibit IEC cell proliferation and increase the sensitivity of IEC cells to apoptosis (42). However, the mechanism by which BC012900 further induces increased apoptosis in IEC cells is unclear. Since PPM1A expression is also increased in cells with increased BC012900 expression, they hypothesized that PPM1A expression may be one of the mechanisms by which BC012900 regulates apoptosis, based on previous reports that overexpression of PPM1A induces G2/M cell cycle arrest and apoptosis (43).

2.1.6 Lnc RNA CRNDE

CRNDE is a gene symbol for Colorectal Neoplasia differentiationally expression (Figure 5) (44). It has been reported that Lnc CRNDE is highly expressed in colorectal cancer, hepatocellular carcinoma, and pancreatic cancer, and decreased in renal pheochromocytoma and ovarian cancer (45). CRNDE may affect tumorigenesis through regulation of miRNAs (46, 47). Studies have found that CRNDE may be related to the progression of IBD (48). In colitis tissue and colonic epithelial cell lines induced by dextran sulfate sodium(DSS), CRNDE can inhibit miRNA-495 expression and increase the expression of cytokine signaling pathway inhibitor (SOCS1) (48). By interfering with the expression of CRNDE, IBD symptoms were alleviated in mice. Chu et al. found that miRNA-495 expression decreased in UC, and miRNA-495 could prevent IEC apoptosis through JAK signaling (49). It has also been suggested that SOCS1 can induce IEC apoptosis by promoting IFN-γ (50). Suppressor of cytokine signaling (SOCS1), a member of the cytokine signaling pathway inhibitor family, is induced by interferon (IFN)-γ-mediated JAK signaling pathway. It is widely considered to be a protein that restricts cytokine receptor signaling (51). In animal models of

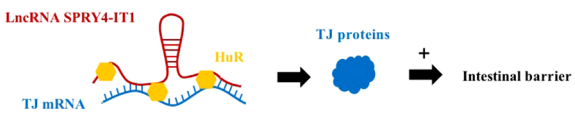

FIGURE 3
LncRNA SPRY4-IT1 has a protective effect on the intestinal barrier. SPRY4-IT1 can directly interact with TJ mRNA to promote the production of TJ proteins to protect the intestinal barrier. Alternatively, the SPRY4-IT1/HuR complex can also bind to TJ mRNA, which protects a protective effect on the intestinal barrier.

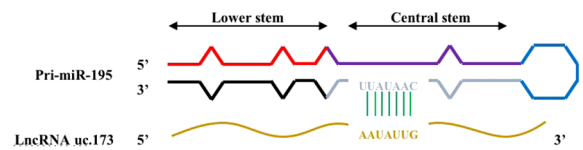

FIGURE 4
Complementary regions of pri-miR-195 interacting with lncRNA uc.173. There is a complementary region in the central stem region of pri-miR-195 that interacts with lncRNA uc.173.

10.3389/fimmu.2024.1406538

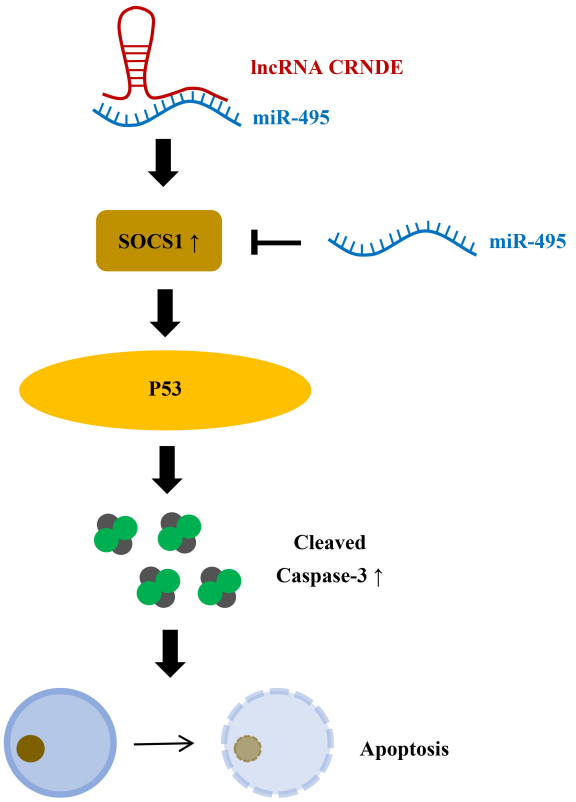

FIGURE 5
LncRNA CRNDE promotes apoptosis of colonic epithelial cells by inhibiting miR-495 and increasing SOCS1. miR-495 can inhibit SOCS1, and LncRNA CRNDE can increase SOCS1 by inhibiting miR-495 to increase P53 phosphorylation, increase activated Caspase-3, and promote apoptosis of colon epithelial cells.

colitis, p53 has been proven to mediate apoptosis of IECs (52). Cui et al. showed that SOCS1 increased p53 phosphorylation and promoted IFN-γ-induced apoptosis of IECs (50). Therefore, it can be speculated that lnc CRNDE regulates IEC apoptosis through the CRNDE/miR-495/SOCS1 axis, which also indicates that CRNDE is a potential target for the treatment of IBD.

2.1.7 Lnc NEAT1

Lnc NEAT1 is a key component in building the ribo-riboprotein complex to regulate DNA-mediated activation of innate immune responses (53) and has also been found to play an important role in innate immune responses (54). Liu et al. found that NEAT1 was overexpressed in both DSS induced mouse models and tumor necrosis factor (TNF) -α-induced inflammatory cell models, and epithelial cell permeability increased in both mice and cell models compared to control cells (55). However, inhibition of NEAT1 can reverse its effects. This suggests that NEAT1 may affect the integrity and permeability of the intestinal epithelial barrier in patients with IBD. They also found that DSS could induce M1 macrophage activation, which was suppressed when NEAT1 expression was suppressed. Favre et al. demonstrated that low-dose photodynamic therapy (LDPDT) can improve T-cell-mediated colitis in mice (56). Subsequent studies have verified that PDT can alleviate DSS induced colitis in mice by regulating PI3K-AKT signaling pathway through Lnc NEAT1-miRNA204–5p axis, but whether PDT can alleviate clinical symptoms of IBD patients still needs further experimental verification (57).

2.1.8 Other Lnc RNAs

CDKN2B-AS1 has more than 20 splicing variants, including typical splicing linear RNA and reverse splicing circular RNA molecules. Some studies have shown that downregulation of CDKN2B-AS1 can destroy Claudin-2 and cause the proliferation of intestinal epithelial cells, thus enhancing the intestinal barrier function (58). Another Lnc RNA, colon cancer-associated transcript 1 (CCAT1), was found to be overexpressed in IBD tissues. Ma et al. reported that CCAT1 expression was positively correlated with myosin light chain kinase (MLCK) (59). MLCK maintained the stability of MLCK mRNA by reducing the binding of miRNA-1853p to MLCK mRNA. MLCK and its phosphorylated products can increase intestinal permeability. CCAT1 and MLCK jointly accelerated the development of IBD (59).

The above studies suggest that lncRNAs not only regulate the apoptosis of epithelial cells in IBD, but also affect intestinal tight junction proteins and regulate the intestinal physical barrier through other mechanisms.

2.2 LncRNAs and immune homeostasis dysregulation

IBD is not only an inflammatory disease of intestinal mucosa, but also an abnormal immune disease caused by immune deficiency of intestinal mucosa (60). Nf-κB is an important immune response factor. When its inhibitory protein is phosphorylated and degraded by proteases, Nf-κB is transferred to the nucleus. It causes transcription of target genes such as interleukin-1β (IL-1β), interleukin-6 (IL-6), interleukin-8 (IL-8), and interferon γ (IFN-γ) (61). Studies have reported that colitis may be caused by excessive inflammatory events such as activation of NF-κB and increased expression of pro-inflammatory factors (62, 63). Since the gut contains complex immune cell populations and inflammatory networks, the precise etiology and pathogenesis of IBD have not been thoroughly studied (64). The intestinal immune system can maintain a complex balance between the intestinal proinflammatory and anti-inflammatory responses. Once the balance is broken, it may lead to the occurrence of IBD. Stimulated by interleukin-1b, IL-6, IL-8, and TNF, NF-κB triggers the transcription of pro-inflammatory cytokines (65). Currently, many studies have revealed that lnc RNAs can affect immune homeostasis in IBD.

2.2.1 IFNG-AS1

IFNG-AS1 is a non-coding transcript located on human chromosome 12 adjacent to the IFNG gene (66). By comparing adult UC patients, Jurkat T cell model and mouse colitis model, Padua et al. found that IFNG-AS1 was associated with IBD susceptibility locus SNP rs7134599, and IFNG-AS1 could

positively regulate the key inflammatory factor IFNG in CD4 T cells (66). Gomez et al. demonstrated that IFNG-AS1 regulates IFNG levels by binding to and actively regulating the histone methyltransferase complex MLL/SET1 (67). The MLL/SET1 complex can turn genes on and off at lysine 4 (K4) through methylation of histone H3 (68). Therefore, IFNG-AS1 may promote the action of Th1 cytokines (IFNG, IL2) and reduce the action of Th2 cytokines (IL10, IL13) through the MLL/SET1 complex (69). These results suggest that lnc RNA IFNG-AS1 is a potential target for the treatment of IBD patients.

2.2.2 LINC01882

There is variation in the genetic locus of protein tyrosine phosphatase 2 (PTPN2) in IBD (70). PTPN2 regulates cytokine signaling by acting on a variety of phosphorylated proteins (71). Scharl et al. demonstrated that PTPN2 regulates autophagy in IECs and that there is a link between SNP rs2542151 and lower levels of PTPN2 protein in colon fibroblasts (72). SNPS at the PTPN2 locus were highly correlated with the DNA methylation level of four CpG sites downstream of PTPN2 and the expression level of the lncRNA LINC01882 downstream of these CpG sites (73). LINC01882, also known as LOC100996324 and RP11–973H3.4, is down-regulated in anti-CD3/CD28-activated CD4+ T cells and can inhibit T cell activation by inhibiting the expression of ZEB1, KLF12 and MAP2K4 to suppress IL-2 expression (73). It has been found that LINC01882 is involved in some autoimmune diseases including IBD. For example, LINC01882 ameliorates acute graft-versus-host disease (aGVHD) via skewing CD4+ T cell differentiation toward Treg cells (74). They also found that LINC01882 promoted Treg differentiation in CD4+ T cells via sponge let-7b-5p (74). This is a target for induction of immune tolerance, which offers the possibility of an effective therapeutic target for patients with aGVHD. LINC01882 is involved in IL-2 expression, which affects the immune response, homeostasis, and differentiation of a variety of lymphocytes, including Tregs. Changes in the number of Tregs contribute to the progression of autoimmune diseases. At present, there are few studies on LINC01882 and IBD, and their relationship still needs to be further explored.

2.2.3 DQ786243

Tregs are important for maintaining intestinal self-tolerance, and their dysfunction is associated with CD and its degree of inflammation (65). Forkhead box P3 (Foxp3) is a major transcription factor controlling the development and function of Tregs. Kim et al. identified a T-cell receptor response enhancer in the first intron of Foxp3 that was dependent on a cyclic-AMP response element binding protein (CREB)/activating transcription factor (ATF) site overlapping a CpG island (75). Therefore, the generation, development, and function of Tregs are dependent on Foxp3 and CREB. Some studies have found that lncRNA DQ786243 and CREB are significantly overexpressed in patients with active CD compared with healthy people or patients with inactive CD (17). However, Foxp3 expression was decreased in inactive CD patients, and there was no significant difference between active CD and healthy people (17). DQ786243 may have a significant effect on the regulation of CREB and Foxp3 genes. Qiao et al. found that DQ786243 could promote CREB and Foxp3 expression and CREB phosphorylation after transfection in Jurkat cells (17). In addition, DQ786243, CREB and Foxp3 mRNAs were all associated with C-reactive protein (CRP), an important serum biomarker of inflammation (17). All these findings suggest that lncRNA DQ786243 is associated with CD, and DQ786243 may regulate the function of Tregs by affecting the expression levels of CREB and Foxp3.

2.2.4 MEG3

Maternally expressed 3(MEG3), a currently concerned lncRNA, has been shown to have anti-inflammatory effects in a variety of inflammatory diseases (76, 77). Wang et al. found that lncRNA-MEG3 was expressed at low levels in a H2O2 -induced Caco-2 cell model and TNBS-induced ulcerative colitis in young rats (78). They injected the lncRNA MEG3 overexpression vector into the UC rat model and found that inflammatory cytokine levels and ROS release were significantly decreased, and IL-10 expression was significantly increased (78). IL-10 is a single-chain glycoprotein that can be produced by adaptive and innate immune cells. It has anti-inflammatory and immunomodulatory effects and can regulate the role of other cytokines in immune and inflammatory diseases. They also found that lncRNA MEG3 may inhibit the release of inflammatory cytokines and ROS by stimulating IL-10 expression (78). Their study similarly confirmed that pyroptosis and apoptosis can be triggered during the pathogenesis of UC, and lncRNA MEG3 can prevent both types of cell death (78). Some studies have reported that miR-98–5p can directly target IL-10 (79). Later they confirmed that lncRNA MEG3 positively regulates IL-10 expression. In addition, knockdown of miR-98–5p was previously shown to alleviate the symptoms of IBD (80). More importantly, the elevation of lncRNA MEG3 inhibited the upregulation of miR-985p expression and promoted the expression of IL-10 by sponging miR-98–5p in UC rats (78). In conclusion, lncRNA-MEG3 can alleviate UC by up-regulating miR-98–5p-loaded IL-10 expression, providing a new potential therapeutic strategy for UC treatment.

2.2.5 LUCAT1

LUCAT1 has previously been identified as a negative feedback regulator of type I interferon (IFN) and inflammatory cytokine expression in human bone marrow cells (Figure 6) (81). It was originally found in lung epithelial cells. Vierbuchen et al. identified the protein important in mRNA processing and alternative splicing as the LUCAT1 binding protein (82). These binding proteins include heterogeneous nuclear ribonucleoprotein (HNRNP) C, M and A2B1, which participate in mRNA splicing and processing, including an mRNA of anti-inflammatory gene NR4A2. At the same time, they found that cells lacking LUCAT1 altered splicing of selected immune genes. For example, splicing of nuclear receptor 4A2 (NR4A2) was particularly affected by lipopolysaccharide (LPS) stimulation (82). In cells lacking LUCAT1, the expression of NR4A2 is reduced and delayed, and the expression of immune genes is elevated in NR4A2-deficient cells. These observations suggest that LUCAT1 is induced to control the splicing and stability of NR4A2, which is partly responsible

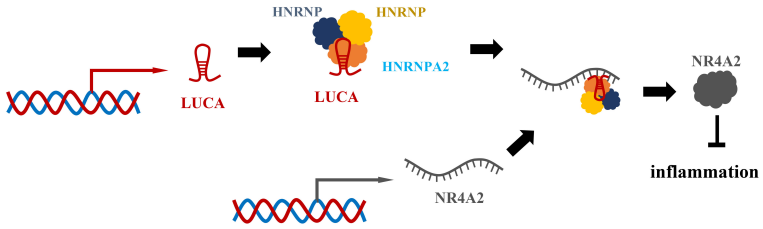

FIGURE 6
LUCAT1 regulates the splicing and stability of NR4A2 to suppress interferon and inflammatory factors. LUCAT1 binds to HNRNPA2B1, HNRNPC, HNRNPM and other proteins, participates in the splicing of NR4A2 mRNA, regulates the splicing and stability of NR4A2, and inhibits interferon and inflammatory factors.

for the anti-inflammatory effects of LUCAT1. They also found that LUCAT1 levels were elevated in patients with chronic obstructive pulmonary disease (COPD) or IBD and that LUCAT1 levels correlated with disease severity (82). Another study revealed lnc RNA-mediated downregulation of innate immunity and inflammatory responses in the SARS-CoV-2 vaccination breakthrough infections (83). They found that LUCAT1 regulates NF-KB-dependent genes by regulating the JAK-STAT pathway in addition to IFN genes (83). In summary, LUCAT1 plays an important role in the regulation of inflammatory diseases. Therefore, LUCAT1 may be used as a potential biomarker and therapeutic target. It is necessary to conduct more studies on the role of LUCAT1 in inflammatory diseases, which can provide new treatment ideas for inflammatory diseases.

2.2.6 Other Lnc RNAs

HIF1A-AS2 is the Roseburia intestinalis flagellin-induced lncRNA in gut epithelium. Quan et al. found that silencing HIF1A-AS2 abrogated the anti-inflammatory effect mediated by intestinal flagellin (84). They also found that HIF1A-AS2 inhibited inflammation by inactivating the NF-κB/JNK pathway and reducing the expression of cytokines such as TNF-a, IL-1b, IL-6, and IL-12 (84). Moreover, knockdown of HIF1A-AS2 significantly increased p65 and Jnk phosphorylation and fully abrogated flagellin-mediated anti-inflammatory effects *in vivo*. Their study provides new insights into the mechanisms by which lncrnas regulate flagellin-mediated resolution of colonic inflammation. Upstream stimulatory factor 1 (USF1) is a class of transcription factors related to coronary artery disease (CAD) (85), which can be used as a mediator to participate in the anti-inflammatory strategy for the treatment of acute lung injury (86). Activating transcription factor 2 (ATF2), a member of basic leucine zipper proteins, is widely expressed in various tissues and participates in inflammatory responses (87). Li et al. demonstrated the proinflammatory role of lncRNA HIF1A-AS2 in atherosclerosis (88). Down-regulation of lncRNA HIF1A-AS2 inhibits atherosclerotic inflammation by reducing the binding of USF1 to the promoter region of ATF2, thereby reducing the expression of ATF2 (88). Therefore, HIF1A-AS2 may be a negative regulator of intestinal inflammation and may be a new target for the treatment of IBD in the future.

LncRNA ANRIL, located on chromosome 9p21, shows significant down-regulation in IBD disease (89). Qiao et al. explored the role of ANRIL and its possible mechanistic studies after stimulating UC to cause inflammatory injury by lipopolysaccharide (LPS) treated human embryonic cells (FHCs) (90). They found that inhibition of ANRIL could negatively regulate miR-323b-5p to alleviate LPS-induced FHCs damage (90). In addition, their results also indicated that miR-323b-5p negatively regulated TLR4 expression (90). TLR4 was the target of miR-323b-5p. It has been shown to be upregulated in UC, causing inflammation and promoting UC development (91). Knockdown of TLR4 reversed the effect of miR-323b-5p in inhibiting LPS-induced injury in FHCs (90). TRL4 is the only TLR capable of activating the MyD88-dependent signaling pathway (92). MyD88 is not only a key downstream signaling ligand of TLR4 receptor complex, but also an important adaptor protein of NF-kB signaling pathway (93). NF-kB pathway is a central mediator involved in immune and inflammatory responses (94), which can play a therapeutic role in UC. Therefore, ANRIL may affect the development of UC by regulating the miR-323b-5p/TLR4/MyD88/NF-κB pathway, which provides new ideas for the treatment of UC in the future. Li et al. found many lncrnas differentially expressed in CD mucosa, indicating that these lncRNAs were all involved in the immune response (95). For example, lncRNA ATG induces stress and apoptotic protease activation in intestinal epithelial cells in the inflammatory environment of CD (96). Caspase-3-mediated cleavage of ATG16L1 is increased, leading to abnormal autophagy in intestinal epithelial cells (96). When the activity of DDX5 in Th17 cells is increased, a large number of lncRNA Rmrp is decomposed, which would bind to RORγ-t, thus causing the latter to undergo nuclear transport, acting on the corresponding promoter, and promoting the development of Th17. Th17 maturation has a protective effect on CD (42, 97, 98). In addition, ENST0000487539_1.1 levels are increased in the serum of CD patients, and they can regulate Treg cell function by regulating Foxp3 levels. They also hypothesized that these lncRNAs might be involved in the regulation of intestinal mucosal function through the genetic network of lncRNA-miRNA/TFs-mRNAs (95).

3 Lnc RNA as an IBD biomarker and a predictor of treatment response

The common methods for the diagnosis and treatment of IBD include clinical manifestations, imaging methods, histopathological

examination, and endoscopic evaluation. Because clinical features of IBD vary among individuals, approximately one quarter of patients have extraintestinal manifestations before diagnosis (99). Histopathology and endoscopy are currently the "gold standard" for diagnosing IBD (100, 101). Because both of these methods rely heavily on skilled clinicians, diagnosis of IBD is difficult. At present, more and more researchers are more inclined to use some biomarkers, such as C-reactive protein (CRP), lactoferrin, calcaretin and so on. However, most current biomarkers reflect systemic inflammation, are present in many diseases, and lack a certain sensitivity and specificity, which can lead to treatment delays and further disease progression. Therefore, it is urgent to find out the biomarkers with high specificity and sensitivity. LncRNAs have been shown to be valuable diagnostic markers for various diseases due to their easy availability, stability, availability by common molecular biology techniques such as qRT-PCR, rapid detection, and quantification (102, 103). A variety of lncRNAs have been shown to be associated with IBD. By monitoring the change of lnc RNA level, the therapeutic effect and prognosis of IBD disease can be evaluated. Many lncRNAs can be used as biomarkers to evaluate clinical evaluation in patients with IBD.

Wang et al. demonstrated that lncRNA KIF9-AS1 and LINC01272 expression was significantly up-regulated, while lncRNA DIO3OS expression was significantly decreased in tissue and plasma samples of IBD patients compared with healthy controls (104). They also used ROC curve analysis to determine the specificity and sensitivity of KIF9-AS1, LINC01272 and DIO3OS, and the results showed that the area under the ROC curve (AUCs) of these three lncRNAs in IBD patients and healthy controls were mostly greater than 0.76 (104). Therefore, lncRNA KIF9-AS1, LINC01272 and DIO3OS may be potential diagnostic biomarkers for IBD. Ge et al. compared the expression of lncRNA ANRIL in CD patients and control group, and the results showed that the area under the curve (AUC) of lncRNA ANRIL expression to distinguish CD patients and control group was 0.803 (95%CI: 0.733–0.874) (105). They also found that lncRNA ANRIL expression could distinguish the active and remission stages of CD (105). They also found that lncRNA ANRIL expression could distinguish the active and remission stages of CD (105). In addition, lncRNA ANRIL expression was negatively correlated with CD disease risk, disease activity, and proinflammatory cytokine levels (105). With the development of the disease, complications such as fistula and stenosis may occur in the late stage of CD. Lncrnas can be used as biomarkers even when complications occur. Visschedijk et al. demonstrated that lncRNA RP11–679B19.1 is associated with recurrent fibrostenosis CD, but its specific mechanism of action remains unclear (106).

Not only can Lnc RNA serve as a biomarker, but it has also been shown to be a predictor of therapeutic response in IBD. Ge et al. found that changes in lncRNA ANRIL expression were associated with infliximab treatment response (105). The expression of lncRNA ANRIL increased in patients who achieved treatment response with infliximab, while it remained stable in patients who failed to achieve treatment response (105). Therefore, the change of intestinal mucosal lncRNA ANRIL is related to the response to infliximab treatment in CD patients, and its up-regulation can be used as a marker of the response to infliximab treatment in CD patients (105). Haberman et al. performed intestinal biopsies from IBD children undergoing endoscopy and treatment and found that the expression of LINC01272 and HNF4A-AS1 was significantly associated with more severe intestinal mucosal injury (89). Calprotectin S100A8 is the most commonly used tissue inflammation biomarker in clinical practice. They also found that HNF4A-AS1 was negatively correlated with the calprotectant S100A8, while LINC01272 was significantly positively correlated with the calprotectant S100A8 (89). HNF4A-AS1 is specifically expressed in epithelial cells, and LINC01272 is specifically expressed in monocytes, neutrophils, and myeloid dendritic cells (DC) (89). Therefore, targeted lncRNA-directed therapy may become potential new tissue-specific targets for RNA-based interventions. Glucocorticoids (GCs) are effective drugs for inducing remission in patients with IBD in clinical practice, which have anti-inflammatory and immunosuppressive effects (107). The level of lncRNA growth inhibition specific 5 (GAS5) was higher in patients with poor GCs response than in those with good response. Therefore, GAS5 may be associated with GCs resistance (108, 109). Some studies have found that the expression of lncRNA GAS5 is different between GCs sensitive cells and GCs resistant cells, and GAS5 is up-regulated in GCs resistant cells and accumulates more in the cytoplasm (110). In conclusion, lncRNA GAS5 can be considered as a novel pharmacogenomic marker that contributes to the personalization of GCs therapy (Table 1).

4 Discussion

IBD is a recurrent chronic inflammatory disease in the gastrointestinal tract. Due to its increasing incidence, it has become a global health problem. Although the current drugs used in the clinical treatment of IBD are effective, they have many limitations. Given the complexity of IBD, *in vivo* approaches to investigate its etiology are essential. Although mouse models of IBD have been gradually developed and refined, the basic understanding of transcriptome differences in these models is still at an early stage, so the exact pathogenesis of these models is not fully understood. Although the exploration of lncRNAs in existing studies is still in the early stage, it has been pointed out that lncRNAs are involved in the pathogenesis of IBD. In IBD, lncRNAs can affect intestinal tight junction proteins, such as lncRNA H19, PLnc RNA1, lnc RNA SPRY4-IT1, etc. LncRNAs can regulate the apoptosis of epithelial cells, such as BC012900, lncRNA CRNDE and so on. LncRNAs also regulate the gut physical barrier through other mechanisms, such as the lncRNA CCAT1. In addition, lncRNAs can affect the immune response in IBD, such as lnc NEAT1, IFNG-AS1, LINC01882 and so on. With the development of molecular biology technology, monitoring the changes of lnc RNAs level can be used to evaluate the efficacy and prognosis of IBD. LncRNA KIF9-AS1, LINC01272 and DIO3OS may be potential diagnostic biomarkers for IBD. LncRNA ANRIL expression is negatively correlated with CD disease risk and disease activity, and is also related to the response to biological agents. Therefore, lncRNAs play an important role in regulating intestinal barrier and immune homeostasis. LncRNAs can not only be used as biomarkers and predictors of treatment response in IBD, but also as targets for IBD. Due to the complexity of IBD

TABLE 1 LncRNAs proposed for IBD biomarkers and therapeutic predictors.

LncRNAs	Disease	Source	Method	Change	Application	Reference
KIF9-AS1	UC&CD	Colonic tissues & blood samples	qPCR	Upgrade	Biomarker between IBD and HC	(102)
LINC01272	UC&CD	Colonic tissues & blood samples	qPCR	Upgrade		
DIO3OS	UC&CD	Colonic tissues & blood samples	qPCR	Downgrade		
ANRIL	CD	Colonic tissues	qPCR	Downgrade	Biomarker between CD and HC, assessed the response to infliximab	(103)
RP11-679B19.1	CD	Ileal tissues	Immunochip	Upgrade	Associated with recurrent fibrous stenosis CD	(104)
LINC01272	CD	Ileal tissues	RNAseq	Downgrade	Associated with more severe intestinal mucosal injury	(105)
HNF4A-AS1	CD	Ileal tissues	RNAseq	Upgrade		
GAS5	UC&CD	Peripheral blood	qPCR	Upgrade	Marker of glucocorticoid therapy in children	(107)

UC, ulcerative colitis; CD, Crohn's Disease; HC, healthy control; qPCR, quantitative real-time PCR; RNAseq, RNA sequencing.

pathogenesis, a single lncRNA may not be able to fully explain IBD. Therefore, based on the close relationship between lncRNAs and IBD, it is essential to clarify the mechanism of lncRNAs in IBD and explore more promising treatment methods.

Author contributions

YH: Writing – original draft, Writing – review & editing. YL: Writing – review & editing. YF: Writing – review & editing. QZ: Writing – review & editing. ZZ: Writing – review & editing. XZ: Writing – review & editing. XY: Writing – review & editing. YC: Methodology, Resources, Writing – review & editing. JD: Methodology, Resources, Writing – review & editing. JY: Methodology, Resources, Writing – review & editing.

Funding

The author(s) declare financial support was received for the research, authorship, and/or publication of this article. This work was supported by the Basic Public Welfare Research Program of Zhejiang Province, China (No. LGF19H160022), Natural Science Foundation of Zhejiang Province, China (No. LQ19H030003), the Key Project of Social Development of Jinhua Science and Technology Bureau of Zhejiang Province, China (No. 2021–3-079).

Conflict of interest

The authors declare that the research was conducted in the absence of any commercial or financial relationships that could be construed as a potential conflict of interest.

Publisher's note

References

1. Chang JT. Pathophysiology of inflammatory bowel diseases. *N Engl J Med*. (2020) 383:2652–64. doi: 10.1056/NEJMra2002697

2. Ng SC, Shi HY, Hamidi N, Underwood FE, Tang W, Benchimol EI, et al. Worldwide incidence and prevalence of inflammatory bowel disease in the 21st century: a systematic review of population-based studies. *Lancet*. (2017) 390:2769–78. doi: 10.1016/S0140–6736(17)32448–0

3. Beiranvand M. A review of the biological and pharmacological activities of mesalazine or 5-aminosalicylic acid (5-ASA): an anti-ulcer and anti-oxidant drug. *Inflammopharmacology*. (2021) 29:1279–90. doi: 10.1007/s10787–021-00856–1

4. Torres J, Bonovas S, Doherty G, Kucharzik T, Gisbert JP, Raine T, et al. ECCO guidelines on therapeutics in crohn's disease: medical treatment. *J Crohns Colitis*. (2020) 14:4–22. doi: 10.1093/ecco-jcc/jjz180

5. Kadmiel M, Cidlowski JA. Glucocorticoid receptor signaling in health and disease. *Trends Pharmacol Sci*. (2013) 34:518–30. doi: 10.1016/j.tips.2013.07.003

6. Keenan GF. Management of complications of glucocorticoid therapy. *Clin Chest Med*. (1997) 18:507–20. doi: 10.1016/s0272–5231(05)70398–1

7. Toruner M, Loftus EV Jr, Harmsen WS, Zinsmeister AR, Orenstein R, Sandborn WJ, et al. Risk factors for opportunistic infections in patients with inflammatory bowel disease. *Gastroenterology*. (2008) 134:929–36. doi: 10.1053/j.gastro.2008.01.012

8. Chen WX, Ren LH, Shi RH. Implication of miRNAs for inflammatory bowel disease treatment: Systematic review. *World J Gastrointest Pathophysiol*. (2014) 5:63–70. doi: 10.4291/wjgp.v5.i2.63

9. Filipowicz W, Bhattacharyya SN, Sonenberg N. Mechanisms of post-transcriptional regulation by microRNAs: are the answers in sight? *Nat Rev Genet*. (2008) 9:102–14. doi: 10.1038/nrg2290

10. Innocenti T, Bigagli E, Lynch EN, Galli A, Dragoni G. MiRNA-Based Therapies for the treatment of inflammatory bowel disease: What are we still missing? *Inflamm Bowel Dis*. (2023) 29:308–23. doi: 10.1093/ibd/izac122

11. Ghosal S, Das S, Chakrabarti J. Long noncoding RNAs: new players in the molecular mechanism for maintenance and differentiation of pluripotent stem cells. *Stem Cells Dev*. (2013) 22:2240–53. doi: 10.1089/scd.2013.0014

12. Song J, Kim D, Han J, Kim Y, Lee M, Jin EJ. PBMC and exosome-derived Hotair is a critical regulator and potent marker for rheumatoid arthritis. *Clin Exp Med*. (2015) 15:121–6. doi: 10.1007/s10238–013-0271–4

13. Steck E, Boeuf S, Gabler J, Werth N, Schnatzer P, Diederichs S, et al. Regulation of H19 and its encoded microRNA-675 in osteoarthritis and under anabolic and catabolic in *vitro* conditions. *J Mol Med (Berl)*. (2012) 90:1185–95. doi: 10.1007/s00109-012-0895-y

14. Tsitsiou E, Williams AE, Moschos SA, Patel K, Rossios C, Jiang X, et al. Transcriptome analysis shows activation of circulating CD8+ T cells in patients with severe asthma. *J Allergy Clin Immunol*. (2012) 129:95–103. doi: 10.1016/j.jaci.2011.08.011

15. Mirza AH, Kaur S, Pociot F. Long non-coding RNAs as novel players in β cell function and type 1 diabetes. *Hum Genomics*. (2017) 11:17. doi: 10.1186/s40246–017-0113–7

16. Soroosh A, Koutsioumpa M, Pothoulakis C, Iliopoulos D. Functional role and therapeutic targeting of microRNAs in inflammatory bowel disease. *Am J Physiol Gastrointest Liver Physiol*. (2018) 314:G256–62. doi: 10.1152/ajpgi.00268.2017

17. Qiao YQ, Huang ML, Xu AT, Zhao D, Ran ZH, Shen J. LncRNA DQ786243 affects Treg related CREB and Foxp3 expression in Crohn's disease. *J BioMed Sci*. (2013) 20:87. doi: 10.1186/1423–0127-20–87

18. Liu Z, Lee J, Krummey S, Lu W, Cai H, Lenardo MJ. The kinase LRRK2 is a regulator of the transcription factor NFAT that modulates the severity of inflammatory bowel disease. *Nat Immunol*. (2011) 12:1063–70. doi: 10.1038/ni.2113

19. Wu F, Huang Y, Dong F, Kwon JH. Ulcerative colitis-associated long noncoding RNA, BC012900, regulates intestinal epithelial cell apoptosis. *Inflamm Bowel Dis*. (2016) 22:782–95. doi: 10.1097/MIB.0000000000000691

20. Wang J, Ghosh SS, Ghosh S. Curcumin improves intestinal barrier function: modulation of intracellular signaling, and organization of tight junctions. *Am J Physiol Cell Physiol*. (2017) 312:C438–45. doi: 10.1152/ajpcell.00235.2016

21. Mittal R, Coopersmith CM. Redefining the gut as the motor of critical illness. *Trends Mol Med*. (2014) 20:214–23. doi: 10.1016/j.molmed.2013.08.004

22. Zeissig S, Bürgel N, Günzel D, Richter J, Mankertz J, Wahnschaffe U, et al. Changes in expression and distribution of claudin 2, 5 and 8 lead to discontinuous tight junctions and barrier dysfunction in active Crohn's disease. *Gut*. (2007) 56:61–72. doi: 10.1136/gut.2006.094375

23. Yadav VK, Kumar A, Tripathi PP, Gupta J. Long noncoding RNAs in intestinal homeostasis, regeneration, and cancer. *J Cell Physiol*. (2021) 236:7801–13. doi: 10.1002/jcp.30393

24. Chen S, He R, He B, Xu L, Zhang S. Potential roles of exosomal lncRNAs in the intestinal mucosal immune barrier. *J Immunol Res*. (2021) 2021:7183136. doi: 10.1155/2021/7183136

25. Gabory A, Ripoche MA, Yoshimizu T, Dandolo L. The H19 gene: regulation and function of a non-coding RNA. *Cytogenet Genome Res*. (2006) 113:188–93. doi: 10.1159/000090831

26. Raveh E, Matouk IJ, Gilon M, Hochberg A. The H19 long non-coding RNA in cancer initiation, progression and metastasis-a proposed unifying theory. *Mol Cancer*. (2015) 14:184. doi: 10.1186/s12943–015-0458–2

27. Pan JX. LncRNA H19 promotes atherosclerosis by regulating MAPK and NF-kB signaling pathway. *Eur Rev Med Pharmacol Sci*. (2017) 21:322–8.

28. Zou T, Jaladanki SK, Liu L, Xiao L, Chung HK, Wang JY, et al. H19 long noncoding RNA regulates intestinal epithelial barrier function via MicroRNA 675 by Interacting with RNA-Binding Protein HuR. *Mol Cell Biol*. (2016) 36:1332–41. doi: 10.1128/MCB.01030–15

29. Chen SW, Wang PY, Liu YC, Sun L, Zhu J, Zuo S, et al. Effect of long noncoding RNA H19 overexpression on intestinal barrier function and its potential role in the pathogenesis of ulcerative colitis. *Inflamm Bowel Dis*. (2016) 22:2582–92. doi: 10.1097/MIB.0000000000000932

30. Zhou X, Ye F, Yin C, Zhuang Y, Yue G, Zhang G. The interaction between MiR-141 and lncRNA-H19 in regulating cell proliferation and migration in gastric cancer. *Cell Physiol Biochem*. (2015) 36:1440–52. doi: 10.1159/000430309

31. Wang SH, Wu XC, Zhang MD, Weng MZ, Zhou D, Quan ZW. Long noncoding RNA H19 contributes to gallbladder cancer cell proliferation by modulated miR-194–5p targeting AKT2. *Tumour Biol*. (2016) 37:9721–30. doi: 10.1007/s13277–016-4852–1

32. Zhi X, Tao J, Li Z, Jiang B, Feng J, Yang L, et al. MiR-874 promotes intestinal barrier dysfunction through targeting AQP3 following intestinal ischemic injury. *FEBS Lett*. (2014) 588:757–63. doi: 10.1016/j.febslet.2014.01.022

33. Su Z, Zhi X, Zhang Q, Yang L, Xu H, Xu Z. LncRNA H19 functions as a competing endogenous RNA to regulate AQP3 expression by sponging miR-874 in the intestinal barrier. *FEBS Lett*. (2016) 590:1354–64. doi: 10.1002/1873–3468.12171

34. Dong L, Ni J, Hu W, Yu C, Li H. Upregulation of long non-coding RNA PlncRNA-1 promotes metastasis and induces epithelial-mesenchymal transition in hepatocellular carcinoma. *Cell Physiol Biochem*. (2016) 38:836–46. doi: 10.1159/000443038

35. Wang CM, Wu QQ, Li SQ, Chen FJ, Tuo L, Xie HW, et al. Upregulation of the long non-coding RNA PlncRNA-1 promotes esophageal squamous carcinoma cell proliferation and correlates with advanced clinical stage. *Dig Dis Sci*. (2014) 59:591–7. doi: 10.1007/s10620–013-2956–7

36. Fang Z, Xu C, Li Y, Cai X, Ren S, Liu H, et al. A feed-forward regulatory loop between androgen receptor and PlncRNA-1 promotes prostate cancer progression. *Cancer Lett*. (2016) 374:62–74. doi: 10.1016/j.canlet.2016.01.033

37. Chen T, Xue H, Lin R, Huang Z. MiR-34c and PlncRNA1 mediated the function of intestinal epithelial barrier by regulating tight junction proteins in inflammatory bowel disease. *Biochem Biophys Res Commun*. (2017) 486:6–13. doi: 10.1016/j.bbrc.2017.01.115

38. Katoh Y, Katoh M. FGF signaling inhibitor, SPRY4, is evolutionarily conserved target of WNT signaling pathway in progenitor cells. *Int J Mol Med*. (2006) 17:529–32. doi: 10.3892/ijmm.17.3.529

39. Xiao L, Rao JN, Cao S, Liu L, Chung HK, Zhang Y, et al. Long noncoding RNA SPRY4-IT1 regulates intestinal epithelial barrier function by modulating the expression levels of tight junction proteins. *Mol Biol Cell*. (2016) 27:617–26. doi: 10.1091/mbc.E15–10-0703

40. Nan A, Zhou X, Chen L, Liu M, Zhang N, Zhang L, et al. A transcribed ultraconserved noncoding RNA, Uc.173, is a key molecule for the inhibition of lead-induced neuronal apoptosis. *Oncotarget*. (2016) 7:112–24. doi: 10.18632/oncotarget.6590

41. Xiao L, Wu J, Wang JY, Chung HK, Kalakonda S, Rao JN, et al. Long Noncoding RNA uc.173 promotes renewal of the intestinal mucosa by inducing degradation of MicroRNA 195. *Gastroenterology*. (2018) 154:599–611. doi: 10.1053/j.gastro.2017.10.009

42. Zacharopoulou E, Gazouli M, Tzouvala M, Vezakis A, Karamanolis G. The contribution of long non-coding RNAs in inflammatory bowel diseases. *Dig Liver Dis*. (2017) 49:1067–72. doi: 10.1016/j.dld.2017.08.003

43. Ofek P, Ben-Meir D, Kariv-Inbal Z, Oren M, Lavi S. Cell cycle regulation and p53 activation by protein phosphatase 2C alpha. *J Biol Chem*. (2003) 278:14299–305. doi: 10.1074/jbc.M211699200

44. Graham LD, Pedersen SK, Brown GS, Ho T, Kassir Z, Moynihan AT, et al. Colorectal neoplasia differentially expressed (CRNDE), a novel gene with elevated expression in colorectal adenomas and adenocarcinomas. *Genes Cancer*. (2011) 2:829–40. doi: 10.1177/1947601911431081

45. Ellis BC, Molloy PL, Graham LD. CRNDE: A long non-coding RNA involved in cancer, neurobiology, and development. *Front Genet*. (2012) 3:270. doi: 10.3389/fgene.2012.00270

46. Chen Z, Yu C, Zhan L, Pan Y, Chen L, Sun C. LncRNA CRNDE promotes hepatic carcinoma cell proliferation, migration and invasion by suppressing miR-384. *Am J Cancer Res*. (2016) 6:2299–309.

47. Han P, Li JW, Zhang BM, Lv JC, Li YM, Gu XY, et al. The lncRNA CRNDE promotes colorectal cancer cell proliferation and chemoresistance via miR-181a-5p-mediated regulation of Wnt/β-catenin signaling. *Mol Cancer*. (2017) 16:9. doi: 10.1186/s12943–017-0583–1

48. Yang F, Li XF, Cheng LN, Li XL. Long non-coding RNA CRNDE promotes cell apoptosis by suppressing miR-495 in inflammatory bowel disease. *Exp Cell Res*. (2019) 382:111484. doi: 10.1016/j.yexcr.2019.06.029

49. Chu XQ, Wang J, Chen GX, Zhang GQ, Zhang DY, Cai YY. Overexpression of microRNA-495 improves the intestinal mucosal barrier function by targeting STAT3 via inhibition of the JAK/STAT3 signaling pathway in a mouse model of ulcerative colitis. *Pathol Res Pract*. (2018) 214:151–62. doi: 10.1016/j.prp.2017.10.003

50. Cui X, Shan X, Qian J, Ji Q, Wang L, Wang X, et al. The suppressor of cytokine signaling SOCS1 promotes apoptosis of intestinal epithelial cells via p53 signaling in Crohn's disease. *Exp Mol Pathol*. (2016) 101:1–11. doi: 10.1016/j.yexmp.2016.05.011

51. Calabrese V, Mallette FA, Deschênes-Simard X, Ramanathan S, Gagnon J, Moores A, et al. SOCS1 links cytokine signaling to p53 and senescence. *Mol Cell*. (2009) 36:754–67. doi: 10.1016/j.molcel.2009.09.044

52. Dirisina R, Katzman RB, Goretsky T, Managlia E, Mittal N, Williams DB, et al. p53 and PUMA independently regulate apoptosis of intestinal epithelial cells in patients and mice with colitis. *Gastroenterology*. (2011) 141:1036–45. doi: 10.1053/j.gastro.2011.05.032

53. Imamura K, Imamachi N, Akizuki G, Kumakura M, Kawaguchi A, Nagata K, et al. Long noncoding RNA NEAT1-dependent SFPQ relocation from promoter region to paraspeckle mediates IL8 expression upon immune stimuli. *Mol Cell*. (2014) 53:393–406. doi: 10.1016/j.molcel.2014.01.009

54. Morchikh M, Cribier A, Raffel R, Amraoui S, Cau J, Severac D, et al. HEXIM1 and NEAT1 long non-coding RNA form a multi-subunit complex that regulates DNA-mediated innate immune response. *Mol Cell*. (2017) 67:387–399.e385. doi: 10.1016/j.molcel.2017.06.020

55. Liu R, Tang A, Wang X, Chen X, Zhao L, Xiao Z, et al. Inhibition of lncRNA NEAT1 suppresses the inflammatory response in IBD by modulating the intestinal epithelial barrier and by exosome-mediated polarization of macrophages. *Int J Mol Med*. (2018) 42:2903–13. doi: 10.3892/ijmm.2018.3829

56. Favre L, Borle F, Velin D, Bachmann D, Bouzourene H, Wagnieres G, et al. Low dose endoluminal photodynamic therapy improves murine T cell-mediated colitis. *Endoscopy*. (2011) 43:604–16. doi: 10.1055/s-0030–1256382

57. Wang K, Zhang Z, Liu K, Yang X, Zou H, Zhou J, et al. Neat1-miRNA204–5p-PI3K-AKT axis as a potential mechanism for photodynamic therapy treated colitis in mice. *Photodiagnosis Photodyn Ther*. (2018) 24:349–57. doi: 10.1016/j.pdpdt.2018.10.020

58. Rankin CR, Lokhandwala ZA, Huang R, Pekow J, Pothoulakis C, Padua D. Linear and circular CDKN2B-AS1 expression is associated with inflammatory bowel disease and participates in intestinal barrier formation. *Life Sci*. (2019) 231:116571. doi: 10.1016/j.lfs.2019.116571

59. Ma D, Cao Y, Wang Z, He J, Chen H, Xiong H, et al. CCAT1 lncRNA promotes inflammatory bowel disease Malignancy by destroying intestinal barrier via downregulating miR-185–3p. *Inflamm Bowel Dis*. (2019) 25:862–74. doi: 10.1093/ibd/izy381

60. Geremia A, Arancibia-Cárcamo CV. Innate lymphoid cells in intestinal inflammation. *Front Immunol*. (2017) 8:1296. doi: 10.3389/fimmu.2017.01296

61. Shih VF, Tsui R, Caldwell A, Hoffmann A. A single NFκB system for both canonical and non-canonical signaling. *Cell Res*. (2011) 21:86–102. doi: 10.1038/cr.2010.161

62. Wang X, Sun Y, Zhao Y, Ding Y, Zhang X, Kong L, et al. Oroxyloside prevents dextran sulfate sodium-induced experimental colitis in mice by inhibiting NF-κB pathway through PPARγ activation. *Biochem Pharmacol*. (2016) 106:70–81. doi: 10.1016/j.bcp.2016.02.019

63. Perše M, Cerar A. Dextran sodium sulphate colitis mouse model: traps and tricks. *J BioMed Biotechnol*. (2012) 2012:718617. doi: 10.1155/2012/718617

64. Abraham C, Cho JH. Inflammatory bowel disease. *N Engl J Med*. (2009) 361:2066–78. doi: 10.1056/NEJMra0804647

65. Boden EK, Snapper SB. Regulatory T cells in inflammatory bowel disease. *Curr Opin Gastroenterol*. (2008) 24:733–41. doi: 10.1097/MOG.0b013e328311f26e

66. Padua D, Mahurkar-Joshi S, Law IK, Polytarchou C, Vu JP, Pisegna JR, et al. A long noncoding RNA signature for ulcerative colitis identifies IFNG-AS1 as an enhancer of inflammation. *Am J Physiol Gastrointest Liver Physiol*. (2016) 311:G446–57. doi: 10.1152/ajpgi.00212.2016

67. Gomez JA, Wapinski OL, Yang YW, Bureau JF, Gopinath S, Monack DM, et al. The NeST long ncRNA controls microbial susceptibility and epigenetic activation of the interferon-γ locus. *Cell*. (2013) 152:743–54. doi: 10.1016/j.cell.2013.01.015

68. Popovic R, Zeleznik-Le NJ. MLL: how complex does it get? *J Cell Biochem*. (2005) 95:234–42. doi: 10.1002/jcb.20430

69. Rankin CR, Shao L, Elliott J, Rowe L, Patel A, Videlock E, et al. The IBD-associated long noncoding RNA IFNG-AS1 regulates the balance between inflammatory and anti-inflammatory cytokine production after T-cell stimulation. *Am J Physiol Gastrointest Liver Physiol*. (2020) 318:G34–40. doi: 10.1152/ajpgi.00232.2019

70. Franke A, Balschun T, Karlsen TH, Hedderich J, May S, Lu T, et al. Replication of signals from recent studies of Crohn's disease identifies previously unknown disease loci for ulcerative colitis. *Nat Genet*. (2008) 40:713–5. doi: 10.1038/ng.148

71. Doody KM, Bourdeau A, Tremblay ML. T-cell protein tyrosine phosphatase is a key regulator in immune cell signaling: lessons from the knockout mouse model and implications in human disease. *Immunol Rev*. (2009) 228:325–41. doi: 10.1111/j.1600-065X.2008.00743.x

72. Scharl M, Wojtal KA, Becker HM, Fischbeck A, Frei P, Arikkat J, et al. Protein tyrosine phosphatase nonreceptor type 2 regulates autophagosome formation in human intestinal cells. *Inflamm Bowel Dis*. (2012) 18:1287–302. doi: 10.1002/ibd.21891

73. Houtman M, Shchetynsky K, Chemin K, Hensvold AH, Ramsköld D, Tandre K, et al. T cells are influenced by a long non-coding RNA in the autoimmune associated PTPN2 locus. *J Autoimmun*. (2018) 90:28–38. doi: 10.1016/j.jaut.2018.01.003

74. Teng Y, Xia L, Huang Z, Yao L, Wu Q. Long noncoding RNA LINC01882 ameliorates aGVHD via skewing CD4+ T cell differentiation toward Treg cells. *Am J Physiol Cell Physiol*. (2023) 324:C395–406. doi: 10.1152/ajpcell.00323.2022

75. Kim HP, Leonard WJ. CREB/ATF-dependent T cell receptor-induced FoxP3 gene expression: a role for DNA methylation. *J Exp Med*. (2007) 204:1543–51. doi: 10.1084/jem.20070109

76. Li Y, Zhang S, Zhang C, Wang M. LncRNA MEG3 inhibits the inflammatory response of ankylosing spondylitis by targeting miR-146a. *Mol Cell Biochem*. (2020) 466:17–24. doi: 10.1007/s11010-019-03681-x

77. Li G, Liu Y, Meng F, Xia Z, Wu X, Fang Y, et al. LncRNA MEG3 inhibits rheumatoid arthritis through miR-141 and inactivation of AKT/mTOR signalling pathway. *J Cell Mol Med*. (2019) 23:7116–20. doi: 10.1111/jcmm.14591

78. Wang Y, Wang N, Cui L, Li Y, Cao Z, Wu X, et al. Long non-coding RNA MEG3 alleviated ulcerative colitis through upregulating miR-98–5p-sponged IL-10. *Inflammation*. (2021) 44:1049–59. doi: 10.1007/s10753-020-01400-z

79. Takuse Y, Watanabe M, Inoue N, Ozaki R, Ohtsu H, Saeki M, et al. Association of IL-10-regulating microRNAs in peripheral blood mononuclear cells with the pathogenesis of autoimmune thyroid disease. *Immunol Invest*. (2017) 46:590–602. doi: 10.1080/08820139.2017.1322975

80. Peng Y, Wang Q, Yang W, Yang Q, Pei Y, Zhang W. MiR-98–5p expression inhibits polarization of macrophages to an M2 phenotype by targeting Trib1 in inflammatory bowel disease. *Acta Biochim Pol*. (2020) 67:157–63. doi: 10.18388/abp.2020_5152

81. Agarwal S, Vierbuchen T, Ghosh S, Chan J, Jiang Z, Kandasamy RK, et al. The long non-coding RNA LUCAT1 is a negative feedback regulator of interferon responses in humans. *Nat Commun*. (2020) 11:6348. doi: 10.1038/s41467–020-20165–5

82. Vierbuchen T, Agarwal S, Johnson JL, Galia L, Lei X, Stein K, et al. The lncRNA LUCAT1 is elevated in inflammatory disease and restrains inflammation by regulating the splicing and stability of NR4A2. *Proc Natl Acad Sci USA*. (2023) 120:e2213715120. doi: 10.1073/pnas.2213715120

83. Chattopadhyay P, Mishra P, Mehta P, Soni J, Gupta R, Tarai B, et al. Transcriptomic study reveals lncRNA-mediated downregulation of innate immune and inflammatory response in the SARS-CoV-2 vaccination breakthrough infections. *Front Immunol*. (2022) 13:1035111. doi: 10.3389/fimmu.2022.1035111

84. Quan Y, Song K, Zhang Y, Zhu C, Shen Z, Wu S, et al. Roseburia intestinalis-derived flagellin is a negative regulator of intestinal inflammation. *Biochem Biophys Res Commun*. (2018) 501:791–9. doi: 10.1016/j.bbrc.2018.05.075

85. Laurila PP, Soronen J, Kooijman S, Forsström S, Boon MR, Surakka I, et al. USF1 deficiency activates brown adipose tissue and improves cardiometabolic health. *Sci Transl Med*. (2016) 8:323ra13. doi: 10.1126/scitranslmed.aad0015

86. Tiruppathi C, Soni D, Wang DM, Xue J, Singh V, Thippegowda PB, et al. The transcription factor DREAM represses the deubiquitinase A20 and mediates inflammation. *Nat Immunol*. (2014) 15:239–47. doi: 10.1038/ni.2823

87. Li M, Zhang D, Ge X, Zhu X, Zhou Y, Zhang Y, et al. TRAF6-p38/JNK-ATF2 axis promotes microglial inflammatory activation. *Exp Cell Res*. (2019) 376:133–48. doi: 10.1016/j.yexcr.2019.02.005

88. Li P, Xing J, Zhang J, Jiang J, Liu X, Zhao D, et al. Inhibition of long noncoding RNA HIF1A-AS2 confers protection against atherosclerosis via ATF2 downregulation. *J Adv Res*. (2020) 26:123–35. doi: 10.1016/j.jare.2020.07.015

89. Haberman Y, BenShoshan M, Di Segni A, Dexheimer PJ, Braun T, Weiss B, et al. Long ncRNA landscape in the ileum of treatment-naive early-onset crohn disease. *Inflamm Bowel Dis*. (2018) 24:346–60. doi: 10.1093/ibd/izx013

90. Qiao C, Yang L, Wan J, Liu X, Pang C, You W, et al. Long noncoding RNA ANRIL contributes to the development of ulcerative colitis by miR-323b-5p/TLR4/MyD88/NF-κB pathway. *Biochem Biophys Res Commun*. (2019) 508:217–24. doi: 10.1016/j.bbrc.2018.11.100

91. Yu ZH, Huang F, Xu N, Zhao DM, Hu FA, Liu J, et al. Expression of Toll-like receptor 4, CD14, and NF-κB in Chinese patients with ulcerative colitis. *J Immunoassay Immunochem*. (2011) 32:47–56. doi: 10.1080/15321819.2010.538108

92. Weighardt H, Jusek G, Mages J, Lang R, Hoebe K, Beutler B, et al. Identification of a TLR4- and TRIF-dependent activation program of dendritic cells. *Eur J Immunol*. (2004) 34:558–64. doi: 10.1002/eji.200324714

93. Han LP, Li CJ, Sun B, Xie Y, Guan Y, Ma ZJ, et al. Protective effects of celastrol on diabetic liver injury via TLR4/MyD88/NF-κB signaling pathway in Type 2 diabetic rats. *J Diabetes Res*. (2016) 2016:2641248. doi: 10.1155/2016/2641248

94. Vallabhapurapu S, Karin M. Regulation and function of NF-kappaB transcription factors in the immune system. *Annu Rev Immunol*. (2009) 27:693–733. doi: 10.1146/annurev.immunol.021908.132641

95. Li N, Shi R. Expression alteration of long non-coding RNAs and their target genes in the intestinal mucosa of patients with Crohn's disease. *Clin Chim Acta*. (2019) 494:14–21. doi: 10.1016/j.cca.2019.02.031

96. Murthy A, Li Y, Peng I, Reichelt M, Katakam AK, Noubade R, et al. A Crohn's disease variant in Atg16l1 enhances its degradation by caspase 3. *Nature*. (2014) 506:456–62. doi: 10.1038/nature13044

97. Calderón-Gómez E, Bassolas-Molina H, Mora-Buch R, Dotti I, Planell N, Esteller M, et al. Commensal-specific CD4(+) cells from patients with Crohn's disease have a T-Helper 17 inflammatory profile. *Gastroenterology*. (2016) 151:489–500.e3. doi: 10.1053/j.gastro.2016.05.050

98. Huang W, Thomas B, Flynn RA, Gavzy SJ, Wu L, Kim SV, et al. DDX5 and its associated lncRNA rmrp modulate TH17 cell effector functions. *Nature*. (2015) 528:517–22. doi: 10.1038/nature16193

99. Vavricka SR, Rogler G, Gantenbein C, Spoerri M, Prinz Vavricka M, Navarini AA, et al. Chronological order of appearance of extraintestinal manifestations relative to the time of IBD diagnosis in the swiss inflammatory bowel disease cohort. *Inflamm Bowel Dis*. (2015) 21:1794–800. doi: 10.1097/MIB.0000000000000429

100. Sinh P, Shen B. Endoscopic evaluation of surgically altered bowel in patients with inflammatory bowel diseases. *Inflamm Bowel Dis*. (2015) 21:1459–71. doi: 10.1097/MIB.0000000000000357

101. Vucelic B. Inflammatory bowel diseases: controversies in the use of diagnostic procedures. *Dig Dis*. (2009) 27:269–77. doi: 10.1159/000228560

102. Bolha L, Ravnik-Glavač M, Glavač D. Long noncoding RNAs as biomarkers in cancer. *Dis Markers*. (2017) 2017:7243968. doi: 10.1155/2017/7243968

103. Ward M, McEwan C, Mills JD, Janitz M. Conservation and tissue-specific transcription patterns of long noncoding RNAs. *J Hum Transcr*. (2015) 1:2–9. doi: 10.3109/23324015.2015.1077591

104. Wang S, Hou Y, Chen W, Wang J, Xie W, Zhang X, et al. KIF9-AS1, LINC01272 and DIO3OS lncRNAs as novel biomarkers for inflammatory bowel disease. *Mol Med Rep*. (2018) 17:2195–202. doi: 10.3892/mmr.2017.8118

105. Ge Q, Dong Y, Lin G, Cao Y. Long noncoding RNA antisense noncoding RNA in the INK4 Locus correlates with risk, severity, inflammation and infliximab efficacy in Crohn's disease. *Am J Med Sci*. (2019) 357:134–42. doi: 10.1016/j.amjms.2018.10.016

106. Visschedijk MC, Spekhorst LM, Cheng SC, van Loo ES, Jansen BHD, Blokzijl T, et al. Genomic and expression analyses identify a disease-modifying variant for fibrostenotic Crohn's disease. *J Crohns Colitis*. (2018) 12:582–8. doi: 10.1093/ecco-jcc/jjy001

107. Ford AC, Bernstein CN, Khan KJ, Abreu MT, Marshall JK, Talley NJ, et al. Glucocorticosteroid therapy in inflammatory bowel disease: systematic review and meta-analysis. *Am J Gastroenterol*. (2011) 106:590–9. doi: 10.1038/ajg.2011.70

108. Lucafò M, Bravin V, Tommasini A, Martelossi S, Rabach I, Ventura A, et al. Differential expression of GAS5 in rapamycin-induced reversion of glucocorticoid resistance. *Clin Exp Pharmacol Physiol*. (2016) 43:602–5. doi: 10.1111/1440–1681.12572

109. Lucafo M, De Iudicibus S, Di Silvestre A, Pelin M, Candussio L, Martelossi S, et al. Long noncoding RNA GAS5: a novel marker involved in glucocorticoid response. *Curr Mol Med*. (2015) 15:94–9. doi: 10.2174/1566524015666150114122354

110. Lucafò M, Di Silvestre A, Romano M, Avian A, Antonelli R, Martelossi S, et al. Role of the long non-coding RNA growth arrest-specific 5 in glucocorticoid response in children with inflammatory bowel disease. *Basic Clin Pharmacol Toxicol*. (2018) 122:87–93. doi: 10.1111/bcpt.12851

frontiers | Frontiers in Immunology

TYPE Review
PUBLISHED 05 September 2024
DOI 10.3389/fimmu.2024.1436437

OPEN ACCESS

EDITED BY
Uzma Saqib,
Indian Institute of Technology Indore, India

REVIEWED BY
Yogesh Saini,
North Carolina State University, United States
Hirohito Kita,
Mayo Clinic Arizona, United States
Remo Castro Russo,
Federal University of Minas Gerais, Brazil

*CORRESPONDENCE
Si Zeng
xzyxyzs@hotmail.com
Peng Zhang
anepengzhang@163.com

†These authors have contributed equally to this work

RECEIVED 22 May 2024
ACCEPTED 22 August 2024
PUBLISHED 05 September 2024

CITATION
Gu S, Wang R, Zhang W, Wen C, Chen C, Liu S, Lei Q, Zhang P and Zeng S (2024) The production, function, and clinical applications of IL-33 in type 2 inflammation-related respiratory diseases.
Front. Immunol. 15:1436437.
doi: 10.3389/fimmu.2024.1436437

The production, function, and clinical applications of IL-33 in type 2 inflammation-related respiratory diseases

Shiyao Gu[1†], Ruixuan Wang[2†], Wantian Zhang[1†], Cen Wen[1], Chunhua Chen[3], Su Liu[4], Qian Lei[1], Peng Zhang[1*] and Si Zeng[1*]

[1]Department of Anesthesiology, Sichuan Provincial People's Hospital, School of Medicine, University of Electronic Science and Technology of China, Chengdu, China, [2]School of Medical and Life Sciences, Chengdu University of Traditional Chinese Medicine, Chengdu, China, [3]Department of Anatomy and Embryology, School of Basic Medical Sciences, Peking University Health Science Center, Beijing, China, [4]Department of Anesthesiology, Affiliated Hospital of Xuzhou Medical University, Xuzhou, China

Epithelial-derived IL-33 (Interleukin-33), as a member of alarm signals, is a chemical substance produced under harmful stimuli that can promote innate immunity and activate adaptive immune responses. Type 2 inflammation refers to inflammation primarily mediated by Type 2 helper T cells (Th2), Type 2 innate lymphoid cells (ILC2), and related cytokines. Type 2 inflammation manifests in various forms in the lungs, with diseases such as asthma and chronic obstructive pulmonary disease chronic obstructive pulmonary disease (COPD) closely associated with Type 2 inflammation. Recent research suggests that IL-33 has a promoting effect on Type 2 inflammation in the lungs and can be regarded as an alarm signal for Type 2 inflammation. This article provides an overview of the mechanisms and related targets of IL-33 in the development of lung diseases caused by Type 2 inflammation, and summarizes the associated treatment methods. Analyzing lung diseases from a new perspective through the alarm of Type 2 inflammation helps to gain a deeper understanding of the pathogenesis of these related lung diseases. This, in turn, facilitates a better understanding of the latest treatment methods and potential therapeutic targets for diseases, with the expectation that targeting IL-33 can propose new strategies for disease prevention.

KEYWORDS

IL-33, type 2 inflammation, respiratory diseases, alarmin, asthma

1 Introduction

IL-33 is an IL-1 family cytokine produced by various cell types, including epithelial cells, endothelial cells, and fibroblasts (1, 2). Human full-length IL-33 consists of 270 amino acids with a relative molecular weight of approximately 30,000. It contains three functional structural domains: the N-terminal nuclear domain (amino acids 1-65), the central domain (amino acids 66-111), and the C-terminal IL-1-like cytokine structural domain (amino acids 112-270) (3). IL-33 mediates signaling by binding to its receptor ST2 (growth STimulation expressed gene 2), which is predominantly expressed on the surface of various immune cells, such as macrophages, natural killer cells, and certain T cell subsets. IL-33 can participate in T2 immunity by activating ST2-expressing immune cells, including type 2 ILC2, Th2 cells, mast cells, eosinophils, basophils, and dendritic cells (4–11).

Type 2 inflammation is a chronic inflammatory process characterized by persistent activation and dysregulation of the immune system. Unlike acute type 1 inflammation, which typically manifests as rapid and transient inflammation, type 2 inflammation progresses slowly and persists over time. It is commonly observed in various chronic diseases, particularly respiratory conditions like asthma, COPD, pulmonary fibrosis, and allergic rhinitis. Type 2 inflammation involves a complex interplay of inflammation-regulating pathways and cytokines. Key players include Th2 cells, IL-4, IL-13, IL-5, IL-9, thymic stromal lymphopoietin (TSLP), and the IL-33 pathway. These pathways and cytokines play critical roles in orchestrating immune responses in respiratory diseases such as asthma and COPD.

The relationship between type 2 inflammation and IL-33 is significant, as IL-33 is considered a key regulator and "alarmin" in type 2 inflammation, particularly in respiratory diseases. In asthma and other respiratory diseases, IL-33 expression is closely associated with the release of cytokines associated with type 2 inflammation, and overexpression of IL-33 can lead to the development of chronic inflammation and airway remodeling, which can exacerbate the severity of the disease (12), increase respiratory mucus secretion, which can aggravate the symptoms of the disease, and participate in the regulation of the immune homeostasis, which can influence the development and progression of respiratory diseases (13, 14). Thus, IL-33 plays an important role in lung inflammation and is closely associated with type 2 inflammation, influencing disease development and progression by regulating the activation of immune cells and the release of pro-inflammatory factors. This review delves into the pivotal role and function of the IL-33 pathway as an "alarmin" in type 2 inflammation within respiratory diseases, exploring its clinical implications and potential for therapeutic interventions.

2 The production of IL-33 in type 2 inflammation in respiratory diseases as "alarmin"

IL-33, also known as high endothelial venous-derived nuclear factor (NF), is a cytokine belonging to the IL-1 family (15). Its primary role involves regulating immune responses, promoting T cell activation, influencing regulatory T cells (Treg), and affecting other immune cells such as macrophages and dendritic cells (16). IL-33 also plays a role in regulating inflammatory responses by promoting the activation of inflammatory cells and enhancing the inflammatory cascade (17). Furthermore, it contributes to tissue repair by promoting wound healing and tissue regeneration (17).

In 2005, Jochen Schmitz and colleagues first proposed that IL-33 could drive Th2responses (18). IL-33 exerts its biological effects through the IL-1 family receptor ST2, which activates NF-κB and MAP kinases, leading to the production of Th2-associated cytokines by polarized Th2 cells *in vitro*. *In vivo*, IL-33 induces the expression of IL-4, IL-5, and IL-13, resulting in severe pathological changes in murine mucosal organs, such as the lung (18). Th2 cells and ILC2s provide protection against worm infections and are involved in allergic reactions; they collaborate at different stages of the immune response (19). Th2 cells primarily induce the expression of IL-25, IL-33, and TSLP through the production of IL-4, while IL-25 and IL-33, in turn, promote the expansion of ILC2s. Therefore, Th2 cell differentiation can occur independently of ILC2s, but the activation of ILC2s can enhance the Th2 response, and Th2 cells can amplify ILC2s by inducing type 2 alarmins (19). The IL-33 signaling pathway in Th2 cells promotes the acquisition of a pro-inflammatory memory state (20). Pathogenic tissue-resident Th2 cells exhibit increased expression of acetyl-CoA carboxylase 1, leading to upregulation of the IL-33 receptor, heightened IL-33 sensitivity, increased IL-5 production, and worsening of airway diseases (21, 22).

The endogenous source of IL-33 is not fully understood; however, it is constitutively active in lymphoid organs, epithelial barrier tissues, brain, and embryos in mice, with epithelial cells being the main source in normal tissues (23). In the human airway, IL-33 is predominantly produced by airway epithelial cells, localized mainly in the nucleus as a full-length precursor. Active full-length IL-33 (IL-33FL) is rapidly released upon cell damage or exposure to environmental stressors like airborne allergens and viruses (24–27).

IL-33FL can be cleaved by serine proteases released by immune cells, such as mast cells, to increase its activity (15). Notably, neutrophil-released elastase, histone G, and protease 3 can also cleave IL-33FL, converting it to a more active, slightly shorter form that is 10-fold more potent (27, 28). Myofibroblasts and endothelial cells may also serve as important sources of IL-33 under inflammatory conditions, while alveolar macrophages can produce high levels of IL-33 in inflamed tissues (23). The release of IL-33 activates Th2 responses, contributing to the onset and progression of inflammation in respiratory diseases.

If we can detect these "alarms" in time and implement appropriate preventive measures proactively, we can effectively reduce and potentially avoid the progression and damage caused by type 2 inflammation in respiratory diseases (Figure 1).

3 IL-33-related pathways

IL-33 binds to its receptor ST2 and triggers downstream signaling pathways, including nuclear factor κB (NF-κB), mitogen-activated protein kinases (MAPKs), and phosphatidylinositol 3-kinase/protein

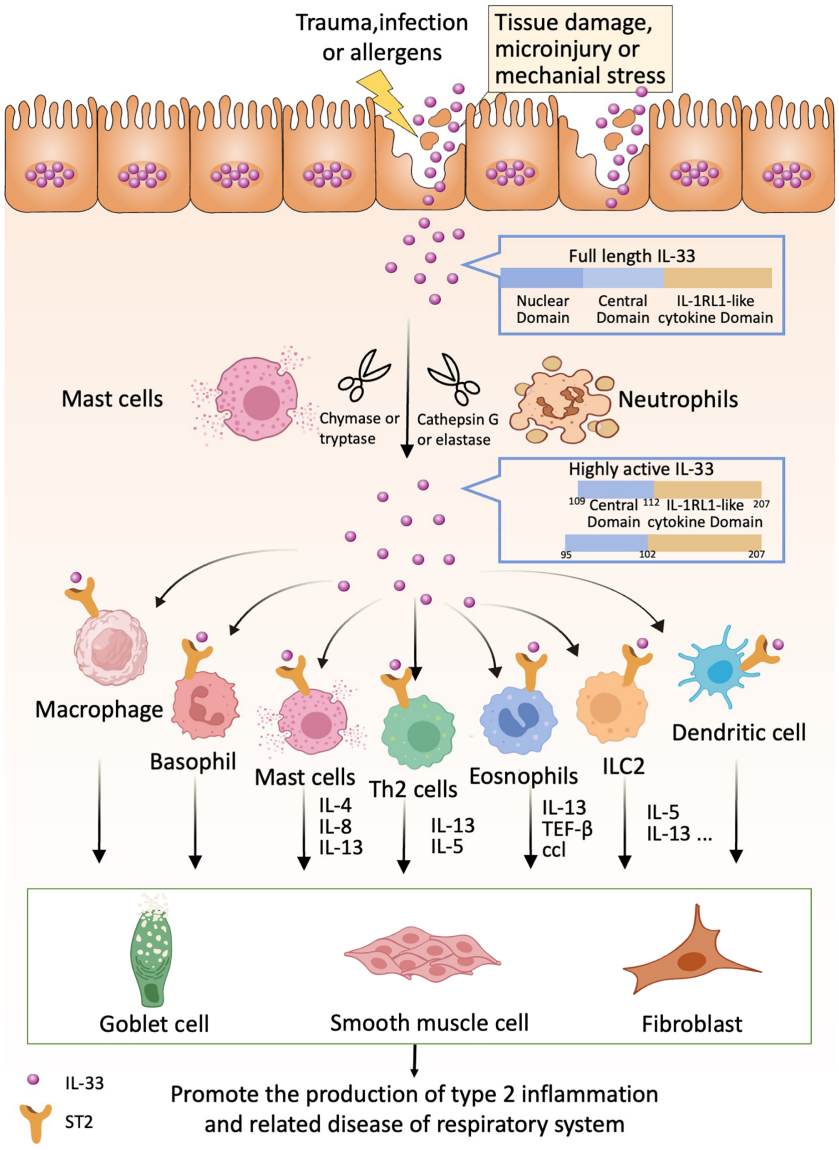

FIGURE 1
IL-33 acts as an alarmin that can be released following cell or tissue damage. Released full-length IL-33 can be processed into highly active forms by proteases produced by neutrophils and mast cells (e.g., IL-33 95-270 and IL-33 109-270). Highly active forms of IL-33 can bind to ST2 receptors on relevant immune cells such as Th2 cells, basophils, eosinophils, ICL2, dendritic cells, macrophages, etc. These immune cells produce the appropriate cytokines, which in turn act on lung cup cells, smooth muscle cells and fibroblasts to promote lung type 2 inflammation-related diseases.

kinase B (PI3K/Akt). Activation of these pathways leads to the production of inflammatory mediators, apoptosis, and activation of immune cells, which play critical roles in the development and progression of respiratory diseases. While IL-33 was traditionally thought to be released passively as a result of cell necrosis, emerging evidence suggests additional mechanisms for IL-33 secretion in response to allergens. This secretion may be mediated by purinergic receptor-dependent signaling or through the activation of the dual oxidase 1 Gene-dependent epidermal growth factor receptor (DUOX1-dependent EGFR) signaling pathway (24, 25) (Figure 2).

The NF-κB pathway is a central pro-inflammatory signaling pathway involved in regulating the expression of genes encoding cytokines, chemokines, and adhesion molecules. NF-κB refers to a family of transcription factors that play crucial roles in various physiological and pathological processes (29, 30). It responds to oxidative stress and regulates the production and expression of inflammatory cytokines and mediators (31). There are two main pathways of NF-κB activation: the classical and non-classical pathways, each with distinct activation mechanisms (32–35). In the classical NF-κB pathway, the key step involves phosphorylation-dependent activation of the I kappa B Kinases (IKKs) complex (36, 37). Once activated, NF-κB translocates into the nucleus, where it binds to target gene promoters and drives transcription, leading to the expression of inflammatory genes (38, 39). On the other hand, the non-classical NF-κB pathway is activated by specific Tumor Necrosis Factor (TNF) superfamily receptors, suggesting a more specialized biological role for this branch of the pathway (32, 33, 35, 40).

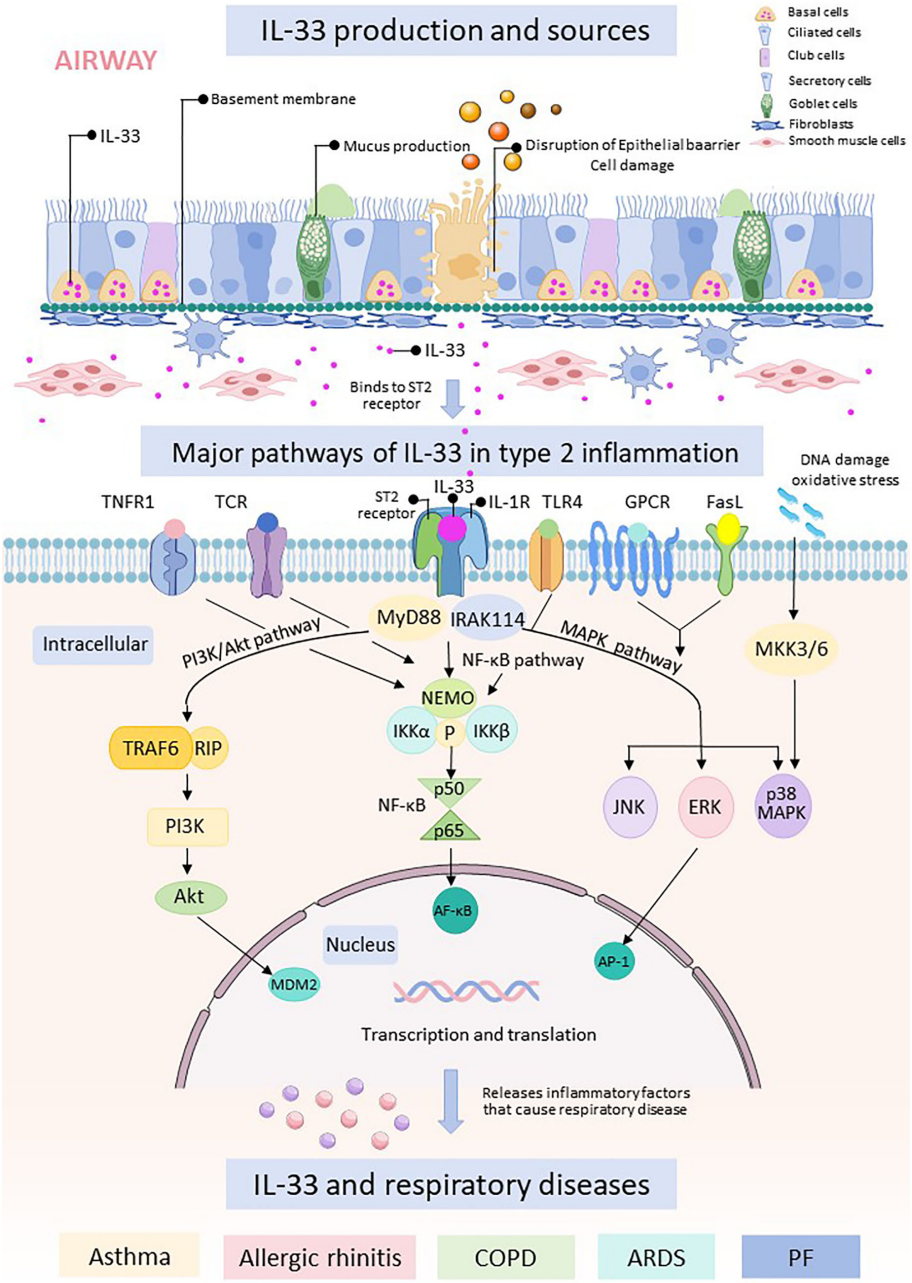

FIGURE 2
The respiratory epithelial barrier is damaged and releases IL-33. Free IL-33 binds to cells containing ST2 receptors and IL-1R, which can cause intranuclear transcription and translation through three pathways, namely, the PI3K/Akt pathway, the NF-κB pathway, and the MAPK.

The MAPKpathway consists of three main components: extracellular regulated protein kinases (ERK), c-Jun N-terminal kinase (JNK), and p38 mitogen-activated protein kinase (p38 MAPK) (30). Studies have implicated the p38 MAPK signaling pathway in olfactory loss associated with allergic rhinitis (AR) in animal models (41). Research has shown elevated expression and activity of p38 MAPK mRNA in rats with olfactory loss due to allergic rhinitis compared to control groups (42).

Additionally, the MAPK signaling pathway is involved in regulating IL-33 expression in airway epithelial cells of COPD patients, particularly during viral infections that worsen the condition (12). Physiologically relevant concentrations of IL-33 can activate the MAPK pathway, enhancing cytokine expression in human NK cells, which may influence disease outcomes in conditions like asthma and COPD (43).

In animal experiments, infusion of 1,4NQ-BC into mice triggered lung inflammation and stimulated IL-33 secretion from lung tissues, primarily from macrophages. This process involved both the MAPK and PI3K/Akt signaling pathways, contributing to pro-inflammatory responses in the lungs (44). Furthermore, IL-33

induces and enhances the secretion of IL-6 and IL-8 in human bronchial epithelial cells (HBEs) and peripheral blood mononuclear cells (PBMCs) from COPD patients via the IL-1 family receptor accessory protein (IL-1RAcP) and MAPK pathways, perpetuating chronic inflammation in the respiratory tract (45).

The PI3K/Akt signaling pathway plays a crucial role as an upstream regulator of nuclear factor E2-related factor 2 (Nrf2), which is involved in mediating oxidative stress responses through the Nrf2/HO-1 pathway (46–48). Studies have demonstrated that β-synephrine can modulate oxidative stress by targeting the PI3K/Akt/Nrf2 signaling pathway (49). In allergic rhinitis (AR), elevated serum leptin levels are observed and positively correlate with clinical symptoms (50, 51). Leptin, along with its receptor, activates multiple signaling pathways including MAPK, JAK2-STAT3, and PI3K/Akt pathways (52 , 47). Specifically, in AR, leptin mediates the activity of type 2 innate lymphoid cells (ILC2) and enhances ILC2-driven inflammation through the PI3K/Akt pathway (53).

In epithelial cells from allergic rhinitis (AR) patients, R. Kamekura et al. discovered that treatment with corticosteroids and various inhibitors targeting receptors such as ERK, p38 MAPK, JNK, NF-κB, and epidermal growth factor receptor led to significant inhibition of IL-8 induced by human nasal epithelial cells (HNECs) and IL-33 induced by granulocyte-macrophage colony-stimulating factor (GM-CSF) (54). Moreover, increased intracellular expression of IL-33 may be linked to altered activation of the innate immune receptor Toll-like receptor 4 (TLR4), particularly influenced by cigarette smoke exposure, notably among smokers (55).

In summary, IL-33 plays a pivotal role in type 2 inflammation by engaging multiple signaling pathways and promoting the development of airway inflammation. Targeting these pathways to inhibit IL-33 expression and production has shown promising results in certain clinical trials, offering a new perspective on effective strategies for treating respiratory diseases driven by IL-33 in the future. By understanding the intricate mechanisms through which IL-33 contributes to inflammation, researchers have identified potential therapeutic targets within the NF-κB, MAPK, PI3K/Akt, and other signaling pathways associated with IL-33 activity. Strategies aimed at blocking IL-33 or modulating its downstream effects hold significant therapeutic potential for managing and potentially preventing the progression of respiratory diseases characterized by type 2 inflammation, such as asthma, COPD, and allergic rhinitis. Further exploration and refinement of these targeted approaches are essential to optimize their clinical efficacy and safety, ultimately providing new avenues for personalized treatment and management of IL-33-mediated respiratory conditions.

4 IL-33 and type 2 inflammation in respiratory diseases

IL-33 plays a key role in type 2 inflammation, especially in respiratory diseases, where it is implicated in common respiratory diseases such as asthma, allergic rhinitis, chronic obstructive pulmonary disease and acute respiratory distress syndrome.

4.1 IL-33 and asthma

Type 2 inflammation is a common feature in patients with asthma, characterized by the activation of group ILC2s in the lungs in response to inhaled allergens, particularly through the production of alarmins such as IL-33 by epithelial cells (56). Activated ILC2s proliferate and secrete IL-5 and IL-13, which contribute to eosinophilic inflammation. In allergic asthma, increased expression of alarmins like TSLP, IL-33, and IL-25 in the airway epithelium is associated with airway obstruction (56). Koji Iijima et al. discovered that IL-33 levels in the lungs of mice rapidly increased within hours after intranasal allergen exposure and continued to rise throughout the chronic inflammation phase. Mice deficient in IL-33R (Il1rl1(-/-)) and thymic stromal lymphopoietin receptor (Tslpr (-/-)) exhibited significantly lower airway inflammation, reduced IgE antibody levels, and decreased airway hyperreactivity (57). Additionally, E. L. Anderson and colleagues found that when naive animals were exposed to airborne allergens, IL-33 in the lungs played a crucial role in promoting the acute bone marrow production of eosinophils. This was achieved through the innate activation of ILC2s and subsequent IL-5 production (58).

Due to the chronic nature of human asthma and challenges in modeling it accurately, researchers primarily rely on mouse models to investigate the role of IL-33 in activating ILC2s and driving type 2 inflammation in the lungs and airways. IL-33 has been shown to activate basophils and mast cells, promoting type 2 inflammation in chronic stable asthma (59). Furthermore, activated mast cells in allergic asthma release serine proteases (chymotrypsin and trypsin) that generate mature, active forms of IL-33, which can potentiate ILC2 activity (15).

IL-33 also stimulates lung CD8 (+) cytotoxic T (Tc) cells to produce type 2 cytokines, which are particularly implicated in severe asthma and asthma exacerbations (60). Increased reprogramming of FoxP3+ regulatory T cells (Tregs) in allergic asthma is associated with IL-33 production, exacerbating airway reactivity (61). Additionally, the RNA-binding protein RBM3 is highly expressed in lung ILCs of asthmatics, induced further by IL-33, and plays a role in regulating ILC function and inflammatory progression (62).

Research has shown that prophylactic or therapeutic administration of P2Y13-R, also known as IL-33 and High-mobility group box1 (HMGB1)'s novel gatekeeper, in experimental asthma models can attenuate the onset and progression of asthma (63). Conversely, intranasal injection of IL-33 or specific allergens in mice leads to increased numbers of ILC2s in the lungs, peripheral blood, and liver. Notably, IL-33-treated mice exhibit proliferation of lung-resident ILC2s and migration of activated ILC2s to the liver, promoting type 2 inflammation and eosinophilic hepatitis (64).

The deterioration of asthma often occurs alongside respiratory viral infections, such as dsRNA challenge or rhinovirus infections,

which can exacerbate allergic asthma in mouse models. In models of house dust mite (HDM)-induced asthma, dsRNA attacks can worsen asthma symptoms, with key upstream Th2 cytokines implicated in aggravation being IL-33, TSLP, and IL-25 (65). IL-33 not only induces antiviral signaling in mast cells (MCs) but also upregulates receptors for human rhinoviruses (HRVs), potentially enhancing viral infection and contributing to viral-induced asthma exacerbation (66).

Studies by Kim A.T. Verheijden and colleagues in HDM-induced asthma mouse models demonstrated that adding galacto-oligosaccharides (GOS) to infant formula diets had intestinal and immune modulatory effects, attenuating IL-33 expression associated with intestinal barrier dysfunction (67). Jackson et al. observed elevated IL-33 levels in asthmatics during experimental rhinovirus (RV) progression, correlating with increased levels of T2 cytokines IL-5 and IL-13 in airway mucosal fluid and the severity of worsening following viral inoculation (68). Similarly, Beale and colleagues (69) reported induction of IL-25 by experimental rhinovirus infection, with higher expression levels at baseline and during infection in asthmatic individuals.

In recent years, the morbidity and severity of asthma have increased alongside rising rates of obesity. Mast cells are implicated as targets and sources of various inflammatory factors and stress molecules in response to metabolic burdens, including adipocytokines, IL-9, IL-33, corticotropin-releasing hormone (CRH) and neurotensin (NT) (70). IL-33, in particular, enhances the release of vascular endothelial growth factor triggered by substance P and promotes the release of TNF promoted by neurotensin. IL-9 and IL-33 contribute to pulmonary mast cell infiltration and worsen allergic inflammation, diminishing the response to glucocorticoids and bronchodilators in obese patients (70). In summary, cytokines such as IL-33 play a critical role in the inflammatory response observed in asthmatic patients, particularly contributing to the enhanced type 2 (T2) inflammatory response seen during the aggravation state of asthma. Asthma is a significant health concern, and innovative studies targeting IL-33 could potentially lead to effective treatments for asthma patients.

4.2 IL-33 and allergic rhinitis

Interleukin (IL)-33 is a novel member of the IL-1 family of cytokines and acts as a ligand for the IL-1 family receptor, ST2. IL-33 is known to induce a type 2 inflammatory response, which is implicated in allergic inflammation observed in conditions like asthma and atopic dermatitis. In allergic rhinitis, IgE is typically associated with early nasal symptoms such as sneezing and a runny nose, whereas Th2 cytokines are linked to reactions like nasal congestion, discomfort, and irritability (71). However, the specific role of IL-33 and its receptor ST2 in allergic rhinitis remains unclear (54).

Dachuan Fan et al. (72) conducted a study using flow cytometry to quantify the frequency of ILC2s in peripheral blood samples from healthy controls and patients with HDMor mugwort monosensitization. Their findings revealed distinct phenotypic and functional differences in ILC2 frequency among patients with allergic rhinitis sensitized to HDM or mugwort allergens (72). R. Kamekura et al. (54) investigated IL-33 and ST2 expression in normal and allergic rhinitis nasal mucosa using reverse transcription and real-time polymerase chain reaction (PCR), as well as immunohistochemistry. Their results indicated an IL-33-mediated inflammatory response and suggested differential regulation of ST2 by various signaling pathways in human nasal epithelial cells (HNECs) (54). In a randomized, double-blind, placebo-controlled trial involving birch pollen-allergic participants, treatment with birch pollen extract led to significantly greater clinical responses compared to placebo. Notably, participants exhibited a significant increase in levels of soluble IL-33 receptor (sST2) in nasal secretions (73). Additionally, baseline IL-33 mRNA levels were strongly associated with late allergic reactions (LAR) in allergic rhinitis, as revealed in studies investigating the molecular basis of LAR (74). In addition to this, genetic factors including cytokine genes influence IL-33 levels and also play an important role in allergic rhinitis (75, 76). Li et al.'s study provided the first evidence that gene expression profiles of AR-derived nasal fibroblasts (NFs) are associated with IL-33 and IL-6 levels, and BARX1 may be an effective target to alleviate the pathogenesis of AR (77).

On the other hand, no significant differences in IL-25 and IL-33 levels were observed between patients with fungal and non-fungal allergic rhinitis. Chronic fungal exposure may regulate innate systemic cytokines in severe persistent allergic rhinitis (78). Furthermore, in studies using Keyhole Limpet Hemocyanin (KLH) as a neoantigen to induce a Th2 response in humans, no differences in IL-1β and IL-33 expression were observed between control and experimental groups (79). IL-33 is closely associated with allergic rhinitis, and interfering with IL-33 may be a new modality for the treatment of allergic rhinitis.

4.3 IL-33 and chronic obstructive pulmonary disease

Senescence is characterized by the gradual decline in lung function due to increased cellular senescence, reduced regenerative capacity, and impaired innate host defenses. The secretion of alarmins, such as IL-33, and the activation of type 2 inflammation represent important mechanisms of innate airway epithelial defense against non-microbial triggers (80). Studies in COPD have demonstrated that exposure to cigarette smoke (CS) promotes IL-33 cytokine responses and contributes to disease development (81). In animal models, CS exposure combined with vascular endothelial growth factor knockout has been shown to recapitulate severe COPD features, including a substantial influx of IL-33-expressing macrophages and neutrophils, highlighting a shift in the CS-induced response towards an uncontrolled, prolonged IL-33-mediated inflammatory reaction from localized surveillance (81). Furthermore, CS-induced pathogenic changes can be notably suppressed by intranasal delivery of neutralizing anti-IL-33 antibodies (82). In summary, IL-33 may play a significant role in influencing the progression of COPD and could be considered a key factor in the disease's development.

4.4 IL-33 and pulmonary fibrosis

PF is a prevalent interstitial lung disease. Recent studies have suggested that IL-33 plays a role in the progression of pulmonary fibrosis, contributing to local inflammation and the formation of fibrotic tissue (83–86). Gao et al. (83) discovered that IL-33 can exacerbate pulmonary fibrosis in mice through the NF-κB pathway. Their experiments inducing pulmonary fibrosis in mice with bleomycin revealed a significant increase in the phosphorylation level of NF-κB p65 protein in lung tissues, along with a marked enhancement in the nuclear translocation of NF-κB p65. Notably, the use of NF-κB inhibitors substantially mitigated these effects (83). Additionally, Yi et al. (87) illustrated that ubiquitin-specific protease 38 (USP38) acts as a negative regulator of IL-33. Their findings demonstrated that mice lacking USP38 displayed more severe pulmonary fibrosis and IL-33-associated lung inflammation following exposure to bleomycin, further solidifying the intricate connection between IL-33 and pulmonary fibrosis (87). Previous research has also indicated that IL-33 can activate transforming growth factor-beta (TGF-β) (86). Recent studies have further suggested that TGF-β1 can induce and sustain the expression of neuropilin-1 (Nrp1), a signaling pathway that upregulates the expression of the IL-33 receptor ST2. This process enhances type 2 immunity and the function of ILC2s, ultimately driving the progression of PF (85). Interestingly, full-length IL-33 seems to have a distinct impact on the pathogenesis of PF compared to processed IL-33. Reports suggest that IL-33 may promote fibrosis development in two forms: full-length IL-33 through both transcription (ST2-dependent) and non-transcription (non-ST2-dependent) mechanisms (88). In conclusion, the relationship between IL-33 and pulmonary fibrosis is intricate, highlighting it as a promising area for further research into the mechanisms and treatment strategies for PF in the future.

Idiopathic pulmonary fibrosis (IPF) is a progressive and highly lethal inflammatory interstitial lung disease characterized by abnormal deposition of the extracellular matrix (89). In the context of idiopathic pulmonary fibrosis, IL-33 may also play a role in its pathogenesis (90). Fanny, M et al. et al. (88) utilized IL-33 in a bleomycin-induced inflammation and Idiopathic pulmonary fibrosis model using mouse IL-33 receptor [tumorigenic 2 (ST2) chain-inhibited] mice compared to C57BL/6 wild-type mice. Unexpectedly, it was found that acute neutrophilic lung inflammation led to the development of IL-33/ST2-dependent pulmonary fibrosis associated with M2-like polarization production, and that 24 hours after bleomycin treatment, ST2-deficient mice exhibited enhanced inflammatory cell recruitment, and MRI showed enhanced inflammation in the lungs with pulmonary edema (91). Lee et al. (90) demonstrated that levels of IL-33 and TSLP in bronchoalveolar lavage fluid may help differentiate IPF from other chronic interstitial lung diseases. Another research has shown that the pro-fibrotic role of IL-25/IL-33/TSLP in IPF represents a novel paradigm, acting directly on two key cells in the fibrotic process: alveolar epithelial cells and (myo) fibroblasts (84).Additionally, Majewski et al. (92) analyzed exhaled breath condensate from IPF patients and found the presence of IL-33, suggesting a potential association between IL-33 and the progression of IPF. Interestingly, full-length IL-33 can contribute to the pathogenesis of IPF by promoting the expression of cytokines such as TGF-β, interleukin-6 (IL-6), monocyte chemotactic protein-1 (MCP-1), macrophage inflammatory protein-1α (MIP-1α), and tumor necrosis factor-alpha (TNF-α) (93). This, in conjunction with bleomycin, leads to the accumulation of lung lymphocytes and collagen production in IPF (93). In contrast, Katherine E. Stephenson et al. utilized a mouse model of bleomycin (BLM)-induced pulmonary fibrosis and evaluated the fibrotic potential of the IL-33-mediated ST2 signaling pathway using a therapeutic dose of ST2-Fc fusion protein. Their findings suggested that this pathway is unlikely to exert a central fibrotic effect in idiopathic pulmonary fibrosis (94). However, further research is needed to elucidate the specific pathways involved. Future studies can build upon this foundation to delve deeper from a broader perspective, increasing the diversity and reliability of research data to contribute to the understanding of the mechanisms and treatment of IPF.

Moreover, IL-33 has been implicated in pulmonary fibrosis associated with systemic sclerosis (SSc). Previous studies have suggested that endothelial cell damage in early SSc patients upregulates IL-33 mRNA expression, leading to the release of IL-33 protein into the bloodstream (95, 96). Recent research has demonstrated elevated levels of IL-33 in SSc patients, with correlations observed between IL-33 levels and the severity of skin sclerosis and pulmonary fibrosis (97, 98). Furthermore, varying degrees of IL-33 upregulation have been identified in patients with cystic fibrosis and silicosis, indicating a potential role for IL-33 in the pathogenesis of these diseases, necessitating further investigation in the future (99, 100).

The treatment of pulmonary fibrosis, encompassing a wide range of diseases, has long posed a significant challenge for the medical community. While numerous research findings have laid the groundwork for understanding these conditions, there remain numerous unexplored avenues that warrant thorough investigation. Advancing our understanding through comprehensive exploration and the accumulation of reliable evidence will be pivotal in unraveling the mechanisms underlying pulmonary fibrosis and related disorders, ultimately aiding in the development of effective treatments in the future.

4.5 IL-33 and other respiratory diseases

In studies of acute respiratory distress syndrome (ARDS), IL-33 has been shown to play a critical role in modulating post-injury inflammation by controlling local cytokine levels and populations of Foxp3+ Tregs (101). Additionally, research in a mouse model of LPS-induced lung injury has revealed that early release of IL-33 in ARDS contributes to an uncontrolled inflammatory response through activation of Invariant natural killer T cells (iNKT cells) (102). This suggests that IL-33 and NKT cells could potentially serve as targets for early intervention in cytokine storms associated with ARDS (102). Brandon W. Lewis et al. studying a cystic fibrosis-like lung disease

model, compared IL-33 gene knockout (IL-33KO) Tg+ mice with IL-33 heterozygous (IL-33HET) Tg+ mice. They found that IL-33KO/Tg+ mice had completely absent eosinophils in bronchoalveolar lavage fluid compared to IL-33HET/Tg+ mice, and mucin staining within airway epithelial cells was completely lost. Additionally, levels of IL-5, IL-4, and Th2-related gene markers (Slc26a4, Clca1, Retnla, and Chi3l4) were significantly reduced, indicating that mucus obstruction was not dependent on IL-33 (103). Moreover, investigations have explored TNFα-induced cytokine production in primary lung fibroblasts from individuals with asthma compared to non-asthmatics, demonstrating significant upregulation of IL-6, IL-8, C-C motif chemokine ligand 5 (CCL5), and TSLP mRNA expression and protein secretion in lung fibroblasts upon TNFα stimulation (104). While numerous studies have confirmed the association of IL-33 with respiratory diseases such as asthma, allergic rhinitis, COPD, and pulmonary fibrosis limited research has investigated the role of IL-33 in other respiratory conditions like ARDS. Consequently, there remains ambiguity regarding the involvement of IL-33 in these diseases, highlighting the need for further studies to elucidate its role and therapeutic implications. Additional investigations are warranted to clarify the relationship between IL-33 and various respiratory disorders beyond the well-established conditions, paving the way for more targeted therapeutic approaches and a comprehensive understanding of IL-33 biology in respiratory pathology.

5 Current status of treatment of type 2 inflammatory respiratory diseases

The treatment of respiratory diseases is confronted with several challenges, encompassing complex etiologies, drug resistance concerns, inflammation, and airway remodeling, as well as individual patient variations such as immune system variability. Moreover, challenges also include issues related to long-term therapy adherence, and the cost and accessibility of treatment. At the heart of type 2 inflammation is the production of cytokines and other inflammatory mediators by T-lymphocytes. These molecules play a pivotal role in the initiation and perpetuation of respiratory diseases by inciting inflammatory responses and influencing the disease trajectory. Addressing these challenges requires a multifaceted approach that integrates insights from immunology, pharmacology, and personalized medicine. Novel therapeutic strategies that specifically target key mediators of inflammation, including cytokines produced by T-lymphocytes, offer promising avenues for improving treatment outcomes and addressing the complexities inherent in managing respiratory diseases. Additionally, efforts to enhance treatment adherence and optimize therapy accessibility are essential for achieving effective disease management and improving patient quality of life.

5.1 Asthma

Asthma is a complex and challenging disease characterized by diverse etiologies and mechanisms. It encompasses various clinical phenotypes, including allergic asthma, nonallergic asthma, adult-onset asthma, asthma with persistent airflow limitation, and obesity-related asthma. Additionally, asthma can be classified based on sputum granulocyte infiltration proportions, such as eosinophilic, neutrophilic, mixed granulocyte, and oligophilic types. The prevalence of asthma is significantly influenced by age and gender. In children, males under thirteen years old tend to have a higher incidence compared to females, whereas in adulthood, females exhibit a higher incidence than males (105–107). Currently, the most effective long-term treatment for asthma management is inhaled corticosteroids (ICS) (108). However, despite high-dose ICS therapy and combination with long-acting β2 agonists or leukotriene modulators, some patients struggle to control their condition. This challenge may be attributed to the heterogeneous nature of asthma, where patients with different asthma phenotypes do not uniformly respond to standard anti-asthma treatments (109). Therefore, further studies are still needed to explore effective drugs and provide new ideas for the treatment of asthma.

5.1.1 Blocking IL-33 production and release in asthma therapy

Fruit and vegetable intake has been associated with a reduced risk of asthma and improved lung function, particularly evidenced by enhanced Forced Expiratory Volume in the first second (FEV1) and decreased wheezing frequency, with notable benefits observed from consuming apples and oranges (110–112). These foods are rich sources of essential vitamins, including vitamin A, vitamin C, vitamin D, and vitamin B6, each of which contributes to protective effects against asthma development (113–116). Recent studies highlight the effectiveness of vitamin B6, particularly its active form pyridoxal phosphate (PLP), in alleviating type 2 inflammatory responses and reducing asthma severity. Healthy individuals tend to exhibit higher concentrations of PLP compared to asthmatics, with the lowest PLP levels observed in patients with severe asthma. Interestingly, serum PLP concentrations positively correlate with FEV1 and negatively correlate with eosinophil levels in asthmatics, indicating a protective role of vitamin B6 in asthma progression (116). Moreover, research by Zhu et al. revealed that PLP inhibits MDM2-mediated ubiquitination of IL-33, a crucial step for IL-33 stability and type 2 inflammatory response regulation. By promoting IL-33 degradation through ubiquitin modification, vitamin B6 attenuates inflammatory responses associated with asthma (116). Given the accessibility and affordability of vitamin B6 through dietary sources, it represents a promising and cost-effective therapeutic strategy for asthma treatment. Incorporating vitamin B6-rich foods into daily nutrition may offer a safe and accessible approach to mitigating asthma symptoms and improving overall respiratory health. Continued research in this area holds potential for advancing personalized nutritional interventions in asthma management.

Upstream of IL-33, drugs primarily act by inhibiting IL-33 expression and activation. Increased SPRR3 gene expression in asthma patients significantly elevates IL-33 levels. Inhibiting SPRR3 suppresses IL-33 expression in lung tissues and bronchoalveolar

lavage fluid (BALF) of asthmatic mice. This inhibition further dampens the activation of the PI3K/Akt/NFκB pathway, reduces expression of IL-25 and TSLP, decreases recruitment of ILC2 cells, and weakens Th2 immune responses (117). Additionally, ascr#7, found in ascarosides produced by parasites like N. brasiliensis, in combination with antigen/gelatin, reduces IL-33 expression in lung epithelial cells. By preventing downstream effector activation by IL-33, it inhibits IL-33-mediated proliferation of ST2+Th2 cells and ILC2 cells (118). The miR-206/cd39/ATP axis regulates airway IL-33, IL-25, and TSLP expression and type 2 inflammation. Elevated ATP levels activate extracellular purinergic receptors, which mediate the release of IL-33. Reduced ATP levels inhibit IL-33, IL-25, and TSLP release, as well as downstream ILC2 amplification (119). Wowbaine, an inhibitor of sodium-potassium ATPase, suppresses the production of IL-33, TSLP, IL-1β, and IL-4 in OVA mice. It also decreases levels of tissue remodeling markers like TNF-α and TGF-β, inhibits cell migration, and reduces vascular permeability (120). Jina et al. (121) found that intranasal inhalation of IFN-λs accelerates the reduction of IL-33 and TSLP levels in the lungs of asthmatic mice, alleviating lung injury induced by Th2 responses. This approach represents a potential method to control Th2-mediated allergic reactions.

Chinese medicines have a long history of use in treating asthma, and recent studies suggest that some Chinese medicines may target the IL-33 pathway upstream. Louki Zupa (LKZP) has been found to inhibit the expression of IL-33 and ST2 in OVA mice. It suppresses the IL-33/ST2-NFκB/GSK3β/mTOR pathway-mediated inflammatory response, thereby attenuating airway inflammation in OVA mice (122). Irisflavin A, another compound, exhibits chemoprotective effects. Treatment of OVA mice with irisflavin A reduces IL-33, IL-4, and IL-5 levels along with their mRNA expression. This treatment also decreases airway hyperresponsiveness in asthmatic mice and exerts a protective effect against airway inflammation and eosinophil chemotaxis (123). Furthermore, in mice sensitized with HDM and undergoing dietary intervention with galacto-oligosaccharides (GOS), levels of IL-33 and ST2 were reduced, and the distribution of IL-33 was altered, leading to a weakened inflammatory response (67).

Another study identified a positive correlation between plasma thrombin-antithrombin complex (TATc) levels and the number and function of innate lymphoid cell type 2 (ILC2) in PBMCs of allergic patients (124). Direct or indirect thrombin inhibitors, such as bivalirudin (TFA) and low molecular weight heparin, were found to inhibit the IL-33-associated type 2 immune response by affecting IL-33 maturation and ILC2 activation *in vivo*. These findings suggest a potential therapeutic approach involving thrombin inhibition to modulate IL-33-mediated immune responses in allergic conditions.

5.1.2 Blocking IL-33/ST2 binding and downstream conduction pathways in asthma therapy

Downstream of the IL-33 pathway, drugs can block IL-33 binding to ST2 and inhibit ILC2 production, thereby attenuating the type 2 inflammatory response. The interleukin family is involved in IL-33-induced allergic asthma, with IL-9 being a downstream cytokine of IL-33. Studies in IL-9-deficient mice have shown that IL-33-induced airway hyperresponsiveness, inflammatory cell infiltration, cuprocyte chemotaxis, collagen deposition, smooth muscle hypertrophy, and downstream cytokine expression were all attenuated, suggesting the involvement of IL-9 in IL-33-induced airway inflammation and asthmatic airway remodeling (125). Mast cells are known to produce interleukin 9 (IL-9), IL-33, and stress molecules. IL-33, in turn, induces mast cells to produce IL-13, which promotes mast cell survival and enhances allergic inflammation by promoting lung mast cell infiltration. Certain flavonoids, such as quercetin and lignans, exhibit potent mast cell inhibitory effects along with anti-inflammatory and antioxidant properties, suggesting a promising therapeutic approach (126, 127). Additionally, blocking the IL-33/RAGE/VCAM-1 pathway inhibits IL-33-induced ILC2-mediated type 2 inflammatory response, leading to the elimination of eosinophilic inflammation and mucous epithelial hyperplasia (128). The mTOR (rapamycin signaling) pathway also plays a role in asthma, where IL-33 induces phosphorylation of rpS6 in bone marrow ILC2s via mTORC1 signaling to initiate the immune response. Rapamycin may attenuate IL-33-induced eosinophilic inflammation by inhibiting IL-5-induced bone marrow ILC2s and reducing mTOR signaling (129). Furthermore, activation of ILC2s downstream of IL-33 and allergic airway inflammation can be inhibited through the adenosine/A2A signaling pathway, likely due to adenosine binding to its receptor, which increases intracellular cAMP production and downregulates the downstream NF-κB pathway (130).

In obese asthma patients, treatment with glucagon-like peptide-1 receptor agonist (GLP-1RA) led to reduced acute release of IL-33 and TSLP, decreased airway hyperresponsiveness, and attenuation of ILC2 activation, providing a potential therapeutic direction for obese asthma treatment (131). Cyclohexane di-gmp (CDG) (132) modulates the downstream ILC2 response to ALT-induced IL-33 release, effectively reducing ALT-induced eosinophilia in bronchoalveolar lavage (BAL) and lungs, along with decreasing IL-5 and IL-13 levels in BAL, attenuating ILC2-driven eosinophilic airway inflammation. Another traditional Chinese medicine, serpentine (133), has been shown to reduce airway hyperresponsiveness and attenuate airway inflammatory response and remodeling by inhibiting IL-33/ST2 signaling, balancing Th1/Th2-associated cytokines, and achieving therapeutic efficacy in mice at 50 mg/kg. Moreover, Fibulin-1 (Fbln1), an ECM protein, stabilizes the deposition of other ECM proteins and collagen. Deletion of Fbln1c in a mouse model of chronic experimental asthma demonstrated protective effects against elevated IL-33, IL-5, IL-13, and TNF, reduced airway remodeling and hyperresponsiveness (AHR), decreased recruitment of neutrophils, eosinophils, and lymphocytes, and lower levels of airway inflammation-related cytokines and chemokines, suggesting a potential therapeutic target for inhibiting chronic asthma airway remodeling and inflammation. Lastly, in patients with mild allergic asthma who discontinued glucocorticoid therapy, the ratios of IL-1β to IL-37 and IL-33 to IL-37 were significantly elevated compared to asthmatics, potentially underlying the persistence of allergic asthma in adults. IL-37 suppresses allergic airway inflammation by balancing the disease-amplifying effects of IL-1β and IL-33 (134). However, the specific mechanism remains unclear,

necessitating further studies to elucidate causation and therapeutic potential.

5.1.3 Monoclonal antibodies in asthma therapy

Blocking TSLP, ST2, and IL-33 can all be effective in treating asthma. Tezepelumab, a monoclonal antibody targeting TSLP, works by directly binding to TSLP and blocking TSLP-TSLPR signaling. It has shown efficacy and long-term safety in treating severe asthma (135). Astegolimab selectively inhibits ST2, reducing the rate of acute asthma deterioration and demonstrating safety and efficacy in patients with severe T2-low type asthma. Antibodies targeting IL-33 that have been studied include itepekimab, tozorakimab, and REGN3500. Although many of these drugs are still in the clinical evaluation stage, itepekimab has demonstrated a significant reduction in the odds of uncontrolled asthma compared to placebo (136). Tozorakimab acts by blocking both IL-33(red) and IL-33(ox) signaling, providing a new strategy for treating inflammation and epithelial dysfunction (137). Interestingly, Vannella et al. (138) studied IL-33, IL-25, and TSLP using the Schistosoma haematobium egg lung granuloma model of allergic airway disease and concluded that targeting only one cytokine is useful but incomplete for reducing allergic airway disease. They suggested that targeting all three cytokines simultaneously could be more meaningful (138). Further studies are needed to confirm the roles of these drugs and provide safer options for pharmacologic asthma treatment.

5.1.4 Allergen immunotherapy in the treatment of asthma

Allergen Immunotherapy (AIT) stands as a pivotal element within asthma treatment, attracting considerable attention within the medical community in recent years, with well-defined international guidelines in place (139). In a retrospective study conducted by Wang et al. involving 112 children diagnosed with allergic rhinitis (AR) and cough variant asthma (CVA), Subcutaneous Immunotherapy (SCIT) was shown to forestall the emergence of new sensitizations and the progression to classic asthma (CA) in this specific pediatric cohort. Moreover, SCIT treatment demonstrated enhancements in serum levels of sIgG4, IL-27, and IL-33, yielding superior clinical outcomes compared to traditional pharmacological approaches (140). Additionally, a study indicated the potential of allergen immunotherapy in reducing the incidence of respiratory infections and mitigating the risk of acute exacerbations in individuals with asthma. Christian and colleagues' (141) research revealed that House Dust Mite Sublingual Immunotherapy (HDM-SLIT) significantly upregulates the expression of bronchial epithelial IFN-β and IFN-λ, thereby dampening the response of IL-33 to the viral mimic poly(I:C). These findings suggest that this therapeutic approach may bolster tolerance to viral infections and enhance the stability of airway epithelium.

In summary, IL-33 plays a critical role in the early stages of asthma development by initiating downstream signaling pathways that contribute to asthma induction and exacerbation. Numerous drugs have demonstrated the ability to lower IL-33 levels and alleviate asthma symptoms. However, the precise mechanisms and targets involved in IL-33 down-regulation remain unclear, necessitating further research to identify these mechanisms and targets. This deeper understanding will pave the way for novel therapeutic options for the treatment of asthma.

5.2 Allergic rhinitis

Given the extensive research on the role of IL-33 in allergic rhinitis (AR) in recent years, targeting IL-33 represents a valuable approach to intervening in the onset and progression of AR (142). In addition to traditional treatments like antihistamines, glucocorticoids, and allergen avoidance, understanding and modulating the IL-33 pathway could offer novel strategies for managing allergic rhinitis effectively. This approach leverages insights into the specific mechanisms underlying AR pathogenesis, potentially leading to more targeted and impactful therapeutic interventions.

5.2.1 Blocking IL-33 production and release in allergic rhinitis

Xiaoqinglongtang (XQLT) is a traditional Chinese herbal formula described in the Shang Han Lun, comprising ephedra, peony, and xixin. Manabu and colleagues (143) found that XQLT administration helped control symptoms and reduced IL-33 levels in serum and nasal lavage fluid in TDI-induced AR mice. Further investigations revealed that XQLT could decrease IL-33 release from nasal epithelial cells. Zhang et al. (144) studied the mechanism of XQLT *in vivo* and discovered that XQLT significantly reduced nasal mucosal tissue damage in an OVA-induced AR mouse model. They observed decreased levels of IL-33, ST2, MYD88, and NF-κB p65 proteins in the XQLT intervention group compared to the control group, suggesting that XQLT might inhibit the IL-33/ST2 signaling pathway through the MYD88/IRAK4/NF-κB p65 pathway (145). Rezwanul et al. (146) demonstrated that wild grape extracts could inhibit IL-33 gene expression in HeLa cells and Swiss 3T3 cells, indicating that wild grapes may contain compounds that inhibit IL-33 expression. Additionally, they found that betuletol, extracted from Brazilian propolis, reduced eosinophil numbers by inhibiting ERK phosphorylation and down-regulating IL-33 expression, thereby improving eosinophilic inflammation symptoms. Some of these substances are already used clinically, while others are still in the laboratory research phase. Further clinical studies are necessary to validate their effectiveness and safety for treating allergic rhinitis and related conditions.

5.2.2 Blocking IL-33/ST2 binding and downstream conduction pathways in allergic rhinitis

MicroRNAs (miRNAs) are small endogenous non-coding molecules that play a crucial role in post-transcriptional regulation (147). Studies have demonstrated that miR-181a-5p can target IL-33, leading to its downregulation and inhibition of the IL-33/ST2/p38

MAPK axis, exerting an anti-inflammatory effect in human RPMI-2650 nasal epithelial cells (148). Another study has shown that Didox reduces cytokine production following IL-33 activation by inhibiting NFκB and AP-1 transcriptional activity in primary mouse mast cells, suggesting that Didox could potentially act as a treatment for ARpatients (142, 148). Additionally, Jin et al. (149) found that Chaenomeles sinensis extract (CSE) could improve rhinitis symptoms in OVA-induced AR mice. Immunohistochemistry revealed that mice gavaged with CSE showed more restricted distribution of ST2 compared to positively treated group mice, along with reduced IL-33 levels, indicating that CSE may be effective in controlling IL-33/ST2 axis-mediated cellular inflammation in nasal epithelial cells. Furthermore, FJE (a yellow flower root extract) is commonly used for allergic inflammation treatment and has been reported to modulate mucus accumulation by reducing inflammatory cell infiltration. It can also inhibit OVA-specific immunoglobulins and modulate the IL-33/TSLP/NF-κB signaling pathway, thereby exerting therapeutic effects on allergic rhinitis (150).

5.2.3 Allergen immunotherapy in the treatment of allergic rhinitis

The pathogenesis of allergic diseases primarily involves allergen-specific IgE and Th2-related cellular inflammation. Allergen-specific immunotherapy primarily targets cellular immunity by inhibiting the production and release of IL-25 and IL-33, reducing the recruitment of inflammatory cells such as ILC2 and eosinophils, and suppressing Th2-related cellular inflammation. This, in turn, alleviates allergic airway inflammation and airway hyperresponsiveness (151, 152). The severity of allergic rhinitis (AR) is positively correlated with IL-33 levels, and a decrease in its levels may indicate improvement in clinical symptoms. Therefore, IL-33 could be considered a crucial predictive factor and a key therapeutic target in the treatment of AR (153, 154).

5.3 Chronic obstructive pulmonary disease

COPD is a prevalent respiratory condition, and emerging research indicates the involvement of type 2 cytokines, including IL-33, in its development (155–157). Current clinical approaches for COPD management primarily involve M-cholinergic inhibitors, β-adrenergic receptor agonists, and glucocorticoids (158). However, specific treatments targeting type 2 inflammation in COPD, such as those involving IL-33, remain lacking. Recent studies have highlighted potential therapeutic strategies targeting IL-33 for COPD. These may include interventions aimed at modulating IL-33 expression, blocking IL-33 signaling pathways, or targeting downstream effectors of IL-33-mediated inflammation. Investigating IL-33 as a therapeutic target could open avenues for developing more tailored and effective treatments for COPD associated with type 2 inflammation (159–164).

5.3.1 Blocking IL-33 production and release in chronic obstructive pulmonary disease

Previous studies have shown that the serum amyloid A (SAA)/IL-33 axis plays a role in the pathological process of steroid-resistant pulmonary inflammation (159). Recent research has indicated that bitterside II could be a potent inhibitor of SAA and IL-33 production. Bitter Glycoside II, a metabolite derived from the plant extract mullein, was found to inhibit LPS-induced SAA1 mRNA expression in human monocytes and SAA-induced IL-33 secretion in human airway epithelial cells. Further investigations revealed that this compound inhibited the TLR2-MAPKp38-ERK1/2 and NF-κB signaling pathways activated by SAA, thereby suppressing IL-33 production and potentially controlling airway remodeling in COPD patients (159). These findings suggest that bitterside II holds promise as a therapeutic agent, although its safety and efficacy require validation through additional animal and clinical trials.

Ella and colleagues (160) observed a significant increase in the secretion of the ceramide biosynthetic enzyme neutral sphingomyelinase 2 (nSMase2) and the IL-33 isoform IL-33Δ34 in patients with COPD following a comprehensive analysis of human airway epithelial cells. Subsequent investigations revealed that nSMase2 promotes IL-33 secretion by integrating into the multivesicular endosomal (MVE) pathway, thereby exacerbating COPD severity in humans. They conducted experiments using the nSMase2 inhibitor, GW6849, which effectively suppressed IL-33 secretion and downstream inflammatory pathways, demonstrating its potential as a novel therapeutic approach for COPD treatment. However, as of now, no relevant drugs targeting this pathway have entered clinical trials.

5.3.2 Blocking IL-33/ST2 binding and downstream conduction pathways in chronic obstructive pulmonary disease

IL-33 plays a role in accelerating the progression of COPD by inducing and enhancing the expression of IL-6 and IL-8 inHBE cells and PBMCs of COPD patients via the ST2/IL-1RacP pathway and MAPKs pathway. In a study conducted by Jin et al. (45), the existence of this pathway was confirmed through cytological experiments. They demonstrated that the expression of IL-6 and IL-8 could be down-regulated by administration of ST2-neutralizing antibody, IL-1RACP-neutralizing antibody, the MAPK inhibitor SB-203580, or the JNK inhibitor SP-600125. These findings suggest that inhibitors targeting these pathways may hold potential therapeutic effects for COPD.

5.3.3 Monoclonal antibodies in chronic obstructive pulmonary disease

Itepekimab, a monoclonal antibody targeting IL-33, has shown potential for COPD treatment in a multicenter, randomized, double-blind, phase 2a clinical trial. In this trial, patients already receiving disease-controlling therapy were additionally treated with Itepekimab (300 mg per injection, twice every two weeks for 24-52 weeks). Subgroup analysis of ex-smokers revealed a 42% reduction in the rate of acute COPD worsening and an improvement in FEV1 by 0.09 L (161). These results suggest potential benefits in lung function improvement for ex-smokers and usefulness in COPD treatment. Astegolimab, a monoclonal antibody against ST2, was investigated in a clinical trial conducted by Aj and colleagues (162). While it did not control the acute exacerbation rate in COPD patients, it showed

promise in improving respiratory function and quality of life. Notably, improvements in Saint George's Respiratory Questionnaire (SGRQ-C) and FEV1 were more significant in patients with higher eosinophils compared to those with lower eosinophils. The study also observed significantly lower blood and sputum eosinophil counts in the drug group compared to the placebo group, contributing to disease control. Further experimental and clinical studies are warranted to explore the potential of anti-ST2 therapy in COPD remission. Tozorakimab, a novel monoclonal antibody, acts by blocking IL-33 formation via the ST2 pathway and inhibiting its signal transduction in the RAGE/EGFR pathway (137). In a recent clinical study by F et al. (163), Tozorakimab demonstrated dose-dependent elevation of serum IL-33/Tozorakimab conjugates and decreased IL-33/ST2 conjugates compared to placebo. The experimental group showed significantly lower serum IL-5 and IL-13 levels and reduced blood eosinophil levels in COPD patients across all dose levels. The safety and tolerability of the drug were also confirmed. Although respiratory function was not examined in this study, ongoing phase 2 and phase 3 clinical trials aim to address these aspects and provide further insights into the efficacy of Tozorakimab for COPD treatment.

5.3.4 Other treatment mechanisms in chronic obstructive pulmonary disease

In COPD treatment regimens, glucocorticoids are considered the most widely used anti-inflammatory agents (164); however, in recent years, many patients have been found to exhibit decreased sensitivity to glucocorticoids, and IL-33 is considered to be a mediator of steroid resistance (165). Recent studies have shown that azithromycin and budesonide, when used alone, cannot inhibit the release of IL-33 from peripheral monocytes, but their combination can reduce the release of IL-33. These findings suggest that azithromycin helps to restore sensitivity to steroids in COPD patients, providing an adjunctive option for disease treatment (164).

5.4 Pulmonary fibrosis

Pulmonary fibrosis represents the end-stage of a lung condition characterized by fibroblast proliferation and extensive accumulation of extracellular matrix, accompanied by inflammatory damage and structural deterioration (166, 167). IL-33, a novel pro-fibrotic cytokine, signals through ST2, facilitating the onset and progression of pulmonary fibrosis by recruiting and guiding the functions of inflammatory cells in a ST2 and macrophage-dependent manner, and amplifying the production of pro-fibrotic cytokines. Attenuating and treating pulmonary fibrosis can be achieved by weakening or blocking its upstream and downstream pathways (166, 167). Bleomycin (BLM) is a critical chemotherapeutic agent used in cancer treatment. However, its cytotoxicity, associated with DNA strand scission and induction of reactive oxygen species, can lead to severe side effects, including pulmonary fibrosis (168–170). IL-33 plays a significant role in the initiation and progression of pulmonary fibrosis. The levels and activity of the IL-33 receptor (IL-33R) are regulated through deubiquitination by ubiquitin-specific protease 38 (USP38) and polyubiquitination by E3 ubiquitin ligase tumor necrosis factor receptor–associated factor 6 (TRAF6) (87). USP38 mediates the deubiquitination of IL-33R via the autophagy-lysosome pathway, promoting receptor downregulation, negatively regulating IL-33-triggered inflammatory signaling, and the inflammatory response; following bleomycin induction, mice with USP38 deficiency exhibit significantly increased transcription of inflammation and fibrosis-related genes in the lungs, heightened inflammatory cell infiltration, collagen deposition, elevated levels of the fibrosis marker α-SMA, and increased mortality (87). Upon IL-33 stimulation, TRAF6 enhances K27-linked polyubiquitination of IL-33R, preventing its autophagic degradation, promoting IL-33R stability, and facilitating effective signal transduction (87). Therefore, USP38 and TRAF6 represent potential drug targets for addressing IL-33-induced pulmonary fibrosis. A study by Zhang JJ et al. (85) revealed that neuropilin-1 (Nrp1) acts as a tissue-specific regulator for lung-resident ILC2. The transforming growth factor beta-1 (TGFβ1)-Nrp1 signaling pathway enhances ILC2 function and type 2 immunity by upregulating IL-33 receptor ST2 expression. Targeting Nrp1 can inhibit the activation of lung ILC2 and attenuate the pulmonary fibrotic response (85). Additionally, eukaryotic initiation factor 3a (eIF3a) serves as a crucial regulatory factor in fibrotic diseases (171, 172). It has been reported that IL-33 can activate the NF-κB pathway to induce eIF3a expression, and the NF-κB pathway inhibitor pyrrolidine dithiocarbamate (PDTC) can reverse this reaction, thereby inhibiting the development of pulmonary fibrosis (173–177). Another pro-apoptotic agent, Dehydrocostus lactone (DHL) (173–177), can downregulate the JNK/p38 MAPK-mediated NF-κB signaling pathway, inhibit macrophage activation, and exert anti-fibrotic effects (178).

Idiopathic pulmonary fibrosis (IPF) is a progressive, irreversible lung disease characterized by respiratory distress and respiratory failure primarily caused by the formation and thickening of lung interstitial tissue scars (179, 180). Currently, pirfenidone and nintedanib are the only treatment options for IPF (179, 180). Researchers are actively exploring new therapeutic drugs and targets. Elamipretide (SS-31) is a novel insulin-targeted antioxidant that protects and repairs damaged mitochondria without affecting healthy mitochondria (181). SS-31 offers protection against pulmonary fibrosis and inflammation by inhibiting the activation of the NLRP3 inflammasome in macrophages mediated by Nuclear factor erythroid 2-related factor 2 (Nrf2) (89). Nuclear factor of activated T cells cytoplasmic member 3 (NFATc3) responds to damaged epithelial cells, IL-33, and Th2 cell stimuli, promoting the production of C-C motif ligand 2 (CCL2) and C-X-C motif chemokine ligand 2 (CXCL2), exacerbating early inflammation, regulating angiogenesis, mediating fibroblast recruitment, and participating in the pathogenesis of pulmonary fibrosis (89). NFATc3 deficiency significantly reduces bleomycin-induced pulmonary fibrosis and inflammation. Tumor Necrosis Factor Superfamily Member 14 (TNFSF14/LIGHT) primarily acts on Lymphotoxin Beta Receptor

TABLE 1 Relevant drugs and their action mechanisms and effects.

Disease	Reference	Medicine	Target /Pathway	Main model/Experiment	Mechanisms and clinical role
Asthma	Zhu S, et al. (116)	Vitamin B6	PLP/MDM2/IL-33 axis	Papain-induced mouse model Human alveolar basal epithelial cell line A549 HEK293FT cell HDM-induced mouse model	Decreases IL-33 stability, promotes IL-33 degradation, reduces eosinophils and ILC2s, and attenuates type 2 inflammation
	Zhu G, et al. (117)	/	SPRR3/PI3K/AKT/NFkB	HDM-induced mouse model	Inhibits IL-33 expression, reduces ILC2s recruitment, and attenuates type 2 inflammation
	Shinoda K, et al. (118)	Ascr#7	Th 2 cells and ILC2 cells	OVA-induced mouse model HDM-induced mouse model	Reduces IL-33 expression and inhibits proliferation of ST2+ Th2 cells and ILC2 cells
	Galvão JGFM, et al. (120)	Wowbaine	Na+-K+-ATPase	OVA-induced mouse model	Inhibits IL-33 production and reduces inflammatory cell migration
	Won J, et al. (121)	IFN- λs	Th 2 cells	OVA-induced mouse model	Accelerates reduction of IL-33 levels
	Huang X, et al. (122)	Louki Zupa	IL-33/ST 2-NFkB/ GSK3b/mTOR	OVA-induced mouse model	Inhibits IL-33, ST 2 expression and down-regulates inflammatory response
	Wuniqiemu T, et al. (123)	Iris flavin A	Th 2 inflammatory factors IL-4, IL-5, IL-33, leukocytes, epithelial transcription factor FOXA3 and mucin MUC5AC	OVA-induced mouse model	Reduces IL-33 expression, reduces infiltration of inflammatory cells and release of inflammatory factors
	Verheijden KA, et al. (67)	GOS	IL-33 mRNA、ST 2 mRNA	HDM-induced mouse model	Reduces IL-33, ST 2 mRNA expression
	Huang Y, et al. (124)	Thrombin inhibitors	IL-33 precursor	ALT-induced mouse model Papain-induced mouse model HDM-induced mouse model OVA-induced mouse model	Inhibits IL-33 precursor activation reduces eosinophils and ILC2s and attenuates type 2 inflammation
	Kimata M, et al. (126) Kempuraj D, et al. (127)	Mast cell inhibitors	Ca2+/PKC	Human cultured mast cells (HCMCs)	Inhibits IL-33 production
	Boberg E, et al. (129)	Rapamycin	mTORC1signaling pathway	IL-33 induced mouse model	Inhibits IL-5-induced bone marrow ILC2s
	Xiao Q, et al. (130)	Adenosine	Adenosine/A2A-cAMP and NFκB	Papain-induced mouse model	Inhibits ILC2s activation
	Toki S, et al. (131)	Glucagon-like peptide-1 receptor agonist	GLP-1RA signaling pathway	ALT - EXT-induced polygenic obese mouse model (TALLYHO mice) and corresponding lean gene control mice (SWR mice)	Reduces acute release of IL-33 and attenuates activation of ILC2s
	Cavagnero KJ, et al. (132)	Cyclic-di-GMP	Interferon gene-stimulating factor (STING) and type 1 IFN signaling pathway	ALT-induced mouse model	Modulates ILCs response
	Yang Q,et al. (132)	Osthole	IL-33/ST 2 signaling pathway	OVA-induced mouse model	Inhibits IL-33/ST 2 signaling
	Liu G, et al. (188)	/	Fibulin-1	HDM-induced mouse model	Reduces IL-33 level
	Kelsen SG, et al.	Astegolimab	ST 2	Multicenter, randomized, double-blind, placebo-controlled, phase 2b study	Selectively inhibits ST 2 , reduces acute asthma exacerbations in a broad population of patients with severe, uncontrolled asthma

(Continued)

TABLE 1 Continued

Disease	Reference	Medicine	Target /Pathway	Main model/Experiment	Mechanisms and clinical role
	Wechsler ME, et al.	Itepekimab	IL-33	Multicenter, randomized, double-blind, placebo-controlled, parallel, phase 2, proof-of-concept trial	Selectively inhibits IL-33, reduces the rate of uncontrolled moderate-to-severe asthma, and improves pre-bronchodilator FEV1
	England E, et al. (149)	Tozorakimab	RAGE / EGFR	ALT-induced mouse model	Blocks IL-33(red) and IL-33(ox) signaling, with good safety and tolerability
Allergic rhinitis	Zhang JJ, et al. (144) Kitano M,et al. (143)	Xiaoqinglongtang	MYD88/IRAK4/NF-κB P65	OVA-induced mouse model TDI-induced mouse model	Reduces IL-33 level
	Shaha A, et al. (146)	Betuletol	PKCδ/ERK and/or IL-33/ ST 2/ERK	PMA-induces swiss 3T3 cell	Down-regulates IL-33 mRNA expression
	Islam R, et al. (145)	Wild grapes	PKCδ	TDI-induced mouse model PMA-induces swiss 3T3 cell	Down-regulates IL-33 mRNA expression
	Long S, et al. (148)	/	miR-181a-5p/IL-33/ST2-p38 MAPK	OVA-induced RPMI-2650 cell	Targeted downregulates IL-33 expression
	Jin J, et al. (149)	Chaenomeles sinensis extract	IL-33/ST 2 signaling pathway	OVA-induced mouse model	Reduces IL-33 levels and inhibits IL-33/ST 2/Th 2 signaling
	Jin J, et al. (150)	F.japonica root extract	IL-33/TSLP/NF-κB	OVA-induced mouse model	Dose-dependent reduces IL-33 level and ST 2 mRNA expression
Chronic obstructive pulmonary disease	Lee K,et al. (159)	Picroside II	SAA-TLR2 - NF-κB SAA-TLR2 - MAPKp38 - ERK1 / 2	SAA-induced human airway epithelial cell	Inhibits IL-33 production
	Katz-Kiriakos E, et al. (160)	GW6849, inhibitor of nSMase2	nSMase 2	ALT-induced human airway epithelial cell	Inhibits IL-33 secretion
	Rabe KF, et al. (161)	Itepekimab	IL-33	Multi-country, randomized, double-blind, placebo-controlled, parallel, phase 2a trial	Selectively inhibits IL-33, reduces exacerbation rates and improves lung function in COPD patients who quit smoking
	Yousuf AJ, et al. (162)	Astegolimab	ST 2	Single-center, randomized, double-blind, placebo-controlled, phase 2a clinical trial	Selectively inhibits ST 2 to improve patients' respiratory function and quality of life
	England E, et al. (137) Reid F, et al. (163)	Tozorakimab	RAGE / EGFR	ALT-induced mouse model Non-clinical, phase I, randomized, double-blind, placebo-controlled study	Neutralizes IL-33, forms IL-β 33 (red)/tozorakimab complex, reduces IL-33/ST2 formation, and has a favorable safety and tolerability profile
Acute respiratory distress syndrome	Lei M, et al. (185)	3-methyladenine	NF-κB	LPS-induced mouse model	Reduces IL-33 level
	Fu J, et al. (186)	Glycyrrhizin	HMGB1	LPS-induced mouse model	Reduces IL-33 level
	Martínez-González I, et al. (187)	Human adipose tissue–derived mesenclymal stem cells overexpressing soluble IL-1 receptor–like–1	IL-33	LPS-induced mouse model	Blocks IL-33 binding to T1/ST2
Pulmonary fibrosis	Yi XM, et al. (87)	/	USP 38 and TRAF 6	Defective Usp38 in Embryonic Fibroblast NIH 3T3 Cells Usp38 Deficient Mouse Model Bleomycin-Induced Mouse Model	Modulating the levels and activity of IL-33R regulates signal transduction, inflammation, and fibrosis.
	Zhang JJ, et al. (85)	/	NRP 1	Id2cre-ert2Nrp1f/f Mouse Model Bleomycin-Induced Mouse Model R5/+ Nrp1f/f Mouse Model	Deficiency in NRP1 downregulates ST2, weakens ILC2 function, and alleviates pulmonary fibrosis.

(Continued)

TABLE 1 Continued

Disease	Reference	Medicine	Target /Pathway	Main model/Experiment	Mechanisms and clinical role
	Nie YJ, et al. (89)	/	NFATc 3	NFATc3-deficient mice Bleomycin-induced mouse model	Deficiency in NFATc3 significantly reduces the levels of fibrotic markers CCL2 and CXCL2 induced by BLM, attenuating BLM-induced pulmonary fibrosis and inflammatory response.
	Gao YX, et al. (83)	Pyrrolidine dithiocarbamate (PTDC)	NF-κB signaling pathway/eIF3a	Bleomycin-induced mouse model.	Inhibit the expression of eIF3a induced by NF-κB pathway activation, thereby alleviating pulmonary fibrosis.
	Nie YJ, et al. (189)	Elamipretide	NRF 2/NLRP 3	Bleomycin-induced mouse model for research purposes.	Inhibit the activation of the NLRP3 inflammasome mediated by NRF2 in macrophages.
	Xiong Y, et al. (178)	Dehydrocostus lactone	JNK/p38 MAPK/NF-κB	A bleomycin-induced mouse model.	Downregulate the NF-κB signaling pathway mediated by JNK/p38 MAPK, reduce the expression of inflammatory cytokines induced by BLM, inhibit macrophage activation, ameliorate lung inflammation, and alleviate pulmonary fibrosis.
	da Silva Antunes R, et al. (182)	/	TNFSF14	Primary human lung fibroblasts (HLF).	LIGHT promotes the proliferation of lung fibroblasts, upregulates the expression of cytokines, amplifying inflammatory and pulmonary fibrotic responses.
	Zheng ZD, et al. (183)	/	IRAK-M	Mouse lung fibroblasts (MLFs).	Inhibit the proliferation and motility of lung fibroblasts, reducing the expression of fibronectin, type I collagen, and α-SMA in MLg cells.

(LTβR), promoting lung fibroblast division, upregulating IL-33 mRNA, and the expression of adhesion molecules intercellular cell adhesion molecule-1 (ICAM-1) and vascular cell adhesion molecule 1 (VCAM-1), inducing the transcription of CC or CXC chemokines in lung fibroblasts, amplifying inflammatory and fibrotic responses. Targeting the blockade of LIGHT activity may provide new therapeutic strategies for pulmonary fibrosis treatment (182). Furthermore, Zheng et al. (183) in an *in vitro* study, unveiled the association between IL-1 receptor-associated kinase (IRAK)-M and pulmonary fibrosis. The overexpression of IRAK-M exerts a beneficial influence on pulmonary fibrosis-related alterations: it notably impedes the proliferation and motility of lung fibroblasts, diminishes the expression of fibronectin, type I collagen, and α-SMA in Murine lung fibroblasts (MLg) cells, and boosts the production of metalloproteinases (MMP9) (183). Essentially, pharmaceutical agents that activate IRAK-M could emerge as a promising avenue for future investigations.

As previously discussed, the ongoing progress in medical research is deepening our comprehension of the pathophysiology of pulmonary fibrosis. Research on associated targets and pathways is progressively broadening, offering valuable insights for the future advancement of clinical practice.

5.5 Other respiratory diseases

In models of acute lung injury (ALI) and ARDS, elevated serum IL-33 levels contribute significantly to the pathogenesis, primarily through the IL-33/STAT3/MMP2/9 pathway (184). Studies have demonstrated that neutralizing IL-33 with specific antibodies can reduce the levels of MMP2 and MMP9, thereby mitigating the severity of lung injury associated with ARDS (184). Additionally, excessive cellular autophagy has been implicated in increased mortality due to ARDS-induced lung injury (185). Liang et al. (185) investigated the role of autophagy modulation in ARDS using rapamycin (RAPA), an autophagy promoter, and 3-methyladenine (3-MA), an autophagy inhibitor. Their findings revealed that 3-MA inhibits NF-κB-mediated IL-33 expression, leading to a reduction in the uncontrolled inflammatory response observed in ARDS.

HMGB1 is an evolutionarily conserved non-histone nuclear protein expressed in nearly all cells. In allergic airway diseases, HMGB1 promotes the release of IL-33 through the HMGB1/RAGE/IL-33 axis. Glycyrrhizic acid has been shown to inhibit HMGB1-mediated IL-33 release and attenuate lung injury (186). Genetic engineering approaches also hold promise for ARDS treatment. The ST2/T1 gene in human mesenchymal stem cells (hASC) can be

selectively spliced using two different promoters to produce two major products: ST2L and sST2. ST2L is a functional component of IL-33 activity induction, while sST2 acts as a decoy receptor for IL-33, inhibiting TLR-4 expression and pro-inflammatory cytokine production by macrophages. Treatment with hASC-sST2 blocks IL-33 binding to ST2, resulting in a protective anti-inflammatory and immunomodulatory effect that reduces pro-inflammatory cellular infiltration and preserves pulmonary vascular barrier integrity (187). This approach offers a potentially effective option for ARDS treatment by inhibiting IL-33 expression and mitigating the inflammatory response.

6 Prospects and the future

In summary, IL-33, a cytokine of the interleukin family, has emerged as a critical player in respiratory type 2 inflammation and is pivotal in the development of asthma, allergic rhinitis, and various other respiratory diseases. This review has illuminated the pathways through which IL-33 contributes to respiratory disease development and has explored the mechanisms and feasibility of drugs targeting IL-33.IL-33 activates the ST2 receptor, initiating a cascade of inflammatory responses that drive the progression and aggravation of respiratory diseases. Therapeutic strategies targeting IL-33 involve blocking IL-33 binding to its receptor, suppressing IL-33 expression, and interrupting IL-33 signaling pathways. Certain drugs, such as monoclonal antibodies and small molecule inhibitors, have demonstrated promising therapeutic effects against IL-33. Looking ahead, further research into the role of IL-33 in respiratory diseases and the clinical application of IL-33-targeted therapies will be crucial. By deepening our understanding of IL-33 regulatory mechanisms, we can develop more effective and personalized treatment approaches, ultimately providing better therapeutic options and improving quality of life for patients with respiratory diseases.

We should recognize that there are currently many shortcomings in targeting the mechanism of action between IL-33 and type 2 inflammation-associated respiratory diseases. For example, the pathways of action have not yet been fully unraveled, as well as insufficient output in translational medicine research.

As an emerging research focus, understanding the role of IL-33 is crucial for gaining deeper insights into respiratory type 2 inflammation-related diseases. However, several challenges remain that require further investigation. Firstly, the mechanism of type 2 inflammation is intricate, and IL-33 represents just one component of this complex process. Exploring interactions with other inflammatory factors and assessing the comparative value of targeting these factors alongside IL-33 warrants future exploration. Secondly, identifying additional pathways influencing IL-33 and disease development requires comprehensive study and validation. To advance the translation of basic research findings, future studies can focus on several key aspects:

Biological Models and Biomarkers: Develop biological models to predict disease prognosis and progression by measuring IL-33 levels in serum or alveolar lavage fluid. Evaluate IL-33 as a potential biomarker for disease diagnosis and severity grading to enhance clinical guidance.

Clinical Trials: Conduct extensive clinical trials on drugs known to affect IL-33 production, release, and downstream pathways. Assess safety, human tolerance, drug distribution, and metabolism to inform treatment protocols and guidelines.

Precision Medicine: Employ personalized medicine approaches by analyzing IL-33 data from individual patients to identify suitable anti-IL-33 drugs, facilitating precision medicine initiatives.

Exploration of IL-33 in Other Diseases: Expand research on IL-33 involvement in type 2-related respiratory diseases like ARDS and pulmonary fibrosis. Investigate IL-33 production, pathways, drug efficacy, safety, and overall patient benefits to improve survival and quality of life.

In conclusion, IL-33 is intricately linked to various respiratory type 2 inflammatory diseases, and further investigation into IL-33 and related pathways holds promise for identifying novel strategies to prevent and manage type 2 inflammation.

Future studies should prioritize investigating undiscovered pathways of IL-33 production and action, assessing drug efficacy and safety, and exploring patient benefits to advance our understanding and clinical management of respiratory diseases associated with type 2 inflammation Table 1.

Author contributions

SG: Data curation, Investigation, Project administration, Writing – original draft. RW: Data curation, Investigation, Project administration, Writing – original draft. WZ: Data curation, Investigation, Project administration, Writing – original draft. CW: Project administration, Supervision, Writing – review & editing. CC: Conceptualization, Resources, Supervision, Writing – review & editing. SL: Conceptualization, Resources, Supervision, Writing – review & editing. QL: Conceptualization, Methodology, Resources, Writing – review & editing. PZ: Conceptualization, Methodology, Resources, Supervision, Writing – review & editing. SZ: Conceptualization, Funding acquisition, Methodology, Resources, Supervision, Writing – review & editing.

Funding

The author(s) declare financial support was received for the research, authorship, and/or publication of this article. This work was supported by The National Natural Science Foundation of China under Grant 82202071 and Sichuan Provincial Science and Technology Program under Grant 2022YFS0237,2023YF0036 and 2022YF50314.

Conflict of interest

The authors declare that the research was conducted in the absence of any commercial or financial relationships that could be construed as a potential conflict of interest.

Publisher's note

References

1. Haenuki Y, Matsushita K, Futatsugi-Yumikura S, Ishii KJ, Kawagoe T, Imoto Y, et al. A critical role of IL-33 in experimental allergic rhinitis. *J Allergy Clin Immunol.* (2012) 130:184–94.e11.

2. Tapiainen T, Dunder T, Möttönen M, Pokka T, Uhari M. Adolescents with asthma or atopic eczema have more febrile days in early childhood: A possible explanation for the connection between paracetamol and asthma? *J Allergy Clin Immunol.* (2010) 125:751–2.

3. Roussel L, Erard M, Cayrol C, Girard JP. Molecular mimicry between IL-33 and KSHV for attachment to chromatin through the H2A–H2B acidic pocket. *EMBO Rep.* (2008) 9:1006–12.

4. Blom L, Poulsen LK. IL-1 family members IL-18 and IL-33 upregulate the inflammatory potential of differentiated human Th1 and Th2 cultures. *J Immunol.* (2012) 189:4331–7.

5. Allakhverdi Z, Smith DE, Comeau MR, Delespesse G. Cutting edge: the ST2 ligand IL-33 potently activates and drives maturation of human mast cells. *J Immunol.* (2007) 179:2051–4.

6. Kurowska-Stolarska M, Kewin P, Murphy G, Russo RC, Stolarski B, Garcia CC, et al. IL-33 induces antigen-specific IL-5+ T cells and promotes allergic-induced airway inflammation independent of IL-4. *J Immunol.* (2008) 181:4780–90.

7. Rank MA, Kobayashi T, Kozaki H, Bartemes KR, Squillace DL, Kita H. IL-33–activated dendritic cells induce an atypical TH2-type response. *J Allergy Clin Immunol.* (2009) 123:1047–54.

8. Besnard AG, Togbe D, Guillou N, Erard F, Quesniaux V, Ryffel B. IL-33-activated dendritic cells are critical for allergic airway inflammation. *Eur J Immunol.* (2011) 41:1675–86.

9. Pecaric-Petkovic T, Didichenko SA, Kaempfer S, Spiegl N, Dahinden CA. Human basophils and eosinophils are the direct target leukocytes of the novel IL-1 family member IL-33. *Blood.* (2009) 113:1526–34.

10. Barlow JL, Peel S, Fox J, Panova V, Hardman CS, Camelo A, et al. IL-33 is more potent than IL-25 in provoking IL-13–producing nuocytes (type 2 innate lymphoid cells) and airway contraction. *J Allergy Clin Immunol.* (2013) 132:933–41.

11. Patial S, Lewis BW, Vo T, Choudhary I, Paudel K, Mao Y, et al. Myeloid-IL4Rα is an indispensable link in IL-33-ILCs-IL-13-IL4Rα axis of eosinophil recruitment in murine lungs. *Sci Rep.* (2021) 11(1):15465.

12. Aizawa H, Koarai A, Shishikura Y, Yanagisawa S, Yamaya M, Sugiura H, et al. Oxidative stress enhances the expression of IL-33 in human airway epithelial cells. *Respir Res.* (2018) 19(1):116.

13. Wechsler ME, Cox GP. Comment on: International ERS/ATS guidelines on definition, evaluation and treatment of severe asthma. *Eur Respir J.* (2014) 44:267–.

14. Boulet L-P. Airway remodeling in asthma. *Curr Opin Pulmonary Med.* (2018) 24:56–62.

15. Lefrançais E, Duval A, Mirey E, Roga S, Espinosa E, Cayrol C, et al. Central domain of IL-33 is cleaved by mast cell proteases for potent activation of group-2 innate lymphoid cells. *Proc Natl Acad Sci.* (2014) 111:15502–7.

16. Drake LY, Kita H. IL-33: biological properties, functions, and roles in airway disease. *Immunol Rev.* (2017) 278:173–84.

17. Glück J, Rymarczyk B, Jura-Szołtys E, Rogala B. Serum levels of interleukin 33 and its receptor ST2 in patients treated with subcutaneous allergen immunotherapy in intermittent allergic rhinitis. *Cent Eur J Immunol.* (2019) 44:214–7.

18. Schmitz J, Owyang A, Oldham E, Song Y, Murphy E, McClanahan TK, et al. IL-33, an interleukin-1-like cytokine that signals via the IL-1 receptor-related protein ST2 and induces T helper type 2-associated cytokines. *Immunity.* (2005) 23:479–90.

19. Gurram RK, Wei D, Yu Q, Butcher MJ, Chen X, Cui K, et al. Crosstalk between ILC2s and Th2 cells varies among mouse models. *Cell Rep.* (2023) 42(2):112073.

20. Endo Y, Hirahara K, Iinuma T, Shinoda K, Tumes DJ, Asou HK, et al. The interleukin-33-p38 kinase axis confers memory T helper 2 cell pathogenicity in the airway. *Immunity.* (2015) 42:294–308.

21. Harker JA, Lloyd CM. T helper 2 cells in asthma. *J Exp Med.* (2023) 220(6): e20221094.

22. Nakajima T, Kanno T, Yokoyama S, Sasamoto S, Asou HK, Tumes DJ, et al. ACC1-expressing pathogenic T helper 2 cell populations facilitate lung and skin inflammation in mice. *J Exp Med.* (2021) 218:e20210639.

23. Pichery M, Mirey E, Mercier P, Lefrancais E, Dujardin A, Ortega N, et al. Endogenous IL-33 is highly expressed in mouse epithelial barrier tissues, lymphoid organs, brain, embryos, and inflamed tissues: *in situ* analysis using a novel il-33–lacZ gene trap reporter strain. *J Immunol.* (2012) 188:3488–95.

24. Kouzaki H, Iijima K, Kobayashi T, O'Grady SM, Kita H. The danger signal, extracellular ATP, is a sensor for an airborne allergen and triggers IL-33 release and innate th2-type responses. *J Immunol.* (2011) 186:4375–87.

25. Hristova M, Habibovic A, Veith C, Janssen-Heininger YMW, Dixon AE, Geiszt M, et al. Airway epithelial dual oxidase 1 mediates allergen-induced IL-33 secretion and activation of type 2 immune responses. *J Allergy Clin Immunol.* (2016) 137:1545–56.e11.

26. Cayrol C, Girard JP. The IL-1-like cytokine IL-33 is inactivated after maturation by caspase-1. *Proc Natl Acad Sci.* (2009) 106:9021–6.

27. Lefrançais E, Roga S, Gautier V, Gonzalez-de-Peredo A, Monsarrat B, Girard J-P, et al. IL-33 is processed into mature bioactive forms by neutrophil elastase and cathepsin G. *Proc Natl Acad Sci.* (2012) 109:1673–8.

28. Lefrançais E, Cayrol C. Mechanisms of IL-33 processing and secretion: differences and similarities between IL-1 family members. *Eur Cytokine Network.* (2012) 23:120–7.

29. Yu H, Lin L, Zhang Z, Zhang H, Hu H. Targeting NF-κB pathway for the therapy of diseases: mechanism and clinical study. *Signal Transduction Targeted Ther.* (2020) 5 (1):209.

30. Qin Z, Xie L, Li W, Wang C, Li Y. New insights into mechanisms traditional chinese medicine for allergic rhinitis by regulating inflammatory and oxidative stress pathways. *J Asthma Allergy.* (2024) 17:97–112.

31. Guo LY, Hung TM, Bae KH, Shin EM, Zhou HY, Hong YN, et al. Anti-inflammatory effects of schisandrin isolated from the fruit of Schisandra chinensis Baill. *Eur J Pharmacol.* (2008) 591:293–9.

32. Sun S-C. Non-canonical NF-κB signaling pathway. *Cell Res.* (2010) 21:71–85.

33. Cildir G, Low KC, Tergaonkar V. Noncanonical NF-κB signaling in health and disease. *Trends Mol Med.* (2016) 22:414–29.

34. Lawrence T. The nuclear factor NF- B pathway in inflammation. *Cold Spring Harbor Perspect Biol.* (2009) 1:a001651–a.

35. Sun SC. The non-canonical NF-κB pathway in immunity and inflammation. *Nat Rev Immunol.* (2017) 17:545–58.

36. Hayden MS, Ghosh S. Shared principles in NF-κB signaling. *Cell.* (2008) 132:344–62.

37. Israel A. The IKK complex, a central regulator of NF- B activation. *Cold Spring Harbor Perspect Biol.* (2009) 2:a000158–a.

38. Chen F, Castranova V, Shi X, Demers LM. New insights into the role of nuclear factor-κB, a ubiquitous transcription factor in the initiation of diseases. *Clin Chem.* (1999) 45:7–17.

39. Wu Y, Su SA, Xie Y, Shen J, Zhu W, Xiang M. Murine models of vascular endothelial injury: Techniques and pathophysiology. *Thromb Res.* (2018) 169:64–72.

40. Dejardin E. The alternative NF-κB pathway from biochemistry to biology: Pitfalls and promises for future drug development. *Biochem Pharmacol.* (2006) 72:1161–79.

41. Gao X, Li N, Zhang J. SB203580, a p38MAPK inhibitor, attenuates olfactory dysfunction by inhibiting OSN apoptosis in AR mice (activation and involvement of the p38 mitogen-activated protein kinase in olfactory sensory neuronal apoptosis of OVA-induced allergic rhinitis). *Brain Behavior.* (2019) 9(6):e01295.

42. Liu J, Liu L, Cui Y, Zhang J, Jiang H. p38 MAPK regulates Th2 cytokines release in PBMCs in allergic rhinitis rats. *J Huazhong Univ Sci Technol [Medical Sciences].* (2010) 30:222–5.

43. Ochayon DE, Ali A, Alarcon PC, Krishnamurthy D, Kottyan LC, Borchers MT, et al. IL-33 promotes type 1 cytokine expression via p38 MAPK in human NK cells. *J Leukocyte Biol.* (2020) 107:663–71.

44. Xiao Q, Song Y, Chu H, Tang M, Jiang J, Meng Q, et al. 1,4NQ-BC enhances Lung Inflammation by mediating secretion IL-33 which derived macrophages. *Environ pollut.* (2020) 265(Pt A):114729.

45. Shang J, Zhao J, Wu X, Xu Y, Xie J, Zhao J. Interleukin-33 promotes inflammatory cytokine production in chronic airway inflammation. *Biochem Cell Biol.* (2015) 93:359–66.

46. Zhang Y, Liu B, Chen X, Zhang N, Li G, Zhang L-H, et al. Naringenin ameliorates behavioral dysfunction and neurological deficits in a d-galactose-induced aging mouse model through activation of PI3K/akt/nrf2 pathway. *Rejuvenation Res.* (2017) 20:462–72.

47. Xi YD, Yu HL, Ding J, Ma WW, Yuan LH, Feng JF, et al. Flavonoids protect cerebrovascular endothelial cells through Nrf2 and PI3K from β-amyloid peptide-induced oxidative damage. *Curr neurovascular Res.* (2012) 9:32–41.

48. Zhao M, Tang X, Gong D, Xia P, Wang F, Xu S. Bungeanum improves cognitive dysfunction and neurological deficits in D-galactose-induced aging mice via activating PI3K/akt/nrf2 signaling pathway. *Front Pharmacol.* (2020) 11.

49. Meng M, Zhang L, Ai D, Wu H, Peng W. [amp]]beta;-asarone ameliorates β-amyloid–induced neurotoxicity in PC12 cells by activating P13K/akt/nrf2 signaling pathway. *Front Pharmacol.* (2021) 12.

50. Hsueh KC, Lin YJ, Lin HC, Lin CY. Serum leptin and adiponectin levels correlate with severity of allergic rhinitis. *Pediatr Allergy Immunol.* (2010) 21(1-Part-II):e155-9.

51. Ciprandi G, De Amici M, Tosca MA, Marseglia G. Serum leptin levels depend on allergen exposure in patients with seasonal allergic rhinitis. *Immunol Investigations.* (2009) 38:681–9.

52. Matarese G, Moschos S, Mantzoros CS. Leptin in immunology. *J Immunol.* (2005) 174:3137–42.

53. Zeng Q, Luo X, Tang Y, Liu W, Luo R. Leptin regulated ILC2 cell through the PI3K/AKT pathway in allergic rhinitis. *Mediators Inflammation.* (2020) 2020:1–9.

54. Kamekura R, Kojima T, Takano K, Go M, Sawada N, Himi T. The role of IL-33 and its receptor ST2 in human nasal epithelium with allergic rhinitis. *Clin Exp Allergy.* (2011) 42:218–28.

55. Pace E, Di Sano C, Sciarrino S, Scafidi V, Ferraro M, Chiappara G, et al. Cigarette smoke alters IL-33 expression and release in airway epithelial cells. *Biochim Biophys Acta (BBA) - Mol Basis Disease.* (2014) 1842:1630–7.

56. Wang W, Li Y, Lv Z, Chen Y, Li Y, Huang K, et al. Bronchial allergen challenge of patients with atopic asthma triggers an alarmin (IL-33, TSLP, and IL-25) response in the airways epithelium and submucosa. *J Immunol.* (2018) 201:2221–31.

57. Iijima K, Kobayashi T, Hara K, Kephart GM, Ziegler SF, McKenzie AN, et al. IL-33 and thymic stromal lymphopoietin mediate immune pathology in response to chronic airborne allergen exposure. *J Immunol.* (2014) 193:1549–59.

58. Anderson EL, Kobayashi T, Iijima K, Bartemes KR, Chen CC, Kita H. IL-33 mediates reactive eosinophilopoiesis in response to airborne allergen exposure. *Allergy.* (2016) 71:977–88.

59. Gordon ED, Simpson LJ, Rios CL, Ringel L, Lachowicz-Scroggins ME, Peters MC, et al. Alternative splicing of interleukin-33 and type 2 inflammation in asthma. *Proc Natl Acad Sci.* (2016) 113:8765–70.

60. van der Ploeg EK, Krabbendam L, Vroman H, van Nimwegen M, de Bruijn MJW, de Boer GM, et al. Type-2 CD8+ T-cell formation relies on interleukin-33 and is linked to asthma exacerbations. *Nat Commun.* (2023) 14:5137.

61. Khumalo J, Kirstein F, Hadebe S, Brombacher F. IL-4Rα signaling in CD4+ CD25+ FoxP3+ T regulatory cells restrains airway inflammation via limiting local tissue IL-33. *JCI insight;.* (2020) 5:e136206.

62. Badrani JH, Strohm AN, Lacasa L, Civello B, Cavagnero K, Haung YA, et al. RNA-binding protein RBM3 intrinsically suppresses lung innate lymphoid cell activation and inflammation partially through CysLT1R. *Nat Commun.* (2022) 13:4435.

63. Werder RB, Ullah MA, Rahman MM, Simpson J, Lynch JP, Collinson N, et al. Targeting the P2Y13 receptor suppresses IL-33 and HMGB1 release and ameliorates experimental asthma. *Am J Respir Crit Care Med.* (2022) 205:300–12.

64. Mathä L, Romera-Hernández M, Steer CA, Yin YH, Orangi M, Shim H, et al. Migration lung resident group 2 innate lymphoid cells link allergic lung inflammation liver immunity. *Front Immunol.* (2021) 12:679509.

65. Mahmutovic Persson I, Akbarshahi H, Menzel M, Brandelius A, Uller L. Increased expression of upstream TH2-cytokines in a mouse model of viral-induced asthma exacerbation. *J Trans Med.* (2016) 14:52.

66. Akoto C, Willis A, Banas C, Bell J, Bryant D, Blume C, et al. IL-33 induces an antiviral signature in mast cells but enhances their permissiveness for human rhinovirus infection. *Viruses.* (2022) 14:2430.

67. Verheijden KAT, Akbari P, Willemsen LEM, Kraneveld AD, Folkerts G, Garssen J, et al. Inflammation-induced expression of the alarmin interleukin 33 can be suppressed by galacto-oligosaccharides. *Int Arch Allergy Immunol.* (2015) 167:127–36.

68. Jackson DJ, Makrinioti H, Rana BM, Shamji BW, Trujillo-Torralbo MB, Footitt J, et al. IL-33–dependent type 2 inflammation during rhinovirus-induced asthma exacerbations in vivo. *Am J Respir Crit Care Med.* (2014) 190:1373–82.

69. Beale J, Jayaraman A, Jackson DJ, Macintyre JDR, Edwards MR, Walton RP, et al. Rhinovirus-induced IL-25 in asthma exacerbation drives type 2 immunity and allergic pulmonary inflammation. *Sci Trans Med.* (2014) 6:256ra134–256ra134.

70. Sismanopoulos N, Delivanis DA, Mavrommati D, Hatziagelaki E, Conti P, Theoharides TC. Do mast cells link obesity and asthma? *Allergy.* (2012) 68:8–15.

71. Eifan AO, Durham SR. Pathogenesis of rhinitis. *Clin Exp Allergy.* (2016) 46:1139–51.

72. Fan D, Wang X, Wang M, Wang Y, Zhang L, Li Y, et al. Allergen-dependent differences in ILC2s frequencies in patients with allergic rhinitis. *Allergy Asthma Immunol Res.* (2016) 8:216–22.

73. Campion NJ, Villazala-Merino S, Thwaites RS, Stanek V, Killick H, Pertsinidou E, et al. Nasal IL-13 production identifies patients with late-phase allergic responses. *J Allergy Clin Immunol.* (2023) 152:1167–78.e12.

74. Leaker BR, Malkov VA, Mogg R, Ruddy MK, Nicholson GC, Tan AJ, et al. The nasal mucosal late allergic reaction to grass pollen involves type 2 inflammation (IL-5 and IL-13), the inflammasome (IL-1β), and complement. *Mucosal Immunol.* (2017) 10:408–20.

75. Li J, Zhang Y, Zhang L. Discovering susceptibility genes for allergic rhinitis and allergy using a genome-wide association study strategy. *Curr Opin Allergy Clin Immunol.* (2015) 15:33–40.

76. Falahi S, Mortazavi SHR, Salari F, Koohyanizadeh F, Rezaeimanesh A, Gorgin Karaji A. Association between IL-33 gene polymorphism (Rs7044343) and risk of allergic rhinitis. *Immunol Investigations.* (2020) 51:29–39.

77. Li Z, Zou W, Sun J, Zhou S, Zhou Y, Cai X, et al. A comprehensive gene expression profile of allergic rhinitis-derived nasal fibroblasts and the potential mechanism for its phenotype. *Hum Exp Toxicol.* (2022) 41:9603271211069038.

78. Abbasi R, Zomorodian K, Zare Shahrabadi Z, Saadat F, Nabavizadeh SH, Esmaeilzadeh H, et al. IL-25 and IL-33 serum levels are not associated with the type of allergen causing allergic rhinitis. *Iranian J Immunol.* (2019) 16:321–6.

79. Spazierer D, Skvara H, Dawid M, Fallahi N, Gruber K, Rose K, et al. T helper 2 biased *de novo* immune response to Keyhole Limpet Hemocyanin in humans. *Clin Exp Allergy.* (2009) 39:999–1008.

80. Schiffers C, Lundblad LKA, Hristova M, Habibovic A, Dustin CM, Daphtary N, et al. Downregulation of DUOX1 function contributes to aging-related impairment of innate airway injury responses and accelerated senile emphysema. *Am J Physiology-Lung Cell Mol Physiol.* (2021) 321:L144–L58.

81. Lee JH, Hailey KL, Vitorino SA, Jennings PA, Bigby TD, Breen EC. Cigarette smoke triggers IL-33–associated inflammation in a model of late-stage chronic obstructive pulmonary disease. *Am J Respir Cell Mol Biol.* (2019) 61:567–74.

82. Qiu C, Li Y, Li M, Li M, Liu X, McSharry C, et al. Anti-interleukin-33 inhibits cigarette smoke-induced lung inflammation in mice. *Immunology.* (2012) 138:76–82.

83. Gao Y, Fu Y, Chen X, Li Z, He X, Li X. IL-33 up-regulates eIF3a expression by activating NF-κB signaling pathway to mediate the proliferation and differentiation of mouse pulmonary myofibroblasts and aggravate pulmonary fibrosis. *Xi Bao Yu Fen Zi Mian Yi Xue Za Zhi.* (2023) 39:693–700.

84. Xu X, Zhang J, Dai H. IL-25/IL-33/TSLP contributes to idiopathic pulmonary fibrosis: Do alveolar epithelial cells and (myo)fibroblasts matter? *Exp Biol Med.* (2020) 245:897–901.

85. Zhang J, Qiu J, Zhou W, Cao J, Hu X, Mi W, et al. Neuropilin-1 mediates lung tissue-specific control of ILC2 function in type 2 immunity. *Nat Immunol.* (2022) 23:237–50.

86. Di Carmine S, Scott MM, McLean MH, McSorley HJ. The role of interleukin-33 in organ fibrosis. *Discovery Immunol.* (2022) 1:kyac006.

87. Yi X-M, Li M, Chen Y-D, Shu H-B, Li S. Reciprocal regulation of IL-33 receptor–mediated inflammatory response and pulmonary fibrosis by TRAF6 and USP38. *Proc Natl Acad Sci.* (2022) 119(10):e2116279119.

88. Luzina IG, Lockatell V, Courneya J-P, Mei Z, Fishelevich R, Kopach P, et al. Full-length IL-33 augments pulmonary fibrosis in an ST2- and Th2-independent, non-transcriptomic fashion. *Cell Immunol.* (2023) 383:104657.

89. Nie Y, Zhai X, Li J, Sun A, Che H, Christman JW, et al. NFATc3 promotes pulmonary inflammation and fibrosis by regulating production of CCL2 and CXCL2 in macrophages. *Aging Dis.* (2023) 14:1441–57.

90. Lee J-U, Chang HS, Lee HJ, Jung CA, Bae DJ, Song HJ, et al. Upregulation of interleukin-33 and thymic stromal lymphopoietin levels in the lungs of idiopathic pulmonary fibrosis. *BMC Pulmonary Med.* (2017) 17(1):39.

91. Fanny M, Nascimento M, Baron L, Schricke C, Maillet I, Akbal M, et al. The IL-33 receptor ST2 regulates pulmonary inflammation and fibrosis to bleomycin. *Front Immunol.* (2018) 9.

92. Majewski S, Tworek D, Szewczyk K, Kurmanowska Z, Antczak A, Górski P, et al. Epithelial alarmin levels in exhaled breath condensate in patients with idiopathic pulmonary fibrosis: A pilot study. *Clin Respir J.* (2019) 13:652–6.

93. Luzina IG, Kopach P, Lockatell V, Kang PH, Nagarsekar A, Burke AP, et al. Interleukin-33 potentiates bleomycin-induced lung injury. *Am J Respir Cell Mol Biol.* (2013) 49:999–1008.

94. Stephenson KE, Porte J, Kelly A, Wallace WA, Huntington CE, Overed-Sayer CL, et al. The IL-33:ST2 axis is unlikely to play a central fibrogenic role in idiopathic pulmonary fibrosis. *Respir Res.* (2023) 24(1):89.

95. Fleischmajer R, Perlish JS, Reeves JR. Cellular infiltrates in scleroderma skin. *Arthritis Rheumatol.* (1977) 20:975–84.

96. Scharffetter K, Lankat-Buttgereit B, Krieg T. Localization of collagen mRNA in normal and scleroderma skin by *in-situ* hybridization. *Eur J Clin Invest.* (1988) 18:9–17.

97. Yanaba K, Yoshizaki A, Asano Y, Kadono T, Sato S. Serum IL-33 levels are raised in patients with systemic sclerosis: association with extent of skin sclerosis and severity of pulmonary fibrosis. *Clin Rheumatol.* (2011) 30:825–30.

98. Versace AG, Bitto A, Ioppolo C, Aragona CO, La Rosa D, Roberts WN, et al. IL-13 and IL-33 serum levels are increased in systemic sclerosis patients with interstitial lung disease. *Front Med.* (2022) 9.

99. Cook DP, Thomas CM, Wu AY, Rusznak M, Zhang J, Zhou W, et al. Cystic fibrosis reprograms airway epithelial IL-33 release and licenses IL-33–dependent inflammation. *Am J Respir Crit Care Med.* (2023) 207:1486–97.

100. Wang Y, Cheng D, Li Z, Sun W, Zhou S, Peng L, et al. IL33-mediated NPM1 promotes fibroblast-to-myofibroblast transition via ERK/AP-1 signaling in silica-induced pulmonary fibrosis. *Toxicol Sci.* (2023) 195:71–86.

101. Liu Q, Dwyer GK, Zhao Y, Li H, Mathews LR, Chakka AB, et al. IL-33-mediated IL-13 secretion by ST2+ Treg controls inflammation after lung injury. *JCI Insight*. (2019) 4:e123919.

102. Zou L, Dang W, Tao Y, Zhao H, Yang B, Xu X, et al. The il-33/st2 axis promotes acute respiratory distress syndrome by natural killer T cells. *Shock*. (2023) 59:902–11.

103. Lewis BW, Vo T, Choudhary I, Kidder A, Bathula C, Ehre C, et al. Ablation of IL-33 suppresses th2 responses but is accompanied by sustained mucus obstruction in the scnn1b transgenic mouse model. *J Immunol*. (2020) 204:1650–60.

104. Drake LY, Koloko Ngassie ML, Roos BB, Teske JJ, Prakash YS. Asthmatic lung fibroblasts promote type 2 immune responses via endoplasmic reticulum stress response dependent thymic stromal lymphopoietin secretion. *Front Physiol*. (2023) 14.

105. Vos T, Abajobir AA, Abate KH, Abbafati C, Abbas KM, Abd-Allah F, et al. Global, regional, and national incidence, prevalence, and years lived with disability for 328 diseases and injuries for 195 countries, 1990–2016: a systematic analysis for the Global Burden of Disease Study 2016. *Lancet*. (2017) 390:1211–59.

106. Schatz M, Camargo CA. The relationship of sex to asthma prevalence, health care utilization, and medications in a large managed care organization. *Ann allergy Asthma Immunol*. (2003) 91:553–8.

107. Wang E, Wechsler ME, Tran TN, Heaney LG, Jones RC, Menzies-Gow AN, et al. Characterization of severe asthma worldwide. *Chest*. (2020) 157:790–804.

108. Reddel HK, Bacharier LB, Bateman ED, Brightling CE, Brusselle GG, Buhl R, et al. Global initiative for asthma strategy 2021: executive summary and rationale for key changes. *Am J Respir Crit Care Med*. (2022) 205:17–35.

109. Chowdhury NU, Guntur VP, Newcomb bnd DC, Wechsler ME. Sex and gender in asthma. *Eur Respir Review*. (2021) 30(20):210067.

110. Romieu I. Fruit and vegetable intakes and asthma in the E3N study. *Thorax*. (2006) 61:209–15.

111. Uddenfeldt M, Janson C, Lampa E, Leander M, Norbäck D, Larsson L, et al. High BMI is related to higher incidence of asthma, while a fish and fruit diet is related to a lower–. *Respir Med*. (2010) 104:972–80.

112. Knekt P, Kumpulainen J, Järvinen R, Rissanen H, Heliövaara M, Reunanen A, et al. Flavonoid intake and risk of chronic diseases. *Am J Clin Nutr*. (2002) 76:560–8.

113. Talaei M, Hughes DA, Mahmoud O, Emmett PM, Granell R, Guerra S, et al. Dietary intake of vitamin A, lung function and incident asthma in childhood. *Eur Respir J*. (2021) 58:2004407.

114. García-García C, Kim M, Baik I. Associations of dietary vitamin A and C intake with asthma, allergic rhinitis, and allergic respiratory diseases. *Nutr Res Practice*. (2023) 17:997–1006.

115. Jolliffe DA, Stefanidis C, Wang Z, Kermani NZ, Dimitrov V, White JH, et al. Vitamin D metabolism is dysregulated in asthma and chronic obstructive pulmonary disease. *Am J Respir Crit Care Med*. (2020) 202:371–82.

116. Zhu S, Zhong S, Cheng K, Zhang L-S, J-w B, Cao Z, et al. Vitamin B6 regulates IL-33 homeostasis to alleviate type 2 inflammation. *Cell Mol Immunol*. (2023) 20:794–807.

117. Zhu G, Cai H, Ye L, Mo Y, Zhu M, Zeng Y, et al. Small proline-rich protein 3 regulates IL-33/ILC2 axis to promote allergic airway inflammation. *Front Immunol*. (2022) 12.

118. Shinoda K, Choe A, Hirahara K, Kiuchi M, Kokubo K, Ichikawa T, et al. Nematode ascarosides attenuate mammalian type 2 inflammatory responses. *Proc Natl Acad Sci*. (2022) 119:e2108686119.

119. Zhang K, Feng Y, Liang Y, Wu W, Chang C, Chen D, et al. Epithelial microRNA-206 targets CD39/extracellular ATP to upregulate airway IL-25 and TSLP in type 2-high asthma. *JCI Insight*. (2021) 6:e148103.

120. Galvão JGFM, Cavalcante-Silva LHA, de Almeida Lima É, Carvalho DCM, Alves AF, Mascarenhas SR. Ouabain modulates airway remodeling caused by Th2-high asthma in mice. *Int Immunopharmacology*. (2022) 109:108808.

121. Won J, Gil CH, Jo A, Kim HJ. Inhaled delivery of Interferon-lambda restricts epithelial-derived Th2 inflammation in allergic asthma. *Cytokine*. (2019) 119:32–6.

122. Huang X, Yu H, Xie C, Zhou Y-L, Chen M-M, Shi H-L, et al. Louki Zupa decoction attenuates the airway inflammation in acute asthma mice induced by ovalbumin through IL-33/ST2-NF-κB/GSK3β/mTOR signalling pathway. *Pharm Biol*. (2022) 60:1520–32.

123. Wuniqiemu T, Teng F, Qin J, lv Y, Nabijan M, Luo Q, et al. Iristectorigenin A exerts novel protective properties against airway inflammation and mucus hypersecretion in OVA-induced asthmatic mice. *Phytomedicine*. (2022) 104:154252.

124. Huang Y, Li X, Zhu L, Huang C, Chen W, Ling Z, et al. Thrombin cleaves IL-33 and modulates IL-33-activated allergic lung inflammation. *Allergy*. (2022) 77:2104–20.

125. Du X, Li C, Wang W, Huang Q, Wang J, Tong Z, et al. IL-33 induced airways Inflammation is partially dependent IL-9. *Cell Immunol*. (2020) 352:104098.

126. Kimata M, Shichijo M, Miura T, Serizawa I, Inagaki N, Nagai H. Effects of luteolin, quercetin and baicalein on immunoglobulin E-mediated mediator release from human cultured mast cells. *Clin Exp Allergy*. (2000) 30:501–8.

127. Kempuraj D, Madhappan B, Christodoulou S, Boucher W, Cao J, Papadopoulou N, et al. Flavonols inhibit proinflammatory mediator release, intracellular calcium ion levels and protein kinase C theta phosphorylation in human mast cells. *Br J Pharmacol*. (2009) 145:934–44.

128. Perkins TN, Oczypok EA, Milutinovic PS, Dutz RE, Oury TD. RAGE-dependent VCAM-1 expression in the lung endothelium mediates IL-33-induced allergic airway inflammation. *Allergy*. (2018) 74:89–99.

129. Boberg E, Weidner J, Malmhäll C, Calvén J, Corciulo C, Rådinger M. Rapamycin dampens inflammatory properties of bone marrow ILC2s in IL-33-induced eosinophilic airway inflammation. *Front Immunol*. (2022) 13.

130. Xiao Q, Han X, Liu G, Zhou D, Zhang L, He J, et al. Adenosine restrains ILC2-driven allergic airway inflammation via A2A receptor. *Mucosal Immunol*. (2022) 15:338–50.

131. Toki S, Newcomb DC, Printz RL, Cahill KN, Boyd KL, Niswender KD, et al. Glucagon-like peptide-1 receptor agonist inhibits aeroallergen-induced activation of ILC2 and neutrophilic airway inflammation in obese mice. *Allergy*. (2021) 76:3433–45.

132. Cavagnero KJ, Badrani JH, Naji LH, Amadeo MB, Leng AS, Lacasa LD, et al. Cyclic-di-GMP induces STING-dependent ILC2 to ILC1 shift during innate type 2 lung inflammation. *Front Immunol*. (2021) 12.

133. Yang Q, Kong L, Huang W, Mohammadtursun N, Li X, Wang G, et al. Osthole attenuates ovalbumin–induced lung inflammation via the inhibition of IL–33/ST2 signaling in asthmatic mice. *Int J Mol Med*. (2020) 46:1389–98.

134. Schröder A, Lunding LP, Zissler UM, Vock C, Webering S, Ehlers JC, et al. IL-37 regulates allergic inflammation by counterbalancing pro-inflammatory IL-1 and IL-33. *Allergy*. (2021) 77:856–69.

135. Gauvreau GM, Bergeron C, Boulet LP, Cockcroft DW, Côté A, Davis BE, et al. Sounding the alarmins—The role of alarmin cytokines in asthma. *Allergy*. (2022) 78:402–17.

136. Wechsler ME, Ruddy MK, Pavord ID, Israel E, Rabe KF, Ford LB, et al. Efficacy and safety of itepekimab in patients with moderate-to-severe asthma. *New Engl J Med*. (2021) 385:1656–68.

137. England E, Rees DG, Scott IC, Carmen S, Chan DTY, Chaillan Huntington CE, et al. Tozorakimab (MEDI3506): an anti-IL-33 antibody that inhibits IL-33 signalling via ST2 and RAGE/EGFR to reduce inflammation and epithelial dysfunction. *Sci Rep*. (2023) 13:9825.

138. Vannella KM, Ramalingam TR, Borthwick LA, Barron L, Hart KM, Thompson RW, et al. Combinatorial targeting of TSLP, IL-25, and IL-33 in type 2 cytokine–driven inflammation and fibrosis. *Sci Trans Med*. (2016) 8:337ra65–337ra65.

139. Alvaro-Lozano M, Akdis CA, Akdis M, Alviani C, Angier E, Arasi S, et al. Allergen immunotherapy in children user's guide. *Pediatr Allergy Immunol*. (2020) 31:1–101.

140. Wang Z, Peng H, Rao K. The secondary prevention effect and influenceon serum slgG4, lL-27 and lL-33 levels of subcutaneous immunotherapy inchildren with allergic rhinitis and cough variant asthmal. *Lin Chuang Er Bi Yan Hou Tou Jing Wai Ke Za Zhi*. (2020) 34:793–8.

141. Woehlk C, Ramu S, Sverrild A, Nieto-Fontarigo JJ, Vázquez-Mera S, Cerps S, et al. Allergen immunotherapy enhances airway epithelial antiviral immunity in patients with allergic asthma (VITAL study): A double-blind randomized controlled trial. *Am J Respir Crit Care Med*. (2023) 207:1161–70.

142. Wise SK, Damask C, Roland LT, Ebert C, Levy JM, Lin S, et al. International consensus statement on allergy and rhinology: Allergic rhinitis – 2023. *Int Forum Allergy Rhinology*. (2023) 13:293–859.

143. Kitano M, Fukuoka S, Adachi N, Hisamitsu T, Sunagawa M. Shoseiryuto ameliorated TDI-induced allergic rhinitis by suppressing IL-33 release from nasal epithelial cells. *Pharmaceutics*. (2022) 14:2083.

144. J-j Z, X-c He, Zhou M, Q-d L, W-z Xu, Y-j Y, et al. Xiao-qing-long-tang ameliorates OVA-induced allergic rhinitis by inhibiting ILC2s through the IL-33/ST2 and JAK/STAT pathways. *Phytomedicine*. (2023) 119:155012.

145. Islam R, Mizuguchi H, Shaha A, Nishida K, Yabumoto M, Ikeda H, et al. Effect of wild grape on the signaling of histamine H1 receptor gene expression responsible for the pathogenesis of allergic rhinitis. *J Med Invest*. (2018) 65:242–50.

146. Shaha A, Islam R, Tanaka N, Kashiwada Y, Fukui H, Takeda N, et al. Betuletol, a propolis component, suppresses IL-33 gene expression and effective against eosinophilia. *Molecules*. (2022) 27:5459.

147. Lu TX, Rothenberg ME. MicroRNA. *J Allergy Clin Immunol*. (2018) 141:1202–7.

148. Long S, Zhang H. MIR-181A-5P attenuates ovalbumin-induced allergic inflammation in nasal epithelial cells by targeting IL-33/P38 MAPK pathway. *Clin Invest Med*. (2021) 44:E31–8.

149. Jin J, Fan YJ, Nguyen TV, Yu ZN, Song CH, Lee S-Y, et al. Chaenomeles sinensis extract ameliorates ovalbumin-induced allergic rhinitis by inhibiting the IL-33/ST2 axis and regulating epithelial cell dysfunction. *Foods*. (2024) 13:611.

150. Jin J, Fan YJ, Nguyen TV, Yu ZN, Song CH, Lee S-Y, et al. Fallopia japonica root extract ameliorates ovalbumin-induced airway inflammation in a CARAS mouse model by modulating the IL-33/TSLP/NF-κB signaling pathway. *Int J Mol Sci*. (2023) 24(15):12514.

151. Tang G, Lan Y, Do B, Lu J, Yang K, Chai L, et al. Observation on the efficacy of sublingual immunotherapy with dust mite allergen for perennial allergic rhinitis and the mechanism of action on ILCs with ILC1s and ILC2s and ILC3s. *Medicine*. (2022) 101:e32019.

152. Baker JR, Rasky AJ, Landers JJ, Janczak KW, Totten TD, Lukacs NW, et al. Intranasal delivery of allergen in a nanoemulsion adjuvant inhibits allergen-specific reactions in mouse models of allergic airway disease. *Clin Exp Allergy*. (2021) 51:1361–73.

153. Nasr W, Sorour S, El Bahrawy A, Boghdadi G, El Shahaway A. The role of the level of interleukin-33 in the therapeutic outcomes of immunotherapy in patients with allergic rhinitis. *Int Arch Otorhinolaryngology*. (2017) 22:152–6.

154. Wang Y, Li C, Xu Y, Xu D, Yang G, Liao F, et al. Sublingual immunotherapy decreases expression of interleukin-33 in children with allergic rhinitis. *Indian J Pediatrics*. (2018) 85:872–6.

155. Pizzichini E, Pizzichini MM, Gibson P, Parameswaran K, Gleich GJ, Berman L, et al. Sputum eosinophilia predicts benefit from prednisone in smokers with chronic obstructive bronchitis. *Am J Respir Crit Care Med*. (1998) 158:1511–7.

156. Saha S, Brightling CE. Eosinophilic airway inflammation in COPD. *Int J chronic obstructive pulmonary disease*. (2006) 1:39–47.

157. Leigh R, Pizzichini MMM, Morris MM, Maltais F, Hargreave FE, Pizzichini E. Stable COPD: predicting benefit from high-dose inhaled corticosteroid treatment. *Eur Respir J*. (2006) 27:964–71.

158. Labaki WW, Rosenberg SR. Chronic obstructive pulmonary disease. *Ann Internal Med*. (2020) 173:ITC17–32.

159. Lee K, Choi J, Choi BK, Gu Y-M, Ryu HW, Oh S-R, et al. Picroside II Isolated from Pseudolysimachion rotundum var. subintegrum Inhibits Glucocorticoid Refractory Serum Amyloid A (SAA) Expression and SAA-induced IL-33 Secretion. *Molecules*. (2019) 24(10):2020.

160. Katz-Kiriakos E, Steinberg DF, Kluender CE, Osorio OA, Newsom-Stewart C, Baronia A, et al. Epithelial IL-33 appropriates exosome trafficking for secretion in chronic airway disease. *JCI Insight*. (2021) 6:e136166.

161. Rabe KF, Celli BR, Wechsler ME, Abdulai RM, Luo X, Boomsma MM, et al. Safety and efficacy of itepekimab in patients with moderate-to-severe COPD: a genetic association study and randomised, double-blind, phase 2a trial. *Lancet Respir Med*. (2021) 9:1288–98.

162. Yousuf AJ, Mohammed S, Carr L, Yavari Ramsheh M, Micieli C, Mistry V, et al. Astegolimab, an anti-ST2, in chronic obstructive pulmonary disease (COPD-ST2OP): a phase 2a, placebo-controlled trial. *Lancet Respir Med*. (2022) 10:469–77.

163. Reid F, Singh D, Albayaty M, Moate R, Jimenez E, Sadiq MW, et al. A randomized phase I study of the anti-interleukin-33 antibody tozorakimab in healthy adults and patients with chronic obstructive pulmonary disease. *Clin Pharmacol Ther*. (2024) 115:565–75.

164. Kadushkin A, Tahanovich A, Movchan L, Talabayeva E, Plastinina A, Shman T. Azithromycin modulates release of steroid-insensitive cytokines from peripheral blood mononuclear cells of patients with chronic obstructive pulmonary disease. *Adv Respir Med*. (2022) 90:17–27.

165. Saglani S, Lui S, Ullmann N, Campbell GA, Sherburn RT, Mathie SA, et al. IL-33 promotes airway remodeling in pediatric patients with severe steroid-resistant asthma. *J Allergy Clin Immunol*. (2013) 132:676–685.e13.

166. Mouratis MA, Aidinis V. Modeling pulmonary fibrosis with bleomycin. *Curr Opin Pulmonary Med*. (2011) 17:355–61.

167. Wynn TA, Ramalingam TR. Mechanisms of fibrosis: therapeutic translation for fibrotic disease. *Nat Med*. (2012) 18:1028–40.

168. Sedhom MAK, Pichery M, Murdoch JR, Foligné B, Ortega N, Normand S, et al. Neutralisation of the interleukin-33/ST2 pathway ameliorates experimental colitis through enhancement of mucosal healing in mice. *Gut*. (2013) 62:1714–23.

169. Zhiguang X, Wei C, Steven R, Wei D, Wei Z, Rong M, et al. Over-expression of IL-33 leads to spontaneous pulmonary inflammation in mIL-33 transgenic mice. *Immunol Letters*. (2010) 131:159–65.

170. Kurowska-Stolarska M, Stolarski B, Kewin P, Murphy G, Corrigan CJ, Ying S, et al. IL-33 amplifies the polarization of alternatively activated macrophages that contribute to airway inflammation. *J Immunol*. (2009) 183:6469–77.

171. Li B, Chen H, Yang X, Wang Y, Qin L, Chu Y. Knockdown of eIF3a ameliorates cardiac fibrosis by inhibiting the TGF-β1/Smad3 signaling pathway. *Cell Mol Biol (Noisy-le-grand)*. (2016) 62:97–101.

172. Zhang YF, Wang Q, Luo J, Yang S, Wang JL, Li HY. Knockdown of eIF3a inhibits collagen synthesis in renal fibroblasts via Inhibition of transforming growth factor-β1/Smad signaling pathway. *Int J Clin Exp Pathol*. (2015) 8:8983–9.

173. Park EJ, Park SW, Kim HJ, Kwak J-H, Lee D-U, Chang KC. Dehydrocostuslactone inhibits LPS-induced inflammation by p38MAPK-dependent induction of hemeoxygenase-1 in *vitro* and improves survival of mice in CLP-induced sepsis in vivo. *Int Immunopharmacol*. (2014) 22:332–40.

174. Singireesu SSNR, Mondal SK, Misra S, Yerramsetty S, K SB. Dehydrocostus lactone induces prominent apoptosis in kidney distal tubular epithelial cells and interstitial fibroblasts along with cell cycle arrest in ovarian epithelial cells. *Biomedicine Pharmacotherapy*. (2018) 99:956–69.

175. Yang M, Zhang J, Li Y, Han X, Gao K, Fang J. Bioassay-guided isolation of dehydrocostus lactone from Saussurea lappa: A new targeted cytosolic thioredoxin reductase anticancer agent. *Arch Biochem Biophysics*. (2016) 607:20–6.

176. Chakravortty D, Lee H-K, Song HE, Lee H-B, Kim C-S, Koketsu M, et al. Growth Inhibitory, Bactericidal, and Morphostructural Effects of Dehydrocostus Lactone from Magnolia sieboldii Leaves on Antibiotic-Susceptible and -Resistant Strains of Helicobacter pylori. *PloS One*. (2014) 9(4):e95530.

177. Jiang E, Sun X, Kang H, Sun L, An W, Yao Y, et al. Dehydrocostus lactone inhibits proliferation, antiapoptosis, and invasion of cervical cancer cells through PI3K/akt signaling pathway. *Int J Gynecologic Cancer*. (2015) 25:1179–86.

178. Xiong Y, Cui X, Zhou Y, Chai G, Jiang X, Ge G, et al. Dehydrocostus lactone inhibits BLM-induced pulmonary fibrosis and inflammation in mice via the JNK and p38 MAPK-mediated NF-κB signaling pathways. *Int Immunopharmacol*. (2021) 98:107780.

179. Ley B, Collard HR, King TE. Clinical course and prediction of survival in idiopathic pulmonary fibrosis. *Am J Respir Crit Care Med*. (2011) 183:431–40.

180. Adegunsoye A, Strek ME. Therapeutic approach to adult fibrotic lung diseases. *Chest*. (2016) 150:1371–86.

181. Zhao K, Zhao G-M, Wu D, Soong Y, Birk AV, Schiller PW, et al. Cell-permeable peptide antioxidants targeted to inner mitochondrial membrane inhibit mitochondrial swelling, oxidative cell death, and reperfusion injury. *J Biol Chem*. (2004) 279:34682–90.

182. da Silva Antunes R, Mehta AK, Madge L, Tocker J, Croft M. TNFSF14 (LIGHT) exhibits inflammatory activities in lung fibroblasts complementary to IL-13 and TGF-β. *Front Immunol*. (2018) 9.

183. Zheng Z, Li J, Cui Y, Wang W, Zhang M, Zhang Y, et al. IRAK-M regulates proliferative and invasive phenotypes of lung fibroblasts. *Inflammation*. (2022) 46:763–78.

184. Liang Y, Yang N, Pan G, Jin B, Wang S, Ji W. Elevated IL-33 promotes expression of MMP2 and MMP9 via activating STAT3 in alveolar macrophages during LPS-induced acute lung injury. *Cell Mol Biol Letters*. (2018) 23:52.

185. Lei M, C-j W, Yu F, Xie K, S-h L, Xu F. Different intensity of autophagy regulate interleukin-33 to control the uncontrolled inflammation of acute lung injury. *Inflammation Res*. (2019) 68:665–75.

186. Fu J, S-h L, C-j W, S-y Li, X-y F, Liu Q, et al. HMGB1 regulates IL-33 expression in acute respiratory distress syndrome. *Int Immunopharmacology*. (2016) 38:267–74.

187. Martínez-González I, Roca O, Masclans JR, Moreno R, Salcedo MT, Baekelandt V, et al. Human mesenchymal stem cells overexpressing the IL-33 antagonist soluble IL-1 receptor–like–1 attenuate endotoxin-induced acute lung injury. *Am J Respir Cell Mol Biol*. (2013) 49:552–62.

188. Liu G, Cooley MA, Nair PM, Donovan C, Hsu AC, Jarnicki AG, et al. Airway remodelling and inflammation in asthma are dependent on the extracellular matrix protein fibulin-1c. *J Pathology*. (2017) 243:510–23.

189. Nie Y, Li J, Zhai X, Wang Z, Wang J, Wu Y, et al. Elamipretide(SS-31) attenuates idiopathic pulmonary fibrosis by inhibiting the nrf2-dependent NLRP3 inflammasome in macrophages. *Antioxidants*. (2023) 12(12):2022.

frontiers | Frontiers in Immunology

TYPE Review
PUBLISHED 31 October 2024
DOI 10.3389/fimmu.2024.1460023

OPEN ACCESS

EDITED BY
Suraj P. Parihar,
University of Cape Town, South Africa

REVIEWED BY
Claudia Carranza,
National Institute of Respiratory Diseases-Mexico (INER), Mexico
Gagandeep Kaur,
University of Rochester Medical Center, United States

*CORRESPONDENCE
Zhongyu Han
hzyczy1997@163.com
Siyu Wang
Horizonwsy0222@126.com
Haoran Chen
chenhrrr@163.com

†These authors have contributed equally to this work

RECEIVED 05 July 2024
ACCEPTED 07 October 2024
PUBLISHED 31 October 2024

CITATION
Lin L, Lin Y, Han Z, Wang K, Zhou S, Wang Z, Wang S and Chen H (2024) Understanding the molecular regulatory mechanisms of autophagy in lung disease pathogenesis. *Front. Immunol.* 15:1460023. doi: 10.3389/fimmu.2024.1460023

Understanding the molecular regulatory mechanisms of autophagy in lung disease pathogenesis

Lin Lin[1†], Yumeng Lin[2†], Zhongyu Han[3,4*†], Ke Wang[5†], Shuwei Zhou[6], Zhanzhan Wang[7], Siyu Wang[8*] and Haoran Chen[4*]

[1]School of Medical and Life Sciences, Chengdu University of Traditional Chinese Medicine, Chengdu, China, [2]Nanjing Tongren Hospital, School of Medicine, Southeast University, Nanjing, China, [3]School of Medicine, Southeast University, Nanjing, China, [4]Science Education Department, Chengdu Xinhua Hospital Affiliated to North Sichuan Medical College, Chengdu, China, [5]Department of Science and Education, Deyang Hospital Affiliated Hospital of Chengdu University of Traditional Chinese Medicine, Deyang, China, [6]Department of Radiology, Zhongda Hospital, Nurturing Center of Jiangsu Province for State Laboratory of AI Imaging & Interventional Radiology, School of Medicine, Southeast University, Nanjing, China, [7]Department of Respiratory and Critical Care Medicine, The First People's Hospital of Lianyungang, Lianyungang, China, [8]Department of Preventive Medicine, Kunshan Hospital of Chinese Medicine, Kunshan, China

Lung disease development involves multiple cellular processes, including inflammation, cell death, and proliferation. Research increasingly indicates that autophagy and its regulatory proteins can influence inflammation, programmed cell death, cell proliferation, and innate immune responses. Autophagy plays a vital role in the maintenance of homeostasis and the adaptation of eukaryotic cells to stress by enabling the chelation, transport, and degradation of subcellular components, including proteins and organelles. This process is essential for sustaining cellular balance and ensuring the health of the mitochondrial population. Recent studies have begun to explore the connection between autophagy and the development of different lung diseases. This article reviews the latest findings on the molecular regulatory mechanisms of autophagy in lung diseases, with an emphasis on potential targeted therapies for autophagy.

KEYWORDS

autophagy, pulmonary diseases, apoptosis, autophagosome, COPD

Introduction

Pulmonary diseases, especially chronic pulmonary diseases, including chronic obstructive pulmonary disease (COPD), pulmonary tuberculosis (PTB), and lung cancer, pose significant threats to human health. Despite notable advancements in research globally in recent years, effective and precise treatments are still insufficient, leaving many lung diseases without a cure.

Autophagy is a common phenomenon in eukaryotic cells that fuses with lysosomes and hydrolyzes intramembrane components by encasing damaged or functionally degenerated organelles and certain proteins and certain macromolecules. Autophagy was first identified in the 1850s and named in 1963 by de Duve et al (1). Recent research has indicated that autophagy is important for maintaining cellular survival and homeostasis (2–4). Through the processing of metabolic precursors from cytoplasmic substrates, this process maintains homeostasis in healthy respiratory cells and ensures survival in conditions of nutrient scarcity (5). In nutrient deficiency, cells acquire nutrients through autophagy; damaged or senescent organelles can be removed by autophagy when cells are damaged or senescent; and these microorganisms or toxins can be cleared by autophagy when cells are infected by microorganisms or invaded by toxins. Eukaryotes have well-preserved degradation and recycling processes critical to maintaining cellular homeostasis and coping with stress. To some extent, autophagy is an effective mechanism to protect cells.

Autophagy is intricately associated with the clearance of organelles and, more significantly, plays a crucial part in the development and progression of various diseases. The relationship between autophagy and disease pathogenesis has not been fully confirmed. Nonetheless, a growing body of evidence indicates that autophagy may play a significant role in various human diseases (2, 6), including inflammatory diseases (7–9), cardiovascular diseases (10, 11), neurodegenerative diseases (12), and cancer (13) (Figure 1). Alterations in autophagic activities may also result from variations in the activation of proteins that regulate autophagy (2, 14). Until now, only limited studies have investigated the role of autophagy in lung disease Figure 2.

This review highlights the most recent developments in the molecular control and the role of autophagy in lung diseases. Additionally, we explore how autophagy-related proteins and regulatory processes may contribute to either the protection against or the advancement of human lung diseases, offering new insights for targeted treatment options.

Phases and classification of autophagy

Autophagy is essential for the process of protein degradation with relatively short half-lives. Morphologically, a significant quantity of dissociative membranous structures appears in the cytoplasm of cells that are about to undergo autophagy, which are called proautophagosomes. The proautophagosome gradually develops into a vacuole with a double membrane structure, which is surrounded by degraded organelles and some cytoplasm (2, 15). This double membrane structure is referred to as the autophagosome (2). Next, after autophagosomes fuse with lysosomes, the inner membranes and their encapsulated substances enter the lysosome and undergo hydrolysis by lysosome enzymes. The lysosomes found in this phagocyte are called autolysosomes. This process leads to the retrieval of soluble cytoplasmic proteins, mitochondria, peroxides, Golgi complexes, and portions of the endoplasmic reticulum, while some digested fragments are released into the cytoplasm for biosynthesis (3, 5, 16).

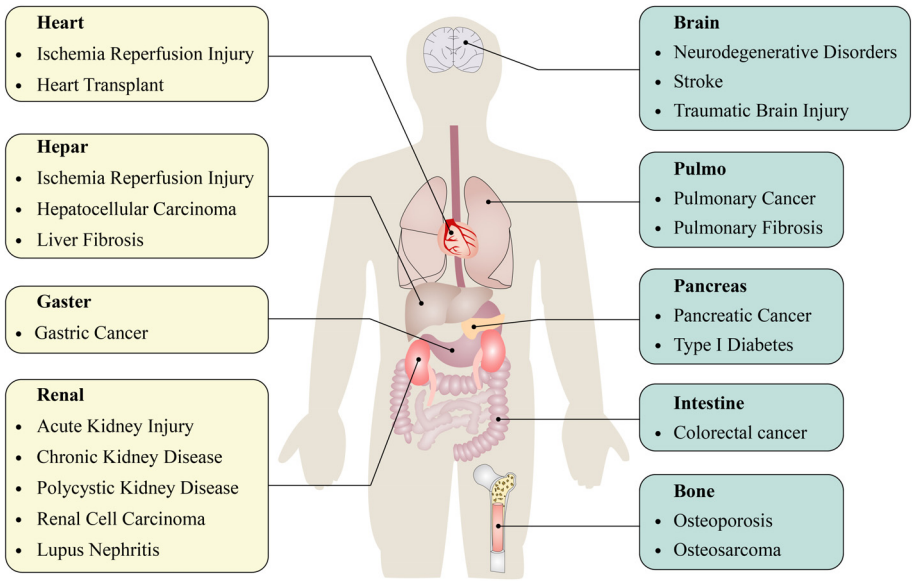

FIGURE 1
Autophagy is involved in the development and progression of multiple diseases.

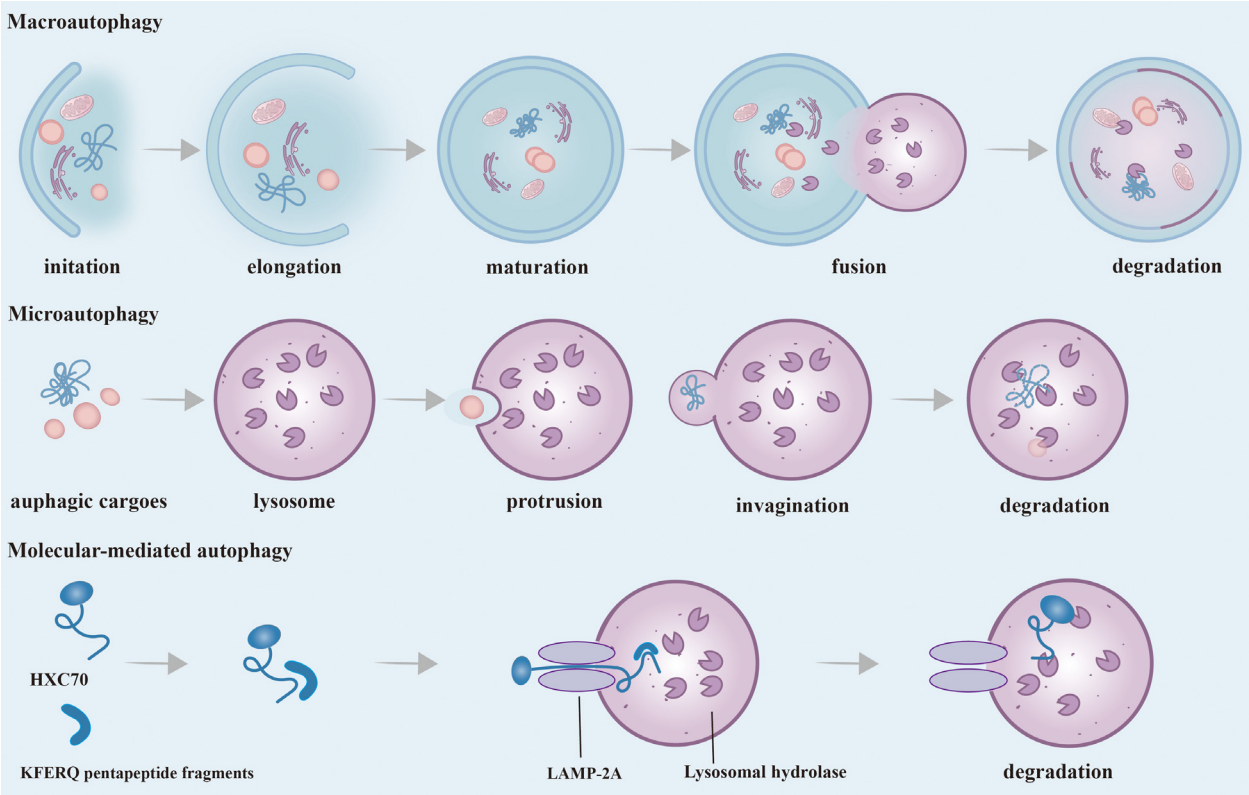

FIGURE 2
Phases and Classification of Autophagy. According to the different ways of transporting substrates to lysosomes, autophagy can be divided into three main ways: macroautophagy, microautophagy and CMA. Macroautophagy: It starts as autophagy-related substances accumulate around misfolded and aggregated proteins, pathogens, non-essential amino acids, etc. to form a barrier membrane. Dysfunctional organelles as well as proteins are surrounded by an isolation membrane and gradually form a bilayer membrane structure, called autophagosomes. The outer membrane of autophagosomes then fuses with lysosomes, and internal material is degraded in autolysosomes. Microautophagy: The process by which membranes of lysosomes encapsulate cargo by direct protrusion or invagination and are degraded in lysosomes. CMA: Substrate proteins containing the KFERQ-like pentapeptide sequence are first recognized by HSC70, then bind to LAMP-2A on the lysosomal membrane and enter the lysosome and eventually are degraded. CMA, Chaperone-mediated autophagy; HSC70, Heat shock cognate protein 70; LAMP-2A, Lysosomal membrane-associated protein 2A.

According to the different ways of transporting substrates to lysosomes, autophagy can be divided into three main ways: macroautophagy, microautophagy, and chaperone-mediated autophagy (CMA) (17). Macroautophagy is the most common autophagy in eukaryotic cells by forming a double-layer membrane around misfolded and aggregated protein pathogens, and non-essential amino acids, and fusing with lysosomes for degradation. Many stresses, such as nutritional deficiency, infection, oxidative stress, and toxic stimulation, can stimulate the occurrence of macroautophagy, which is generally referred to as autophagy. Different from macroautophagy, there is no formation process of autophagy membrane in microautophagy. A characteristic aspect is that the lysosome membrane is straight taken in by lysosomes and late endosomes via membrane protrusion and invagination, and it is then broken down within the endolysosomal lumen. During the dependent multivesicular body (MVB) formation, a significant quantity of cytoplasmic proteins is selectively integrated into the lumens of endosomes in substantial amounts (18). CMA represents a highly selective mechanism of autophagy with two core members: the heat shock cognate protein 70 (HSC70) and the lysosomal membrane-associated protein 2A (LAMP-2A). HSC70 is a molecular chaperone protein. The process of CMA degrades proteins that contain KFERQ pentapeptide fragments in the peptide chain. First, the heat shock protein HSC70 specifically recognizes and binds to proteins containing KFERQ five-peptide fragments, and transports the target protein into the lysosome for degradation through interaction with LAMP2A (17). Macroautophagy is considered to be the predominant form of autophagy compared to microautophagy and molecular-mediated autophagy, and this has also been the subject of extensive research. Therefore, what we usually call “autophagy” is macroautophage.

In addition, autophagy can be classified into selective autophagy, aggregative autophagy, and xenophagy, etc. Recent research has demonstrated that several denatured proteins, organelles, and certain bacteria can be selectively destroyed by autophagy. This process is called “selective autophagy”, the most representative of which is mitophagy (17, 19, 20). Mitophagy is a specific degradation targeting depolarized mitochondria (21). Xenophagy involves the digestion of extracellular components containing pathogens or bacteria that invade the body (22).

Molecular involvement in autophagy and molecular regulation

The process of autophagy is modulated and governed by various relative proteins. In mammalian cells, starvation-induced autophagy is regulated by approximately 20 core Atg genes (23). These gene products are persistently incorporated into vacuoles and assembled to construct pre-autophagosomes. In addition, the modification of microtubule-associated protein-1 light chain 3 (LC3) is an important step in forming autophagic vacuole. In autophagosomes, LC3 and its homologues act on autophagic substrates or proteins to facilitate the selection of autophagic cargoes (24).

The elongation stage of autophagosome formation relies on two ubiquitin-like conjugation systems (Figure 3), (2, 3). Besides the proteins mentioned in Figure 3, the maturation and fusion of autophagosomes also depend on various other proteins, such as small GTPases (like Rab7), class C Vps proteins, ultraviolet radioresistance-associated gene protein (UVRAG), and lysosome-associated membrane proteins (for instance, LAMP-2A) (25, 26). In recent years, additional proteins associated with autophagy have been progressively identified alongside the aforementioned proteins. In a complicated regulatory network, these proteins regulate the initiation and execution of autophagy (2, 27). We will describe this in detail in the following paragraphs (Figure 3).

Mammalian target of rapamycin signaling pathway

Many studies have demonstrated that mTOR negatively regulates autophagy in nutrient-rich environments (28). mTOR is

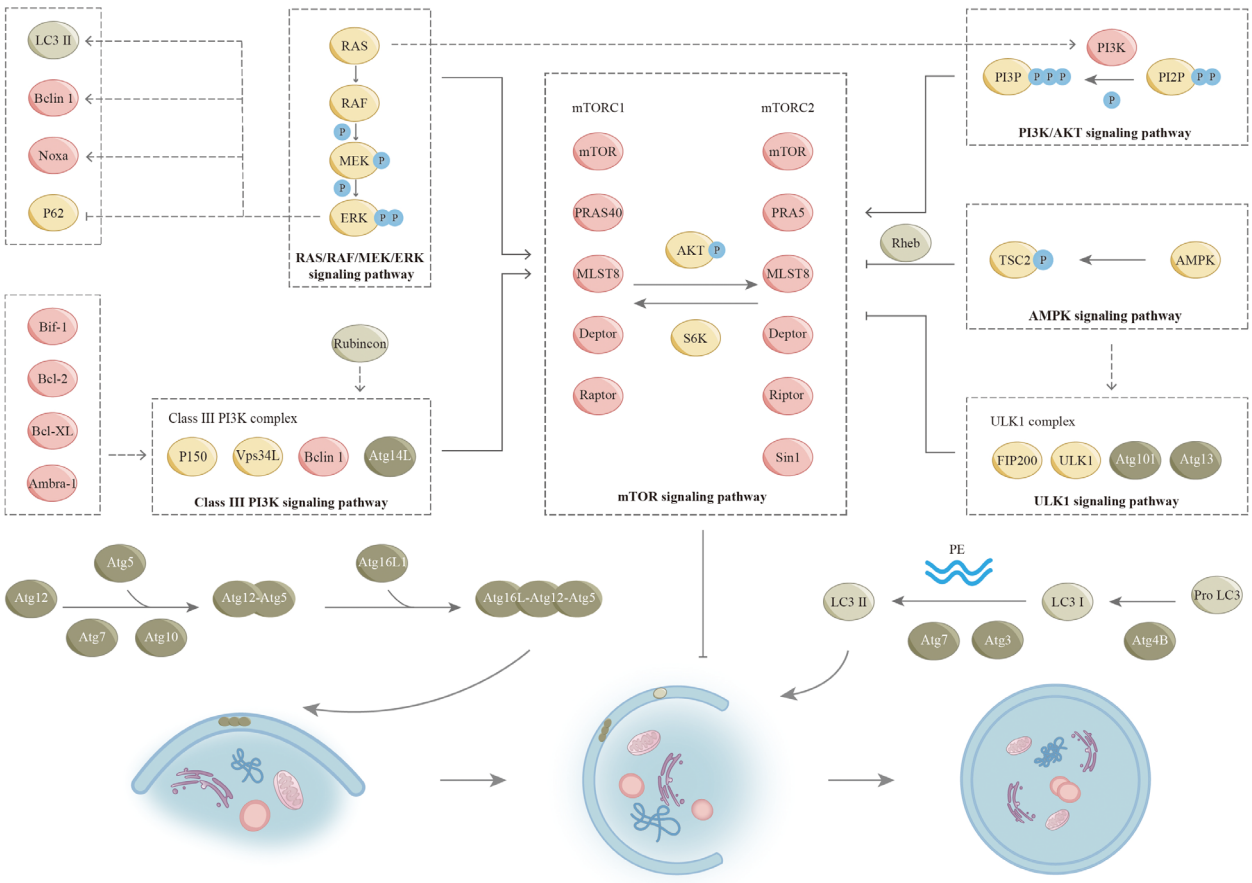

FIGURE 3
Signaling pathways for autophagy. The process of autophagy is regulated by many signaling pathways (as shown), and there is also complex crosstalk between various pathways. Two ubiquitin-like conjugation systems involved in the formation of autophagosome: In the first system, the ubiquitin-like protein Atg12 is enzymatically coupled to Atg5 by Atg7 (E1 ubiquitin-activating enzyme-like) and Atg10 (E2 ubiquitin-conjugating enzyme-like) to produce the Atg5-Atg12 complex. The Atg5-Atg12 complex interacts with Atg16L1 to form a complex that plays a role in the formation of autophagic membranes. As part of the maturation process, these factors are separated from autophagosomes. The second coupling system requires the ubiquitin-like protein LC3. LC3 and its homologues, including the isozymes of LC3 and associated proteins (e.g., GABARAP), are modified by cellular lipid PE. An important regulatory step in the formation of autophagosomes is the transformation of LC3-I (free form) to LC3-II (PE conjugated form). The precursor form of LC3 is cleaved by the protease ATG4B to yield LC3- I (not shown). ATG7 and ATG3 participate in conjugating PE with LC3-I to LC3-II. LC3-II cytoplasmic redistribution, characterized by punctate LC3 staining, is indicative of autophagosome formation. GABARAP, (GABA type A receptor-associated protein); LC3, (Microtubule-associated protein 1 light chain 3;
PE, (Phosphatidylethanolamine).

an atypical serine/threonine protein kinase that is evolutionarily relatively conserved. Cell cycle regulation, proliferation, differentiation, motility, and invasion are among its physiological functions. Two unique complexes, mTORC1 and mTORC2, exist within the cell and are distinguished by distinct components. mTORC1 and mTORC2 are two signaling complexes that play a major role in the mTOR pathway. Ribosomal protein S6 kinase (S6K) and kinase B (AKT) are key enzymes in the interaction between mTORC1 and mTORC2. S6K is activated by mTORC1, which subsequently activates mTORC2. Conversely, mTORC2 facilitates the phosphorylation of AKT, leading to the activation of mTORC1. mTORC1 is responsive to energy levels and stress, and it is significantly inhibited by rapamycin. A substantial body of research has indicated that mTORC1 exerts an inhibitory influence on the process of autophagy (29, 30). Unlike mTORC1, mTORC2 is not susceptible to both rapamycin and nutrients because of the presence of Rictor (31). However, long-term rapamycin treatment ultimately inhibits mTORC2 activity (32). mTOR is a key molecule during autophagy induction. Many signaling pathways have the capacity to either promote or inhibit the process of autophagy through their interactions with mTOR (Figure 3). Nonetheless, the enhancement or suppression of autophagy by these pathways is not definitive. In some specific cases, the opposite effect may also be exerted. We will describe it further in the following sections.

mTOR is integral to numerous physiological functions, such as cell proliferation, survival, and autophagy, which is intricately linked to various lung diseases through its regulatory effects on cell growth, inflammation, and fibrosis. We will describe it in the following sections. The mTOR signaling pathway plays a critical role in the development and maintenance of lung function. It regulates the growth and differentiation of lung epithelial cells and fibroblasts to maintain normal lung function. Moreover, mTOR signaling is involved in the immune response to pulmonary pathogens, which regulates the activation of immune cells and the inflammatory response. Given its central role in lung diseases, mTOR signaling has become a target for therapeutic intervention.

The phosphoinositide-3-kinase protein/kinase B signaling pathway

PI3K/AKT was discovered in the 1980s and plays an important role in major physiological activities of cells (33). PI3K-AKT signaling mainly involves two metabolites, phosphatidylinositol-4,5-bisphosphate (PIP2) and phosphatidylinositol-3,4,5-bisphosphate (PIP3), and two coding genes, lipid phosphatase (PTEN) and 3-phosphoinositide-dependent protein kinase-1 (PDK1). PIP2 is converted to PIP3 by phosphorylation in response to PI3K. Next, PIP3 on autophagosome membranes recruits ATG18 and binds to bilayer membranes, allowing autophagosomes to extend and complete (34). PDK1 is a key regulatory molecule of the PI3K-AKT signal transduction pathway and plays an important part in the activation of AKT (35–37). In addition, mTORC2 can directly activate AKT by phosphorylating Ser-473 (36). PTEN is an important negative regulator of PIP2 conversion to PIP3. PTEN acts to promote dephosphorylation of PIP3 thereby inhibiting its accumulation in cells (38). Once activated, AKT acts on various cytoplasmic proteins to mediate cell growth and survival. The main downstream effector is mTOR. Furthermore, AKT influences the interaction between phosphorylated tuberous sclerosis complex 1 (TSC1) and phosphorylated tuberous sclerosis complex 2 (TSC2), consequently facilitating the activation of mTORC1 via the H-Ras-like GTPase (Rheb) (39). Subsequently, active mTORC1 inhibits autophagy by blocking the uncoordinated 51-like protein kinase (ULK1) (40).

The PI3K/AKT signaling has a tight relationship in regulating cell growth, survival, and metabolism. This pathway is involved in numerous cellular processes and has significant implications for various lung diseases. In certain pathological conditions, the PI3K/AKT signaling pathway is frequently activated in reaction to inflammatory stimuli and oxidative stress, which results in airway remodeling and contributes to the pathophysiology of the disease, including mucus hypersecretion and smooth muscle cell proliferation, therefore enhancing the survival of inflammatory cells in the lungs. The PI3K/AKT pathway presents multiple potential therapeutic targets for treating lung diseases. Inhibitors of PI3K, AKT, or associated pathways are currently undergoing investigation to reduce inflammation, fibrosis, and tumor growth in lung diseases.

RAS/RAF/MEK/ERK signaling pathway

As a significant signaling pathway of mitogen-activated protein kinase (MAPK), RAS/RAF/MEK/ERK is involved in regulating cell proliferation, differentiation, apoptosis, and numerous signaling pathways (41, 42). RAS is a small GTPase that is activated by several factors, including receptor tyrosine kinases, growth factors, heterotrimeric G proteins, integrins, serpentine receptors, and cytokine receptors. Furthermore, oxidative stress activates the RAS/RAF/MEK/ERK signaling pathway. Notably, certain growth receptors are not required for ROS-induced RAS activation (43). In addition, ROS can uncouple MAPK pathway activity from RAS expression (44). Activated RAS further recruits RAF (MAPKKK) to the plasma membrane for activation. Following this, RAF activates and phosphorylates MEK (MAPKK), followed by ERK (MAPK). As ERK is activated, it translocates to the nucleus and triggers transcription and expression of target genes (45, 46). The expression products of these genes regulate various physiological functions of cells, including the regulation of autophagy (45, 46). PI3K and TSC2 are regulated by the RAS/RAF/MEK/ERK pathway, thereby activating mTORC1 activity. In addition, the activated RAS/RAF/MEK/ERK signaling pathway up-regulates LC3, Beclin1, and Noxa, and directly down-regulates p62 to induce autophagy (47, 48). Following induction by lindane, the formation of autophagosomes within cells is closely linked to the prolonged activation of ERK (49). Notably, this phenomenon occurs independently of both mTOR and p38 (49). These seemingly contradictory findings indicate that specific

environmental conditions may directly influence the regulation of autophagy via the RAS/RAF/MEK/ERK signaling pathway.

Dysregulation of this pathway has been implicated in various diseases, including lung cancer. Mutations in genes encoding components of this pathway, such as KRAS, BRAF, and MEK, are commonly found in lung cancer patients. Mutations in BRAF and MEK are also observed in a subset of lung cancer patients. Furthermore, aberrant activation of the RAS/RAF/MEK/ERK pathway has been linked to other lung diseases, such as pulmonary fibrosis and COPD. In these conditions, dysregulated signaling through this pathway can lead to inflammation, tissue remodeling, and fibrosis in the lungs.

Adenosine 5'monophosphate-activated protein kinase signaling pathway

AMPK is recognized as one of the primary substrates of LKB1 (liver kinase B1), which functions as an intrinsic energy sensor and regulator of cellular homeostasis (50, 51). AMPK is a heterotrimeric serine/threonine kinase that consists of a catalytic αsubunit and two regulatory subunits, which are β and γ. The activation of AMPK occurs in reaction to elevated levels of intracellular AMP and reduced levels of ATP, particularly during conditions of nutrients. LKB1 implements the involvement of this process by phosphorylating the α-activating loop (52). The activation of AMPK affects multiple processes, including mTOR pathway regulation and p53 phosphorylation (53). Further, AMPK is capable of directly phosphorylating Raptor or TSC2. Next, TSC2 signals to inhibit mTOC1 activity (44, 45, 54). In this pathway, AMPK negatively regulates mTORC1 by adenosine 5' -monophosphate levels, thereby positively regulating autophagy upon energy depletion (55). Research indicates that AMPK exerts direct regulation over ULK1 in a manner that is sensitive to nutrient availability, thereby contributing to the intricate nature of regulatory mechanisms, as elaborated upon in the subsequent sections (56–58).

AMPK is a dominant y regulator of cellular energy metabolism and plays a crucial role in maintaining cellular homeostasis. Within the realm of pulmonary disorders, AMPK signaling has been demonstrated to exhibit both preventive and pathogenic effects. In several lung diseases, including COPD, asthma, and pulmonary fibrosis, dysregulation of AMPK signaling has been implicated. However, the relationship between AMPK signaling and lung disease is complex and disease-specific. Additional investigation is necessary to elucidate the specific mechanisms by which AMPK influences lung function, as well as to assess the feasibility of marking this pathway for therapeutic strategies.

Uncoordinated-51-like protein kinase signaling pathway

ULK1 is a master regulator of autophagy initiation among mTORC1 downstream regulatory targets (59). Among the components of autophagy, ATG1, ATG13, and ATG17 are critical regulators of autophagy initiation (44, 60–62). In mammals, ULK1 and ULK2 are homologues of ATG1, and mATG13 and 200 kDa adhesion kinase family interacting protein (FIP200) are homologues of ATG13 and ATG17, respectively (59, 63–66). The importance of ULK1 in the autophagy pathway is reflected in its involvement in forming mTOR substrate complexes (60, 66, 67). mTORC1 has been reported to inhibit its pre-autophagic effect by phosphorylating ULK1 under normal and nutrient-rich conditions (68). mTORC1 is also able to directly phosphorylate and inhibit ATG13, one of the activators of ULK1. ULK1 can activate autophagy by phosphorylating Beclin-1 indirectly involved in the formation of VPS34-Beclin-1-ATG14 (29, 69, 70). In addition, AMPK can directly interact with ULK1 to regulate ULK1 in a nutrient-sensitive manner. Activating ULK1 by phosphorylating Ser 317/Ser 777, AMPK acts by triggering autophagy in response to glucose and amino acid starvation (58). Interestingly, mTORC1 blocks the cellular collection between ULK1 and AMPK by phosphorylating Ser 757. Consequently, it can be inferred that ULK1 equips cells with the capacity to effectively respond to intricate environmental alterations in conjunction with mTORC1 and AMPK.

Recent studies denote that ULK1 signaling may be implicated in the development of several pulmonary disorders. In conditions like IPF, COPD, and lung cancer, dysregulation of autophagy, including ULK1 signaling, has been implicated in disease progression. Investigating the function of ULK1 signaling in lung diseases may facilitate the creation of targeted therapies designed to regulate autophagy and improve outcomes for patients with these conditions.

Type III phosphatidylinositol triphosphate kinase signaling pathway

Autophagosome formation is closely dependent on class III PI3K complexes. Activated class III PI3K complexes lead to increased PI3P formation, and PI3P-recruiting protein factors initiate autophagosome formation, including WD repeat protein interacting with inosine phosphate (WIPI-1/2), Atg18, and protein 1 containing double FYVE (DFCP1) (71, 72). Class III PI3K complexes exist in two distinct types in mammalian cells, where complexes consisting of VPS34L, p150, Beclin1, and ATG14L are closely associated with autophagy. We refer here to this complex collectively as the class III PI3K complex. Beclin 1 serves as a significant regulator of autophagy. It is also defined as a tumor suppressor protein, exhibiting the capacity to engage with a wide variety of proteins, including ATG14L, ultraviolet resistance-associated gene protein (UVRAG), Rubicon, and Bcl-2 (73–76). Three domains play important roles in Beclin1 function, including the Bcl-2 homology 3 (BH3) domain and the central coiled-coil domain (CCD) that mediates interactions with ATG14L and UVRAG (77–80). In addition, the active ULK1 results in the recruitment of class III PI3K complexes to autophagosomes, forming alternating Beclin 1-Vps34L complexes with UVRAG and promoting autophagy (75, 81–83). Evolutionarily conserved domain (ECD) mediates communication between Beclin 1 and VPS34, which in turn activates VPS34 kinase to regulate

autophagosome formation. Furthermore, class III PI3K complexes can negatively regulate autophagy in response to the newly identified factor Rubicon (84, 85). Ambra-1, Bif-1, Bcl-2, and Bcl-XL can also act on class III PI3K complexes to modulate their activity (76, 86, 87).

In the context of lung disease, dysregulation of Class III PI3K signaling has been implicated in various respiratory conditions. In diseases like IPF, COPD, and lung cancer, altered Class III PI3K signaling has been associated with disease pathogenesis and progression. Understanding the role of Class III PI3K signaling in lung diseases is important for identifying potential therapeutic targets and developing targeted interventions to modulate this pathway for the treatment of respiratory disorders.

Wild-type p53 signaling pathway

p53 functions as a tumor suppressor protein and serves as a transcription factor that regulates gene networks in response to various cellular stresses, thereby maintaining genome stability and integrity. However, p53 not only prevents tumorigenesis but also plays a critical regulatory part in primary signaling and metabolic adaptation (88, 89). The effect of wild-type p53 on autophagy is complex, highly dependent on the environment, and determined by the cellular microenvironment and stressful conditions. The progression of the cell cycle and the subcellular localization of p53 serve dual functions in the regulation of autophagy. The dual effect of wild-type p53 on autophagy is reflected in its transcriptional activity against a range of downstream target genes with autophagic regulatory effects. The dual role of p53 in autophagy is presented in Table 1.

p53 signaling plays a significant role in the development and progression of various lung diseases. Mutations in the p53 gene can disrupt its tumor-suppressor function, leading to uncontrolled cell growth, evasion of cell death, and genomic instability, all of which are hallmarks of cancer. Dysregulated p53 signaling has been linked to a poorer prognosis in lung cancer patients and resistance to certain anticancer therapies. Dysregulation of p53 contributes to abnormal repair processes in the lung tissue, leading to excessive collagen deposition, fibrosis, and impaired lung function. Moreover, activation of p53 can promote cell cycle arrest, DNA repair, or apoptosis, depending on the extent of damage while disruption of p53 function may impair the lung's ability to repair and regenerate, exacerbating lung injury and contributing to disease progression.

Function of autophagy

Autophagy serves as a mechanism for maintaining a stable pool of organelles by regenerating metabolic precursors and eliminating subcellular debris in response to diverse environmental stressors. In the presence of such stress, autophagy initiates cellular defense mechanisms by facilitating the removal of damaged organelles and ubiquitinated protein aggregates (90, 91). Under specific conditions of glucose or amino acid starvation, autophagy is compensatory to participate in the basic metabolic cycle of cells by acting on

TABLE 1 The dual effects of wild-type p53 on autophagy.

Effect	Signaling pathway	Mechanism	References
Promoted	mTOR	Wild-type p53 uses AICAR to stimulate AMPK activity to inhibit key downstream effectors of mTOR signaling, such as phosphorylation of 4E-BP1 and RPS6. p53 can induce secretion of IGF-BP3 and indirectly affect the autophagic process regulated by IGF (s).	(256, 257)
Promoted	AMPK	Wild-type p53 stimulates signaling through AMPK to the β1/β2 subunit (Sestrin1/2).	(258, 259)
Promoted	DAPK-1	DAPK-1 promotes Wild-type p53 accumulation in an ARF-dependent manner, followed by stimulation of autophagy through ARF.	(260, 261)
Promoted	Bcl-2 protein family	Wild-type p53 activates multiple pro-apoptotic protein production, including Bax as well as the BH3-only proteins Bad, Bnip3, and Puma.	(262, 263)
Promoted	PI3K	Wild-type p53 in the nucleus is able to up-regulate PTEN through a transcription-dependent pathway, which in turn inhibits the PI3K pathway.	(264, 265)
Promoted	HIF-1	HIF-1 can stabilize p53, which in turn promotes the autophagic process.	(266, 267)
Promoted	ULK1	In response to DNA damage, p53 upregulates ULK1 and ULK2 expression.	(268)
Promoted	HSF-1	Wild-type p53 is involved in the induction of (Isg20L1 and HSF1), which in turn transactivates autophagy-related genes (ATG7).	(269)
Promoted	TGM2	Wild-type p53 promotes autophagic flux by enhancing autophagic protein degradation and autophagosome clearance by inducing TGM2	(270)
Inhibited	mTOR	Wild-type p53 inhibits AMP-dependent kinases, thereby activating mTOR	(271)
Inhibited	TIGAR	Wild-type p53 induced TIGAR (TP53-induced glycolytic and apoptotic modulator) regulates glycolysis and cellular ROS levels	(272)
Inhibited	miR-34a series and miR-34a/34c-5p	Wild-type p53 impacts transcriptional regulation of microRNAs (miR-34a series and miR-34a/34c-5p, against	(273, 274)

(Continued)

TABLE 1 Continued

Effect	Signaling pathway	Mechanism	References
		ATG9A and ATG4B, respectively)	
Inhibited	Beclin-1	Wild-type p53 interacts with Beclin-1 and subsequently promotes its ubiquitination and proteasome-mediated degradation	(275)
Inhibited	RB1CC1/ FIP200	Wild-type p53 inhibits autophagy by interacting with the human ortholog of yeast Atg17, RB1CC1/FIP200	(276)
Inhibited	PKR	Wild-type p53 inhibits autophagy by reducing double-stranded RNA accumulation and PKR (protein kinase RNA activation) activation	(277)

AICAR, 5-Aminoimidazole-4-carboxamide1-β-D-ribofuranoside; AMPK, Adenosine 5'-monophosphate-activated protein kinas; ARF, Auxin response factor; Bcl-2, B-cell lymphoma-2; DAPK-1, Death associated protein kinase 1; HIF-1, Hypoxia-inducible factor 1 ; HSF-1, Heat shock factor 1; IGF-BP3, Insulin-like growth factor binding-protein-3; mTOR, Mammalian target of rapamycin; PI3K, Phosphoinositide 3-kinase; PKR, Protein kinase R; PTEN, Phosphatase and tensin homolog; RB1CC1, RB1-inducible coiled-coil 1; RPS6, Ribosomal protein S6; TIGAR, TP53 induced glycolysis regulatory phosphatase Gene; ULK1, Unc-51-like kinase 1; 4E-BP1, Recombinant human eukaryotic translation initiation factor 4E-binding protein 1.

intracellular proteins, lipids, and other organic macromolecules (5). Specifically, autophagy plays a very important role in apoptosis, inflammation, and immunity. We will describe this in detail below.

Autophagy in apoptosis

Cells can undergo apoptosis in response to intracellular signaling, extracellular signaling, and endoplasmic reticulum (ER) stress (Figure 4). Cysteine protease (caspase) induction and activation play a critical role in apoptosis. Endogenous apoptosis is also known as the mitochondrial pathway due to a mechanism closely related to the permeability of the mitochondrial membrane. This process is also strongly associated with the Bcl-2 protein family. Bcl-2, Bcl-XL, and Mcl-1 are negative regulators of apoptosis and protect cells from apoptosis when multiple types of cells are stimulated. Bax and Bak can undergo apoptosis by penetrating the mitochondrial membrane, releasing cytochrome c, and subsequently activating caspases. However, the exact mechanism by which these proteins promote apoptosis is unknown. Exogenous apoptosis requires the formation of a critical complex, the death-inducing signaling complex (DISC). Death receptors, including Fas, TNFR1, and TRAIL, are located on the cell surface and mediate apoptosis when activated. The production of DISC is initiated by the binding of death receptors to their corresponding ligands. When Fas binds to its ligand, activated Fas forms a DISC by binding connexin to the death domain (FADD). DISC then binds recruited pro-caspase 8 by interacting with another motif called the death effector domain (DED). Next, Pro-caspase 8 dimerizes and gains catalytic activity after degrading downstream substrates, producing and releasing heterotetrameric active caspase 8. Eventually, cells undergo extrinsic apoptosis. The ER stress pathway involves the buildup of incorrectly folded or unfolded proteins within the ER, which can arise from various factors such as infection, hypoxia, starvation, chemical influences, and deviations from homeostatic regulation of ER secretory functions. This accumulation leads to ER stress-induced apoptosis and triggers the unfolded protein response (UPR) pathway in response to the misfolding of proteins within the ER.

Recent research has indicated a strong connection between autophagy and apoptosis (92, 93). According to different experimental models, autophagy is associated with anti-apoptotic and pro-apoptotic effects (94). Several signaling mechanisms interact between apoptosis and autophagy. Autophagy proteins are involved in the regulation of apoptosis, while apoptotic proteins also influence the process of autophagy (95). Bcl-2 family members Bcl-2 and Bcl-XL, can directly interact with Beclin 1 by binding to the BH3 domain in the intrinsic apoptotic pathway (96, 97). Further studies showed that the anti-autophagic function of Bcl-2 mainly occurs in the ER and stabilizes Beclin-1 interaction with Bcl-2 through its 2Fe-2S cluster binding to Bcl-2. The c-Jun-NH2-terminal kinase (JNK) pathway is closely linked to apoptosis signaling. The JNK pathway can regulate the function of autophagy by affecting several key proteins (98). The JNK pathway promotes autophagy by preventing the association between Beclin 1 and Bcl-2 family proteins (99). In addition, AMPK can dissociate the Bcl-2-Beclin1 complex and promote the formation of the Beclin1-PI3K complex (100). Notably, mTOR is key in linking apoptosis and autophagy. It has been shown that loss of Raptor activates caspase 3, leading to mitochondrial abnormalities, which positively regulate apoptosis and autophagy (101).

Additionally, there is a complex link between the extrinsic apoptotic pathway and autophagy. Critical components of DISC regulate autophagy in this process. Excess autophagy occurs in fibroblasts, macrophages, and T cells when caspase 8 is inhibited or deficient (102, 103). DED is a protein interaction domain that can be found in pro-caspases and proteins in the apoptotic cascade that regulate caspase activation. Apoptosis and autophagy are also affected by FADD mutations, which produce abnormal death domains (DD). Mutants (FADD-DD) were recruited to DISC without DED. By interacting with pro-caspase 8 and cellular FADD-like IL-1β converting enzyme inhibitor protein (c-FLIP), this domain prevented the development of death receptor-induced apoptosis. Besides, it can cause excessive autophagy in epithelial cells and T cells (102, 104). Exogenous apoptotic signaling pathways can be affected by several autophagic proteins such as Atg5 (105). The knockdown of Atg5 exerts different effects on cell survival under different study conditions (106). Typically, proteolytic fragments of Atg5 can promote apoptosis by inhibiting Bcl-XL (107).

Autophagy in inflammation and immunity

The autophagy process influences immune and inflammatory responses in many diseases (Figure 5) (7). There is a complex

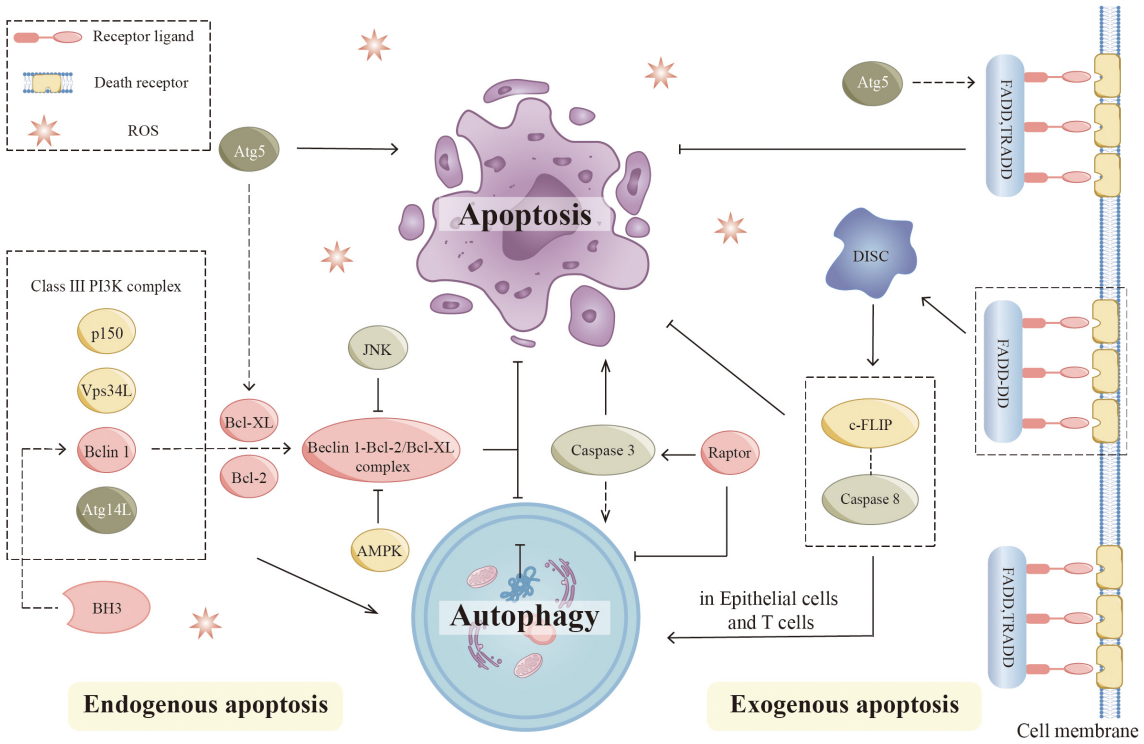

FIGURE 4
Autophagy and apoptosis. In endogenous apoptosis, the interaction of autophagic proteins with apoptotic proteins regulates this process. Bcl-2 family members, including Bcl-2 and Bcl-XL, can directly interact with Beclin 1 by binding to the BH3 domain. The JNK pathway promotes autophagy by preventing the association between Beclin 1 and Bcl-2 family proteins. AMPK also dissociates the Bcl-2-Beclin1 complex and promotes Beclin1-PI3K complex formation. Apoptosis signaling pathways may be affected by various autophagic proteins such as Atg5. Proteolytic fragments of Atg5 are able to promote apoptosis by inhibiting Bcl-XL. In extrinsic apoptosis, key components of DISC regulate autophagy during this process. Apoptosis and autophagy are affected by mutations in FADD, which create DD. The mutant (FADD-DD) was recruited to DISC in the absence of DED. By interacting with caspase 8 precursor and c-FLIP, this domain prevents the development of death receptor-induced apoptosis, while it can lead to excessive autophagy in epithelial cells and T cells. Atg5 can form a complex with FADD to affect the apoptosis process. AMPK, (Adenosine 5′-monophosphate-activated protein kinase); Bcl-2, (B-cell lymphoma-2); BH3, (Bcl-2 homolog3r); Caspase, (Cysteine protease); c-FLIP, (Cellular FADD-like IL-1β-converting enzyme-inhibitory protein); DD, (Death domain); DED, (Death effector domain); DISC, (Death-inducing signaling complex); JNK, (c-Jun-NH2-terminal kinase).

interrelationship among autophagy, immunity, and inflammation. Autophagic proteins play a role in inducing and suppressing immune and inflammatory responses. Similarly, immune and inflammatory signals play a role in inducing and inhibiting autophagy. Autophagy provides new insights into the prevention and treatment of infectious, autoimmune, and inflammatory diseases by balancing the benefits and drawbacks of immune and inflammatory responses.

Autophagy regulates various immune responses during infection. In many experiments, we have found that mutations in autophagy genes increase susceptibility to certain diseases (108–112). Studies performed on human genetics have revealed important clues regarding xenophagy, autophagic proteins that affect pathogen replication or survival, and the general immune system. Numerous studies have demonstrated the significance of autophagy in the human cellular defense mechanisms against mycobacterial infections (113). Autophagy genes play a significant role in regulating host genes for Mycobacterium tuberculosis (Mtb) replication (114). Autophagy may be a crucial component of TB drug resistance. At the same time, to survive *in vivo*, some viruses and bacteria have evolved different methods of adaptation to autophagy. They can prevent the occurrence of autophagy by inhibiting the foremost steps of autophagy or/and the production of autophagosomes, avoid protein modification or interfere with the recognition of autophagy by autophagy signaling, and even promote self-replication and survival using autophagy-related proteins. For example, human immunodeficiency virus (HIV), Kaposi's sarcoma-associated herpes virus inhibits antiviral capacity and immune properties *in vivo* by affecting key pathways of autophagy. HIV envelope proteins activate mTOR signaling and prevent HIV transfer to CD4 + T cells. Kaposi's sarcoma-associated herpesvirus prevents LC3-II production by interacting with Atg3 (115). Bacteria also have multiple strategies to avoid degradation. By disguising themselves, several bacteria can evade autophagic recognition in the cytoplasm. For example, VirG is a protein present on the bacterial surface and is necessary for Shigella to be targeted by autophagosomes. Atg5 can prevent its interaction with VirG by competitively binding to IcsB, an effector of Shigella (116). Several cytoskeletal proteins of cells are ActA-dependent (117). This feature allows bacteria to masquerade as their host organelle (117). Listeria protein ActA interacts with the intracytoplasmic actin polymerization machinery, thereby blocking binding to ubiquitin, recruitment of p62, and autophagy targeting (117). Several pathogens

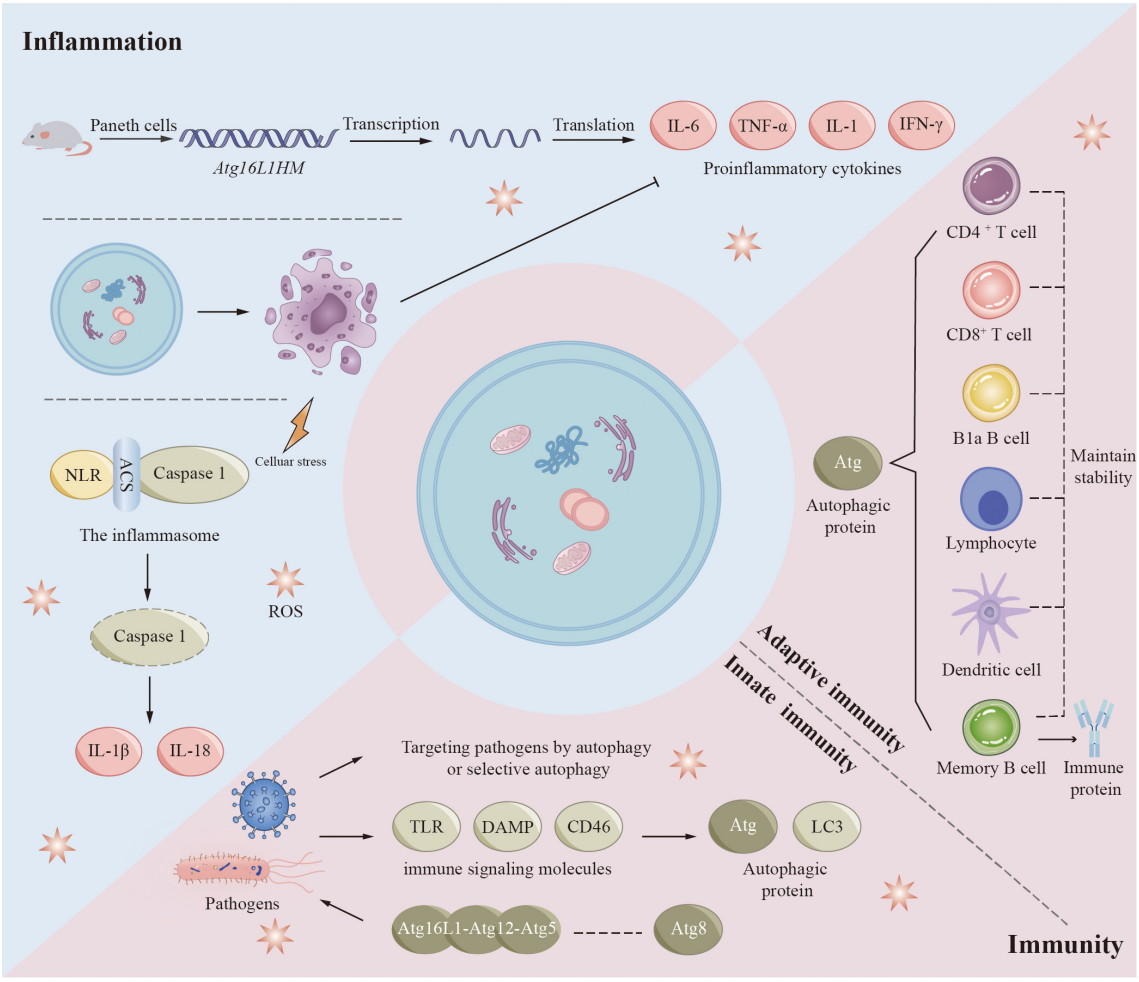

FIGURE 5
Autophagy in inflammation and immunity. Autophagy proteins play a role in inducing and suppressing immune and inflammatory responses, and immune and inflammatory signals play a role in inducing and inhibiting autophagy. Autophagic proteins play an important role in adaptive immunity, mainly including maintaining the normal number and function of immune-related cells such as B1a B cells, $CD4^+$ T cells, and $CD8^+$ T cells. Autophagy also plays a role in innate immunity when pathogens such as bacteria and viruses invade the human body. However, some pathogens are able to achieve their own survival by inhibiting, evading or even utilizing the autophagic process. Autophagy pathways and associated proteins also play crucial roles in regulating inflammatory responses. Increased transcription of pro-inflammatory cytokines and adipokines has been observed in mouse Paneth cells (Atg16L1HM), which contribute to the development of inflammation. Inflammasomes are important substances in the development of inflammation, and inflammasomes activated by various factors mediate the degradation and activation of caspase-1 and ultimately promote the synthesis and secretion of inflammatory factors (IL-1β and IL-18). Autophagy also removes cell debris generated by apoptosis, which in turn inhibits tissue inflammation.

are also able to benefit themselves using components of autophagy in membrane trafficking, including poliovirus, rotavirus, coronavirus, dengue virus, and hepatitis B and C viruses (113, 118).

Autophagy is also regulated by immune signaling molecules, including innate and adaptive immunity. Although the regulatory mechanism of autophagy by most immune-related signaling molecules is currently unknown, some findings provide clues. NOD1 and NOD2, two typical NLRs (NOD-like receptor cryopyrin protein), can be activated by specific components of bacterial peptidoglycan. In response to bacterial infection, activated NOD1 and NOD2 interact with ATG16L1 to induce autophagy (119). NOD2 mutations associated with Crohn's disease have been found to influence ATG16L1 recruitment and bacterial co-localization with LC3 (119). Presumably, in innate immunity, the ATG5-ATG12-ATG16L1 complex interacts with members of the ATG8 family and may stimulate pathogen-induced autophagy or enhance the ability of selective autophagy to target pathogens (120). Various cytokines, including but not limited to CLCF1, LIF, IGF1, FGF2, and the chemokine SDF1 (also called CXCL12) may have a broader role in controlling autophagy (121). Autophagy also plays a crucial role in adaptive immunity. Multiple regulatory pathways of autophagy possess the capacity to affect both the functionality and stability of the immune system, in addition to influencing antigen presentation. B1a B cells, CD4 + T cells, CD8 + T cells, and fetal hematopoietic stem cells rely on autophagic proteins to maintain their numbers (122–124). Thymic clearance of autoreactive T cells is an important function of autophagy in immune system development and homeostasis (123). Epithelial cells of the thymus are highly autophagic. Mutations in Atg5 in thymic epithelial cells result in altered autoimmunity and specific immunity of certain

MHC class II-restricted T cells (125). In addition, autophagy may play an important role in the differentiation of lymphocytes by indirectly affecting the expression of cytokines. During antigen presentation, autophagy proteins present endogenous antigen MHC class II to CD4 + T cells, enhance cross-presentation of antigen-providing cells with CD8 + T cells, and facilitate cross-presentation of phagocytosed antigens by dendritic cells to CD4 + T cells (126–128). Autophagy also contributes to memory B cell maintenance and regulates immunoglobulin secretion (129–131).

Recent findings have shown that autophagy is closely associated with the development of certain chronic inflammatory diseases, such as Crohn's disease, systemic lupus erythematosus (SLE), and other autoimmune diseases (132, 133). In animal models and human diseases, autophagic failure is usually characterized by dysregulation of inflammation (134). Its main role is to regulate inflammatory transcriptional responses. Increased transcription of proinflammatory cytokines and adipokines has been observed in Paneth cells (Atg16L1HM) of Atg16L1 subtype mice (119, 135–137). Inflammasomes are another important target of autophagic proteins in inflammatory signaling. Inflammasomes are multiprotein complexes containing NLR, adaptor protein ASC, and caspase 1. Inflammasomes can be stimulated by infection or other stress-related pathways. Activated inflammasomes mediate the degradation and activation of caspase-1 and ultimately promote synthesis and secretion of IL-1β and IL-18 (138, 139). In addition, activation of the NALP3 inflammasome is increased in Beclin 1 and LC3B gene-deficient monocytes (140, 141). This enhancement ultimately facilitates the activation of IL-1β and IL-18. The autophagic process can also suppress tissue inflammation by removing apoptotic corpses. During developmentally programmed cell death, autophagy induces xenophagic clearance in dying apoptotic cells by generating ATP-dependent phagocytic signals (142). Increasing evidence suggests that autophagic proteins are required for TLRs mediated phagolysosomal pathways (142). To clear inflammatory sources such as exogenous inflammatory sources (e.g., bacterial viruses) and endogenous pro-inflammatory sources (e.g., damaged organelles, aggregates), autophagic cargoes are usually regulated by ubiquitin and are regulated by a type called SLR (sequestrate-like receptor: p62 [SQSTM1], NBR1, OPTN, NDP52, TAX1BP1, etc.) (143).

Methods for measuring autophagic activity

Currently, the most effective methods for analyzing autophagy *in vitro* and *in vivo* remain significantly controversial, due to the complexity of the autophagic process. The measurement of autophagic activity can be divided into two categories: counting autophagosomes and measuring autophagic flux.

Currently, three primary methodologies are employed to assess the number of autophagosomes: electron microscopy (144), Western blot (WB) analysis (145), and fluorescent protein labeling techniques (146). Electron microscopy observation of autophagic structures is the most traditional method. Morphological alterations occurring at various stages of autophagy can be directly visualized using a transmission electron microscope, allowing for an initial assessment of the autophagic phase. Electron microscopy showed damaged organelles in cells undergoing autophagy. In the case of mitochondria, vacuolated bilayer membrane-like structures, or vacuolated structures of bilayer membranes, i.e., autophagosomes, can be observed around them (146, 147). LC3 runs through the whole autophagic process and is currently recognized as an autophagic marker. Changes in the LC3-II/I ratio can be detected using WB to assess the intensity of autophagy. In addition, autophagy can be detected using the property of green fluorescent protein (GFP) quenching in acidic environments (146). Based on GFP-LC3, the researchers developed the GFP-RFP-LC3 tool, a method that allows observation of autophagy in individual cells. Keima is a unique fluorescent protein that is independent of LC3 and suitable for monitoring nonselective autophagy and microautophagy (148). Keima can additionally serve as a tool for the detection of organelle autophagy when conjugated with organelle-specific markers. Scholarly investigations have indicated that an increased presence of autophagosomes or LC3B-II within the system correlates with enhanced proteolytic activity. However, there is no clear correlation between autophagy activity and the abundance of autophagosomes or LC3B proteins (24, 146, 149). For this reason, dynamic measurements of autophagic flux are required (146).

A prominent contemporary approach for assessing autophagic flux involves the observation of LC3 turnover. This approach relies on LC3B-II pooling at autophagosome membranes. When cells were treated with lysosomal reagents (e.g., ammonium chloride) or lysosomal protease inhibitors (e.g., chloroquine), the degradation of LC3-II was blocked, resulting in the accumulation of LC3-II. Thus, the difference in LC3-II amounts between samples represents the amount of LC3 that is delivered to lysosomes for degradation (150). Second, the amount of total cellular LC3 can be quantified by immunoblot analysis or flow cytometry or qualitatively observed by fluorescence microscopy, which is inversely proportional to autophagic flux. In addition to LC3, several groups have developed some specific macrophage substrates to monitor autophagic flux, such as p62/SQSTM1 (151, 152), BRCA1 gene 1 protein (NBR1) (151), betaine-homocysteine s-methyltransferase (153), and polyglutamine protein aggregates (154).

Autophagy in lung diseases

COPD

COPD is a chronic inflammatory pulmonary disease connected with smoking, which is the third most common death factor around the world and consists of 3 primary disease states: chronic bronchitis or proximal airway mucus hypersecretion; emphysema or peripheral lung destruction and loss of alveolar attachments; and small airway disease characterized by inflammation and airway remodeling (Figure 6) (155, 156).

In 2000, autophagic vacuoles were detected in liver specimens lacking alpha-1 antitrypsin, indicating the potential role of autophagy

in lung disease (157). COPD pathogenesis is not fully understood but may be associated with aberrant cellular responses of bronchial cells and lung cells to CS (cigarette smoke) (158, 159). In the setting of COPD, autophagy-promoting epithelial cell death was shown to be a potential mechanism (160, 161). As compared to healthy individuals, COPD patients have increased levels of LC3B-II and autophagy-related proteins including ATG4, ATG5-ATG12, and ATG7 (160). In addition, it was observed under electron microscopy that the formation of autophagosomes was also markedly increased in lung tissues from COPD patients compared with control lung tissues (160). Mice exposed to CS are usually used as an experimental model of COPD. In lung tissue, mice subjected to cigarette smoke exposure exhibit elevated levels of autophagic proteins and an increased presence of autophagosomes. Interestingly, mice deficient in LC3B and autophagy proteins are resistant to CS-induced pathological changes (161, 162). These findings indicate that the autophagy pathway may contribute to the progress toward COPD in some specific circumstances (160, 161).

Histone deacetylase 6 (HDAC6) is a critical regulator of primary ciliary uptake. Studies have shown that HDAC6 is involved in the degradation of autophagy in cells (162). Shortened cilia and increased HDAC6 are observed in respiratory epithelial cells treated with CS exposure. Cilia shortening induced by CS is inhibited in mice that lack autophagic protein and HDAC6 (162). This result reflects the importance of pathological changes of HDAC6 in respiratory epithelial cells. Consequently, autophagy plays a role in the HDAC6-mediated degradation of cilia within airway epithelial cells in experimental models of COPD (163). Some studies have reported the involvement of mitochondrial in (164, 165). A key mitophagy protein, phosphatase and angiotensin homolog (PTEN) -induced putative kinase 1 (PINK1), has been found to be increased in the lungs of COPD patients (166). Genetic defects in PINK1 and inhibition of mitophagy with drugs showed resistance to COPD pathology in CS-exposed mice (166).

Cystic fibrosis

Cystic fibrosis (CF) is an autosomal recessive disorder due to mutations in the CF gene located in the 7th pair of chromosomes, which can cause serious damage to the lungs, digestive system, and other organs of the body (167–169). Mutations in related CF genes affect the expression of cystic fibrosis transmembrane conductance regulators (CFTR). It is most typical to have a 508-phenylalanine

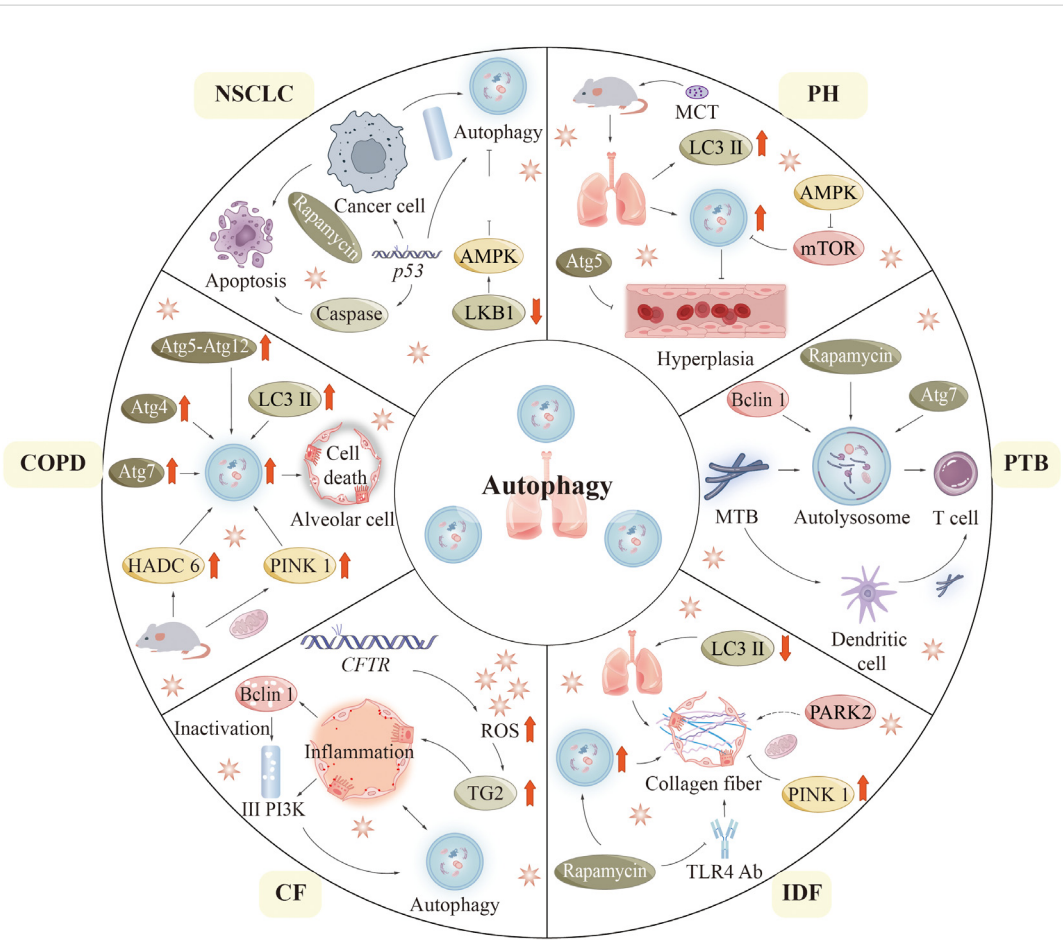

FIGURE 6
Autophagy in lung diseases. In this figure, we summarize the pathogenesis related to the process of autophagy in six pulmonary diseases: COPD, CF, IPF, PTB, PH, and NSCLC. CF, (Cystic fibrosis); COPD, (Chronic obstructive pulmonary disease); IPF, (Idiopathic pulmonary fibrosis); NSCLC, (Non-small cell lung cancer); PH, (Pulmonary hypertension); PTB, (Pulmonary tuberculosis).

deletion in the CFTR gene ($CFTRF^{508del}$) (168). The primary characteristic of cystic fibrosis (CF) within the respiratory system is the overproduction and subsequent accumulation of mucus in the airways. This pathological change can secondarily cause recurrent bronchial infections and airway obstruction. In epithelial cells, mutations in CFTR lead to increased ROS formation. Accumulated ROS promotes tissue transglutaminase 2 (TG2) production. Excessive TG2 is an important cause of inflammatory reactions in CF (170, 171). These complex responses lead to the loss of Beclin 1 and class III PI3K complex function, further affecting autophagic function. Notably, the enhancement of autophagy through the overexpression of Beclin 1 has been shown to enhance inflammatory responses (170), indicating that the autophagic system is essential for the clearance of protein aggregates. In a similar vein, mice with the F508del-CFTR mutation demonstrate reduced levels of Beclin 1 expression (172). Significant risk of morbidity and mortality exists in CF patients due to pseudomonas aeruginosa infection. Experimentally, defective autophagic function resulting from reduced levels or loss of function of BECN1 renders mice lungs more vulnerable to pseudomonas aeruginosa infection (173).

Idiopathic pulmonary fibrosis

Idiopathic pulmonary fibrosis (IPF) is the most common form of idiopathic interstitial pneumonia in clinical practice and is a chronic pulmonary disease of unrecognized etiology (174, 175). Although IPF has epithelial origins, it displays abnormal adaptive immune responses, such as T-cell and B-cell dysregulation (176). The levels of LC3-II expression in lung tissue from patients diagnosed with IPF are significantly reduced compared to those observed in healthy individuals (160, 177). Autophagy seems to play a protective role in the development of IPF. In experimental models of IPF, rapamycin inhibits lung fibroblasts' expression of fibronectin and alpha-smooth muscle actin through its up-regulation of autophagy (178). In addition, the pro-autophagic effect of rapamycin is shown to promote collagen formation in lung epithelial cells (177). Rapamycin also inhibits pulmonary fibrosis induced by Toll-like receptor 4 (TLR4) antibodies or bleomycin in mice (177–179). Furthermore, in the absence of autophagy genes or when autophagy is suppressed pharmacologically, transforming growth factor (TGF) activates lung fibroblasts (177, 178).

In IPF, researchers found clusters of malformed mitochondria in lung epithelial cells, particularly in alveolar type II cells (AECIIs) (180). In addition, microarray analysis showed decreased PINK1 in lung tissues from IPF patients (180). The knock-down PINK1 mice displayed increased mitochondrial depolarization and expression of pro-fibrotic factors (180, 181). The mechanism of the antifibrotic effect of PINK1 in lung epithelial cells is reflected in the prevention of cell death by preserving the morphology and function of mitochondria (180, 181). It has been suggested that PARK2, an important mitophagy-related molecule may be linked to the pathogenesis of IPF (182). Mitophagy is activated in alveolar macrophages from IPF patients and mice treated with bleomycin. Whereas increased apoptosis of macrophages is found in mitophagy-deficient mice, which prevents them from pulmonary fibrosis.

Pulmonary hypertension

Pulmonary hypertension (PH) is a disease of abnormally high blood pressure in the pulmonary arteries. PH is predominantly defined by the remodeling of pulmonary vasculature, a multifaceted and progressive phenomenon that ultimately results in right heart failure and mortality. Studies have investigated how autophagy acts in PAH pathogenesis, but conclusions remain disputed. Experimental mice with chronic hypoxia showed increased levels of LC3B and autophagosomes in their lungs (183). Furthermore, a higher prevalence of autophagic vacuoles was noted in lung tissue subjected to hypoxia. Mice deficient in MAP1LC3B (MAP1LC3B –/–) that were exposed to chronic hypoxic conditions demonstrated more pronounced PH values in comparison to their wild-type counterparts. PH values included right ventricular systolic pressure and vessel wall thickness. An elevation in angiogenesis within pulmonary artery endothelial cells has been noted in cases of persistent PH in Beclin 1-null mice (184). ATG5-targeting siRNA has been found to directly disrupt autophagy to inhibit the proliferation process of rat pulmonary artery smooth muscle cells. The AMPK signaling pathway, recognized as a crucial component of autophagy, significantly results in the process of autophagy in cardiomyocytes. Research has shown that pharmacological inhibition of the AMPK pathway increases cardiomyocyte mortality, suggesting a protective effect on AMPK-associated cardiomyocyte autophagy. Monocrotaline (MCT) is a commonly used drug in animal experimental models of induced PH. Recent research indicates that in rats treated with monocrotaline (MCT), the expression of phospho-mTOR in the right ventricle is down-regulated, while the expression of phospho-AMPK is elevated at the 2 and 4-week marks. Conversely, at the 6-week interval, there is an up-regulation of phospho-mTOR expression and a decrease in phospho-AMPK expression in the right ventricle of MCT-treated rats (185). This suggests that the AMPK-mTOR autophagy signaling pathway is involved in regulating autophagy in pulmonary hypertension rats. It has already been demonstrated that rapamycin treatment can prevent right ventricular hypertrophy and dysfunction through activation of the autophagy pathway in animal models. The findings indicate that autophagy could potentially be a contributing factor to human vascular disease (186). However, these findings are derived from static measurements. Additional experimental investigations are necessary to elucidate the relationship between human vascular disease and autophagy (183).

Pulmonary tuberculosis

PTB is a chronic and long-term pulmonary disease caused by Mtb infecting the human lung, and it is the predominant manifestation of tuberculosis. Mtb is classified as an intracellular pathogen that releases a diverse array of effector proteins within host cells. These proteins subsequently disrupt cellular signaling pathways, thereby influencing normal cellular functions. It

ultimately promotes its survival in host cells and leads to host cell pathology. During the initial stages of infection, innate immune responses are stimulated, and inflammatory cells are recruited to the lungs. Mtb evades and eliminates innate immune cells, spreads to the draining lymph nodes, and triggers a specific T-cell response that promotes the formation of granulomas at the sites of pulmonary infection (187). Inflammatory granulomas are believed to lead to lung tissue damage, and pulmonary fibrosis, and progressively develop chronic and persistent clinical manifestations of PTB (188).

Mtb inhibits phagosome-lysosome fusion, allowing it to persist in the phagosome during maturation. Autophagy is important for the elimination of Mtb. *In vitro*, rapamycin or starvation-induced autophagy promotes the conversion of Mtb phagosomes into autolysosomes, which contain more antimicrobial chambers (e.g., antimicrobial peptides) than conventional phagosomes (129, 189). Macrophages are also enhanced in their ability to present mycobacterial antigens by autophagy (197). Moreover, phagolysosomal fusion is found to be inhibited when cells are infected with Mtb in macrophages lacking Beclin 1 and ATG7 (189). This result could preliminarily prove that autophagy is advantageous for killing tubercle bacilli. However, the specific mechanism of the defense effect of autophagy proteins on Mtb in humans is unknown. In addition, recent *in vitro* studies have demonstrated increased Mtb replication in HIV-infected macrophages co-infected with Mtb when autophagy is activated by the suppression of the mTOR pathway (190). A recent study found that certain autophagic mechanisms acting on phagocytes are critical mechanisms to target Mtb, known as xenophagy. The embryonic exogenic homeobox 1 (ESX-1) secretion system is a virulence factor of Mtb (191). ESX-1 causes Mtb DNA exposure to the host cytoplasm through phagosome permeation (192). DNA exposed to the cytoplasm is detected and ubiquitinated by cytoplasmic DNA sensor molecules (e.g., STING) (192). Ubiquitinated DNA attaches to LC3 via several proteins like p62 and nucleoporin 52. Consequently, it is encapsulated in autophagosomes to fuse with lysosomes (192).

Non-small cell lung cancer

The mechanism of action of autophagy in cancer has repeatedly been described as a double-edged sword. The role that autophagy-related cellular pathways play in the pathological progression of NSCLC is being extensively investigated. Mutations in genes involved in the mTOR signaling pathway may be associated with malignant proliferation of cells. Mutations in genes in the mTOR pathway, such as KRAS, epidermal growth factor receptor (EGFR), LKB1, PTEN, PIK3CA, AKT1, EGFR, PIK3CA, and PTEN, have some relationship with the development of NSCLC (29). Research indicates that the anticancer efficacy of LKB1 is diminished in NSCLC. The researchers propose that this reduction may facilitate tumor proliferation via the LKB1-AMPK-mTOR signaling pathway (193). Rapamycin causes endogenous apoptosis of cancerous cells, which in turn inhibits tumor growth in mouse models of NSCLC (194, 195). *In vitro* lung cancer models, rapamycin enhances apoptosis and autophagy (196). The PI3K signaling pathway serves as a primary regulator of autophagy, with its activation leading to the inhibition of autophagic processes in cancerous cells. Furthermore, the activation of this pathway enhances the production of tumor-promoting antigens, thereby facilitating the process of carcinogenesis. Mutations in p53 are also important correlates of tumorigenesis. p53 is one of the most frequently mutated genes and is present in 45% – 70% of adenocarcinomas and 60% – 80% of squamous cell carcinomas (196). The pathogenesis of NSCLC depends heavily on the absence of the p53 gene (197). p53 can be present in the cytoplasm and nucleus. Under cellular stress, p53 can translocate into the nucleus (197). The p53 protein, located in the nucleus, experiences conformational alterations that enable it to function as a transcription factor. This activity facilitates the upregulation of numerous pro-apoptotic proteins, thereby making sense in the regulation of both endogenous and exogenous apoptotic pathways (197). p53 can also translocate to the mitochondrial surface and directly bind to Bcl-2 family proteins to promote endogenous apoptosis (197, 198). In addition to this, p53 promotes the expression of Apaf-1 and caspase-6 and promotes extrinsic apoptosis (198). p53 also plays a role in regulating the autophagic process. An autophagy-induced response was observed in mice whose p53 expression was blocked using cypermethrin-α. And p53-null cells also showed enhanced autophagy compared with wild-type cells. In addition, cytoplasmic p53 can interact with FIP200, which in turn competitively inactivates autophagy.

Other lung diseases

In addition to the above lung diseases, autophagy is also greatly related to the occurrence and development of many other lung diseases, such as asthma, COVID-19, and atypical pneumonia.

Autophagy plays a complex role in the pathophysiology of asthma and may be deleterious or beneficial. Autophagy can affect inflammatory response, airway remodeling, immune regulation, and other aspects, and is an important field of asthma treatment research. Polymorphisms in the autophagy-related gene Atg5 are strongly associated with asthma (199). In respiratory epithelial cells of patients with severe asthma, the expression level of Atg5 protein is increased, and this phenomenon is closely related to the deepening of the degree of fibrosis in the lower cell layer as well as the increase of collagen-1 expression (200). IL-13 plays a crucial role in the development of T2 asthma (201). *In vitro*, IL-13 stimulated goblet cell production and secretion of MUC5AC protein from human respiratory epithelial cells (202). This process is associated with activation of the autophagic process, which is blocked when expression of Atg5 is inhibited. In addition, inhibition of autophagy also affects IL-13 production in response to ROS (203). In addition, in asthmatic patients, airway epithelial cells initiate autophagy by inhibiting mTORC1 signaling in response to IL-13 or IL-33 (204). Bronchial fibroblasts showed enhanced mitophagy accompanied by increased expression levels of PINK1

and Parkin protein in severe asthma, which may be an adaptive response against mitochondrial dysfunction in asthmatic cells (205).

COVID-19 is caused by a coronavirus called SARS-CoV-2, and prior research has indicated that autophagy may play a dual role in the context of coronavirus infection (206). Autophagy can degrade coronavirus, enhance inflammatory responses, and modulate inflammation in neutrophils (207). At the same time, it also promotes antigen presentation and provokes immunity against coronavirus (208). However, double-membrane vesicles of autophagosomes facilitate the sequestration of the virus from external immune responses, thereby serving as sites for viral replication and transcription (207). In addition, nonstructural protein 6 (NSP6) of novel coronavirus assists the virus in escaping host innate immunity by activating autophagy. Recent studies have shown that overexpression of SARS-CoV-2 papain-like protease cleaves ULK1 and disrupts the formation of ULK1-ATG13 complex to block intact host autophagy (209). Corona virus also inhibits BECN1 and activates autophagy inhibitors (SKP2 and AKT1) to prevent autophagosome fusion with lysosomes to limit autophagy signal transduction (210, 211). Interestingly, compared with classical SARS-CoV, ORF3a of SARS-CoV-2 can separate homotypic fusion and protein classification components, thereby inhibiting fusion of autophagosomes and lysosomes, which is a unique feature of SARS-CoV-2 inhibition of autophagy (212, 213).

Autophagy is also important in atypical pneumonia, for example, infections caused by Chlamydia pneumonia(CP), Mycoplasma pneumonia, and Legionella. In CP, it has been shown to limit intracellular CP growth *in vitro* by inhibiting autophagy, but *in vivo*, research has demonstrated that the impairment of autophagy in myeloid cells is associated with increased mortality, potentially resulting from intricate antagonistic interactions between inflammasomes and autophagy (214). Post-infection with Mycoplasma pneumonia, the activation of autophagy may correlate with the severity of the disease, and both excessive activation and suppression of autophagy could influence the progression of the illness. Membrane lipids of Mycoplasma pneumonia can activate autophagy through TLR4 and promote the production of inflammatory factors such as TNF-α and IL-1β, exacerbating the inflammatory response (215). Legionella can inject effector proteins into host cells via its type IV secretion system (Dot/Icm) to avoid autophagy and survive. Nevertheless, the autophagy gene Atg7 can also exert its effect by assisting macrophages to clear bacteria (216).

Autophagy as a potential therapeutic target for the treatment of lung diseases

In the human body, autophagy is essential to maintain the normal functioning of tissues and organs as well as the development of diseases. Thus, targeting autophagy may be useful in the treatment of disease, but may also exacerbate disease deterioration. Because the autophagic process can help clear harmful protein aggregates and damaged organelles. However, excessive autophagy or dysregulation of autophagy may be harmful to cells. In lung diseases, the role of autophagy is particularly complex. On the one hand, it can clear pathogens and damaged cells in the lungs and help resist infection and inflammation. On the other hand, if the autophagic process is dysregulated, it may lead to damage and dysfunction of lung tissue. Therefore, using autophagy as a target for the treatment of lung diseases requires great caution. If the treatment strategy is not appropriate, it may exacerbate the condition rather than improve it. How to balance the activation and inhibition of autophagy to achieve the best therapeutic effect is currently a major difficulty in autophagy-targeted therapy (Table 2).

COPD

Based on the available findings, it may be possible to hypothesize that selective targeting of autophagy-related proteins at the genetic or pharmacological level may serve as a basis for the formulation of novel therapies for COPD. In mouse models, many studies have attempted to mitigate the occurrence of abnormal autophagy during smoke exposure by different approaches. However, these investigations have primarily focused on preventive interventions related to the duration of smoking. These studies included the chemical chaperone 4-phenylbutyrate (162); antioxidant drug, cysteine (217); arachidonic acid-derived epoxyeicosatrienoic acid (218); HDAC6 inhibitor tubastatin (219); mitophagy inhibitor Mdivi134; and sodium channel inhibitor carbamazepine. In addition, studies using the mTOR inhibitor rapamycin suggested that increasing autophagy during CS exposure could reduce lung tissue inflammation, which may be of assistance. However, rapamycin increased the number of apoptotic and inflammatory cells compared with controls at baseline. To clarify the pathophysiological function of autophagy in disease, it is essential to carefully time the activation of autophagy and the targeting of lung cells. Further investigation is required to assess the impact of these agents on dysregulated autophagy in COPD.

CF

Treatments for CF have been extensively investigated. The restoration of autophagic functionality may provide additional therapeutic options for treating CF. The antioxidant n-acetyl-l-cysteine has been shown to improve airway phenotypes in CFTR mutant mice. In addition, oral cysteamine was found to restore Beclin 1 expression and prolonged the survival of CFTR ^{F508del} mutant mice (220). Hence, it may be worthwhile to investigate cysteamine drugs' mechanism through restoring autophagy (221). In addition, regular and continuous use of azithromycin has been demonstrated to enhance the health condition of CF patients (222, 223). However, It has been reported that mycobacterial infection increases synchronously with the onset of CF in some studies (224, 225). The seemingly contradictory results observed in cystic fibrosis patients treated with azithromycin

TABLE 2 The mechanism of autophagy-related targets in lung diseases.

Lung diseases	Drug	Autophagy-related targets	Study subject	Mechanism	Reference
COPD	Cysteamine	ROS, Beclin-1, p62	Beas2b cells, C57BL/6 mice, and human (GOLD 0-IV) lung tissues	Cysteamine-induced autophagy can reduce aggregate formation, CS-induced alveolar senescence/death, and emphysema progression.	(278)
	Parkin activators (Preclinical)	PRKN	HBEC	PRKN levels attenuate COPD progression by modulating PINK1-PRKN-mediated mitophagy.	(279)
	NaHS, PAG	COX2	Human lung cells, Bronchial epithelial BEAS-2B cells	H2S inhibits the iron autophagy pathway mediated by NCOA4 and inhibits the ferritin response mediated by lipid peroxidation by activating Nrf2 and PPAR-γ signaling pathways.	(280)
	U75302	LTB4, TFEB	HBE	Inhibition of the LTB4/BLT1 pathway by U75302 promotes autolysosome formation and degradation in response to CS exposure.	(281)
	Gemfibrozil/Laccatin	TFEB	Beas2b cells and C57BL/6 mice	Gemfibrozil/laccein can control CS-induced airway inflammation and autophagic injury by up-regulating TFEB.	(282)
	Ghrelin	NF-κB, AP-1	HBEC	Ghrelin inhibits excessive inflammatory pathways and autophagy induced by particulate matter and/or cigarette extracts in bronchial epithelial cells.	(283)
	Klotho	AKT, ERK	MH-S cells	Klotho inhibits CSE-induced autophagy by down-regulating IGF-1R, Akt and ERK phosphorylation in alveolar macrophages.	(284)
	PFI-103	FSTL1	Human lung cells, C57BL/6 mice	FSTL1 can activate PI3K/Akt signaling pathway and AMPK signaling pathway to regulate autophagy.	(285)
	HMGB1	NF-κB	Human lung cells, C57BL/6 mice	HMGB1 abrogates migration and NF-κB activation in CSE-treated lung macrophages by inhibiting autophagy.	(286)
	Puerarin	FUNDC1	HBEC	Puerarin inhibits FUNDC1-mediated mitochondrial autophagy and CSE-induced apoptosis of human bronchial epithelial cells by activating the PI3K/AKT/mTOR signaling pathway.	(287)
	MitoQ	ROS	HUVEC	MitoQ maintains mitochondrial function by reducing ROS production and excessive autophagy.	(288)
	Vardenafil	AMPK, mTOR	16 HBE cells, C57BL/6 mice	Vardenafil activates autophagy via the AMPK/mTOR signalling pathway	(289)
	Sodium tanshinone IIA sulfonate	PI3K, mTOR	ARPE-19 cells	Sodium tanshinone IIA sulfonate can increase PI3K and mTOR transcription, activate the PI3K/AKT/mTOR pathway, and reduce autophagy.	(290)
	Silymarin	ERK, p38	Beas-2B cells	Silymarin can attenuate inflammatory responses by intervening in crosstalk between autophagy and the ERK MAPK pathway	(291)
	Tiotropium, Olodaterol	JNK	BEAS-2B cells	Tiotropium/olodaterol protects bronchial epithelial cells from CSE-induced injury by inhibiting activation of autophagy and upregulation of JNK phosphorylation.	(292)
	Taurine	NADH	HBEC	Taurine triggers autophagy in C/EBPα/mitochondria/ATG7 pathway.	(293)
	Resveratrol	Notch1	HUVEC	RESV protects against CSE-induced apoptosis by regulating Notch1-mediated autophagy priming.	(294)

(Continued)

10.3389/fimmu.2024.1460023

TABLE 2 Continued

Lung diseases	Drug	Autophagy-related targets	Study subject	Mechanism	Reference
	Epoxyeicosatrienoic acids	PI3K/Akt, mTOR, p62	BEAS-2B cells	EETs inhibit autophagy via PI3K/Akt/mTOR signaling	(295)
	Quercetogetin	PINK1, DRP-1	BEAS-2B cells	QUE inhibits CSE-induced mitochondrial dysfunction and mitophagy by inhibiting phosphorylated (p) -DRP-1 and PINK1 expression.	(296)
CF	Azithromycin	A53T α-synuclein, Q74 huntingtin protein	HeLa, COS-7 cells	Azithromycin blocks autophagic clearance and autophagosome acidification,	(297)
	Myriocin	FA, SREBPF1	IB3-1 cells	Myriocin attenuates inflammation and activates TFEB-induced stress responses, enhances fatty acid oxidation and promotes autophagy.	(298)
	AR-13	CFTR, LC3-II	Human heparinized blood samples	AR-13 treatment increases CFTR and LC3-II expression in epithelial cells.	(299)
	Fatty Acid Cysteamine Conjugates	CFTR	HBEC	It enhances correction of misfolded F508del cystic fibrosis transmembrane conductance regulator (CFTR) by activating autophagy.	(300)
	cysteamine plus epigallocatechin gallate	CFTR	Human nasal epithelial cells	cysteamine plus epigallocatechin gallate rescues CFTR function when autophagy is active and improves CFTR function by expressing proteins that are rescuable	(301)
	Givinostat	CFTR	R77C fibroblasts	Givinostat synergistically improves trafficking efficiency by inducing the F508del CFTR mutant.	(302)
	Cysteamine	CFTR	CF mice	Cysteamine can rescue the function of the F508del-CFTR mutant, thereby restoring bacterial internalization and clearance through processes involving upregulation of the pro-autophagic protein Beclin 1 and reconstitution of the autophagic pathway.	(303)
IPF	Spermidine	mTOR, PI3K/AKT, ATG7	Primary human lung fibroblasts, C57BL/6 mice	Spermidine modulated autophagy by activating the expression of key autophagic molecules such as LC3-II, beclin-1, and ATG7 as well as inhibiting mTOR, a downstream mediator of PI3K/AKT signaling.	(304)
	Eupatilin	Sestrin2, PI3K/Akt, mTOR	MRC-5 cells	Eupatilin ameliorates lung fibrosis by activating the Sestrin2/PI3K/Akt/mTOR-dependent autophagy pathway.	(305)
	Fu-Zheng-Tong-Luo formula	Janus kinase 2, transcription 3	Growth factor-β-induced lung fibroblast model	Fu-zheng-Tong-luo formula promotes autophagy by controlling Janus kinase 2/signal transducer and activator of transcription 3 pathway.	(306)
	Niclosamide Ethanolamine Salt	PI3K, mTOR, Beclin-1	A549 cells, C57BL-6J mice	NEN inhibits PI3K-mTORC1 downstream signaling and Beclin-1 independent autophagy, contributing to inhibition of TGF-β1-induced EMT and collagen deposition in epithelial cells and primary human fibroblasts	(307)
	Fibroblast growth factor 21	PI3K/AKT, mTOR	C57BL/6 mice	FGF21 ameliorates IPF by inhibiting PI3K-AKT-mTOR signaling pathway and activating autophagy	(308)
	Astragaloside IV	PTEN, PI3K/AKT, mTOR		Astragaloside IV activates autophagy by miR-21-mediated PTEN/PI3K/AKT/mTOR pathway	(309)
	Supramolecular Nanofibers	TRB3	MRC-5 cells	Supramolecular Nanofibers interfere with aberrant TRB3/p62 PPIs to restore autophagy.	(310)
	Naringin	ATF3, PINK1	C57BL/6 mice		(311)

(Continued)

10.3389/fimmu.2024.1460023

TABLE 2 Continued

Lung diseases	Drug	Autophagy-related targets	Study subject	Mechanism	Reference
				Naringin represses expression of ERS and mitophagy-related genes as well as ERS downstream proteins, thereby activating transcription factor (ATF) 3 and repressing PTEN-induced transcription of kinase 1 (PINK1).	
	Tetrandrine	PINK1, Parkin	MLE-12 cells	Tetrandrine alleviates IPF by inhibiting alveolar epithelial cell senescence through PINK1/Parkin-mediated mitophagy.	(312)
	Zanubrutinib	TGF-β1	Human fibroblasts	It inhibits collagen deposition and myofibroblast activation by inhibiting the TGF-β1/Smad pathway, and induces autophagy through the TGF-β1/mTOR pathway.	(313)
	Bergenin	TGF-β1	Human fibroblasts	Bergenin inhibits myofibroblast activation and promotes autophagy and apoptosis in myofibroblasts.	(314)
	Ellagic Acid	Wnt	Mlg cells, NIH-3T3 cells	Ellagic acid inhibits fibroblast activation and induces autophagy and apoptosis in myofibroblasts mainly by regulating the Wnt pathway.	(315)
	Astragalin	Beclin-1, LC3A/B	BEAS-2B cells	Astragalutin inhibits autophagosome formation in oxidant-exposed airway epithelial cells by reducing beclin-1 and LC3A/B induction.	(316)
	Tubastatin	TGF-β, PI3K/AKT	Human lung tissue samples	Tubastatin ameliorates lung fibrosis by targeting TGFβ-PI3K-Akt pathway via an HDAC6-independent mechanism.	(317)
	Nintedanib	Beclin-1, ATG7, TGF-β	Primary human fibroblasts, IMR-90 cells	Nintedanib inhibits TGF-β signaling, downregulates ECM gene/protein expression, and promotes non-canonical autophagy.	(318)
	Pirfenidone	PARK2, ROS	Human lung tissue	Pirfenidone induces autophagy/mitophagy activation by enhancing PARK2 expression.	(319)
	Dihydroartemisinin	ROS, Fe2 +	HFL1 cells	DHA treatment resulted in Fe2 + deficiency which then triggered ferritin autophagy D in activated HFL1 cells to inhibit fibroblast differentiation into myofibroblasts.	(320)
PH	ROC-325	HIF-1α, HIF-2α, p62	SD rats	ROC-325 exerts vasodilation and antagonizes pulmonary vascular remodeling by inhibiting autophagy, degrading HIF, and activating eNOS-NO signaling.	(321)
	Piperlongumine	LC3B	PASMCs	Piperlongumine may be effective in inhibiting the proliferation of PASMCs by regulating autophagy, reducing pulmonary artery systolic pressure and right ventricular hypertrophy, and improving pulmonary vascular remodeling.	(322)
	Rhodiola crenulata extract	PPARγ, LC3B, ATG7	PAH rats	RCE administration reversed high levels of decadienoyl-L-carnitine by modulating the metabolic enzyme CPT1A in mRNA and protein levels in serum and lung in PAH rats.	(323)
	Metformin	AMPK	PAH rats	Metformin inhibited hypoxia-induced pulmonary vascular remodeling, collagen deposition, pulmonary artery smooth muscle cell proliferation, increased BECN-1 and LC3B-II/-I ratios, and down-regulation of p62 by inhibiting autophagy through activation of the AMPK signaling pathway.	(324)
	Umbelliferone	ROCK	PASMCs	Umbelliferone could ameliorate hypoxia-induced pulmonary hypertension by inhibiting RhoA/ROCK signaling pathway and autophagy.	(325)
	liraglutide	NADPH, NOX	PASMCs		(326)

(Continued)

10.3389/fimmu.2024.1460023

TABLE 2 Continued

Lung diseases	Drug	Autophagy-related targets	Study subject	Mechanism	Reference
				Liraglutide can reduce the proliferation of PASMCs by inhibiting cellular Drp1/nicotinamide adenine dinucleotide phosphate (NADPH) oxidase (NOX) pathway and Atg-5/Atg-7/Beclin-1/LC3β-dependent pathway of autophagy in PAH.	
	Docetaxel	LC3B-II, p62	PAH rats	Docetaxel decreased autophagy as monitored by LC3B-II and p62 expression.	(327)
	Puerarin	LC3B-II, BECN-1, SQSTM1	PASMCs	Puerarin reverses pulmonary vascular remodeling induced by hypoxia in an autophagy-dependent manner.	(328)
	Chloroquine	p62, LC3B-II, BMPR-II	SD rats	Chloroquine prevents the progression of experimental pulmonary hypertension by inhibiting autophagy and lysosomal bone morphogenetic protein type II receptor degradation.	(329)
	Carfilzomib	LC3B-II	SD rats	TP53INP1 specifically drives autophagy to cell death by interacting with LC3B-II in response to Carfilzomib.	(330)
	Quercetin	FOXO1	PASMCs	Quercetin enhanced hypoxia-induced autophagy via the FOXO1-SENS3-mTOR pathway.	(331)
	Apelin	PI3K/Akt, mTOR	PASMCs	Exogenous apelin inhibits autophagy and reduces cell proliferation by activating the APJ receptor-dependent PI3K/Akt/mTOR signaling pathway.	(332)
	Trifluoperazine	AKT	Human pulmonary artery smooth muscle cells	Trifluoperazine reduces activation of the multitasking kinase AKT, resulting in nuclear translocation and slowed proliferation of FOXO3.	(333)
	Iloprost	TGF-β1, LC3B	SD rats	Iloprost significantly induced metalloproteinase-9 gene expression and activity and increased expression of autophagy genes associated with collagen degradation.	(334)
PTB	1,25-dihydroxyvitamin D3	ATG5, Beclin-1	PTB Patient Monocytes	Vitamin D enhances innate immune function, promotes the expression of autophagy-related genes, and may help to control the intracellular growth of Mycobacterium bovis in macrophages.	(335)
	Nordihydroguaiaretic acid	PI3K/AKT, mTOR	THP-1 cells, MDM	Nordihydroguaiaretic acid enhances the immune response by promoting autophagy.	(336)
	MIR144*	DRAM2	ATCC, CRL-3213	MIR144* inhibits the antimicrobial response against Mycobacterium tuberculosis in human monocytes and macrophages by targeting the autophagy protein DRAM2.	(337)
	BTLA	AKT, mTOR	Whole blood of PTB patients, C57/BL6 mice	BTLA promotes host defense against Mycobacterium by enhancing autophagy.	(338)
	Loperamide	LC3, ATG16L1	Balb/c mice	The effect of loperamide on human AM bactericidal activity is associated with degradative autophagy, including ectopic expression and degradation of endogenous p62.	(339)
	Curcumin	NFκB, LC3B	THP-1 human monocytes	Curcumin enhances control of Mycobacterium tuberculosis-infected human macrophages by inducing autophagy.	(340)
NSCLC	Apatinib	ROS/Nrf2/p62 signaling	A549 cells, H1299 cells	Apatinib induces autophagy and apoptosis in NSCLC by modulating ROS/Nrf2/p62 signaling.	(341)
	Andrographolide	p62			(342)

(Continued)

10.3389/fimmu.2024.1460023

TABLE 2 Continued

Lung diseases	Drug	Autophagy-related targets	Study subject	Mechanism	Reference
			H1975cells, H1299cells, H1650cells, H460cells, BEAS-2B cells	Andrographolide regulates P62-dependent selective autophagic degradation of PD-L1 by inhibiting STAT3 phosphorylation.	
	Schizandrin A	p62, AMPK	A549, H1299, H1975, BEAS-2B cells	SchA can induce autophagy by activating the AMPK signal, the autophagy process induced by SchA remains incomplete and fails to promote cell survival.	(343)
	Curcumin	Beclin1, LC3	A549 cells, H1299 cells	Curcumin induces iron death by activating autophagy in NSCLC.	(344)
	Rocaglamide	cGAS-STING, ULK1	A549cells, H1299 cells, H1975 cells	RocA promotes NK cell infiltration by targeting ULK1 to inhibit autophagy.	(345)
	Tryptanthrin	ROS, LC3	A549 cells	Tryptanthrin increases autophagy triggered by the transition from LC3-I to LC3-II to inhibit proliferation and induce apoptosis in non-small cell lung cancer (NSCLC) cells.	(346)
	Polyphyllin VI	ROS, NF-κB	A549 cells, H1299 cells	PPVI-induced caspase-1-mediated pyroptosis in NSCLC by inducing ROS/NF-κB/NLRP3/GSDMD signaling axis	(347)
	Crizotinib	AMPK	CCC-HEH-2	Crizotinib-impaired autophagic process leads to cardiomyocyte death and cardiac injury through inhibition of MET protein degradation, and a novel function of blocking autophagosome-lysosome fusion is demonstrated in drug-induced cardiotoxicity.	(348)
	Tubeimoside-1	mTOR	A549 cells, H157cells, H1299cells, H460 cells, LLC	TBM-1 selectively binds to the mammalian target of rapamycin (mTOR) kinase and suppresses the activation of mTORC1, leading to the nuclear translocation of TFEB and lysosome biogenesis.	(349)
	Ginsenoside Rg5	PI3K/Akt, mTOR	H1650 cells, A549 cells, BEAS-2B cells	Rg5 induces autophagy and caspase-dependent apoptosis in NSCLC cells by inhibiting the PI3K/Akt/mTOR signaling pathway.	(350)
	Resveratrol	AMPK, mTOR	A549 cells	RSV antagonizes NGFR knockdown-induced enhanced autophagy and apoptosis via AMPK, mTOR pathway.	(351)
	Pseudolaric acid B	ROS, AMPK, mTOR	BEAS-2B cells, H1975 cells, H1650 cells	PAB induces apoptosis and autophagic cell death in NSCLC cells via the ROS-triggered AMPK/mTOR signaling pathway.	(352)
	Corynoxine	AKT, mTOR, GSK3β	A549 cells, H1975 cells	Corynoxine triggers cell death by activating PP2A and inhibiting the AKT-mTOR/GSK3β axis.	(353)
	Morusin	JNK, ERK, PI3K/Akt	A549 cells, NCI-H292	Morusin induces apoptosis and autophagy through JNK, ERK and PI3K/Akt signaling in human lung cancer cells.	(354)
	Sophflarine A	ROS	A549cells, H820 cells	Sophflarine A mediates pyroptosis and autophagy via regulating ROS.	(355)

(Continued)

10.3389/fimmu.2024.1460023

TABLE 2 Continued

Lung diseases	Drug	Autophagy-related targets	Study subject	Mechanism	Reference
	DFIQ	ROS, LAMP2	H1299cells, A549cells, H460 cells	DFIQ induces ROS production through autophagy activation and LAMP2 depletion.	(356)
	Carnosic Acid	LKB1, AMPK	H1299 cells, H460 cells	CA can induce apoptosis through a mechanism involving sestrin-2/LKB1/AMPK signaling and autophagy induction.	(357)
	Muyin extract	P53, Bcl-2	A549 cells, NCI-H460 cells	Muyin extract induces apoptosis and autophagy by blocking the Akt/mTOR pathway to enhance immunity.	(358)
	ABTL0812	ATF4-DDIT3-TRIB3	A549 cells, MRC5	ABTL0812 inhibits the AKT-mTORC1 axis via upregulation of TRIB3 in cancer cells and tumor models.	(359)
	(+)-anthrabenzoxocinone	PI3K/AKT, mTOR	A549 cells, NCI-H1299, NCI-H226	The PI3K/AKT/mTOR signaling pathway is targeted and suppressed by (+)-ABX, resulting in the induction of S and G2/M phase arrest, apoptosis, and autophagy in NSCLC cells.	(360)
	ASP4132	AMPK	A549cells and NCI-H1944	ASP4132 acts through AMPK activation, mTORC1 inhibition and EGFR-PDGFRα degradation, as well as Akt inhibition and autophagy induction.	(361)
	Baicalein	MAP4K3, mTOR	H1299 cells, A549 cells	Baicalein regulates autophagy in NSCLC via the MAP4K3/mTORC1/TFEB axis.	(362)
	pegaharoline A	PI3K/AKT, mTOR	A549 cells, PC9	PA can inhibit NSCLC cell growth by blocking PI3K/AKT/mTOR and EMT pathways.	(363)
	Ailanthone	ULK1	H1975, A549, HCT-8, MDA-MB-231, BEAS-2B, 293T cells	Ailanthone inhibits ULK1-mediated autophagy and subsequently inhibits NSCLC cells	(364)
	DSTYK	P62, mTOR	H2009 cells, H226 cells	DSTYK inhibits mTORC1, which promotes autophagy, and its defects result in disruption of autophagy, leading to progressive accumulation of autophagosomes.	(365)

10.3389/fimmu.2024.1460023

may be attributed to the drug's capacity to inhibit lysosomal acidification. This inhibition subsequently disrupts autophagy and the degradation processes within phagosomes. More therapeutic options targeting autophagy-related pathways need to be investigated in greater depth.

IPF

Promoting autophagy may be beneficial in the treatment of IPF. Currently, drugs that may be active include IL17A neutralizing antibodies (177), MIR449A(microRNA 449a) (226), or PDGFRB (platelet-derived growth factor receptor beta) inhibitors. Bleomycin-mediated increases in mortality and decreases in fibrotic resistance in mice have been observed in experimental models (178, 227). However, rapamycin appears to potentiate silica-induced effects, exacerbating inflammation and fibrosis (228). In individuals diagnosed with IPF, the rapamycin analog everolimus has been observed to contribute to the progression of the disease. Therefore, further studies are required to assess whether targeted autophagy agents are beneficial in IPF.

Pulmonary hypertension

Numerous studies utilizing animal models have investigated the impact of rapamycin, mTOR inhibitors, and autophagy activators on the prevention of PAH development (229). In clinical settings, everolimus, a derivative of rapamycin, has been shown to enhance outcomes in patients with strict PH resulting from chronic thromboembolic disease, while also decreasing pulmonary vascular resistance (230). The suppression of the autophagy pathway may offer potential targeted therapeutic strategies for the disease.

Pulmonary tuberculosis

Therapeutic regimens targeting pulmonary tuberculosis by autophagy-related pathways are being widely investigated. Vitamin D stimulates autophagy activation in Mycobacterium tuberculosis by inducing antibiotics (231). Vitamin D deficiency has been linked to a heightened threat of active TB (232). The conversion time of sputum cultures is not affected by vitamin D supplementation according to recent research (233, 234). However, it has also been reported that vitamin D supplementation given to patients with vitamin D receptor polymorphisms shortens sputum culture conversion time (234). Isoniazid and pyrazinamide are recognized as primary agents in the treatment of tuberculosis. These compounds facilitate the activation of autophagy and the maturation of autophagosomes within host cells infected by Mtb (235). This may constitute a component of the fundamental mechanism associated with the treatment involving these agents. Although the activation of autophagy has been previously proposed as a viable therapeutic approach for patients infected with Mtb, recent findings cast uncertainty on this hypothesis and impede the progression of further research.

Non-small cell lung cancer

The development of novel compounds aimed at targeting mutant p53 and reinstating its wild-type functionality represents a promising therapeutic approach for cancer treatment, particularly in the context of NSCLC, which is characterized by a significant mutation frequency (236–238). This therapeutic potential has already been demonstrated in many compounds. Nutlins are cis-imidazoline analogs that inhibit the interaction between MDM2 and wild-type p53 *in vivo*, which in turn enhances the anti-tumor ability of p53 (239). We speculate that the development of targeted agents against aberrant p53 or promoting anti-tumor activity of wild-type p53 may be helpful in the treatment of cancer. RETRA was found to inhibit the malignant proliferation of cancer cells carrying aberrant p53 via a p73-dependent salvage pathway (240). The reactivating small molecule PRIMA-1 of mutant p53 can be combined to convert it into a wild-type construct, thereby achieving inhibition of tumor growth (241, 242). In addition, restoring and stabilizing the DNA binding domain (DBD) of p53 is also a promising tumor suppressor strategy.

Rapamycin has great potential in cancer therapy, which activates mitochondria-mediated apoptosis independent of p53 in NSCLC cells, stressing its effectiveness in disease (29). It has been shown that mouse models of NSCLC have reduced tumor growth and apoptosis following rapamycin treatment (232). Furthermore, certain anticancer agents have demonstrated markedly enhanced efficacy when administered in conjunction with rapamycin. This includes Bcl-2 inhibitors such as ABT-737, pemetrexed, and lipophilic bisphosphonates (196). Additionally, EGFR tyrosine kinase inhibitors (TKIs) have received approval for the treatment of patients with NSCLC who possess particular EGFR mutations (243). However, resistance to this drug is a major problem in clinical treatment. Notably, erlotinib combined with rapamycin enhanced autophagy and restored sensitivity to EGFR-TKIs (244). Erlotinib in combination with rapamycin has also been shown to help overcome resistance due to p53 deficiency *in vitro*.

In addition to rapamycin, drugs targeting proteins related to other signaling pathways of autophagy, such as AZD8055 (PI3K inhibitor), NVP-BEZ235 (PI3K and mTORC1 inhibitors), perifosine (AKT inhibitor), and GSK-690693 (AKT inhibitor), have been investigated in NSCLC. In certain instances, these targeted therapies modulate autophagy-related pathways as a component of the treatment regimen for NSCLC (245–248). The effects of some traditional Chinese medicine compounds in NSCLC have also been largely investigated. Curcumin is a phenolic compound derived from the plant Curcuma longa (249, 250). Curcumin treatment showed a promoting effect of autophagy as well as a pro-apoptotic effect in lung adenocarcinoma A549 cells, allowing us to speculate its therapeutic potential in NSCLC (251).

Cytoprotective autophagy in NSCLC cells is also activated by cucurbitacin E and glycerinic acid (252). Licochalcone A, a flavonoid derived from the traditional Chinese medicinal plant Glycyrrhiza uralensis Fisch, has been shown to promote apoptosis and autophagy through the induction of ER stress (253). Thick acid from Poria cocos halted lung cancer cell growth by boosting ROS and activating JNK (254). Platycodin-D can induce autophagy in H460 and A549 NSCLC cells, as shown by stimulating the formation of ATG3, ATG7, Beclin-1, and LC3-II (255).

Conclusion

Autophagy plays a dual role in lung diseases, exhibiting both potentially harmful effects in certain pathophysiological conditions and serving as a protective mechanism that promotes cell survival. Recent advancements in research have significantly enhanced our understanding of the role of autophagy in the pathophysiological mechanisms underlying various diseases, thereby offering novel insights for the development of targeted therapies for pulmonary diseases. However, assessing the actual clinical effects of targeted agents for autophagy-related pathways on lung diseases is challenging. The challenge arises from the observation that autophagic responses occurring in various compartments of the lung may yield markedly distinct effects. Accurate measurements of autophagy also need to be updated. It is critical to revise the precise assessments of autophagy. Understanding the impact of highly specific autophagy modulators on disease models characterized by particular autophagy deficiencies is vital for formulating clinically relevant approaches to either stimulate or suppress autophagy.

Author contributions

LL: Writing – original draft. YL: Writing – original draft. ZH: Writing – review & editing, Writing – original draft. KW: Writing – original draft. SZ: Writing – original draft. ZW: Writing – original draft. SW: Writing – review & editing. HC: Writing – review & editing.

Funding

The author(s) declare that no financial support was received for the research, authorship, and/or publication of this article.

Conflict of interest

The authors declare that the research was conducted in the absence of any commercial or financial relationships that could be construed as a potential conflict of interest.

Publisher's note

All claims expressed in this article are solely those of the authors and do not necessarily represent those of their affiliated organizations, or those of the publisher, the editors and the reviewers. Any product that may be evaluated in this article, or claim that may be made by its manufacturer, is not guaranteed or endorsed by the publisher.

References

1. He C, Klionsky DJ. Regulation mechanisms and signaling pathways of autophagy. *Annu Rev Genet*. (2009) 43:67–93. doi: 10.1146/annurev-genet-102808-114910

2. Ravikumar B, Sarkar S, Davies JE, Futter M, Garcia-Arencibia M, Green-Thompson ZW, et al. Regulation of mammalian autophagy in physiology and pathophysiology. *Physiol Rev*. (2010) 90:1383–435. doi: 10.1152/physrev.00030.2009

3. Eskelinen EL, Saftig P. Autophagy: a lysosomal degradation pathway with a central role in health and disease. *Biochim Biophys Acta*. (2009) 1793:664–73. doi: 10.1016/j.bbamcr.2008.07.014

4. Pattison CJ, Korolchuk VI. Autophagy: 'Self-eating' Your way to longevity. *Subcell Biochem*. (2018) 90:25–47. doi: 10.1007/978-981-13-2835-0_2

5. Rabinowitz JD, White E. Autophagy and metabolism. *Science*. (2010) 330:1344–8. doi: 10.1126/science.1193497

6. Mizushima N, Levine B, Cuervo AM, Klionsky DJ. Autophagy fights disease through cellular self-digestion. *Nature*. (2008) 451:1069–75. doi: 10.1038/nature06639

7. Levine B, Mizushima N, Virgin HW. Autophagy in immunity and inflammation. *Nature*. (2011) 469:323–35. doi: 10.1038/nature09782

8. Rioux JD, Xavier RJ, Taylor KD, Silverberg MS, Goyette P, Huett A, et al. Genome-wide association study identifies new susceptibility loci for Crohn disease and implicates autophagy in disease pathogenesis. *Nat Genet*. (2007) 39:596–604. doi: 10.1038/ng2032

9. Alula KM, Theiss AL. Autophagy in crohn's disease: converging on dysfunctional innate immunity. *Cells*. (2023) 12:1779. doi: 10.3390/cells12131779

10. Martinet W, De Meyer GR. Autophagy in atherosclerosis: a cell survival and death phenomenon with therapeutic potential. *Circ Res*. (2009) 104:304–17. doi: 10.1161/CIRCRESAHA.108.188318

11. Tang Y, Xu W, Liu Y, Zhou J, Cui K, Chen Y. Autophagy protects mitochondrial health in heart failure. *Heart Fail Rev*. (2024) 29:113–23. doi: 10.1007/s10741-023-10354-x

12. Diab R, Pilotto F, Saxena S. Autophagy and neurodegeneration: Unraveling the role of C9ORF72 in the regulation of autophagy and its relationship to ALS-FTD pathology. *Front Cell Neurosci*. (2023) 17:1086895. doi: 10.3389/fncel.2023.1086895

13. Rosenfeldt MT, Ryan KM. The multiple roles of autophagy in cancer. *Carcinogenesis*. (2011) 32:955–63. doi: 10.1093/carcin/bgr031

14. Liang C. Negative regulation of autophagy. *Cell Death Differ*. (2010) 17:1807–15. doi: 10.1038/cdd.2010.115

15. Lin Z, Long F, Kang R, Klionsky DJ, Yang M, Tang D. The lipid basis of cell death and autophagy. *Autophagy*. (2024) 20:469–88. doi: 10.1080/15548627.2023.2259732

16. Klionsky DJ. Autophagy: from phenomenology to molecular understanding in less than a decade. *Nat Rev Mol Cell Biol*. (2007) 8:931–7. doi: 10.1038/nrm2245

17. Mizushima N, Komatsu M. Autophagy: renovation of cells and tissues. *Cell*. (2011) 147:728–41. doi: 10.1016/j.cell.2011.10.026

18. Sahu R, Kaushik S, Clement CC, Cannizzo ES, Scharf B, Follenzi A, et al. Microautophagy of cytosolic proteins by late endosomes. *Dev Cell*. (2011) 20:131–9. doi: 10.1016/j.devcel.2010.12.003

19. Choi AM, Ryter SW, Levine B. Autophagy in human health and disease. *N Engl J Med*. (2013) 368:1845–6. doi: 10.1056/NEJMra1205406

20. Stolz A, Ernst A, Dikic I. Cargo recognition and trafficking in selective autophagy. *Nat Cell Biol*. (2014) 16:495–501. doi: 10.1038/ncb2979

21. Vargas JNS, Hamasaki M, Kawabata T, Youle RJ, Yoshimori T. The mechanisms and roles of selective autophagy in mammals. *Nat Rev Mol Cell Biol*. (2023) 24:167–85. doi: 10.1038/s41580-022-00542-2

22. Rubio-Tomás T, Sotiriou A, Tavernarakis N. The interplay between selective types of (macro)autophagy: Mitophagy and xenophagy. *Int Rev Cell Mol Biol*. (2023) 374:129–57. doi: 10.1016/bs.ircmb.2022.10.003

23. Tanida I. Autophagy basics. *Microbiol Immunol*. (2011) 55:1–11. doi: 10.1111/j.1348-0421.2010.00271.x

24. Li W, Zhou C, Yu L, Hou Z, Liu H, Kong L, et al. Tumor-derived lactate promotes resistance to bevacizumab treatment by facilitating autophagy enhancer protein RUBCNL expression through histone H3 lysine 18 lactylation (H3K18la) in colorectal cancer. *Autophagy*. (2024) 20:114–30. doi: 10.1080/15548627.2023.2249762

25. Liang C, Lee JS, Inn KS, Gack MU, Li Q, Roberts EA, et al. Beclin1-binding UVRAG targets the class C Vps complex to coordinate autophagosome maturation and endocytic trafficking. *Nat Cell Biol*. (2008) 10:776–87. doi: 10.1038/ncb1740

26. Grochowska KM, Sperveslage M, Raman R, Failla AV, Głów D, Schulze C, et al. Chaperone-mediated autophagy in neuronal dendrites utilizes activity-dependent lysosomal exocytosis for protein disposal. *Cell Rep*. (2023) 42:112998. doi: 10.1016/j.celrep.2023.112998

27. Yang Z, Klionsky DJ. Mammalian autophagy: core molecular machinery and signaling regulation. *Curr Opin Cell Biol*. (2010) 22:124–31. doi: 10.1016/j.ceb.2009.11.014

28. Jung CH, Ro SH, Cao J, Otto NM, Kim DH, Mtor Regulation of Autophagy. mTOR regulation of autophagy. *FEBS Lett*. (2010) 584:1287–95. doi: 10.1016/j.febslet.2010.01.017

29. Fumarola C, Bonelli MA, Petronini PG, Alfieri RR. Targeting PI3K/AKT/mTOR pathway in non small cell lung cancer. *Biochem Pharmacol*. (2014) 90:197–207. doi: 10.1016/j.bcp.2014.05.011

30. Shimobayashi M, Hall MN. Making new contacts: the mTOR network in metabolism and signalling crosstalk. *Nat Rev Mol Cell Biol*. (2014) 15:155–62. doi: 10.1038/nrm3757

31. Loewith R, Jacinto E, Wullschleger S, Lorberg A, Crespo JL, Bonenfant D, et al. Two TOR complexes, only one of which is rapamycin sensitive, have distinct roles in cell growth control. *Mol Cell*. (2002) 10:457–68. doi: 10.1016/S1097-2765(02)00636-6

32. Mendoza MC, Er EE, Blenis J. The Ras-ERK and PI3K-mTOR pathways: cross-talk and compensation. *Trends Biochem Sci*. (2011) 36:320–8. doi: 10.1016/j.tibs.2011.03.006

33. Vivanco I, Sawyers CL. The phosphatidylinositol 3-Kinase AKT pathway in human cancer. *Nat Rev Cancer*. (2002) 2:489–501. doi: 10.1038/nrc839

34. Proikas-Cezanne T, Haas ML, Pastor-Maldonado CJ, Schüssele DS. Human WIPI β-propeller function in autophagy and neurodegeneration. *FEBS Lett*. (2024) 598:127–39. doi: 10.1002/1873-3468.14782

35. Franke TF, Yang SI, Chan TO, Datta K, Kazlauskas A, Morrison DK, et al. The protein kinase encoded by the Akt proto-oncogene is a target of the PDGF-activated phosphatidylinositol 3-kinase. *Cell*. (1995) 81:727–36. doi: 10.1016/0092-8674(95)90534-0

36. Sarbassov DD, Guertin DA, Ali SM, Sabatini DM. Phosphorylation and regulation of Akt/PKB by the rictor-mTOR complex. *Science*. (2005) 307:1098–101. doi: 10.1126/science.1106148

37. Fei C, Zhen X, Shiqiang Z, Jun P. Frontier knowledge and future directions of programmed cell death in clear cell renal cell carcinoma. *Cell Death Discovery*. (2024) 10:113. doi: 10.1038/s41420-024-01880-0

38. Liu P, Cheng H, Roberts TM, Zhao JJ. Targeting the phosphoinositide 3-kinase pathway in cancer. *Nat Rev Drug Discovery*. (2009) 8:627–44. doi: 10.1038/nrd2926

39. Inoki K, Li Y, Zhu T, Wu J, Guan KL. TSC2 is phosphorylated and inhibited by Akt and suppresses mTOR signalling. *Nat Cell Biol*. (2002) 4:648–57. doi: 10.1038/ncb839

40. Laplante M, Sabatini DM. mTOR signaling in growth control and disease. *Cell*. (2012) 149:274–93. doi: 10.1016/j.cell.2012.03.017

41. McCubrey JA, Steelman LS, Chappell WH, Abrams SL, Wong EW, Chang F, et al. Roles of the Raf/MEK/ERK pathway in cell growth, Malignant transformation and drug resistance. *Biochim Biophys Acta*. (2007) 1773:1263–84. doi: 10.1016/j.bbamcr.2006.10.001

42. Asati V, Mahapatra DK, Bharti SK. PI3K/Akt/mTOR and Ras/Raf/MEK/ERK signaling pathways inhibitors as anticancer agents: Structural and pharmacological perspectives. *Eur J Med Chem*. (2016) 109:314–41. doi: 10.1016/j.ejmech.2016.01.012

43. Lander HM, Milbank AJ, Tauras JM, Hajjar DP, Hempstead BL. Redox regulation of cell signalling. *Nature*. (1996) 381:380–1. doi: 10.1038/381380a0

44. Livingston MJ, Zhang M, Kwon SH, Chen JK, Li H, Manicassamy S, et al. Autophagy activates EGR1 via MAPK/ERK to induce FGF2 in renal tubular cells for fibroblast activation and fibrosis during maladaptive kidney repair. *Autophagy*. (2024) 20:1032–53. doi: 10.1080/15548627.2023.2281156

45. Roach PJ. AMPK -> ULK1 -> autophagy. *Mol Cell Biol*. (2011) 31:3082–4. doi: 10.1128/MCB.05565-11

46. Li H, Zhu H, Xu CJ, Yuan J. Cleavage of BID by caspase 8 mediates the mitochondrial damage in the Fas pathway of apoptosis. *Cell*. (1998) 94:491–501. doi: 10.1016/S0092-8674(00)81590-1

47. Goulielmaki M, Koustas E, Moysidou E, Vlassi M, Sasazuki T, Shirasawa S, et al. BRAF associated autophagy exploitation: BRAF and autophagy inhibitors synergise to efficiently overcome resistance of BRAF mutant colorectal cancer cells. *Oncotarget*. (2016) 7:9188–221. doi: 10.18632/oncotarget.6942

48. Elgendy M, Sheridan C, Brumatti G, Martin SJ. Oncogenic Ras-induced expression of Noxa and Beclin-1 promotes autophagic cell death and limits clonogenic survival. *Mol Cell*. (2011) 42:23–35. doi: 10.1016/j.molcel.2011.02.009

49. Corcelle E, Nebout M, Bekri S, Gauthier N, Hofman P, Poujeol P, et al. Disruption of autophagy at the maturation step by the carcinogen lindane is associated with the sustained mitogen-activated protein kinase/extracellular signal-regulated kinase activity. *Cancer Res*. (2006) 66:6861–70. doi: 10.1158/0008-5472.CAN-05-3557

50. Shaw RJ, Bardeesy N, Manning BD, Lopez L, Kosmatka M, DePinho RA, et al. The LKB1 tumor suppressor negatively regulates mTOR signaling. *Cancer Cell*. (2004) 6:91–9. doi: 10.1016/j.ccr.2004.06.007

51. Woods A, Johnstone SR, Dickerson K, Leiper FC, Fryer LG, Neumann D, et al. LKB1 is the upstream kinase in the AMP-activated protein kinase cascade. *Curr Biol*. (2003) 13:2004–8. doi: 10.1016/j.cub.2003.10.031

52. Shackelford DB, Shaw RJ. The LKB1-AMPK pathway: metabolism and growth control in tumour suppression. *Nat Rev Cancer*. (2009) 9:563–75. doi: 10.1038/nrc2676

53. Jones RG, Plas DR, Kubek S, Buzzai M, Mu J, Xu Y, et al. AMP-activated protein kinase induces a p53-dependent metabolic checkpoint. *Mol Cell*. (2005) 18:283–93. doi: 10.1016/j.molcel.2005.03.027

54. Corradetti MN, Inoki K, Bardeesy N, DePinho RA, Guan KL. Regulation of the TSC pathway by LKB1: evidence of a molecular link between tuberous sclerosis complex and Peutz-Jeghers syndrome. *Genes Dev*. (2004) 18:1533–8. doi: 10.1101/gad.1199104

55. Gwinn DM, Shackelford DB, Egan DF, Mihaylova MM, Mery A, Vasquez DS, et al. AMPK phosphorylation of raptor mediates a metabolic checkpoint. *Mol Cell*. (2008) 30:214–26. doi: 10.1016/j.molcel.2008.03.003

56. Lee JW, Park S, Takahashi Y, Wang HG. The association of AMPK with ULK1 regulates autophagy. *PloS One*. (2010) 5:e15394. doi: 10.1371/journal.pone.0015394

57. Shang L, Chen S, Du F, Li S, Zhao L, Wang X. *Nutrient starvation elicits an acute autophagic response mediated by Ulk1 dephosphorylation and its subsequent dissociation from AMPK*. *Proc Natl Acad Sci U S A*. (2011) 108:4788–93. doi: 10.1073/pnas.1100844108

58. Kim J, Kundu M, Viollet B, Guan KL. AMPK and mTOR regulate autophagy through direct phosphorylation of Ulk1. *Nat Cell Biol*. (2011) 13:132–41. doi: 10.1038/ncb2152

59. Chan EY, Kir S, Tooze SA. siRNA screening of the kinome identifies ULK1 as a multidomain modulator of autophagy. *J Biol Chem*. (2007) 282:25464–74. doi: 10.1074/jbc.M703663200

60. Mizushima N. The role of the Atg1/ULK1 complex in autophagy regulation. *Curr Opin Cell Biol*. (2010) 22:132–9. doi: 10.1016/j.ceb.2009.12.004

61. Chan EY, Tooze SA. Evolution of Atg1 function and regulation. *Autophagy*. (2009) 5:758–65. doi: 10.4161/auto.8709

62. Yao W, Chen Y, Chen Y, Zhao P, Liu J, Zhang Y, et al. TOR-mediated Ypt1 phosphorylation regulates autophagy initiation complex assembly. *EMBO J*. (2023) 42:e112814. doi: 10.15252/embj.2022112814

63. Hara T, Takamura A, Kishi C, Iemura S, Natsume T, Guan JL, et al. FIP200, a ULK-interacting protein, is required for autophagosome formation in mammalian cells. *J Cell Biol*. (2008) 181:497–510. doi: 10.1083/jcb.200712064

64. Young AR, Chan EY, Hu XW, Köchl R, Crawshaw SG, High S, et al. Starvation and ULK1-dependent cycling of mammalian Atg9 between the TGN and endosomes. *J Cell Sci*. (2006) 119:3888–900. doi: 10.1242/jcs.03172

65. Ganley IG, Lam du H, Wang J, Ding X, Chen S, Jiang X. ULK1.ATG13.FIP200 complex mediates mTOR signaling and is essential for autophagy. *J Biol Chem*. (2009) 284:12297–305. doi: 10.1074/jbc.M900573200

66. Hosokawa N, Sasaki T, Iemura S, Natsume T, Hara T, Mizushima N. Atg101, a novel mammalian autophagy protein interacting with Atg13. *Autophagy*. (2009) 5:973–9. doi: 10.4161/auto.5.7.9296

67. Chan EY, Longatti A, McKnight NC, Tooze SA. Kinase-inactivated ULK proteins inhibit autophagy via their conserved C-terminal domains using an Atg13-independent mechanism. *Mol Cell Biol*. (2009) 29:157–71. doi: 10.1128/MCB.01082-08

68. Chang YY, Neufeld TP. An Atg1/Atg13 complex with multiple roles in TOR-mediated autophagy regulation. *Mol Biol Cell*. (2009) 20:2004–14. doi: 10.1091/mbc.e08-12-1250

69. Randall-Demllo S, Chieppa M, Eri R. Intestinal epithelium and autophagy: partners in gut homeostasis. *Front Immunol*. (2013) 4:301. doi: 10.3389/fimmu.2013.00301

70. Sarbassov DD, Ali SM, Sengupta S, Sheen JH, Hsu PP, Bagley AF, et al. Prolonged rapamycin treatment inhibits mTORC2 assembly and Akt/PKB. *Mol Cell*. (2006) 22:159–68. doi: 10.1016/j.molcel.2006.03.029

71. Proikas-Cezanne T, Waddell S, Gaugel A, Frickey T, Lupas A, Nordheim A. WIPI-1alpha (WIPI49), a member of the novel 7-bladed WIPI protein family, is aberrantly expressed in human cancer and is linked to starvation-induced autophagy. *Oncogene*. (2004) 23:9314–25. doi: 10.1038/sj.onc.1208331

72. Polson HE, de Lartigue J, Rigden DJ, Reedijk M, Urbé S, Clague MJ, et al. Mammalian Atg18 (WIPI2) localizes to omegasome-anchored phagophores and positively regulates LC3 lipidation. *Autophagy*. (2010) 6:506–22. doi: 10.4161/auto.6.4.11863

73. Liang XH, Jackson S, Seaman M, Brown K, Kempkes B, Hibshoosh H, et al. Induction of autophagy and inhibition of tumorigenesis by beclin 1. *Nature*. (1999) 402:672–6. doi: 10.1038/45257

74. Furuya N, Yu J, Byfield M, Pattingre S, Levine B. The evolutionarily conserved domain of Beclin 1 is required for Vps34 binding, autophagy and tumor suppressor function. *Autophagy*. (2005) 1:46–52. doi: 10.4161/auto.1.1.1542

75. He C, Levine B. The beclin 1 interactome. *Curr Opin Cell Biol*. (2010) 22:140–9. doi: 10.1016/j.ceb.2010.01.001

76. Prerna K, Dubey VK. Beclin1-mediated interplay between autophagy and apoptosis: New understanding. *Int J Biol Macromol*. (2022) 204:258–73. doi: 10.1016/j.ijbiomac.2022.02.005

77. Liang XH, Kleeman LK, Jiang HH, Gordon G, Goldman JE, Berry G, et al. Protection against fatal Sindbis virus encephalitis by beclin, a novel Bcl-2-interacting protein. *J Virol*. (1998) 72:8586–96. doi: 10.1128/JVI.72.11.8586-8596.1998

78. Feng W, Huang S, Wu H, Zhang M. Molecular basis of Bcl-xL's target recognition versatility revealed by the structure of Bcl-xL in complex with the BH3 domain of Beclin-1. *J Mol Biol*. (2007) 372:223–35. doi: 10.1016/j.jmb.2007.06.069

79. Li X, He L, Che KH, Funderburk SF, Pan L, Pan N, et al. Imperfect interface of Beclin1 coiled-coil domain regulates homodimer and heterodimer formation with Atg14L and UVRAG. *Nat Commun*. (2012) 3:662. doi: 10.1038/ncomms1648

80. González-King H, Rodrigues PG, Albery T, Tangruksa B, Gurrapu R, Silva AM, et al. VHL suppresses autophagy and tumor growth through PHD1-dependent Beclin1 hydroxylation. *EMBO J*. (2024) 43:931–55. doi: 10.1038/s44318-024-00051-2

81. Liang C, Feng P, Ku B, Dotan I, Canaani D, Oh BH, et al. Autophagic and tumour suppressor activity of a novel Beclin1-binding protein UVRAG. *Nat Cell Biol*. (2006) 8:688–99. doi: 10.1038/ncb1426

82. Itakura E, Kishi C, Inoue K, Mizushima N. Beclin 1 forms two distinct phosphatidylinositol 3-kinase complexes with mammalian Atg14 and UVRAG. *Mol Biol Cell*. (2008) 19:5360–72. doi: 10.1091/mbc.e08-01-0080

83. Itakura E, Mizushima N. Atg14 and UVRAG: mutually exclusive subunits of mammalian Beclin 1-PI3K complexes. *Autophagy*. (2009) 5:534–6. doi: 10.4161/auto.5.4.8062

84. Zhong Y, Wang QJ, Li X, Yan Y, Backer JM, Chait BT, et al. Distinct regulation of autophagic activity by Atg14L and Rubicon associated with Beclin 1-phosphatidylinositol-3-kinase complex. *Nat Cell Biol*. (2009) 11:468–76. doi: 10.1038/ncb1854

85. Matsunaga K, Saitoh T, Tabata K, Omori H, Satoh T, Kurotori N, et al. Two Beclin 1-binding proteins, Atg14L and Rubicon, reciprocally regulate autophagy at different stages. *Nat Cell Biol*. (2009) 11:385–96. doi: 10.1038/ncb1846

86. Maiuri MC, Le Toumelin G, Criollo A, Rain JC, Gautier F, Juin P, et al. Functional and physical interaction between Bcl-X(L) and a BH3-like domain in Beclin-1. *EMBO J*. (2007) 26:2527–39. doi: 10.1038/sj.emboj.7601689

87. Pattingre S, Tassa A, Qu X, Garuti R, Liang XH, Mizushima N, et al. Bcl-2 antiapoptotic proteins inhibit Beclin 1-dependent autophagy. *Cell*. (2005) 122:927–39. doi: 10.1016/j.cell.2005.07.002

88. Vousden KH, Lane DP. p53 in health and disease. *Nat Rev Mol Cell Biol*. (2007) 8:275–83. doi: 10.1038/nrm2147

89. Freed-Pastor WA, Prives C. Mutant p53: one name, many proteins. *Genes Dev*. (2012) 26:1268–86. doi: 10.1101/gad.190678.112

90. Kroemer G, Mariño G, Levine B. Autophagy and the integrated stress response. *Mol Cell*. (2010) 40:280–93. doi: 10.1016/j.molcel.2010.09.023

91. Johansen T, Lamark T. Selective autophagy mediated by autophagic adapter proteins. *Autophagy*. (2011) 7:279–96. doi: 10.4161/auto.7.3.14487

92. Scarlatti F, Granata R, Meijer AJ, Codogno P. Does autophagy have a license to kill mammalian cells? *Cell Death Differ*. (2009) 16:12–20. doi: 10.1038/cdd.2008.101

93. Galluzzi L, Vicencio JM, Kepp O, Tasdemir E, Maiuri MC, Kroemer G. To die or not to die: that is the autophagic question. *Curr Mol Med*. (2008) 8:78–91. doi: 10.2174/156652408783769616

94. Chen R, Zou J, Zhong X, Li J, Kang R, Tang D. HMGB1 in the interplay between autophagy and apoptosis in cancer. *Cancer Lett*. (2024) 581:216494. doi: 10.1016/j.canlet.2023.216494

95. Maiuri MC, Zalckvar E, Kimchi A, Kroemer G. Self-eating and self-killing: crosstalk between autophagy and apoptosis. *Nat Rev Mol Cell Biol*. (2007) 8:741–52. doi: 10.1038/nrm2239

96. Shvets E, Elazar Z. Flow cytometric analysis of autophagy in living mammalian cells. *Methods Enzymol*. (2009) 452:131–41. doi: 10.1016/S0076-6879(08)03609-4

97. Farkas T, Høyer-Hansen M, Jäättelä M. Identification of novel autophagy regulators by a luciferase-based assay for the kinetics of autophagic flux. *Autophagy*. (2009) 5:1018–25. doi: 10.4161/auto.5.7.9443

98. Shimizu S, Konishi A, Nishida Y, Mizuta T, Nishina H, Yamamoto A, et al. Involvement of JNK in the regulation of autophagic cell death. *Oncogene*. (2010) 29:2070–82. doi: 10.1038/onc.2009.487

99. Wei Y, Sinha S, Levine B. Dual role of JNK1-mediated phosphorylation of Bcl-2 in autophagy and apoptosis regulation. *Autophagy*. (2008) 4:949–51. doi: 10.4161/auto.6788

100. He C, Zhu H, Li H, Zou MH, Xie Z. Dissociation of Bcl-2-Beclin1 complex by activated AMPK enhances cardiac autophagy and protects against cardiomyocyte apoptosis in diabetes. *Diabetes*. (2013) 62:1270–81. doi: 10.2337/db12-0533

101. Shende P, Plaisance I, Morandi C, Pellieux C, Berthonneche C, Zorzato F, et al. Cardiac raptor ablation impairs adaptive hypertrophy, alters metabolic gene expression, and causes heart failure in mice. *Circulation*. (2011) 123:1073–82. doi: 10.1161/CIRCULATIONAHA.110.977066

102. Bell BD, Leverrier S, Weist BM, Newton RH, Arechiga AF, Luhrs KA, et al. *FADD and caspase-8 control the outcome of autophagic signaling in proliferating T cells. Proc Natl Acad Sci U S A*. (2008) 105:16677–82. doi: 10.1073/pnas.0808597105

103. Yu L, Alva A, Su H, Dutt P, Freundt E, Welsh S, et al. Regulation of an ATG7-beclin 1 program of autophagic cell death by caspase-8. *Science*. (2004) 304:1500–2. doi: 10.1126/science.1096645

104. Thorburn J, Moore F, Rao A, Barclay WW, Thomas LR, Grant KW, et al. Selective inactivation of a Fas-associated death domain protein (FADD)-dependent apoptosis and autophagy pathway in immortal epithelial cells. *Mol Biol Cell*. (2005) 16:1189–99. doi: 10.1091/mbc.e04-10-0906

105. Pyo JO, Jang MH, Kwon YK, Lee HJ, Jun JI, Woo HN, et al. Essential roles of Atg5 and FADD in autophagic cell death: dissection of autophagic cell death into vacuole formation and cell death. *J Biol Chem*. (2005) 280:20722–9. doi: 10.1074/jbc.M413934200

106. Wang F, Trosdal ES, Paddar MA, Duque TLA, Allers L, Mudd M, et al. The role of ATG5 beyond Atg8ylation and autophagy. *Autophagy*. (2024) 20:448–50. doi: 10.1080/15548627.2023.2273703

107. Yousefi S, Perozzo R, Schmid I, Ziemiecki A, Schaffner T, Scapozza L, et al. Calpain-mediated cleavage of Atg5 switches autophagy to apoptosis. *Nat Cell Biol*. (2006) 8:1124–32. doi: 10.1038/ncb1482

108. Zhao Z, Fux B, Goodwin M, Dunay IR, Strong D, Miller BC, et al. Autophagosome-independent essential function for the autophagy protein Atg5 in cellular immunity to intracellular pathogens. *Cell Host Microbe*. (2008) 4:458–69. doi: 10.1016/j.chom.2008.10.003

109. Shelly S, Lukinova N, Bambina S, Berman A, Cherry S. Autophagy is an essential component of Drosophila immunity against vesicular stomatitis virus. *Immunity*. (2009) 30:588–98. doi: 10.1016/j.immuni.2009.02.009

110. Orvedahl A, MacPherson S, Sumpter R Jr., Tallóczy Z, Zou Z, Levine B, et al. Autophagy protects against Sindbis virus infection of the central nervous system. *Cell Host Microbe*. (2010) 7:115–27. doi: 10.1016/j.chom.2010.01.007

111. Yano T, Mita S, Ohmori H, Oshima Y, Fujimoto Y, Ueda R, et al. Autophagic control of listeria through intracellular innate immune recognition in drosophila. *Nat Immunol*. (2008) 9:908–16. doi: 10.1038/ni.1634

112. Jia K, Thomas C, Akbar M, Sun Q, Adams-Huet B, Gilpin C, et al. *Autophagy genes protect against Salmonella typhimurium infection and mediate insulin signaling-regulated pathogen resistance. Proc Natl Acad Sci U S A*. (2009) 106:14564–9. doi: 10.1073/pnas.0813319106

113. Deretic V, Levine B. Autophagy, immunity, and microbial adaptations. *Cell Host Microbe*. (2009) 5:527–49. doi: 10.1016/j.chom.2009.05.016

114. Dwivedi R, Baindara P. Differential regulation of TFEB-induced autophagy during mtb infection and starvation. *Microorganisms*. (2023) 11:2944. doi: 10.3390/microorganisms11122944

115. Lee JS, Li Q, Lee JY, Lee SH, Jeong JH, Lee HR, et al. FLIP-mediated autophagy regulation in cell death control. *Nat Cell Biol*. (2009) 11:1355–62. doi: 10.1038/ncb1980

116. Sumpter R Jr., Levine B. Autophagy and innate immunity: triggering, targeting and tuning. *Semin Cell Dev Biol*. (2010) 21:699–711. doi: 10.1016/j.semcdb.2010.04.003

117. Yoshikawa Y, Ogawa M, Hain T, Yoshida M, Fukumatsu M, Kim M, et al. Listeria monocytogenes ActA-mediated escape from autophagic recognition. *Nat Cell Biol*. (2009) 11:1233–40. doi: 10.1038/ncb1967

118. Dreux M, Chisari FV. Viruses and the autophagy machinery. *Cell Cycle*. (2010) 9:1295–307. doi: 10.4161/cc.9.7.11109

119. Travassos LH, Carneiro LA, Ramjeet M, Hussey S, Kim YG, Magalhães JG, et al. Nod1 and Nod2 direct autophagy by recruiting ATG16L1 to the plasma membrane at the site of bacterial entry. *Nat Immunol*. (2010) 11:55–62. doi: 10.1038/ni.1823

120. Behrends C, Sowa ME, Gygi SP, Harper JW. Network organization of the human autophagy system. *Nature*. (2010) 466:68–76. doi: 10.1038/nature09204

121. Lipinski MM, Hoffman G, Ng A, Zhou W, Py BF, Hsu E, et al. A genome-wide siRNA screen reveals multiple mTORC1 independent signaling pathways regulating autophagy under normal nutritional conditions. *Dev Cell*. (2010) 18:1041–52. doi: 10.1016/j.devcel.2010.05.005

122. Virgin HW, Levine B. Autophagy genes in immunity. *Nat Immunol*. (2009) 10:461–70. doi: 10.1038/ni.1726

123. Mizushima N, Levine B. Autophagy in mammalian development and differentiation. *Nat Cell Biol*. (2010) 12:823–30. doi: 10.1038/ncb0910-823

124. Liu F, Lee JY, Wei H, Tanabe O, Engel JD, Morrison SJ, et al. FIP200 is required for the cell-autonomous maintenance of fetal hematopoietic stem cells. *Blood*. (2010) 116:4806–14. doi: 10.1182/blood-2010-06-288589

125. Nedjic J, Aichinger M, Emmerich J, Mizushima N, Klein L. Autophagy in thymic epithelium shapes the T-cell repertoire and is essential for tolerance. *Nature*. (2008) 455:396–400. doi: 10.1038/nature07208

126. Lee HK, Mattei LM, Steinberg BE, Alberts P, Lee YH, Chervonsky A, et al. In vivo requirement for Atg5 in antigen presentation by dendritic cells. *Immunity*. (2010) 32:227–39. doi: 10.1016/j.immuni.2009.12.006

127. Münz C. Antigen processing via autophagy–not only for MHC class II presentation anymore? *Curr Opin Immunol*. (2010) 22:89–93. doi: 10.1016/j.coi.2010.01.016

128. Lo TH, Weng IC, Chen HL, Liu FT. The role of galectins in the regulation of autophagy and inflammasome in host immunity. *Semin Immunopathol*. (2024) 46:6. doi: 10.1007/s00281-024-01018-5

129. Deretic V, Kimura T, Timmins G, Moseley P, Chauhan S, Mandell M. Immunologic manifestations of autophagy. *J Clin Invest*. (2015) 125:75–84. doi: 10.1172/JCI73945

130. Pengo N, Scolari M, Oliva L, Milan E, Mainoldi F, Raimondi A, et al. Plasma cells require autophagy for sustainable immunoglobulin production. *Nat Immunol*. (2013) 14:298–305. doi: 10.1038/ni.2524

131. Chen M, Hong MJ, Sun H, Wang L, Shi X, Gilbert BE, et al. Essential role for autophagy in the maintenance of immunological memory against influenza infection. *Nat Med*. (2014) 20:503–10. doi: 10.1038/nm.3521

132. Barrett JC, Hansoul S, Nicolae DL, Cho JH, Duerr RH, Rioux JD, et al. Genome-wide association defines more than 30 distinct susceptibility loci for Crohn's disease. *Nat Genet*. (2008) 40:955–62. doi: 10.1038/ng.175

133. Keller CW, Adamopoulos IE, Lünemann JD. Autophagy pathways in autoimmune diseases. *J Autoimmun*. (2023) 136:103030. doi: 10.1016/j.jaut.2023.103030

134. Deretic V, Levine B. Autophagy balances inflammation in innate immunity. *Autophagy*. (2018) 14:243–51. doi: 10.1080/15548627.2017.1402992

135. Saitoh T, Fujita N, Jang MH, Uematsu S, Yang BG, Satoh T, et al. Loss of the autophagy protein Atg16L1 enhances endotoxin-induced IL-1beta production. *Nature*. (2008) 456:264–8. doi: 10.1038/nature07383

136. Cadwell K, Liu JY, Brown SL, Miyoshi H, Loh J, Lennerz JK, et al. A key role for autophagy and the autophagy gene Atg16l1 in mouse and human intestinal Paneth cells. *Nature*. (2008) 456:259–63. doi: 10.1038/nature07416

137. Paludan C, Schmid D, Landthaler M, Vockerodt M, Kube D, Tuschl T , et al. Endogenous MHC class II processing of a viral nuclear antigen after autophagy. *Science*. (2005) 307:593–6. doi: 10.1126/science.1104904

138. Schroder K, Tschopp J. The inflammasomes. *Cell*. (2010) 140:821–32. doi: 10.1016/j.cell.2010.01.040

139. Saitoh T, Akira S. Regulation of innate immune responses by autophagy-related proteins. *J Cell Biol*. (2010) 189:925–35. doi: 10.1083/jcb.201002021

140. Nakahira K, Haspel JA, Rathinam VA, Lee SJ, Dolinay T, Lam HC, et al. Autophagy proteins regulate innate immune responses by inhibiting the release of mitochondrial DNA mediated by the NALP3 inflammasome. *Nat Immunol*. (2011) 12:222–30. doi: 10.1038/ni.1980

141. Zhou R, Yazdi AS, Menu P, Tschopp J. A role for mitochondria in NLRP3 inflammasome activation. *Nature*. (2011) 469:221–5. doi: 10.1038/nature09663

142. Qu X, Zou Z, Sun Q, Luby-Phelps K, Cheng P, Hogan RN, et al. Autophagy gene-dependent clearance of apoptotic cells during embryonic development. *Cell*. (2007) 128:931–46. doi: 10.1016/j.cell.2006.12.044

143. Birgisdottir Å B, Lamark T, Johansen T. The LIR motif - crucial for selective autophagy. *J Cell Sci*. (2013) 126:3237–47. doi: 10.1242/jcs.126128

144. Swanlund JM, Kregel KC, Oberley TD. Investigating autophagy: quantitative morphometric analysis using electron microscopy. *Autophagy*. (2010) 6:270–7. doi: 10.4161/auto.6.2.10439

145. Mizushima N, Yoshimori T. How to interpret LC3 immunoblotting. *Autophagy*. (2007) 3:542–5. doi: 10.4161/auto.4600

146. Mizushima N, Yoshimori T, Levine B. Methods in mammalian autophagy research. *Cell*. (2010) 140:313–26. doi: 10.1016/j.cell.2010.01.028

147. Martinet W, De Meyer GR, Andries L, Herman AG, Kockx MM. In situ detection of starvation-induced autophagy. *J Histochem Cytochem*. (2006) 54:85–96. doi: 10.1369/jhc.5A6743.2005

148. Yoshii SR, Mizushima N. Monitoring and measuring autophagy. *Int J Mol Sci*. (2017) 18:1865. doi: 10.3390/ijms18091865

149. Rubinsztein DC, Cuervo AM, Ravikumar B, Sarkar S, Korolchuk V, Kaushik S, et al. In search of an "autophagomometer. *Autophagy*. (2009) 5:585–9. doi: 10.4161/auto.5.5.8823

150. Haspel J, Shaik RS, Ifedigbo E, Nakahira K, Dolinay T, Englert JA, et al. Characterization of macroautophagic flux in vivo using a leupeptin-based assay. *Autophagy*. (2011) 7:629–42. doi: 10.4161/auto.7.6.15100

151. Larsen KB, Lamark T, Øvervatn A, Harneshaug I, Johansen T, Bjørkøy G. A reporter cell system to monitor autophagy based on p62/SQSTM1. *Autophagy*. (2010) 6:784–93. doi: 10.4161/auto.6.6.12510

152. Bjørkøy G, Lamark T, Pankiv S, Øvervatn A, Brech A, Johansen T. Monitoring autophagic degradation of p62/SQSTM1. *Methods Enzymol*. (2009) 452:181–97. doi: 10.1016/S0076-6879(08)03612-4

153. Dennis PB, Mercer CA. The GST-BHMT assay and related assays for autophagy. *Methods Enzymol*. (2009) 452:97–118. doi: 10.1016/S0076-6879(08)03607-0

154. Ju JS, Miller SE, Jackson E, Cadwell K, Piwnica-Worms D, Weihl CC. Quantitation of selective autophagic protein aggregate degradation in vitro and in vivo using luciferase reporters. *Autophagy*. (2009) 5:511–9. doi: 10.4161/auto.5.4.7761

155. Burney PG, Patel J, Newson R, Minelli C, Naghavi M. *Global and regional trends in COPD mortality, 1990-2010. Eur Respir J*. (2015) 45:1239–47. doi: 10.1183/09031936.00142414

156. Lareau SC, Fahy B, Meek P, Wang A. *Chronic obstructive pulmonary disease (COPD). Am J Respir Crit Care Med*. (2019) 199:P1–p2. doi: 10.1164/rccm.1991P1

157. Teckman JH, Perlmutter DH. *Retention of mutant alpha(1)-antitrypsin Z in endoplasmic reticulum is associated with an autophagic response. Am J Physiol Gastrointest Liver Physiol*. (2000) 279:G961–74. doi: 10.1152/ajpgi.2000.279.5.G961

158. Hogg JC, Timens W. The pathology of chronic obstructive pulmonary disease. *Annu Rev Pathol*. (2009) 4:435–59. doi: 10.1146/annurev.pathol.4.110807.092145

159. Barnes PJ. Immunology of asthma and chronic obstructive pulmonary disease. *Nat Rev Immunol*. (2008) 8:183–92. doi: 10.1038/nri2254

160. Chen ZH, Kim HP, Sciurba FC, Lee SJ, Feghali-Bostwick C, Stolz DB, et al. Egr-1 regulates autophagy in cigarette smoke-induced chronic obstructive pulmonary disease. *PloS One*. (2008) 3:e3316. doi: 10.1371/journal.pone.0003316

161. Chen ZH, Lam HC, Jin Y, Kim HP, Cao J, Lee SJ, et al. *Autophagy protein microtubule-associated protein 1 light chain-3B (LC3B) activates extrinsic apoptosis during cigarette smoke-induced emphysema. Proc Natl Acad Sci U S A*. (2010) 107:18880–5. doi: 10.1073/pnas.1005574107

162. Lam HC, Cloonan SM, Bhashyam AR, Haspel JA, Singh A, Sathirapongsasuti JF, et al. Histone deacetylase 6-mediated selective autophagy regulates COPD-associated cilia dysfunction. *J Clin Invest*. (2013) 123:5212–30. doi: 10.1172/JCI69636

163. Cloonan SM, Lam HC, Ryter SW, Choi AM. Ciliophagy": The consumption of cilia components by autophagy. *Autophagy*. (2014) 10:532–4. doi: 10.4161/auto.27641

164. Wiegman CH, Michaeloudes C, Haji G, Narang P, Clarke CJ, Russell KE, et al. Oxidative stress-induced mitochondrial dysfunction drives inflammation and airway smooth muscle remodeling in patients with chronic obstructive pulmonary disease. *J Allergy Clin Immunol*. (2015) 136:769–80. doi: 10.1016/j.jaci.2015.01.046

165. Sureshbabu A, Bhandari V. Targeting mitochondrial dysfunction in lung diseases: emphasis on mitophagy. *Front Physiol*. (2013) 4:384. doi: 10.3389/fphys.2013.00384

166. Mizumura K, Cloonan SM, Nakahira K, Bhashyam AR, Cervo M, Kitada T, et al. Mitophagy-dependent necroptosis contributes to the pathogenesis of COPD. *J Clin Invest*. (2014) 124:3987–4003. doi: 10.1172/JCI74985

167. Stoltz DA, Meyerholz DK, Welsh MJ. Origins of cystic fibrosis lung disease. *N Engl J Med*. (2015) 372:351–62. doi: 10.1056/NEJMra1300109

168. Cutting GR. Cystic fibrosis genetics: from molecular understanding to clinical application. *Nat Rev Genet*. (2015) 16:45–56. doi: 10.1038/nrg3849

169. Fiedorczuk K, Chen J. Molecular structures reveal synergistic rescue of Δ508 CFTR by Trikafta modulators. *Science*. (2022) 378:284–90. doi: 10.1126/science.ade2216

170. Luciani A, Villella VR, Esposito S, Brunetti-Pierri N, Medina D, Settembre C, et al. Defective CFTR induces aggresome formation and lung inflammation in cystic fibrosis through ROS-mediated autophagy inhibition. *Nat Cell Biol*. (2010) 12:863–75. doi: 10.1038/ncb2090

171. Feng Y, et al. Interplay of energy metabolism and autophagy. *Autophagy*. (2024) 20:4–14. doi: 10.1080/15548627.2023.2247300

172. De Stefano D, Villella VR, Esposito S, Tosco A, Sepe A, De Gregorio F, et al. Restoration of CFTR function in patients with cystic fibrosis carrying the F508del-CFTR mutation. *Autophagy*. (2014) 10:2053–74. doi: 10.4161/15548627.2014.973737

173. Junkins RD, Shen A, Rosen K, McCormick C, Lin TJ. Autophagy enhances bacterial clearance during P. aeruginosa lung infection. *PLoS One*. (2013) 8:e72263. doi: 10.1371/journal.pone.0072263

174. Wolters PJ, Collard HR, Jones KD. Pathogenesis of idiopathic pulmonary fibrosis. *Annu Rev Pathol*. (2014) 9:157–79. doi: 10.1146/annurev-pathol-012513-104706

175. Raghu G, Remy-Jardin M, Richeldi L, Thomson CC, Inoue Y, Johkoh T, et al. Idiopathic pulmonary fibrosis (an update) and progressive pulmonary fibrosis in adults: an official ATS/ERS/JRS/ALAT clinical practice guideline. *Am J Respir Crit Care Med*. (2022) 205:e18–47. doi: 10.1164/rccm.202202-0399ST

176. Gross TJ, Hunninghake GW. Idiopathic pulmonary fibrosis. *N Engl J Med*. (2001) 345:517–25. doi: 10.1056/NEJMra003200

177. Mi S, Li Z, Yang HZ, Liu H, Wang JP, Ma YG, et al. Blocking IL-17A promotes the resolution of pulmonary inflammation and fibrosis via TGF-beta1-dependent and -independent mechanisms. *J Immunol*. (2011) 187:3003–14. doi: 10.4049/jimmunol.1004081

178. Patel AS, Lin L, Geyer A, Haspel JA, An CH, Cao J, et al. Autophagy in idiopathic pulmonary fibrosis. *PloS One*. (2012) 7:e41394. doi: 10.1371/journal.pone.0041394

179. Yang HZ, Wang JP, Mi S, Liu HZ, Cui B, Yan HM, et al. TLR4 activity is required in the resolution of pulmonary inflammation and fibrosis after acute and chronic lung injury. *Am J Pathol*. (2012) 180:275–92. doi: 10.1016/j.ajpath.2011.09.019

180. Bueno M, Lai YC, Romero Y, Brands J, St Croix CM, Kamga C, et al. PINK1 deficiency impairs mitochondrial homeostasis and promotes lung fibrosis. *J Clin Invest*. (2015) 125:521–38. doi: 10.1172/JCI74942

181. Patel AS, Song JW, Chu SG, Mizumura K, Osorio JC, Shi Y, et al. Epithelial cell mitochondrial dysfunction and PINK1 are induced by transforming growth factor-beta1 in pulmonary fibrosis. *PloS One*. (2015) 10:e0121246. doi: 10.1371/journal.pone.0121246

182. Kobayashi K, Araya J, Minagawa S, Hara H, Saito N, Kadota T, et al. Involvement of PARK2-mediated mitophagy in idiopathic pulmonary fibrosis pathogenesis. *J Immunol*. (2016) 197:504–16. doi: 10.4049/jimmunol.1600265

183. Lee SJ, Smith A, Guo L, Alastalo TP, Li M, Sawada H, et al. Autophagic protein LC3B confers resistance against hypoxia-induced pulmonary hypertension. *Am J Respir Crit Care Med*. (2011) 183:649–58. doi: 10.1164/rccm.201005-0746OC

184. Teng RJ, Du J, Welak S, Guan T, Eis A, Shi Y, et al. *Cross talk between NADPH oxidase and autophagy in pulmonary artery endothelial cells with intrauterine persistent pulmonary hypertension. Am J Physiol Lung Cell Mol Physiol*. (2012) 302:L651–63. doi: 10.1152/ajplung.00177.2011

185. Deng Y, Wu W, Guo S, Chen Y, Liu C, Gao X, et al. Altered mTOR and Beclin-1 mediated autophagic activation during right ventricular remodeling in monocrotaline-induced pulmonary hypertension. *Respir Res*. (2017) 18:53. doi: 10.1186/s12931-017-0536-7

186. Lee SJ, Kim HP, Jin Y, Choi AM, Ryter SW. Beclin 1 deficiency is associated with increased hypoxia-induced angiogenesis. *Autophagy*. (2011) 7:829–39. doi: 10.4161/auto.7.8.15598

187. Hunter RL. Pathology of post primary tuberculosis of the lung: an illustrated critical review. *Tuberculosis (Edinb)*. (2011) 91:497–509. doi: 10.1016/j.tube.2011.03.007

188. Sasindran SJ, Torrelles JB. Mycobacterium tuberculosis infection and inflammation: what is beneficial for the host and for the bacterium? *Front Microbiol*. (2011) 2:2. doi: 10.3389/fmicb.2011.00002

189. Fabri M, Stenger S, Shin DM, Yuk JM, Liu PT, Realegeno S, et al. Vitamin D is required for IFN-gamma-mediated antimicrobial activity of human macrophages. *Sci Transl Med*. (2011) 3:104ra102. doi: 10.1126/scitranslmed.3003045

190. Andersson AM, Andersson B, Lorell C, Raffetseder J, Larsson M, Blomgran R. Autophagy induction targeting mTORC1 enhances Mycobacterium tuberculosis replication in HIV co-infected human macrophages. *Sci Rep*. (2016) 6:28171. doi: 10.1038/srep28171

191. Tzfadia O, Gijsbers A, Vujkovic A, Snobre J, Vargas R, Dewaele K, et al. Single nucleotide variation catalog from clinical isolates mapped on tertiary and quaternary structures of ESX-1-related proteins reveals critical regions as putative Mtb therapeutic targets. *Microbiol Spectr*. (2024) 12:e0381623. doi: 10.1128/spectrum.03816-23

192. Watson RO, Manzanillo PS, Cox JS. Extracellular M. tuberculosis DNA targets bacteria for autophagy by activating the host DNA-sensing pathway. *Cell*. (2012) 150:803–15. doi: 10.1016/j.cell.2012.06.040

193. Dong LX, Sun LL, Zhang X, Pan L, Lian LJ, Chen Z, et al. Negative regulation of mTOR activity by LKB1-AMPK signaling in non-small cell lung cancer cells. *Acta Pharmacol Sin*. (2013) 34:314–8. doi: 10.1038/aps.2012.143

194. Wang L, Wang R. Effect of rapamycin (RAPA) on the growth of lung cancer and its mechanism in mice with A549. *Int J Clin Exp Pathol*. (2015) 8:9208–13.

195. Abadi AH, Mahdavi M, Khaledi A, Esmaeili SA, Esmaeili D, Sahebkar A. Study of serum bactericidal and splenic activity of Total-OMP- CagA combination from Brucella abortus and Helicobacter pylori in BALB/c mouse model. *Microb Pathog*. (2018) 121:100–5. doi: 10.1016/j.micpath.2018.04.050

196. Kim KW, Moretti L, Mitchell LR, Jung DK, Lu B. Combined Bcl-2/mammalian target of rapamycin inhibition leads to enhanced radiosensitization via induction of apoptosis and autophagy in non-small cell lung tumor xenograft model. *Clin Cancer Res*. (2009) 15:6096–105. doi: 10.1158/1078-0432.CCR-09-0589

197. Kruse JP, Gu W. Modes of p53 regulation. *Cell*. (2009) 137:609–22. doi: 10.1016/j.cell.2009.04.050

198. Vaseva AV, Marchenko ND, Ji K, Tsirka SE, Holzmann S, Moll UM. p53 opens the mitochondrial permeability transition pore to trigger necrosis. *Cell*. (2012) 149:1536–48. doi: 10.1016/j.cell.2012.05.014

199. Zhao H, Dong F, Li Y, Ren X, Xia Z, Wang Y, et al. Inhibiting ATG5 mediated autophagy to regulate endoplasmic reticulum stress and CD4(+) T lymphocyte differentiation: Mechanisms of acupuncture's effects on asthma. *BioMed Pharmacother*. (2021) 142:112045. doi: 10.1016/j.biopha.2021.112045

200. Poon AH, Choy DF, Chouiali F, Ramakrishnan RK, Mahboub B, Audusseau S, et al. Increased autophagy-related 5 gene expression is associated with collagen expression in the airways of refractory asthmatics. *Front Immunol*. (2017) 8:355. doi: 10.3389/fimmu.2017.00355

201. Chung KF, Dixey P, Abubakar-Waziri H, Bhavsar P, Patel PH, Guo S, et al. Characteristics, phenotypes, mechanisms and management of severe asthma. *Chin Med J (Engl)*. (2022) 135:1141–55. doi: 10.1097/CM9.0000000000001990

202. Dickinson JD, Alevy Y, Malvin NP, Patel KK, Gunsten SP, Holtzman MJ, et al. IL13 activates autophagy to regulate secretion in airway epithelial cells. *Autophagy*. (2016) 12:397–409. doi: 10.1080/15548627.2015.1056967

203. Dickinson JD, Sweeter JM, Warren KJ, Ahmad IM, De Deken X, Zimmerman MC, et al. Autophagy regulates DUOX1 localization and superoxide production in airway epithelial cells during chronic IL-13 stimulation. *Redox Biol*. (2018) 14:272–84. doi: 10.1016/j.redox.2017.09.013

204. Li W, Wu Y, Zhao Y, Li Z, Chen H, Dong L, et al. MTOR suppresses autophagy-mediated production of IL25 in allergic airway inflammation. *Thorax*. (2020) 75:1047–57. doi: 10.1136/thoraxjnl-2019-213771

205. Eltokhy AK, Toema O, El-Deeb OS. The correlation between PINK-1/parkin mediated mitophagy, endoplasmic reticulum stress and total polyamines in pediatric bronchial asthma: an integrated network of pathways. *Mol Biol Rep*. (2022) 49:227–35. doi: 10.1007/s11033-021-06861-5

206. Choi Y, Bowman JW, Jung JU. Autophagy during viral infection - a double-edged sword. *Nat Rev Microbiol*. (2018) 16:341–54. doi: 10.1038/s41579-018-0003-6

207. García-Pérez BE, González-Rojas JA, Salazar MI, Torres-Torres C, Castrejón-Jiménez NS. Taming the autophagy as a strategy for treating COVID-19. *Cells*. (2020) 9:2679. doi: 10.3390/cells9122679

208. Ahmad L, Mostowy S, Sancho-Shimizu V. Autophagy-virus interplay: from cell biology to human disease. *Front Cell Dev Biol*. (2018) 6:155. doi: 10.3389/fcell.2018.00155

209. Mohamud Y, Xue YC, Liu H, Ng CS, Bahreyni A, Jan E, et al. The papain-like protease of coronaviruses cleaves ULK1 to disrupt host autophagy. *Biochem Biophys Res Commun*. (2021) 540:75–82. doi: 10.1016/j.bbrc.2020.12.091

210. Gassen NC, Niemeyer D, Muth D, Corman VM, Martinelli S, Gassen A, et al. SKP2 attenuates autophagy through Beclin1-ubiquitination and its inhibition reduces MERS-Coronavirus infection. *Nat Commun*. (2019) 10:5770. doi: 10.1038/s41467-019-13659-4

211. Gassen NC, Papies J, Bajaj T, Emanuel J, Dethloff F, Chua RL, et al. SARS-CoV-2-mediated dysregulation of metabolism and autophagy uncovers host-targeting antivirals. *Nat Commun*. (2021) 12:3818. doi: 10.1038/s41467-021-24007-w

212. Miao G, Zhao H, Li Y, Ji M, Chen Y, Shi Y, et al. ORF3a of the COVID-19 virus SARS-CoV-2 blocks HOPS complex-mediated assembly of the SNARE complex required for autolysosome formation. *Dev Cell*. (2021) 56:427–442.e5. doi: 10.1016/j.devcel.2020.12.010

213. Zhao Z, Lu K, Mao B, Liu S, Trilling M, Huang A, et al. The interplay between emerging human coronavirus infections and autophagy. *Emerg Microbes Infect*. (2021) 10:196–205. doi: 10.1080/22221751.2021.1872353

214. Crother TR, Porritt RA, Dagvadorj J, Tumurkhuu G, Slepenkin AV, Peterson EM, et al. Autophagy limits inflammasome during chlamydia pneumoniae infection. *Front Immunol*. (2019) 10:754. doi: 10.3389/fimmu.2019.00754

215. Shimizu T. Inflammation-inducing factors of mycoplasma pneumoniae. *Front Microbiol*. (2016) 7:414. doi: 10.3389/fmicb.2016.00414

216. Thomas DR, Newton P, Lau N, Newton HJ. Interfering with Autophagy: The Opposing Strategies Deployed by Legionella pneumophila and Coxiella burnetii Effector Proteins. *Front Cell Infect Microbiol*. (2020) 10:599762. doi: 10.3389/fcimb.2020.599762

217. Vij N, Chandramani-Shivalingappa P, Van Westphal C, Hole R, Bodas M. *Cigarette smoke-induced autophagy impairment accelerates lung aging, COPD-emphysema exacerbations and pathogenesis. Am J Physiol Cell Physiol*. (2018) 314:C73–c87. doi: 10.1152/ajpcell.00110.2016

218. Li Y, Yu G, Yuan S, Tan C, Lian P, Fu L, et al. Cigarette smoke-induced pulmonary inflammation and autophagy are attenuated in ephx2-deficient mice. *Inflammation*. (2017) 40:497–510. doi: 10.1007/s10753-016-0495-z

219. Lo S, Yuan SS, Hsu C, Cheng YJ, Chang YF, Hsueh HW, et al. Lc3 over-expression improves survival and attenuates lung injury through increasing autophagosomal clearance in septic mice. *Ann Surg*. (2013) 257:352–63. doi: 10.1097/SLA.0b013e318269d0e2

220. Chen X, Tsvetkov AS, Shen HM, Isidoro C, Ktistakis NT, Linkermann A, et al. International consensus guidelines for the definition, detection, and interpretation of autophagy-dependent ferroptosis. *Autophagy*. (2024) 20:1213–46. doi: 10.1080/15548627.2024.2319901

221. Maule G, Arosio D, Cereseto A. Gene therapy for cystic fibrosis: progress and challenges of genome editing. *Int J Mol Sci*. (2020) 21:3903. doi: 10.3390/ijms21113903

222. Martinez FJ, Curtis JL, Albert R. Role of macrolide therapy in chronic obstructive pulmonary disease. *Int J Chron Obstruct Pulmon Dis*. (2008) 3:331–50. doi: 10.2147/COPD.S681

223. McArdle JR, Talwalkar JS. Macrolides in cystic fibrosis. *Clin Chest Med*. (2007) 28:347–60. doi: 10.1016/j.ccm.2007.02.005

224. Esther CR Jr., Esserman DA, Gilligan P, Kerr A, Noone PG. Chronic Mycobacterium abscessus infection and lung function decline in cystic fibrosis. *J Cyst Fibros*. (2010) 9:117–23. doi: 10.1016/j.jcf.2009.12.001

225. Roux AL, Catherinot E, Ripoll F, Soismier N, Macheras E, Ravilly S, et al. Multicenter study of prevalence of nontuberculous mycobacteria in patients with cystic fibrosis in France. *J Clin Microbiol*. (2009) 47:4124–8. doi: 10.1128/JCM.01257-09

226. Han R, Ji X, Rong R, Li Y, Yao W, Yuan J, et al. MiR-449a regulates autophagy to inhibit silica-induced pulmonary fibrosis through targeting Bcl2. *J Mol Med (Berl)*. (2016) 94:1267–79. doi: 10.1007/s00109-016-1441-0

227. Gui YS, Wang L, Tian X, Li X, Ma A, Zhou W, et al. mTOR overactivation and compromised autophagy in the pathogenesis of pulmonary fibrosis. *PloS One*. (2015) 10:e0138625. doi: 10.1371/journal.pone.0138625

228. Liu H, Cheng Y, Yang J, Wang W, Fang S, Zhang W, et al. BBC3 in macrophages promoted pulmonary fibrosis development through inducing autophagy during silicosis. *Cell Death Dis*. (2017) 8:e2657. doi: 10.1038/cddis.2017.78

229. Spiekerkoetter E, Tian X, Cai J, Hopper RK, Sudheendra D, Li CG, et al. FK506 activates BMPR2, rescues endothelial dysfunction, and reverses pulmonary hypertension. *J Clin Invest*. (2013) 123:3600–13. doi: 10.1172/JCI65592

230. Seyfarth HJ, Hammerschmidt S, Halank M, Neuhaus P, Wirtz HR. Everolimus in patients with severe pulmonary hypertension: a safety and efficacy pilot trial. *Pulm Circ*. (2013) 3:632–8. doi: 10.1086/674311

231. Samimi R, Hosseinpanahi A, Zaboli R, Peymani A, Rouhi S, Ahmadi Gooraji S, et al. Prevalence of vitamin D receptor genes polymorphisms in people with pulmonary tuberculosis: A systematic review and meta-analysis. *Med J Islam Repub Iran*. (2024) 38:32. doi: 10.47176/mjiri.38.32

232. Nnoaham KE, Clarke A. Low serum vitamin D levels and tuberculosis: a systematic review and meta-analysis. *Int J Epidemiol*. (2008) 37:113–9. doi: 10.1093/ije/dym247

233. Daley P, Jagannathan V, John KR, Sarojini J, Latha A, Vieth R, et al. Adjunctive vitamin D for treatment of active tuberculosis in India: a randomised, double-blind, placebo-controlled trial. *Lancet Infect Dis*. (2015) 15:528–34. doi: 10.1016/S1473-3099(15)70053-8

234. Martineau AR, Timms PM, Bothamley GH, Hanifa Y, Islam K, Claxton AP, et al. High-dose vitamin D(3) during intensive-phase antimicrobial treatment of pulmonary tuberculosis: a double-blind randomised controlled trial. *Lancet*. (2011) 377:242–50. doi: 10.1016/S0140-6736(10)61889-2

235. Kim JJ, Lee HM, Shin DM, Kim W, Yuk JM, Jin HS, et al. Host cell autophagy activated by antibiotics is required for their effective antimycobacterial drug action. *Cell Host Microbe*. (2012) 11:457–68. doi: 10.1016/j.chom.2012.03.008

236. Pflaum J, Schlosser S, Müller M. p53 family and cellular stress responses in cancer. *Front Oncol*. (2014) 4:285. doi: 10.3389/fonc.2014.00285

237. Parrales A, Iwakuma T. Targeting oncogenic mutant p53 for cancer therapy. *Front Oncol*. (2015) 5:288. doi: 10.3389/fonc.2015.00288

238. Gibbons DL, Byers LA, Kurie JM. Smoking, p53 mutation, and lung cancer. *Mol Cancer Res*. (2014) 12:3–13. doi: 10.1158/1541-7786.MCR-13-0539

239. Vassilev LT, Vu BT, Graves B, Carvajal D, Podlaski F, Filipovic Z, et al. In vivo activation of the p53 pathway by small-molecule antagonists of MDM2. *Science*. (2004) 303:844–8. doi: 10.1126/science.1092472

240. Kravchenko JE, Ilyinskaya GV, Komarov PG, Agapova LS, Kochetkov DV, Strom E, et al. *Small-molecule RETRA suppresses mutant p53-bearing cancer cells through a p73-dependent salvage pathway*. *Proc Natl Acad Sci U S A*. (2008) 105:6302–7. doi: 10.1073/pnas.0802091105

241. Lambert JM, Gorzov P, Veprintsev DB, Söderqvist M, Segerbäck D, Bergman J, et al. PRIMA-1 reactivates mutant p53 by covalent binding to the core domain. *Cancer Cell*. (2009) 15:376–88. doi: 10.1016/j.ccr.2009.03.003

242. Meher RK, Mir SA, Anisetti SS. In silico and in vitro investigation of dual targeting Prima-1(MET) as precision therapeutic against lungs cancer. *J Biomol Struct Dyn*. (2024) 42:4169–84. doi: 10.1080/07391102.2023.2219323

243. Nagano T, Tachihara M, Nishimura Y. Dacomitinib, a second-generation irreversible epidermal growth factor receptor tyrosine kinase inhibitor (EGFR-TKI) to treat non-small cell lung cancer. *Drugs Today (Barc)*. (2019) 55:231–6. doi: 10.1358/dot.2019.55.4.2965337

244. Fung C, Chen X, Grandis JR, Duvvuri U. EGFR tyrosine kinase inhibition induces autophagy in cancer cells. *Cancer Biol Ther*. (2012) 13:1417–24. doi: 10.4161/cbt.22002

245. Chresta CM, Davies BR, Hickson I, Harding T, Cosulich S, Critchlow SE, et al. AZD8055 is a potent, selective, and orally bioavailable ATP-competitive mammalian target of rapamycin kinase inhibitor with in vitro and in vivo antitumor activity. *Cancer Res*. (2010) 70:288–98. doi: 10.1158/0008-5472.CAN-09-1751

246. Sini P, James D, Chresta C, Guichard S. Simultaneous inhibition of mTORC1 and mTORC2 by mTOR kinase inhibitor AZD8055 induces autophagy and cell death in cancer cells. *Autophagy*. (2010) 6:553–4. doi: 10.4161/auto.6.4.11671

247. Jin HO, Lee YH, Park JA, Kim JH, Hong SE, Kim HA, et al. Blockage of Stat3 enhances the sensitivity of NSCLC cells to PI3K/mTOR inhibition. *Biochem Biophys Res Commun*. (2014) 444:502–8. doi: 10.1016/j.bbrc.2014.01.086

248. Xu CX, Zhao L, Yue P, Fang G, Tao H, Owonikoko TK, et al. Augmentation of NVP-BEZ235's anticancer activity against human lung cancer cells by blockage of autophagy. *Cancer Biol Ther*. (2011) 12:549–55. doi: 10.4161/cbt.12.6.16397

249. Wu SH, Hang LW, Yang JS, Chen HY, Lin HY, Chiang JH, et al. Curcumin induces apoptosis in human non-small cell lung cancer NCI-H460 cells through ER stress and caspase cascade- and mitochondria-dependent pathways. *Anticancer Res*. (2010) 30:2125–33.

250. Lin SS, Huang HP, Yang JS, Wu JY, Hsia TC, Lin CC, et al. DNA damage and endoplasmic reticulum stress mediated curcumin-induced cell cycle arrest and apoptosis in human lung carcinoma A-549 cells through the activation caspases cascade- and mitochondrial-dependent pathway. *Cancer Lett*. (2008) 272:77–90. doi: 10.1016/j.canlet.2008.06.031

251. Su Q, Pan J, Wang C, Zhang M, Cui H, Zhao X. Curcumin and baicalin co-loaded nanoliposomes for synergistic treatment of non-small cell lung cancer. *Pharmaceutics*. (2024) 16:973. doi: 10.3390/pharmaceutics16080973

252. Lin Y, Wang Y, Liu X, Yan J, Su L, Liu X. A novel derivative of tetrandrine (H1) induces endoplasmic reticulum stress-mediated apoptosis and prosurvival autophagy in human non-small cell lung cancer cells. *Tumour Biol*. (2016) 37:10403–13. doi: 10.1007/s13277-016-4950-0

253. Tang ZH, Chen X, Wang ZY, Chai K, Wang YF, Xu XH, et al. Induction of C/EBP homologous protein-mediated apoptosis and autophagy by licochalcone A in non-small cell lung cancer cells. *Sci Rep*. (2016) 6:26241. doi: 10.1038/srep26241

254. Ma J, Liu J, Lu C, Cai D. Pachymic acid induces apoptosis via activating ROS-dependent JNK and ER stress pathways in lung cancer cells. *Cancer Cell Int*. (2015) 15:78. doi: 10.1186/s12935-015-0230-0

255. Zhao R, Chen M, Jiang Z, Zhao F, Xi B, Zhang X, et al. Platycodin-D induced autophagy in non-small cell lung cancer cells via PI3K/akt/mTOR and MAPK signaling pathways. *J Cancer*. (2015) 6:623–31. doi: 10.7150/jca.11291

256. Buckbinder L, Talbott R, Velasco-Miguel S, Takenaka I, Faha B, Seizinger BR, et al. Induction of the Growth Inhibitor Igf-Binding Protein 3 by P53. *Nature*. (1995) 377:646–9. doi: 10.1038/377646a0

257. Drakos E, Atsaves V, Li J, Leventaki V, Andreeff M, Medeiros LJ, et al. Stabilization and Activation of P53 Downregulates Mtor Signaling through Ampk in Mantle Cell Lymphoma. *Leukemia*. (2009) 23:784–90. doi: 10.1038/leu.2008.348

258. Feng Z, Hu W, de Stanchina E, Teresky AK, Jin S, Lowe S, et al. The Regulation of Ampk Beta1, Tsc2, and Pten Expression by P53: Stress, Cell and Tissue Specificity, and the Role of These Gene Products in Modulating the Igf-1-Akt-Mtor Pathways. *Cancer Res*. (2007) 67:3043–53. doi: 10.1158/0008-5472.Can-06-4149

259. Budanov AV, Karin M. P53 Target Genes Sestrin1 and Sestrin2 Connect Genotoxic Stress and Mtor Signaling. *Cell*. (2008) 134:451–60. doi: 10.1016/j.cell.2008.06.028

260. Martoriati A, Doumont G, Alcalay M, Bellefroid E, Pelicci PG, Marine JC. Dapk1, Encoding an Activator of a P19arf-P53-Mediated Apoptotic Checkpoint, Is a Transcription Target of P53. *Oncogene*. (2005) 24:1461–6. doi: 10.1038/sj.onc.1208256

261. Reef S, Zalckvar E, Shifman O, Bialik S, Sabanay H, Oren M, et al. A Short Mitochondrial Form of P19arf Induces Autophagy and Caspase-Independent Cell Death. *Mol Cell*. (2006) 22:463–75. doi: 10.1016/j.molcel.2006.04.014

262. Yee KS, Wilkinson S, James J, Ryan KM, Vousden KH. Puma- and Bax-Induced Autophagy Contributes to Apoptosis. *Cell Death Differ*. (2009) 16:1135–45. doi: 10.1038/cdd.2009.28

263. Maiuri MC, Criollo A, Tasdemir E, Vicencio JM, Tajeddine N, Hickman JA, et al. Bh3-Only Proteins and Bh3 Mimetics Induce Autophagy by Competitively Disrupting the Interaction between Beclin 1 and Bcl-2/Bcl-X(L). *Autophagy*. (2007) 3:374–6. doi: 10.4161/auto.4237

264. Abraham AG, O'Neill E. Pi3k/Akt-Mediated Regulation of P53 in Cancer. *Biochem Soc Trans*. (2014) 42:798–803. doi: 10.1042/bst20140070

265. Stambolic V, MacPherson D, Sas D, Lin Y, Snow B, Jang Y, et al. Regulation of Pten Transcription by P53. *Mol Cell*. (2001) 8:317–25. doi: 10.1016/s1097-2765(01)00323-9

266. An WG, Kanekal M, Simon MC, Maltepe E, Blagosklonny MV, Neckers LM. Stabilization of Wild-Type P53 by Hypoxia-Inducible Factor 1alpha. *Nature*. (1998) 392:405–8. doi: 10.1038/32925

267. Chen D, Li M, Luo J, Gu W. Direct Interactions between Hif-1 Alpha and Mdm2 Modulate P53 Function. *J Biol Chem*. (2003) 278:13595–8. doi: 10.1074/jbc.C200694200

268. Gao W, Shen Z, Shang L, Wang X. Upregulation of Human Autophagy-Initiation Kinase Ulk1 by Tumor Suppressor P53 Contributes to DNA-Damage-Induced Cell Death. *Cell Death Differ*. (2011) 18:1598–607. doi: 10.1038/cdd.2011.33

269. Desai S, Liu Z, Yao J, Patel N, Chen J, Wu Y, et al. Heat Shock Factor 1 (Hsf1) Controls Chemoresistance and Autophagy through Transcriptional Regulation of Autophagy-Related Protein 7 (Atg7). *J Biol Chem*. (2013) 288:9165–76. doi: 10.1074/jbc.M112.422071

270. Yeo SY, Itahana Y, Guo AK, Han R, Iwamoto K, Nguyen HT, et al. Transglutaminase 2 Contributes to a Tp53-Induced Autophagy Program to Prevent Oncogenic Transformation. *Elife*. (2016) 5:e07101. doi: 10.7554/eLife.07101

271. Tasdemir E, Maiuri MC, Galluzzi L, Vitale I, Djavaheri-Mergny M, D'Amelio M, et al. Regulation of Autophagy by Cytoplasmic P53. *Nat Cell Biol*. (2008) 10:676–87. doi: 10.1038/ncb1730

272. Bensaad K, Tsuruta A, Selak MA, Vidal MN, Nakano K, Bartrons R, et al. Tigar, a P53-Inducible Regulator of Glycolysis and Apoptosis. *Cell*. (2006) 126:107–20. doi: 10.1016/j.cell.2006.05.036

273. Xu J, Wang Y, Tan X, Jing H. Micrornas in Autophagy and Their Emerging Roles in Crosstalk with Apoptosis. *Autophagy*. (2012) 8:873–82. doi: 10.4161/auto.19629

274. Liao JM, Cao B, Zhou X, Lu H. New Insights into P53 Functions through Its Target Micrornas. *J Mol Cell Biol*. (2014) 6:206–13. doi: 10.1093/jmcb/mju018

275. Liu J, Xia H, Kim M, Xu L, Li Y, Zhang L, et al. Beclin1 Controls the Levels of P53 by Regulating the Deubiquitination Activity of Usp10 and Usp13. *Cell*. (2011) 147:223–34. doi: 10.1016/j.cell.2011.08.037

276. Morselli E, Shen S, Ruckenstuhl C, Bauer MA, Mariño G, Galluzzi L, et al. P53 Inhibits Autophagy by Interacting with the Human Ortholog of Yeast Atg17, Rb1cc1/Fip200. *Cell Cycle*. (2011) 10:2763–9. doi: 10.4161/cc.10.16.16868

277. Galluzzi L, Kepp O. Kroemer G. *A New Role Cytoplasmic P53: Binding Destroying Double-Stranded Rna. Cell Cycle*. (2010) 9:2491–2. doi: 10.4161/cc.9.13.12191

278. Vij N, Chandramani-Shivalingappa P, Van Westphal C, Hole R, Bodas M. Cigarette Smoke-Induced Autophagy Impairment Accelerates Lung Aging, Copd-Emphysema Exacerbations and Pathogenesis. *Am J Physiol Cell Physiol*. (2018) 314: C73–c87. doi: 10.1152/ajpcell.00110.2016

279. Araya J, Tsubouchi K, Sato N, Ito S, Minagawa S, Hara H, et al. Prkn-Regulated Mitophagy and Cellular Senescence During Copd Pathogenesis. *Autophagy*. (2019) 15:510–26. doi: 10.1080/15548627.2018.1532259

280. Wang Y, Liao S, Pan Z, Jiang S, Fan J, Yu S, et al. Hydrogen Sulfide Alleviates Particulate Matter-Induced Emphysema and Airway Inflammation by Suppressing Ferroptosis. *Free Radic Biol Med*. (2022) 186:1–16. doi: 10.1016/j.freeradbiomed.2022.04.014

281. Zhang L, Huang J, Dong R, Feng Y, Zhou M. Therapeutic Potential of Blt1 Antagonist for Copd: Involvement of Inducing Autophagy and Ameliorating Inflammation. *Drug Des Devel Ther*. (2019) 13:3105–16. doi: 10.2147/dddt.S215433

282. Bodas M, Patel N, Silverberg D, Walworth K, Vij N. Master Autophagy Regulator Transcription Factor Eb Regulates Cigarette Smoke-Induced Autophagy Impairment and Chronic Obstructive Pulmonary Disease-Emphysema Pathogenesis. *Antioxid Redox Signal*. (2017) 27:150–67. doi: 10.1089/ars.2016.6842

283. Song B, Yan X, Li R, Zhang H. Ghrelin Ameliorates Chronic Obstructive Pulmonary Disease-Associated Infllammation and Autophagy. *Biotechnol Appl Biochem*. (2021) 68:356–65. doi: 10.1002/bab.1933

284. Li L, Zhang M, Zhang L, Cheng Y, Tu X, Lu Z. Klotho Regulates Cigarette Smoke-Induced Autophagy: Implication in Pathogenesis of Copd. *Lung*. (2017) 195:295–301. doi: 10.1007/s00408-017-9997-1

285. Liu Y, Xu J, Liu T, Wu J, Zhao J, Wang J, et al. Fstl1 Aggravates Cigarette Smoke-Induced Airway Inflammation and Airway Remodeling by Regulating Autophagy. *BMC Pulm Med*. (2021) 21:45. doi: 10.1186/s12890-021-01409-6

286. Le Y, Wang Y, Zhou L, Xiong J, Tian J, Yang X, et al. Cigarette Smoke-Induced Hmgb1 Translocation and Release Contribute to Migration and Nf-κb Activation through Inducing Autophagy in Lung Macrophages. *J Cell Mol Med*. (2020) 24:1319–31. doi: 10.1111/jcmm.14789

287. Wang L, Jiang W, Wang J, Xie Y, Wang W. Puerarin Inhibits Fundc1-Mediated Mitochondrial Autophagy and Cse-Induced Apoptosis of Human Bronchial Epithelial Cells by Activating the Pi3k/Akt/Mtor Signaling Pathway. *Aging (Albany NY)*. (2022) 14:1253–64. doi: 10.18632/aging.203317

288. Chen S, Wang Y, Zhang H, Chen R, Lv F, Li Z, et al. The Antioxidant Mitoq Protects against Cse-Induced Endothelial Barrier Injury and Inflammation by Inhibiting Ros and Autophagy in Human Umbilical Vein Endothelial Cells. *Int J Biol Sci*. (2019) 15:1440–51. doi: 10.7150/ijbs.30193

289. Li W, Yan J, Xu J, Zhu L, Zhai C, Wang Y, et al. Vardenafil Alleviates Cigarette Smoke-Induced Chronic Obstructive Pulmonary Disease by Activating Autophagy Via the Ampk/Mtor Signalling Pathway: An in Vitro and in Vivo Study. *In Vitro Cell Dev Biol Anim*. (2023) 59:717–28. doi: 10.1007/s11626-023-00820-z

290. Han D, Wu X, Liu L, Shu W, Huang Z. Sodium Tanshinone Iia Sulfonate Protects Arpe-19 Cells against Oxidative Stress by Inhibiting Autophagy and Apoptosis. *Sci Rep*. (2018) 8:15137. doi: 10.1038/s41598-018-33552-2

291. Li D, Hu J, Wang T, Zhang X, Liu L, Wang H, et al. Silymarin Attenuates Cigarette Smoke Extract-Induced Inflammation Via Simultaneous Inhibition of Autophagy and Erk/P38 Mapk Pathway in Human Bronchial Epithelial Cells. *Sci Rep*. (2016) 6:37751. doi: 10.1038/srep37751

292. Chen CH, Li YR, Lin SH, Chang HH, Chai WH, Chan PC, et al. Tiotropium/Olodaterol Treatment Reduces Cigarette Smoke Extract-Induced Cell Death in Beas-2b Bronchial Epithelial Cells. *BMC Pharmacol Toxicol*. (2020) 21:74. doi: 10.1186/s40360-020-00451-0

293. Li X, Yang H, Sun H, Lu R, Zhang C, Gao N, et al. Taurine Ameliorates Particulate Matter-Induced Emphysema by Switching on Mitochondrial Nadh Dehydrogenase Genes. *Proc Natl Acad Sci U.S.A*. (2017) 114:E9655–e64. doi: 10.1073/pnas.1712465114

294. Zong DD, Liu XM, Li JH, Ouyang RY, Long YJ, Chen P, et al. Resveratrol Attenuates Cigarette Smoke Induced Endothelial Apoptosis by Activating Notch1 Signaling Mediated Autophagy. *Respir Res*. (2021) 22:22. doi: 10.1186/s12931-021-01620-3

295. Li Y, Yu G, Yuan S, Tan C, Xie J, Ding Y, et al. 14,15-Epoxyeicosatrienoic Acid Suppresses Cigarette Smoke Condensate-Induced Inflammation in Lung Epithelial Cells by Inhibiting Autophagy. *Am J Physiol Lung Cell Mol Physiol*. (2016) 311:L970–l80. doi: 10.1152/ajplung.00161.2016

296. Son ES, Kim SH, Ryter SW, Yeo EJ, Kyung SY, Kim YJ, et al. Quercetogetin Protects against Cigarette Smoke Extract-Induced Apoptosis in Epithelial Cells by Inhibiting Mitophagy. *Toxicol In Vitro*. (2018) 48:170–8. doi: 10.1016/j.tiv.2018.01.011

297. Renna M, Schaffner C, Brown K, Shang S, Tamayo MH, Hegyi K, et al. Azithromycin Blocks Autophagy and May Predispose Cystic Fibrosis Patients to Mycobacterial Infection. *J Clin Invest*. (2011) 121:3554–63. doi: 10.1172/jci46095

298. Signorelli P, Pivari F, Barcella M, Merelli I, Zulueta A, Dei Cas M, et al. Myriocin Modulates the Altered Lipid Metabolism and Storage in Cystic Fibrosis. *Cell Signal*. (2021) 81:109928. doi: 10.1016/j.cellsig.2021.109928

299. Assani K, Shrestha CL, Rinehardt H, Zhang S, Robledo-Avila F, Wellmerling J, et al. Ar-13 Reduces Antibiotic-Resistant Bacterial Burden in Cystic Fibrosis Phagocytes and Improves Cystic Fibrosis Transmembrane Conductance Regulator Function. *J Cyst Fibros*. (2019) 18:622–9. doi: 10.1016/j.jcf.2018.10.010

300. Vu CB, Bridges RJ, Pena-Rasgado C, Lacerda AE, Bordwell C, Sewell A, et al. Fatty Acid Cysteamine Conjugates as Novel and Potent Autophagy Activators That Enhance the Correction of Misfolded F508del-Cystic Fibrosis Transmembrane Conductance Regulator (Cftr). *J Med Chem*. (2017) 60:458–73. doi: 10.1021/acs.jmedchem.6b01539

301. Tosco A, De Gregorio F, Esposito S, De Stefano D, Sana I, Ferrari E, et al. A Novel Treatment of Cystic Fibrosis Acting on-Target: Cysteamine Plus Epigallocatechin Gallate for the Autophagy-Dependent Rescue of Class Ii-Mutated Cftr. *Cell Death Differ*. (2016) 23:1380–93. doi: 10.1038/cdd.2016.22

302. Hoch L, Bourg N, Degrugillier F, Bruge C, Benabides M, Pellier E, et al. Dual Blockade of Misfolded Alpha-Sarcoglycan Degradation by Bortezomib and Givinostat Combination. *Front Pharmacol*. (2022) 13:856804. doi: 10.3389/fphar.2022.856804

303. Ferrari E, Monzani R, Villella VR, Esposito S, Saluzzo F, Rossin F, et al. Cysteamine Re-Establishes the Clearance of Pseudomonas Aeruginosa by Macrophages Bearing the Cystic Fibrosis-Relevant F508del-Cftr Mutation. *Cell Death Dis*. (2017) 8: e2544. doi: 10.1038/cddis.2016.476

304. Baek AR, Hong J, Song KS, Jang AS, Kim DJ, Chin SS, et al. Spermidine Attenuates Bleomycin-Induced Lung Fibrosis by Inducing Autophagy and Inhibiting Endoplasmic Reticulum Stress (Ers)-Induced Cell Death in Mice. *Exp Mol Med*. (2020) 52:2034–45. doi: 10.1038/s12276-020-00545-z

305. Gong H, Lyu X, Liu Y, Peng N, Tan S, Dong L, et al. Eupatilin Inhibits Pulmonary Fibrosis by Activating Sestrin2/Pi3k/Akt/Mtor Dependent Autophagy Pathway. *Life Sci*. (2023) 334:122218. doi: 10.1016/j.lfs.2023.122218

306. Zhang X, Su J, Lin J, Liu L, Wu J, Yuan W, et al. Fu-Zheng-Tong-Luo Formula Promotes Autophagy and Alleviates Idiopathic Pulmonary Fibrosis by Controlling the Janus Kinase 2/Signal Transducer and Activator of Transcription 3 Pathway. *J Ethnopharmacol*. (2023) 314:116633. doi: 10.1016/j.jep.2023.116633

307. Pei X, Zheng F, Li Y, Lin Z, Han X, Feng Y, et al. Niclosamide Ethanolamine Salt Alleviates Idiopathic Pulmonary Fibrosis by Modulating the Pi3k-Mtorc1 Pathway. *Cells*. (2022) 11:346. doi: 10.3390/cells11030346

308. Qi J, Wu Y, Guo Z, Zhu S, Xiong J, Hu F, et al. Fibroblast Growth Factor 21 Alleviates Idiopathic Pulmonary Fibrosis by Inhibiting Pi3k-Akt-Mtor Signaling and Stimulating Autophagy. *Int J Biol Macromol*. (2024) 273:132896. doi: 10.1016/j.ijbiomac.2024.132896

309. Li T, Gao X, Jia R, Sun Y, Ding Y, Wang F, et al. Astragaloside Iv Inhibits Idiopathic Pulmonary Fibrosis through Activation of Autophagy by Mir-21-Mediated Pten/Pi3k/Akt/Mtor Pathway. *Cell Mol Biol (Noisy-le-grand)*. (2024) 70:128–36. doi: 10.14715/cmb/2024.70.2.18

310. Zheng D, Guo J, Liang Z, Jin Y, Ding Y, Liu J, et al. Supramolecular Nanofibers Ameliorate Bleomycin-Induced Pulmonary Fibrosis by Restoring Autophagy. *Adv Sci (Weinh)*. (2024) 11:e2401327. doi: 10.1002/advs.202401327

311. Wei Y, Sun L, Liu C, Li L. Naringin Regulates Endoplasmic Reticulum Stress and Mitophagy through the Atf3/Pink1 Signaling Axis to Alleviate Pulmonary Fibrosis. *Naunyn Schmiedebergs Arch Pharmacol*. (2023) 396:1155–69. doi: 10.1007/s00210-023-02390-z

312. Chu L, Zhuo J, Huang H, Chen W, Zhong W, Zhang J, et al. Tetrandrine Alleviates Pulmonary Fibrosis by Inhibiting Alveolar Epithelial Cell Senescence through Pink1/Parkin-Mediated Mitophagy. *Eur J Pharmacol*. (2024) 969:176459. doi: 10.1016/j.ejphar.2024.176459

313. Chen S, Wei Y, Li S, Miao Y, Gu J, Cui Y, et al. Zanubrutinib Attenuates Bleomycin-Induced Pulmonary Fibrosis by Inhibiting the Tgf-β1 Signaling Pathway. *Int Immunopharmacol*. (2022) 109316. doi: 10.1016/j.intimp.2022.109316

314. Li X, Wang Y, Liang J, Bi Z, Ruan H, Cui Y, et al. Bergenin Attenuates Bleomycin-Induced Pulmonary Fibrosis in Mice Via Inhibiting Tgf-β1 Signaling Pathway. *Phytother Res*. (2021) 35:5808–22. doi: 10.1002/ptr.7239

315. Zhao X, Gao M, Liang J, Chen Y, Wang Y, Wang Y, et al. Slc7a11 Reduces Laser-Induced Choroidal Neovascularization by Inhibiting Rpe Ferroptosis and Vegf Production. *Front Cell Dev Biol*. (2021) 9:639851. doi: 10.3389/fcell.2021.639851

316. Cho IH, Choi YJ, Gong JH, Shin D, Kang MK, Kang YH. Astragalin Inhibits Autophagy-Associated Airway Epithelial Fibrosis. *Respir Res*. (2015) 16:51. doi: 10.1186/s12931-015-0211-9

317. Saito S, Zhuang Y, Shan B, Danchuk S, Luo F, Korfei M, et al. Tubastatin Ameliorates Pulmonary Fibrosis by Targeting the Tgfβ-Pi3k-Akt Pathway. *PloS One*. (2017) 12:e0186615. doi: 10.1371/journal.pone.0186615

318. Rangarajan S, Kurundkar A, Kurundkar D, Bernard K, Sanders YY, Ding Q, et al. Novel Mechanisms for the Antifibrotic Action of Nintedanib. *Am J Respir Cell Mol Biol*. (2016) 54:51–9. doi: 10.1165/rcmb.2014-0445OC

319. Kurita Y, Araya J, Minagawa S, Hara H, Ichikawa A, Saito N, et al. Pirfenidone Inhibits Myofibroblast Differentiation and Lung Fibrosis Development During Insufficient Mitophagy. *Respir Res*. (2017) 18:114. doi: 10.1186/s12931-017-0600-3

320. Yu N, Wang N, Zhang W, Xue J, Zhou Q, Hu F, et al. Dihydroartemisinin (Dha) Inhibits Myofibroblast Differentiation through Inducing Ferroptosis Mediated by Ferritinophagy. *Heliyon*. (2024) 10:e27276. doi: 10.1016/j.heliyon.2024.e27276

321. Bao C, Liang S, Han Y, Yang Z, Liu S, Sun Y, et al. The Novel Lysosomal Autophagy Inhibitor (Roc-325) Ameliorates Experimental Pulmonary Hypertension. *Hypertension*. (2023) 80:70–83. doi: 10.1161/hypertensionaha.122.19397

322. Ye W, Tang T, Li Z, Li X, Huang Q. Piperlongumine Attenuates Vascular Remodeling in Hypoxic Pulmonary Hypertension by Regulating Autophagy. *J Cardiol*. (2022) 79:134–43. doi: 10.1016/j.jjcc.2021.08.023

323. Ren HH, Niu Z, Guo R, Fu M, Li HR, Zhang XY, et al. Rhodiola Crenulata Extract Decreases Fatty Acid Oxidation and Autophagy to Ameliorate Pulmonary Arterial Hypertension by Targeting Inhibiton of Acylcarnitine in Rats. *Chin J Nat Med*. (2021) 19:120–33. doi: 10.1016/s1875-5364(21)60013-4

324. Liu Y, Xu Y, Zhu J, Li H, Zhang J, Yang G, et al. Metformin Prevents Progression of Experimental Pulmonary Hypertension Via Inhibition of Autophagy and Activation of Adenosine Monophosphate-Activated Protein Kinase. *J Vasc Res*. (2019) 56:117–28. doi: 10.1159/000498894

325. Shang P, Sun SB, Liu BH. Umbelliferone Improves Chronic Hypoxia-Induced Pulmonary Hypertension by Inhibiting the Rhoa/Rock Signaling Pathway and Autophagy. *Sheng Li Xue Bao*. (2022) 74:555–62.

326. Wu YC, Wang WT, Lee SS, Kuo YR, Wang YC, Yen SJ, et al. Glucagon-Like Peptide-1 Receptor Agonist Attenuates Autophagy to Ameliorate Pulmonary Arterial Hypertension through Drp1/Nox- and Atg-5/Atg-7/Beclin-1/Lc3β Pathways. *Int J Mol Sci*. (2019) 20:3435. doi: 10.3390/ijms20143435

327. Ibrahim YF, Shults NV, Rybka V, Suzuki YJ. Docetaxel Reverses Pulmonary Vascular Remodeling by Decreasing Autophagy and Resolves Right Ventricular Fibrosis. *J Pharmacol Exp Ther*. (2017) 363:20–34. doi: 10.1124/jpet.117.239921

328. Zhang X, Liu Q, Zhang C, Sheng J, Li S, Li W, et al. Puerarin Prevents Progression of Experimental Hypoxia-Induced Pulmonary Hypertension Via Inhibition of Autophagy. *J Pharmacol Sci*. (2019) 141:97–105. doi: 10.1016/j.jphs.2019.09.010

329. Long L, Yang X, Southwood M, Lu J, Marciniak SJ, Dunmore BJ, et al. Chloroquine Prevents Progression of Experimental Pulmonary Hypertension Via Inhibition of Autophagy and Lysosomal Bone Morphogenetic Protein Type Ii Receptor Degradation. *Circ Res*. (2013) 112:1159–70. doi: 10.1161/circresaha.111.300483

330. Wang X, Ibrahim YF, Das D, Zungu-Edmondson M, Shults NV, Suzuki YJ. Carfilzomib Reverses Pulmonary Arterial Hypertension. *Cardiovasc Res*. (2016) 110:188–99. doi: 10.1093/cvr/cvw047

331. He Y, Cao X, Guo P, Li X, Shang H, Liu J, et al. Quercetin Induces Autophagy Via Foxo1-Dependent Pathways and Autophagy Suppression Enhances Quercetin-Induced Apoptosis in Pasmcs in Hypoxia. *Free Radic Biol Med*. (2017) 103:165–76. doi: 10.1016/j.freeradbiomed.2016.12.016

332. Zhang H, Gong Y, Wang Z, Jiang L, Chen R, Fan X, et al. Apelin Inhibits the Proliferation and Migration of Rat Pasmcs Via the Activation of Pi3k/Akt/Mtor Signal and the Inhibition of Autophagy under Hypoxia. *J Cell Mol Med*. (2014) 18:542–53. doi: 10.1111/jcmm.12208

333. Grobs Y, Awada C, Lemay SE, Romanet C, Bourgeois A, Toro V, et al. Preclinical Investigation of Trifluoperazine as a Novel Therapeutic Agent for the Treatment of Pulmonary Arterial Hypertension. *Int J Mol Sci*. (2021) 22:2919. doi: 10.3390/ijms22062919

334. Gomez-Arroyo J, Sakagami M, Syed AA, Farkas L, Van Tassell B, Kraskauskas D, et al. Iloprost Reverses Established Fibrosis in Experimental Right Ventricular Failure. *Eur Respir J*. (2015) 45:449–62. doi: 10.1183/09031936.00188013

335. Afsal K, Selvaraj P. Effect of 1,25-Dihydroxyvitamin D3 on the xpression of Mannose Receptor, Dc-Sign and Autophagy Genes in Pulmonary Tuberculosis. *Tuberculosis (Edinb)*. (2016) 99:1–10. doi: 10.1016/j.tube.2016.03.010

336. Guzmán-Beltrán S, Rubio-Badillo M, Juárez E, Hernández-Sánchez F, Torres M. Nordihydroguaiaretic Acid (Ndga) and α-Mangostin Inhibit the Growth of Mycobacterium Tuberculosis by Inducing Autophagy. *Int Immunopharmacol*. (2016) 31:149–57. doi: 10.1016/j.intimp.2015.12.027

337. Kim JK, Lee HM, Park KS, Shin DM, Kim TS, Kim YS, et al. Mir144* Inhibits Antimicrobial Responses against Mycobacterium Tuberculosis in Human Monocytes and Macrophages by Targeting the Autophagy Protein Dram2. *Autophagy*. (2017) 13:423–41. doi: 10.1080/15548627.2016.1241922

338. Liu J, Ming S, Song W, Meng X, Xiao Q, Wu M, et al. B and T Lymphocyte Attenuator Regulates Autophagy in Mycobacterial Infection Via the Akt/Mtor Signal Pathway. *Int Immunopharmacol*. (2021) 91:107215. doi: 10.1016/j.intimp.2020.107215

339. Juárez E, Carranza C, Sánchez G, González M, Chávez J, Sarabia C, et al. Loperamide Restricts Intracellular Growth of Mycobacterium Tuberculosis in Lung Macrophages. *Am J Respir Cell Mol Biol*. (2016) 55:837–47. doi: 10.1165/rcmb.2015-0383OC

340. Bai X, Oberley-Deegan RE, Bai A, Ovrutsky AR, Kinney WH, Weaver M, et al. Curcumin Enhances Human Macrophage Control of Mycobacterium Tuberculosis Infection. *Respirology*. (2016) 21:951–7. doi: 10.1111/resp.12762

341. Xie C, Zhou X, Liang C, Li X, Ge M, Chen Y, et al. Apatinib Triggers Autophagic and Apoptotic Cell Death Via Vegfr2/Stat3/Pd-L1 and Ros/Nrf2/P62 Signaling in Lung Cancer. *J Exp Clin Cancer Res*. (2021) 40:266. doi: 10.1186/s13046-021-02069-4

342. Wang XR, Jiang ZB, Xu C, Meng WY, Liu P, Zhang YZ, et al. Andrographolide Suppresses Non-Small-Cell Lung Cancer Progression through Induction of Autophagy and Antitumor Immune Response. *Pharmacol Res*. (2022) 179:106198. doi: 10.1016/j.phrs.2022.106198

343. Zhu L, Wang Y, Lv W, Wu X, Sheng H, He C, et al. Schizandrin a Can Inhibit Non–Small Cell Lung Cancer Cell Proliferation by Inducing Cell Cycle Arrest, Apoptosis and Autophagy. *Int J Mol Med*. (2021) 48:214. doi: 10.3892/ijmm.2021.5047

344. Tang X, Ding H, Liang M, Chen X, Yan Y, Wan N, et al. Curcumin Induces Ferroptosis in Non-Small-Cell Lung Cancer Via Activating Autophagy. *Thorac Cancer*. (2021) 12:1219–30. doi: 10.1111/1759-7714.13904

345. Yan X, Yao C, Fang C, Han M, Gong C, Hu D, et al. Rocaglamide Promotes the Infiltration and Antitumor Immunity of Nk Cells by Activating Cgas-Sting Signaling in Non-Small Cell Lung Cancer. *Int J Biol Sci*. (2022) 18:585–98. doi: 10.7150/ijbs.65019

346. Zou Y, Zhang G, Li C, Long H, Chen D, Li Z, et al. Discovery of Tryptanthrin and Its Derivatives and Its Activities against Nsclc in Vitro Via Both Apoptosis and Autophagy Pathways. *Int J Mol Sci*. (2023) 24:1450. doi: 10.3390/ijms24021450

347. Teng JF, Mei QB, Zhou XG, Tang Y, Xiong R, Qiu WQ, et al. Polyphyllin Vi Induces Caspase-1-Mediated Pyroptosis Via the Induction of Ros/Nf-κb/Nlrp3/Gsdmd Signal Axis in Non-Small Cell Lung Cancer. *Cancers (Basel)*. (2020) 12:193. doi: 10.3390/cancers12010193

348. Xu Z, Pan Z, Jin Y, Gao Z, Jiang F, Fu H, et al. Inhibition of Prkaa/Ampk (Ser485/491) Phosphorylation by Crizotinib Induces Cardiotoxicity Via Perturbing Autophagosome-Lysosome Fusion. *Autophagy*. (2024) 20:416–36. doi: 10.1080/15548627.2023.2259216

349. Liu X, Yin M, Dong J, Mao G, Min W, Kuang Z, et al. Tubeimoside-1 Induces Tfeb-Dependent Lysosomal Degradation of Pd-L1 and Promotes Antitumor Immunity by Targeting Mtor. *Acta Pharm Sin B*. (2021) 11:3134–49. doi: 10.1016/j.apsb.2021.03.039

350. Zhang C, Jin Y. Ginsenoside Rg5 Induces Nsclc Cell Apoptosis and Autophagy through Pi3k/Akt/Mtor Signaling Pathway. *Hum Exp Toxicol*. (2024) 43:9603271241229140. doi: 10.1177/09603271241229140

351. Li J, Fan Y, Zhang Y, Liu Y, Yu Y, Ma M. Resveratrol Induces Autophagy and Apoptosis in Non-Small-Cell Lung Cancer Cells by Activating the Ngfr-Ampk-Mtor Pathway. *Nutrients*. (2022) 14:2413. doi: 10.3390/nu14122413

352. Luo D, He F, Liu J, Dong X, Fang M, Liang Y, et al. Pseudolaric Acid B Suppresses Nsclc Progression through the Ros/Ampk/Mtor/Autophagy Signalling Pathway. *BioMed Pharmacother*. (2024) 175:116614. doi: 10.1016/j.biopha.2024.116614

353. Hou G, Hu W, Sang Y, Gan X, Xu H, Hu Q, et al. Corynoxine Triggers Cell Death Via Activating Pp2a and Regulating Akt-Mtor/Gsk3β Axes in Nsclc. *Biochem Pharmacol*. (2024) 222:116110. doi: 10.1016/j.bcp.2024.116110

354. Wang J, Liu X, Zheng H, Liu Q, Zhang H, Wang X, et al. Morusin Induces Apoptosis and Autophagy Via Jnk, Erk and Pi3k/Akt Signaling in Human Lung Carcinoma Cells. *Chem Biol Interact*. (2020) 331:109279. doi: 10.1016/j.cbi.2020.109279

355. Luo D, Dai X, Tian H, Fan C, Xie H, Chen N, et al. Sophflarine a, a Novel Matrine-Derived Alkaloid from Sophora Flavescens with Therapeutic Potential for Non-Small Cell Lung Cancer through Ros-Mediated Pyroptosis and Autophagy. *Phytomedicine*. (2023) 116:154909. doi: 10.1016/j.phymed.2023.154909

356. Huang HW, Bow YD, Wang CY, Chen YC, Fu PR, Chang KF, et al. Dfiq, a Novel Quinoline Derivative, Shows Anticancer Potential by Inducing Apoptosis and Autophagy in Nsclc Cell and in Vivo Zebrafish Xenograft Models. *Cancers (Basel)*. (2020) 12:1348. doi: 10.3390/cancers12051348

357. O'Neill EJ, Sze NSK, MacPherson REK, Tsiani E. Carnosic Acid against Lung Cancer: Induction of Autophagy and Activation of Sestrin-2/Lkb1/Ampk Signalling. *Int J Mol Sci*. (2024) 25:1950. doi: 10.3390/ijms25041950

358. Kan Y, Song M, Cui X, Yang Q, Zang Y, Li Q, et al. Muyin Extract Inhibits Non-Small-Cell Lung Cancer Growth by Inducing Autophagy and Apoptosis in Vitro and in Vivo. *Phytomedicine*. (2022) 96:153834. doi: 10.1016/j.phymed.2021.153834

359. Muñoz-Guardiola P, Casas J, Megías-Roda E, Solé S, Perez-Montoyo H, Yeste-Velasco M, et al. The Anti-Cancer Drug Abtl0812 Induces Er Stress-Mediated Cytotoxic Autophagy by Increasing Dihydroceramide Levels in Cancer Cells. *Autophagy*. (2021) 17:1349–66. doi: 10.1080/15548627.2020.1761651

360. Li XQ, Cheng XJ, Wu J, Wu KF, Liu T. Targeted Inhibition of the Pi3k/Akt/Mtor Pathway by (+)-Anthrabenzoxocinone Induces Cell Cycle Arrest, Apoptosis, and Autophagy in Non-Small Cell Lung Cancer. *Cell Mol Biol Lett*. (2024) 29:58. doi: 10.1186/s11658-024-00578-6

361. Xia YC, Zha JH, Sang YH, Yin H, Xu GQ, Zhen J, et al. Ampk Activation by Asp4132 Inhibits Non-Small Cell Lung Cancer Cell Growth. *Cell Death Dis*. (2021) 12:365. doi: 10.1038/s41419-021-03655-2

362. Li J, Yan L, Luo J, Tong L, Gao Y, Feng W, et al. Baicalein Suppresses Growth of Non-Small Cell Lung Carcinoma by Targeting Map4k3. *BioMed Pharmacother*. (2021) 133:110965. doi: 10.1016/j.biopha.2020.110965

363. Wu Z, Li W, Tang Q, Huang L, Zhan Z, Li Y, et al. A Novel Aniline Derivative from Peganum Harmala L. Promoted Apoptosis Via Activating Pi3k/Akt/Mtor-Mediated Autophagy in Non-Small Cell Lung Cancer Cells. *Int J Mol Sci*. (2023) 24:12626. doi: 10.3390/ijms241612626

364. Fang C, Wu W, Ni Z, Liu Y, Luo J, Zhou Y, et al. Ailanthone Inhibits Non-Small Cell Lung Cancer Growth and Metastasis through Targeting Upf1/Gas5/Ulk1 Signaling Pathway. *Phytomedicine*. (2024) 128:155333. doi: 10.1016/j.phymed.2023.155333

365. Valencia K, Echepare M, Teijeira Á, Pasquier A, Bértolo C, Sainz C, et al. Dstyk Inhibition Increases the Sensitivity of Lung Cancer Cells to T Cell-Mediated Cytotoxicity. *J Exp Med*. (2022) 219:e20220726. doi: 10.1084/jem.20220726

frontiers | Frontiers in Immunology

TYPE Original Research
PUBLISHED 15 January 2025
DOI 10.3389/fimmu.2024.1475195

OPEN ACCESS

EDITED BY
Mirza S. Baig,
Indian Institute of Technology Indore, India

REVIEWED BY
Prabhugouda Siriyappagouder,
Nord University, Norway
Ze Fan,
Heilongjiang River Fisheries Research Institute, China

*CORRESPONDENCE
Yongchao Yuan
yyc@mail.hzau.edu.cn

RECEIVED 03 August 2024
ACCEPTED 16 December 2024
PUBLISHED 15 January 2025

CITATION
Yi L, Mo A, Yang H, Yang Y, Xu Q and Yuan Y (2025) Integrative RNA, miRNA, and 16S rRNA sequencing reveals immune-related regulation network for glycinin-induced enteritis in hybrid yellow catfish, *Pelteobagrus fulvidraco* ♀ × *Pelteobagrus vachelli* ♂. *Front. Immunol.* 15:1475195. doi: 10.3389/fimmu.2024.1475195

Integrative RNA, miRNA, and 16S rRNA sequencing reveals immune-related regulation network for glycinin-induced enteritis in hybrid yellow catfish, *Pelteobagrus fulvidraco* ♀ × *Pelteobagrus vachelli* ♂

Linyuan Yi[1], Aijie Mo[1], Huijun Yang[1], Yifan Yang[1], Qian Xu[1] and Yongchao Yuan[1,2,3]*

[1]College of Fisheries, Key Lab of Freshwater Animal Breeding, Ministry of Agriculture, Huazhong Agricultural University, Wuhan, Hubei, China, [2]Shuangshui Shuanglu Institute, Huazhong Agricultural University, Wuhan, China, [3]National Demonstration Center for Experimental Aquaculture Education, Huazhong Agricultural University, Wuhan, China

Glycinin-induced foodborne enteritis is a significant obstacle that hinders the healthy development of the aquatic industry. Glycinin causes growth retardation and intestinal damage in hybrid yellow catfish (*Pelteobagrus fulvidraco* ♀ × *Pelteobagrus vachelli* ♂), but its immune mechanisms are largely unknown. In the current study, five experimental diets containing 0% (CK), 1.74% (G2), 3.57% (G4), 5.45% (G6), and 7.27% (G8) immunological activity of glycinin were fed to juvenile hybrid yellow catfish to reveal the mechanism of the intestinal immune response to glycinin through RNA and microRNA (miRNA) sequencing and to explore the interrelation between immune molecules and intestinal microbiota. The results demonstrated that glycinin content in the posterior intestine increased significantly and linearly with the rise of dietary glycinin levels. More than 5.45% of dietary glycinin significantly reduced the nutritional digestion and absorption function of the posterior intestine. Notably, an obvious alteration in the expression levels of inflammatory genes (*tnf-α*, *il-1β*, *il-15*, and *tgf-β1*) of the posterior intestine was observed when dietary glycinin exceeded 3.57%. Sequencing results of RNA and miRNA deciphered 4,246 differentially expressed genes (DEGs) and 28 differentially expressed miRNAs (DEmiRNAs) between the CK and G6 groups. Furthermore, enrichment analysis of DEGs and DEmiRNA target genes exhibited significant responses of the MAPK, NF-κB, and WNT pathways following experimental fish exposure to 5.45% dietary glycinin. Additionally, at the level of 3.57% in the diet, glycinin obviously inhibited the increase of microbiota, especially potential probiotics such as *Ruminococcus bromii*, *Bacteroides plebeius*, *Faecalibacterium prausnitzii*, and *Clostridium clostridioforme*. In sum, 5.45% dietary glycinin through the MAPK/NF-κB/WNT

pathway induces enteritis, and inflammatory conditions could disrupt micro-ecological equilibrium through miRNA secreted by the host in hybrid yellow catfish. This study constitutes a comprehensive transcriptional perspective of how intestinal immunity responds to excessive glycinin in fish intestines.

KEYWORDS

hybrid yellow catfish, glycinin, foodborne enteritis, intestinal immunity, intestinal microbiata

1 Introduction

The substitution of fish meal with plant protein in aquafeeds leads to intestinal inflammation and growth inhibition, which poses major obstacles hindering the progress of the aquaculture sector. Soybean meal has emerged as the predominant alternative plant protein source to fish meal in aquafeeds, owing to its abundant yield, elevated protein content, and reliable availability (1). However, soybean antigenic proteins, as the main anti-nutritional factor with significant abundance, resistance to heat and strong immunogenicity in soybean meal, and prolonged and increased consumption can predispose aquatic organisms to allergic reactions in their gastrointestinal tracts, culminating in intestinal damage and related complications (2, 3). As one of the most important soybean antigen proteins, glycinin accounts for nearly 41.9% of soybean protein (4), possesses an extremely compact molecular structure, and is difficult to enzymatically hydrolyze (5). Recent research reported that 3.08%–6.04% immunologically active glycinin in the diet caused intestinal inflammation and oxidative damage, destroyed immune and digestive functions, and ultimately hindered the growth of *Rhynchocypris lagowskii* Dybowski (6). Accumulating lines of evidence suggest that excessive dietary glycinin could increase intestinal mucosal permeability, trigger intestinal inflammatory pathology, or disrupt microbial balance in various aquatic animals such as turbot (*Scophthalmus maximus* L) (7), Chinese mitten crabs (*Eriocheir sinensis*) (8), grass carp (*Ctenopharyngodon idella*) (9), and orange-spotted grouper (*Epinephelus coioides*) (10).

As the largest immune organ, the intestine accompanying the strongest mucosal immune system plays a crucial role in preserving host immune homeostasis and preventing pathological immune responses (11). However, owing to the fragile digestive tract of juvenile animals, a small proportion of glycinin that has not been fully digested maintains macromolecular activity and directly crosses the intestinal mucosal barrier, thereby stimulating the immune response in the blood, lymph, and intestine, causing inflammatory tissue damage (12, 13). It is a remarkable fact that previous studies on grass carp (9, 12) and *R. lagowskii* Dybowski (6) revealed that inflammation in the posterior intestine caused by glycinin appears more serious compared with that in the anterior and mid intestines, attributed to reasons such as that epithelial cells of the posterior intestine are more sensitive to antigen binding, leading to the strongest inflammatory response (14). The resistance of fish growth to the nutrient composition and immune status may form an intestinal environment conducive to the reproduction of potentially pathogenic bacteria, thereby impacting the homeostasis of the intestinal microbial community (15). Although certain studies have reported that 8% or 10% dietary glycinin disturbs the micro-ecological equilibrium of the intestine in aquatic animals (8, 10, 16), the specific action mechanism of this process and the relationship between microbes and intestinal inflammation still have many limitations, and more explorations are needed to enrich the understanding of this active field.

New omics technologies, including RNA sequencing (RNA-seq) and microRNA sequencing (microRNA-seq), hold notable potential to explore and interpret the complex relationship between fish nutrition and immunity (17). Ambient changes can trigger changes in transcriptional expression patterns (18). Nevertheless, to date, the effects of glycinin on the intestinal transcriptome and immunomodulatory networks have not been reported, and further research is needed. MicroRNAs (miRNAs), endogenous ~22-nucleotide non-coding RNAs, directly inhibit the gene expression via mRNA cleavage and/or translation (19). MiRNAs play a cardinal role in regulating pathological processes, and their dysregulation is connected with many diseases, including inflammation (20). It is worth noting that gradually increasing studies indicated that miRNAs are cardinal communication mediators of host–microbe interactions (21–23). Host-derived miRNAs are transferred into intestinal bacteria through extracellular vesicles, modulating their gene expression and affecting the replication of intestinal microbiota (21, 24). Conversely, the microbiota can alter host miRNA expression to promote epithelial proliferation and regulate its permeability, affecting intestinal homeostasis (25). Despite that the importance of this interaction is continuously emerging, the response mechanism between miRNA and intestinal microbiota in glycinin-induced enteritis remains elusive in fish.

Hybrid yellow catfish (*Pelteobagrus fulvidraco* ♀ × *Pelteobagrus vachelli* ♂) is a new species with fast growth, strong disease resistance, high quality, and market acceptance (26). In spite of this, cultured hybrid yellow catfish frequently cause foodborne enteritis attributed to its vigorous ingestion, which causes huge

10.3389/fimmu.2024.1475195

economic losses to the aquaculture industry. Our previous study found that more than 5.45% dietary glycinin eminently reduced the growth performance, accompanied by the aggravation of intestinal oxidative stress and apoptosis, and the impairment of intestinal structural integrity (27). Information on how glycinin causes gastrointestinal inflammation of hybrid yellow catfish is still unclear. Hence, the aim of this research was to use omics technology to explore the immunomodulatory networks and microbial imbalance mechanism of glycinin-induced foodborne enteritis and to provide essential insight into the breakthrough of intestinal health disorders in fish.

2 Materials and methods

2.1 Diet production and breeding trial

Glycinin was isolated from soybeans obtained from Wuhan Alpha Agri-tech Co., Ltd., and the specific extraction method was the same as that described in Yi et al. (27). Additionally, this research utilized the diet preparation and growth experiment in our previous study (27). Briefly, five different levels of glycinin diets were created based on the nutritional needs of the hybrid yellow catfish being studied (Table 1). They included 0%, 2.08%, 4.16%, 6.24%, and 8.32% glycinin, which corresponded to substituting 0%, 20%, 40%, 60%, and 80% fish meal proteins with soybean meal proteins, recording as the CK, G2, G4, G6, and G8 groups, respectively. Raw materials were provided by Wuhan Aohua Technology Co., Ltd. (Wuhan, China). The method of feed production was described in our previous study (27). Immunological activities of dietary glycinin in the groups of CK, G2, G4, G6, and G8 were consistent with those of our previous experiment, which were 0%, 1.74%, 3.57%, 5.45%, and 7.27%, respectively (27).

Juvenile hybrid yellow catfish (1.02 ± 0.01 g) were from Hubei Huangyouyuan Fisheries Development Co., Ltd. (Wuhan, China). The breeding trial took place in the Huazhong Agricultural University aquaculture base. A total of 450 fish were randomly placed into 15 glass tanks (1.20 × 0.60 × 0.45 m) at 30 fish per tank. Experimental fish were temporarily fed with the control group feed for 2 weeks to adapt to the experimental environment. Then, five experimental diets were randomly divided into triplicate tanks. During the rearing period, the feeding management and water quality testing methods for fish were the same as those in our previous study (27).

TABLE 1 Formulation and nutritional content of experimental feeds (air-dry basis, %).

Components	Experimental diets				
	CK	G2	G4	G6	G8
White fishmeal	40.00	32.00	24.00	16.00	8.00
Chicken powder	10.00	10.00	10.00	10.00	10.00
Corn gluten flour	8.00	8.00	8.00	8.00	8.00
Glycinin	0.00	2.08	4.16	6.24	8.32
Casein	0.00	2.72	5.44	8.16	10.88
Soybean phospholipid oil	5.00	5.60	6.20	6.80	7.40
High gluten flour	27.50	30.10	32.70	35.30	37.90
Choline chloride	1.00	1.00	1.00	1.00	1.00
Vitamin premix [1]	2.00	2.00	2.00	2.00	2.00
Mineral premix [2]	2.00	2.00	2.00	2.00	2.00
Sodium alginate	2.00	2.00	2.00	2.00	2.00
Antioxidant	0.50	0.50	0.50	0.50	0.50
Anti-mildew agent	0.50	0.50	0.50	0.50	0.50
Betaine	1.00	1.00	1.00	1.00	1.00
Chromium trioxide	0.50	0.50	0.50	0.50	0.50
Nutritional composition					
Moisture	12.59	12.96	12.51	12.92	12.88
Crude protein	42.41	42.19	42.39	42.17	42.62
Crude lipid	9.23	9.14	9.73	9.13	9.38
Ash	8.80	8.92	8.71	8.30	8.14

[1]Vitamin premix (mg/kg diet): vitamin A, 1.67; vitamin D, 0.027; vitamin E, 50.20; vitamin K, 11.10; vitamin C, 100.50; folic acid, 5.20; calcium pantothenate, 50.20; inositol, 100.50; niacin, 100.50; biotin, 0.12; cellulose, 645.25.
[2]Mineral premix (mg/kg diet): NaCl, 500.15; $MgSO_4·7H_2O$, 8,155.55; $NaH_2PO_4·2H_2O$, 12,500.51; KH_2PO_4, 16,000.51; $Ca(H_2PO_4)_2·H_2O$, 7,650.50; $FeSO_4·7H_2O$, 2,286.15; $C_6H_{10}CaO_6·5H_2O$, 1,750.12; $ZnSO_4·7H_2O$, 178.12; $MnSO_4·H_2O$, 61.35; $CuSO_4·5H_2O$, 15.45; $CoSO_4·7H_2O$, 0.89; KI, 1.5; Na_2SeO_3, 0.59.

2.2 Sample collection

In the eighth week, three fish were chosen at random from each group to be anesthetized using 100 mg/L MS-222 (tricaine methanesulfonate, Sigma, St. Louis, MO, USA) solutions. Subsequently, the intestinal contents were separated to detect intestinal microbes. Six fish after 24 hours of fasting were randomly selected from each tank and anesthetized to isolate posterior intestinal tissue for detection of gene expression, RNA-seq, miRNA-seq, and the activities of ATPase and Na^+-K^+-ATPase. The differentiation and separation of the posterior intestine referred to the method of Li et al. (28). The aforementioned samples were kept at −80°C until testing.

2.3 Enzyme activity determination

Posterior intestine tissue soaked in 9 volumes of phosphate-buffered saline (PBS) was disrupted and centrifuged to prepare tissue homogenate solution. It was used to determine glycinin contents with the plant glycinin ELISA kit (Jingmei Biological Technology Co., Ltd., Jiangsu, China), and the activities of ATPase and Na^+-K^+-ATPase were determined using the kit of Nanjing Jiancheng Bioengineering Institute (Nanjing, China; Cat. No. A070-1 and A070-2). Experimentation and computation were conducted following the instructions.

2.4 Real-time quantitative PCR

Detailed steps for real-time quantitative PCR (RT-qPCR) of inflammation-related mRNA and miRNA in the posterior intestine are provided in the Supplementary Material. Specific primers were designed according to the National Center for Biotechnology Information (NCBI) based on the yellow catfish gene sequences (Supplementary Table S1). The reference genes of mRNA and miRNA were *β-actin* (29) and U6 (30), respectively. The expression levels were quantitated by the $2^{-\Delta\Delta CT}$ method (31).

2.5 RNA-seq and miRNA-seq analysis

The isolation, library construction, sequence determination, and function enrichment of RNA and miRNA were completed by Shanghai Meiji Biomedical Technology Co., Ltd. (Shanghai, China). Detailed instructions can be obtained from the Supplementary Material.

2.6 16S rRNA sequencing

Microbial 16S rRNA sequencing was conducted by Shanghai Personalbio Technology Co., Ltd. The specific steps can be obtained in the Supplementary Material.

2.7 Statistical analysis

Data were analyzed using the SPSS Statistics 26.0 software. The analysis methodology was similar to that of our previous study (27). In short, the normality distribution and variance homogeneity of data were examined using the Shapiro–Wilk and Levene's tests, respectively. One-way ANOVA was employed to analyze the differences between different levels of glycinin groups. Multiple comparative analyses were executed by Tukey's test. Linear and quadratic tendencies were assessed using orthogonal polynomial contrasts. Experimental data were presented as means ± standard error (means ± SE). Additionally, a difference was regarded as significant if $p \leq 0.05$. Pearson's correlation coefficient (PCC) was used to uncover the correlations between inflammatory cytokine gene expressions, the posterior intestinal microbiota abundance, and differentially expressed miRNA (DEmiRNA) expressions.

3 Results

3.1 Enzyme activities of posterior intestine

With the rise of dietary glycinin level, the posterior intestinal glycinin content increased significantly and linearly (Figure 1A). In comparison to that in the CK group, ATPase activity was notably reduced in the G4, G6, and G8 groups (Figure 1B), and Na^+-K^+-ATPase activity was dramatically decreased in the G6 and G8 groups (Figure 1C). Additionally, significant linear and quadratic relationships were presented between the dietary glycinin levels and the activities of ATPase and Na^+-K^+-ATPase.

3.2 Relative expressions of inflammatory cytokine mRNAs in posterior intestine

The impacts of glycinin in the diet on the mRNA expressions of inflammatory cytokines in the posterior intestine are presented in Figure 2. The expressions of *tumor necrosis factor* (*tnf-α*), *interleukin-1β* (*il-1β*), and *interleukin-15* (*il-15*) in the G4, G6, and G8 groups were considerably elevated in comparison to those in the CK group, but the expression of *transforming growth factor-β1* (*tgf-β1*) obviously dropped in the glycinin-added groups. Notably, the expressions of *tnf-α* and *il-1β* in the G6 and G8 groups were considerably elevated compared to those in the G4 group, while the *tgf-β1* expression was considerably reduced. Relative to that in the CK group, the expression of *interleukin-10* (*il-10*) was remarkably enhanced in the G2, G4, and G6 groups, with no obvious variation in the G8 group. Strong linear relationships were demonstrated among the levels of dietary glycinin and the expressions of *tnf-α*, *il-1β*, *il-15*, and *tgf-β1*. A notable quadratic trend was displayed in the expression of *il-10* with the increase of dietary glycinin levels. No considerable variation was noted in the expression of *interleukin-8* (*il-8*).

3.3 RNA-seq analysis of posterior intestine

Our previous study indicated that 5.45% feed glycinin significantly reduced the growth rate of hybrid yellow catfish and induced cell apoptosis (27), significantly reduced posterior intestinal ATPase and Na^+-K^+-ATPase activities, and induced the highest significance of pro-inflammatory factors level in this paper. RNA-seq was performed on the CK and G6 groups. A total of 38.75 Gb of high-quality data was acquired (Supplementary Table S2). Principal component analysis (PCA) suggested the variations in gene expression profiles among two groups (Figure 3A). Moreover, 8.09% and 6.07% of specific gene expressions were sequenced in the CK and G6 groups, respectively (Figure 3B). A total of 4,246 differentially expressed genes (DEGs) were obtained, with 2,246 upregulated and 2,000 downregulated genes (Figure 3C). In the cluster analysis, it was evident that a noticeable portion of the DEGs showed absolutely converse expression patterns between the CK and G6 groups (Figure 3D).

Analysis using the Kyoto Encyclopedia of Genes and Genomes (KEGG) disclosed that there was a considerable enrichment of elevated genes in 43 KEGG pathways. Remarkably enriched immune- and human disease-related pathways primarily included Coronavirus disease-COVID-19, Complement and coagulation cascades, *Staphylococcus aureus* infection, NF-kappa B (NF-κB) signaling pathway, B cell receptor signaling pathway, Natural killer cell mediated cytotoxicity, Fc epsilon RI signaling pathway, Inflammatory mediator regulation of TRP channels, MAPK (mitogen-activated protein kinase) signaling pathway, and Intestinal immune network for IgA production (Figure 4A; Supplementary Table S3). Additionally, the first 20 pathways

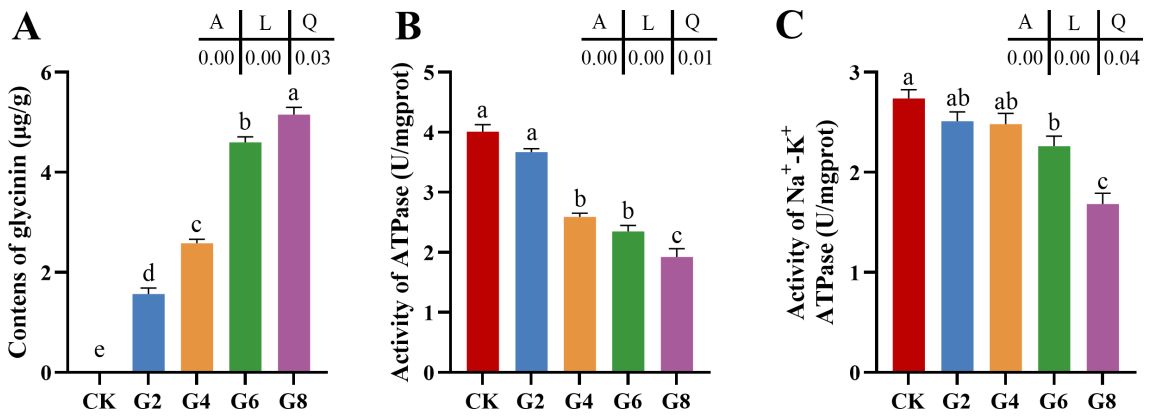

FIGURE 1
Glycinin contents **(A)** and the activities of ATPase **(B)** and Na^+-K^+-ATPase **(C)** in posterior intestine of *Pelteobagrus fulvidraco* ♀ × *Pelteobagrus vachelli* ♂. Obvious differences among groups are denoted by a, b, c, d, and e ($p < 0.05$). A indicates the *p*-value assayed via one-way ANOVA; L indicates a linear tendency assayed via orthogonal polynomial contrasts; Q indicates a quadratic tendency assayed via orthogonal polynomial contrasts.

obviously enriched by downregulated genes mainly involved nutrient absorption and metabolism, including Fat digestion and absorption, Endocytosis, Protein digestion and absorption, Protein processing in endoplasmic reticulum, Citrate cycle (TCA cycle), Glycerophospholipid metabolism, ABC transporters, Mineral absorption, Selenocompound metabolism, Alanine, aspartate and glutamate metabolism, and Vitamin digestion and absorption, as well as immune- and human disease-related pathways including Lipid and atherosclerosis, MicroRNAs in cancer, Focal adhesion, and Adherens junction (Figure 4B, Supplementary Table S3).

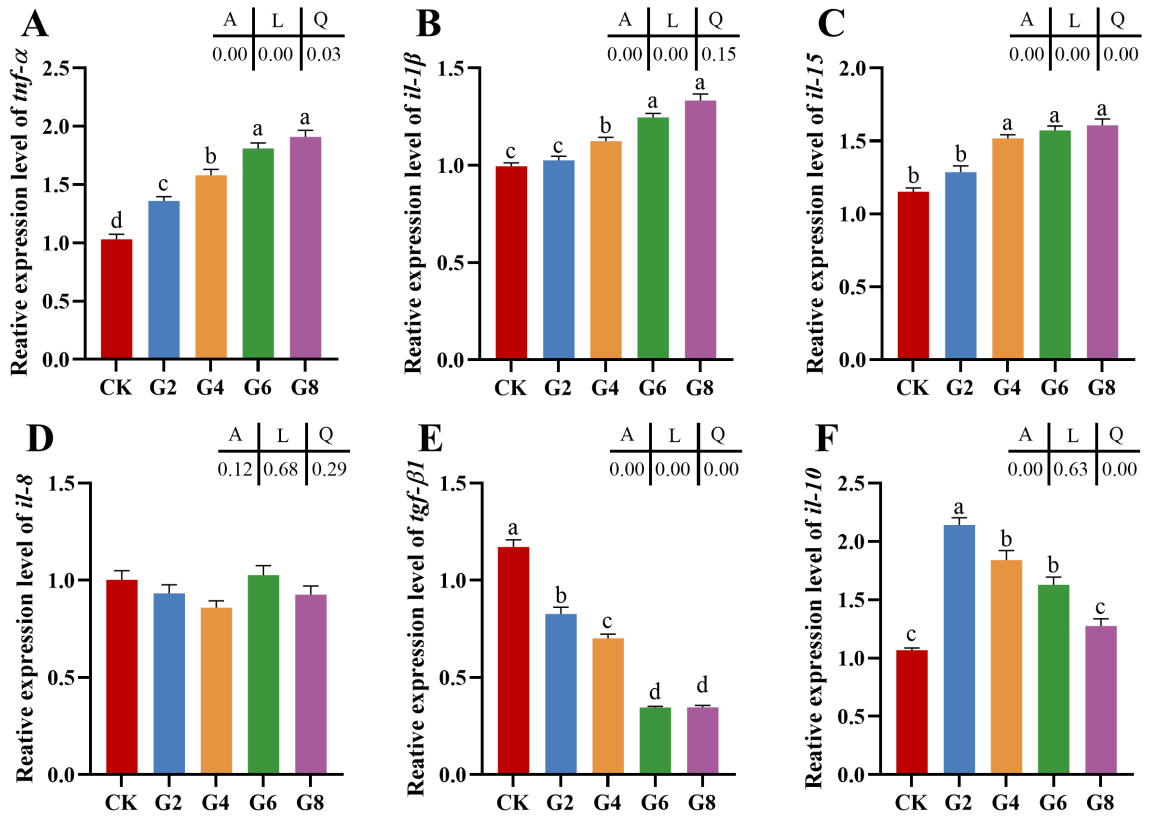

FIGURE 2
RT-qPCR of tnf-α **(A)**, il-1β **(B)**, il-15 **(C)**, il-8 **(D)**, tgf-β1 **(E)**, il-10 **(F)** mRNAs in posterior intestine of *Pelteobagrus fulvidraco* ♀ × *Pelteobagrus vachelli* ♂ (n = 3). The obvious differences among groups are denoted by a, b, c, and d ($p < 0.05$). A indicates the p-value assayed via one-way ANOVA; L indicates a linear tendency assayed via orthogonal polynomial contrasts; Q indicates a quadratic tendency assayed via orthogonal polynomial contrasts.

10.3389/fimmu.2024.1475195

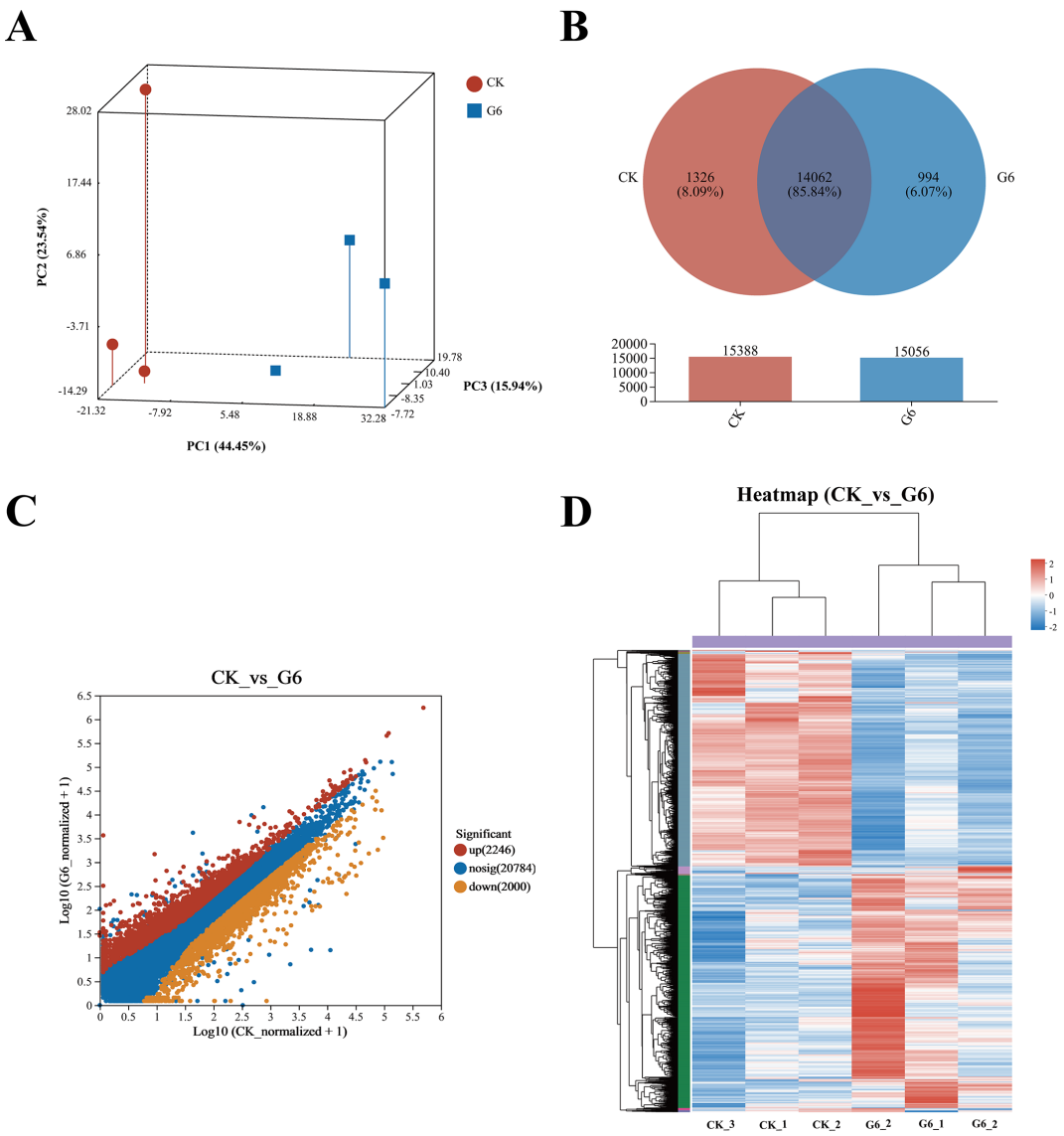

FIGURE 3
RNA-seq analysis of posterior intestine in the CK and G6 groups. **(A)** Principal component analysis (PCA). **(B)** Venn analysis. **(C)** Scatter diagram of differentially expressed genes (DEGs): red stands for upregulation, and yellow stands for downregulation ($p < 0.05$). **(D)** Cluster analysis of DEGs (heatmap): red indicates upregulation of DEGs, while blue represents downregulation.

3.4 MiRNA-seq analysis of posterior intestine

Six samples from the CK and G6 groups were sequenced with miRNA, and a total of 170 known miRNAs and 335 novel miRNAs were obtained (Supplementary Table S4). Analysis of miRNA expression results presented that 224 miRNAs were co-expressed between the CK and G6 groups, accounting for 76.45% of the total miRNAs, and the unique miRNAs of the G6 group were 8.53% higher than those of the CK group (Figure 5A). The top 10 expressed miRNAs in different samples were ipu-miR-192, ipu-miR-194a, ipu-miR-143, ipu-miR-21, ipu-miR-146a, ipu-miR-22a, ipu-miR-26a, ipu-miR-126a, NW_020848201_1_3371, ipu-miR-200b, ipu-miR-10b, ipu-miR-26b, ipu-miR-458, and ipu-let-7e (Figure 5B). DEmiRNAs were screened by differential expression analysis, with the involvement of 20 upregulated and eight downregulated genes (Figure 5C). Among the seven known DEmiRNAs discovered, ipu-miR-216b, ipu-miR-29c, ipu-miR-216a, ipu-miR-217, ipu-miR-184, and ipu-miR-459 were significantly reduced, and ipu-miR-489 was significantly enhanced (Supplementary Table S4).

A total of 15,466 target genes were predicted using miRanda and RNAhybrid software, including 1,736 DEmiRNA targets. DEmiRNA targets were enriched into 108 KEGG pathways (Supplementary Table S5), of which significantly enriched immune- and human disease-related pathways included Cushing syndrome and Gastric cancer (Figure 5D). Interestingly, the signaling pathways mainly involved in DEmiRNA targets were almost identical to those involved in DEGs in the aforesaid

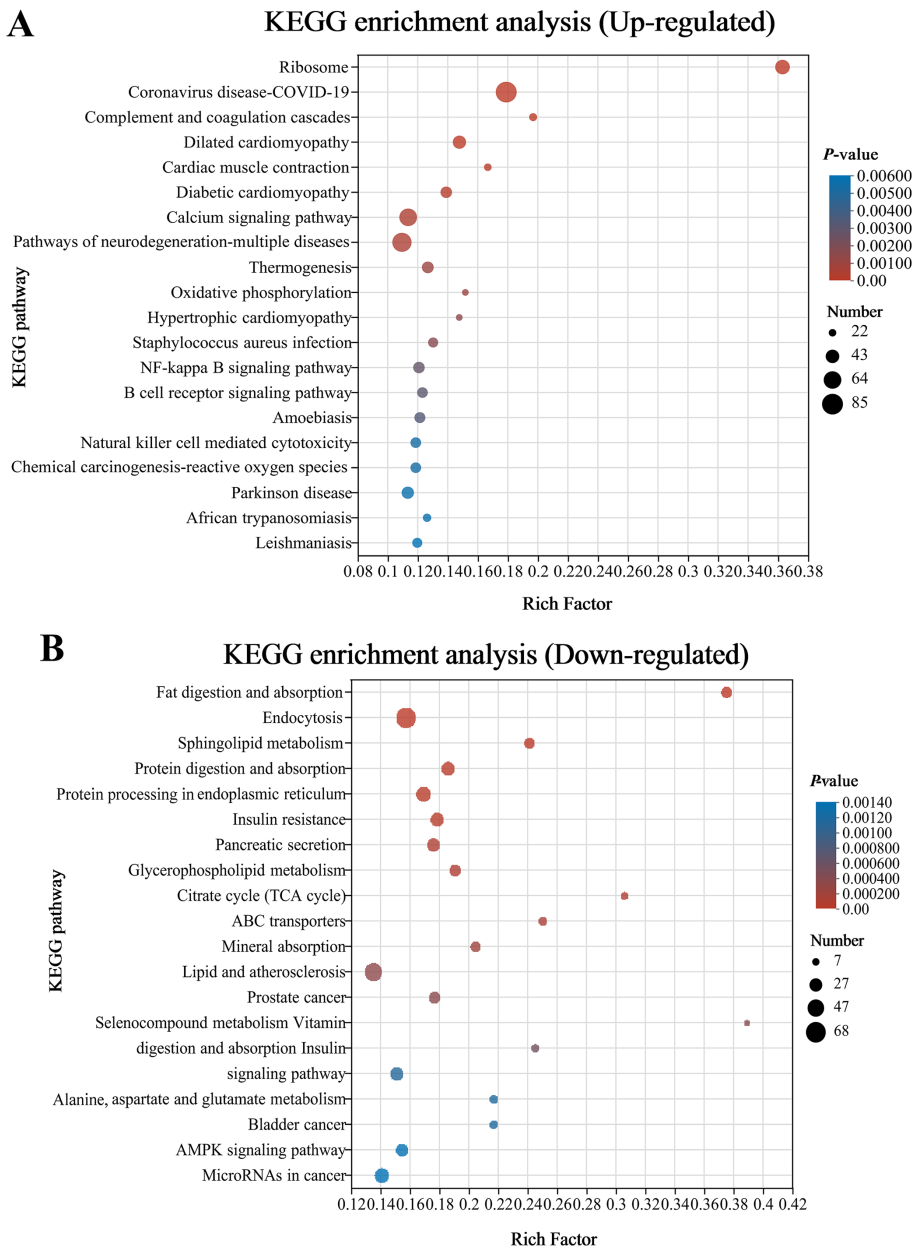

FIGURE 4
Bubble chart of top 20 Kyoto Encyclopedia of Genes and Genomes (KEGG) pathways concentrated with upward **(A)** and downward genes **(B)** in the CK and G6 groups. The more significant the rich factor, the higher the level of enrichment. The sizes of the dots represent the quantity of genes, and the colors of the dots are associated with various *p*-values. $p < 0.05$ is regarded as considerably enriched.

immune pathways, such as MAPK, WNT, PI3K-AKT, and TGF-β (Supplementary Table S5).

3.5 DEmiRNAs targeting DEGs

Association analysis of DEmiRNAs and targeting DEGs revealed 366 DEmiRNA–DEG interactions. We selected known DEmiRNAs to construct their interactome with DEGs (Figure 6) and screened for DEmiRNA–DEG pairs associated with inflammation. For instance, miRNA-216b could negatively regulate the expression of *wnt3a* (|PCCs| = 0.66, $p = 0.16$). Ipu-miR-29c may be the regulator of *smad3* (PCCs = 1, $p = 0.00$), *traf4* (PCCs = 0.88, $p = 0.02$), *txndc5* (PCCs = 0.83, $p = 0.04$), etc. Additionally, ipu-miR-217 could negatively direct the expression of *ehf* (|PCCs| = 0.83, $p = 0.04$).

3.6 RT-qPCR verification of DEGs and DEmiRNAs

To confirm the reliability of RNA-seq and miRNA-seq, the DEG expressions associated with the MAPK, NF-κB, and WNT pathways and known DEmiRNAs were validated by RT-qPCR. Our

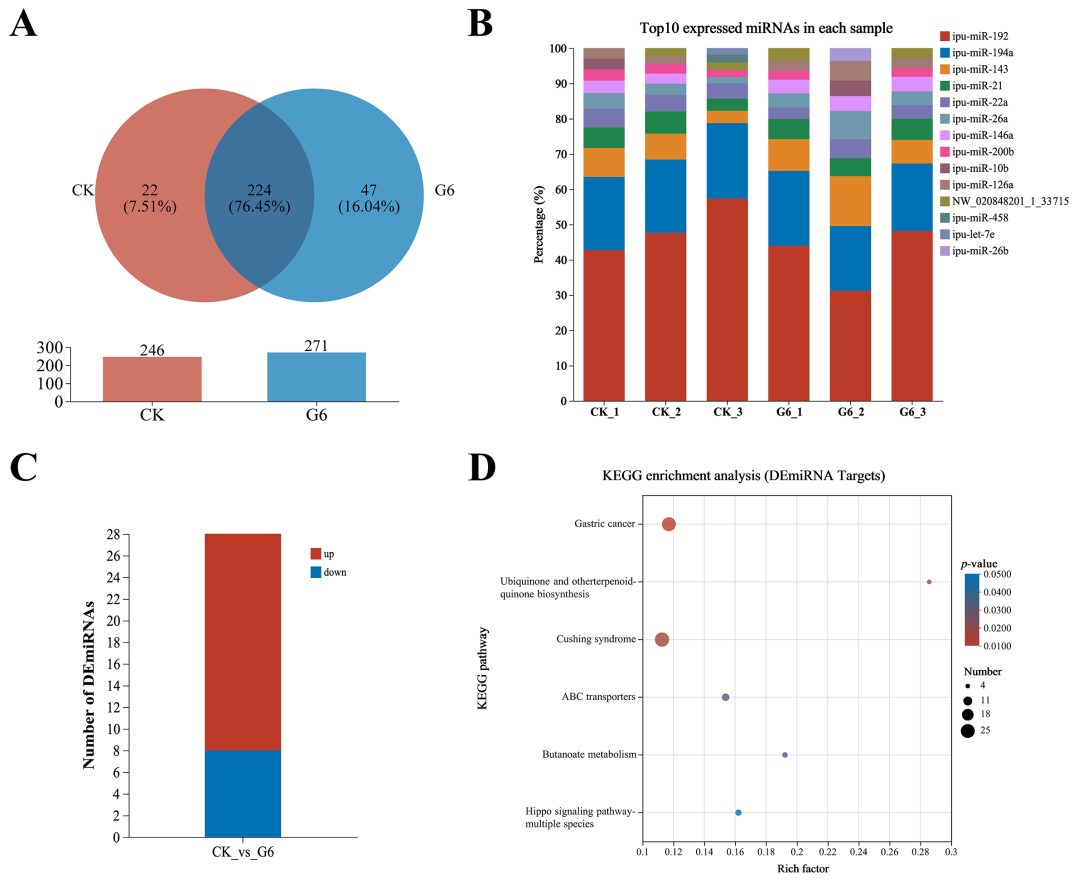

FIGURE 5
MiRNA-seq analysis of posterior intestine in the CK and G6 groups. **(A)** Venn analysis. **(B)** Top 10 expressed miRNAs in each sample. **(C)** Differentially expressed miRNAs (DEmiRNAs). **(D)** Top 20 Kyoto Encyclopedia of Genes and Genomes (KEGG) enrichment pathways of DEmiRNAs. Significant enrichment is indicated as –log10(*p*) > 0.

findings exhibited almost identical expression patterns between RT-qPCR results of DEmiRNAs and DEGs and their respective transcriptome sequencing data, except for up-miR-489 (Figure 7).

3.7 Microbial analysis of posterior intestine

Inflammation may contribute to the loss of intestinal microbiota balance; similarly, dysregulation of the microbiota may directly or indirectly affect the development of inflammation and immune-mediated pathologies. Thus, 16S rRNA sequencing was conducted in all groups to analyze the microbial composition of the posterior intestine. Our data presented that the highest number of 2,479 unique operational taxonomic units (OTUs) was observed in the CK group; interestingly, a reduced number of OTUs was presented in the glycinin-added groups (Figure 8A). There were 115 most shared OTUs between the G2 and CK groups. Principal coordinate analysis (PCoA) based on Unweighted_uniFrac further presented that the coordinates of the CK group were separated from the glycinin-added groups (Figure 8B). Alpha-diversity analysis suggested that there were no considerable differences between groups (Figure 8C). However, compared with those in the CK group, the indices such as Chao 1, Faith_pd, Shannon, and Observed_species displayed a downtrend in the glycinin-added groups (Figure 8C).

Microbial composition analysis showed that Proteobacteria (41.50% ± 8.05%), Fusobacteria (29.76% ± 8.74%), and Firmicutes (26.73% ± 7.81%) were identified as the predominant bacterial phyla of the posterior intestine from all groups (Figure 9A; Supplementary Table S6). *Cetobacterium* (29.56% ± 8.71%) had the highest abundance in all groups. However, the subdominant genera were different in different groups, with *Plesiomonas* (3.46% ± 1.18%) and Clostridiaceae *Clostridium* (1.87% ± 0.77%) in the CK group; *Lactococcus* (11.32% ± 1.86%), *Aeromonas* (11.41% ± 8.90%), and *Plesiomonas* (4.28% ± 2.69%) in the G2 group; and *Lactococcus* (31.33% ± 11.01%) and *Plesiomonas* (2.74% ± 0.85%) in the G4, G6, and G8 groups (Figure 9B; Supplementary Table S6). The average abundance at the species level was mainly dominated by *Cetobacterium somerae* (29.02% ± 8.54%) (Figure 9C; Supplementary Table S6).

Linear discriminant analysis effect size (LEfSe) was performed to identify the steady difference in species between different groups (Figure 10). The results indicated that the phylum level abundances including Actinobacteria, Bacteroidetes, Acidobacteria, Chloroflexi,

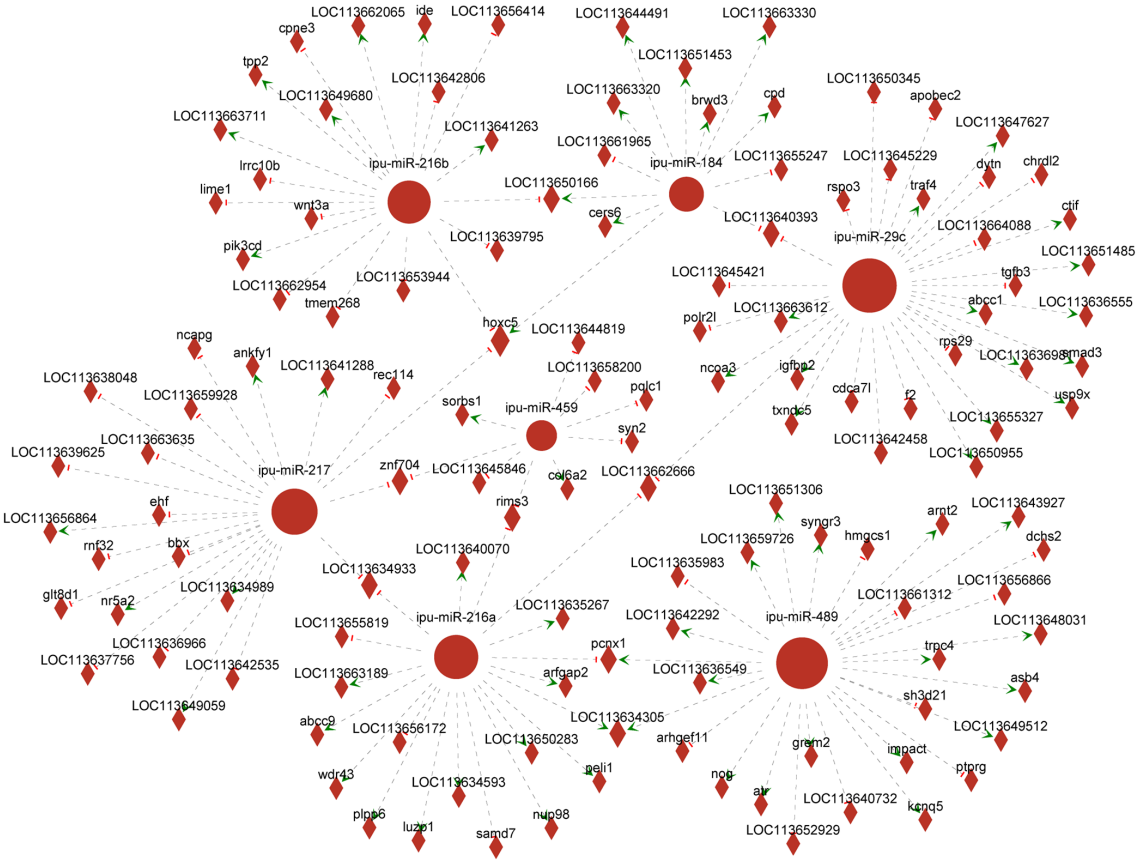

FIGURE 6
Network analysis of the association between known differentially expressed miRNAs (DEmiRNAs) and their targeting differentially expressed genes (DEGs). Circular nodes represent known DEmiRNAs; diamond nodes represent target genes; short red vertical bars represent negative regulation, and green arrows represent positive correlation.

Chlamydia, Cyanobacteria, and TM6 presented significant reductions in the glycinin-added groups relative to the CK group. At the species level, based on the presence of a certain level of glycinin in this experimental diet, the relative abundances of *Prauserella rugosa*, *Ruminococcus bromii*, *Bacteroides plebeius*, *Faecalibacterium prausnitzii*, *Reyranella massiliensis*, *Aliihoeflea aestuarii*, *Collinsella aerofaciens*, *Dorea formicigenerans*, *Clostridium perfringens*, *Clostridium clostridioforme*, and *Gemmiger formicilis* were downward significantly comparable with those in the CK group. It is worth mentioning that the abundance of *Leuconostoc fallax* in the G6 group was remarkably upward compared to that in the CK group.

Pearson's correlation analysis was employed to estimate the association between the expressions of inflammatory cytokine mRNAs and the abundances of differential species microbes (Figure 11). Significantly negative correlations were discovered between the abundances of *R. bromii* and *C. perfringens* and the *il-10* expression ($0.57 \geq |PCCs| \geq 0.52$). Similarly, the abundance changes in *P. rugosa*, *R. bromii*, *F. prausnitzii*, *A. aestuarii*, *C. perfringens*, *C. clostridioforme*, and *G. formicilis* presented noticeable negative correlations with the *tnf-α* and *il-15* expressions ($0.78 \geq |PCCs| \geq 0.53$). The abundances of *P. rugosa* and *A. aestuarii* showed an eminent opposite connection with the *il-1β* expression ($0.63 \geq PCCs \geq 0.58$). Contrarily, remarkable positive connections were displayed between the abundances of *A. aestuarii*, *P. rugosa*, and *C. perfringens* and the *tgf-β1* expression ($0.75 \geq PCCs \geq 0.65$). The *L. fallax* abundance and the *il-15* expression also showed an obvious positive relationship (PCCs = 0.53). The aforementioned results confirmed that dietary glycinin levels were associated with microbial modulation that was in turn associated with induced inflammation.

The KEGG pathway function annotation displayed that the microbial functional potential is primarily enriched in material metabolism, such as amino acids, carbohydrates, cofactors, and vitamins (Supplementary Figure S1A). Subsequently, MetagenomeSeq was performed to identify the metabolic pathways with significant differences between the CK group and the glycinin-added groups (Supplementary Figure S1, Supplementary Table S7). Results showed that relative to those in the CK group, 2, 16, 19, and 17 significant metabolic pathways were observed in the G2, G4, G6, and G8 groups, respectively. The *S. aureus* infection pathway was noticeably enhanced in the G2 and G6 groups (Supplementary Figures S1B, D). Nevertheless, more downregulated differential pathways were screened out in the G4, G6, and G8 groups, including

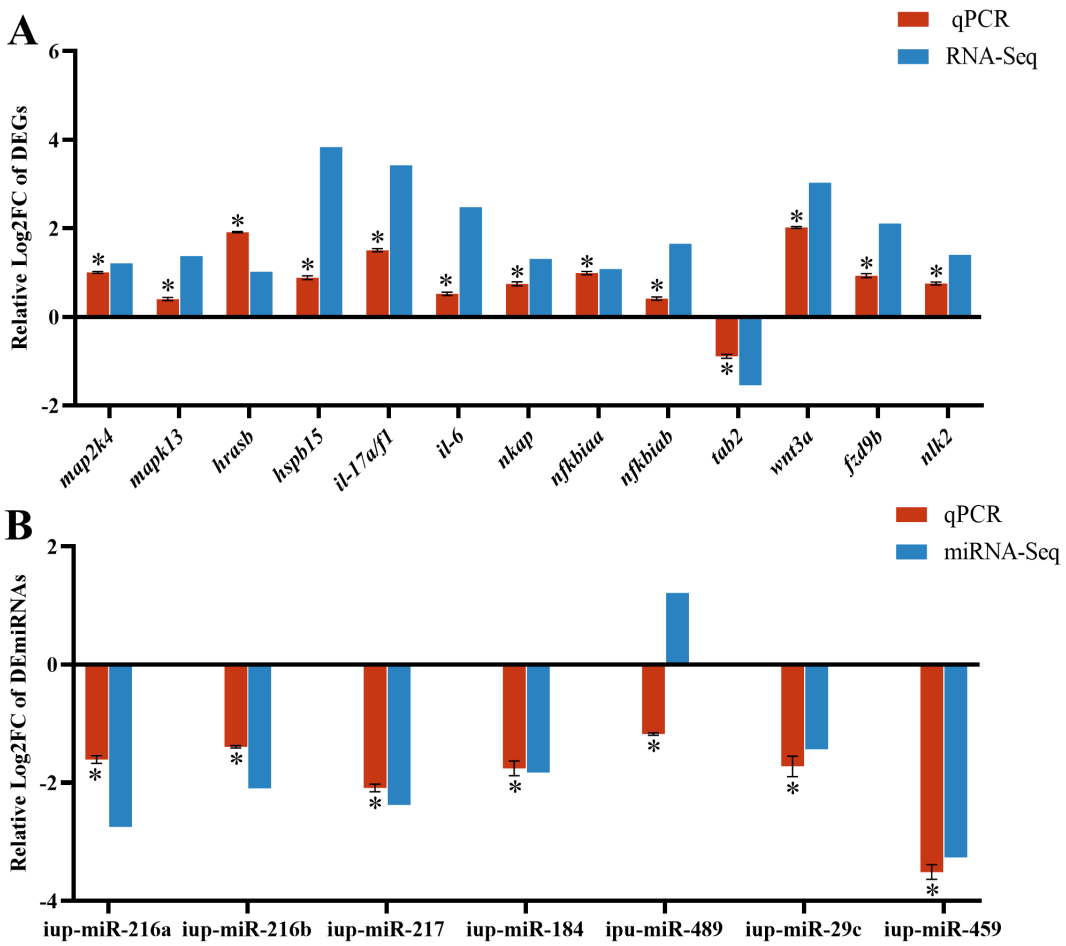

FIGURE 7
RT-qPCR results of differentially expressed genes (DEGs) **(A)** and differentially expressed miRNAs (DEmiRNAs) **(B)** in the CK and G6 groups. Data describe mean ± SE (n = 3). Relative log2Fold Chang (log2FC) reveals the changes between two groups of samples in expression levels and normalized by change in the reference gene of mRNA (*β-actin*) or miRNA (U6). Asterisks indicate obvious differences in DEGs or DEmiRNAs validated by qPCR between two groups of samples ($p < 0.05$).

Lysosome, Atrazine degradation, Cyanoamino acid metabolism, Proteasome, Polyketide sugar unit biosynthesis, NOD-like receptor signaling pathway, Protein digestion and absorption, Apoptosis, and Steroid biosynthesis (Supplementary Figures S1C–E).

3.8 Correlation analysis of DEmiRNAs and microbiota

Correlations between the expressions of DEmiRNAs and the abundances of differential species microbes in the posterior intestine are shown in Figure 12. The ipu-miR-29c expression showed a robust negative correlation with the *L. fallax* abundance (|PCCs| = 0.90); contrastingly, it was eminently positively correlated with the abundances of *P. rugosa* and *C. perfringens* (0.83 ≥ PCCs ≥ 0.82). Additionally, noticeable positive relationships were observed between the expressions of ipu-miR-217 and ipu-miR-216b and the abundances of *P. rugosa* and *R. bromii* (0.88 ≥ PCCs ≥ 0.85). Furthermore, there were dramatic positive correlations between the expressions of ipu-miR-216a and ipu-miR-459 and the abundances of *R. bromii*, *B. plebeius*, *F. prausnitzii*, *R. massiliensis*, *A. aestuarii*, *C. aerofaciens*, *D. formicigenerans*, *C. clostridioforme*, and *G. formicilis* (0.99 ≥ PCCs ≥ 0.83).

4 Discussion

4.1 High levels of dietary glycinin reduced the activities of ATPase and Na^+-K^+-ATPase in posterior intestine

Homeostasis of fish intestinal function is an important defense line against exogenous antigen invasion. As a foreign antigen with strong immunogenicity, a small portion of glycinin that is difficult to enzymatically hydrolyze would maintain macromolecular activity and directly cross the intestinal barrier, stimulating the immune response of blood, lymph, and intestinal mucosa to generate intestinal dysfunction (12, 32). In this study, a significant

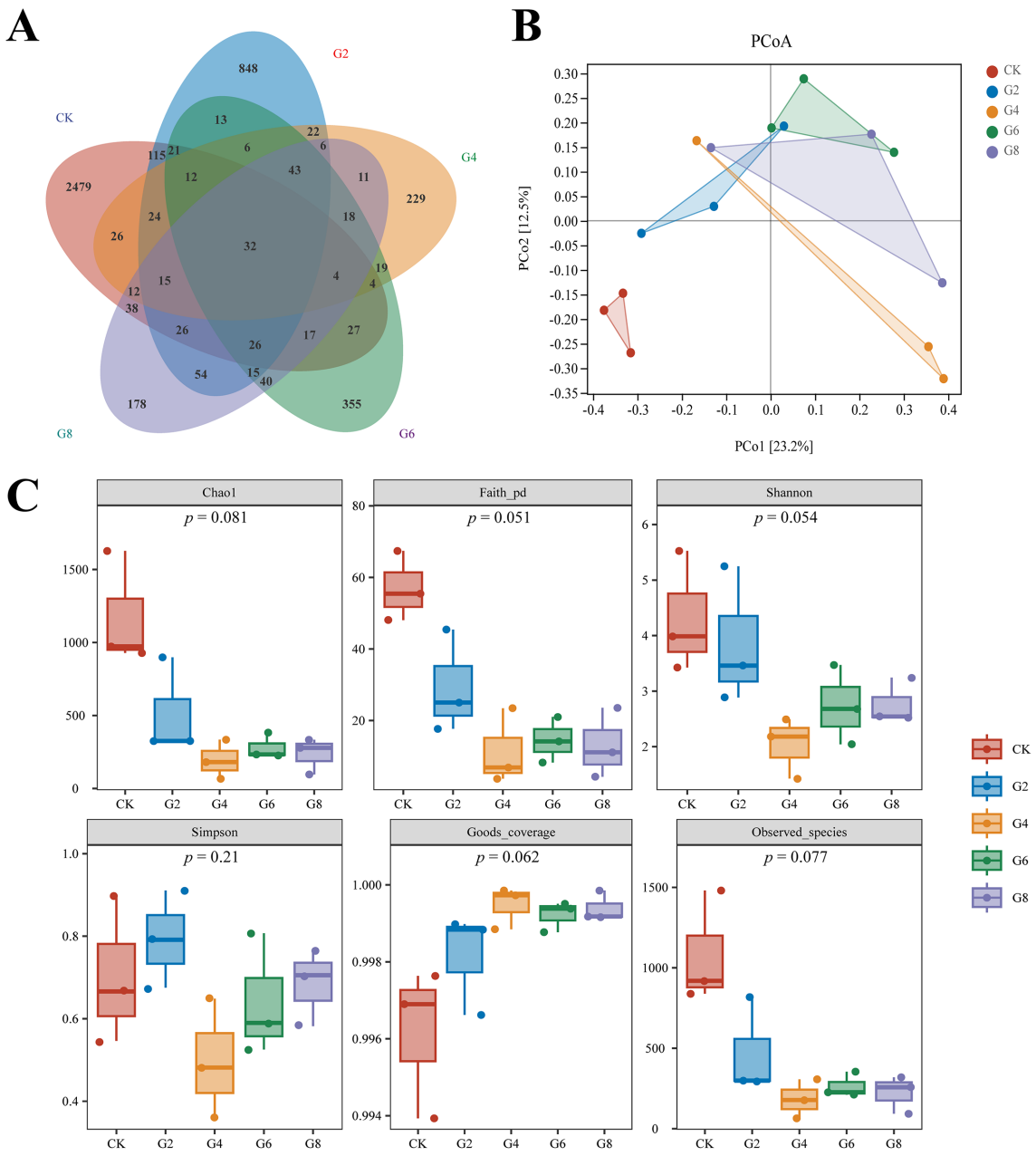

FIGURE 8
Microbial diversity in posterior intestine of *Pelteobagrus fulvidraco* ♀ × *Pelteobagrus vachelli* ♂. **(A)** Venn analysis. **(B)** Principal coordinate analysis (PCoA). **(C)** Alpha-diversity analysis.

positive correlation was observed between the glycinin contents in the posterior intestine and the levels of dietary glycinin, indicating that glycinin may exist in the form of macromolecules to damage the intestine. It should be emphasized that specific IgM against glycinin was notably increased in the blood of turbot that was given 8.31% dietary glycinin (7), suggesting that glycinin induced an immune response in fish.

To further explore the effect of dietary glycine on the absorption of intestinal nutrients in hybrid catfish, we examined the activities of ATPase and Na^+-K^+-ATPase in this study. ATPases are a type of membrane proteins that play an essential role in the transport of substances during cellular metabolism (33). Na^+-K^+-ATPase creates a beneficial transcellular Na gradient that is essential for the effective operation of Na-dependent nutrient co-transporters on the brush border membrane of intestinal epithelial cells and can indirectly indicate the absorptive ability of intestinal mucosa (34, 35). Our assay results presented that the activities of ATPase and Na^+-K^+-ATPase were dramatically diminished linearly with the increase of the dietary glycinin levels, suggesting that glycinin may interrupt the absorption of nutrients. The consistent results have also been reported in a study of mirror carp (*Cyprinus carpio*) (36). Consistently, RNA-seq results revealed that pathways associated

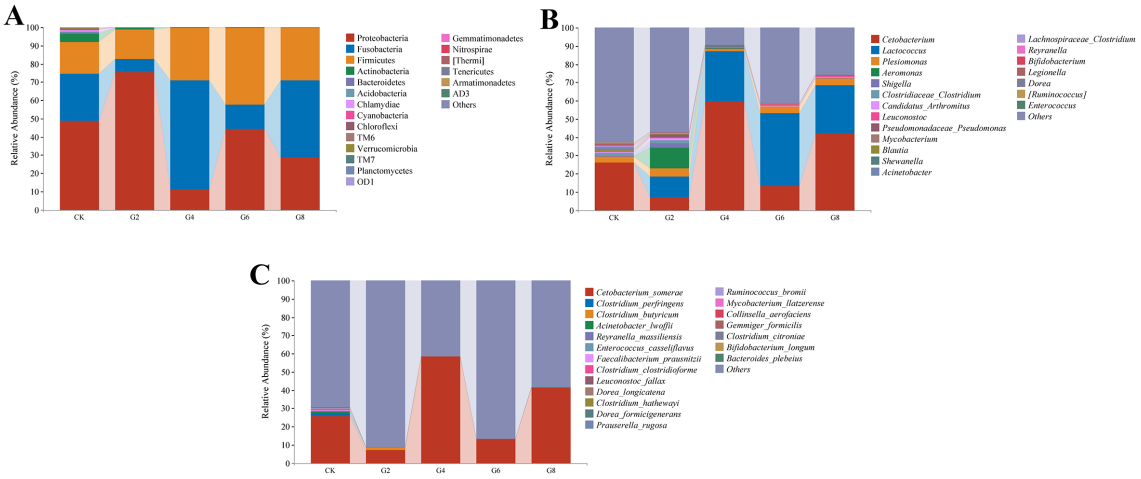

FIGURE 9
Microbial composition in posterior intestine of *Pelteobagrus fulvidraco* ♀ × *Pelteobagrus vachelli* ♂. **(A)** Phylum level. **(B)** Genus level. **(C)** Species level.

with nutrient absorption and metabolism were obviously enriched by downregulated genes, including those related to fats, proteins, glycerophospholipids, minerals, amino acids, and vitamins. Furthermore, our earlier study indicated that high levels of dietary glycinin considerably reduced the protein efficiency ratio of feed and the crude lipid content of whole fish. These findings supported the additional lines of evidence that glycinin may influence the nutrient transport and absorption capabilities of enterocytes. It is notable that inhibited Na^+-K^+-ATPase activity in the inflamed mucosa was attributed to the elevation of specific inflammatory mediators (37). Similarly, the diminishment of Na^+-K^+-ATPase in chronic enteritis of rabbits inhibited the brush border membrane Na-glucose cotransport pathway (38).

4.2 High levels of dietary glycinin disturb the expressions of inflammatory cytokine mRNAs in posterior intestine

Glycinin entering the blood and lymph stimulated the intestinal mucosa to produce an immunologic response and cause changes in cytokines (8, 32). Cytokines of the intestine are central players in the regulation of immunological responses after mucosal insults and the dominance of homeostatic or inflammatory conditions (39). In a previous study, we noticed that the integrity of posterior intestinal conformation was impacted by 3.57% glycinin, while 5.45% and 7.27% dietary glycinin groups were more serious (27). Our results of this paper validated that the expressions of the pro-inflammatory

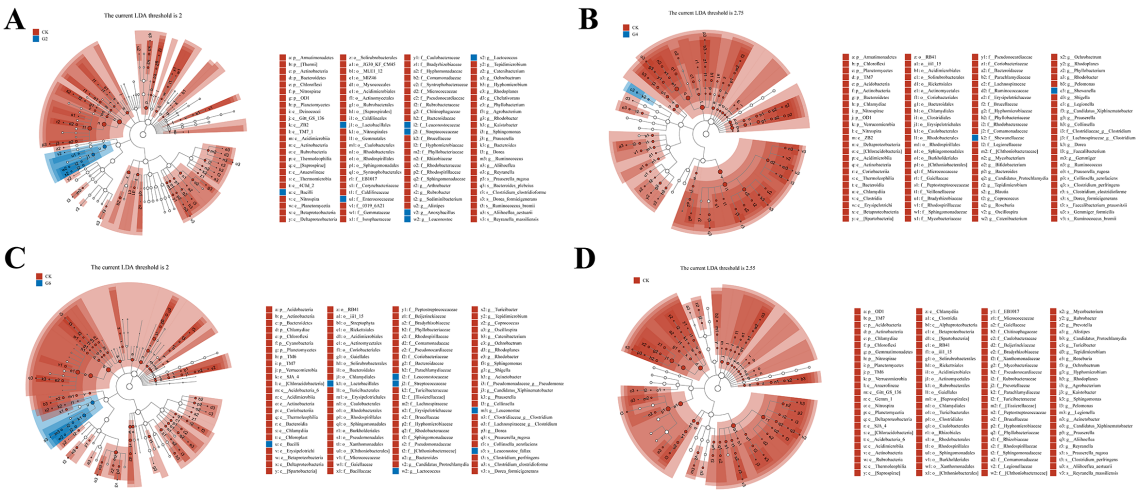

FIGURE 10
Linear discriminant analysis (LDA) effect size (LEfSe) analysis of posterior intestinal microbes in *Pelteobagrus fulvidraco* ♀ × *Pelteobagrus vachelli* ♂. **(A)** CK vs. G2. **(B)** CK vs. G4. **(C)** CK vs. G6. **(D)** CK vs. G8. Blue or red nodes represent a notable rise in the abundance of the group represented by that color. Letters indicate the name of the flora or species with significant differences between groups. LEfSe scores of the significantly different microbiota are higher than the LDA threshold.

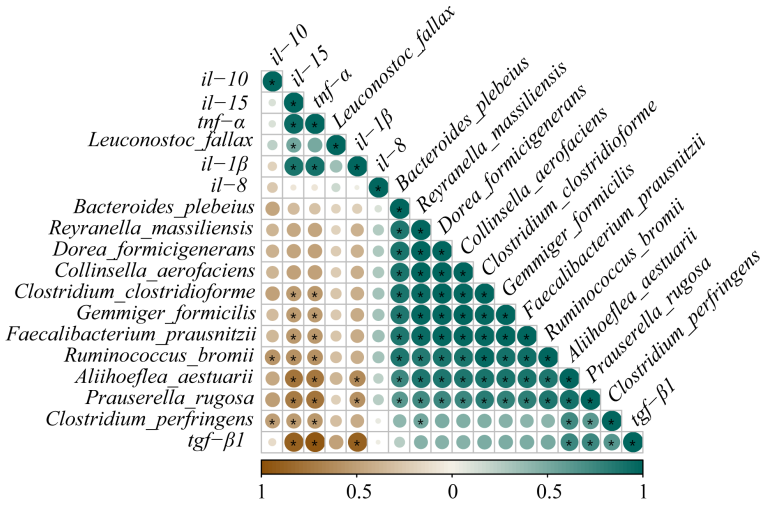

FIGURE 11
Correlation analysis between differential species microbes and the expressions of inflammatory cytokine mRNAs in posterior intestine of *Pelteobagrus fulvidraco* ♀ × *Pelteobagrus vachelli* ♂. Brown indicates negative correlation, and green indicates positive correlation. The size of circle is positively correlated with Pearson's correlation coefficient (PPC). Asterisks indicate notable distinctions ($p < 0.05$).

genes (*tnf-α* and *il-1β*) and immunoregulatory gene (*il-15*) increased dramatically at 3.57% or higher dietary glycinin levels, whereas the expression of anti-inflammatory cytokine *tgf-β1* was depressed by dietary glycinin, suggesting that excessive dietary glycinin may induce the occurrence of enteritis in hybrid yellow catfish. These were consistent with the research outcomes on golden crucian carp (*C. carpio* × *Carassius auratus*) (3), grass carp (12), hybrid grouper (*Epinephelus fuscoguttatus* ♀ × *Epinephelus lanceolatus* ♂) (32), and *R. lagowskii* Dybowski (6). During inflammation, immune cells rush into the intestinal mucosa, affecting the function of epithelial cells by producing IL-1 and TNF-α (40). Meanwhile, T lymphocytes mediate inflammatory suppression by secreting cytokines (IL-10 and TGF-β) to maintain intestinal homeostasis (41). IL-15, an immunoregulatory cytokine with multiple functions, evokes improved innate immunity to shape adaptive immunity, which is accompanied by the rise of its level following pathogenic encounters with the host (42). Furthermore, a prior study has shown that the administration of IL-15 results in the development of severe inflammatory arthritis (43).

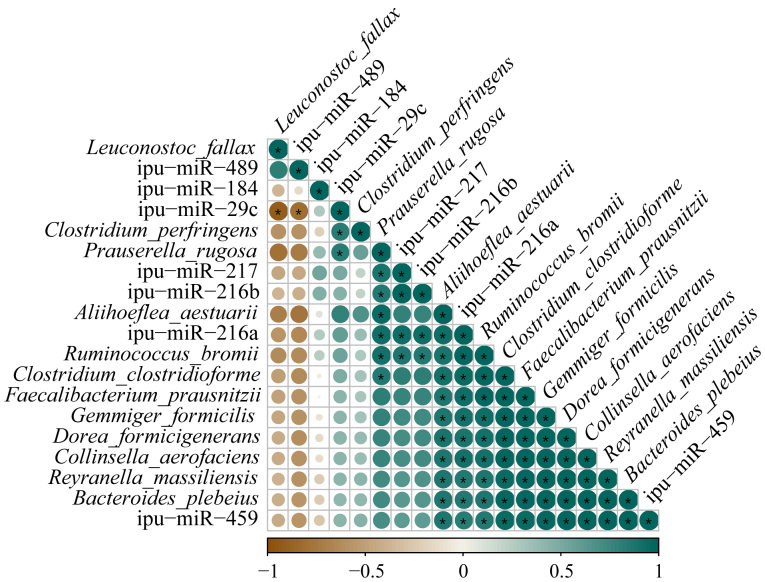

FIGURE 12
Correlation analysis between the expressions of known differentially expressed miRNAs (DEmiRNAs) and the abundances of differential species microbes in posterior intestine of *Pelteobagrus fulvidraco* ♀ × *Pelteobagrus vachelli* ♂. Brown indicates negative correlation, and green indicates positive correlation. The size of circle is positively correlated with Pearson's correlation coefficients (PPCs). Asterisks indicate notable distinctions ($p < 0.05$).

Interestingly, the *il-10* expression was considerably elevated in the G2, G4, and G6 groups in this research, while no notable distinction was observed in the CK and G8 groups. Activated monocytes and lymphocytes secrete IL-10 to inhibit the formation of pro-inflammatory cytokines (IL-1, IL-6, TNF-α, etc.); otherwise, the balance of pro- and anti-inflammatory systems may be disrupted with the continuous increase of pro-inflammatory cytokines, which may exacerbate the inflammation (44). Correspondingly, the high expression of *il-10* mRNA under the stimulation of dietary glycinin may be an adaptive mechanism for the body to suppress the persistence and severity of inflammation, while 7.27% dietary glycinin may severely destroy the immune system homeostasis. Inconsistently, high levels of dietary glycinin induced an attenuated *il-10* expression in the posterior intestine of turbot (7) and *C. carpio* var. Jian (45), which may be associated with the stage of the body's inflammatory resistance mechanism or different exposure times to glycinin.

4.3 RNA-seq analysis of posterior intestine

To obtain insights into the underlying mechanisms of enteritis activated by glycinin, RNA-seq identified 4,246 DEGs between the CK and G6 groups in the posterior intestine of hybrid yellow catfish. As is well known, under the stimulation of exogenous heat sources, inflammatory neurotransmitters are released, activating immune cells and causing sustained tissue damage or repair. In this study, numerous upregulated DEGs by dietary glycinin were eminently enriched in the immune cell response-related KEGG pathways such as Complement and coagulation cascades, B cell receptor signaling pathway, Natural killer cell mediated cytotoxicity, Inflammatory mediator regulation of TRP channels, and Intestinal immune network for IgA production. Foreign antigens activate myeloid leukocytes, which are then degraded by leukocytes and presented to T cells (46). Subsequently, CD4+ T cells polarize and secrete special cytokines to execute immune function (47). As in higher vertebrates, natural killer (NK)-like cells and CD8+ T cells enable the elimination of infected cells and protect the host from severe damage (48). DEGs also were partly amassed in the T-cell receptor signaling pathway, Th1 and Th2 cell differentiation, and Th17 cell differentiation in this study (Supplementary Table S2), suggesting that glycinin activates the cellular immune response of fish intestine. B-cell receptors recognize pathogenic signals and trigger a series of intricate biological responses to play a role in humoral defense (49). Antigen–antibody binding activates the complement system, promoting processes such as inflammation and apoptosis (50). The interplay of complement and coagulation is crucial in the development and treatment of inflammation, which also involves the modulation of inflammatory cytokines (51). TRP channels in immune cells mediate the production and release of inflammatory mediators (52). The intestinal immune network for IgA production contributes to maintaining a peaceful bacteria–host interaction (53). Similarly, the response of the aforementioned pathways to pathogens has been pointed in fish such as *P. vachelli* (54), hybrid grouper (55), and Mandarin fish (*Siniperca chuatsi*) (56). It is a wonder that *S. aureus* infection was found in both the enrichment pathway of DEGs and the prediction of microbial functional potential, revealing that glycinin may increase the susceptibility of the fish intestine to pathogenic bacteria.

Differently, downregulated DEGs were noticeably enriched in the nutrient metabolism such as proteins, lipids, and amino acids. Significantly, downregulated microbial functional pathways in the G4, G6, and G8 groups were also clustered in metabolism including proteins and steroids. Consistently, our prior study validated that 6% or higher dietary glycinin significantly reduced feed protein conversion efficiency and the crude lipid content in entire fish and muscle of experimental fish (27), suggesting that glycinin not only caused the immunoreaction of the body but also led to the disorder of nutrient metabolism. Similar results were observed in enteritis induced by soybean meal in hybrid grouper (55).

Furthermore, the co-enrichment of DEGs and DEmiRNA target genes yielded intriguing results as the significant responses of the MAPK, NF-κB, and WNT pathways in glycinin-induced enteritis. MAPK and NF-κB, as classical signaling pathways of inflammation (57), have been declared on their response mechanism to glycinin in piglets (58), grass carp (12), *C. carpio* (59), etc. IL-17A/F1 promotes the expressions of *il-1β*, *tnf-α*, *il-6*, chemokines, and antibacterial peptides and activates the MAPK and NF-κB signal pathways in fish (60). Consistently, the validation of RT-qPCR indicated that the expressions of MAPK (*map2k4*, *mapk13*, *hrasb*, and *hspb15*) and NF-κB (*il-17a/f1*, *il-6*, *nakp*, *nfkbiaa*, and *nfkbiab*) pathway-related genes were upregulated by 5.45% dietary glycinin in hybrid yellow catfish intestine. Intriguingly, MAPK13 is one of the four p38 MAPKs that exert its function acting on pro-inflammatory signaling (61). As a subfamily of the MAPK superfamily, the p38 MAPK is essential in the inflammatory stress response (62), activated by various growth factors, inflammatory cytokines, or a range of environmental pressures (63). The p38 MAPK has been previously identified as being able to elevate the approachability of the hidden NF-κB binding sites to activate the NF-κB pathway (64). A recent study reported that hypoxic–ischemic conditions induce inflammation and enhance cytotoxicity through the p38MAPK/NF-κB pathways in microglial cells (65). Additionally, the present study demonstrated that glycinin exposure stimulated the WNT signaling pathway, involving the immunomodulation of inflammation characterized by increased *wnt3a*, *fzd9b*, and *nlk2* mRNA expressions. Indeed, the WNT pathway and inflammatory signaling cascades interact significantly with each other (66). Wnt signaling is essential for modulating the immune system by controlling inflammatory cytokines including NF-κB and its associated genes (*il-6*, *il-8*, and *tnf-α*) (67) and manipulating the proliferation and differentiation of intestinal epithelial cells under inflammation conditions (66). Ayers et al. (68) reported that suppressing WNT signaling alleviates cholestatic injury by destroying the NF-κB-dependent inflammatory axis. Notably, past studies have suggested that WNT can synergistically drive tumorigenesis with ERK signaling (69) and can also cooperate with p38 MAPK to regulate cell proliferation (70). Nevertheless, further research is required to validate the significance of these findings in relation to inflammatory diseases.

4.4 MiRNA-seq analysis of posterior intestine

The role of miRNA has been considered in inflammation (71). It is well known that miRNA disturbances may affect multiple cellular pathways, as a single miRNA can control several target genes simultaneously. Lines of evidence suggest that numerous miRNAs, such as miR-192, miR-143, miR-21, miR-146a, miR-26a/26b, miR-126, and miR-200b, contribute to protecting or destroying the tight junctions of the intestine and involve the process of inflammation by inhibiting or stimulating immune cells such as T cells, neutrophils, macrophages, or monocytes (72). Apparently, abundant expressions of these miRNAs were also found in this study. Furthermore, our study suggested that 5.45% dietary glycinin noticeably attenuated the known miRNA expressions of ipu-miR-216a, ipu-miR-216b, ipu-miR-217, ipu-miR-184, ipu-miR-29c, and ipu-miR-459, showing that high levels of dietary glycinin may disrupt host miRNA expression patterns. Related studies have reported that the overexpression of miR-216a can inhibit lipopolysaccharide (LPS)-induced cell apoptosis and autophagy and regulate JAK2-STAT3 and NF-κB signal transduction to reduce inflammatory damage (73). MiR-216b has been extensively studied and identified as a regulator of inflammation as well as a factor that suppresses tumors (74). Additionally, miR-217 knockdown aggravated the inflammation in the endothelial cells of the human aorta, increasing IL-16, IL-β, and TNF-α levels (75). Similarly, miR-184 and miR-29c potentially participate in the signal transduction related to inflammation and apoptosis, and their overexpression suppressed pro-inflammatory cytokine release (IL-16, IL-β, etc.) in microglial inflammation triggered by LPS (76, 77). These results suggest that excessive feed glycinin may regulate the occurrence and development of intestinal inflammation by inhibiting inflammation-related miRNAs.

Correlation network analysis displayed that DEmiRNAs may regulate the inflammation-related genes to participate in glycinin-induced enteritis. Recent research indicated that hsa–miR–216a–3p manipulates cell hyperplasia in oral cancer through Wnt3a/β–catenin signaling (78). In our study, the expression of *wnt3a* may be regulated by ipu-miR-216b. Additionally, the *smad3* gene controls inflammatory cell recruitment through TGF-β signaling (79). Earlier research about Crohn's disease showed that TRAF4 represses the stimulation of NF-κB caused by NOD2 (80). TXNDC5 plays a role in initiating and progressing inflammation (81). The mRNA expression of the aforementioned regulatory factors may be regulated by ipu-miR-29c in glycinin-induced enteritis. Additionally, EHF is crucial for preserving the balance of epidermal and colonic epithelial tissues (82), and this gene may be regulated by ipu-miR-217 in this research. However, the specific miRNAs targeting regulatory relationships mentioned above need to be further studied.

4.5 Microbial analysis of posterior intestine

A plethora of studies have revealed a connection between intestinal microflora dysbiosis and inflammation (83–85). Exploring the response mechanisms of intestinal microbiota to glycinin-induced enteritis is a key process for understanding intestinal health. The diversity and stability of intestinal microbiota are closely related to fish diseases (86). In the present study, the alpha diversity of microflora in the posterior intestine was not eminently affected by dietary glycinin, but the richness indices (Chao 1 and Observed_species), the evolutionary diversity index (Faith_pd), and the number of OTUs showed a certain decreasing trend in the glycinin-added groups, especially in the high-level glycinin groups. In comparison to healthy fish, lower alpha diversity was detected in diseased fish including salmon (*Plecoglossus altivelis*) (86), yellow catfish (*P. fulvidraco*) (28), and grouper (*E. coioides*) (87). Microbial diversity may be reduced by high levels of glycinin to induce dysbiosis and inflammation. Previous research has reported that the active antimicrobial peptide segments produced by glycinin decomposition can inactivate microbial cells through cell membrane pores or membrane permeability (88).

In order to discover bacteria susceptible to glycinin, we explored phyla displaying significant reactions to dietary glycinin regardless of dosage. The results revealed that Proteobacteria, Fusobacteria, and Firmicutes were the main phyla, which is consistent with the core microbiota found in the intestine of *P. fulvidraco* (89), grass carp (90), and common carp (*C. carpio* L.) (91). It is noteworthy that relative abundances of Actinobacteria, Bacteroidetes, Acidobacteria, Chloroflexi, Chlamydia, Cyanobacteria, and TM6 significantly dwindled after adding a certain level of dietary glycinin in this experiment, which may be a specific manifestation of reduced microbial community richness by dietary glycinin. A study on Chinese mitten crab claimed that 80 g/kg dietary glycinin considerably increased the abundances of Actinobacteria and Proteobacteria in the intestine, while the abundance of Bacteroidetes was decreased (8). Nonetheless, the overall structure of intestinal microbiota was not significantly affected by dietary glycinin in turbot (7). These inconsistent results may be partly associated with differences in dietary glycinin levels, species, or aquaculture environment.

Correspondingly, the levels of dietary glycinin changed to varying degrees in the dominant microbiota at the genus level. *Cetobacterium* was identified as a superior genus in each group, with the representative being *C. somerae*. The metabolism of *C. somerae* produces acetic acid, which promotes insulin expression and glycometabolism and plays an important regulatory role in fish health (92). Clostridiaceae encompassing *Clostridium* appeared in higher abundance in the feces of dogs fed meat diets, indicating its potential correlation with protein digestibility (93). Intriguingly, both microbial function prediction and RNA-seq validated that the protein digestion and absorption pathway was significantly downregulated by dietary glycinin, which may be related to the attenuation of *Clostridium* abundance. The stimulation of *Leuconostoc* abundance in the G6 group should be noted. The inflammatory cases of *Leuconostoc* infection have been continuously reported (94, 95), and they are associated with potential and frequent gastrointestinal diseases (95).

Similar to the phylum level, most microbial species were significantly inhibited by the dietary glycinin of different levels, which further indicated that glycinin causes disruption of intestinal microbiota. Among them, *R. bromii*, *F. prausnitzii*, *C. clostridioforme*, and *B. plebeius* are potential probiotics, which produce secondary metabolites with strong biological activity such as short-chain fatty

acids, mainly in the antibacterial, anti-tumor, or anti-inflammatory role, and protect the intestinal mucosal barrier from damage by foreign antigens (96–98). In addition, *R. massiliensis* was considered to enhance the stress resistance of tropical gars (*Atractosteus tropicus*) in adverse environments (99). A recent study also found the absence of most microflora, including *D. formicigenerans*, in Saudi inflammatory bowel disease (IBD0 patients (100). In contrast, *C. perfringens*, a conditioned pathogen secreting virulent toxins, triggers related intestinal diseases (101). There is relatively little research on *P. rugosa*, *A. aestuarii*, *C. aerofaciens*, and *G. formicilis*, particularly in the intestine of fish. All aforesaid results demonstrated that the ecological balance of microbial communities may be disrupted by dietary glycinin by inhibiting the intestinal microbiota reproduction of hybrid yellow catfish, especially potential probiotics.

Correlation analysis addressed the noticeable negative relationships among the remarkably different bacteria and the mRNA expressions of *tnf-α*, *il-1β*, and *il-15*. Khan et al. (102) found that *F. prausnitzii* inhibits the secretion of IL-8 activated by IL-1β in Caco-2 cells. In rheumatoid arthritis, with higher IL-6 levels, attenuated *R. bromii* was identified by machine learning (103). Additionally, the possible cause of inhibited *C. perfringens* could be an increase in *il-10* expression. A study in chicken revealed *il-10* production in necrotic enteritis induced by *C. perfringens* (104). These findings suggest that the reduced intestinal microbiota may be related to the occurrence of enteritis, but whether inflammatory cytokines are the direct factors that inhibit or facilitate the growth of intestinal microbes needs to be studied more comprehensively.

4.6 Correlation analysis of DEmiRNAs and microbiota

Past studies have revealed that host-derived miRNAs are vital for maintaining normal intestinal microbiota (21, 23). MiR-21, an important factor involved in the pathogenesis of intestinal inflammation, aggravated dextran sodium sulfate (DSS)-induced colitis in mice by affecting the intestinal microflora (105). Released miRNA is taken up by bacteria, e.g., *Fusobacterium nucleatum* and *Escherichia coli*, and combines with DNA to specifically manipulate gene expression and, consequently, alter microbial adaptability (24). Additionally, it is important to highlight that miRNA may indirectly affect microbial dysbiosis by regulating the production of cytokines (106). MiR-21 activates macrophages and naive CD4+ cells to release inflammatory mediators, intensifying colitis, which may indirectly influence the homeostasis of the microbiota (107).

Intriguingly enough, host miRNA expression is also affected by intestinal microbiota (108). A study demonstrated that probiotics including *Lactobacillus fermentum* and *Lactobacillus salivarius* restored the miRNA expression such as miR-143 in mice with DSS-induced colitis (109). Additionally, a certain study reported a strongly positive relationship between *Faecalibacterium* and hsa-miR-6833-5p (25). In our study, *F. prausnitzii* presented significant positive correlations with the expressions of ipu-miR-216a and ipu-miR-459. However, so far, there is no literature exploring the direct relationship between the microbes and the DEmiRNAs of this study. The microbiota may affect host miRNA expression through metabolites (e.g., short-chain fatty acids), bacterial endotoxins, and other factors, thereby influencing the host's intestinal health (110, 111). Anzola et al. (112) deciphered that bacterial component LPS via TLR4/MyD88/NF-κB-AKT enhances miR-146a levels in non-tumoral rat ileal cells to affect inflammation. Nonetheless, the exact interaction mechanism between specific miRNAs and microorganisms still needs further research.

5 Conclusion

Taken together, dietary 5.45% or higher levels of glycinin induced enteritis through the MAPK/NF-κB/WNT pathway, and inflammatory state could disrupt micro-ecology balance by host-secreted miRNA in hybrid yellow catfish. Otherwise, the observations in this study regarding the partial immune regulatory network of intestinal mRNA, miRNA, and microbes are based on the transcriptional profiles obtained and should be further verified in future studies by *in vitro* experiments, luciferase assay, or fecal microbiota transplant experiments.

Data availability statement

The data of Transcriptome and Small RNA sequencing are deposited in the NCBI SRA database. The names of the repository/repositories and accession number(s) can be found below: https://www.ncbi.nlm.nih.gov/, PRJNA1207723; https://www.ncbi.nlm.nih.gov/, PRJNA1207605. And the other data can be found in the link: https://www.jianguoyun.com/p/DdZdUyQQ1JKXDRiFl-cFIAA.

Ethics statement

The animal study was approved by the Ethics Committee of Huazhong Agricultural University. The study was conducted in accordance with the local legislation and institutional requirements.

Author contributions

LY: Data curation, Investigation, Methodology, Writing – original draft, Writing – review & editing. AM: Methodology, Visualization, Writing – review & editing. HY: Project administration, Validation, Writing – review & editing. YFY: Data curation, Methodology, Writing – original draft. QX: Investigation, Methodology, Writing – review & editing. YCY: Formal analysis, Funding acquisition, Project administration, Supervision, Writing – review & editing.

Funding

The author(s) declare financial support was received for the research, authorship, and/or publication of this article. This work was supported by the National Natural Science Foundation of

China (32273167) and the Fundamental Research Funds for the Central Universities (2662022SCYJ003).

Acknowledgments

The authors would like to thank all the collaborators and supporters who provided funding, experimental testing platforms, and equipment for this study.

Conflict of interest

The authors declare that the research was conducted in the absence of any commercial or financial relationships that could be construed as a potential conflict of interest.

Publisher's note

Supplementary material

The Supplementary Material for this article can be found online at: https://www.frontiersin.org/articles/10.3389/fimmu.2024.1475195/full#supplementary-material

References

1. Booman M, Forster I, Vederas JC, Groman DB, Jones SRM. Soybean meal induced enteritis in Atlantic salmon (*Salmo salar*) and Chinook salmon (*Oncorhynchus tshawytscha*) but not in pink salmon (O. *gorbuscha) Aquaculture*. (2018) 483:238–43. doi: 10.1016/j.aquaculture.2017.10.025

2. Zhang Y, Duan X, Jiang W, Feng L, Wu P, Liu Y, et al. Soybean glycinin decreased growth performance, impaired intestinal health, and amino acid absorption capacity of juvenile grass carp (*Ctenopharyngodon idella*). *Fish Physiol Biochem*. (2019) 45:1589–602. doi: 10.1007/s10695-019-00648-z

3. Li M, Li L, K YD, Zhu R, Yu Z, Wang JY, et al. Effects of glycinin on growth performance, immunity and antioxidant capacity in juvenile golden crucian carp, *cyprinus carpio* × *Carassius auratus*. *Aquaculture*. (2020) 51:465–79. doi: 10.1111/are.14390

4. Zhou Y, Liao Y, Bai J, Xia X, Wu Z, Li X, et al. Effects of active soybean isoflavones on the structure and potential allergenicity of glycinin. *LWT*. (2024) 198:116050. doi: 10.1016/j.lwt.2024.116050

5. Wang T, Qin GX, Sun ZW, Zhao Y. Advances of research on glycinin and β-conglycinin: a review of two major soybean allergenic proteins. *Crit Rev Food Sci Nutr*. (2014) 54:850–62. doi: 10.1080/10408398.2011.613534

6. Zhu R, Li L, Li M, Yu Z, Wang HH, Quan YN, et al. Effects of dietary glycinin on the growth performance, immunity, hepatopancreas and intestinal health of juvenile *Rhynchocypris lagowskii* Dybowski. *Aquaculture*. (2021) 54:737030. doi: 10.1016/j.aquaculture.2021.737030

7. Li YX, Yang P, Zhang YJ, Ai QH, Xu W, Zhang WB, et al. Effects of dietary glycinin on the growth performance, digestion, intestinal morphology and bacterial community of juvenile turbot, *Scophthalmus maximus* L. *Aquaculture*. (2017) 479:125–33. doi: 10.1016/j.aquaculture.2017.05.008

8. Han F, Wang X, Guo J, Qi C, Xu C, Luo Y, et al. Effects of glycinin and β-conglycinin on growth performance and intestinal health in juvenile Chinese mitten crabs (*Eriocheir sinensis*). *Fish Shellfish Immunol*. (2019) 84:269–79. doi: 10.1016/j.fsi.2018.10.013

9. Zhang YL, Duan XD, Feng L, Jiang WD, Wu P, Liu Y, et al. Soybean glycinin disrupted intestinal structural integrity related to aggravation of apoptosis and downregulated transcription of tight junction proteins in the intestine of juvenile grass carp (*Ctenopharyngodon idella*). *Aquaculture*. (2021) 531:735909. doi: 10.1016/j.aquaculture.2020.735909

10. Yin Y, Zhao X, Yang L, Wang K, Sun Y, Ye J. Dietary high glycinin reduces growth performance and impairs liver and intestinal health status of Orange-spotted grouper (*Epinephelus coioides*). *Anim (Basel)*. (2023) 13:2605. doi: 10.3390/ani13162605

11. Wang S, Xia P, Chen Y, Qu Y, Xiong Z, Ye B, et al. Regulatory innate lymphoid cells control innate intestinal inflammation. *Cell*. (2017) 171:201–216.e18. doi: 10.1016/j.cell.2017.07.027

12. Zhang YL, Duan XD, Feng L, Jiang WD, Wu P, Liu Y, et al. Soybean glycinin impaired immune function and caused inflammation associated with PKC-ζ/NF-κb and mTORC1 signaling in the intestine of juvenile grass carp (*Ctenopharyngodon idella*). *Front Immunol*. (2020) 106:393–403. doi: 10.1016/j.fsi.2020.08.008

13. Wang L, Li W, Xin S, Wu S, Peng C, Ding H, et al. Soybean glycinin and β-conglycinin damage the intestinal barrier by triggering oxidative stress and inflammatory response in weaned piglets. *Eur J Nutr*. (2023) 62:2841–54. doi: 10.1007/s00394-023-03188-8

14. Bakke-Mckellep AM, Sperstad S, Penn MH, Salas PM, Refstie S, Landsverk T, et al. Effects of dietary soybean meal, inulin and oxytetracycline on gastrointestinal histological characteristics, distal intestine cell proliferation and intestinal microbiota in Atlantic salmon (*Salmo salar* L.). *Br J Nutr*. (2007) 97:699–713. doi: 10.1017/S0007114507381397

15. Sommer F, Bäckhed F. The gut microbiota–masters of host development and physiology. *Nat Rev Microbiol*. (2013) 11:227–38. doi: 10.1038/nrmicro2974

16. He Y, Liang J, Dong X, Liu H, Yang Q, Zhang S, et al. Soybean β-conglycinin and glycinin reduced growth performance and the intestinal immune defense and altered microbiome in juvenile pearl gentian groupers *Epinephelus fuscoguttatus*♀ × *Epinephelus lanceolatus*♂. *Anim Nutr*. (2021) 9:193–203. doi: 10.1016/j.aninu.2021.11.001

17. Martin SAM, Król E. Nutrigenomics and immune function in fish: new insights from omics technologies. *Dev Comp Immunol*. (2017) 75:86–98. doi: 10.1016/j.dci.2017.02.024

18. Gill N, Dhillon B. RNA-seq data analysis for differential expression. *Methods Mol Biol*. (2022) 2391:45–54. doi: 10.1007/978-1-0716-1795-3_4

19. Rezaee D, Saadatpour F, Akbari N, Zoghi A, Najafi S, Beyranvand P, et al. The role of microRNAs in the pathophysiology of human central nervous system: A focus on neurodegenerative diseases. *Ageing Res Rev*. (2023) 92:102090. doi: 10.1016/j.arr.2023.102090

20. Hwang H, Chang HR, Baek D. Determinants of functional microRNA targeting. *Mol Cells*. (2023) 46:21–32. doi: 10.14348/molcells.2023.2157

21. Dong J, Tai JW, Lu LF. MiRNA-microbiota interaction in gut homeostasis and colorectal cancer. *Trends Cancer*. (2019) 5:666–9. doi: 10.1016/j.trecan.2019.08.003

22. Sirufo MM, Ginaldi L, De Martinis M. Microbiota-miRNA interactions: Opportunities in ankylosing spondylitis. *Autoimmun Rev*. (2021) 20:102905. doi: 10.1016/j.autrev.2021.102905

23. Oliveira ECS, Quaglio AEV, Magro DO, Di Stasi LC, Sassaki LY. Intestinal microbiota and miRNA in IBD: A narrative review about discoveries and perspectives for the future. *Int J Mol Sci*. (2023) 24:7176. doi: 10.3390/ijms24087176

24. Liu S, da Cunha AP, Rezende RM, Cialic R, Wei Z, Bry L, et al. The host shapes the gut microbiota via fecal microRNA. *Cell Host Microbe*. (2016) 19:32–43. doi: 10.1016/j.chom.2015.12.005

25. Wortelboer K, Bakker GJ, Winkelmeijer M, van Riel N, Levin E, Nieuwdorp M, et al. Fecal microbiota transplantation as tool to study the interrelation between microbiota composition and miRNA expression. *Microbiol Res*. (2022) 257:126972. doi: 10.1016/j.micres.2022.126972

26. Zheng T, Song Z, Qiang J, Tao Y, Zhu H, Ma J, et al. Transport stress induces skin innate immunity response in hybrid yellow catfish (*Tachysurus fulvidraco*♀ × P. vachellii♂) through TLR/NLR signaling pathways and regulation of mucus secretion. *Front Immunol*. (2021) 12:740359. doi: 10.3389/fimmu.2021.740359

27. Yi L, Liu J, Yang H, Mo A, Zhai Y, Wang S, et al. Effects of dietary glycinin on oxidative damage, apoptosis and tight junction in the intestine of juvenile hybrid yellow catfish, *Pelteobagrus fulvidraco* ♀ × *Pelteobaggrus vachelli* ♂. *Int J Mol Sci*. (2022) 23:11198. doi: 10.3390/ijms231911198

28. Li W, Liu B, Liu Z, Yin Y, Xu G, Han M, et al. Effect of dietary histamine on intestinal morphology, inflammatory status, and gut microbiota in yellow catfish (*Pelteobagrus fulvidraco*). *Fish Shellfish Immunol*. (2021) 117:95–103. doi: 10.1016/j.fsi.2021.07.017

29. Guo C, Zhang Z, Zhang M, Guo G, Yu G, Zhao D, et al. Screening and stability analysis of reference genes for gene expression normalization in hybrid yellow catfish (*Pelteobagrus fulvidraco* ♀ × *Pelteobagrus vachelli* ♂) fed diets containing different soybean meal levels. *Aquac Nutr*. (2023) 2023:1232518. doi: 10.1155/2023/1232518

30. Zhang G, Li J, Zhang J, Liang X, Zhang X, Wang T, et al. Integrated analysis of transcriptomic, miRNA and proteomic changes of a novel hybrid yellow catfish uncovers key roles for miRNAs in heterosis. *Mol Cell Proteomics*. (2019) 18:1437–53. doi: 10.1074/mcp.RA118.001297

31. Schefe JH, Lehmann KE, Buschmann IR, Unger T, Funke-Kaiser H. Quantitative real-time RT-PCR data analysis: current concepts and the novel "gene expression's CT difference" formula. *J Mol Med*. (2006) 84:901–10. doi: 10.1007/s00109-006-0097-6

32. Yin B, Liu H, Tan B, Dong X, Chi S, Yang Q, et al. MHC II-PI3K/Akt/mTOR signaling pathway regulates intestinal immune response induced by soy glycinin in hybrid grouper: Protective effects of sodium butyrate. *Front Immunol*. (2021) 11:615980. doi: 10.3389/fimmu.2020.615980

33. Ishmukhametov R. ATPase: Overview. In: Roberts GCK, editor. *Encyclopedia of Biophysics*. Springer, Berlin, Heidelberg (2013). doi: 10.1007/978-3-642-16712-6_207

34. Nepal N, Arthur S, Sundaram U. Unique regulation of Na-K-ATPase during growth and maturation of intestinal epithelial cells. *Cells*. (2019) 8:593. doi: 10.3390/cells8060593

35. Veillette PA, Young G. Temporal changes in intestinal Na^+, K^+-ATPase activity and *in vitro* responsiveness to cortisol in juvenile chinook salmon. *Comp Biochem Phys A*. (2004) 138:297–303. doi: 10.1016/j.cbpb.2004.04.007

36. Luo Q, Qian R, Qiu Z, Yamamoto FY, Du Y, Lin X, et al. Dietary α-ketoglutarate alleviates glycinin and β-conglycinin induced damage in the intestine of mirror carp (*Cyprinus carpio*). *Front Immunol*. (2023) 14:1140012. doi: 10.3389/fimmu.2023.1140012

37. Nepal N, Arthur S, Haynes J, Palaniappan B, Sundaram U. Mechanism of Na-K-ATPase inhibition by PGE2 in intestinal epithelial cells. *Cells*. (2021) 10:752. doi: 10.3390/cells10040752

38. Manoharan P, Gayam S, Arthur S, Palaniappan B, Singh S, Dick GM, et al. Chronic and selective inhibition of basolateral membrane Na-K-ATPase uniquely regulates brush border membrane Na absorption in intestinal epithelial cells. *Am J Physiol Cell Physiol*. (2015) 308:C650–6. doi: 10.1152/ajpcell.00355.2014

39. Bamias G, Cominelli F. Cytokines and intestinal inflammation. *Curr Opin Gastroenterol*. (2016) 32:437–42. doi: 10.1097/mog.0000000000000315

40. Bruewer M, Luegering A, Kucharzik T, Parkos CA, Madara JL, Hopkins AM, et al. Proinflammatory cytokines disrupt epithelial barrier function by apoptosis-independent mechanisms. *J Immunol*. (2003) 171:6164–72. doi: 10.4049/jimmunol.171.11.6164

41. Izcue A, Coombes JL, Powrie F. Regulatory lymphocytes and intestinal inflammation. *Annu Rev Immunol*. (2009) 27:313–38. doi: 10.1146/annurev.immunol.021908.132657

42. Patidar M, Yadav N, Dalai SK. Interleukin 15: A key cytokine for immunotherapy. *Cytokine Growth Factor Rev*. (2016) 31:49–59. doi: 10.1016/j.cytogfr.2016.06.001

43. Yang XK, Xu WD, Leng RX, Liang Y, Liu YY, Fang XY, et al. Therapeutic potential of IL-15 in rheumatoid arthritis. *Hum Immunol*. (2015) 76:812–8. doi: 10.1016/j.humimm.2015.09.041

44. Cicchese JM, Evans S, Hult C, Joslyn LR, Wessler T, Millar JA, et al. Dynamic balance of pro- and anti-inflammatory signals controls disease and limits pathology. *Immunol Rev*. (2018) 285:147–67. doi: 10.1111/imr.12671

45. Jiang WD, Hu K, Zhang JX, Liu Y, Jiang J, Wu P, et al. Soyabean glycinin depresses intestinal growth and function in juvenile Jian carp (*Cyprinus carpio* var Jian): Protective effects of glutamine. *Br J Nutr*. (2015) 114:1569–83. doi: 10.1017/S0007114515003219

46. Chan JTH, Kadri S, Köllner B, Rebl A, Korytář T. RNA-seq of single fish cells - seeking out the leukocytes mediating immunity in teleost fishes. *Front Immunol*. (2022) 13:798712. doi: 10.3389/fimmu.2022.798712

47. Ruterbusch M, Pruner KB, Shehata L, Pepper M. *In vivo* CD4+ T cell differentiation and function: Revisiting the Th1/Th2 paradigm. *Annu Rev Immunol*. (2020) 38:705–25. doi: 10.1146/annurev-immunol-103019-085803

48. Koh CH, Lee S, Kwak M, Kim BS, Chung Y. CD8 T-cell subsets: heterogeneity, functions, and therapeutic potential. *Exp Mol Med*. (2023) 55:2287–99. doi: 10.1038/s12276-023-01105-x

49. Kwak K, Akkaya M, Pierce SK. B cell signaling in context. *Nat Immunol*. (2019) 20:963–9. doi: 10.1038/s41590-019-0427-9

50. Goldberg BS, Ackerman ME. Antibody-mediated complement activation in pathology and protection. *Immunol Cell Biol*. (2020) 98:305–17. doi: 10.1111/imcb.12324

51. Oikonomopoulou K, Ricklin D, Ward PA, Lambris JD. Interactions between coagulation and complement-their role in inflammation. *Semin Immunopathol*. (2012) 34:151–65. doi: 10.1007/s00281-011-0280-x

52. Partida-Sanchez S, BN D, Schwab A, Zierler S. Editorial: TRP channels in inflammation and immunity. *Front Immunol*. (2021) 12:684172. doi: 10.3389/fimmu.2021.684172

53. Gutzeit C, Magri G, Cerutti A. Intestinal IgA production and its role in host-microbe interaction. *Immunol Rev*. (2014) 260:76–85. doi: 10.1111/imr.12189

54. Qin C, Gong Q, Wen Z, Yuan D, Shao T, Wang J, et al. Transcriptome analysis of the spleen of the darkbarbel catfish *Pelteobagrus vachellii* in response to *Aeromonas hydrophila* infection. *Fish Shellfish Immunol*. (2017) 70:498–506. doi: 10.1016/j.fsi.2017.09.042

55. He Y, Ye G, Chi S, Tan B, Dong X, Yang Q, et al. Integrative transcriptomic and small RNA sequencing reveals immune-related miRNA-mRNA regulation network for soybean meal-induced enteritis in hybrid grouper, *Epinephelus fuscoguttatus*♀ × *Epinephelus lanceolatus*♂. *Front Immunol*. (2020) 11:1502. doi: 10.3389/fimmu.2020.01502

56. Zhou Y, Fu HC, Wang YY, Huang HZ, Fu XZ, Li NQ. The dynamic immune responses of Mandarin fish (*Siniperca chuatsi*) to ISKNV in early infection based on full-length transcriptome analysis and weighted gene co-expression network analysis. *Fish Shellfish Immunol*. (2022) 122:191–205. doi: 10.1016/j.fsi.2022.02.017

57. Kunnumakkara AB, Sailo BL, Banik K, Harsha C, Prasad S, Gupta SC, et al. Chronic diseases, inflammation, and spices: how are they linked? *J Transl Med*. (2018) 16:14. doi: 10.1186/s12967-018-1381-2

58. Peng C, Sun Z, Wang L, Shu Y, He M, Ding H, et al. Glycinin-induced porcine IPEC-J2 cells damage via the NF-κB/MAPK signaling pathway. *Res square*. (2020). doi: 10.21203/rs.3.rs-16881/v2

59. Li DL, Liu SY, Zhu R, Meng ST, Wang YT, Yang ZY, et al. Potential protective effects of sodium butyrate on glycinin-induced oxidative stress, inflammatory response, and growth inhibition in. *Cyprinus carpio Fish Physiol Biochem*. (2024) 50:273–93. doi: 10.1007/s10695-023-01276-4

60. Zhou X, Zhang GR, Ji W, Shi ZC, Ma XF, Luo ZL, et al. Expression and function analysis of interleukin-17A/F1, 2, and 3 genes in yellow catfish (*Pelteobagrus fulvidraco*): Distinct bioactivity of recombinant IL-17A/F1, 2, and 3. *Front Immunol*. (2021) 12:626895. doi: 10.3389/fimmu.2021.626895

61. Yurtsever Z, Scheaffer SM, Romero AG, Holtzman MJ, Brett TJ. The crystal structure of phosphorylated MAPK13 reveals common structural features and differences in p38 MAPK family activation. *Acta Crystallogr D Biol Crystallogr*. (2015) 71:790–9. doi: 10.1107/S1399004715001212

62. Yong HY, Koh MS, Moon A. The p38 MAPK inhibitors for the treatment of inflammatory diseases and cancer. *Expert Opin Investig Drugs*. (2009) 18:1893–905. doi: 10.1517/13543780903321490

63. Cuadrado A, Nebreda AR. Mechanisms and functions of p38 MAPK signalling. *Biochem J*. (2010) 429:403–17. doi: 10.1042/BJ20100323

64. Saccani S, Pantano S, Natoli G. p38-Dependent marking of inflammatory genes for increased NF-kappa B recruitment. *Nat Immunol*. (2002) 3:69–75. doi: 10.1038/ni748

65. Aoki Y, Dai H, Furuta F, Akamatsu T, Oshima T, Takahashi N, et al. LOX-1 mediates inflammatory activation of microglial cells through the p38-MAPK/NF-κB pathways under hypoxic-ischemic conditions. *Cell Commun Signal*. (2023) 21:126. doi: 10.1186/s12964-023-01048-w

66. Moparthi L, Koch S. Wnt signaling in intestinal inflammation. *Differentiation*. (2019) 108:24–32. doi: 10.1016/j.diff.2019.01.002

67. Di Bartolomeo L, Vaccaro F, Irrera N, Borgia F, Li Pomi F, Squadrito F, et al. Wnt signaling pathways: from inflammation to non-melanoma skin cancers. *Int J Mol Sci*. (2023) 24:1575. doi: 10.3390/ijms24021575

68. Ayers M, Kosar K, Xue Y, Goel C, Carson M, Lee E, et al. Inhibiting wnt signaling reduces cholestatic injury by disrupting the inflammatory axis. *Cell Mol Gastroenterol Hepatol*. (2023) 16:895–921. doi: 10.1016/j.jcmgh.2023.08.004

69. Jeong WJ, Yoon J, Park JC, Lee SH, Lee SH, Kaduwal S, et al. Ras stabilization through aberrant activation of Wnt/β-catenin signaling promotes intestinal tumorigenesis. *Sci Signal*. (2012) 5:ra30. doi: 10.1126/scisignal.2002242

70. Ehyai S, Dionyssiou MG, Gordon JW, Williams D, Siu KW, McDermott JC. A p38 mitogen-activated protein kinase-regulated myocyte enhancer factor 2-β-catenin interaction enhances canonical Wnt signaling. *Mol Cell Biol*. (2015) 36:330–46. doi: 10.1128/MCB.00832-15

71. Das K, Rao LVM. The role of microRNAs in inflammation. *Int J Mol Sci*. (2022) 23:15479. doi: 10.3390/ijms232415479

72. Moein S, Vaghari-Tabari M, Qujeq D, Majidinia M, Nabavi SM, Yousefi B. MiRNAs and inflammatory bowel disease: An interesting new story. *J Cell Physiol*. (2019) 234:3277–93. doi: 10.1002/jcp.27173

73. Kong F, Sun Y, Song W, Zhou Y, Zhu S. MiR-216a alleviates LPS-induced acute lung injury via regulating JAK2/STAT3 and NF-κB signaling. *Hum Cell*. (2020) 33:67–78. doi: 10.1007/s13577-019-00289-7

74. Liu H, Ye T, Yang X, Liu J, Jiang K, Lu H, et al. H19 promote calcium oxalate nephrocalcinosis-induced renal tubular epithelial cell injury via a ceRNA pathway. *EBioMedicine*. (2019) 50:366–78. doi: 10.1016/j.ebiom.2019.10.059

75. Yang X, Li D, Qi YZ, Chen W, Yang CH, Jiang YH. MicroRNA-217 ameliorates inflammatory damage of endothelial cells induced by oxidized LDL by targeting EGR1. *Mol Cell Biochem*. (2020) 475:41–51. doi: 10.1007/s11010-020-03857-w

76. Danis B, van Rikxoort M, Kretschmann A, Zhang J, Godard P, Andonovic L, et al. Differential expression of miR-184 in temporal lobe epilepsy patients with and without hippocampal sclerosis - Influence on microglial function. *Sci Rep*. (2016) 6:33943. doi: 10.1038/srep33943

77. Wang R, Li Q, He Y, Yang Y, Ma Q, Li C. MiR-29c-3p inhibits microglial NLRP3 inflammasome activation by targeting NFAT5 in Parkinson's disease. *Genes Cells*. (2020) 25:364–74. doi: 10.1111/gtc.12764

78. Wang Y, Liu S, Lv F, Zhai W, Wang W, Duan Y, et al. hsa–miR–216a–3p regulates cell proliferation in oral cancer via the Wnt3a/β–catenin pathway. *Mol Med Rep*. (2023) 27:128. doi: 10.3892/mmr.2023.13015

79. Graf K, Schaefer-Graf UM. Is Smad3 the key to inflammation and fibrosis in hypertensive heart disease? *Hypertension*. (2010) 5):1088–9. doi: 10.1161/HYPERTENSIONAHA.110.150466

80. Marinis JM, Homer CR, McDonald C, Abbott DW. A novel motif in the Crohn's disease susceptibility protein, NOD2, allows TRAF4 to down-regulate innate immune responses. *J Biol Chem*. (2011) 286:1938–50. doi: 10.1074/jbc.M110.189308

81. Jiao M, Zhang Y, Song X, Xu B. The role and mechanism of TXNDC5 in disease progression. *Front Immunol*. (2024) 15:1354952. doi: 10.3389/fimmu.2024.1354952

82. Reehorst CM, Nightingale R, Luk IY, Jenkins L, Koentgen F, Williams DS, et al. EHF is essential for epidermal and colonic epithelial homeostasis, and suppresses Apc-initiated colonic tumorigenesis. *Development*. (2021) 148:dev199542. doi: 10.1242/dev.199542

83. Schirmer M, Garner A, Vlamakis H, Xavier RJ. Microbial genes and pathways in inflammatory bowel disease. *Nat Rev Microbiol*. (2019) 17:497–511. doi: 10.1038/s41579-019-0213-6

84. Caruso R, Lo BC, Núñez G. Host-microbiota interactions in inflammatory bowel disease. *Nat Rev Immunol*. (2020) 20:411–26. doi: 10.1038/s41577-019-0268-7

85. Nishida A, Nishino K, Sakai K, Owaki Y, Noda Y, Imaeda H. Can control of gut microbiota be a future therapeutic option for inflammatory bowel disease? *World J Gastroenterol*. (2021) 27:3317–26. doi: 10.3748/wjg.v27.i23.3317

86. Nie L, Zhou QJ, Qiao Y, Chen J. Interplay between the gut microbiota and immune responses of ayu (*Plecoglossus altivelis*) during Vibrio Anguillarum infection. *Fish Shellfish Immunol*. (2017) 68:479–87. doi: 10.1016/j.fsi.2017.07.054

87. Xiao Joe JT, Tseng YC, Wu JL, Lu MW. The alteration of intestinal microbiota profile and immune response in *Epinephelus coioides* during pathogen infection. *Life*. (2021) 11:99. doi: 10.3390/life11020099

88. Xiang N, Lyu Y, Zhu X, Bhunia AK, Narsimhan G. Methodology for identification of pore forming antimicrobial peptides from soy protein subunits β-conglycinin and glycinin. *Peptides*. (2016) 85:27–40. doi: 10.1016/j.peptides.2016.09.004

89. Wu S, Gao T, Zheng Y, Wang W, Cheng Y, Wang G. Microbial diversity of intestinal contents and mucus in yellow catfish (*Pelteobagrus fulvidraco*). *Aquaculture*. (2010) 303:1–7. doi: 10.1016/j.aquaculture.2009.12.025

90. Wu S, Wang G, Angert ER, Wang W, Li W, Zou H. Composition, diversity, and origin of the bacterial community in grass carp intestine. *PloS One*. (2012) 7:e30440. doi: 10.1371/journal.pone.0030440

91. Li XM, Yan QY, Xie SQ, Hu W, Yu YH, Hu ZH. Gut microbiota contributes to the growth of fast-growing transgenic common carp (*Cyprinus carpio* L.). *PloS One*. (2013) 8:e64577. doi: 10.1371/journal.pone.0064577

92. Wang A, Zhang Z, Ding Q, Yang Y, Bindelle J, Ran C, et al. Intestinal *Cetobacterium* and acetate modify glucose homeostasis via parasympathetic activation in zebrafish. *Gut Microbes*. (2021) 13:1–15. doi: 10.1080/19490976.2021

93. Bermingham EN, Maclean P, Thomas DG, Cave NJ, Young W. Key bacterial families (Clostridiaceae, Erysipelotrichaceae and Bacteroidaceae) are related to the digestion of protein and energy in dogs. *Peer J*. (2017) 5:e3019. doi: 10.7717/peerj.3019

94. García-Granja PE, López J, Ladrón R, San Román JA. Infective endocarditis due to *Leuconostoc* species. *Rev Esp Cardiol (Engl Ed)*. (2018) 71:592–4. doi: 10.1016/j.rec.2017.04.013

95. Abouradi S, Ejjebli S, Chawki K, Drighil A. Urothelial carcinoma associated with infective endocarditis due to a *Leuconostoc* Species: A rare case report. *Ann Med Surg (Lond)*. (2022) 76:103430. doi: 10.1016/j.amsu.2022.103430

96. Kumari M, Singh P, Nataraj BH, Kokkiligadda A, Naithani H, Azmal Ali S, et al. Fostering next-generation probiotics in human gut by targeted dietary modulation: An emerging perspective. *Food Res Int*. (2021) 150:110716. doi: 10.1016/j.foodres.2021.110716

97. Leonard MM, Valitutti F, Karathia H, Pujolassos M, Kenyon V, Fanelli B, et al. Microbiome signatures of progression toward celiac disease onset in at-risk children in a longitudinal prospective cohort study. *Proc Natl Acad Sci U S A*. (2021) 118:e2020322118. doi: 10.1073/pnas.2020322118

98. Pei T, Zhu D, Yang S, Hu R, Wang F, Zhang J, et al. *Bacteroides plebeius* improves muscle wasting in chronic kidney disease by modulating the gut-renal muscle axis. *J Cell Mol Med*. (2022) 26:6066–78. doi: 10.1111/jcmm.17626

99. Méndez-Pérez R, García-López R, Bautista-López JS, Vázquez-Castellanos JF, Peña-Marín ES, Martínez-García R, et al. Gut microbiome analysis in adult tropical gars (*Atractosteus tropicus*). *BioRxiv*. (2019), 557629. doi: 10.1101/557629

100. Al-Amrah H, Saadah OI, Mosli M, Annese V, Al-Hindi R, Edris S, et al. Composition of the gut microbiota in patients with inflammatory bowel disease in Saudi Arabia: A pilot study. *Saudi J Gastroenterol*. (2023) 29:102–10. doi: 10.4103/sjg.sjg_368_22

101. Kiu R, Hall LJ. An update on the human and animal enteric pathogen. *Clostridium perfringens Emerg Microbes Infect*. (2018) 7:141. doi: 10.1038/s41426-018-0144-8

102. Khan MT, Dwibedi C, Sundh D, Pradhan M, Kraft JD, Caesar R, et al. Synergy and oxygen adaptation for development of next-generation probiotics. *Nature*. (2023) 620:381–5. doi: 10.1038/s41586-023-06378-w

103. Guan Y, Zhang Y, Zhu Y, Wang Y. CXCL10 as a shared specific marker in rheumatoid arthritis and inflammatory bowel disease and a clue involved in the mechanism of intestinal flora in rheumatoid arthritis. *Sci Rep*. (2023) 13:9754. doi: 10.1038/s41598-023-36833-7

104. Lee Y, Kim WH, Lee SJ, Lillehoj HS. Detection of chicken interleukin-10 production in intestinal epithelial cells and necrotic enteritis induced by *Clostridium perfringens* using capture ELISA. *Vet Immunol Immunopathol*. (2018) 204:52–8. doi: 10.1016/j.vetimm.2018.10.001

105. Johnston DGW, Williams MA, Thaiss CA, Cabrera-Rubio R, Raverdeau M, McEntee C, et al. Loss of microRNA-21 influences the gut microbiota, causing reduced susceptibility in a murine model of colitis. *J Crohns Colitis*. (2018) 12:835–48. doi: 10.1093/ecco-jcc/jjy038

106. Casado-Bedmar M, Viennois E. MicroRNA and gut microbiota: Tiny but mighty-novel insights into their cross-talk in inflammatory bowel disease pathogenesis and therapeutics. *J Crohns Colitis*. (2022) 16:992–1005. doi: 10.1093/ecco-jcc/jjab223

107. Smigielska-Czepiel K, van den Berg A, Jellema P, Slezak-Prochazka I, Maat H, van den Bos H, et al. Dual role of miR-21 in CD4+ T-cells: activation-induced miR-21 supports survival of memory T-cells and regulates CCR7 expression in naive T-cells. *PloS One*. (2013) 8:e76217. doi: 10.1371/journal.pone.0076217

108. Mody D, Verma V, Rani V. Modulating host gene expression via gut microbiome-microRNA interplay to treat human diseases. *Crit Rev Microbiol*. (2021) 47:596–611. doi: 10.1080/1040841X.2021.1907739

109. Rodríguez-Nogales A, Algieri F, Garrido-Mesa J, Vezza T, Utrilla MP, Chueca N, et al. Differential intestinal anti-inflammatory effects of *Lactobacillus fermentum* and *Lactobacillus salivarius* in DSS mouse colitis: impact on microRNAs expression and microbiota composition. *Mol Nutr Food Res*. (2017) 61:1700144. doi: 10.1002/mnfr.201700144

110. Dalmasso G, Cougnoux A, Delmas J, Darfeuille-Michaud A, Bonnet R. The bacterial genotoxin colibactin promotes colon tumor growth by modifying the tumor microenvironment. *Gut Microbes*. (2014) 5:675–80. doi: 10.4161/19490976.2014.969989

111. Hu S, Liu L, Chang EB, Wang JY, Raufman JP. Butyrate inhibits pro-proliferative miR-92a by diminishing c-Myc-induced miR-17-92a cluster transcription in human colon cancer cells. *Mol Cancer*. (2015) 14:180. doi: 10.1186/s12943-015-0450-x

112. Anzola A, González R, Gámez-Belmonte R, Ocón B, Aranda CJ, Martínez-Moya P, et al. MiR-146a regulates the crosstalk between intestinal epithelial cells, microbial components and inflammatory stimuli. *Sci Rep*. (2018) 8:17350. doi: 10.1038/s41598-018-35338-y

frontiers | Frontiers in Immunology

TYPE Review
PUBLISHED 07 February 2025
DOI 10.3389/fimmu.2025.1425901

OPEN ACCESS

EDITED BY
Suraj P. Parihar,
University of Cape Town, South Africa

REVIEWED BY
Wei-Ting Kuo,
National Taiwan University, Taiwan
Alireza Haghparast,
Ferdowsi University of Mashhad, Iran
Soodeh Alidadi,
Ferdowsi University of Mashhad, Iran

*CORRESPONDENCE
Changfa Wang
wangchangfa@lcu.edu.cn
Muhammad Zahoor Khan
zahoorkhattak91@yahoo.com
Muhammad Zahoor
muhammad.zahoor@medisin.uio.no

RECEIVED 30 April 2024
ACCEPTED 20 January 2025
PUBLISHED 07 February 2025

CITATION
Khan MZ, Li L, Zhan Y, Binjiang H, Liu X, Kou X, Khan A, Qadeer A, Ullah Q, Alzahrani KJ, Wang T, Wang C and Zahoor M (2025) Targeting Nrf2/KEAP1 signaling pathway using bioactive compounds to combat mastitis. *Front. Immunol.* 16:1425901. doi: 10.3389/fimmu.2025.1425901

Targeting Nrf2/KEAP1 signaling pathway using bioactive compounds to combat mastitis

Muhammad Zahoor Khan[1*], Liangliang Li[1], Yandong Zhan[1], Huang Binjiang[1], Xiaotong Liu[1], Xiyan Kou[1], Adnan Khan[2], Abdul Qadeer[3], Qudrat Ullah[4], Khalid J. Alzahrani[5], Tongtong Wang[1], Changfa Wang[1*] and Muhammad Zahoor[6*]

[1]Liaocheng Research Institute of Donkey High-Efficiency Breeding and Ecological Feeding, Liaocheng University, Liaocheng, China, [2]Genome Analysis Laboratory of the Ministry of Agriculture, Agricultural Genomics Institute at Shenzhen, Chinese Academy of Agricultural Sciences, Shenzhen, China, [3]Department of Cell Biology, School of Life Sciences, Central South University, Changsha, China, [4]Department of Theriogenology, Faculty of Veterinary and Animal Sciences, Cholistan University of Veterinary and Animal Sciences, Bahawalpur, Punjab, Pakistan, [5]Department of Clinical Laboratories Sciences, College of Applied Medical Sciences, Taif University, Taif, Saudi Arabia, [6]Department of Molecular Medicine, Institute of Basic Medical Sciences, University of Oslo, Oslo, Norway

Mastitis is a common inflammation of mammary glands that has a significantly impact on dairy production and animal health, causing considerable economic burdens worldwide. Elevated reactive oxygen species (ROS) followed by oxidative stress, apoptosis, inflammatory changes and suppressed immunity are considered the key biomarkers observed during mastitis. The Nrf2/KEAP1 signaling pathway plays a critical role in regulating antioxidant responses and cellular defense mechanisms. When activated by bioactive compound treatment, Nrf2 translocates to the nucleus and induces the expression of its target genes to exert antioxidant responses. This reduces pathogen-induced oxidative stress and inflammation by inhibiting NF-kB signaling in the mammary glands, one of the prominent pro-inflammatory signaling pathway. Here, we summarize recent studies to highlight the therapeutic potential of Nrf2/KEAP1 pathway in the prevention and treatment of mastitis. Collectively this review article aims to explore the potential of bioactive compounds in mitigating mastitis by targeting the Nrf2/KEAP1 signaling pathway.

KEYWORDS

mastitis, inflammation, immunity, oxidative stress, antioxidants, bioactive compounds, Nrf2/Keap1 signaling pathway

1 Introduction

Mastitis, an inflammation of the mammary glands, is characterized by increased inflammation, reactive oxygen species (ROS), and reduced immune effectiveness in the mammary gland tissues (1). This condition poses a significant challenge to the global dairy industry, leading to considerable financial burdens due to decreased milk yield, the need for

therapies, reproductive issues, and the necessity for animal culling, as indicated by various studies (2–6). Globally, mastitis incurs substantial economic costs, estimated to be between US$19.7 billion and US$32 billion annually. In the United States alone, the annual economic loss due to mastitis is estimated at around US$2 billion (7, 8). In Canada, the dairy industry faces an annual financial loss of Can$400 million (equivalent to US$318 million), while in China, the estimated annual fiscal losses due to mastitis range between 15 (2.1 billion USD) and 45 (6.3 billion USD) billion Chinese Yuan (CNY) (9).

The multifaceted nature of mastitis as a disease is widely recognized in the scientific community (10). Mastitis is typically classified into clinical and sub-clinical forms. Clinical mastitis is characterized by pronounced pathological (redness, pain and fever) and physical changes (swollen and hot) in mammary gland tissues, while sub-clinical mastitis, particularly when caused by *Staphylococcus aureus*, often presents more subtly, with no obvious symptoms except for elevated milk somatic cell counts and a decrease in milk yield (11–17). The primary bacterial pathogens associated with mastitis include *Escherichia coli, Streptococcus uberis, S. dysgalactiae*, and *S. aureus* (18). The susceptibility of animals to mastitis is influenced by various factors such as the anatomical positioning of the udder, lactation stages, age, and conditions during the periparturient period (18–20).

The periparturient period is particularly critical, as animals experience a negative energy balance, leading to suppressed immunity, enhanced inflammatory responses, and an overproduction of ROS (21). This imbalance necessitates increased oxygen consumption for cellular respiration, thereby inducing oxidative stress (22). Factors such as a high body condition score (BCS), elevated levels of non-esterified fatty acids (NEFA), and β-hydroxybutyric acid (BHB) have been identified as significant contributors to the augmentation of ROS production during periparturient period (21–24). The elevated levels of oxidative stress activate the nuclear factor kappa B (NF-κB) signaling pathways, which in turn promote inflammatory changes in the mammary glands (25, 26). Additionally, the relationship between negative energy balance-induced oxidative stress, suppressed immunity, and heightened inflammatory changes is clearly depicted in Figure 1. Oxidative stress is a pivotal factor associated with compromised immunity and the intensification of inflammatory responses, thereby facilitate the pathogenesis of mastitis (1, 21, 22, 27). In response, several recent investigations have underscored the efficacy of antioxidant supplementation in mitigating oxidative stress and, consequently, alleviating mastitis (28–32).

Given the complex genetic mechanisms of mastitis, the erythroid-2 related factor 2/Kelch-like ECH-associated protein 1 (Nrf2/KEAP1) signaling pathway has received significant attention due to its crucial role in regulating antioxidant responses and reducing oxidative distress (33, 34). Notably, several bioactive compounds such as Metformin and Resveratrol have been demonstrated to significantly upregulate Nrf2 levels and activate antioxidant response elements, thereby attenuating oxidative stress and ameliorating mastitis induced by lipopolysaccharide (LPS) (35, 36). In light of the critical function of Nrf2/KEAP1 signaling pathway in the context of mastitis, the present study endeavors to elucidate the research trajectory concerning key pharmacological agents and antioxidants targeting this pathway as a preventative strategy against mastitis in animals.

2 Methodology

This review article was synthesized based on an extensive examination of literature primarily published from 2018 to 2024. Additionally, seven articles published between 2015 and 2017, and one study from 2009, were also considered for discussion in current review article. The search for relevant literature was conducted through distinguished academic databases such as X-MOL, Web of Science, Google Scholar, and PubMed. Keywords utilized in this search included 'Nrf2/KEAP1 signaling pathway,' 'inflammation,' 'apoptosis,' 'antioxidant,' 'oxidative stress,' 'mastitis,' and 'bioactive compounds,' with a focus on their antioxidant and anti-inflammatory properties. Inclusion criteria were restricted to articles published in journals indexed in the Science Citation Index (SCI) and in the English language. Exclusions were made for book chapters, articles published in non-SCI indexed journals, and those written in languages other than English. This methodological approach ensured a focused and comprehensive review of the relevant scientific literature.

3 Role of oxidative stress in the pathogenesis of mastitis

During bacterial infections, there is a marked increase in the production of ROS, which play a crucial role in pathogen clearance while also contributing significantly to the initiation and amplification of inflammatory signaling pathways (37, 38). Mastitis, often caused by bacterial pathogens such as *S. aureus or E. coli*, elicits a robust immune response. This response is primarily characterized by the recruitment and activation of innate immune cells, especially neutrophils and macrophages, at the site of infection (39, 40). These immune cells utilize ROS generation as a critical mechanism to combat invading pathogens (41–43). Immune cells like neutrophils, upon encountering pathogens, undergo a process known as the oxidative or respiratory burst. This rapid release of ROS, including hydrogen peroxide (H_2O_2) and superoxide radicals, acts as a powerful antimicrobial strategy aimed at destroying the invading microorganisms. However, while ROS are essential in pathogen clearance, excessive or prolonged production can result in tissue damage. In mastitis, the inflammatory process leads to the activation of endothelial cells in the mammary gland, which in turn increases vascular permeability. This heightened permeability facilitates the infiltration of immune cells to the infection site, but it also contributes to increased ROS production from both endothelial cells and the infiltrating immune cells.

Inflammation and infection also stimulate the release of various cytokines and chemokines, which are signaling molecules that regulate the immune response. Some of these molecules further activate immune cells, resulting in additional ROS production. Notably, cytokines such as tumor necrosis factor α (TNF-α), interleukin-1 β (IL-1β), and interleukin-6 (IL-6)—all of which are

10.3389/fimmu.2025.1425901

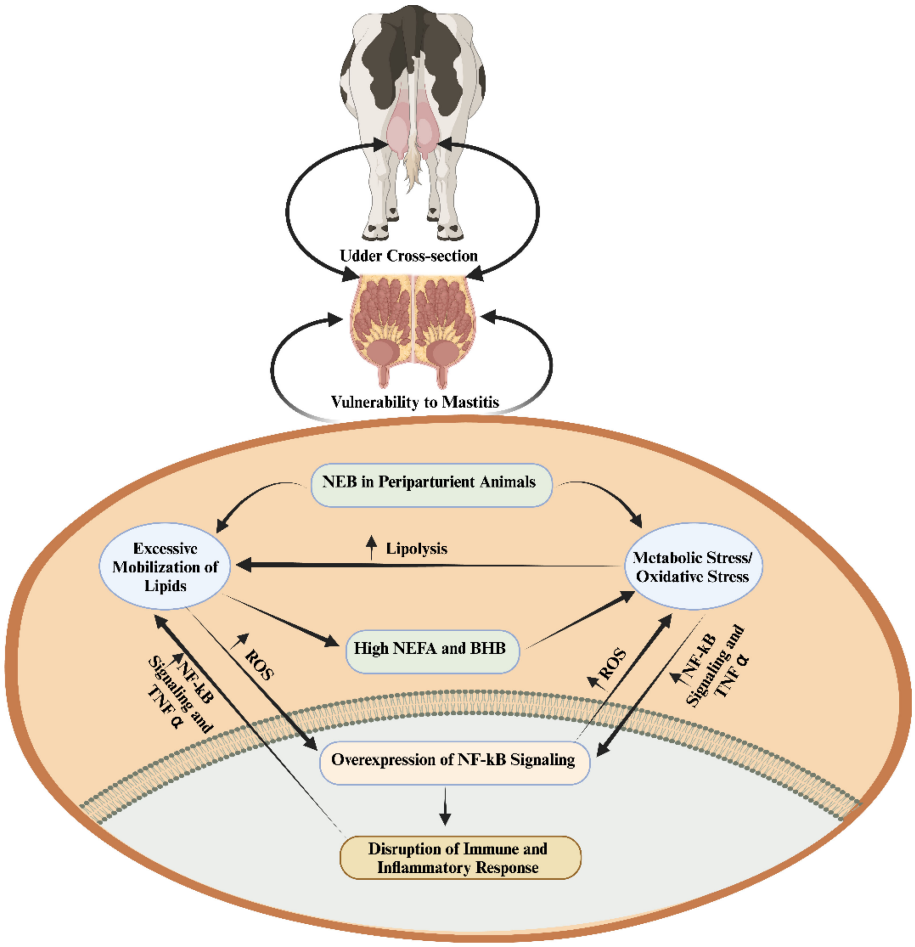

FIGURE 1
The interplay among negative energy balance induced oxidative stress, immunity and inflammation during periparturient period (1). When there is a negative energy balance, the process of lipolysis is enhanced by metabolic/oxidative stress. The excessive lipid mobilization elevates inflammation and disrupts the immunity via regulation of nuclear factor kappa-light-chain-enhancer of activated B cells (NF-kB) signaling. non-esterified fatty acids (NEFA); β-Hydroxybutyrate (BHB); tumor necrosis factor α (TNF-α); negative energy balance (NEB); reactive oxygen species (ROS).

commonly elevated during mastitis—can enhance ROS production through immune cell activation. The combined effects of pathogen presence and immune system activation can lead to tissue damage and cellular stress within the mammary gland. Stressed and damaged cells, as a result of altered metabolic and physiological states, can produce ROS as a byproduct. Under normal physiological conditions, the body's antioxidant defenses maintain a balance to prevent excessive ROS production and subsequent tissue damage. However, during mastitis, the increased ROS levels can overwhelm these natural defenses, leading to oxidative stress (44). In brief, when LPS enters the body, it activates Toll-like receptors (TLRs) on immune cells such as mast cells, macrophages, and epithelial cells, leading to the production of ROS. These ROS contribute to oxidative stress, which drives tissue damage and inflammation in mastitis. Elevated ROS damages cellular components, including lipids, proteins, and DNA, while also activating IKK (IκB kinase), which leads to the degradation of IκB proteins. This allows NF-κB to move into the nucleus, where it promotes the expression of pro-inflammatory cytokines like TNF-α, IL-6, and IL-1β, as well as chemokines that recruit immune cells—key events in the inflammatory phase of mastitis. Additionally, excessive ROS, often resulting from mitochondrial dysfunction and chronic inflammation, can prevent the degradation of Keap1. This inhibits NRF2 from dissociating from Keap1, impairing its ability to activate antioxidant defense mechanisms (Figure 2).

Several recent studies have demonstrated that LPS, not only triggers innate immune responses but also induces oxidative damage and apoptosis (45–49). The imbalance between the antioxidant capabilities of the mammary gland and the excessive ROS production—driven by the high metabolic activity of the gland—contributes significantly to the development of mastitis. This imbalance is a major factor leading to decreased milk yield and quality (50, 51). Beyond bacterial infections, other factors such as negative energy balance, heat stress, and environmental toxins can also induce oxidative stress in the mammary gland, leading to further cellular damage (28, 52–56). Given these insights, reducing oxidative stress within mammary gland tissue represents a promising strategy for mitigating mastitis in animals. To effectively combat this condition, it is essential to conduct

10.3389/fimmu.2025.1425901

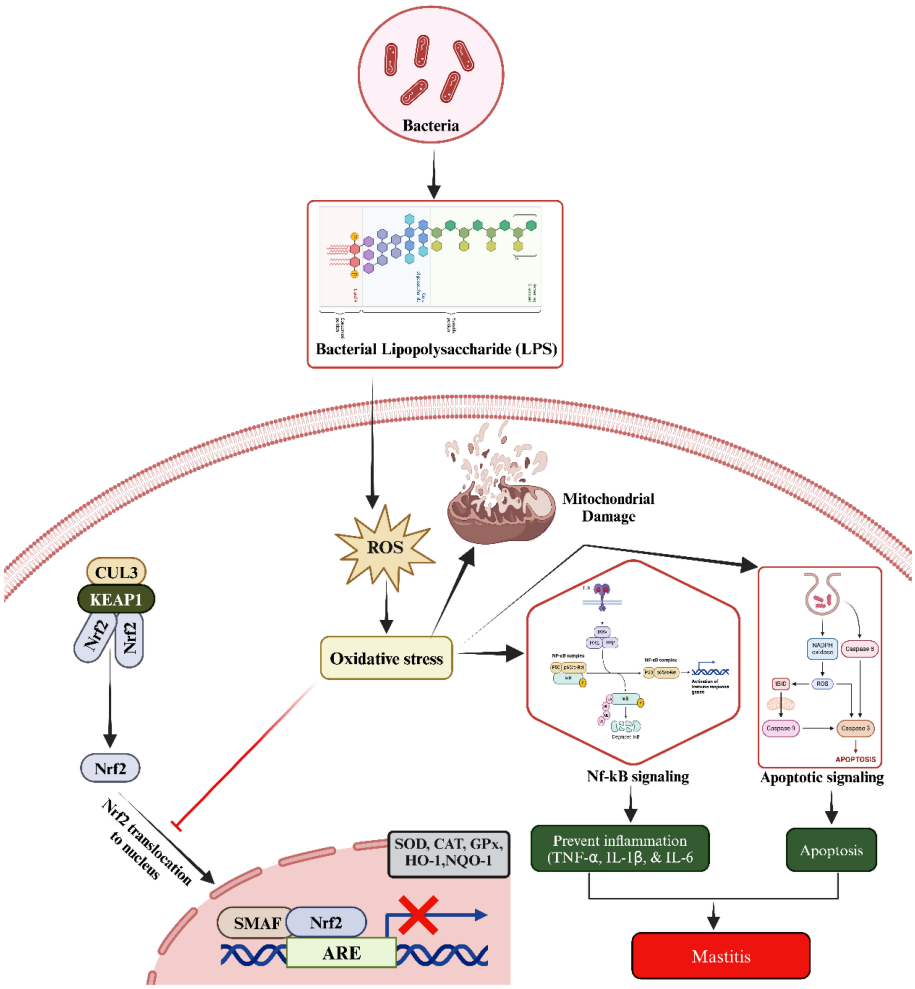

FIGURE 2
The underlined molecular mechanism during mastitis development. The LPS increased the ROS production. Elevated ROS disrupts the oxidant and antioxidant balance via blocking the entry of Nrf2 to nucleus. Additionally, elevated oxidative stress triggers the activation of NF-κB and apoptotic signaling pathways, leading to inflammatory changes, injury to mammary gland cells, and subsequent development of mastitis. Kelch-like ECH-associated protein 1 (KEAP1), tumor necrosis factor α (TNF-α), interleukin-1 β (IL-1β), and interleukin-6 (IL-6), nuclear factor erythroid 2-related factor 2 (Nrf2), cullin 3 (CUL3), heme oxygenase 1 (HO-1), antioxidant response elements (AREs), superoxide dismutase (SOD), catalase (CAT), glutathione peroxidase (GPX), and NAD(P)H quinone oxidoreductase 1 (NQO1).

comprehensive research into the mechanisms underlying oxidative stress and apoptosis in the mammary glands. Understanding these pathways will aid in developing targeted interventions aimed at reducing oxidative damage and improving overall animal health and productivity (57).

4 Bioactive compounds boost antioxidant and anti-inflammatory responses by activating Nrf2/KEAP1 signaling pathway to combat mastitis

Bioactive compounds interact with and inhibit the activity of KEAP1, a cytoplasmic repressor that binds to NRF2 under normal conditions. When KEAP1 is inhibited, NRF2 is released and translocates to the nucleus. Nrf2, upon translocating to the nucleus, binds to antioxidant response elements (AREs) located in the promoter regions of various genes (52). This binding activates the expression of key antioxidant genes, including heme oxygenase-1 (HO-1), superoxide dismutase (SOD), catalase (CAT), glutathione peroxidase (GPX), and NAD(P)H quinone oxidoreductase 1 (NQO1) (Figure 3) (58, 59). The increase in these enzymes enhances the cell's antioxidant capacity, reducing oxidative stress by neutralizing ROS. Bioactive compounds can inhibit the activation of the NF-κB pathway by preventing the degradation of inhibitor of kappa B (IκBα), which keeps NF-κB inactive in the cytoplasm. The one possible mechanism associated with suppression might be due to the inhibition of ROS via upregulating the antioxidant status. By inhibiting the translocation of NF-κB to the nucleus, the transcription of pro-inflammatory genes (such as TNF-α, IL-1β, and IL-6) is reduced (60–63). This result in a decrease in the production of inflammatory cytokines and chemokines, leading to reduced inflammation. Considering the critical role of the Nrf2/KEAP1

10.3389/fimmu.2025.1425901

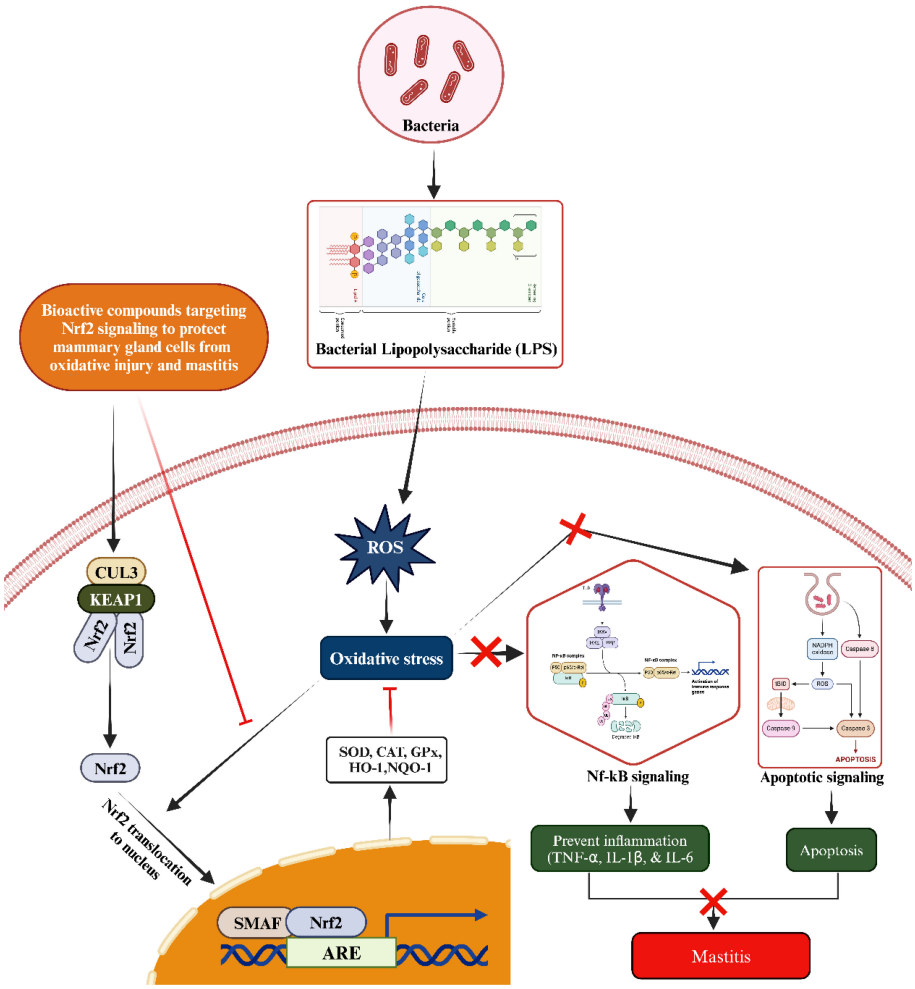

FIGURE 3
Mechanism of activating the Nrf2/KEAP1 signaling pathway to counteract oxidative stress and subsequent inflammatory reactions, including mastitis, induced by LPS through the administration of bioactive compounds from an external source. Upon administration, the bioactive compound triggers the activation of Nrf2. This activated Nrf2 then translocates to the nucleus, where it forms a heterodimer with small Maf proteins (sMaf) by binding to SMAF. This Nrf2/sMaf heterodimer specifically binds to a cis-acting enhancer known as the antioxidant response element (ARE), initiating the transcription of a range of antioxidant genes. These ARE-regulated genes play a crucial role in blocking oxidative stress and inhibiting the NF-kB signaling pathway activated by LPS. Additionally, they enhance antioxidant and anti-inflammatory responses, thereby preventing inflammatory changes in mammary epithelial cells.

signaling pathway, a large number of bioactive compounds such as phytoncide, melatonin, Chinese propolis, bergenin, and resveratrol etc., have been systematically evaluated for their regulatory effects on this pathway to alleviate mastitis in animals (64–68).

4.1 Bioactive compounds boost antioxidant and anti-inflammatory responses by activating Nrf2/KEAP1 signaling to combat mastitis: *in vitro* evidence

It has been well established through *in vitro* experiments that bioactive compounds can enhance the activation of the Nrf2/KEAP1 signaling pathway. This activation leads to improved antioxidant defenses and potential therapeutic benefits in mastitis. This section focuses on the specific mechanisms by which these compounds influence the Nrf2/KEAP1 signaling cascade. By providing insights into their role in combating mastitis at the cellular level, this section enhances our understanding of how these compounds work.

Consistently, the administration of *Tanshinone IIa* to LPS-stimulated cow mammary epithelial cells (CMECs) was observed to have positive effects (62). In addition, it was found that *Tanshinone IIa* reduced oxidative stress markers, restored mitochondrial function, and enhanced antioxidant enzyme activity by activating the Nrf2/Keap1 signaling pathway (62). The study conducted by Kang et al. (64) explored the effects of phytoncide extracted from pinecones on BMECs, specifically focusing on its anti-inflammatory and antioxidant properties using an *in vitro* model. To induce inflammation, the cells were treated with LPS. Their findings revealed that phytoncide significantly reduced the expression of pro-inflammatory cytokines such as TNF-α, IL-6, and IL-1β. Moreover, it inhibited the NF-κB signaling pathway (64). Furthermore, phytoncide was

found to activate Nrf2 and enhance the antioxidant response in BMECs. Similarly, in a study conducted by Yu et al. (65), BMECs were pre-treated with melatonin (43 μM and 430 μM) for 12 hours prior to LPS stimulation (100 ng/mL) for an additional 12 hours to induce inflammation. Their results showed that melatonin inhibited the LPS-binding protein–CD14–TLR4 signaling pathway, leading to a decrease in pro-inflammatory mediators and an increase in anti-inflammatory responses, followed by enhanced antioxidant defenses through the activation Nrf2 pathway (65). The protective effects of Chinese propolis on BMECs against damage caused by LPS- induced mastitis. Briefly, Chinese propolis preserved cell viability in bovine mammary cells exposed to pathogens and reduced pro-inflammatory cytokine expression (IL-6, TNF-α). It also boosted antioxidant gene expression (HO-1, Txnrd-1, GCLM) and inhibited NF-κB activation while enhancing Nrf2-ARE activity, which are key pathways in inflammation and oxidative stress defense (66). In a related study, Ma X et al. (69) explored the protective effects of selenomethionine against inflammatory injury and oxidative damage in BMECs induced by *Klebsiella pneumoniae* (*K. pneumoniae*). Their findings revealed that *K. pneumoniae* suppresses the Nrf2 signaling pathway and antioxidant enzyme activity, resulting in elevated inflammatory cytokine levels and activation of the NF-κB pathway. However, pre-treatment with 4 μM selenomethionine prior to infection effectively protected BMECs by activating Nrf2 signaling and inhibiting NF-κB activation, thus mitigating both inflammation and oxidative stress (69).

A study investigated the cytoprotective effects of resveratrol on BMECs exposed to oxidative stress induced by H_2O_2 (67). Resveratrol pretreatment rescued cell viability, reduced intracellular ROS accumulation, and prevented endoplasmic reticulum stress and mitochondria-related apoptosis. It also upregulated the expression of multiple antioxidant defense genes (Nrf2, HO-1, TrxR-1 and xCT), playing a key role in bolstering the cells' antioxidant mechanisms. Furthermore, they noticed that the protective effects of resveratrol were dependent on the activation of the Nrf2, with its induction mediated by the phosphoinosi-tide-3-kinase/protein kinase B (PI3K/Akt) and ERK/MAPK pathways and negatively regulated by the p38/MAPK pathway (67). Furthermore, Ma Y et al. (70) demonstrated that green tea polyphenols (GTPs) protect BMECs from inflammation, oxidative stress, and apoptosis induced by H_2O_2 (500 μM for 12 h). The BMECs were pre-treated with various concentrations of GTPs before being exposed to H_2O_2 to induce oxidative damage. It was found that GTPs treatment significantly decreased the level of MDA and increased the expressions of Nrf2, HO-1, SOD, CAT, and GSH-Px, indicating enhanced antioxidant capacity and reduced oxidative stress in BMECs (70). Moreover, Zhu et al. (71) elucidated the role of Ubiquitin-specific protease 14 (USP14) in mediating LPS-induced oxidative stress and ferroptosis, leading to the regulation of IL-6. They found that Ferrostatin-1 (Fer-1) upregulated Nrf2 levels following the suppression of oxidative stress, highlighting its potential in mitigating oxidative stress-induced damage in the goat MECs (71). Supplementation with methionine and arginine has been evidenced to ameliorate oxidative stress and inflammation provoked by LPS in BMECs (72). They administered methionine and arginine and incubated for 12 hours followed by LPS (1 μg/mL) treatment obtained from *E. coli*. These nutrients downregulated the expressions of chemokine (C-X-C motif) ligand 2 (CXCL2) and IL-1β and upregulated the levels of solute carrier family 36 member 1 (SLC36A1) and solute carrier family 7 member 1 (SLC7A1), thereby mitigating inflammatory alterations in the mammary gland. Additionally, Dai et al. (72) observed heightened levels of NFE2L2, SOD2, NQO1, and GPX1, indicative of enhanced antioxidant status following methionine and arginine supplementation. Consequently, a study has shown that LPS (1μg/mL) induced inflammatory changes such as elevated expressions of TNF-α, IL-1β, and IL-6 and heightened oxidative stress through the inhibition of Nrf2, HO-1, NQO-1, and thioredoxin reductase 1 (TXNRD1) in BMECs. However, hydroxytyrosol (10 and 25 μM) treatment prevented LPS-induced mastitis by increasing the levels of Nrf2, HO-1, NQO-1, TXNRD1, TNF-α, IL-1β, and IL-6 in mammary gland tissue (73). Similarly, Guo et al. (74) demonstrated that butyrate mitigates oxidative stress and inflammatory responses by reducing the levels of TNF-α, IL-1β, and IL-6, while enhancing the expression of SOD2, Nrf2, and AMP-activated protein kinase (AMPK) in BMECs. These actions contribute to protecting the mammary gland against LPS-induced mastitis. Additionally, vitamin A supplementation was shown to prevent LPS-induced oxidative stress by upregulating Nrf2 and GPX expression and downregulating NF-κB, IL-1, and IL-1β (75, 76).

Astragaloside IV, an extract from *Astragalus membranaceus* (Fisch) Bunge, prevented ammonia-induced oxidative stress and apoptosis by augmenting the expression of HO-1, xCT (also known as SLC7A11), and Nrf2 signaling, and suppressing Bax, caspase 3, p53, while upregulating Bcl2 levels (77). Furthermore, they elucidated that Astragaloside IV regulates Nrf2 signaling via the activation of PI3K/AKT and mitogen-activated protein kinase/extracellular signal-regulated kinase (MAPK/ERK) pathways in BMECs (77). Consequently, it has been documented that melatonin (1 mM) inhibited LPS-induced oxidative stress and inflammation in mouse mammary gland tissue (78). Furthermore, the melatonin treatment significantly downregulated the levels of TNF-α, IL-1β, IL-6, CXCL1, monocyte chemoattractant protein-1 (MCP-1), and regulated upon activation normal T-cell expressed and secreted (RANTES), enhanced Nrf2 levels, and suppressed inducible nitric oxide synthase (iNOS) and cyclooxygenase-2 (COX-2) (78). Puerarin supplementation (400 mg mixed with a standard diet daily) has been shown to significantly reduce inflammatory cytokines and somatic cell count (SCC) in the milk of cows with mastitis. Additionally, Puerarin (40 μM) treatment was found to decrease the expression of NF-κB-associated inflammatory factors (IL-6 and IL-8) while increasing the levels of Nrf2 and its associated antioxidant genes (GSH, SOD, CAT), thereby mitigating inflammation and oxidative stress induced by H_2O_2 (400 μM) in BMECs (79). This *in-vitro* compilation emphasizes the therapeutic potential of targeting Nrf2/KEAP1 signaling as a strategy for managing mastitis in animals. It also highlights the need for additional research in this field to fully utilize the benefits of bioactive compounds in animal health and disease management. For ease of reference, the roles of various bioactive compounds in preventing and reducing mastitis, particularly through the regulation of Nrf2/KEAP1 signaling pathway, are summarized in Table 1.

4.2 Bioactive compounds boost antioxidant and anti-inflammatory responses by activating Nrf2/KEAP1 signaling to combat mastitis: *in vivo* evidence

Recent *in vivo* studies have demonstrated that bioactive compounds can significantly enhance antioxidant and anti-inflammatory responses by activating the Nrf2/KEAP1 signaling pathway, offering a promising therapeutic approach for combating mastitis. For example, a study conducted by Ding et al. (102) investigated the effects of Rutin supplementation on goat mammary gland tissue during the periparturient period. The researchers administered Rutin at doses of 50 and 100 mg/kg body weight per day for 28 days prior to and 28 days after parturition. The results showed significant reductions in the levels of BHB and MDA, two markers of oxidative stress, and increased expressions of Nrf2, CAT, GSH-Px, SOD, and T-AOC, indicating enhanced antioxidant activity in the mammary gland tissue. Furthermore, the study found that Rutin treatment effectively prevented apoptosis and inflammation in the mammary gland. This was evidenced by the suppression of pro-apoptotic proteins Bax, caspase-3, and caspase-9, and the elevation of the anti-apoptotic protein Bcl2. These changes in apoptotic markers contributed to the preservation of mammary gland health (102). In addition to its anti-apoptotic effects, Rutin also exhibited anti-inflammatory properties. It downregulated the expressions of the pro-inflammatory cytokine TNF-α and the transcription factor NF-κB, thus mitigating inflammatory changes in the mammary tissue of goats during the periparturient period (102). In a separate study, Lebda et al. (103) established an LPS-induced rat mastitis model and supplemented it with nanocurcumin at a dose of 35 mg/kg body weight, administered orally for a 14-day period. They found that nanocurcumin increased antioxidant activity by increasing the expressions of Nrf2 and GSH-Px and decreasing MDA levels. Additionally, nanocurcumin reduced inflammation by decreasing the expressions of TNF-α, IL-1β, TLR4, NF-κB p65, and high mobility group box 1 (HMGB1) (103). Moreover, extensive research has demonstrated that supplementation with cis-9, trans-11 conjugated linoleic acid (CLA) at a dosage of 70 g can enhance the anti-inflammatory and antioxidant responses in BMECs in response to LPS-induced inflammation and oxidative stress (104–106). Additionally, these studies have reported elevated blood glucose levels and reduced concentrations of BHB in cows receiving CLA supplementation (104–106). Additionally, it was observed that the positive effects mentioned above were a result of the upregulation of Nrf2 and the suppression of autophagy induced by ROS when CLA supplementation was introduced. This, in turn, contributed to the promotion of mammary gland health (107). Consistently a study found that sulforaphane administration to mice at a dose of 50 mg/kg/day/intraperitoneally 7 days LPS in mice. Following sulforaphane administration, to create mastitis model, LPS was injected into the mammary ducts of the mice (108). These findings were further validated *in vitro* using primary goat mammary epithelial cells (GMECs) treated with both sulforaphane (20 μM) and LPS. In both *in vivo* and *in vitro* experiments, sulforaphane significantly decreased the expression of inflammatory cytokines and the protein levels of key inflammatory mediators (101, 108). A study found that corynoline intraperitoneal injection in mice significantly reduced the expression of pro-inflammatory cytokines, such as TNF-α, IL-1β, and IL-6, in the mammary tissues of LPS (intramammary)-induced mice. Furthermore, the findings of the study showed that corynoline exerted its protective effect to enhance antioxidant response by regulating the AKT/GSK3β/Nrf2 signaling pathway (33). Furthermore, a study used *in vivo* experiments where cows were treated with rumen-bypassed niacin (30g/day), and *in vitro* studies using primary BMECs (34). They documented that niacin reduced somatic cell counts (SCCs) and inflammatory markers (IL-6, IL-1β, TNF-α) in both blood and milk of mastitis infected cows. Niacin activated the GPR109A receptor, phosphorylated AMPK, and promoted NRF-2 nuclear import, ultimately reducing inflammation through enhanced autophagy (34). Another study demonstrated the effectiveness of resveratrol in reducing the inflammatory response and oxidative damage caused by *S. uberis* infection in mice mammary gland tissues and both *in vitro* and *in vivo* trials supported these findings (36). The study also revealed that resveratrol activates the Nrf2 signaling pathway, which is responsible for regulating cellular antioxidant responses. Additionally, resveratrol was found to promote the degradation of Keap1 through p62 activation. This, in turn, led to increased expression of Nrf2 and its downstream antioxidant pathways (36). Therefore, it can be concluded that resveratrol's activation of the p62-Keap1/Nrf2 signaling pathway successfully reduces oxidative damage and inflammation caused by *S. uberis* infection. Consistently, another study reported that LPS (10 μg/mL)-induced mastitis in mouse model was effectively treated with Caffeic acid at a dosage of 10 mg/kg administered intramammarily. This treatment modulated the NF-κB/Nrf2 signaling pathway, significantly reducing LPS-induced ROS production, which drives inflammatory changes and oxidative stress in mammary gland epithelial cells. Caffeic acid prevented the activation of NF-κB by activating IκBα and promoted the dissociation of Nrf2 from its cytoplasmic inhibitor Keap1 (47). By elevating Nrf2 levels and suppressing NF-κB activity, caffeic acid enhanced the antioxidant response, alleviated inflammation, and mitigated damage to mammary tissue. Furthermore, it inhibited the oxidative burst and neutrophil chemotaxis, demonstrating protective effects in MMECs (47). In a study on LPS-induced mastitis (100 μg/intramammary), Wogonin, a flavonoid derived from medicinal plants (also known as 5,7-dihydroxy-8-methoxyflavone), was administered intraperitoneally at a dosage of 40 mg/kg. They found that Wogonin treatment by targeting NF-κB/Nrf2/HO-1 signaling pathway, significantly inhibited of inflammation by reducing the expression of NF-κB, TNF-α, and IL-1β. Moreover, it enhanced the antioxidant response by increasing levels of Nrf2, HO-1, GSH, and SOD, while simultaneously decreasing MDA levels in MMECs (108). All of the studies that reported the *in vivo* effects of bioactive compounds in the treatment of mastitis by targeting Nrf2 signaling pathway have been summarized in Table 2.

TABLE 1 Bioactive compounds targeting Nrf2/KEAP1/HO1 signaling pathway to combat mastitis*: In vitro* evidence.

Causative Agent	Therapeutic Agent/dosage/ method of administration	Target pathway	Outcomes	Experimental model	References
Lipoteichoic Acid (100 μg/mL of LTA for 6 hours)–induced mastitis	Metformin (1,1-Dimethylbiguanide hydrochloride, derived from *Galega officinalis*) 3 mM for 12 hours prior to LTA exposure/cell culture	AMPK/Nrf2/NF-κB Signaling Pathway	◇ Metformin activates the NRF2 pathway by affecting cellular energy status. It does this by inhibiting mitochondrial complex I, which reduces ATP production and increases the AMP/ATP ratio. This, in turn, activates AMP-activated protein kinase (AMPK), a crucial regulator of cellular energy balance. ◇ When AMPK is activated by metformin, it can phosphorylate and activate NRF2. Additionally, metformin has been found to inhibit the activation of NF-κB, mainly through the activation of AMPK. This inhibition can prevent the phosphorylation and degradation of IκB by inhibiting IκB kinase ◇ Collectively metformin significantly downregulated the expression of NF-κB, cyclooxygenase-2, IL-1β, and IL-6 and upregulated the levels of AMPK, Nrf2 and HO-1 to enhance antioxidant and anti-inflammatory responses in BMECs	BMECs	(35)
LPS (10 μg/mL)-induced mastitis	Chlorogenic acid (Traditional Chinese medicinal herbs such as honeysuckle, Eucommia ulmoides leaves, and chrysanthemum)/10 μg/mL/cell culture	NF-κB/Nrf2/HO-1 signaling pathway	◇ Prevented the degradation of IκBα to inhibit the activation of NF-κB and promote the degradation of Keap1 to facilitate the release of Nrf2 ◇ Suppressed the inflammatory changes by reducing the expressions of NF-κB, IL-6, IL-8, TNF-α, IL-1β, and iNOS ◇ Enhanced Antioxidant responses by elevation the level of CHOP, Nrf2 and HO-1	BMECs	(57)
LPS (10 μg/mL)-induced mastitis	Tanshinone IIa (Diterpene quinone derived from the roots of *Salvia miltiorrhiza)* 2.5 μM/cell culture	Nrf2/Keap1 signaling pathway	◇ The Tanshinone IIa Nrf2 signaling pathway potentially leads to the upregulation of antioxidant enzymes like HO-1, NQO1, and glutathione S-transferase (GST). These enzymes play a crucial role in neutralizing ROS and reducing oxidative stress, which is a significant factor in the development and progression of mastitis. ◇ Furthermore, the activation of Nrf2 by Tanshinone IIa also results in the suppression of pro-inflammatory cytokines. This occurs because the antioxidant enzymes induced by Nrf2 can decrease oxidative stress levels, consequently reducing the activation of NF-κB, which is a major transcription factor responsible for the expression of these inflammatory cytokines. ◇ Prevented mastitis via regulation of Keap1/Nrf2 signaling pathways	BMECs	(61)
LPS (10 μg/mL)-induced mastitis	Sodium butyrate (sodium salt of butyric acid)/2 mM/cell culture	Nrf2 signaling pathway	◇ Upregulated the expression of Nrf2, SOD, GSH-Px, CAT, HO-1, and NQO1 suppressed the level of MDA to promote antioxidant response ◇ Inflammatory changes were reversed by downregulating the levels of IL-6, IL-Iβ, TNF-α, NF-κB ◇ Apoptosis was prevented by inhibiting the levels of caspases and Bax and elevated the expression of Bcl2 ◇ By activating Nrf2, Sodium butyrate helps in reducing the production of pro-inflammatory cytokines like TNF-α, IL-1β, and IL-6. This effect is partly due to the crosstalk between Nrf2 and NF-κB pathways, where Nrf2 activation can inhibit NF-κB-mediated inflammatory signaling. ◇ Sodium butyrate is also a well-known histone deacetylase (HDAC) inhibitor. By inhibiting HDACs, it can increase the acetylation of histones, which relaxes chromatin structure and facilitates the transcription of Nrf2 target genes	BMECs	(80)
LPS-induced mastitis	Lentinan (β-1,3-glucan)/20 μg/mL/direct addition to the cell culture medium	Nrf2 pathway	◇ Lentinan blocked the expression of NF-κB and MAPK to relieve inflammatory changes ◇ Enhanced Nrf2 and HO-1 level to suppress to oxidative stress and MBECs injury	BMECs	(81)

(Continued)

10.3389/fimmu.2025.1425901

TABLE 1 Continued

Causative Agent	Therapeutic Agent/dosage/ method of administration	Target pathway	Outcomes	Experimental model	References
LPS-induced mastitis	2-methyl nonyl ketone (Derived from Houttuynia Cordata Thunb) 25 μg/mL/ administered directly to cell culture medium	TLR4-NF-κB and Nrf2/ HO-1 signaling pathway	◇ Enhanced the expression of TLR4-NF-κB and suppressed Nrf2/HO-1 level by LPS levels. ◇ 2-Methyl Nonyl Ketone modify Keap1, which can lead to the release of Nrf2 ◇ Nrf2/HO-1 level was improved by 2-methyl nonyl ketone in mammary cells, and prevented inflammatory changes caused by activated NF-κB and TLR4 to inflammatory changes in the mammary gland tissue ◇ Finally prevented cell injury from inflammation and oxidative stress	BMECs	(82)
LPS-induced mastitis	Betaine (Trimethylglycine, a product derived from *Beta vulgaris*)/25 mM/administered directly to cell culture medium	Nrf2/HO-1 signaling pathway	◇ Promoting the dissociation of Nrf2 from Keap1 ◇ Activated Nrf2 regulates the levels of SOD, GSH-Px, and reduced the levels of MDA, IL-1β, IL-6 and TNFα to relieve inflammatory changes and oxidative stress in BMECs via activation Nrf2/HO-1 and suppressing signaling pathways	BMECs	(83)
LPS-induced mastitis	Niacin (Vitamin B3/nicotinic acid)/50 mg/kg/ administered intraperitoneally	AMPK/Nrf2 signaling pathway	◇ Niacin, particularly through its role in NAD+ synthesis, supports the cellular redox state and energy metabolism. ◇ NAD+ is a cofactor for the activity of sirtuins, which are involved in the deacetylation of proteins, including those that can influence NRF2 activity. ◇ Activate the expression of GPR109A, which suppress the proinflammatory cytokines (TNF-α, IL-6 and IL-1β) and regulated the Nrf2 to enhance the anti-inflammatory and antioxidant responses to mitigate mastitis	MMECs	(84)
LPS (100 μg/mL)-induced mastitis	Curcumin (Diferuloylmethane, a compound derived from rhizomes of turmeric)/10 μM/ administration directly into cell culture	Nrf2 signaling pathway	◇ The electrophilic properties of the α, β-unsaturated carbonyl group in curcumin can modify cysteine residues in Keap1, leading to the disruption of the Keap1-NRF2 complex. This allows NRF2 to accumulate and translocate to the nucleus ◇ Once activated, NRF2 increases the expression of several genes involved HO-1 and NQO-1 to improve the antioxidant activity ◇ Apoptosis was inhibited via upregulation of Bcl2 and suppression of Bax ◇ The inflammatory changes were prevented via downregulation of TNF-α, IL-8, IL-6 and IL-1β ◇ Protected BMECs from oxidative damage	BMECs	(85)
LPS (50 μg/mL of LPS for 12 hours)-induced mastitis	Ferulic acid (4-hydroxy-3-methoxycinnamic acid, plant based) 15 μg/mL/administered into cell culture 2 hours before LPS treatment	NF-κB/Nrf2 signaling pathways	◇ Antioxidant ability was enhanced through regulation of Nrf2 followed by elevated levels of its downstream genes SOD, GPX, COX2 and suppressed the expression of MDA ◇ Reduced the level of Bax and elevated the expression of Bcl2 ◇ Anti-inflammatory response was promoted via regulation of NF-kB, TNF-α, IL-6, and IL-1β	BMECs	(86)
LPS (12 μg/mL of LPS for 12 hours)-induced mastitis	Menthol (2-Isopropyl-5-methylcyclohexanol, a compound extracted from the essential oils of mint plants)/200 μM/administered into cell culture	AMPK/ULK1/Nrf-2/ autophagy pathway	◇ Suppressed the levels of TNF-α, IL-6, and IL-1β ◇ Promoted the expressions of ULK1, AMPK, and Nrf2 ◇ Restored synthesis of milk fat and milk protein	BMECs	(87)
LPS (100 ng/mL of LPS)-induced mastitis	Dandelion (medicinal plant based)/10μg/mL/ applied directly to the cultured cells *in vitro*	Nrf2 signaling pathway	◇ Dandelions contains Chicoric Acid and Beta-Carotene, which are known for their strong antioxidant effects. By scavenging free radicals and reducing oxidative stress, these compounds can help activate NRF2. ◇ Taraxasterol and Luteolin in Dandelions by reducing inflammation, these compounds can help to modulate NRF2 signaling	BMECs	(88)

(Continued)

10.3389/fimmu.2025.1425901

TABLE 1 Continued

Causative Agent	Therapeutic Agent/dosage/ method of administration	Target pathway	Outcomes	Experimental model	References
			◇ Ameliorated the level ROS production and enhanced Nrf2 expression. ◇ Protected mammary gland damage from oxidative stress		
Streptococcus lutetiensis induced oxidative stress and autophagy	N-Acetyl-L-cysteine (NAC)/5 Mm/ cell culture	Nrf2/Keap1 signaling pathway	◇ NAC promotes the activation and nuclear translocation of Nrf2 by modifying cysteine residues on Keap1, a protein that normally inhibits Nrf2 ◇ NAC serves as a precursor to GSH, a critical antioxidant that neutralizes ROS and reduces oxidative stress. By replenishing GSH levels, NAC helps maintain redox balance in the mammary gland during mastitis. ◇ NAC promotes the activation and nuclear translocation of Nrf2 by modifying cysteine residues on Keap1 ◇ Its ability to activate Nrf2 indirectly inhibits the NF-κB signaling pathway, reducing the inflammatory response and preventing excessive tissue damage. ◇ Enhanced the antioxidant response by elevating the level of Nrf2, HO1, and NQO1, and reduced ROS production	BMECs	(89)
γ-d-Glutamyl-meso-diaminopimelic acid induced oxidative stress and inflammation	Glutamine/0.6 mM for 12/administration directly into cell culture	NOD1/NF-κB and ERK/Nrf2 pathways	◇ Downregulated the levels of NF-κB, NOD1, IL-6 and TNF-α by glutamine treatment and inflammatory changes were relieved ◇ Enhanced the expression of ERK, Nrf2, SOD, CAT, NQO1 and HO-1 to improve the antioxidant response	BMECs	(90)
H_2O_2 (100 μμ) induced oxidative stress and inflammation	Quercetin (Plant based polyphenolic flavonoid, composed of two benzene rings (A and B) connected by a three-carbon chain that forms a closed pyran ring)/20 μμ/ cell culture	MAPK/Nrf2 Signaling Pathway	◇ Modified cysteine residues on Keap1 allow Nrf2 to escape degradation. ◇ Alleviated oxidative stress. ◇ Improved mice mammary epithelial cell viability and antioxidant capacity. ◇ Restored mammary health by enhancing Nrf2, T-AOC, and MAPK expression.	MMECs	(91)
H_2O_2 (500 μM)-induced oxidative stress	Taurine/2.0 mM taurine for 12 h/cell culture	Nrf2-MAPK signaling pathway	◇ Upregulated the expression on Nrf2 and inactivated the p38/MAPK pathway ◇ Relieved the oxidative stress and guard the mammary gland tissue	PMECs	(92)
H2O2 (100 μM)-induced oxidative stress and apoptosis	Myricetin (3,5,7,3′,4′,5′-hexahydroxyflavone, a plant-based flavonoid)/5 μM/administration directly into cell culture	AMPK/Nrf2 signaling pathway	◇ Reduced MDA and ROS level ◇ Enhanced antioxidant response via the elevated expressions of Nrf2, T-AOC, SOD and CAT ◇ Myricetin reduces the production of pro-inflammatory cytokines and also inhibits the activation of NF-κB	BMECs	(93)
H_2O_2-induced ROS production	Baicalin (5,6-Dihydroxy-4-oxoflav-2-en-7-yl β-D-glucopyranosiduronic acid, a flavonoid compound, primarily derived from the roots of ***Scutellaria baicalensis***, commonly known as Baikal skullcap or Chinese skullcap)/ cell culture	Nrf2 signaling pathway	◇ Baicalin can inhibit the Keap1-Nrf2 interaction, leading to stabilization and accumulation of Nrf2 in the cytoplasm. ◇ Suppressed level of ROS and oxidative stress via activation of Nrf2 signaling pathway ◇ Baicalin, through its action on Nrf2, can modulate the expression of inflammatory cytokines and other mediators, thereby contributing to a reduction in inflammation associated with mastitis	BMECs	(94)
H_2O_2 (500 μM)-induced oxidative stress, inflammation and apoptosis	Lycopene (Plant based carotenoid) 24 hours for 24 hours/cell culture	Nrf2/NF-κB signaling Pathway	◇ Lycopene causes modifications in Keap1's cysteine residues and as a result Nrf2 translocates to nucleus, and binds to antioxidant response elements (AREs) in the promoter regions of target genes. ◇ Enhanced the antioxidant response through activation of Nrf2 ◇ Relieved inflammation via downregulation the levels of NF-κB, TNF-α, IL-6, and IL-1β	BMECs	(95)

(Continued)

10.3389/fimmu.2025.1425901

TABLE 1 Continued

Causative Agent	Therapeutic Agent/dosage/ method of administration	Target pathway	Outcomes	Experimental model	References
			◇ Prevented apoptosis via upregulation of Bcl2 and decreased the expressions of Bax and caspase-3 ◇		
H_2O_2 (400 μM for 24 hours)-induced Oxidative Stress and Apoptosis	Sulforaphane (1-isothiocyanato-4-methylsulfinylbutane, medicinal plant based) 5 μM/cell culture/*in vivo*	AMPK/Nrf2 Signaling Pathway	◇ Improved antioxidant response via upregulation of Nrf2, SOD, GSH and AMPK and inhibition of MDA ◇ Reduced apoptosis via downregulating Bax and caspase-3, and elevated the level of Bcl2 ◇ Protected mammary epithelial cells from oxidative damage	GMECs	(96)
Deoxynivalenol (0.25 μg/mL)-induced oxidative stress and inflammatory response	Pterostilbene (4'-Methoxy-4-hydroxystilbene, derivative of resveratrol)/2.0504 μg/mL for 9 hours/cell culture	NF-κB/Nrf2/Keap1 signaling pathway	◇ Relieved inflammatory changes via downregulation of NF-κB P65, NF-κB P50, MCP-1, COX-2, TNF-α, IL-6, and IL-1β ◇ Enhanced Antioxidant response and inhibited ROS production by elevated levels of Nrf2, Keap1, T-AOC, SOD1, SOD2, and GSH and reduced MDA content	BMECs	(97)
Heat stress induced oxidative stress and apoptosis	Methionine/120 mg/L/cell culture	Nrf2 Signaling Pathway	◇ Elevated the expression of Nrf2, GSH-Px, SOD, SLC7A11 and FTH1 ◇ Inhibit the level of MDA ◇ Met treatment further restored mitochondrial function, iron homeostasis imbalance caused by heat treatment in BMECs	BMECs	(98)
Heat (42°C)-induced oxidative stress in BMECs	Procyanidin B2/25 μM/administration directly into cell culture	Nrf2 signaling pathway	◇ Procyanidin B2 treatment reversed the inflammatory changes and oxidative damage caused by heat stress in BMECs via activating Nrf2/HO-1 pathway	BMECs	(99)
Heat stress-induced oxidative damage	S-allyl cysteine (a natural organosulfur compound primarily derived from aged garlic (*Allium sativum*)./15 μg/mL/applied *in vitro* for 2 hours prior to the induction of heat stress.	Nrf2/HO-1 signaling pathway	◇ Reduced ROS production, caspase-3 and Bax levels ◇ Enhanced Nrf2, SOD, CAT, GSH-Px, HSP70, HO-1, Bcl2 expressions. ◇ Overall enhance antioxidant efficiency and prevent apoptosis via regulation of Nrf2/HO-1 signaling pathway and prevented cell injury	BMECs	(100)
Heat stress (42°C)–induced oxidative stress and apoptosis	Betaine (Trimethylglycine, a product derived from Beta vulgaris)/25 mM/applied directly to the cultured cells *in vitro*	Nrf-2/HO-1 signaling pathway	◇ Enhanced antioxidant activity via upregulation of SOD, CAT, HO-1, and Nrf2 and decreased MDA contents ◇ Increased the expressions HSP70, HSP27 and Bcl2 and suppressed the Bax to relieve apoptosis	BMECs	(101)

CHOP, C/EBP Homologous Protein; MMECs, Mice mammary epithelial cells; BMECs, Bovine mammary epithelial cells; GMECs, goat mammary epithelial cells; TNF-α, necrosis factor-α; interleukin (IL)-1β and IL-6); COX2, cyclooxygenase-2; iNOS, inducible nitric oxide synthase; NF-κB, nuclear factor kappa-B; MAPK, mitogen-activated protein kinase; SLC7A11, solute carrier family 7, member 11; FTH1, ferritin heavy chain 1; PMECs, porcine mammary epithelial cells; MPO, myeloperoxidase; NLRP3, Nucleotide-binding oligomerization domain-like receptor containing pyrin domain 3; ULK1, unc-51 like kinase 1; GSK-3 beta, Glycogen synthase kinase-3 beta; MCP-1, monocyte chemotactic protein 1; NLRP3, NOD-like receptor protein 3.

10.3389/fimmu.2025.1425901

TABLE 2 Bioactive compounds targeting Nrf2/KEAP1 signaling pathway to combat mastitis: *in vivo* evidence.

Causative Agent	Therapeutic Agent/dosage/ method of administration	Target pathway	Outcomes	Experimental model	References
LPS (100 μg/intramammary)-induced mastitis	Corynoline (Benzylisoquinoline, extracted from *Corydalis bungeana* Turcz)/60 mg/kg/intraperitoneally	AKT/GSK3β/Nrf2 signaling pathway	◇ Inhibited inflammatory changes via downregulation of NF- kB, TNF-α and IL-1β expressions ◇ Upregulated the expressions of Nrf2, AKT and GSK3β and reduced the level of MDA ◇ Finally, the Corynoline ameliorated mastitis by promoting antioxidant activity and anti-inflammatory response via AKT/GSK3β/Nrf2 signaling pathway	Mouse	(33)
LPS (100 μg/intramammary)-induced mastitis	Niacin (Vitamin B3/nicotinic acid)/24 g/day/orally	GPR109A/AMPK/NRF2	◇ Elevated levels of GPR109A, Nrf2 and AMPK to enhanced antioxidant response and relieve oxidative stressed ◇ Ameliorated the inflammatory changes via downregulating IL-6, IL-1β, and TNF-α ◇ Prevented mastitis via regulating the GPR109A/AMPK/NRF-2 in mammary epithelial cells	Mouse	(34)
Streptococcus uberis (1×10^7 CFU/intramammary injection)-induced mastitis	Resveratrol (3,5,4'-trihydroxy-trans-stilbene, medicinal plant based) 100 mg/kg/orally	Nrf2/Keap1 signaling pathway	◇ Suppressed via inflammation and oxidative stress via activation of Nrf2/Keap1 signaling pathway ◇ Protected mouse mammary gland from oxidative damage and mastitis	Mouse	(36)
LPS (10 μg/mL)-induced mastitis	Caffeic acid (Hydroxycinnamic acid, composed of A carboxylic acid group attached to phenyl ring through a two-carbon alkene chain) 10 mg/kg/intramammary administration	NF-κB/Nrf2 signaling pathway	◇ Significantly reduced LPS-induced ROS production which promote the inflammatory changes and oxidative stress in mammary gland epithelial cells ◇ Prevented the activation of NF-κB by activating IκBα and promote the dissociation of Nrf2 from its cytoplasmic inhibitor Keap1 ◇ By elevating level of Nrf2 and suppression of NF-κB activity, caffeic acid enhanced the antioxidant response and relieved inflammation ◇ Alleviated mammary tissue damage and inhibited the oxidative burst and neutrophil chemotaxis	Mouse	(47)
LPS-induced mastitis *in vivo* and *in vitro*	Sulforaphane (1-isothiocyanato-4-methylsulfinylbutane, medicinal plant based) 50 mg/kg/day via intraperitoneal injection for 7 days (*in vivo*) and 20 μM/cell culture (*in vitro*)	Nrf2 Signaling Pathway	◇ Suppressed ROS level and enhanced antioxidant response ◇ Prevented inflammatory changes by downregulating the expression levels of TNF-α, IL-1β, IL-6, COX2, iNOS, and NF-κB ◇ Up-regulated the expression level of Nrf2	Mouse and GMECs	(108)
LPS (100 μg/intramammary)-induced mastitis	Wogonin (5,7-dihydroxy-8-methoxyflavone, medicinal plant-based flavonoid) 40 mg/kg/intraperitoneally	NF-κB/Nrf2/HO-1 signaling pathway	◇ Inhibited inflammation (downregulated the NF-κB, TNF-α and IL-1β levels) and enhanced the antioxidant response (increased the Nrf2, HO-1, GSH, SOD and decreased MDA levels)	Mouse	(109)
LPS (2.5 mg/kg)-induced inflammation and oxidative stress	Resveratrol (3,5,4'-trihydroxy-trans-stilbene) 2 mg/kg/orally for 15 days	NF-κb/Nrf2 Signaling	◇ Upregulated the level of Nrf2 by inhibiting oxidative stress via enhancing antioxidant response ◇ Enhanced the levels of Nrf2 and T-AOC and combat oxidative stress ◇ By activating Nrf2, resveratrol can inhibit the production of pro-inflammatory cytokines (e.g., TNF-α, IL-6) and reduce the expression of inflammatory mediators like NF-κB.	Mouse	(110)

(Continued)

10.3389/fimmu.2025.1425901

TABLE 2 Continued

Causative Agent	Therapeutic Agent/dosage/ method of administration	Target pathway	Outcomes	Experimental model	References
LPS-induced oxidative stress	Sanguinarine (A benzophenanthridine alkaloid derived from *Sanguinaria canadensis* and *poppy Fumaria* species)/50 μM/intraperitoneally	Nrf2/HO-1 signaling pathway	◇ Sanguinarine modifies Keap1, leading to the release of NRF2. ◇ Enhanced the level of Nrf2 followed by elevated antioxidant response ◇ Suppressed TNF-α and IL-1β expression followed by inhibition of inflammatory changes in MMECs	Mouse	(111)
LPS- induced mastitis	Kynurenic acid (2-Hydroxy-3-carboxy-6-methoxybenzeneacetic acid, a metabolite of tryptophan)/100 mg/kg/intraperitoneally	NF-κB/Nrf2/HO-1 signaling pathway	◇ NF-κB, TNF-α and IL-1β mRNA expressions were inhibited ◇ Blood-milk barrier integrity was protected from oxidative stress damage induced by LPS via activating Nrf2/HO-1 signaling pathway	Mouse	(112)
LPS (10 μg)-induced mastitis	Dioscin (a natural compound extracted from the tubers of *Dioscorea japonica*)/45 mg/kg/ day/orally	AMPK/Nrf2/NF-κB signaling Pathway	◇ Promoted the expressions of AMPK and Nrf2 and ameliorated oxidative stress ◇ Inhibited the levels of NLRP3, IL-6, IL-1β, TNF-α, and NF-κB to relieve inflammatory changes ◇ Prevented mastitis via activation of AMPK/Nrf2/NF-κB signaling Pathway	Mouse	(113)
LPS-induced mastitis	Schisandrin A (dibenzocyclooctadiene lignane, derived from the plant *Schisandra chinensis*)/40 mg/kg/administered via intraperitoneal injection	Nrf2 signaling pathway	◇ Enhanced antioxidant and anti-inflammatory response via activated AMPK/ULK1/Nrf2 signaling pathway ◇ Protected mammary gland from oxidative injury and mitigated mastitis	Mouse	(114)
LPS (100 μL)-induced mastitis via nipple duct injection in 5–7 days postpartum mice	Dimethyl itaconate (Cell-permeable derivative of itaconate and a metabolite of the tricarboxylic acid cycle)/25 mg/kg/intraperitoneal	MAPKs/Nrf2/NF-κB signaling pathways	◇ Activates Nrf2 via alkylation of KEAP1. ◇ Reduced inflammatory changes by downregulating the levels of TLR4, NF-κB, TNF-α and IL-1β. ◇ Relieved oxidative response and enhance antioxidant response via regulation of MAPK and Nrf2 ◇ Overall, dimethyl itaconate prevented mastitis via activation of MAPKs/Nrf2 and inhibition of NF-κB signaling pathways	Mouse	(115)
S. uberis (1×10^7 CFU/ intramammary injection)-induced mastitis	Taurine (2-aminoethanesulfonic acid) 100 mg/kg body weight/intraperitoneally	NF-κB/AMPK/Nrf2 signaling pathway	◇ Decreased the expressions of TLR2, CXCL2, MAPK and NF-κB to relieve the inflammation ◇ Regulated the expression of AMPK/Nrf2 to enhance the antioxidant response ◇ Protected mammary tissue from oxidative damage	Murine mammary glands	(116)
S. aureus (1×10^7 CFU)-induced mastitis	Diosmetin (3′,5,7-trihydroxy-4′-methoxyflavone, plant based)/25 mg/kg/intramammary one hour before S. aureus treatment	NF-κb/Nrf2/HO-1 Signaling pathway	◇ Promoted the dissociation of Nrf2 from Keap1. ◇ Upregulated the expressions of SIRT1, GPX4, HO-1 and Nrf2 and downregulated the level of MDA and promoted the antioxidant response ◇ Suppressed the level of MPO, TNF-α and IL-1β, and NF-kB and alleviated the inflammation	Mouse	(117)
S. aureus (1×10^7 CFU)-induced oxidative stress and apoptosis	Saikosaponin (Triterpene saponin, derived from the roots of *Bupleurum falcatum*)/20 mg/ kg/intramammary	SIRT1/Nrf2 Signaling pathway	◇ Disrupted the interaction between Nrf2 and Keap1. This disruption leads to the stabilization and nuclear translocation of Nrf2. ◇ Enhanced the level of SIRT1, Nrf2, HO-1 and GPX4 to promote antioxidant response ◇ Suppressed the level of MPO, TNF-α and IL-1β, and NF-kB and alleviated the inflammation	Mouse	(118)

10.3389/fimmu.2025.1425901

5 Limitations and future directions

Most of the evidence presented is based on preclinical studies involving cell cultures and animal models. However, there is a lack of clinical trials in actual dairy herds, which limits the direct applicability of these findings to real-world farming practices. The transition from laboratory research to practical applications in dairy farming remains underexplored. To translate preclinical findings into practical applications, it is essential to conduct well-designed clinical trials and field studies in dairy herds. These studies should assess the effectiveness, safety, and economic viability of bioactive compounds in preventing and treating mastitis in real-world settings.

The review emphasizes the beneficial effects of bioactive compounds in reducing oxidative stress and inflammation. However, it does not fully address the potential unintended effects, such as toxicity or interference with other cellular pathways. These aspects require careful consideration, especially in long-term or high-dose applications.

Several studies have shown that Nrf2 signaling plays a complex and multifaceted role in cancer development and progression (119–122). When Nrf2 is overactivated, it can enhance antioxidant responses. While this is beneficial under normal circumstances, it may inadvertently support tumor growth and resistance to therapy by promoting cellular survival pathways. On the other hand, some research suggests that Nrf2 could be a potential target for cancer treatment, indicating that regulating its activity could suppress tumor progression (123). These findings highlight the dual nature of Nrf2 in cancer biology. Given these insights, it is crucial to carefully assess the biological impact of Nrf2, particularly its overactivation, in future research on mastitis mitigation. Understanding the potential negative effects of Nrf2 overactivation will be essential to prevent unintended consequences and ensure the effectiveness of therapeutic interventions.

Future studies should explore the potential synergistic effects of combining multiple bioactive compounds or integrating them with existing therapeutic strategies. Such combinations might enhance efficacy and reduce the likelihood of resistance or side effects. Investigating the long-term impact and safety of bioactive compound supplementation in animals is crucial. These studies should consider potential off-target effects, the impact on milk quality and yield, and overall animal health and welfare. Beyond the biological effects, future research should assess the economic feasibility of using bioactive compounds on a large scale in dairy farming. Additionally, the environmental impact of their use, including any potential residues in milk and their effects on ecosystems, should be thoroughly evaluated.

6 Conclusion

In conclusion, the review highlights the pivotal role of the Nrf2/KEAP1 signaling pathway in combating mastitis through the regulation of antioxidant and anti-inflammatory responses. The evidence underscores the therapeutic potential of bioactive compounds, which activate Nrf2/KEAP1 signaling pathway, in enhancing antioxidant defenses, reducing inflammation, and mitigating cellular damage in mammary tissues. These compounds offer promising avenues for improving the health of dairy animals, particularly in the context of mastitis management. However, despite the significant progress in understanding the molecular mechanisms by which these bioactive compounds exert their effects, further research is needed to optimize their use in practical settings. Future studies should focus on combination strategies of these compounds to maximize their efficacy in preventing and treating mastitis. Moreover, the exploration of additional bioactive compounds and their interactions with other cellular pathways could provide deeper insights into their broader applications in animal health. Finally, to translate the findings from preclinical research into practical applications, it is crucial to carry out meticulously designed clinical trials and field studies within dairy herds in future.

Author contributions

MK: Conceptualization, Data curation, Formal analysis, Funding acquisition, Investigation, Methodology, Project administration, Resources, Software, Supervision, Validation, Visualization, Writing – original draft, Writing – review & editing. LL: Data curation, Investigation, Methodology, Software, Validation, Writing – review & editing. YZ: Conceptualization, Data curation, Software, Validation, Writing – review & editing. HB: Data curation, Investigation, Methodology, Software, Writing – review & editing. XL: Investigation, Methodology, Software, Validation, Writing – review & editing. XK: Conceptualization, Data curation, Investigation, Software, Validation, Writing – review & editing. AK: Conceptualization, Data curation, Investigation, Software, Validation, Writing – review & editing. AQ: Conceptualization, Software, Validation, Writing – review & editing. QU: Conceptualization, Investigation, Validation, Writing – review & editing. KA: Conceptualization, Data curation, Validation, Writing – review & editing. TW: Conceptualization, Investigation, Software, Validation, Writing – review & editing. CW: Conceptualization, Funding acquisition, Project administration, Resources, Supervision, Validation, Visualization, Writing – original draft, Writing – review & editing. MZ: Conceptualization, Funding acquisition, Project administration, Resources, Supervision, Validation, Visualization, Writing – original draft, Writing – review & editing.

Funding

The author(s) declare financial support was received for the research, authorship, and/or publication of this article. This research was funded by the National Key R&D Program of China (grant number 2022YFD1600103; 2023YFD1302004), The Shandong

Province Modern Agricultural Technology System Donkey Industrial Innovation Team (grant no. SDAIT-27), Livestock and Poultry Breeding Industry Project of the Ministry of Agriculture and Rural Affairs (grant number 19211162), The National Natural Science Foundation of China (grant no. 31671287), The Open Project of Liaocheng University Animal Husbandry Discipline (grant no. 319312101- 14), The Open Project of Shandong Collaborative Innovation Center for Donkey Industry Technology (grant no. 3193308), Research on Donkey Pregnancy Improvement (grant no. K20LC0901), Key R&D Program Project of Shandong Province (2021TZXD012), Liaocheng University scientific research fund (grant no. 318052025) and Shandong Province Agricultural Major Technology Collaborative Promotion Plan (SDNYXTTG-2024-13), Natural Science Foundation of Shandong Province (ZR2024MC162).

Conflict of interest

The authors declare that the research was conducted in the absence of any commercial or financial relationships that could be construed as a potential conflict of interest.

Publisher's note

References

1. Khan MZ, Huang B, Kou X, Chen Y, Liang H, Ullah Q, et al. Enhancing bovine immune, antioxidant and anti-inflammatory responses with vitamins, rumen-protected amino acids, and trace minerals to prevent periparturient mastitis. *Front Immunol.* (2024) 14:1290044. doi: 10.3389/fimmu.2023.1290044

2. Corrêa DC, Nunes GT, Barcelos RA, Dos Santos JR, Vogel FS, Cargnelutti JF. Economic losses caused by mastitis and the influence of climate variation on the occurrence of the disease in a dairy cattle farm in southern Brazil. *Trop Anim Health Production.* (2024) 56:1–9. doi: 10.1007/s11250-024-03914-2

3. Kour S, Sharma N NB, Kumar P, Soodan JS, Santos MV, Son YO. Advances in diagnostic approaches and therapeutic management in bovine mastitis. *Veterinary Sci.* (2023) 10:449. doi: 10.3390/vetsci10070449

4. Richardet M, Solari HG, Cabrera VE, Vissio C, Agüero D, Bartolomé JA, et al. The economic evaluation of mastitis control strategies in holstein-friesian dairy herds. *Animals.* (2023) 13:1701. doi: 10.3390/ani13101701

5. Samaraweera AM, van der Werf JH, Boerner V, Hermesch S. Economic values for production, fertility and mastitis traits for temperate dairy cattle breeds in tropical Sri Lanka. *J Anim Breed Genet.* (2022) 139:330–41. doi: 10.1111/jbg.v139.3

6. Hogeveen H, Steeneveld W, Wolf CA. Production diseases reduce the efficiency of dairy production: a review of the results, methods, and approaches regarding the economics of mastitis. *Annu Rev Resour Econ.* (2019) 11:289–312. doi: 10.1146/annurev-resource-100518-093954

7. Puerto MA, Shepley E, Cue RI, Warner D, Dubuc J, Vasseur E. The hidden cost of disease: I. Impact of the first incidence of mastitis on production and economic indicators of primiparous dairy cows. *J dairy science.* (2021) 104:7932–43. doi: 10.3168/jds.2020-19584

8. Rollin E, Dhuyvetter KC, Overton MW. The cost of clinical mastitis in the first 30 days of lactation: An economic modeling tool. *Prev veterinary Med.* (2015) 122:257–64. doi: 10.1016/j.prevetmed.2015.11.006

9. Wang L, Yang F, Wei XJ, Luo YJ, Guo WZ, Zhou XZ, et al. Prevalence and risk factors of subclinical mastitis in lactating cows in Northwest China. *Israel J Veterinary Med.* (2019) 74:17–22.

10. De Vliegher S, Ohnstad I, Piepers S. Management and prevention of mastitis: A multifactorial approach with a focus on milking, bedding and data-management. *J Integr Agriculture.* (2018) 17:1214–33. doi: 10.1016/S2095-3119(17)61893-8

11. Cobirka M, Tancin V, Slama P. Epidemiology and classification of mastitis. *Animals.* (2020) 10:2212. doi: 10.3390/ani10122212

12. Khan MZ, Wang J, Ma Y, Chen T, Ma M, Ullah Q, et al. Genetic polymorphisms in immune-and inflammation-associated genes and their association with bovine mastitis resistance/susceptibility. *Front Immunol.* (2023) 14:1082144. doi: 10.3389/fimmu.2023.1082144

13. Khan MZ, Khan A, Xiao J, Ma J, Ma Y, Chen T, et al. Overview of research development on the role of NF-κB signaling in mastitis. *Animals.* (2020) 10:1625. doi: 10.3390/ani10091625

14. Khan MZ, Khan A, Xiao J, Ma Y, Ma J, Gao J, et al. Role of the JAK-STAT pathway in bovine mastitis and milk production. *Animals.* (2020) 10:2107. doi: 10.3390/ani10112107

15. Khan MZ, Dari G, Khan A, Yu Y. Genetic polymorphisms of TRAPPC9 and CD4 genes and their association with milk production and mastitis resistance phenotypic traits in Chinese Holstein. *Front Veterinary Science.* (2022) 9:1008497. doi: 10.3389/fvets.2022.1008497

16. Wang D, Wei Y, Shi L, Khan MZ, Fan L, Wang Y, et al. Genome-wide DNA methylation pattern in a mouse model reveals two novel genes associated with Staphylococcus aureus mastitis. *Asian-Australasian J Anim Sci.* (2020) 33:203. doi: 10.5713/ajas.18.0858

17. Khan MZ, Wang D, Liu L, Usman T, Wen H, Zhang R, et al. Significant genetic effects of JAK2 and DGAT1 mutations on milk fat content and mastitis resistance in Holsteins. *J Dairy Res.* (2019) 86:388–93. doi: 10.1017/S0022029919000682

18. Tommasoni C, Fiore E, Lisuzzo A, Gianesella M. Mastitis in dairy cattle: On-farm diagnostics and future perspectives. *Animals.* (2023) 13:2538. doi: 10.3390/ani13152538

19. Khan MZ, Khan A, Xiao J, Dou J, Liu L, Yu Y. Overview of folic acid supplementation alone or in combination with vitamin B12 in dairy cattle during periparturient period. *Metabolites.* (2020) 10:263. doi: 10.3390/metabo10060263

20. Khan MZ, Zhang Z, Liu L, Wang D, Mi S, Liu X, et al. Folic acid supplementation regulates key immunity-associated genes and pathways during the periparturient period in dairy cows. *Asian-Australasian J Anim Sci.* (2020) 33:1507. doi: 10.5713/ajas.18.0852

21. Khan MZ, Ma Y, Xiao J, Chen T, Ma J, Liu S, et al. Role of selenium and vitamins E and B9 in the alleviation of bovine mastitis during the periparturient period. *Antioxidants.* (2022) 11:657. doi: 10.3390/antiox11040657

22. Xiao J, Khan MZ, Ma Y, Alugongo GM, Ma J, Chen T, et al. The antioxidant properties of selenium and vitamin E; their role in periparturient dairy cattle health regulation. *Antioxidants.* (2021) 10:1555. doi: 10.3390/antiox10101555

23. Ster C, Loiselle MC, Lacasse P. Effect of postcalving serum nonesterified fatty acids concentration on the functionality of bovine immune cells. *J Dairy Sci.* (2012) 95:708–17. doi: 10.3168/jds.2011-4695

24. Ospina PA, McArt JA, Overton TR, Stokol T, Nydam DV. Using nonesterified fatty acids and β-hydroxybutyrate concentrations during the transition period for herd-level monitoring of increased risk of disease and decreased reproductive and milking performance. *Vet Clin N Am Food Anim. Pract.* (2013) 29:387–412. doi: 10.1016/j.cvfa.2013.04.003

25. Song Y, Loor JJ, Li C, Liang Y, Li N, Shu X, et al. Enhanced mitochondrial dysfunction and oxidative stress in the mammary gland of cows with clinical ketosis. *J Dairy Science.* (2021) 104:6909–18. doi: 10.3168/jds.2020-19964

26. Shi Z, Li XB, Peng ZC, Fu SP, Zhao CX, Du XL, et al. Berberine protects against NEFA-induced impairment of mitochondrial respiratory chain function and insulin signaling in bovine hepatocytes. *Int J Mol Sci.* (2018) 19:1691. doi: 10.3390/ijms19061691

27. Khan MZ, Liu S, Ma Y, Ma M, Ullah Q, Khan IM, et al. Overview of the effect of rumen-protected limiting amino acids (methionine and lysine) and choline on the immunity, antioxidative, and inflammatory status of periparturient ruminants. *Front Immunol.* (2023) 13:1042895. doi: 10.3389/fimmu.2022.1042895

28. Khan MZ, Khan A, Chen W, Chai W, Wang C. Advancements in genetic biomarkers and exogenous antioxidant supplementation for safeguarding mammalian cells against heat-induced oxidative stress and apoptosis. *Antioxidants.* (2024) 13:258. doi: 10.3390/antiox13030258

29. Abeyta MA, Al-Qaisi M, Horst EA, Mayorga EJ, Rodriguez-Jimenez S, Goetz BM, et al. Effects of dietary antioxidant supplementation on metabolism and inflammatory biomarkers in heat-stressed dairy cows. *J Dairy Science.* (2023) 106:1441–52. doi: 10.3168/jds.2022-22338

30. Vašková J, Klepcová Z, Špaková I, Urdzík P, Štofilová J, Bertková I, et al. The importance of natural antioxidants in female reproduction. *Antioxidants.* (2023) 12:907. doi: 10.3390/antiox12040907

31. Meli R, Monnolo A, Annunziata C, Pirozzi C, Ferrante MC. Oxidative stress and BPA toxicity: an antioxidant approach for male and female reproductive dysfunction. *Antioxidants.* (2020) 9:405. doi: 10.3390/antiox9050405

32. Mohd Mutalip SS, Ab-Rahim S, Rajikin MH. Vitamin E as an antioxidant in female reproductive health. *Antioxidants.* (2018) 7:22. doi: 10.3390/antiox7020022

33. Wu Y, He T, Fu Y, Chen J. Corynoline protects lipopolysaccharide-induced mastitis through regulating AKT/GSK3β/Nrf2 signaling pathway. *Environ Toxicology.* (2021) 36:2493–9. doi: 10.1002/tox.v36.12

34. Guo W, Liu J, Li W, Ma H, Gong Q, Kan X, et al. Niacin alleviates dairy cow mastitis by regulating the GPR109A/AMPK/NRF2 signaling pathway. *Int J Mol Sci.* (2020) 21:3321. doi: 10.3390/ijms21093321

35. Arbab AA, Lu X, Abdalla IM, Idris AA, Chen Z, Li M, et al. Metformin inhibits lipoteichoic acid–induced oxidative stress and inflammation through AMPK/NRF2/NF-κB signaling pathway in bovine mammary epithelial cells. *Front Veterinary Science.* (2021) 8:661380. doi: 10.3389/fvets.2021.661380

36. Zhou Y, Lan R, Xu Y, Zhou Y, Lin X, Miao J. Resveratrol alleviates oxidative stress caused by Streptococcus uberis infection via activating the Nrf2 signaling pathway. *Int Immunopharmacology.* (2020) 89:107076. doi: 10.1016/j.intimp.2020.107076

37. Silwal P, Kim JK, Kim YJ, Jo EK. Mitochondrial reactive oxygen species: double-edged weapon in host defense and pathological inflammation during infection. *Front Immunol.* (2020) 11:554462. doi: 10.3389/fimmu.2020.01649

38. Mirza Z, Walhout AJ, Ambros V. A bacterial pathogen induces developmental slowing by high reactive oxygen species and mitochondrial dysfunction in Caenorhabditis elegans. *Cell Rep.* (2023) 42:113189. doi: 10.1016/j.celrep.2023.113189

39. Srithanasuwan A, Tata L, Tananupak W, Jaraja W, Suriyasathaporn W, Chuammitri P. Exploring the distinct immunological reactions of bovine neutrophils towards major and minor pathogens responsible for mastitis. *Int J Veterinary Sci Med.* (2023) 11:106–20. doi: 10.1080/23144599.2023.2262250

40. Rainard P, Foucras G, Martins RP. Adaptive cell-mediated immunity in the mammary gland of dairy ruminants. *Front Veterinary Science.* (2022) 9:854890. doi: 10.3389/fvets.2022.854890

41. Chen Y, Yang J, Huang Z, Yin B, Umar T, Yang C, et al. Vitexin mitigates Staphylococcus aureus-induced mastitis via regulation of ROS/ER stress/NF-κB/MAPK pathway. *Oxid Med Cell Longevity.* (2022) 2022:7977433. doi: 10.1155/2022/7977433

42. Ma F, Yang S, Zhou M, Lu Y, Deng B, Zhang J, et al. NADPH oxidase-derived reactive oxygen species production activates the ERK1/2 pathway in neutrophil extracellular traps formation by Streptococcus agalactiae isolated from clinical mastitis bovine. *Veterinary Microbiol.* (2022) 268:109427. doi: 10.1016/j.vetmic.2022.109427

43. Li B, Wan Z, Wang Z, Zuo J, Xu Y, Han X, et al. TLR2 signaling pathway combats Streptococcus uberis infection by inducing mitochondrial reactive oxygen species production. *Cells.* (2020) 9:494. doi: 10.3390/cells9020494

44. Biswas S, Mukherjee R, Chakravarti S, Bera AK, Bandyopadhyay S, De UK, et al. Influence of pathogens specific subclinical mastitis on oxidative status and mineral metabolism of yak. *Emerging Anim Species.* (2023) 8:100028. doi: 10.1016/j.eas.2023.100028

45. Ma Y, Cheng L, Gao X, Elsabagh M, Feng Y, Li Z, et al. Melatonin modulates lipopolysaccharides-induced inflammatory response and maintains circadian rhythm associated with histone H3 acetylation in bovine mammary epithelial cells. *J Funct Foods.* (2024) 116:106156. doi: 10.1016/j.jff.2024.106156

46. Cai X, Zhou Z, Kan X, Xu P, Guo W, Fu S, et al. Daidzein relieves lipopolysaccharide-induced mastitis through inhibiting MAPKs and AKT/NF-κB P65 signaling pathways. *Rev Bras Farmacognosia.* (2024) 29:1–2. doi: 10.1007/s43450-024-00529-4

47. Yu C, Zhang C, Huai Y, Liu D, Zhang M, Wang H, et al. The inhibition effect of caffeic acid on NOX/ROS-dependent macrophages M1-like polarization contributes to relieve the LPS-induced mice mastitis. *Cytokine.* (2024) 174:156471. doi: 10.1016/j.cyto.2023.156471

48. Luo H, Li Y, Xie J, Xu C, Zhang Z, Li M, et al. Effect and mechanism of Prunella vulgaris L. extract on alleviating lipopolysaccharide-induced acute mastitis in protecting the blood-milk barrier and reducing inflammation. *J Ethnopharmacology.* (2024) 12:117998. doi: 10.1016/j.jep.2024.117998

49. Choudhary RK, Olszanski L, McFadden TB, Lalonde C, Spitzer A, Shangraw EM, et al. Systemic and local responses of cytokines and tissue histology following intramammary lipopolysaccharide challenge in dairy cows. *J Dairy Science.* (2024) 107:1299–310. doi: 10.3168/jds.2023-23543

50. Abuelo A, Hernández J, Benedito JL, Castillo C. Redox biology in transition periods of dairy cattle: Role in the health of periparturient and neonatal animals. *Antioxidants.* (2019) 8:20. doi: 10.3390/antiox8010020

51. Aitken SL, Karcher EL, Rezamand P, Gandy JC, VandeHaar MJ, Capuco AV, et al. Evaluation of antioxidant and proinflammatory gene expression in bovine mammary tissue during the periparturient period. *J dairy science.* (2009) 92:589–98. doi: 10.3168/jds.2008-1551

52. Huang Q, Liu J, Peng C, Han X, Tan Z. Hesperidin ameliorates H2O2-induced bovine mammary epithelial cell oxidative stress via the Nrf2 signaling pathway. *J Anim Sci Biotechnol.* (2024) 15:57. doi: 10.1186/s40104-024-01012-9

53. Senthamilan S, Aggarwal A, Grewal S, Rani S, Vats P, Pal P, et al. Pre-treatment but not co-treatment with vitexin alleviates hyperthermia induced oxidative stress and inflammation in buffalo mammary epithelial cells. *J Reprod Immunol.* (2023) 158:103979. doi: 10.1016/j.jri.2023.103979

54. Ayemele AG, Tilahun M, Lingling S, Elsaadawy SA, Guo Z, Zhao G, et al. Oxidative stress in dairy cows: insights into the mechanistic mode of actions and mitigating strategies. *Antioxidants.* (2021) 10:1918. doi: 10.3390/antiox10121918

55. Rakib MR, Zhou M, Xu S, Liu Y, Khan MA, Han B, et al. Effect of heat stress on udder health of dairy cows. *J dairy Res.* (2020) 87:315–21. doi: 10.1017/S0022029920000886

56. Zhu H, Cao W, Huang Y, Karrow NA, Yang Z. Involvement of pyocyanin in promoting LPS-induced apoptosis, inflammation, and oxidative stress in bovine mammary epithelium cells. *Agriculture.* (2023) 13:2192. doi: 10.3390/agriculture13122192

57. Liu D, Lin J, He W, Huang K. Selenium and taurine combination is better than alone in protecting lipopolysaccharide-induced mammary inflammatory lesions via activating PI3K/Akt/mTOR signaling pathway by scavenging intracellular ROS. *Oxid Med Cell Longevity.* (2021) 2021:5048375. doi: 10.1155/2021/5048375

58. Lyu CC, Ji XY, Che HY, Meng Y, Wu HY, Zhang JB, et al. CGA alleviates LPS-induced inflammation and milk fat reduction in BMECs through the NF-κB signaling pathway. *Heliyon.* (2024) 10:e25004. doi: 10.1016/j.heliyon.2024.e25004

59. Zhou M, Barkema HW, Gao J, Yang J, Wang Y, Kastelic JP, et al. MicroRNA miR-223 modulates NLRP3 and Keap1, mitigating lipopolysaccharide-induced inflammation and oxidative stress in bovine mammary epithelial cells and murine mammary glands. *Veterinary Res.* (2023) 1454:78. doi: 10.1186/s13567-023-01206-5

60. Zhao W, Deng Z, Barkema HW, Xu M, Gao J, Liu G, et al. Nrf2 and NF-κB/NLRP3 inflammasome pathways are involved in Prototheca bovis infections of mouse mammary gland tissue and mammary epithelial cells. *Free Radical Biol Med.* (2022) 1184:148–57. doi: 10.1016/j.freeradbiomed.2022.04.005

61. Ko YC, Choi HS, Kim SL, Yun BS, Lee DS. Anti-inflammatory effects of (9Z, 11E)-13-Oxooctadeca-9, 11-dienoic acid (13-KODE) derived from Salicornia herbacea L. @ on lipopolysaccharide-stimulated murine macrophage via NF-kB and MAPK inhibition and Nrf2/HO-1 signaling activation. *Antioxidants.* (2022) 11:180. doi: 10.3390/antiox11020180

62. Fu K, Sun Y, Wang J, Cao R. Tanshinone IIa alleviates LPS-induced oxidative stress in dairy cow mammary epithelial cells by activating the Nrf2 signalling pathway. *Res Veterinary Science.* (2022) 151:149–55. doi: 10.1016/j.rvsc.2022.08.008

63. Khan MZ, Li L, Wang T, Liu X, Chen W, Ma Q, et al. Bioactive compounds and probiotics mitigate mastitis by targeting NF-κB signaling pathway. *Biomolecules.* (2024) 14:1011. doi: 10.3390/biom14081011

64. Kang S, Lee JS, Lee HC, Petriello MC, Kim BY, Do JT, et al. Phytoncide extracted from pinecone decreases LPS-induced inflammatory responses in bovine mammary epithelial cells. *J Microbiol Biotechnol.* (2017) 26:579–87. doi: 10.4014/jmb.1510.10070

65. Yu GM, Kubota H, Okita M, Maeda T. The anti-inflammatory and antioxidant effects of melatonin on LPS-stimulated bovine mammary epithelial cells. *PloS One.* (2017) 12:e0178525. doi: 10.1371/journal.pone.0178525

66. Wang K, Jin XL, Shen XG, Sun LP, Wu LM, Wei JQ, et al. Effects of Chinese propolis in protecting bovine mammary epithelial cells against mastitis pathogens-induced cell damage. *Mediators inflammation.* (2016) 2016:8028291. doi: 10.1155/2016/8028291

67. Jin X, Wang K, Liu H, Hu F, Zhao F, Liu J. Protection of bovine mammary epithelial cells from hydrogen peroxide-induced oxidative cell damage by resveratrol. *Oxid Med Cell Longevity.* (2016) 2016:2572175. doi: 10.1155/2016/2572175

68. Gao XJ, Guo MY, Zhang ZC, Wang TC, Cao YG, Zhang NS. Bergenin plays an anti-inflammatory role via the modulation of MAPK and NF-κB signaling pathways in a mouse model of LPS-induced mastitis. *Inflammation.* (2015) 38:1142–50. doi: 10.1007/s10753-014-0079-8

69. Ma X, Xu S, Li J, Cui L, Dong J, Meng X, et al. Selenomethionine protected BMECs from inflammatory injury and oxidative damage induced by Klebsiella pneumoniae by inhibiting the NF-κB and activating the Nrf2 signaling pathway. *Int Immunopharmacology.* (2022) 109027. doi: 10.1016/j.intimp.2022.109027

70. Ma Y, Ma X, An Y, Sun Y, Dou W, Li M, et al. Green tea polyphenols alleviate hydrogen peroxide-induced oxidative stress, inflammation, and apoptosis in bovine mammary epithelial cells by activating erk1/2–nfe2l2–hmox1 pathways. *Front Veterinary Science.* (2022) 8:804241. doi: 10.3389/fvets.2021.804241

71. Zhu G, Sui S, Shi F, Wang Q. Inhibition of USP14 suppresses ferroptosis and inflammation in LPS-induced goat mammary epithelial cells through ubiquitylating the IL-6 protein. *Hereditas.* (2022) 159:21. doi: 10.1186/s41065-022-00235-y

72. Dai H, Coleman DN, Hu L, Martinez-Cortés I, Wang M, Parys C, et al. Methionine and arginine supplementation alter inflammatory and oxidative stress responses during lipopolysaccharide challenge in bovine mammary epithelial cells *in vitro*. *J Dairy Sci.* (2020) 103:676–89. doi: 10.3168/jds.2019-16631

73. Fusco R, Cordaro M, Siracusa R, Peritore AF, D'Amico R, Licata P, et al. Effects of hydroxytyrosol against lipopolysaccharide-induced inflammation and oxidative stress in bovine mammary epithelial cells: A natural therapeutic tool for bovine mastitis. *Antioxidants.* (2020) 9:693. doi: 10.3390/antiox9080693

74. Guo W, Liu J, Sun J, Gong Q, Ma H, Kan X, et al. Butyrate alleviates oxidative stress by regulating NRF2 nuclear accumulation and H3K9/14 acetylation via GPR109A in bovine mammary epithelial cells and mammary glands. *Free Radical Biol Med*. (2020) 152:728–42. doi: 10.1016/j.freeradbiomed.2020.01.016

75. Shi H, Guo X, Yan S, Guo Y, Shi B, Zhao Y. VA inhibits LPS-induced oxidative stress via modulating Nrf2/NF-κB-signalling pathways in bovine mammary epithelial cells. *Ital J Anim Science*. (2019) 18:1099–110. doi: 10.1080/1828051X.2019.1619490

76. Shi HY, Yan SM, Guo YM, Zhang BQ, Guo XY, Shi BL. Vitamin A pretreatment protects NO-induced bovine mammary epithelial cells from oxidative stress by modulating Nrf2 and NF-κB signaling pathways. *J Anim Science*. (2018) 96:1305–16. doi: 10.1093/jas/sky037

77. Wang F, Zhao Y, Chen S, Chen L, Sun L, Cao M, et al. Astragaloside IV alleviates ammonia-induced apoptosis and oxidative stress in bovine mammary epithelial cells. *Int J Mol Sci*. (2019) 20:600. doi: 10.3390/ijms20030600

78. Yu GM, Tan W. Melatonin inhibits lipopolysaccharide-induced inflammation and oxidative stress in cultured mouse mammary tissue. *Mediators Inflammation*. (2019) 2019(1):8597159. doi: 10.1155/2019/8597159

79. Lyu C, Yuan B, Meng Y, Cong S, Che H, Ji X, et al. Puerarin alleviates H2O2-induced oxidative stress and blood–milk barrier impairment in dairy cows. *Int J Mol Sci*. (2023) 24:7742. doi: 10.3390/ijms24097742

80. Ali I, Li C, Kuang M, Shah AU, Shafiq M, Ahmad MA, et al. Nrf2 Activation and NF-Kb & caspase/bax signaling inhibition by sodium butyrate alleviates LPS-induced cell injury in bovine mammary epithelial cells. *Mol Immunol*. (2022) 148:54–67. doi: 10.1016/j.molimm.2022.05.121

81. Meng M, Huo R, Wang Y, Ma N, Shi X, Shen X, et al. Lentinan inhibits oxidative stress and alleviates LPS-induced inflammation and apoptosis of BMECs by activating the Nrf2 signaling pathway. *Int J Biol Macromolecules*. (2022) 222:2375–91. doi: 10.1016/j.ijbiomac.2022.10.024

82. Wang N, Zhu Y, Li D, Basang W, Huang Y, Liu K, et al. 2-methyl nonyl ketone from houttuynia cordata thunb alleviates LPS-induced inflammatory response and oxidative stress in bovine mammary epithelial cells. *Front Chem*. (2022) 9:793475. doi: 10.3389/fchem.2021.793475

83. Zhao N, Yang Y, Xu H, Li L, Hu Y, Liu E, et al. Betaine protects bovine mammary epithelial cells against LPS-induced inflammatory response and oxidative damage via modulating NF-κB and Nrf2 signalling pathway. *Ital J Anim science*. (2022) 21:859–69. doi: 10.1080/1828051X.2022.2070035

84. Guo W, Li W, Su Y, Liu S, Kan X, Ran X, et al. GPR109A alleviate mastitis and enhances the blood milk barrier by activating AMPK/Nrf2 and autophagy. *Int J Biol Sci*. (2021) 17:4271. doi: 10.7150/ijbs.62380

85. Li R, Fang H, Shen J, Jin Y, Zhao Y, Wang R, et al. Curcumin alleviates LPS-induced oxidative stress, inflammation and apoptosis in bovine mammary epithelial cells via the NFE2L2 signaling pathway. *Toxins*. (2021) 13:208. doi: 10.3390/toxins13030208

86. Liu M, Zhang C, Xu X, Zhao X, Han Z, Liu D, et al. Ferulic acid inhibits LPS-induced apoptosis in bovine mammary epithelial cells by regulating the NF-κB and Nrf2 signalling pathways to restore mitochondrial dynamics and ROS generation. *Veterinary Res*. (2021) 52:1–1. doi: 10.1186/s13567-021-00973-3

87. Liu S, Guo W, Jia Y, Ye B, Liu S, Fu S, et al. Menthol targeting AMPK alleviates the inflammatory response of bovine mammary epithelial cells and restores the synthesis of milk fat and milk protein. *Front Immunol*. (2021) 12:782989. doi: 10.3389/fimmu.2021.782989

88. Sun Y, Wu Y, Wang Z, Chen J, Yang Y, Dong G. Dandelion extract alleviated lipopolysaccharide-induced oxidative stress through the Nrf2 pathway in bovine mammary epithelial cells. *Toxins*. (2020) 12:496. doi: 10.3390/toxins12080496

89. Chen P, Yang J, Wu N, Han B, Kastelic JP, Gao J. Streptococcus lutetiensis induces autophagy via oxidative stress in bovine mammary epithelial cells. *Oxid Med Cell Longevity*. (2022) 72022:2549772. doi: 10.1155/2022/2549772

90. Cheng X, Aabdin ZU, Wang Y, Ma N, Dai H, Shi X, et al. Glutamine pretreatment protects bovine mammary epithelial cells from inflammation and oxidative stress induced by γ-d-glutamyl-meso-diaminopimelic acid (iE-DAP). *J Dairy Science*. (2021) 104:2123–39. doi: 10.3168/jds.2020-18402

91. Li Y, Han N, Hou P, Zhao FQ, Liu H. Roles of MAPK and Nrf2 signaling pathways in quercetin alleviating redox imbalance induced by hydrogen peroxide in mammary epithelial cells. *Anim Nutriomics*. (2024) 1:e1. doi: 10.1017/anr.2024.2

92. Xu M, Che L, Gao K, Wang L, Yang X, Wen X, et al. Taurine alleviates oxidative stress in porcine mammary epithelial cells by stimulating the Nrf2-MAPK signaling pathway. *Food Sci Nutr*. (2023) 11:1736–46. doi: 10.1002/fsn3.v11.4

93. Kan X, Liu J, Chen Y, Guo W, Xu D, Cheng J, et al. Myricetin protects against H2O2-induced oxidative damage and apoptosis in bovine mammary epithelial cells. *J Cell Physiol*. (2021) 236:2684–95. doi: 10.1002/jcp.v236.4

94. Perruchot MH, Gondret F, Robert F, Dupuis E, Quesnel H, Dessauge F. Effect of the flavonoid baicalin on the proliferative capacity of bovine mammary cells and their ability to regulate oxidative stress. *PeerJ*. (2019) 7:e6565. doi: 10.7717/peerj.6565

95. Sun X, Jia H, Xu Q, Zhao C, Xu C. Lycopene alleviates H2O2-induced oxidative stress, inflammation and apoptosis in bovine mammary epithelial cells via the NFE2L2 signaling pathway. *Food Funct*. (2019) 10:6276–85. doi: 10.1039/C9FO01922G

96. Shao D, Gao Z, Zhao Y, Fan M, Zhao X, Wei Q, et al. Sulforaphane suppresses H2O2-induced oxidative stress and apoptosis via the activation of AMPK/NFE2L2 signaling pathway in goat mammary epithelial cells. *Int J Mol Sci*. (2023) 24:1070. doi: 10.3390/ijms24021070

97. Zhang J, Wang J, Fang H, Yu H, Zhao Y, Shen J, et al. Pterostilbene inhibits deoxynivalenol-induced oxidative stress and inflammatory response in bovine mammary epithelial cells. *Toxicon*. (2021) 189:10–8. doi: 10.1016/j.toxicon.2020.11.002

98. Xu J, Wang XL, Zeng HF, Han ZY. Methionine alleviates heat stress-induced ferroptosis in bovine mammary epithelial cells through the Nrf2 pathway. *Ecotoxicology Environ Safety*. (2023) 256:114889. doi: 10.1016/j.ecoenv.2023.114889

99. Wang H, Hao W, Yang L, Li T, Zhao C, Yan P, et al. Procyanidin B2 alleviates heat-induced oxidative stress through the Nrf2 pathway in bovine mammary epithelial cells. *Int J Mol Sci*. (2022) 23:7769. doi: 10.3390/ijms23147769

100. Wang Y, Wang HL, Xing GD, Qian Y, Zhong JF, Chen KL. S-allyl cysteine ameliorates heat stress-induced oxidative stress by activating Nrf2/HO-1 signaling pathway in BMECs. *Toxicol Appl Pharmacol*. (2021) 416:115469. doi: 10.1016/j.taap.2021.115469

101. Li C, Wang Y, Li L, Han Z, Mao S, Wang G. Betaine protects against heat exposure–induced oxidative stress and apoptosis in bovine mammary epithelial cells via regulation of ROS production. *Cell Stress Chaperones*. (2019) 24:453–60. doi: 10.1007/s12192-019-00982-4

102. Ding H, Li Y, Zhao C, Yang Y, Xiong C, Zhang D, et al. Rutin supplementation reduces oxidative stress, inflammation and apoptosis of mammary gland in sheep during the transition period. *Front veterinary science*. (2022) 279:907299. doi: 10.3389/fvets.2022.907299

103. Lebda MA, Elmassry IH, Taha NM, Elfeky MS. Nanocurcumin alleviates inflammation and oxidative stress in LPS-induced mastitis via activation of Nrf2 and suppressing TLR4-mediated NF-κB and HMGB1 signaling pathways in rats. *Environ Sci pollut Res*. (2022) F1:1–2. doi: 10.1007/s11356-021-16309-9

104. Gross JJ, Grossen-Rösti L, Héritier R, Tröscher A, Bruckmaier RM. Inflammatory and metabolic responses to an intramammary lipopolysaccharide challenge in early lactating cows supplemented with conjugated linoleic acid. *J Anim Physiol Anim Nutr*. (2018) 102:102–48. doi: 10.1111/jpn.2018.102.issue-2

105. Hanschke N, Kankofer M, Ruda L, Höltershinken M, Meyer U, Frank J, et al. The effect of conjugated linoleic acid supplements on oxidative and antioxidative status of dairy cows. *J Dairy Sci*. (2016) 99:8090–102. doi: 10.3168/jds.2015-10685

106. Basiricò L, Morera P, Dipasquale D, Tröscher A, Serra A, Mele M, et al. Conjugated linoleic acid isomers strongly improve the redox status of bovine mammary epithelial cells (BME-UV1). *J Dairy Sci*. (2015) 98:7071–82. doi: 10.3168/jds.2015-9787

107. Ma N, Wei G, Zhang H, Dai H, Roy AC, Shi X, et al. Cis-9, trans-11 CLA alleviates lipopolysaccharide-induced depression of fatty acid synthesis by inhibiting oxidative stress and autophagy in bovine mammary epithelial cells. *Antioxidants*. (2021) 11:55. doi: 10.3390/antiox11010055

108. Shao D, Shen W, Miao Y, Gao Z, Pan M, Wei Q, et al. Sulforaphane prevents LPS-induced inflammation by regulating the Nrf2-mediated autophagy pathway in goat mammary epithelial cells and a mouse model of mastitis. *J Anim Sci Biotechnol*. (2023) 14:61. doi: 10.1186/s40104-023-00858-9

109. He X, Wang J, Sun L, Ma W, Li M, Yu S, et al. Wogonin attenuates inflammation and oxidative stress in lipopolysaccharide-induced mastitis by inhibiting Akt/NF-κB pathway and activating the Nrf2/HO-1 signaling. *Cell Stress Chaperones*. (2023) 28:989–99. doi: 10.1007/s12192-023-01391-4

110. Malik MU, Hashmi N, Khan M, Aabdin ZU, Sami R, Aljahani AH, et al. Nutraceutical effect of resveratrol on the mammary gland: focusing on the NF-κb/nrf2 signaling pathways. *Animals*. (2023) 13:1266. doi: 10.3390/ani13071266

111. Zheng Z, Zheng Y, Liang X, Xue G, Wu H. Sanguinarine enhances the integrity of the blood–milk barrier and inhibits oxidative stress in lipopolysaccharide-stimulated mastitis. *Cells*. (2022) 11:3658. doi: 10.3390/cells11223658

112. Zhao C, Wu K, Bao L, Chen L, Feng L, Liu Z, et al. Kynurenic acid protects against mastitis in mice by ameliorating inflammatory responses and enhancing blood-milk barrier integrity. *Mol Immunol*. (2021) 134–44. doi: 10.1016/j.molimm.2021.06.022

113. Ran X, Zhang Y, Yang Y, Hu G, Liu J, Hou S, et al. Dioscin improves pyroptosis in LPS-induced mice mastitis by activating AMPK/Nrf2 and inhibiting the NF-κB signaling pathway. *Oxid Med Cell longevity*. (2020) 2020:1–25. doi: 10.1155/2020/8845521

114. Xu D, Liu J, Ma HE, Guo W, Wang J, Kan X, et al. Schisandrin A protects against lipopolysaccharide-induced mastitis through activating Nrf2 signaling pathway and inducing autophagy. *Int Immunopharmacology*. (2020) 78:105983. doi: 10.1016/j.intimp.2019.105983

115. Zhao C, Jiang P, He Z, Yuan X, Guo J, Li Y, et al. Dimethyl itaconate protects against lippolysacchride-induced mastitis in mice by activating MAPKs and Nrf2 and inhibiting NF-κB signaling pathways. *Microbial pathogenesis*. (2019) 133:103541. doi: 10.1016/j.micpath.2019.05.024

116. Li M, Wang Z, Fu S, Sun N, Li W, Xu Y, et al. Taurine reduction of injury from neutrophil infiltration ameliorates Streptococcus uberis-induced mastitis. *Int Immunopharmacology*. (2023) 124:111028. doi: 10.1016/j.intimp.2023.111028

117. Zhao L, Jin L, Yang B. Diosmetin alleviates S. aureus-induced mastitis by inhibiting SIRT1/GPX4 mediated ferroptosis. *Life Sci*. (2023) 331:122060. doi: 10.1016/j.lfs.2023.122060

118. Zhao L, Jin L, Yang B. Saikosaponin A alleviates Staphylococcus aureus-induced mastitis in mice by inhibiting ferroptosis via SIRT1/Nrf2 pathway. *J Cell Mol Med*. (2023) 27:3443–50. doi: 10.1111/jcmm.v27.22

119. Glorieux C, Enríquez C, González C, Aguirre-Martínez G, Buc Calderon P. The multifaceted roles of NRF2 in Cancer: friend or foe? *Antioxidants*. (2024) 13:70. doi: 10.3390/antiox13010070

120. Occhiuto CJ, Moerland JA, Leal AS, Gallo KA, Liby KT. The multi-faceted consequences of NRF2 activation throughout carcinogenesis. *Molecules Cells*. (2023) 46:176–86. doi: 10.14348/molcells.2023.2191

121. Wu S, Lu H, Bai Y. Nrf2 in cancers: A double-edged sword. *Cancer Med*. (2019) 8:2252–67. doi: 10.1002/cam4.2019.8.issue-5

122. Jeddi F, Soozangar N, Sadeghi MR, Somi MH, Samadi N. Contradictory roles of Nrf2/Keap1 signaling pathway in cancer prevention/promotion and chemoresistance. *DNA repair*. (2017) 54:13–21. doi: 10.1016/j.dnarep.2017.03.008

123. Lin L, Wu Q, Lu F, Lei J, Zhou Y, Liu Y, et al. Nrf2 signaling pathway: current status and potential therapeutic targetable role in human cancers. *Front Oncol*. (2023) 13:1184079. doi: 10.3389/fonc.2023.1184079

frontiers | Frontiers in Immunology

TYPE Review
PUBLISHED 26 February 2025
DOI 10.3389/fimmu.2025.1506500

OPEN ACCESS

EDITED BY
Uzma Saqib,
Indian Institute of Technology Indore, India

REVIEWED BY
Sutripta Sarkar,
Barrackpore Rastraguru Surendranath College, India
Xinxing Wan,
Central South University, China

*CORRESPONDENCE
Yue Qiu
15179280806@163.com

†These authors have contributed equally to this work

RECEIVED 05 October 2024
ACCEPTED 12 February 2025
PUBLISHED 26 February 2025

CITATION
Zhuo Y, Fu S and Qiu Y (2025) Regulation of the immune microenvironment by SUMO in diabetes mellitus. *Front. Immunol.* 16:1506500. doi: 10.3389/fimmu.2025.1506500

Regulation of the immune microenvironment by SUMO in diabetes mellitus

Yuting Zhuo[1,2†], Shangui Fu[2†] and Yue Qiu[1*]

[1]Department of Endocrinology and Metabolism, Jiujiang Hospital of Traditional Chinese Medicine, Jiujiang, Jiangxi, China, [2]The Second School of Clinical Medicine, Jiangxi Medical College, Nanchang University, Nanchang, Jiangxi, China

Post-translational modifications such as SUMOylation are crucial for the functionality and signal transduction of a diverse array of proteins. Analogous to ubiquitination, SUMOylation has garnered significant attention from researchers and has been implicated in the pathogenesis of various human diseases in recent years, such as cancer, neurological lesions, cardiovascular diseases, diabetes mellitus, and so on. The pathogenesis of diabetes, particularly type 1 and type 2 diabetes, has been closely associated with immune dysfunction, which constitutes the primary focus of this review. This review will elucidate the process of SUMOylation and its impact on diabetes mellitus development and associated complications, focusing on its regulatory effects on the immune microenvironment. This article summarizes various signaling pathways at both cellular and molecular levels that are implicated in these processes. Furthermore, it proposes potential new targets for drug development aimed at the prevention and treatment of diabetes mellitus based on insights gained from the SUMOylation process.

KEYWORDS

immune, SUMOylation, diabetes mellitus, inflammation, posttranslation modification, signaling pathway

1 Introduction

In the context of globalization, diabetes mellitus (DM) has emerged as a critical public health issue and a substantial economic burden on healthcare systems worldwide. The estimated prevalence of DM in the adult population was 10.5% in 2021, with projections indicating a continued rise in prevalence, as reported in the survey (1). From 2007 to 2017, there was a notable increase in the prevalence of DM among Chinese adults, and the number of diabetes-related risk factors remained uncontrolled (2). Therefore, addressing the challenge posed by DM has emerged as an urgent priority for the public health protection system. DM is a group of metabolic disorders that are characterized by hyperglycemia. Based on the diagnostic and classification criteria set forth by the American Diabetes Association (ADA),

DM is classified into four categories: type 1 diabetes mellitus (T1DM), type 2 diabetes mellitus(T2DM), gestational diabetes mellitus (GDM), and other types of DM. T1DM is regarded as an autoimmune disease, which is characterized by the autoimmune destruction of pancreatic β-cells. T2DM constitutes over 90% of all DM types, with a more intricate underlying mechanism than that of T1DM. This condition is marked by insulin resistance and a relative insulin deficiency (3, 4). DM is frequently a multifactorial disease that can present in various forms, including immune dysregulation, glucose metabolism disorders, insulin resistance, and β-cell destruction (5). In these cases, immune dysfunction exerts an influence on the development of DM, which is caused by various factors and contributes to the onset of DM and its associated complications (6, 7).

Since the initial identification of small ubiquitin-like modifier (SUMO) proteins in 1996, these proteins have increasingly been recognized as versatile and important post-translation modifications (PTMs) (8). SUMO proteins constitute a family of proteins that modulate their function through the processes of associating with other proteins (SUMOylation) and dissociating from them (deSUMOylation) (9). The modification of the substrate protein is reversible. Similar to ubiquitination, SUMOylation plays a critical role in regulating various cellular processes by modulating distinct substrates. This modulation influences the stability and subcellular localization of proteins, as well as impacting essential processes such as cell cycle regulation (10), DNA synthesis and repair (11), signal transduction, and cellular immunity (12).

2 SUMOylation

2.1 Overview of SUMOylation

The attachment of SUMO proteins to a cysteine residue within a protein is termed SUMOylation. In contrast, the removal of SUMO proteins from the substrate is referred to as deSUMOylation. *In vivo*, the SUMOylation and deSUMOylation processes reciprocally regulate the SUMOylated state of proteins.

The three-dimensional structure of SUMO proteins exhibits a similarity to that of ubiquitin, as both proteins belong to the conserved ubiquitin-like protein (UBL) family. SUMO proteins covalently bind to the lysine residues of target proteins through a cascade reaction facilitated by a series of enzymes. SUMO1, SUMO2, SUMO3, SUMO4 (13), and SUMO5 (14) are the five isoforms of SUMO proteins that have been described. Of these, there is widespread expression of SUMO1, SUMO2, and SUMO3 *in vivo*. The amino acid sequences of SUMO2 and SUMO3 are essentially identical but have only 46% homogeneity with SUMO1 (15–17). The expression of SUMO4 is predominantly observed in immune tissues, including the kidneys, spleen, and lymph nodes (18). Numerous studies have demonstrated a strong association between SUMO4 and the development of T1DM and T2DM (19–22). Additionally, SUMO5 is tissue-specific, highly conserved in primates, and is also involved in the formation and destruction of promyelocytic leukemia nuclear body (PML-NB) (14).

2.2 Mechanism of SUMOylation

The process of SUMOylation is analogous to ubiquitination, as the SUMO protein binds to the substrate protein through a series of enzymatic reactions. (Table 1) The principal enzymes involved in this process are, in order: the activation enzyme 1 (E1, Aos1/Uba2 heterodimer), conjugation enzyme 2 (E2, Ubc9), and SUMO ligation enzyme 3 (E3, such as PIAS, ZNF451, and RanBP2) (23–28). The PIAS family is the major SUMO E3 ligase and comprises PIAS1, PIAS2 (PIASx), PIAS3, and PIAS4 (PIASy) (29, 30). Subsequently, SUMO-specific proteases (SENPs) execute the deSUMOylation process.

The process of SUMOylation can be categorized into four principal stages: the maturation of SUMO, activation of SUMO by the E1 enzyme, the activated SUMO binds to the E2 enzyme and promotion of the conjugation of SUMO to the substrate by the E3 enzyme. (Figure 1) (i) The first step in SUMO maturation begins with SENPs degrading several amino acids at the C-terminus of SUMOs to expose the diglycine residues. (ii) Next, in the presence of ATP, the diglycine residues of mature SUMOs interact with the cysteine residue of the E1 enzyme, forming high-energy thioester bonds. E1s are constituted by two subunits: the SUMO-activating enzyme subunit 1 (SAE1 or Aos1) and the SUMO-activating enzyme subunit 2 (SAE2 or Uba2). Typically, these two subunits assemble into ATP-dependent heterodimers consisting of SAE1 and SAE2 (31, 32). The process of SUMO activation is accomplished through the mechanism above (33). (iii) Subsequently, SUMOs are transferred from the E1 to the E2, resulting in the formation of a SUMO-E2 complex. The only E2 binding enzyme identified is ubiquitin conjugating enzyme 9 (Ubc9) (34–36). (iv) Ultimately, under the catalytic influence of E3 ligases, Ubc9 directly recognizes the conserved sequence Ψ-Kx-D/E (Ψ represents a hydrophobic group, K denotes lysine conjugated to SUMO, x signifies any amino acid, and D/E indicates an acidic amino acid, either aspartic acid or glutamic acid) within the substrate. This recognition facilitates the conjugation of SUMO proteins to lysine residues of the substrate, forming isopeptide bonds and thereby completing the transfer of SUMO from the E2 enzyme to the substrate (37). The process of deSUMOylation is defined as the dissociation of SUMO from the substrate protein. The SENPs encompass various species, with seven members of the SENP family identified in the human genome, specifically SENPs 1–3 and 5–7 (38). In summary, SUMOylation is characterized by two major features: specificity and reversibility. The specificity is determined by the combined action of Ubc9 and E3 ligases, while the reversibility is achieved through the deSUMOylation process mediated by SENPs. This ensures the dynamic regulation of SUMOylation.

SUMOylation, a crucial post-translational modification of proteins, regulates key cellular processes through diverse molecular mechanisms. Notably, the fragile replication fork structure becomes particularly susceptible to chromosomal rearrangements and mutations during DNA replication. Studies have revealed that Pli1, an E3 SUMO ligase, mediates SUMOylation to perform dual functions: it not only maintains replication fork integrity but also promotes their translocation to nuclear pore complexes (NPCs) via

TABLE 1 The enzymes of SUMOylation in mammal cells.

Enzyme	Homo sapiens	Mechanisms of enzymes in inflammation and diabetes	References
E1 activating enzymes	SAE1-SAE2 (Aos1/Uba2 heterodimer)	Overexpression of SAE1/Uba2 promotes glycolysis in cells, increases lactate secretion and enhances the expression of proinflammatory cytokines.	(133)
E2 conjugating enzymes	Ubc9	Both conditional ablation and overexpression of Ubc9 in pancreatic β cells impair β cell function and subsequently lead to diabetes.	(66)
E3 ligases	PIAS1, PIASx (2), PIAS3, PIASy (4)	PIAS-family proteins mediate the SUMOylation of Glis3, leading to decreased insulin transcription.	(134)
	ZNF451	ZNF451 inhibits the transcription of Smad3/4 and negatively regulates TGF-β signaling.	(135)
	RanBP2	Inhibition of the Insulin-like Growth Factor 1 Receptor (IGF1R)/RanBP2/SUMO1 complex formation restricts the expression of proinflammatory cytokines.	(136)
	STAT	SAE1/Uba2 promotes the phosphorylation and nuclear translocation of PKM2 through SUMOylation, thereby enhancing STAT5A expression and regulating glycolysis.	(133)
	Pc2	——	——
	MAPL	MAPL regulates inflammatory responses by suppressing NLRP3 inflammasome activity through SUMOylation.	(74)
deSUMOylation	SENPs 1–3 and 5–7	SENP2 modulates diabetes-associated lipid metabolism through regulating the deSUMOylation of SET domain bifurcated 1 (Setdb1).	(106)
		SENP6 and SENP7 regulate NLRP3 inflammasome activity through their deSUMOylation modification function.	(74)

poly-SUMOylation-induced SUMO chain formation. This regulatory mechanism orchestrates the precise repair of replication forks and is essential for preserving genomic stability (11).

Emerging evidence has highlighted the pivotal role of SUMOylation regulation in cell cycle control. Mechanistically, lactate has been shown to inhibit the deSUMOylation activity of SENP1 through zinc ion chelation at its active site, leading to enhanced APC4 SUMOylation. This post-translational modification triggers structural remodeling of the anaphase-promoting complex (APC/C), facilitating its interaction with UBE2C and thereby orchestrating proper cell cycle progression and mitotic regulation (10). Capitalizing on the essential role of SUMOylation in cell cycle regulation, scientists have developed TAK-981, a novel SUMO E1 inhibitor. This small molecule exhibits dual anti-tumor mechanisms: it not only arrests the cancer cell cycle through SUMOylation inhibition but also potentiates anti-tumor immunity by stimulating immune activation, with a specific emphasis on cellular immune responses. These pharmacological properties underscore its promising clinical applications in oncology (12).

3 Regulation of immune microenvironment by SUMOylation

3.1 Regulation of immune cells by SUMOylation

3.1.1 SUMOylation and regulatory T cells

Regulation of immune homeostasis is well known to be the function of regulatory T (Treg) cells, which can exert immunosuppressive and inflammatory control effects by promoting the formation of anti-inflammatory (M2) macrophages (39), inhibiting T helper (Th) cell populations (40), and secreting inhibitory cytokines, such as interleukin-10 (IL-10) and IL-35 (41). SUMOylation is involved in maintaining peripheral T cell homeostasis and immune tolerance. Stimulation of the T-cell receptor (TCR) and cluster of differentiation 28 (CD28) can induce the production of reactive oxygen species (ROS), resulting in the accumulation of SENP3. SENP3 promotes the nuclear localization of BACH2 by mediating the deSUMOylation of the transcriptional repressor BACH2, thereby preserving the stability of Treg cells and their immunosuppressive function (42).

3.1.2 SUMOylation and CD8+ T cells

TCR-induced ROS also prompts rapid translocation of SENP7 to the cytoplasm, thereby mediating the deSUMOylation, ubiquitination, and subsequent degradation of phosphatase and tensin homolog (PTEN) protein. In CD8 T cells, SENP7-dependent reduction of PTEN maintains metabolic fitness and effector function. Moreover, SENP7 enhances the activation of PI3K/mTOR signal transduction and is involved in the maintenance of glycolysis and oxidative phosphorylation (OXPHOS) in CD8 T cells (43). Several studies have indicated that SUMOylation can impede the presentation of major histocompatibility complex class I (MHC I) antigens, thereby promoting immune evasion by tumor cells. Conversely, the inhibition of SUMOylation has been shown to repair the MHC I antigen presentation mechanism, activate CD8+ T cells, and augment their cytotoxic efficacy against target cells (44).

SUMOylation is crucial for the growth of hepatocellular carcinoma (HCC) cells, and SUMOylation inhibitors TAK-981

and ML-792 effectively reduce SUMOylation in HCC cells. Furthermore, they enhance anti-tumor immunity by restoring the killing ability of T cells, promoting the activity of natural killer (NK) cells and inflammatory (M1) macrophages, activating innate immune cells, and modulating the intestinal microbiota (45). Moreover, the inhibitory effect of TAK-981 on SUMOylation in T cells has been demonstrated. The interferon (IFN)-like response mediated by TAK-981 inhibits the differentiation of Treg cells while enhancing various cytotoxic features of primary chronic lymphocytic leukemia (CLL)-derived CD8+ T cells, including degranulation (CD107a), and upregulated perforin, Granzyme B, and IFN-γ expression activity (46).

3.1.3 SUMOylation and Th17 cell differentiation

Th cell subsets are important players in chronic inflammation and insulin resistance in DM, with the Th17 cell population garnering significant interest from researchers due to its heterogeneity (47, 48). Th17 cells represent a critical component of the pathogenic T cell population. A variety of parenteral autoimmune diseases and tissue inflammation have been linked to Th17 cells[48]. In the absence of SENP2, the co-transcriptional factor Smad4 serves as the modification site of SUMO1 to up-regulate the expression level and nuclear localization of Smad4 and promote the differentiation of T cells to pathogenic Th17 cells (49). PIAS4 catalyzes SUMO3 transcription factor retinoic acid-related orphan receptor gamma t (RORγt) to SUMOylation at the lysine residue 31 (K31), promoting the binding of two RORγt binding proteins (KAT2A and SRC1) to RORγt, which drives the differentiation and development of Th17 cells (50). Under the catalysis of two SUMO E3 ligases, PIASxβ and PIAS3, SUMO1 modifies the K54 of phospholipase C-γ1 (PLC-γ1) to regulate T cell activation and induce IL-2 production by facilitating the assembly of PLC-γ1 microclusters (51).

3.1.4 SUMOylation and macrophage polarization

Macrophages are of significant importance in the regulation of the body's immune response and metabolism. After polarization, macrophages form different subtypes: Th17 cells represent a critical component of the pathogenic T cell population. A variety of parenteral autoimmune diseases and tissue inflammation have been linked to Th17 cells, while M2 macrophages play an anti-inflammatory role (52). Studies have demonstrated that mice with conditional knockout of SENP3 exhibit diminished polarization of M1 macrophages and reduced production of pro-inflammatory cytokines under lipopolysaccharide (LPS) induction, thereby indicating that SENP3 plays an important pro-inflammatory role in LPS-induced lung injury and regulates M1 macrophage polarization by activating pyruvate kinase M2 (PKM2) in a hypoxia-inducible factor-1α(HIF-1α)dependent manner (53).

3.1.5 Summary

SUMOylation exerts distinct effects on various types of immune cells, with regulatory mechanisms that differ across cell types and involve multiple aspects such as activation, differentiation and functional activities, affecting the secretion of downstream cytokines (such as IL-2, IL-6, IL-8, IL-10, etc.) or direct killing effects. While maintaining or breaking immune tolerance, SUMOylation also regulates the production and quantity of various inflammatory mediators, affecting the inflammatory response.

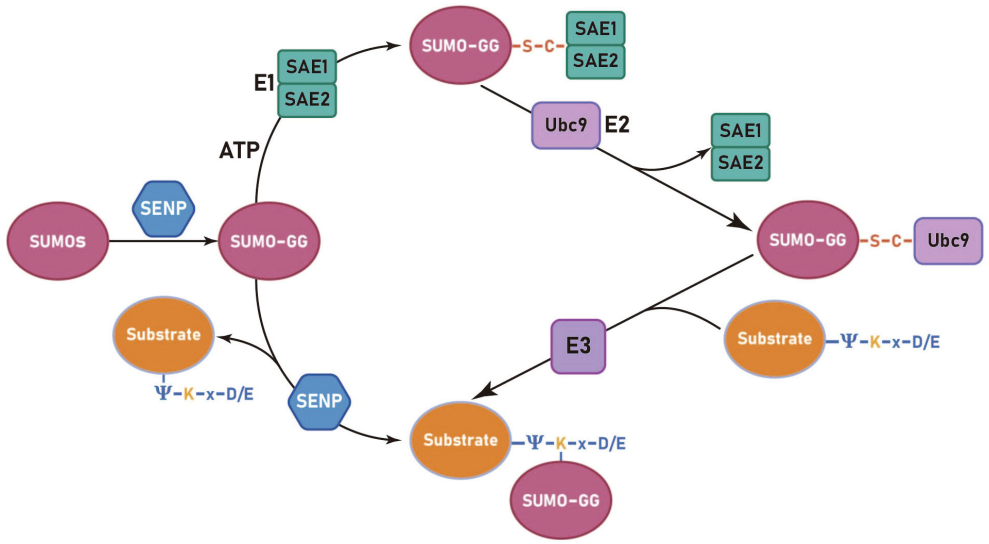

FIGURE 1
The SUMOylation cycle in mammalian cells involves several sequential steps. Initially, SUMO paralogues are cleaved by a SUMO-specific protease (SENP) to expose carboxy-terminal diglycine residues (GG). Subsequently, an ATP-dependent activation step is carried out by the activation enzyme 1 (SAE1 and SAE2), resulting in the formation of a high-energy thioester bond. The activated SUMO is then transferred from the E1 to the E2, forming a SUMO-E2 complex through a thioester linkage. Finally, the E2 enzyme, Ubc9, recognizes the conserved sequence Ψ-K-x-D/E (Ψ represents a hydrophobic group, K denotes lysine conjugated to SUMO, x signifies any amino acid, and D/E indicates an acidic amino acid, either aspartic acid or glutamic acid) on the substrate protein and facilitates the formation of an isopeptide bond between the SUMO and substrate protein, a reaction catalyzed by the E3 ligase.

The above analysis reveals an antagonistic relationship between Treg cells and Th17 cells. SUMOylation has been demonstrated to regulate both of these cell types, suggesting that the modulation of Treg/Th17 cells under SUMOylation conditions may prove beneficial for the advancement and prognosis of autoimmune diseases. Additionally, the opposite effects on macrophage polarization and activated cells indicate that it is feasible to create an environment conducive to M2 macrophage polarization rather than M1 macrophage polarization by influencing SUMOylation, thereby controlling chronic inflammation or excessively amplified inflammatory responses.

3.2 SUMOylation and inflammatory response

3.2.1 SUMOylation and the NF-KB signaling pathway

Post-translational modifications serve as critical regulators of immune signaling-related proteins. SUMOylated nuclear factor kappa B (NF-κB) p65 inhibits NF-κB activation and its downstream pathways in HCC cells by assembling with mesencephalic astrocyte-derived neurotrophic factor (MANF). As a transcription factor, NF-κB regulates gene expression activity, and its activation can result in the production of numerous inflammatory factors. The NF-κB signaling pathway is a classic pathway for regulating immune and inflammatory responses and is also key to the pathogenesis of DM and its complications. SUMO1 overexpression can also SUMOylate MANF and promote the nuclear import of MANF (54, 55).

Further study revealed that SUMOylated annexin-A1 (ANXA1) promotes inhibitory kappa B (IκB) kinase α (IKKα) degradation through selective autophagy, while numerous studies have indicated that IKKα/β-mediated phosphorylation-dependent degradation of IκB is the most critical step in canonical NF-κB signaling pathway activation, thereby inhibiting its overall activation (56).

Additionally, SENP6 could stabilize IKKα by deSUMOylating ANXA1, leading to inflammation (57). Under the regulation of the telomere-associated protein SLX4IP, the SUMO E3 ligase PIAS1 SUMOylates the telomere-binding protein RAP1, facilitating its interaction with IKK and subsequently leading to the activation of the transcription factor NF-κB (58). NF-κB essential molecule (NEMO) is a critical regulator in NF-κB. Intermittent hypoxia (IH) conditions enhance the SUMOylation of NEMO, resulting in NF-κB activation and upregulating the expression levels of tumor necrosis factor-alpha (TNF-α) and IL-6. SENP1-mediated deSUMOylation of NEMO can reduce the inflammatory response of microglia (59, 60). SENP2 can also inhibit the activation of the NF-κB signaling pathway through NEMO deSUMOylation, a mechanism that plays a crucial role in reducing doxorubicin resistance in breast cancer (61). The SUMO E3 ligase tripartite motifcontaining protein 60 (TRIM60) mediates the SUMOylation of TAK1 binding protein TAB2 at K329 and K562, and the SUMOylation of TAB2 interferes with the formation of TRAF6/TAB2/TAK1 complex to inhibit the MAPK/NF-κB pathway. This negatively regulates the innate immune response to toll-like receptor (TLR) signaling (62) (Figure 2).

3.2.2 SUMOylation and the JNK signaling pathway

C-Jun-N-Terminal kinase (JNK) is a member of the mitogen-activated protein kinase (MAPK) family and serves as a critical component of the inflammatory signaling system. Under conditions of elevated H2O2, JNK can be activated as a substrate for SUMO1, with both molecules participating in the apoptotic death pathway caused by oxidative stress. Curcumin acts as an antiinflammatory antioxidant molecule to counteract this effect, which has important implications in retinal layer associated diseases (63, 64).

3.2.3 SUMOylation and the NRF2 signaling pathway

Nuclear factor erythroid 2-related factor 2 (NRF2) has been demonstrated to be a key regulatory factor in maintaining redox homeostasis, typically existing in a low-activity state due to the negative regulation by kelch-like ECH-associated protein 1 (KEAP1), the substrate recognition component of the ubiquitin E3 ligase (65). Researchers have found that SUMOylation preserves and enhances the survival and function of β-cells while reducing the risk of DM. This process largely depends on the SUMOylation process of NRF2, a critical antioxidant factor, which plays a protective role in β-cells (66). SUMO2 has been demonstrated to modify NRF2 at K110 and K533, thereby influencing its transcriptional activity and effective nucleocytoplasmic localization (67). In addition, studies have shown that amyloid-β (aβ) can inhibit the binding of NRF2 and its activation signaling pathway by reducing the SUMOylation of both NRF2 and small musculoaponeurotic fibrosarcoma (sMaf) protein, which is essential for NRF2 activation. This process plays an important role in the onset and progression of Alzheimer's disease (AD) (68). ROS could induce abnormal nucleolar activation of NRF2 through deSUMOylation of NRF2 mediated by SENP3 (69). Serine starvation diminishes SENP1 expression in HCC cells, facilitates SUMO1 modification of NRF2 at the conserved K110, enhances *de novo* serine synthesis, and perpetuates HCC tumorigenesis (70).

3.2.4 SUMOylation and the inflammasome

The assembly of inflammasome is a critical factor in immune response, and SUMOylation is also involved in the activation of inflammasome as a post-translational modification mechanism. The non-obese diabetic (NOD)-like receptor (NLR) family pyrin domain-containing 3 (NLRP3) is essential for the activation of the NLRP3 inflammasome (71). The SUMO E3 ligase tripartite motifcontaining protein 28 (TRIM28) interacts with NLRP3, facilitating the SUMO1- and SUMO2/3catalyzed SUMOylation of NLRP3, thereby inhibiting its ubiquitination and subsequent proteasomal degradation. Consequently, TRIM28 stabilizes NLRP3 protein expression and enhances subsequent inflammasome activation (72). Other studies have similarly demonstrated that SUMO1 can mediate the SUMOylation of NLRP3 (73). In addition, previous studies have demonstrated that SUMOylation exerts an inhibitory effect on the

activation of the NLRP3 inflammasome. For instance, the SUMOylation of NLRP3 mediated by mitochondrial-anchored protein ligase (MAPL), identified as the first mitochondrial-anchored SUMO E3 ligase, negatively regulates inflammasome formation, while SUMO-specific proteases SENP6 and SENP7 reverse this phenomenon (74). Additional experiments have also shown that the knockdown of SENP7 inhibits the activation of the NLRP3 inflammasome pathway (75). The nuclear zinc-finger and BTB domaincontaining protein 16 (ZBTB16) serves a positive regulatory role in the assembly of inflammasomes. The underlying mechanism involves ZBTB16 facilitating inflammasome assembly through the regulation of the adaptor protein ASC (apoptosis-associated speck-like protein containing a CARD) by SUMO1 modification at K21 and/or K109 (76) (Table 2).

4 Diabetes and immune system interactions

4.1 Overview of diabetes

Diabetes mellitus represents a group of metabolic disorders characterized primarily by chronic hyperglycemia, which serves as a key diagnostic criterion. In addition, patients with diabetes have typical clinical manifestations including polydipsia, polyphagia and polyuria. Diabetes-associated complications, categorized into macrovascular (primarily cardiovascular disease) and microvascular complications (including diabetic nephropathy, retinopathy, and neuropathy), can lead to multi-organ damage. These complications significantly impair patients' quality of life while increasing morbidity

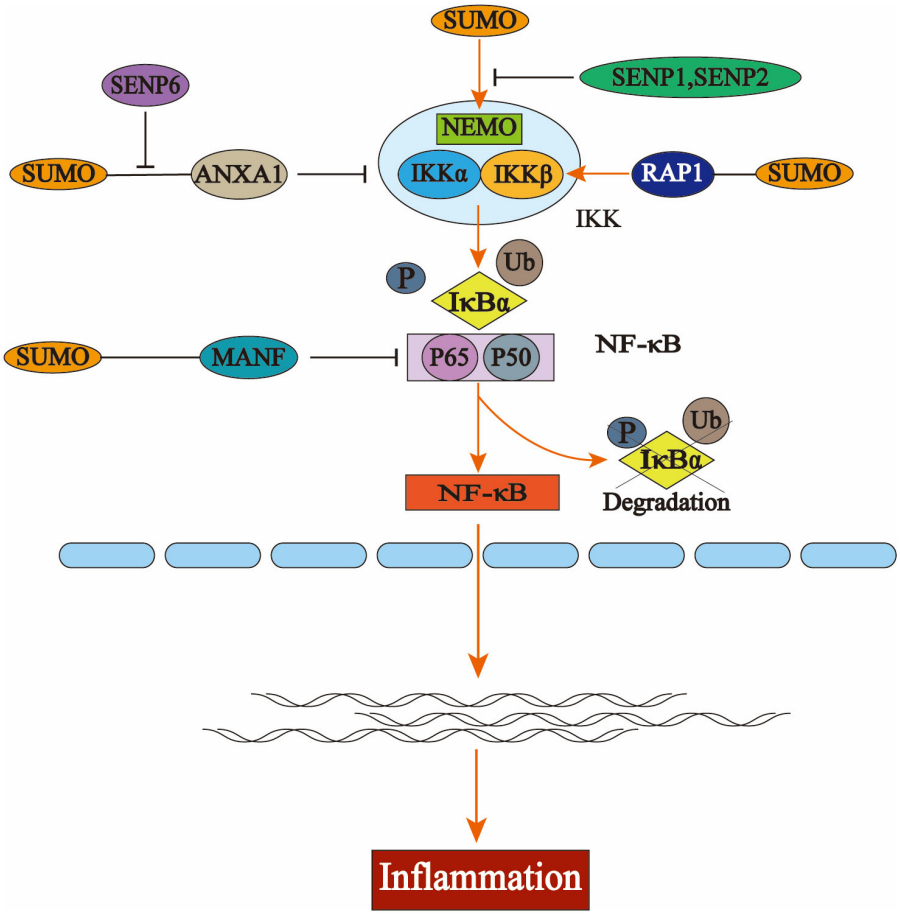

FIGURE 2
The activation process of nuclear factor kappa B (NF-κB) and the regulation of the NFκB signaling pathway by the small ubiquitin-like modifier (SUMO). In the resting state, NF-κB binds to the inhibitory protein IκBα to form an inactive trimer in the cytoplasm, thereby preventing its translocation into the nucleus. Upon stimulation by extracellular stressors, the inhibitory kappa Bn(IκB) kinase complex (IKK) is activated, resulting in phosphorylation and subsequent degradation of IκBα via the ubiquitin-proteasome system. This leads to dissociation of the trimer, allowing for nuclear translocation of the p50-p65 heterodimer that exhibits NF-κB activity and engages in gene transcription and protein synthesis. Several key components within the NF-κB pathway—including IκBα, NF-κB essential molecule (NEMO), P65, IKKα, and IKKβ—are subject to SUMO modification. The interaction between NEMO and SUMO facilitates the activation of IKK; similarly, SUMO-modified RAP1 enhances this activation process which ultimately promotes the degradation of IκBα and triggers NF-κB pathway activation. Additionally, the binding of annexin-A1 (ANXA1) or mesencephalic astrocyte-derived neurotrophic factor (MANF) to SUMO inhibits this pathway's activation by interfering with key signaling molecules involved in NF-κB regulation.

TABLE 2 SUMOylation and inflammatory response.

Inflammatory responses	SUMO	Enzymes	Findings	References
JNK signaling pathway	SUMO1	——	They both participate in the apoptotic death pathway caused by oxidative stress.	(63, 64)
NRF2 signaling pathway	SUMO1	——	Serine starvation induces SUMO1 to modify NRF2 for self-*de novo* synthesis.	(70)
	——	Ubc9	Amyloid β (Aβ) inhibits the signaling of the endogenous antioxidant Nrf2 by decreasing its SUMO modification levels	(68)
	——	SENP3	ROS induces abnormal nucleolar activation of NRF2 through deSUMOylation.	(69)
	SUMO2	——	SUMO2 modifies NRF2 to affect its transcriptional activity and effective nucleocytoplasmic localization.	(67)
Inflammasomes	——	TRIM28	TRIM28 stabilizes NLRP3 protein expression and enhances subsequent inflammasome activation.	(72)
	SUMO1	——	SUMO1 mediates SUMOylation of NLRP3 protein.	(73)
	——	MAPL,SENP6, SENP7	SENP6 and SENP7 reverse MAPL negative regulation of inflammasome formation.	(74, 75)
	SUMO1	——	ZBTB16 promotes inflammasome by controlling the modification of the ASC.	(76)

and mortality rates (77). Diabetes is generally divided into four clinical categories, namely type 1 diabetes(T1DM), type 2 diabetes (T2DM), gestational diabetes (GDM) and other specific types of diabetes, and the vast majority of them are type II diabetes, accounting for 90%-95% of all diabetes (3, 78). This review primarily focuses on type 1 and type 2 diabetes, which represent the most clinically significant forms of the disease.

T1DM and T2DM exhibit distinct heterogeneity, with significant differences in their pathogenesis, clinical manifestations, and disease progression. T1DM predominantly affects younger populations, particularly children and adolescents, although its prevalence is highest in adults due to patient longevity (79). Autoimmune mediated beta cell destruction leading to insufficient insulin secretion is a recognized mechanism, symptoms include polydipsia, polyuria, weight loss, and in severe cases, diabetic ketoacidosis. Currently, the main treatment is insulin replacement therapy (80, 81).

In contrast, T2DM typically manifests later in life and is frequently associated with obesity. Its pathogenesis involves progressive insulin secretory dysfunction coupled with insulin resistance. Notably, patients with T2DM exhibit a significantly higher risk of cardiovascular events compared to their T1DM counterparts (82).

4.2 Interaction between diabetes and the immune system

4.2.1 Interaction between T1DM and the immune system

It is well established that T1DM is an autoimmune disorder characterized by the destruction of β-cells mediated by T lymphocytes. T cells recognize islet antigens, drive islet autoimmunity and islet inflammatory infiltration, while activated autoreactive CD8+ T cells induce β-cell apoptosis through various mechanisms (83, 84), resulting in impaired insulin secretion. In addition to T cells, other immune components including innate immune cells (B cells, NK cells, macrophages, and neutrophils) and pro-inflammatory cytokines (such as TNF-α, IL-6, IFN-γ, and CXCL10) significantly contribute to disease progression by amplifying the autoimmune cascade (85–88).

Recent studies have demonstrated that β-cells are not merely passive 'victims' of autoimmunity, rather, they can also exacerbate the condition (89). Cellular alterations in β-cells, including enhanced immunogenicity, cellular senescence, oxidative stress, and endoplasmic reticulum dysfunction, can trigger the formation of novel antigenic epitopes, thereby amplifying immune responses. This self-perpetuating process represents a crucial mechanism through which β-cells contribute to T1DM pathogenesis (90). These results indicated that the islet - immune cell interaction promoted the progression of T1DM to a great extent, and the occurrence of T1DM could not be attributed to the immune system, and the involvement and metabolic changes of β cells were also worthy of consideration.

4.2.2 Interaction between T2DM and the immune system

T2DM is acknowledged as a metabolic disorder characterized by insulin resistance and progressive insulin insufficiency, with obesity identified as the primary risk factor predisposing individuals to T2DM (91). Adipose tissue hyperplasia results in elevated free fatty acid (FFA) levels, triggering the release of monocyte chemokines and subsequent macrophage activation (92), while also facilitating macrophage polarization (93) that exacerbates the inflammatory response. Research has demonstrated that cytokines secreted by activated macrophages not only reduce adipocyte insulin sensitivity but also promote further macrophage infiltration and inflammatory signaling amplification. This cascade ultimately disrupts insulin

receptor signaling pathways in adipocytes, resulting in systemic insulin resistance (94). Macrophages can also directly or indirectly cause β-cell dysfunction, leading to impaired insulin secretion (95, 96). In addition, other immune cells (B cells and T cells) and their secreted cytokines have also been shown to contribute to the development of insulin resistance and T2DM (97, 98).

T2DM is characterized by complex metabolic disorders, and in addition to obesity, the gut microbiome has also been shown to be involved in the development of T2DM (99). Disruption of the intestinal barrier leads to bacterial penetration, and recognition of bacterial components [mainly lipopolysaccharide (LPS)] by Toll-like receptors (TLRS) and their adaptor molecules leads to the activation of inflammasomes and inflammatory signaling pathways, resulting in insulin resistance and chronic inflammation (100). Furthermore, studies have demonstrated that IL-17 receptor deficiency under high-fat diet (HFD) conditions disrupts neutrophil migration in the intestinal mucosa. This impairment results in gut microbiota dysbiosis and subsequent LPS translocation to adipose tissue, ultimately contributing to insulin resistance and metabolic dysfunction. Additionally, IL-17 receptor deficiency impairs the phosphorylation and activation of key kinases in insulin signaling pathways, leading to compensatory hyperinsulinemia and exacerbation of insulin resistance (101).

4.3 Summary of the role of SUMOylation regulating the immune microenvironment in the development of diabetes mellitus

4.3.1 The impact of SUMOylation on lipid metabolism

The function of adipose tissue is intricately linked to the pathogenesis of DM, with peripancreatic adipocytes (PAT) secreting pro-inflammatory cytokines that recruit immune cells, resulting in damage to pancreatic islet β-cells and exacerbating the progression of T1DM. The elevated SUMOylation of the component NEMO at the lysine-277/309 sites is pivotal in this process, as it induces NF-κB activation and cytokine expression in SENP1-deficient adipocytes. Moreover, NEMO SUMOylation and NF-κB activation in PAT exhibit greater sensitivity to variations in SENP1 expression and activity compared to other adipose depots (54). Relevant studies have also elaborated and summarized the role of SENP1-mediated protein SUMOylation in the pancreatic immune response, β-cell damage, and the progression of DM, while also proposing the use of NEMO inhibitory peptides or NF-κB inhibitors as potential therapeutic strategies for T1DM (102).

It is well established that inflammation plays a significant role in the pathogenesis of T2DM. In particular, inflammation within adipose tissue, resulting from both malnutrition and obesity, can impair insulin receptor function and diminish insulin sensitivity through the action of inflammatory mediators and immune cell infiltration (103). Recent evidence indicates that ubiquitin-conjugating enzyme E2 I (Ube2i) plays a crucial role in the maintenance of growth and normal function of white adipose tissue (WAT). Impaired WAT expansion, inflammatory responses, and adipocyte apoptosis were observed in Ube2i-deficient mice with adipocyte-specific deletion. These alterations led to metabolic abnormalities such as ectopic lipid deposition and insulin resistance in the liver, mirroring the insulin resistance seen in patients with adipose dystrophy. Notably, a sex difference was evident, with effects being more pronounced in females. This underscores the critical role of Ube2i in maintaining functional stability and normal expansion of adipose tissue, however, its specific downstream transcription factors and mechanisms of action require further investigation (104).

Another study demonstrated that adipocyte Ubc9 enhances the SUMOylation of Endoplasmic reticulum protein44 (ERp44) and promotes its covalent binding to endoplasmic reticulum oxidoreductase 1 (Ero1α), thereby exacerbating cell-to-cell transmission of endoplasmic reticulum stress (ER) signals and retention of Ero1α, which ultimately leads to disorders associated with ER stress. ER stress and impaired ER function disrupt systemic glucose homeostasis, resulting in abnormalities in lipid metabolism and insulin resistance. Ubc9 knockdown in adipocytes demonstrated that inhibition of SUMO modification attenuated high-fat-induced ER stress, facilitated lipolysis and energy metabolism, and restored ER function, ultimately leading to the alleviation of insulin resistance and obesity. These findings suggest that modulation of ERp44's SUMOylation may represent a viable strategy for ameliorating obesity and insulin resistance in clinical settings (105). SUMOylation of SET structural domain bifurcation 1 (Setdb1) promotes Setdb1 to occupy the promoter site of the Pparg and Cebpa genes. Setdb1 functions as a histone methyltransferase responsible for H3K9 trimethylation, which increases H3K9 trimethylation in adipocytes and represses the expression of Pparg and Cebpa, ultimately leading to a reduction in lipid storage capacity. This process was validated in adipocyte-specific SENP2 knockout mice subjected to a diet rich in fats, which exhibited ectopic fat accumulation and insulin resistance pathology (106).

SUMOylation exerts diverse effects on lipid metabolism through its regulation of various target proteins. The primary mechanisms involve activation of adipose tissue inflammatory signaling pathways, induction of endoplasmic reticulum stress, and dysregulation of lipid homeostasis. Both adipose tissue inflammation and lipid metabolism dysregulation contribute to insulin receptor impairment, disrupted insulin signaling pathways, and subsequent development of insulin resistance and T2DM. Furthermore, adipose-derived inflammatory infiltration can induce pancreatic β-cell dysfunction, potentially exacerbating T1DM progression. These findings suggest that modulation of protein SUMOylation in adipocytes may represent a promising therapeutic strategy for mitigating insulin resistance and protecting β-cell function.

4.3.2 The impact of SUMOylation on transcription factors and their downstream effectors

It has been reported that under high glucose conditions, retinal microvascular endothelial cells (mRMEC) exhibit significantly elevated levels of SUMO1 and SUMO2/3 proteins, along with enhanced stabilization of RUNX family transcription factor 1 (RUNX1) protein through SUMO2/3dependent SUMOylation, a process that is heavily reliant on the K182 and K144 residues of

RUNX1. RUNX1 protein enhances the proliferation, migration, and angiogenesis of mRMECs, contributing to the exacerbation of diabetic retinopathy (DR) symptoms. This process can be alleviated by SENP1 overexpression, suggesting a potential correlation between SUMOylation and the severity of DR (107, 108). Similarly, high glucose induction can elevate the expression levels of SUMO1 and silent information regulator 1 (SIRT1) proteins in human lens epithelial cells (HLECs), moreover, SUMO1 overexpression enhances the SUMOylation of IκBα, thereby stabilizing this protein and facilitating its binding to NF-κB p65, which inhibits NF-κB p65 activation and oxidative stress. This mechanism protects the lens from high glucose-induced oxidative damage. Collectively, these findings suggest that SUMO1 may represent a novel therapeutic target for the treatment of diabetic cataracts (DC) (109).

NF-κB functions as a transcription factor that regulates gene expression activity, and its activation can result in the production of substantial amounts of inflammatory factors. It has been previously mentioned that several signaling molecules within the NF-κB pathway, including IKKα, NEMO, and p65, are subject to modification by SUMOylation. Contrary to previous reports indicating that high glucose and high osmolality diminish the interaction between IκBα and SUMO1, reduced SUMOylation of IκBα leads to decreased expression levels of IκBα, resulting in the activation of NF-κB signaling, which is implicated in the pathogenesis of diabetic nephropathy (DN). Therefore, novel therapeutic strategies targeting specific regulators of the NF-κB pathway may prove effective in treating DN (110).

Previous studies have also investigated the complex role of mouse SUMO2 (mSUMO2) in the development of autoimmune diabetes by establishing genetically modified mice with a enhanced repressor of NF-κB (IκBαΔN) and overexpression of mSUMO2, which demonstrated that Th1 cytokines were suppressed in the IκBαΔN T cells. Conversely, T cells with elevated levels of mSUMO2 showed a reduction in both Th1 and Th2 cytokine production. Furthermore, IκBαΔN completely prevented diabetes regardless of mSUMO2 overexpression, however, mice expressing only mSUMO2 exhibited susceptibility to diabetes comparable to that of wild-type mice. It is suggested that SUMO2 may differentially inhibit NF-κB expression at least in T cells, but the specific regulatory mechanism and the signaling molecules involved remain to be clearly elucidated (111). Similarly, the further development of DM and its complications through activation of the NF-κB pathway can also be observed through the enhanced phosphorylation and SUMOylation of IκB kinase γ (IKKγ) (30).

The NF-κB pathway plays a vital role in the development of DM through various mechanisms. For instance, deficiency of thioredoxin 2 (Trx2) in adipose tissue results in the stimulation of NFκB, which mediates the accumulation of the autophagy receptor p62, leading to mitochondrial autophagy and subsequently promotes insulin resistance and lipid metabolism disorders in T2DM, thereby linking NF-κB to metabolic disorders associated with insulin resistance (112). NF-κB also upregulates the expression of complement C3, thereby promoting the development of DM (113), C3 is a crucial component in the activation process of all three complement pathways and is not only associated with insulin resistance (114), reflecting the progression of metabolic derangement but also serves as a biomarker for T1DM and T2DM (115, 116). Epidemiological studies have demonstrated that elevated plasma levels of complement C3 can increase the risk of diabetic retinopathy, diabetic nephropathy, and neuropathy (113) in the general population (117). Furthermore, the pathogenesis of diabetes-related periodontitis mediated by C3 in patients with T2DM is supported by existing studies (118). Induced by hyperglycemia, the NF-κB signaling pathway mediates the activation of valvular interstitial cells (VICs), resulting in valvular calcification and dysfunction, which significantly contributes to the exacerbation of valvular calcification in patients with T2DM suffering from aortic stenosis (AS) (119).

Moreover, the NF-κB signaling pathway, along with its related inflammatory mediators, could represent a critical nexus in microRNA-92a-mediated diabetic cardiovascular disease (120). The aforementioned findings suggest that inhibition of the NF-κB signaling pathway may serve as an effective therapeutic target for DM. The mechanisms underlying NF-κB pathway activation are intricate and involve a diverse array of signaling molecules. It is anticipated that further investigation into potential sumo-chemical modifications regulating the NF-κB pathway will yield significant insights, particularly regarding their critical roles in the pathogenesis of TM and its associated complications.

The age-related decrease in c-Maf SUMOylation within CD4 T cells negatively correlates with IL-21 expression, which facilitates the differentiation of T follicular helper (Tfh) cells and the proliferation of granzyme B-producing effector/memory CD8+ T cells, thereby contributing to the development of autoimmune diabetes in NOD mice. Moreover, the findings indicate that SUMOdeficient c-Maf inhibits Death domain-associated protein 6 (Daxx)/Histone Deacetylase (HDAC) recruitment to the IL-21 promoter (IL-21p) and enhances histone acetylation mediated by CREBbinding protein (CBP) and p300. It is hypothesized that inhibitors of CBP/p300 may mitigate several effects induced by IL-21 (121). This study elucidates a potential link between the SUMO status of a single transcription factor and the pathogenesis of autoimmune diabetes, detailing the downstream signaling molecules involved (e.g., IL-21, Daxx, etc.) and their pathogenic effects supported by experimental data. It suggests that the low SUMOylation levels of c-Maf may serve as a precursor to autoimmune diabetes, thereby facilitating early preventive and therapeutic interventions. Additionally, the role and downstream effects of IL-21 offer novel insights for the treatment of T1DM.

The role of transcription factor c-Maf in the pathogenesis of autoimmune diabetes is further corroborated by reports indicating that c-Maf directly influences the expression of glucose transporter genes Sglt2 and Glut2. Additionally, c-Maf deficiency has been shown to ameliorate diabetic nephropathy associated with hyperglycemia and oxidative stress by downregulating Sglt2 and Glut2 expression (122).

IL-21, a cytokine primarily produced by Tfh, is an essential element of the immune system that modulates various immune subpopulations, including B cells and CD8+ T cells. It is instrumental in the pathogenesis of multiple autoimmune diseases, including DM (123). IL-21 has been demonstrated to exhibit pro-diabetic activity, contributing to β-cell destruction

and the onset of spontaneous T1DM (124). Additionally, it is implicated in Tfh cell-mediated chronic vascular inflammatory responses and the progression of diabetic retinopathy (125). Clinical trials have demonstrated that the combination of anti-IL-21 antibodies and liraglutide preserves β-cell activity and enhances islet function, offering a promising approach to addressing the treatment of T1DM (126).

Besides IL-21, other cytokines, including members of the IL-12 family members (IL-12, IL23, IL-27 and IL-35) (127), along with IL-6 (128), TNF-α (129), have been closely associated with DM and its complications. Identifying these cytokines in relation to the development of diabetes mellitus also provides targeted therapeutic avenues for managing diabetes and its related conditions.

Similarly in NOD mouse CD4+ T cells, SUMO1 reduces IL-4 production by enhancing its interaction with c-Maf, thereby inhibiting c-Maf from binding to the IL-4p half-MARE site. This reduction is detrimental to the normal development of protective Th2 cells. Numerous studies have demonstrated that T1DM is associated with an attenuated Th2 response, and thus this pathway may be involved in the immune bias of T1DM (130).

SENP1 has been demonstrated to enhance cell death in the insulin secreting cell line (INS-1 832/13) and human islet cells, leading to islet secretory dysfunction that correlates with decreased expression of inducible nitric oxide synthase (iNOS) and nuclear translocation of NF-κB. In contrast, up-regulation of SUMO1 or knockdown of SENP1 can reduce the nuclear translocation of NF-κB and its target gene expression, suggesting that preservation of islet activity and restoration of islet survival can be achieved through the processes of SUMOylation and de-SUMOylation (131). Glycolipotoxicity and the pro-inflammatory cytokine TNF-α convert extracellular stress into pattern recognition receptor (PKR) activation via the second messenger ceramide and activated PKR interacts with the conjugating enzyme Ubc9 to promote SUMOylation-dependent stabilization of p53, whose enhanced transcriptional activity leads to cell cycle arrest and disrupts β-cell proliferation, thereby contributing to the progression of T2DM. These findings indicate that targeting the ceramide/PKR/Ubc9/p53 signaling pathway may represent an effective strategy for the treatment of T2DM (132) (Table 3).

5 Conclusions and future perspectives

Recently, significant advancements in SUMOylation research has led to a deeper insight into the molecular mechanisms and enzymatic systems that are involved. More importantly, SUMOylation, as a novel reversible protein regulation process, plays a crucial role in the development of various physiopathological states within the body, offering new insights into the pathogenesis of multiple diseases. Building on this foundation, the present paper offers a comprehensive overview of how SUMO chemical modifications influence downstream signaling molecules by regulating the functions of proteins within the immune environment, thereby potentially impacting the pathogenesis of DM.

This review comprehensively examines the molecular mechanisms of SUMOylation and its regulatory effects on the immune system, with particular emphasis on their pivotal roles in the pathogenesis of both T1DM and T2DM. By exploring the intricate relationships among these components, we aim to clarify the critical function of SUMOylation in modulating the immune microenvironment and its implications for diabetes progression and associated complications.

Additionally, it summarizes several intricate molecular mechanisms, the majority of which are classical signaling pathways linked to immune homeostasis and inflammation, including adipose tissue inflammatory factors, NF-κB pathway activation, Tfh cytokines, and other cellular signaling pathways. This underscores the significant potential of SUMO in diabetes-related therapies. SUMOylation influences the activity of key protein kinases involved in the pathogenesis by disrupting downstream signaling pathways. Although several studies have supported this notion, most

TABLE 3 Molecular mechanism and pathogenesis of SUMOylation on diabetes mellitus and its complications.

Diseases	Molecular mechanisms	Pathogenesis	References
Diabetic retinopathy	SUMO2/3-dependent SUMOylation enhances RUNX1 protein stability.	RUNX1 protein promotes mRMEC proliferation, migration and angiogenesis.	(107, 108)
Diabetic cataract	IκBα SUMOylates and inhibits NF-κB p65 activation and oxidative stress.	Stabilization of IκBα protects the lens from high glucose-induced oxidative damage.	(109)
Diabetic nephropathy	SUMOylation of IκBα is reduced.	It is involved in the development of DN by activating the NF-κB signaling pathway.	(110)
	c-Maf deletion reduces the expression of glucose transport genes Sglt2 and Glut2.	It improves hyperglycemia and oxidative stress.	(122)
Autoimmune diabetes	SUMO2 differentially regulates NF-κB expression in T cells.	The role of SUMOylation in developing autoimmune diabetes *in vivo* remains to be investigated.	(111)
	Attenuation of c-Maf SUMOylation induces CD8 T cells to produce granzyme B.	Granzyme B causes β cell apoptosis.	(121)
T1DM	The enhanced SUMO1 conjugation to c-Maf resulted in decreased IL-4 production.	This is detrimental to the normal development of protective Th2 cells.	(130)
T2DM	PKR interacts with Ubc9 to promote SUMOylation-dependent stabilization of P53.	Enhanced transcriptional activity of P53 arrests the cell cycle of β-cell proliferation.	(132)

are based on similar animal models, and the detailed mechanisms of SUMO modification on the regulation of various physiological and pathological states of the organism remain inadequately elucidated. Furthermore, the proteins subject to this modification warrant further investigation. In future research, it is anticipated that a more comprehensive understanding of how SUMO-regulated key proteins induce islet inflammation and autoimmunity will be achieved, leading to the identification of new therapeutic targets for diabetes based on these key proteins and existing knowledge.

Author contributions

YZ: Writing – original draft, Writing – review & editing. SF: Writing – original draft, Writing – review & editing. YQ: Writing – review & editing.

Funding

The author(s) declare that no financial support was received for the research, authorship, and/or publication of this article.

Conflict of interest

The authors declare that the research was conducted in the absence of any commercial or financial relationships that could be construed as a potential conflict of interest.

Generative AI statement

The author(s) declare that no Generative AI was used in the creation of this manuscript.

Publisher's note

References

1. Ong KL, Stafford LK, McLaughlin SA, Boyko EJ, Vollset SE, Smith AE, et al. Global, regional, and national burden of diabetes from 1990 to 2021, with projections of prevalence to 2050: A systematic analysis for the global burden of disease study 2021. *Lancet (London England)*. (2023) 402:203–34. doi: 10.1016/s0140-6736(23)01301-6

2. Jin C, Lai Y, Li Y, Teng D, Yang W, Teng W, et al. Changes in the prevalence of diabetes and control of risk factors for diabetes among chinese adults from 2007 to 2017: an analysis of repeated national cross-sectional surveys. *J Diabetes*. (2024) 16: e13492. doi: 10.1111/1753-0407.13492

3. ElSayed NA, Aleppo G, Bannuru RR, Bruemmer D, Collins BS, Ekhlaspour L, et al. Diagnosis and classification of diabetes: standards of care in diabetes-2024. *Diabetes Care*. (2024) 47:S20–s42. doi: 10.2337/dc24-S002

4. American Diabetes Association. Classification and diagnosis of diabetes: standards of medical care in diabetes-2019. *Diabetes Care*. (2019) 42:S13–s28. doi: 10.2337/dc19-S002

5. Guo H, Wu H, Li Z. The pathogenesis of diabetes. *Int J Mol Sci*. (2023) 24(8):6978. doi: 10.3390/ijms24086978

6. Ruze R, Liu T, Zou X, Song J, Chen Y, Xu R, et al. Obesity and type 2 diabetes mellitus: connections in epidemiology, pathogenesis, and treatments. *Front Endocrinol (Lausanne)*. (2023) 14:1161521. doi: 10.3389/fendo.2023.1161521

7. Sticht J, Álvaro-Benito M, Konigorski S. Type 1 diabetes and the hla region: genetic association besides classical hla class ii genes. *Front Genet*. (2021) 12:683946. doi: 10.3389/fgene.2021.683946

8. Okura T, Gong L, Kamitani T, Wada T, Okura I, Wei CF, et al. Protection against fas/apo-1- and tumor necrosis factor-mediated cell death by a novel protein, sentrin. *J Immunol (Baltimore Md: 1950)*. (1996) 157:4277–81. doi: 10.4049/jimmunol.157.10.4277

9. Su HL, Li SS. Molecular features of human ubiquitin-like sumo genes and their encoded proteins. *Gene*. (2002) 296:65–73. doi: 10.1016/s0378-1119(02)00843-0

10. Liu W, Wang Y, Bozi LHM, Fischer PD, Jedrychowski MP, Xiao H, et al. Lactate regulates cell cycle by remodelling the anaphase promoting complex. *Nature*. (2023) 616:790–7. doi: 10.1038/s41586-023-05939-3

11. Kramarz K, Schirmeisen K, Boucherit V, Ait Saada A, Lovo C, Palancade B, et al. The nuclear pore primes recombination-dependent DNA synthesis at arrested forks by promoting sumo removal. *Nat Commun*. (2020) 11:5643. doi: 10.1038/s41467-020-19516-z

12. Kumar S, Schoonderwoerd MJA, Kroonen JS, de Graaf IJ, Sluijter M, Ruano D, et al. Targeting pancreatic cancer by tak-981: A sumoylation inhibitor that activates the immune system and blocks cancer cell cycle progression in a preclinical model. *Gut*. (2022) 71:2266–83. doi: 10.1136/gutjnl-2021-324834

13. Guo D, Li M, Zhang Y, Yang P, Eckenrode S, Hopkins D, et al. A functional variant of sumo4, a new I kappa B alpha modifier, is associated with type 1 diabetes. *Nat Genet*. (2004) 36:837–41. doi: 10.1038/ng1391

14. Liang YC, Lee CC, Yao YL, Lai CC, Schmitz ML, Yang WM. Sumo5, a novel poly-sumo isoform, regulates pml nuclear bodies. *Sci Rep*. (2016) 6:26509. doi: 10.1038/srep26509

15. Tatham MH, Jaffray E, Vaughan OA, Desterro JM, Botting CH, Naismith JH, et al. Polymeric chains of sumo-2 and sumo-3 are conjugated to protein substrates by sae1/sae2 and ubc9. *J Biol Chem*. (2001) 276:35368–74. doi: 10.1074/jbc.M104214200

16. Saitoh H, Hinchey J. Functional heterogeneity of small ubiquitin-related protein modifiers sumo-1 versus sumo-2/3. *J Biol Chem*. (2000) 275:6252–8. doi: 10.1074/jbc.275.9.6252

17. Kamitani T, Kito K, Nguyen HP, Fukuda-Kamitani T, Yeh ET. Characterization of a second member of the sentrin family of ubiquitin-like proteins. *J Biol Chem*. (1998) 273:11349–53. doi: 10.1074/jbc.273.18.11349

18. Bohren KM, Nadkarni V, Song JH, Gabbay KH, Owerbach D. A M55v polymorphism in a novel sumo gene (Sumo-4) differentially activates heat shock transcription factors and is associated with susceptibility to type I diabetes mellitus. *J Biol Chem*. (2004) 279:27233–8. doi: 10.1074/jbc.M402273200

19. Li H, Ning M, Li Q, Wang T, Li W, Xiao J, et al. The association of five polymorphisms with diabetic retinopathy in a chinese population. *Ophthalmic Genet*. (2023) 44:346–51. doi: 10.1080/13816810.2023.2194494

20. Tong Z, Qi J, Ma W, Wang D, Hu B, Li Y, et al. Sumo4 gene snp rs237025 and the synergistic effect with weight management: A study of risk factors and interventions for mets. *Front Genet*. (2021) 12:786393. doi: 10.3389/fgene.2021.786393

21. Li YY, Wang H, Yang XX, Geng HY, Gong G, Kim HJ, et al. Small ubiquitin-like modifier 4 (Sumo4) gene M55v polymorphism and type 2 diabetes mellitus: A meta-analysis including 6,823 subjects. *Front Endocrinol*. (2017) 8:303. doi: 10.3389/fendo.2017.00303

22. Coppola A, Tomasello L, Pizzolanti G, Pucci-Minafra I, Albanese N, Di Cara G, et al. *In vitro* phenotypic, genomic and proteomic characterization of a cytokine-resistant murine B-tc3 cell line. *PloS One*. (2012) 7:e32109. doi: 10.1371/journal.pone.0032109

23. Schmidt D, Müller S. Members of the pias family act as sumo ligases for C-jun and P53 and repress P53 activity. *Proc Natl Acad Sci U.S.A*. (2002) 99:2872–7. doi: 10.1073/pnas.052559499

24. Karvonen U, Jääskeläinen T, Rytinki M, Kaikkonen S, Palvimo JJ. Znf451 is a novel pml body- and sumo-associated transcriptional coregulator. *J Mol Biol*. (2008) 382:585–600. doi: 10.1016/j.jmb.2008.07.016

25. Zeng W, Gu S, Yu Y, Feng Y, Xiao M, Feng XH. Znf451 stabilizes twist2 through sumoylation and promotes epithelial-mesenchymal transition. *Am J Cancer Res*. (2021) 11:898–915.

26. Moreno-Oñate M, Herrero-Ruiz AM, García-Dominguez M, Cortés-Ledesma F, Ruiz JF. Ranbp2-mediated sumoylation promotes human DNA polymerase lambda nuclear localization and DNA repair. *J Mol Biol*. (2020) 432:3965–79. doi: 10.1016/j.jmb.2020.03.020

27. Liu X, Liu J, Xiao W, Zeng Q, Bo H, Zhu Y, et al. Sirt1 regulates N(6) -methyladenosine rna modification in hepatocarcinogenesis by inducing ranbp2-dependent fto sumoylation. *Hepatol (Baltimore Md)*. (2020) 72:2029–50. doi: 10.1002/hep.31222

28. Werner A, Flotho A, Melchior F. The ranbp2/rangap1*Sumo1/ubc9 complex is a multisubunit sumo E3 ligase. *Mol Cell*. (2012) 46:287–98. doi: 10.1016/j.molcel.2012.02.017

29. Wu R, Fang J, Liu M, A J, Liu J, Chen W, et al. Sumoylation of the transcription factor zfhx3 at lys-2806 requires sae1, ubc9, and pias2 and enhances its stability and function in cell proliferation. *J Biol Chem*. (2020) 295:6741–53. doi: 10.1074/jbc.RA119.012338

30. Huang W, Liang Y, Dong J, Zhou L, Gao C, Jiang C, et al. Sumo E3 ligase piasy mediates high glucose-induced activation of nf-Kb inflammatory signaling in rat mesangial cells. *Mediators Inflammation*. (2017) 2017:1685194. doi: 10.1155/2017/1685194

31. Desterro JM, Rodriguez MS, Kemp GD, Hay RT. Identification of the enzyme required for activation of the small ubiquitin-like protein sumo-1. *J Biol Chem*. (1999) 274:10618–24. doi: 10.1074/jbc.274.15.10618

32. Gong L, Li B, Millas S, Yeh ET. Molecular cloning and characterization of human aos1 and uba2, components of the sentrin-activating enzyme complex. *FEBS Lett*. (1999) 448:185–9. doi: 10.1016/s0014-5793(99)00367-1

33. Johnson ES, Schwienhorst I, Dohmen RJ, Blobel G. The ubiquitin-like protein smt3p is activated for conjugation to other proteins by an aos1p/uba2p heterodimer. *EMBO J*. (1997) 16:5509–19. doi: 10.1093/emboj/16.18.5509

34. Lin D, Tatham MH, Yu B, Kim S, Hay RT, Chen Y. Identification of a substrate recognition site on ubc9. *J Biol Chem*. (2002) 277:21740–8. doi: 10.1074/jbc.M108418200

35. Bernier-Villamor V, Sampson DA, Matunis MJ, Lima CD. Structural basis for E2-mediated sumo conjugation revealed by a complex between ubiquitin-conjugating enzyme ubc9 and rangap1. *Cell*. (2002) 108:345–56. doi: 10.1016/s0092-8674(02)00630-x

36. Desterro JM, Thomson J, Hay RT. Ubch9 conjugates sumo but not ubiquitin. *FEBS Lett*. (1997) 417:297–300. doi: 10.1016/s0014-5793(97)01305-7

37. Li O, Ma Q, Li F, Cai GY, Chen XM, Hong Q. Progress of small ubiquitin-related modifiers in kidney diseases. *Chin Med J (Engl)*. (2019) 132:466–73. doi: 10.1097/cm9.0000000000000094

38. Nayak A, Müller S. Sumo-specific proteases/isopeptidases: senps and beyond. *Genome Biol*. (2014) 15:422. doi: 10.1186/s13059-014-0422-2

39. Song J, Gong YH, Yan X, Liu Y, Zhang M, Luo J, et al. Regulatory T cells accelerate the repair process of renal fibrosis by regulating mononuclear macrophages. *Am J Med Sci*. (2021) 361:776–85. doi: 10.1016/j.amjms.2021.01.022

40. Jiao WE, Xu S, Qiao YL, Kong YG, Sun L, Deng YQ, et al. Notch2-dependent gata3+ Treg cells alleviate allergic rhinitis by suppressing the th2 cell response. *Int Immunopharmacol*. (2022) 112:109261. doi: 10.1016/j.intimp.2022.109261

41. Sawant DV, Yano H, Chikina M, Zhang Q, Liao M, Liu C, et al. Adaptive plasticity of il-10(+) and il-35(+) T(Reg) cells cooperatively promotes tumor T cell exhaustion. *Nat Immunol*. (2019) 20:724–35. doi: 10.1038/s41590-019-0346-9

42. Yu X, Lao Y, Teng XL, Li S, Zhou Y, Wang F, et al. Senp3 maintains the stability and function of regulatory T cells via bach2 desumoylation. *Nat Commun*. (2018) 9:3157. doi: 10.1038/s41467-018-05676-6

43. Wu Z, Huang H, Han Q, Hu Z, Teng XL, Ding R, et al. Senp7 senses oxidative stress to sustain metabolic fitness and antitumor functions of cd8+ T cells. *J Clin Invest*. (2022) 132(7):e155224. doi: 10.1172/jci155224

44. Demel UM, Böger M, Yousefian S, Grunert C, Zhang L, Hotz PW, et al. Activated sumoylation restricts mhc class I antigen presentation to confer immune evasion in cancer. *J Clin Invest*. (2022) 132(9):e152383. doi: 10.1172/jci152383

45. Wang Z, Pan B, Su L, Yu H, Wu X, Yao Y, et al. Sumoylation inhibitors activate anti-tumor immunity by reshaping the immune microenvironment in a preclinical model of hepatocellular carcinoma. *Cell Oncol (Dordr)*. (2023) 47(2):513–32. doi: 10.1007/s13402-023-00880-z

46. Lam V, Roleder C, Liu T, Bruss N, Best S, Wang X, et al. T cell-intrinsic immunomodulatory effects of tak-981 (Subasumstat), a sumo-activating enzyme inhibitor, in chronic lymphocytic leukemia. *Mol Cancer Ther*. (2023) 22:1040–51. doi: 10.1158/1535-7163.Mct-22-0762

47. Schnell A, Huang L, Singer M, Singaraju A, Barilla RM, Regan BML, et al. Stem-like intestinal th17 cells give rise to pathogenic effector T cells during autoimmunity. *Cell*. (2021) 184:6281–98.e23. doi: 10.1016/j.cell.2021.11.018

48. Schnell A, Littman DR, Kuchroo VK. T(H)17 cell heterogeneity and its role in tissue inflammation. *Nat Immunol*. (2023) 24:19–29. doi: 10.1038/s41590-022-01387-9

49. Yang TT, Chiang MF, Chang CC, Yang SY, Huang SW, Liao NS, et al. Senp2 restrains the generation of pathogenic th17 cells in mouse models of colitis. *Commun Biol*. (2023) 6:629. doi: 10.1038/s42003-023-05009-4

50. He Z, Zhang J, Huang Z, Du Q, Li N, Zhang Q, et al. Sumoylation of rorγt regulates T(H)17 differentiation and thymocyte development. *Nat Commun*. (2018) 9:4870. doi: 10.1038/s41467-018-07203-z

51. Wang QL, Liang JQ, Gong BN, Xie JJ, Yi YT, Lan X, et al. T cell receptor (Tcr)-induced plc-Γ1 sumoylation via piasxβ and pias3 sumo E3 ligases regulates the microcluster assembly and physiological function of plc-Γ1. *Front Immunol*. (2019) 10:314. doi: 10.3389/fimmu.2019.00314

52. Yunna C, Mengru H, Lei W, Weidong C. Macrophage M1/M2 polarization. *Eur J Pharmacol*. (2020) 877:173090. doi: 10.1016/j.ejphar.2020.173090

53. He S, Fan C, Ji Y, Su Q, Zhao F, Xie C, et al. Senp3 facilitates M1 macrophage polarization via the hif-1α/pkm2 axis in lipopolysaccharide-induced acute lung injury. *Innate Immun*. (2023) 29:25–34. doi: 10.1177/17534259231166212

54. Shao L, Zhou HJ, Zhang H, Qin L, Hwa J, Yun Z, et al. Senp1-mediated nemo desumoylation in adipocytes limits inflammatory responses and type-1 diabetes progression. *Nat Commun*. (2015) 6:8917. doi: 10.1038/ncomms9917

55. Liu J, Wu Z, Han D, Wei C, Liang Y, Jiang T, et al. Mesencephalic astrocyte-derived neurotrophic factor inhibits liver cancer through small ubiquitin-related modifier (Sumo)Ylation-related suppression of nf-Kb/snail signaling pathway and epithelial-mesenchymal transition. *Hepatol (Baltimore Md)*. (2020) 71:1262–78. doi: 10.1002/hep.30917

56. Li X, Xia Q, Mao M, Zhou H, Zheng L, Wang Y, et al. Annexin-A1 sumoylation regulates microglial polarization after cerebral ischemia by modulating ikkα Stability via selective autophagy. *Sci Adv*. (2021) 7(4):eabc5539. doi: 10.1126/sciadv.abc5539

57. Mao M, Xia Q, Zhan GF, Chu QJ, Li X, Lian HK. Senp6 Induces Microglial Polarization and Neuroinflammation through De-Sumoylation of Annexin-A1 after Cerebral Ischaemia-Reperfusion Injury. *Cell bioscience*. (2022) 12:113. doi: 10.1186/s13578-022-00850-2

58. Robinson NJ, Miyagi M, Scarborough JA, Scott JG, Taylor DJ, Schiemann WP. Slx4ip promotes rap1 sumoylation by pias1 to coordinate telomere maintenance through nf-Kb and notch signaling. *Sci Signaling*. (2021) 14(689):eabe9613. doi: 10.1126/scisignal.abe9613

59. Yang T, Sun J, Wei B, Liu S. Senp1-mediated nemo de-sumoylation inhibits intermittent hypoxia induced inflammatory response of microglia *in vitro*. *J Cell Physiol*. (2020) 235:3529–38. doi: 10.1002/jcp.29241

60. Wang H, Yang T, Sun J, Zhang S, Liu S. Senp1 Modulates Microglia-Mediated Neuroinflammation toward Intermittent Hypoxia-Induced Cognitive Decline through the De-Sumoylation of Nemo. *J Cell Mol Med*. (2021) 25:6841–54. doi: 10.1111/jcmm.16689

61. Gao X, Wu Y, Qiao L, Feng X. Senp2 suppresses nf-Kb activation and sensitizes breast cancer cells to doxorubicin. *Eur J Pharmacol*. (2019) 854:179–86. doi: 10.1016/j.ejphar.2019.03.051

62. Gu Z, Chen X, Yang W, Qi Y, Yu H, Wang X, et al. The sumoylation of tab2 mediated by trim60 inhibits mapk/nf-Kb activation and the innate immune response. *Cell Mol Immunol*. (2021) 18:1981–94. doi: 10.1038/s41423-020-00564-w

63. Buccarello L, Dragotto J, Iorio F, Hassanzadeh K, Corbo M, Feligioni M. The pivotal role of sumo-1-jnk-tau axis in an *in vitro* model of oxidative stress counteracted by the protective effect of curcumin. *Biochem Pharmacol*. (2020) 178:114066. doi: 10.1016/j.bcp.2020.114066

64. Buccarello L, Dragotto J, Hassanzadeh K, Maccarone R, Corbo M, Feligioni M. Retinal ganglion cell loss in an ex vivo mouse model of optic nerve cut is prevented by curcumin treatment. *Cell Death Discovery*. (2021) 7:394. doi: 10.1038/s41420-021-00760-1

65. Yamamoto M, Kensler TW, Motohashi H. The keap1-nrf2 system: A thiol-based sensor-effector apparatus for maintaining redox homeostasis. *Physiol Rev*. (2018) 98:1169–203. doi: 10.1152/physrev.00023.2017

66. He X, Lai Q, Chen C, Li N, Sun F, Huang W, et al. Both conditional ablation and overexpression of E2 sumo-conjugating enzyme (Ubc9) in mouse pancreatic beta cells result in impaired beta cell function. *Diabetologia*. (2018) 61:881–95. doi: 10.1007/s00125-017-4523-9

67. Walters TS, McIntosh DJ, Ingram SM, Tillery L, Motley ED, Arinze IJ, et al. Sumo-modification of human nrf2 at K(110) and K(533) regulates its nucleocytoplasmic localization, stability and transcriptional activity. *Cell Physiol biochemistry: Int J Exp Cell physiology biochemistry Pharmacol*. (2021) 55:141–59. doi: 10.33594/000000351

68. Wang P, Wang X, Qiao K, Zhang Y, Nie Q, Cui J, et al. Reduced sumoylation of nrf2 signaling contributes to its inhibition induced by amyloid-B. *Neurosci Lett*. (2023) 799:137118. doi: 10.1016/j.neulet.2023.137118

69. Zhou Z, Xu J, Bao X, Shi J, Liu B, Chen Y, et al. Nuclear nrf2 activity in laryngeal carcinoma is regulated by senp3 after cisplatin-induced reactive oxygen species stress. *J Cancer*. (2019) 10:3427–34. doi: 10.7150/jca.30318

70. Guo H, Xu J, Zheng Q, He J, Zhou W, Wang K, et al. Nrf2 sumoylation promotes *de novo* serine synthesis and maintains hcc tumorigenesis. *Cancer Lett*. (2019) 466:39–48. doi: 10.1016/j.canlet.2019.09.010

71. Agostini L, Martinon F, Burns K, McDermott MF, Hawkins PN, Tschopp J. Nalp3 forms an il-1beta-processing inflammasome with increased activity in muckle-

wells autoinflammatory disorder. *Immunity*. (2004) 20:319–25. doi: 10.1016/s1074-7613(04)00046-9

72. Qin Y, Li Q, Liang W, Yan R, Tong L, Jia M, et al. Trim28 sumoylates and stabilizes nlrp3 to facilitate inflammasome activation. *Nat Commun*. (2021) 12:4794. doi: 10.1038/s41467-021-25033-4

73. Shao L, Liu Y, Wang W, Li A, Wan P, Liu W, et al. Sumo1 sumoylates and senp3 desumoylates nlrp3 to orchestrate the inflammasome activation. *FASEB journal: Off Publ Fed Am Societies Exp Biol*. (2020) 34:1497–515. doi: 10.1096/fj.201901653R

74. Barry R, John SW, Liccardi G, Tenev T, Jaco I, Chen CH, et al. Sumo-mediated regulation of nlrp3 modulates inflammasome activity. *Nat Commun*. (2018) 9:3001. doi: 10.1038/s41467-018-05321-2

75. Li X, Jiao F, Hong J, Yang F, Wang L, Gong Z. Senp7 knockdown inhibited pyroptosis and nf-Kb/nlrp3 inflammasome pathway activation in raw 264.7 cells. *Sci Rep*. (2020) 10:16265. doi: 10.1038/s41598-020-73400-w

76. Dong D, Du Y, Fei X, Yang H, Li X, Yang X, et al. Inflammasome activity is controlled by zbtb16-dependent sumoylation of asc. *Nat Commun*. (2023) 14:8465. doi: 10.1038/s41467-023-43945-1

77. Cole JB, Florez JC. Genetics of diabetes mellitus and diabetes complications. *Nat Rev Nephrol*. (2020) 16:377–90. doi: 10.1038/s41581-020-0278-5

78. Harreiter J, Roden M. Diabetes mellitus: definition, classification, diagnosis, screening and prevention (Update 2023). *Wiener klinische Wochenschrift*. (2023) 135:7–17. doi: 10.1007/s00508-022-02122-y

79. Vanderniet JA, Jenkins AJ, Donaghue KC. Epidemiology of type 1 diabetes. *Curr Cardiol Rep*. (2022) 24:1455–65. doi: 10.1007/s11886-022-01762-w

80. Zajec A, Trebušak Podkrajšek K, Tesovnik T, Šket R, Čugalj Kern B, Jenko Bizjan B, et al. Pathogenesis of type 1 diabetes: established facts and new insights. *Genes*. (2022) 13(4):706. doi: 10.3390/genes13040706

81. Stene LC, Lernmark A. Epidemiology and pathogenesis of type 1 diabetes. In: Gruessner RWG, Gruessner AC, editors. *Transplantation of the Pancreas*., vol. . p . Springer International Publishing, Cham (2023). p. 13–39.

82. Galicia-Garcia U, Benito-Vicente A, Jebari S, Larrea-Sebal A, Siddiqi H, Uribe KB, et al. Pathophysiology of type 2 diabetes mellitus. *Int J Mol Sci*. (2020) 21(17):6275. doi: 10.3390/ijms21176275

83. Knight RR, Kronenberg D, Zhao M, Huang GC, Eichmann M, Bulek A, et al. Human B-cell killing by autoreactive preproinsulin-specific cd8 T cells is predominantly granule-mediated with the potency dependent upon T-cell receptor avidity. *Diabetes*. (2013) 62:205–13. doi: 10.2337/db12-0315

84. Trivedi P, Graham KL, Krishnamurthy B, Fynch S, Slattery RM, Kay TW, et al. Perforin facilitates beta cell killing and regulates autoreactive cd8+ T-cell responses to antigen in mouse models of type 1 diabetes. *Immunol Cell Biol*. (2016) 94:334–41. doi: 10.1038/icb.2015.89

85. Kendall PL, Woodward EJ, Hulbert C, Thomas JW. Peritoneal B cells govern the outcome of diabetes in non-obese diabetic mice. *Eur J Immunol*. (2004) 34:2387–95. doi: 10.1002/eji.200324744

86. Serreze DV, Chapman HD, Varnum DS, Hanson MS, Reifsnyder PC, Richard SD, et al. B lymphocytes are essential for the initiation of T cell-mediated autoimmune diabetes: analysis of a new "Speed congenic" Stock of nod.Ig mu null mice. *J Exp Med*. (1996) 184:2049–53. doi: 10.1084/jem.184.5.2049

87. Bruggeman Y, Martens PJ, Sassi G, Viaene M, Wasserfall CH, Mathieu C, et al. Footprint of pancreas infiltrating and circulating immune cells throughout type 1 diabetes development. *Front Endocrinol*. (2023) 14:1275316. doi: 10.3389/fendo.2023.1275316

88. Bender C, Rajendran S, von Herrath MG. New insights into the role of autoreactive cd8 T cells and cytokines in human type 1 diabetes. *Front Endocrinol*. (2020) 11:606434. doi: 10.3389/fendo.2020.606434

89. Roep BO, Thomaidou S, van Tienhoven R, Zaldumbide A. Type 1 diabetes mellitus as a disease of the B-cell (Do not blame the immune system)? *Nat Rev Endocrinol*. (2021) 17:150–61. doi: 10.1038/s41574-020-00443-4

90. Atkinson MA, Mirmira RG. The pathogenic "Symphony" in type 1 diabetes: A disorder of the immune system, B Cells, and exocrine pancreas. *Cell Metab*. (2023) 35:1500–18. doi: 10.1016/j.cmet.2023.06.018

91. Okamura T, Hashimoto Y, Hamaguchi M, Obora A, Kojima T, Fukui M. Ectopic fat obesity presents the greatest risk for incident type 2 diabetes: A population-based longitudinal study. *Int J Obes (2005)*. (2019) 43:139–48. doi: 10.1038/s41366-018-0076-3

92. Jiao P, Chen Q, Shah S, Du J, Tao B, Tzameli I, et al. Obesity-related upregulation of monocyte chemotactic factors in adipocytes: involvement of nuclear factor-kappab and C-jun nh2-terminal kinase pathways. *Diabetes*. (2009) 58:104–15. doi: 10.2337/db07-1344

93. Lumeng CN, Bodzin JL, Saltiel AR. Obesity induces a phenotypic switch in adipose tissue macrophage polarization. *J Clin Invest*. (2007) 117:175–84. doi: 10.1172/jci29881

94. Xu H, Barnes GT, Yang Q, Tan G, Yang D, Chou CJ, et al. Chronic inflammation in fat plays a crucial role in the development of obesity-related insulin resistance. *J Clin Invest*. (2003) 112:1821–30. doi: 10.1172/jci19451

95. Ying W, Fu W, Lee YS, Olefsky JM. The role of macrophages in obesity-associated islet inflammation and B-cell abnormalities. *Nat Rev Endocrinol*. (2020) 16:81–90. doi: 10.1038/s41574-019-0286-3

96. Wentworth JM, Fourlanos S, Harrison LC. Reappraising the stereotypes of diabetes in the modern diabetogenic environment. *Nat Rev Endocrinol*. (2009) 5:483–9. doi: 10.1038/nrendo.2009.149

97. DeFuria J, Belkina AC, Jagannathan-Bogdan M, Snyder-Cappione J, Carr JD, Nersesova YR, et al. B cells promote inflammation in obesity and type 2 diabetes through regulation of T-cell function and an inflammatory cytokine profile. *Proc Natl Acad Sci U.S.A*. (2013) 110:5133–8. doi: 10.1073/pnas.1215840110

98. Kintscher U, Hartge M, Hess K, Foryst-Ludwig A, Clemenz M, Wabitsch M, et al. T-lymphocyte infiltration in visceral adipose tissue: A primary event in adipose tissue inflammation and the development of obesity-mediated insulin resistance. *Arteriosclerosis thrombosis Vasc Biol*. (2008) 28:1304–10. doi: 10.1161/atvbaha.108.165100

99. Zhong H, Ren H, Lu Y, Fang C, Hou G, Yang Z, et al. Distinct gut metagenomics and metaproteomics signatures in prediabetics and treatment-naïve type 2 diabetics. *EBioMedicine*. (2019) 47:373–83. doi: 10.1016/j.ebiom.2019.08.048

100. Scheithauer TPM, Rampanelli E, Nieuwdorp M, Vallance BA, Verchere CB, van Raalte DH, et al. Gut microbiota as a trigger for metabolic inflammation in obesity and type 2 diabetes. *Front Immunol*. (2020) 11:571731. doi: 10.3389/fimmu.2020.571731

101. Pérez MM, Martins LMS, Dias MS, Pereira CA, Leite JA, Gonçalves ECS, et al. Interleukin-17/interleukin-17 receptor axis elicits intestinal neutrophil migration, restrains gut dysbiosis and lipopolysaccharide translocation in high-fat diet-induced metabolic syndrome model. *Immunology*. (2019) 156:339–55. doi: 10.1111/imm.13028

102. Shao L, Feng B, Zhang Y, Zhou H, Ji W, Min W. The role of adipose-derived inflammatory cytokines in type 1 diabetes. *Adipocyte*. (2016) 5:270–4. doi: 10.1080/21623945.2016.1162358

103. Kahn CR, Wang G, Lee KY. Altered adipose tissue and adipocyte function in the pathogenesis of metabolic syndrome. *J Clin Invest*. (2019) 129:3990–4000. doi: 10.1172/jci129187

104. Cox AR, Chernis N, Kim KH, Masschelin PM, Saha PK, Briley SM, et al. Ube2i deletion in adipocytes causes lipoatrophy in mice. *Mol Metab*. (2021) 48:101221. doi: 10.1016/j.molmet.2021.101221

105. Xie H, Wang YH, Liu X, Gao J, Yang C, Huang T, et al. Sumoylation of erp44 enhances ero1α Er retention contributing to the pathogenesis of obesity and insulin resistance. *Metabolism*. (2023) 139:155351. doi: 10.1016/j.metabol.2022.155351

106. Zheng Q, Cao Y, Chen Y, Wang J, Fan Q, Huang X, et al. Senp2 regulates adipose lipid storage by de-sumoylation of setdb1. *J Mol Cell Biol*. (2018) 10:258–66. doi: 10.1093/jmcb/mjx055

107. Zhang W, Li F, Hou J, Cheng Y, Zhang W, Liang X, et al. Aberrant sumo2/3 modification of runx1 upon senp1 inhibition is linked to the development of diabetic retinopathy in mice. *Exp Eye Res*. (2023) 237:109695. doi: 10.1016/j.exer.2023.109695

108. Zhang W, Zhang D, Cheng Y, Liang X, Wang J. Runx1 regulates tff1 expression to expedite viability of retinal microvascular endothelial cells in mice with diabetic retinopathy. *Exp Eye Res*. (2022) 217:108969. doi: 10.1016/j.exer.2022.108969

109. Han X, Dong XX, Shi MY, Feng L, Wang XL, Zhang JS, et al. Sumoylation and deacetylation affect nf-Kb P65 activity induced by high glucose in human lens epithelial cells. *Int J Ophthalmol*. (2019) 12:1371–9. doi: 10.18240/ijo.2019.09.01

110. Huang W, Xu L, Zhou X, Gao C, Yang M, Chen G, et al. High glucose induces activation of nf-Kb inflammatory signaling through Iκbα Sumoylation in rat mesangial cells. *Biochem Biophys Res Commun*. (2013) 438:568–74. doi: 10.1016/j.bbrc.2013.07.065

111. Hwang KW, Won TJ, Kim H, Chun HJ, Chun T, Park Y. Erratum to "Characterization of the regulatory roles of the sumo. *Diabetes Metab Res Rev*. (2012) 28:196–202. doi: 10.1002/dmrr.2273

112. He F, Huang Y, Song Z, Zhou HJ, Zhang H, Perry RJ, et al. Mitophagy-mediated adipose inflammation contributes to type 2 diabetes with hepatic insulin resistance. *J Exp Med*. (2021) 218(3):e20201416. doi: 10.1084/jem.20201416

113. Jiang T, Li Y, He S, Huang N, Du M, Zhai Q, et al. Reprogramming astrocytic ndrg2/nf-Kb/C3 signaling restores the diabetes-associated cognitive dysfunction. *EBioMedicine*. (2023) 93:104653. doi: 10.1016/j.ebiom.2023.104653

114. Wlazlo N, van Greevenbroek MM, Ferreira I, Feskens EJ, van der Kallen CJ, Schalkwijk CG, et al. Complement factor 3 is associated with insulin resistance and with incident type 2 diabetes over a 7-year follow-up period: the codam study. *Diabetes Care*. (2014) 37:1900–9. doi: 10.2337/dc13-2804

115. Sarkar S, Elliott EC, Henry HR, Ludovico ID, Melchior JT, Frazer-Abel A, et al. Systematic review of type 1 diabetes biomarkers reveals regulation in circulating proteins related to complement, lipid metabolism, and immune response. *Clin Proteomics*. (2023) 20:38. doi: 10.1186/s12014-023-09429-6

116. Jiang J, Wang H, Liu K, He S, Li Z, Yuan Y, et al. Association of complement C3 with incident type 2 diabetes and the mediating role of bmi: A 10-year follow-up study. *J Clin Endocrinol Metab*. (2023) 108:736–44. doi: 10.1210/clinem/dgac586

117. Rasmussen KL, Nordestgaard BG, Nielsen SF. Complement C3 and risk of diabetic microvascular disease: A cohort study of 95202 individuals from the general population. *Clin Chem*. (2018) 64:1113–24. doi: 10.1373/clinchem.2018.287581

118. Li Y, Wang X, Wang S, Zhu C, Guo J, Li K, et al. Complement 3 mediates periodontal destruction in patients with type 2 diabetes by regulating macrophage polarization in periodontal tissues. *Cell proliferation*. (2020) 53:e12886. doi: 10.1111/cpr.12886

119. Kopytek M, Mazur P, Ząbczyk M, Undas A, Natorska J. Diabetes concomitant to aortic stenosis is associated with increased expression of nf-Kb and more pronounced valve calcification. *Diabetologia*. (2021) 64:2562–74. doi: 10.1007/s00125-021-05545-w

120. Wang WY, Zheng YS, Li ZG, Cui YM, Jiang JC. Mir-92a contributes to the cardiovascular disease development in diabetes mellitus through nf-Kb and downstream inflammatory pathways. *Eur Rev Med Pharmacol Sci*. (2019) 23:3070–9. doi: 10.26355/eurrev_201904_17589

121. Hsu CY, Yeh LT, Fu SH, Chien MW, Liu YW, Miaw SC, et al. Sumo-defective C-maf preferentially transactivates il21 to exacerbate autoimmune diabetes. *J Clin Invest*. (2018) 128:3779–93. doi: 10.1172/jci98786

122. Fujino M, Morito N, Hayashi T, Ojima M, Ishibashi S, Kuno A, et al. Transcription factor C-maf deletion improves streptozotocin-induced diabetic nephropathy by directly regulating sglt2 and glut2. *JCI Insight*. (2023) 8(6):e163306. doi: 10.1172/jci.insight.163306

123. Ren HM, Lukacher AE, Rahman ZSM, Olsen NJ. New developments implicating il-21 in autoimmune disease. *J Autoimmun*. (2021) 122:102689. doi: 10.1016/j.jaut.2021.102689

124. Sutherland AP, Van Belle T, Wurster AL, Suto A, Michaud M, Zhang D, et al. Interleukin-21 is required for the development of type 1 diabetes in nod mice. *Diabetes*. (2009) 58:1144–55. doi: 10.2337/db08-0882

125. Liu Y, Yang Z, Lai P, Huang Z, Sun X, Zhou T, et al. Bcl-6-directed follicular helper T cells promote vascular inflammatory injury in diabetic retinopathy. *Theranostics*. (2020) 10:4250–64. doi: 10.7150/thno.43731

126. von Herrath M, Bain SC, Bode B, Clausen JO, Coppieters K, Gaysina L, et al. Anti-interleukin-21 antibody and liraglutide for the preservation of B-cell function in adults with recent-onset type 1 diabetes: A randomised, double-blind, placebo-controlled, phase 2 trial. *Lancet Diabetes Endocrinol*. (2021) 9:212–24. doi: 10.1016/s2213-8587(21)00019-x

127. Luo J, Ning T, Li X, Jiang T, Tan S, Ma D. Targeting il-12 family cytokines: A potential strategy for type 1 and type 2 diabetes mellitus. *Biomedicine pharmacotherapy = Biomedecine pharmacotherapie*. (2024) 170:115958. doi: 10.1016/j.biopha.2023.115958

128. Gunes A, Schmitt C, Bilodeau L, Huet C, Belblidia A, Baldwin C, et al. Il-6 trans-signaling is increased in diabetes, impacted by glucolipotoxicity, and associated with liver stiffness and fibrosis in fatty liver disease. *Diabetes*. (2023) 72:1820–34. doi: 10.2337/db23-0171

129. Roca-Rivada A, Marín-Cañas S, Colli ML, Vinci C, Sawatani T, Marselli L, et al. Inhibition of the type 1 diabetes candidate gene ptpn2 aggravates tnf-A-induced human beta cell dysfunction and death. *Diabetologia*. (2023) 66:1544–56. doi: 10.1007/s00125-023-05908-5

130. Leavenworth JW, Ma X, Mo YY, Pauza ME. Sumo conjugation contributes to immune deviation in nonobese diabetic mice by suppressing C-maf transactivation of il-4. *J Immunol*. (2009) 183:1110–9. doi: 10.4049/jimmunol.0803671

131. Hajmrle C, Ferdaoussi M, Plummer G, Spigelman AF, Lai K, Manning Fox JE, et al. Sumoylation protects against il-1β-induced apoptosis in ins-1 832/13 cells and human islets. *Am J Physiol Endocrinol Metab*. (2014) 307:E664–73. doi: 10.1152/ajpendo.00168.2014

132. Song Y, Wan X, Gao L, Pan Y, Xie W, Wang H, et al. Activated pkr inhibits pancreatic B-cell proliferation through sumoylation-dependent stabilization of P53. *Mol Immunol*. (2015) 68:341–9. doi: 10.1016/j.molimm.2015.09.007

133. Wang C, Xiao Y, Lao M, Wang J, Xu S, Li R, et al. Increased sumo-activating enzyme sae1/uba2 promotes glycolysis and pathogenic behavior of rheumatoid fibroblast-like synoviocytes. *JCI Insight*. (2020) 5(18):e135935. doi: 10.1172/jci.insight.135935

134. Hoard TM, Yang XP, Jetten AM, ZeRuth GT. Pias-family proteins negatively regulate glis3 transactivation function through sumo modification in pancreatic B Cells. *Heliyon*. (2018) 4:e00709. doi: 10.1016/j.heliyon.2018.e00709

135. Feng Y, Wu H, Xu Y, Zhang Z, Liu T, Lin X, et al. Zinc finger protein 451 is a novel smad corepressor in transforming growth factor-B Signaling. *J Biol Chem*. (2014) 289:2072–83. doi: 10.1074/jbc.M113.526905

136. Chen Y, Chen X, Luo Z, Kang X, Ge Y, Wan R, et al. Exercise-induced reduction of igf1r sumoylation attenuates neuroinflammation in app/ps1 transgenic mice. *J advanced Res*. (2024) S2090-1232(24)00127-9. doi: 10.1016/j.jare.2024.03.025

frontiers | Frontiers in Immunology

TYPE Original Research
PUBLISHED 08 May 2025
DOI 10.3389/fimmu.2025.1493950

OPEN ACCESS

EDITED BY
Uzma Saqib,
Indian Institute of Technology Indore, India

REVIEWED BY
Sadiq Umar,
University of Illinois Chicago, United States
Laura Andrea Dada,
Northwestern University, United States

*CORRESPONDENCE
Yogesh Saini
ysaini@ncsu.edu

RECEIVED 10 September 2024
ACCEPTED 09 April 2025
PUBLISHED 08 May 2025

CITATION
Choudhary I, Paudel K, Kumar R, Sharma A, Patial S and Saini Y (2025) Airway epithelial cell-specific deletion of EGFR modulates mucoinflammatory features of cystic fibrosis-like lung disease in mice.
Front. Immunol. 16:1493950.
doi: 10.3389/fimmu.2025.1493950

Airway epithelial cell-specific deletion of EGFR modulates mucoinflammatory features of cystic fibrosis-like lung disease in mice

Ishita Choudhary[1], Kshitiz Paudel[1], Rahul Kumar[1], Amit Sharma[1], Sonika Patial[2] and Yogesh Saini[1]*

[1]Department of Population Health and Pathobiology, College of Veterinary Medicine, North Carolina State University, Raleigh, NC, United States, [2]Division of Translational Toxicology, National Institute of Environmental Health Sciences, Research Triangle Park, Durham, NC, United States

Mucoinflammatory lung disease in cystic fibrosis (CF) is characterized by airway surface liquid (ASL) layer dehydration and mucins hyperconcentration, which leads to airway obstruction, inflammation, bronchiectasis, and increased susceptibility to recurrent bacterial infections. Epidermal growth factor receptor (EGFR) is known to regulate airway mucous cell metaplasia (MCM) and mucins expression, but the role of EGFR pathway in the pathogenesis of CF-like lung disease remains unclear. Therefore, we hypothesized that airway epithelial cell-specific deficiency of EGFR mitigates mucoinflammatory responses in *Scnn1b*-transgenic (Tg+) mice that phenocopy human CF-like lung disease. To test this hypothesis, we examined the effect of airway epithelial cell-specific EGFR deficiency on the manifestation of mucoinflammatory outcomes in Tg+ mice. The airway epithelial cell-specific EGFR-deficient wild-type (WT) mice did not exhibit any obvious structural and functional defects in the lungs. The deletion of EGFR in airway epithelial cells in Tg+ mice, however, resulted in increased recruitment of neutrophils and macrophages into the lung airspaces, which was accompanied by significantly increased bronchoalveolar lavage fluid (BALF) levels of inflammatory mediators, including KC, G-CSF, MIP-2, MIP-1α, TNF-α, and MIP-1β. Additionally, as compared with the EGFR-sufficient Tg+ mice, the airway epithelial cell-specific EGFR-deficient Tg+ mice exhibited significantly increased postnatal mortality and compromised bacterial clearance. The deletion of EGFR in the airway epithelial cells of Tg+ mice resulted in an increased degree of mucus obstruction, which was associated with an increase in MCM and MUC5B production. Some of the molecular markers of type 2 inflammation, including *Il13*, *Slc26a4*, and *Retnla*, were significantly increased in airway epithelial cell-

specific EGFR-deficient Tg+ mice versus EGFR-sufficient Tg+ mice. Taken together, our data show that EGFR deletion in the airway epithelial cells compromises postnatal survival, delays bacterial clearance, and modulates inflammatory and mucus obstruction-relevant endpoints, i.e., MCM, MUC5B production, and mucus obstruction, in Tg+ mice.

KEYWORDS

EGFR, cystic fibrosis, *Scnn1b*-Tg+, airway epithelium, mucus obstruction

Introduction

Cystic fibrosis (CF) is an autosomal recessive genetic disorder caused by various mutations in the cystic fibrosis transmembrane conductance regulator (*CFTR*) gene, which results in reduced chloride and bicarbonate ions secretion and increased sodium ions absorption (1, 2). The resulting ionic imbalance leads to the dehydration of the airway surface liquid layer (ASL), causing mucins hyperconcentration, mucostasis, defective mucociliary clearance, airway inflammation, and recurrent bacterial infections (2, 3). Mucins hypersecretion is another key characteristic of CF, where the excessive release of mucins into the hyperconcentrated ASL results in the formation of static mucus plugs, which in turn contributes to airflow obstruction (3). IL-4Rα and epidermal growth factor receptor (EGFR) pathways are known to contribute to mucins hypersecretion via coordinated promotion of mucous cell metaplasia (MCM) (4–10). While the role of IL-4Rα signaling pathway has been investigated in mouse model of human CF-like lung disease (11), the role of EGFR signaling pathway in inducing mucins production and other inflammatory outcomes remains unclear.

EGFR, one of the four members of the receptor tyrosine kinase (RTK) superfamily, binds to a variety of ligands, including epidermal growth factor (EGF), transforming growth factor-α (TGF-α), amphiregulin (AREG), epiregulin (EREG), β-cellulin (BTC), heparin-binding EGF (HB-EGF), and epigen (EPGN) (12, 13). EGFR is critically important for embryonic development, tissue differentiation, and cellular function, and EGFR loss causes either embryonic or postnatal mortality depending on the genetic background of the mice (14–16). In normal airways, EGFR signaling constitutes a critical developmental pathway in lung epithelial cells by controlling lung development and maintaining airway homeostasis (15, 17–20). Dysregulated EGFR signaling is associated with the pathogenesis of airway hypersecretory and mucoinflammatory diseases such as asthma and COPD (12). EGFR signaling is critical for inducing MCM in animal models and for mucins expression in human airway epithelial cells in response to IL-13, viruses, TGF-α, and cigarette smoke (6, 21–24). Increased EGFR signaling, TGF-α production, and mucins (MUC5AC and MUC5B) expression have been reported in the airways of CF patients (25); however, the causative role of EGFR in CF-like lung disease has not been demonstrated, thus warranting further investigation. Accordingly, we investigated the role of airway epithelial cell-specific EGFR in the pathogenesis of mucoinflammatory lung disease in *Scnn1b*-transgenic (*Scnn1b*-Tg +) mice, a mouse model of human CF-like lung disease.

The *Scnn1b*-Tg+ (Tg+) mouse overexpresses sodium channel, non-voltage gated 1, beta subunit (*Scnn1b*) transgene in club cell secretory protein (CCSP)-expressing airway epithelial cells (26). The *Scnn1b* overexpression dictates the hyperabsorption of sodium ions into the airway epithelial cells, resulting in an osmotic gradient-driven dehydration of ASL. As a consequence, within the first week of postnatal life, the Tg+ neonates exhibit mucoinflammatory lung disease features, including MCM, mucins hypersecretion, mucus obstruction, defective mucociliary clearance, airway inflammation characterized by activated macrophages, granulocytes, and lymphocytes, and spontaneous bacterial infections (26–30). In this study, we hypothesized that airway epithelial cell-specific deficiency of EGFR mitigates mucoinflammatory responses in Tg+ mice. Towards this, we examined the effects of airway epithelial cell-specific EGFR deletion on key features of Tg+ mice, including postnatal survival, genes relevant to mucoinflammatory responses, mucus obstruction, MCM, immune cell recruitment, cytokine levels, and bacterial load. The results from this study highlight the contribution of airway epithelial cell-specific EGFR in the pathogenesis of CF-like mucoinflammatory lung disease in Tg+ mice.

Materials and methods

Generation of mice and animal husbandry

Scnn1b-Tg+ (Tg+) mice [B6N.Cg-Tg(Scgb1a1-Scnn1b) 6608Bouc/J] were procured from the Jackson Laboratory (Bar Harbor, ME) and maintained at the Division of Laboratory Animal Medicine (DLAM) vivarium of Louisiana State University (LSU). Club cell-specific Cre recombinase (CCSP-Cre^{+}) mice were provided by Dr. Francesco J. DeMayo (NIEHS, North Carolina (NC)), and *Egfr* floxed (*Egfr*$^{fl/fl}$) mice were provided by Dr. David Threadgill (Texas A&M University, Texas). All three mice strains were interbred to generate various parental genotypes. EGFR-sufficient Tg+ (CCSP-Cre^{-}/*Egfr*$^{fl/fl}$/Tg+) and airway epithelial cell-

specific EGFR-deficient Tg+ (CCSP-Cre^{+}/*Egfr*$^{fl/fl}$/Tg+) and their wild-type (WT) counterparts, i.e., CCSP-Cre^{-}/*Egfr*$^{fl/fl}$/WT and CCSP-Cre^{+}/*Egfr*$^{fl/fl}$/WT, were generated by reciprocal crosses between CCSP-Cre^{+}/*Egfr*$^{fl/fl}$/WT and CCSP-Cre^{-}/*Egfr*$^{fl/fl}$/Tg+ (or CCSP-Cre^{-}/*Egfr*$^{fl/fl}$/WT and CCSP-Cre^{+}/*Egfr*$^{fl/fl}$/Tg+) parental genotypes. The CCSP-Cre^{+}/*Egfr*$^{fl/fl}$/Tg+ mice are expected to have EGFR deficiency only in the CCSP+ cells. However, our previous study employing CCSP-Cre mice (31) have shown that the CCSP-Cre^{+} causes recombination in almost all the airway epithelial cells. Therefore, we will be using the term "airway epithelial cell-specific EGFR-deficient mice" and not "Club cell-specific EGFR deficient mice". Genotypes of all four experimental groups were confirmed with polymerase chain reaction (PCR). Nucleotide sequences of primers used for genotyping are included in Supplementary Table 1. Mice were housed in hot-washed and individually ventilated cages on 12h day/night cycle at DLAM vivarium of LSU. Mice were provided with a regular diet and water *ad libitum*. All the animal experiments were approved by the Institutional Animal Care and Use Committee (IACUC) of Louisiana State University.

Bronchoalveolar lavage fluid analyses and tissue collection

Juvenile mice (Postnatal day 21, PND21) were anesthetized via intraperitoneal (IP) injection of 2,2,2-tribromoethanol (Millipore Sigma, Burlington, MA). The left main stem bronchus was ligated, and the right lung lobes were aseptically lavaged with a body weight-adjusted volume of Dulbecco's Phosphate Buffered Saline (DPBS) (Corning, Manassas, VA). A fraction of the harvested bronchoalveolar lavage fluid (BALF) was used for the estimation of colony forming units (CFUs), and the remaining BALF was centrifuged at 4°C for 500 x *g* for 5 min. Cell-free BALF supernatant was collected and stored at -80°C for the total protein, dsDNA, and cytokine analyses. Cell pellets were resuspended in 250 µl of DPBS and used for total and differential cell counts estimation as described previously (32). Lavaged right lung lobes were snap-frozen and stored at -80°C for gene expression analyses. Unlavaged left lung lobes were fixed in 10% neutral buffered formalin and processed for histological analyses, as described previously (33).

Total protein and dsDNA estimation

Total protein and dsDNA contents in the BALF were determined by Bradford assay (Bio-Rad, Hercules, CA) and spectrophotometric assay using NanoDrop 8000 (Thermo Fisher Scientific, Waltham, MA), respectively.

Cytokine analyses

Cell-free BALF samples were assayed for various soluble mediators as previously described (34). Briefly, the BALF levels of various cytokines and chemokines were determined using Luminex XMAP-based assay (MCYTOMAG-70K), according to the manufacturer's instructions (EMD Millipore, Billerica, MA). The list of cytokines and chemokines is included in Supplementary Table 2.

Enzyme-linked immunosorbent assay

IL-13 levels were analyzed in the cell-free BALF samples using Mouse IL-13 ELISA Kit-Quantikine (Cat # M1300CB, R&D systems, Minneapolis, MN), according to the manufacturer's instructions.

Bacterial burden analyses

The aseptically harvested BALF was serially diluted and plated onto Columbia blood agar (CBA) plates (Hardy Diagnostics, Santa Maria, CA). The plates were incubated in anaerobic candle jars at 37°C for 48h. The CFUs were counted, and the morphological characteristics of the colonies were recorded, as previously described (32).

Histopathological analyses

The formalin-fixed left lung lobes were embedded in paraffin and sectioned at 5µm thickness. Alcian blue-periodic acid-Schiff (AB-PAS) staining was performed to stain mucopolysaccharide materials in the airway lumen and mucins content within the airway epithelial cells. Mucus obstruction was graded using the histological semiquantitative grading strategy as previously described (32). For MCM analyses, the photographs of AB-PAS-stained large airways were captured under the 40X objective of the ECLIPSE Ci-L microscope with DS-Fi2 camera attachment (Nikon, Melville, NY). Thereafter, the analyses were performed by quantifying the number of mucous cells per millimeter (mm) of basement membrane using the Fiji software (35). All the slides were graded by a board-certified anatomic pathologist in a blinded manner.

Immunohistochemical analyses

Formalin-fixed paraffin-embedded left lung sections were used for the immunohistochemical localization of MUC5AC, MUC5B, and E-cadherin. The sections were stained with the corresponding primary antibodies: rabbit polyclonal MUC5AC antibody (UNC 294, a kind gift by Dr. Camille Ehre, University of North Carolina, Chapel Hill, NC), rabbit polyclonal MUC5B antibody (UNC223, a kind gift by Dr. Camille Ehre, University of North Carolina, Chapel Hill, NC), and Rabbit monoclonal E-cadherin primary antibody (3195, Cell Signaling Technology, Danvers, MA) using previously published procedure (36–38). The immunostained slides were analyzed by a board-certified anatomic pathologist without prior knowledge of genotypes. The photographs were

captured under the 40X or 4X objective of the ECLIPSE Ci-L microscope with DS-Fi2 camera attachment (Nikon, Melville, NY). Thereafter, captured images were processed using the Fiji software (35) to determine the percentage of stained area (MUC5B and MUC5AC).

Gene expression analyses

Total RNA isolation from right lungs, analysis of quantity and purity of isolated total RNA, cDNA generation, and reverse transcription quantitative polymerase chain reaction (RT-qPCR) were done as described previously (39). The nucleotide sequences of primers used in RT-qPCR are included in Supplementary Table 1.

BaseScope (RNA *in situ* hybridization) assay for the detection of *Egfr* mRNA

Left lungs were fixed in 10% neutral buffered formalin for 24 hrs. and embedded in paraffin. These formalin-fixed, paraffin-embedded left lung sections were used to perform RNA *in situ* localization of *Egfr* mRNA using BaseScope technology (ACD, Newark, CA). Briefly, the lung sections were baked at 60°C in a hybridization oven, deparaffinized in xylene and dehydrated in 100% ethanol followed by air-drying the slides for 5 min at 60°C. The slides were then incubated for 10 min at room temperature (RT) with 3% hydrogen peroxide (322335; ACD, Newark, CA) to quench the endogenous peroxidase activity. Target retrieval was performed using a 1X RNAscope Target Retrieval Reagent (322000; ACD, Newark, CA) at 98-102°C for 15 minutes, followed by three washes in distilled water. RNAscope Protease IV (322336; ACD, Newark, CA) was added to the lung sections and incubated at 40°C in a hybridization oven for 30 minutes followed by two washes of distilled water. Custom designed *Egfr* probe (1307511-C1; ACD, Newark, CA) equilibrated to room temperature was subsequently added to the lung sections and incubated in a hybridization oven for 2 hours at 40°C. After two washes with the wash buffer (310091, ACD, Newark, CA), the sections underwent eight amplification steps to enhance the signals. BaseScopeTM Detection Reagents v2–RED (Cat. No. 323910; ACD, Newark, CA) were used to detect the red signal. Finally, the sections were counterstained with 50% Gill's Hematoxylin I for 2 min at RT followed by 3–5 times rinse with tap water. The slides were further washed 2–3 times in 0.02% Ammonia water, followed by 3-time wash in tap water. The slides were dehydrated at 60°C in a hybridization oven until the slides were completely dry, and coverslipped using VectaMount mounting media (H-5000; Vector Laboratories, Burlingame, CA). The stained slides were analyzed by a board-certified anatomic pathologist without prior knowledge of genotypes. The stained slides were captured under the 100X objective of the ECLIPSE Ci-L microscope with DS-Fi2 camera attachment (Nikon, Melville, NY).

Statistical analyses

One-way analysis of variance (ANOVA) followed by Tukey's *post hoc* test was used to determine statistically significant differences among the groups. All data were presented as mean ± standard error of the mean (SEM). Grubbs' test was used to remove the outliers. To reduce the number of horizontal bars indicating statistically significant differences between experimental groups, we used a single bar when one group showed significant differences compared to multiple other groups (with vertical ticks). A p-value of less than 0.05 was considered statistically significant. All statistical analyses were performed using GraphPad Prism 10.0 (GraphPad Software Inc., La Jolla, CA).

Results

EGFR deletion in airway epithelial cells increases postnatal mortality in Tg+ mice

The airway epithelial cell-specific EGFR-deficient Tg+ (Cre^+/Tg+) and control (Cre^-/Tg+, Cre^+/WT, and Cre^-/WT) mice were generated (Figure 1A), and three-week-old juveniles (Postnatal day 21; PND21) were assessed for endpoints including postnatal survival, RT-qPCR for genes relevant to mucoinflammatory responses, mucus obstruction, MCM, immune cell recruitment, cytokine levels, and bacterial load. The deletion of EGFR in the airway epithelial cells was confirmed by BaseScope assay (Figure 1B).

The germline deletion of EGFR in mice results in mortality between midgestation and PND 20, depending on the genetic background of the mice (14). Therefore, to determine whether the airway-epithelial cell-specific EGFR deficiency contributes to the embryonic mortality, we analyzed the possibility of embryonic mortality by calculating the mendelian ratio of the expected genotypes of neonates, i.e., Cre^-/WT (n=80), Cre^+/WT (n=72), Cre^-/Tg+ (n=83), and Cre^+/Tg+ (n=66). The mendelian ratio for the Cre^-/WT, Cre^+/WT, Cre^-/Tg+, and Cre^+/Tg+ progeny was 1.06:0.96:1.10:0.88, respectively. The calculated $\chi 2$ value of 0.498 suggested that the observed mendelian ratio was not significantly deviated from the expected mendelian ratio of 1:1:1:1. These data suggest that airway epithelial cell-specific deletion of EGFR doesn't compromise embryonic viability.

The Tg+ mice exhibit significant postnatal mortality within the first 3 weeks of life (11, 26, 27). To determine the effect of airway epithelial cell-specific EGFR deletion on postnatal survivability of the Tg+ mice, we observed pups until PND20. The survivability was comparable between Cre^-/WT and Cre^+/WT pups (Figure 1C), suggesting that airway epithelial cell-specific EGFR deletion does not compromise postnatal survival in WT pups. Consistent with the previous studies (11, 26, 27, 39), Cre^-/Tg+ exhibited ~41.5% mortality between PND0-PND20, with most of the deaths observed between PND7-PND17 (Figure 1C). As compared with the Cre^-/Tg+ group, the Cre^+/Tg+ mice showed significantly higher mortality rate of ~56.1% (Figure 1C). However, similar to the Cre^-/

10.3389/fimmu.2025.1493950

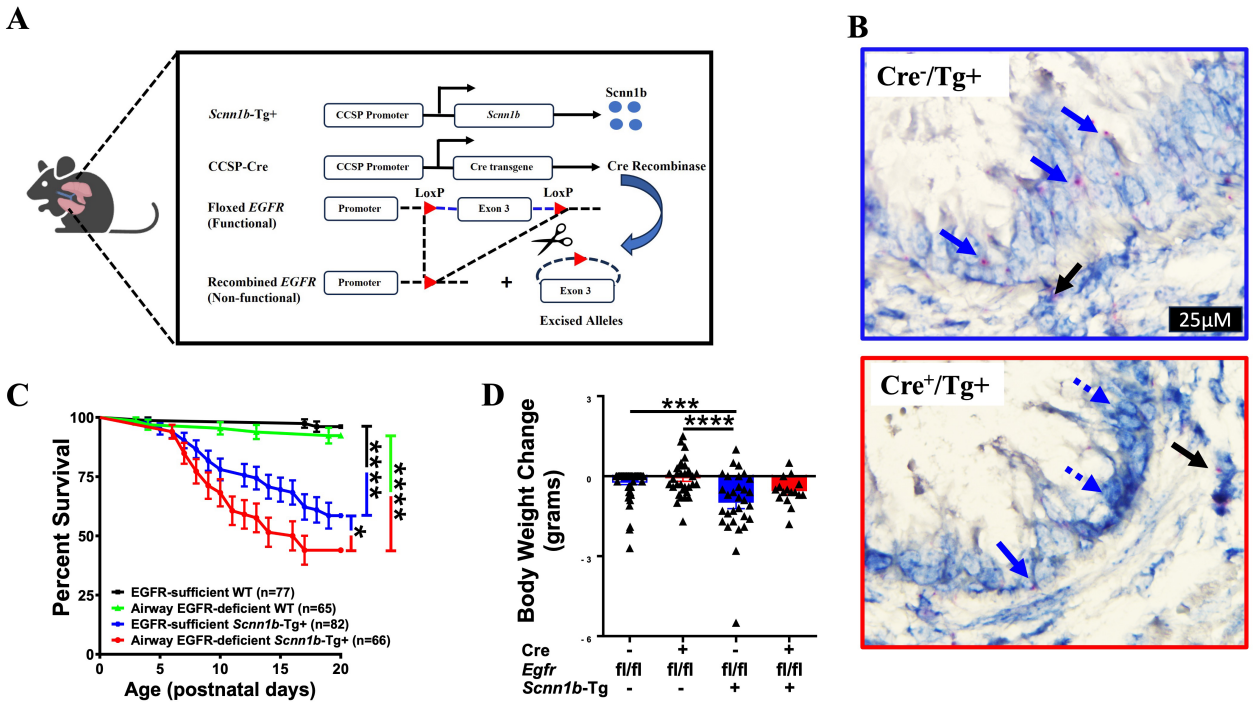

FIGURE 1
EGFR deletion in airway epithelial cells increases postnatal mortality but does not affect body weight change in *Scnn1b*-Tg+ (Tg+) mice. **(A)** Schematic diagram for the generation of airway epithelial cell-specific EGFR-deficient *Scnn1b*-Tg+ (CCSP-Cre^{+}/*Egfr*$^{fl/fl}$/Tg+) mice were generated by interbreeding club cell-specific Cre recombinase (CCSP-Cre^{+}), floxed *Egfr* (*Egfr*$^{fl/fl}$), and *Scnn1b*-Tg+ mice. **(B)** *In situ BaseScope* hybridization for *Egfr* transcripts [red dots representing punctate staining for *Egfr* mRNA in airway epithelial cells (blue arrows) and alveolar epithelial cells (black arrows)] in EGFR-sufficient Tg+ (top panel) and airway epithelial cell-specific EGFR-deficient (bottom panel) Tg+ mice. **(C)** Survival curve for the progeny of the crosses between CCSP-Cre^{+}/*Egfr*$^{fl/fl}$/WT and CCSP-Cre^{-}/*Egfr*$^{fl/fl}$/Tg+ (or CCSP-Cre^{+}/*Egfr*$^{fl/fl}$/Tg+ and CCSP-Cre^{-}/*Egfr*$^{fl/fl}$/WT) mice. n= number of pups per genotype. ****$p < 0.0001$ (EGFR-sufficient WT (CCSP-Cre^{-}/*Egfr*$^{fl/fl}$/WT; Cre^{-}/WT) vs EGFR-sufficient *Scnn1b*-Tg+ (CCSP-Cre^{-}/*Egfr*$^{fl/fl}$/Tg+; Cre^{-}/Tg+)) and (EGFR-deficient WT (CCSP-Cre^{+}/*Egfr*$^{fl/fl}$/WT; Cre^{+}/WT) vs EGFR-deficient *Scnn1b*-Tg+ (CCSP-Cre^{+}/*Egfr*$^{fl/fl}$/Tg+; Cre^{+}/Tg+)), *$p < 0.05$ (Cre^{-}/Tg+ vs Cre^{+}/Tg+) by Gehan-Breslow-Wilcoxon test. Cre^{-}/WT (black), Cre^{+}/WT (green), Cre^{-}/Tg+ (blue), and Cre^{+}/Tg+ neonates (red). **(D)** Body weight change values represent body weight gain (positive value) or loss (negative value) as compared to gender- and age- matched Cre^{-}/WT littermates. The body weights of the healthiest Cre^{-}/WT male or female mice were set to 0. Individual body weight values for other littermates were generated by subtracting the body weight of Cre^{-}/WT from body weight of each gender-matched littermates. Cre^{-}/WT [blue open bar], Cre^{+}/WT [red open bar], Cre^{-}/Tg+ [solid blue bar], and Cre^{+}/Tg+ [solid red bar] mice. Sample size (n=16-59/group). Error bars represent Mean ± SEM. One-way ANOVA followed by Tukey's *post hoc* test was used for the statistical analysis. ***$p < 0.001$, ****$p < 0.0001$.

Tg+ group, most of the deaths in Cre^{+}/Tg+ mice occurred between PND7-PND17. We also investigated the effect of airway epithelial cell-specific deletion of EGFR on postnatal distress in mice by recording their body weights at PND21. Although the Tg+ pups of both genotypes displayed lower body weight at PND21, the airway epithelial cell-specific deletion of EGFR did not alter the postnatal body weight in WT and Tg+ juveniles (Figure 1D). These data suggest that the EGFR deletion promotes mucus obstruction, a pathogenic pathway that contributes to the neonatal mortality in Tg + mice (11, 26, 27).

EGFR deletion in airway epithelial cells increases expression of type 2 inflammation-associated gene signatures and mucus obstruction in Tg+ juveniles

The Tg+ mice predominantly exhibit type 2 inflammation characterized by increased levels of Th2 cytokines, i.e., IL-4 and IL-13, and elevated type 2 inflammation-associated gene signatures (27, 30, 32, 39). Indeed, type 2 inflammation-associated mucus obstruction is known to be the primary cause of postnatal mortality in Tg+ mice (11, 26, 27). Here, we hypothesized that the exaggerated type 2 inflammation in the Cre^{+}/Tg+ mice contributes to excessive mucus obstruction, which results in their increased mortality.

First, we analyzed the expression levels of type 2 inflammation-associated gene signatures, including *Slc26a4*, *Retnla, Chi3l4*, and *Clca1*. The mRNA levels for *Slc26a4*, *Retnla, Chi3l4*, and *Clca1* were comparable in Cre^{-}/WT and Cre^{+}/WT mice (Figures 2A–D), which suggest that the EGFR deletion in the healthy airways does not induce type 2 inflammation. As reported previously (30, 32), the *Slc26a4* mRNA levels trended higher in Cre^{-}/Tg+ mice as compared with Cre^{-}/WT and Cre^{+}/WT mice (Figure 2A). The *Slc26a4* mRNA levels were significantly higher in Cre^{+}/Tg+ mice as compared with all the other three experimental groups (Figure 2A). The mRNA levels of *Retnla* and *Chi3l4* were higher in Cre^{-}/Tg+ versus Cre^{-}/WT mice (Figures 2B, C). As compared with the Cre^{-}/Tg+ mice, the mRNA levels of *Retnla, Chi3l4*, and *Clca1* were higher in Cre^{+}/Tg+

10.3389/fimmu.2025.1493950

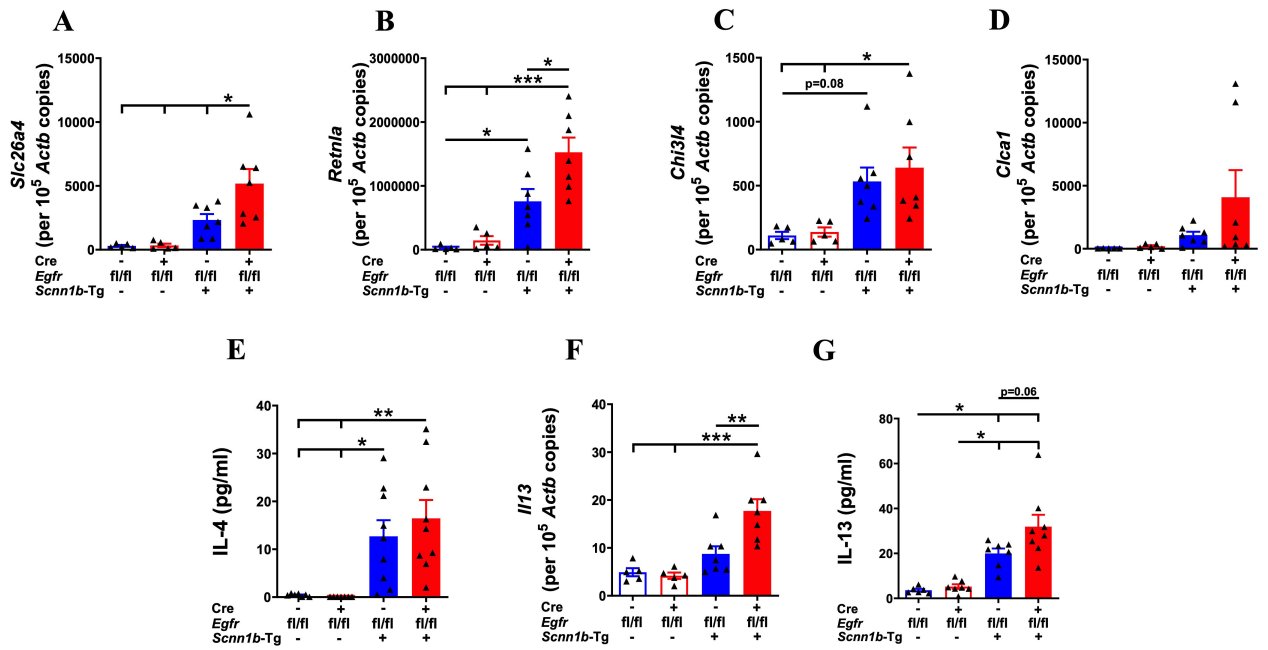

FIGURE 2
EGFR deletion in airway epithelial cells increases the expression of markers associated with type 2 inflammation in Tg+ juveniles. Absolute quantification of *Slc26a4* mRNA **(A)**, *Retnla* mRNA **(B)**, *Chi3l4* mRNA **(C)**, and *Clca1* mRNA **(D)** in the lungs from WT mice (with Cre^- or Cre^+ status) and Tg+ mice (with Cre^- or Cre^+ status) (n=5-7/group). BALF cytokine levels (in pg/ml; picograms per milliliter) of IL-4 (n=7-9/group) **(E)** and absolute quantification of *Il13* mRNA **(F)** in the lungs from WT mice (with Cre^- or Cre^+ status) and Tg+ mice (with Cre^- or Cre^+ status). Sample size (n=5-7/group). **(G)** BALF cytokine levels (in pg/ml; picograms per milliliter) of IL-13 (n=6-8/group) in the lungs from WT mice (with Cre^- or Cre^+ status) and Tg+ mice (with Cre^- or Cre^+ status). Error bars represent Mean ± SEM. One-way ANOVA followed by Tukey's *post hoc* test was used for the statistical analysis. $*p < 0.05$, $**p < 0.01$, $***p < 0.001$. To minimize the number of horizontal lines in various panels (e.g., **A**), single horizontal line with small vertical ticks were used to indicate statistically significant differences. The positioning of small vertical ticks indicates the group that is significantly different from the reference group (with no vertical line). In **(A)**, single horizontal significance line with three vertical ticks suggests significant difference for three comparisons, i.e., Cre^+/Tg+ vs Cre^-/Tg+, Cre^+/Tg+ vs Cre^+/WT, and Cre^+/Tg+ vs Cre^-/WT.

mice, with only *Retnla* showing a significant increase (Figures 2B–D). Because IL4Rα, a common receptor subunit for IL-4 and IL-13, is known to cause mucous cell metaplasia in Tg+ mice (11), we assessed the levels of IL-4 and IL-13. The IL-4 protein levels were comparable in BALF from Cre^-/WT and Cre^+/WT mice (Figure 2E). As reported previously (32, 40), Cre^-/Tg+ mice had elevated IL-4 levels as compared with their WT counterparts (Figure 2E). As compared with the Cre^-/Tg+ mice, the Cre^+/Tg+ mice had insignificantly elevated (p =0.77) IL-4 levels (Figure 2E). The *Il13* mRNA levels in the lung homogenates were comparable among Cre^-/WT and Cre^+/WT mice and significantly higher in the Cre^+/Tg+ group versus the other three experimental groups (Figure 2F). Consistent with the mRNA levels, the IL-13 protein levels showed higher trend in Cre^+/Tg+ mice compared to Cre^-/Tg+ (p =0.06) (Figure 2G).

Airway mucous cell metaplasia (MCM) and mucus obstruction are consistent features of lung disease in Tg+ mice, where two gel-forming mucins, i.e., MUC5B and MUC5AC, primarily contribute to airway mucus obstruction (27). To investigate the effect of airway epithelial cell-specific EGFR deletion on MCM and mucus obstruction, we performed AB-PAS, MUC5B, and MUC5AC staining on the lung sections. While only a very small proportion of Cre^-/WT and Cre^+/WT mice showed minimal airway mucus obstruction, Cre^-/Tg+ mice had a marked increase in the proportion of mucous cells (AB-PAS+, MUC5B+, and MUC5AC+) and the degree of airway mucus obstruction (Figures 3A–G, Supplementary Figure 1). The extent of MCM, as indicated by the proportion of AB-PAS+ and MUC5B+ airway epithelial cells, and the degree of airway mucus obstruction, as indicated by AB-PAS- and MUC5B-stained airway luminal contents, were significantly higher in Cre^+/Tg+ mice compared with Cre^-/Tg+ mice (Figures 3A, B, D–F). The proportion of MUC5AC+ airway epithelial cells was comparable between Cre^+/Tg+ mice versus Cre^-/Tg+ mice (Figures 3C, G). These data suggest that airway epithelial cell-specific EGFR deficiency results in increased MUC5B production and mucus obstruction in Tg+ juveniles.

EGFR deletion in airway epithelial cells worsens inflammatory features in Tg+ juveniles

Increased total protein and dsDNA contents in the BALF are indicative of lung inflammation (32, 41, 42). Therefore, to determine the effect of airway epithelial cell-specific EGFR deletion on lung inflammation, we assessed total protein and dsDNA contents in the BALF. BALF total protein and dsDNA contents were comparable among Cre^-/WT and Cre^+/WT mice

10.3389/fimmu.2025.1493950

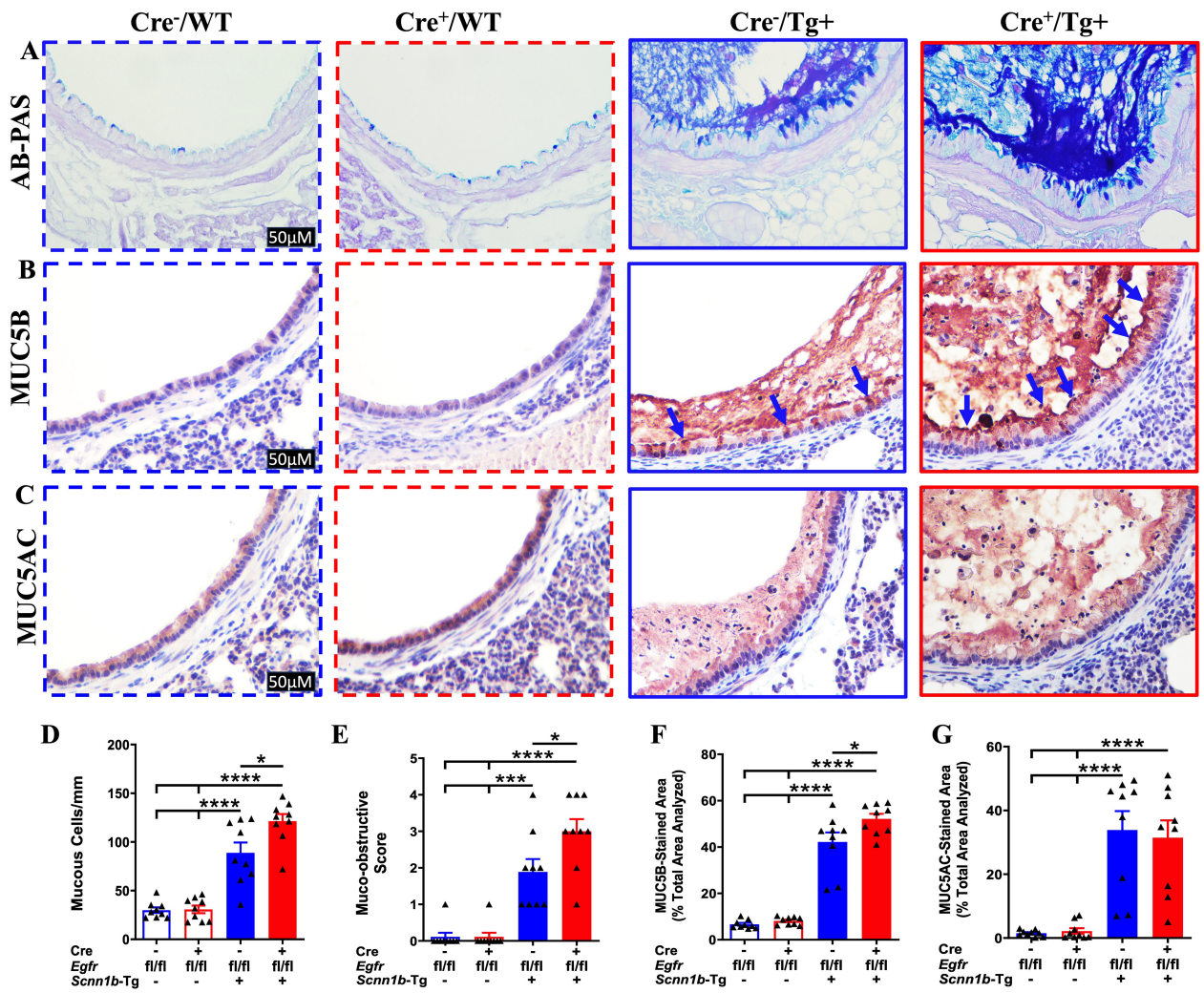

FIGURE 3
EGFR deletion in airway epithelial cells promotes mucus obstruction in Tg+ juveniles. Representative photomicrographs of AB-PAS-stained **(A)**, MUC5B-immunostained **(B)**, and MUC5AC-immunostained **(C)** left lung lobe sections from Cre$^-$/WT, Cre$^+$/WT, Cre$^-$/Tg+, and Cre$^+$/Tg+ mice. All photomicrographs for each stain across all four groups were taken at the same magnification. (Cre$^-$/WT [blue dotted border], Cre$^+$/WT [red dotted border], Cre$^-$/Tg+ [blue solid border], and Cre$^+$/Tg+ [red solid border] mice). Blue arrows indicate MUC5B+ airway epithelial cells. **(D)** Semiquantitative histological scoring for airway mucus obstruction from AB-PAS-stained left lung sections from Cre$^-$/WT, Cre$^+$/WT, Cre$^-$/Tg+, and Cre$^+$/Tg+ mice. Sample size (n=9/group). **(E)** Number of mucous cells per millimeter of basement membrane from AB-PAS-stained left lung sections from Cre$^-$/WT, Cre$^+$/WT, Cre$^-$/Tg+, and Cre$^+$/Tg+ mice. Sample size (n=9/group). **(F)** Percent MUC5B-stained area in the first-generation airway section calculated using Fiji software. Sample size (n=9/group). **(G)** Percent MUC5AC-stained area in the first-generation airway section was calculated using Fiji software. Sample size (n=9/group). Different groups are shown as: Cre$^-$/WT (blue open bar), Cre$^+$/WT (red open bar), Cre$^-$/Tg+ (blue solid bar), and Cre$^+$/Tg+ (red solid bar). Error bars represent Mean ± SEM. One-way ANOVA followed by Tukey's *post hoc* test was used for the statistical analysis. *$p < 0.05$, ***$p < 0.001$, ****$p < 0.0001$. To minimize the number of horizontal lines in various panels (e.g., **D**), single horizontal line with small vertical ticks were used to indicate statistically significant differences. The positioning of small vertical ticks indicates the group that is significantly different from the reference group (with no vertical line). In **(D)**, single horizontal significance line with three vertical ticks suggests significant difference for two comparisons, i.e., Cre$^-$/Tg+ vs Cre$^+$/WT, and Cre$^-$/Tg+ vs Cre$^-$/WT.

(Figures 4A, B). Cre$^-$/Tg+ mice, on the other hand, had significantly elevated BALF total protein and an increasing trend of dsDNA contents, as compared with Cre$^-$/WT and Cre$^+$/WT mice (Figures 4A, B). Deletion of EGFR in the airway epithelial cells significantly increased the BALF total protein and dsDNA contents in Cre$^+$/Tg+ mice compared with all other experimental groups (Figures 4A, B), suggesting that airway epithelial cell-specific deletion of EGFR contributes to exaggerated lung inflammation in Tg+ juveniles.

To determine whether the increase in the BALF protein levels in Cre$^+$/Tg+ mice is caused by epithelial barrier dysfunction, we assessed the mRNA levels of key apical junction complex proteins that are critical for epithelial barrier function. The mRNA levels of genes encoding adherens junction (AJ) proteins, i.e., E-Cadherin (*Cdh1*), were significantly reduced in Cre$^+$/Tg+ mice as compared with Cre$^-$/Tg+ mice (Supplementary Figure 2A). The mRNA levels of genes encoding tight junction (TJ) proteins, including Claudin 5 (*Cldn5*), Occludin (*Ocln*), and ZO1 (*Tjp1*), adherens junction (AJ)

10.3389/fimmu.2025.1493950

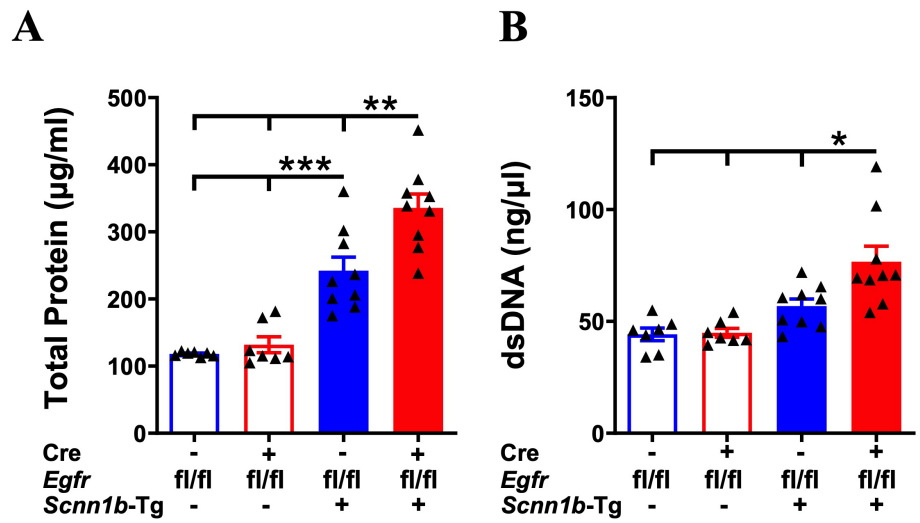

FIGURE 4
Airway epithelial cell-specific EGFR-deficient Tg+ mice exhibit elevated BALF protein and dsDNA contents. The total protein contents (µg/ml) **(A)** and dsDNA contents (ng/µl) **(B)** in cell-free BALF from WT mice (with Cre^- or Cre^+ status) and Tg+ mice (with Cre^- or Cre^+ status). Sample size (n=7-9/group). Error bars represent Mean ± SEM. One-way ANOVA followed by Tukey's *post hoc* test was used for the statistical analysis. *$p < 0.05$, **$p < 0.01$, ***$p < 0.001$. To minimize the number of horizontal lines in various panels (e.g., **A**), single horizontal line with small vertical ticks were used to indicate statistically significant differences. The positioning of small vertical ticks indicates the group that is significantly different from the reference group (with no vertical line). In **(A)**, single horizontal significance line with three vertical ticks suggests significant difference for two comparisons, i.e., Cre^-/Tg+ vs Cre^+/WT, and Cre^-/Tg+ vs Cre^-/WT.

proteins, i.e., Beta-catenin (*Ctnnb1*), and gap junction protein, i.e., Connexin 43 (*Cx43*) trended lower in Cre^+/Tg+ mice as compared with Cre^-/Tg+ mice (Supplementary Figures 2B–F). Consistent with the reduced *Cdh1* mRNA levels, the immunohistochemical staining of E -Cadherin showed reduced staining intensity in Cre^+/Tg+ mice as compared with Cre^-/Tg+ mice (Supplementary Figure 2G).

Next, we determined the effect of airway epithelial cell-specific EGFR deletion on immune cell recruitment into the airspaces by performing immune cell analyses in the BALF from all four experimental groups. Cre^-/WT and Cre^+/WT mice had comparable total immune cells in the BALF (Figures 5A, D). The proportion of four types of immune cells, i.e., macrophages, neutrophils, eosinophils, and lymphocytes, were also comparable among Cre^-/WT and Cre^+/WT mice (Figures 5B–D). These data suggest that the airway epithelial cell-specific deletion of EGFR doesn't alter immune cell composition in the airspaces of WT mice. Consistent with previous reports (26, 27, 32, 40), as compared with the Cre^-/WT and Cre^+/WT mice, the total cell counts were significantly increased in Cre^-/Tg+ mice, which was mainly attributable to increase in macrophages, neutrophils, eosinophils, and lymphocytes (Figures 5A–D). The total cell counts were significantly increased in Cre^+/Tg+ as compared with Cre^-/Tg+ mice (Figures 5A–D), which was attributable to the increased numbers of macrophages and neutrophils (Figures 5B–D). These data suggest that airway epithelial cell-specific deficiency of EGFR enhances neutrophil and macrophage recruitment into the airspaces of Tg+ mice.

Next, we assessed the effect of airway epithelial cell-specific EGFR deletion on inflammatory mediators released into the lung airspaces by determining BALF cytokines and chemokines levels. The levels of primary neutrophil-specific chemokines, including KC/CXCL1, G-CSF, and MIP-2/CXCL2, were comparable among Cre^-/WT and Cre^+/WT mice (Figures 6A–C). Consistent with the increased neutrophil counts in Cre^-/Tg+ mice, KC/CXCL1, G-CSF, and MIP-2/CXCL2 levels trended higher in Cre^-/Tg+ compared with Cre^-/WT and Cre^+/WT mice (Figures 6A–C). Mirroring the additional increase in neutrophil counts in Cre^+/Tg+ mice compared with Cre^-/Tg+ mice, KC/CXCL1, G-CSF, and MIP-2/CXCL2 levels were significantly increased in Cre^+/Tg+ mice compared with Cre^-/Tg+ mice (Figures 6A–C). Consistent with the increased macrophage counts, the levels of MIP-1α/CCL3 and MIP-1β/CCL4, the chemokines reported to drive macrophage/monocyte recruitment (43–45), were significantly increased in Cre^+/Tg+ mice compared with all other three experimental groups (Figures 6D, E). Other inflammatory mediators, such as TNF-α, showed significantly higher expression levels in Cre^+/Tg+ mice compared with all other experimental groups (Figure 6F), and IL-6 showed significantly higher expression levels in Cre^+/Tg+ mice compared with WT groups and a higher trend in Cre^+/Tg+ mice than Cre^-/Tg+ mice (Figure 6G). We also assessed the levels of IL-5, a type 2 cytokine that plays a key role in the proliferation, maturation, and differentiation of eosinophils (46, 47). IL-5 levels were significantly higher in Cre^-/Tg+ mice and trended higher in Cre^+/Tg+ mice versus their WT counterparts (Figure 6H). Consistent with the comparable eosinophil counts, IL-5 levels did not differ significantly between Cre^-/Tg+ and Cre^+/Tg+ mice (Figure 6H). These data suggest that the airway epithelial cell-specific deletion of EGFR promotes a pro-inflammatory microenvironment in Tg+ airways that dictates the recruitment of inflammatory immune cells into the airspaces.

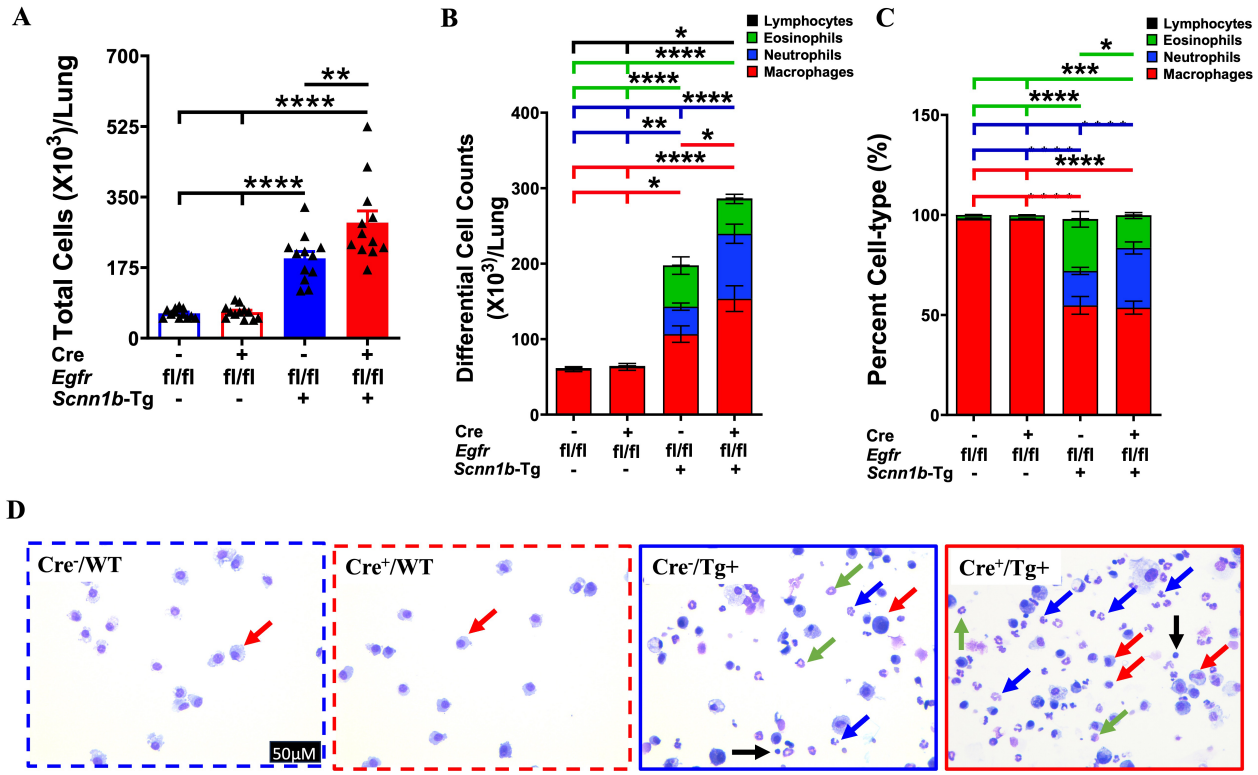

FIGURE 5
EGFR deletion in airway epithelial cells modulates immune cell recruitment in airspaces of Tg+ mice. Total cell counts **(A)** are shown for Cre$^-$/WT [blue open bar], Cre$^+$/WT [red open bar], Cre$^-$/Tg+ [solid blue bar], and Cre$^+$/Tg+ [solid red bar] mice (n=12/group). Differential cell counts **(B)** and the relative percentages **(C)** are presented as a stacked bar graph (macrophages [red bar], neutrophils [blue bar], eosinophils [green bar], and lymphocytes [black bar]) in the harvested BALF from Cre$^-$/WT, Cre$^+$/WT, Cre$^-$/Tg+, and Cre$^+$/Tg+ mice. Sample size (n=11-12/group). Error bars represent Mean ± SEM. One-way ANOVA followed by Tukey's *post hoc* test was used for the statistical analysis. *$p < 0.05$, **$p < 0.01$, ***$p < 0.001$, ****$p < 0.0001$. **(D)** Representative photomicrographs of Wright-Giemsa-stained BALF cytospins from Cre$^-$/WT, Cre$^+$/WT, Cre$^-$/Tg+, and Cre$^+$/Tg+ mice. Macrophages (red arrows), neutrophils (blue arrows), eosinophils (green arrows), and lymphocytes (black arrows). All photomicrographs in panel D were taken at the same magnification. To minimize the number of horizontal lines in various panels (e.g., **A**), single horizontal line with small vertical ticks were used to indicate statistically significant differences. The positioning of small vertical ticks indicates the group that is significantly different from the reference group (with no vertical line). In **(A)** single horizontal significance line with three vertical ticks suggests significant difference for two comparisons, i.e., Cre$^-$/Tg+ vs Cre$^+$/WT, and Cre$^-$/Tg+ vs Cre$^-$/WT.

EGFR deletion in airway epithelial cells compromises bacterial clearance in airspaces of Tg+ mice

Spontaneous bacterial infections due to a defect in the mucociliary clearance resulting from mucostasis are a consistent feature of Tg+ lung disease (29, 31, 32, 39, 40, 48). These bacterial infections are, however, reported to be cleared in the early adulthood (29). To determine the effect of airway epithelial cell-specific EGFR deletion on the clearance of spontaneous bacterial infections, we estimated airspace bacterial burden by determining the colony-forming unit (CFU) counts in BALF at PND21. The BALF collected from Cre$^-$/WT and Cre$^+$/WT mice were devoid of bacterial colonies (Figure 7). Approximately 50% (6 out of 12) of Cre$^-$/Tg+ mice still had lower bacterial counts (mean CFU= ~108/ml) (Figure 7). In contrast, 91.6% (11 out of 12 mice) of Cre$^+$/Tg+ mice showed bacterial burden (mean CFU= ~3907/ml), which was significantly higher as compared with Cre$^-$/Tg+ mice (Figure 7). These data suggest that the airway epithelial cell-specific EGFR deletion delays bacterial clearance in Tg+ mice.

Discussion

The EGFR signaling is implicated in the pathogenesis of airway hypersecretory and mucoinflammatory diseases such as asthma and COPD (12). The expression of EGFR and its ligands, including amphiregulin and heparin-binding EGF (HB-EGF), is increased in airway epithelial cells in asthmatics compared with non-asthmatic patients (49). EGFR signaling is also critical for inducing mucous cell metaplasia (MCM) in animal models and for mucins expression in human airway epithelial cells (6, 21–24). The levels of gel-forming mucins, i.e., MUC5AC and MUC5B, and the expression of EGFR and its ligands, i.e., TGF-α and amphiregulin, are elevated in the CF patients (25, 50). However, the pathogenic role of EGFR signaling in mucoinflammatory lung diseases remains unknown.

In this study, we investigated the role of airway epithelial cell-specific EGFR signaling in the pathogenesis of mucoinflammatory lung disease in *Scnn1b*-transgenic (Tg+) mice, a mouse model of human CF-like lung disease. More specifically, we attempted to answer the following questions: 1) Does airway epithelial cell-specific deletion of EGFR affect the respiratory tract homeostasis

10.3389/fimmu.2025.1493950

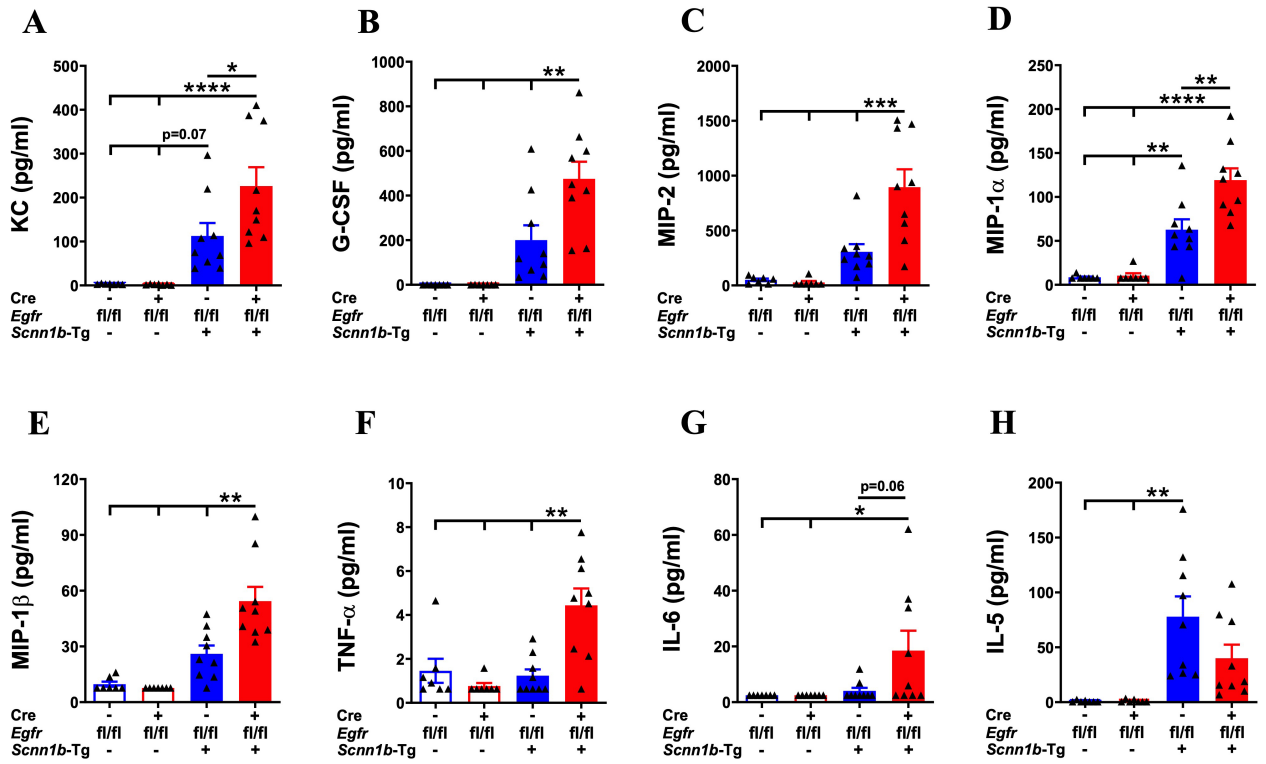

FIGURE 6
EGFR deletion in airway epithelial cells alters the levels of inflammatory mediators in the airspaces of Tg+ mice. Cell-free BALF cytokine levels (pg/ml; picograms per milliliter) of KC **(A)**, G-CSF **(B)**, MIP-2 **(C)**, MIP-1α **(D)**, MIP-1β **(E)**, TNF-α **(F)**, IL-6 **(G)**, and IL-5 **(H)** in WT mice (with Cre^- or Cre^+ status) and Tg+ mice (with Cre^- or Cre^+ status). Sample size (n=7-9/group). Error bars represent Mean ± SEM. One-way ANOVA followed by Tukey's *post hoc* test was used for the statistical analysis. *$p < 0.05$, **$p < 0.01$, ***$p < 0.001$, ****$p < 0.0001$. To minimize the number of horizontal lines in various panels (e.g., **B**), single horizontal line with small vertical ticks were used to indicate statistically significant differences. The positioning of small vertical ticks indicates the group that is significantly different from the reference group (with no vertical line). In **(B)** single horizontal significance line with three vertical ticks suggests significant difference for three comparisons, i.e., Cre^+/Tg+ vs Cre^-/Tg+, Cre^+/Tg+ vs Cre^+/WT, and Cre^+/Tg+ vs Cre^-/WT.

in WT mice? 2) Does airway epithelial cell-specific deletion of EGFR affect the embryonic and postnatal survivability in Tg+ mice? 3) Does airway epithelial cell-specific deletion of EGFR affect the MCM, mucins production, and mucus obstruction in Tg+ mice? 4) Does airway epithelial cell-specific deletion of EGFR affect the inflammatory outcomes in Tg+ mice? 5) Does airway epithelial cell-specific deletion of EGFR affect bacterial clearance in Tg+ mice? To answer these questions, we examined the effect of airway epithelial cell-specific EGFR deficiency on the manifestation of mucoinflammatory outcomes in Tg+ mice.

First, we assessed the effect of airway epithelial cell-specific EGFR deficiency on the composition of mucous cells, a cell type specialized in the synthesis and secretion of mucins (51), in WT mice. Consistent with previous studies (11, 26, 27, 32), the mucous cells were minimal and comparable in EGFR-sufficient WT (Cre^-/WT) and airway epithelial cell-specific EGFR-deficient WT (Cre^+/WT) mice. These data suggest that airway epithelial cell-specific EGFR deficiency does not alter the epithelial cell composition in the WT mice. Next, we assessed the effect of airway epithelial cell-specific EGFR deficiency on the numbers and composition of immune cells in the airspaces of WT mice. The Cre^-/WT and Cre^+/WT mice had a comparable total number of immune cells dominated by macrophages, suggesting that airway epithelial cell-specific EGFR deficiency does not alter the immune cell composition in WT mice. Additionally, the BALF levels of total protein, dsDNA, and inflammatory mediators were also comparable between Cre^-/WT and Cre^+/WT mice. These data suggest that airway epithelial cell-specific deletion of EGFR does not affect the respiratory tract homeostasis in WT mice.

Next, we examined the effect of airway epithelial cell-specific EGFR deficiency on the embryonic and postnatal survivability. Although the germ-line deletion of EGFR results in embryonic lethality (14), as indicated by the mendelian ratio of expected progeny obtained, the airway epithelial cell-specific EGFR deficiency did not result in any embryonic lethality. However, the airway epithelial cell-specific EGFR deficiency compromised the postnatal survival in Tg+ mice. Earlier studies have shown that the postnatal mortality in Tg+ mice is mainly attributed to sudden respiratory collapse due to airway mucus obstruction (11, 26, 27). Therefore, we next compared the severity of mucus obstruction between EGFR-sufficient Tg+ (Cre^-/Tg+) and airway epithelial cell-specific EGFR-deficient Tg+ (Cre^+/Tg+) mice. We found that

10.3389/fimmu.2025.1493950

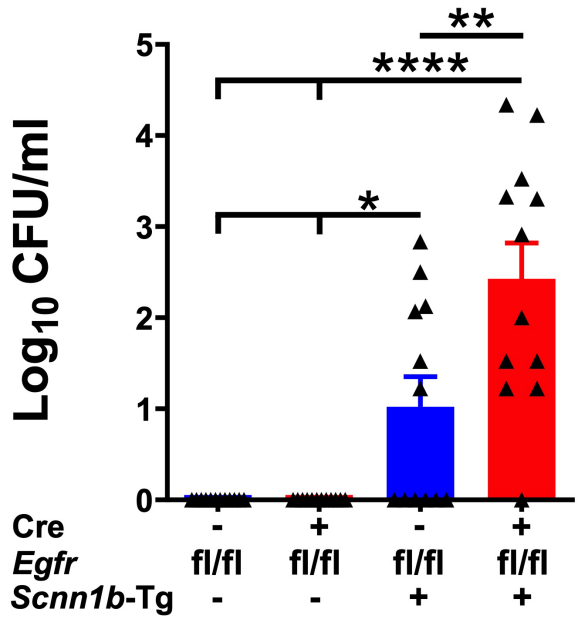

FIGURE 7
Airway epithelial cell-specific deletion of EGFR compromises bacterial clearance in Tg+ mice. Colony Forming Units (CFU) were counted in BALF from Cre^-/WT [blue open bar], Cre^+/WT [red open bar], Cre^-/Tg+ [solid blue bar], and Cre^+/Tg+ [solid red bar] mice. The CFU values were log10-transformed. Sample size (n=12/group). Error bars represent Mean ± SEM. One-way ANOVA followed by Tukey's *post hoc* test was used for the statistical analysis. *$p < 0.05$, **$p < 0.01$, ****$p < 0.0001$. To minimize the number of horizontal lines in various panels, single horizontal line with small vertical ticks were used to indicate statistically significant differences. The positioning of small vertical ticks indicates the group that is significantly different from the reference group (with no vertical line). In Figure 7, single horizontal significance line with three vertical ticks suggests significant difference for two comparisons, i.e., Cre^-/Tg+ vs Cre^+/WT, and Cre^-/Tg+ vs Cre^-/WT.

airway epithelial cell-specific EGFR deficiency results in increased mucus obstruction in Tg+ mice, which was likely a factor in their increased postnatal mortality.

The static mucus in the Tg+ mice primarily consists of mixed mucopolysaccharide material that stains positive for two major gel-forming mucins, i.e., MUC5B and MUC5AC (31, 32, 40). The absence of MUC5B, not MUC5AC, significantly reduces the extent of mucus plugging or airway mucus obstruction in Tg+ mice, suggesting the unique contribution of MUC5B to the mucoinflammatory phenotype of these mice (52). Consistent with this report, the airway epithelial cell-specific deletion of EGFR significantly increased MUC5B levels without altering the MUC5AC levels. Our previous reports also found a strong association between MUC5B expression and mucus obstruction (39, 40). These findings suggest that increased MUC5B levels in Cre^+/Tg+ mice might have contributed to the exaggerated mucus obstruction and postnatal mortality.

Earlier studies have shown that Tg+ mice exhibit mucus obstruction along with MCM, suggesting that MCM, in part, may contribute to mucus obstruction (26, 27, 32, 48). The mucous cells, indicative of MCM, stain positive for mucopolysaccharide material (MUC5B and MUC5AC) in the Tg+ mice (31, 32, 40). Pharmacological inhibition of EGFR signaling, using drugs such as AG-1478, gefitinib, or BIBX1522, has been demonstrated to reduce MCM in both acute and chronic asthma models (6, 53–55), suggesting a contributory role of EGFR in MCM. Consequently, we compared MCM between Cre^-/Tg+ and Cre^+/Tg+ mice. In contradiction to the pharmacological EGFR inhibition reports in experimental asthma models (6, 53–55), the airway epithelial cell-specific EGFR deficiency resulted in an enhanced MCM in Tg+ mice, a trend consistent with the increased mucus obstruction in these mice. These opposing effects observed between cell-specific genetic deletion and broad-spectrum pharmacological inhibition indicate that EGFR pathway in non-airway epithelial cells may also contribute to the manifestation of MCM.

IL-4 and IL-13 via IL4Rα signaling have been known to drive MCM in 10-day-old Tg+ mice (11) and mice models of allergic asthma (10, 56). In our study, the *Il13* mRNA levels were significantly upregulated in Cre^+/Tg+ versus Cre^-/Tg+ mice. IL-13 and IL-4 levels also showed a higher trend in Cre^+/Tg+ versus Cre^-/Tg+ mice. The mRNA levels of *Slc26a4* and *Retnla*, markers of type 2 inflammation, were also significantly upregulated in Cre^+/Tg+ versus Cre^-/Tg+ mice. These data suggest that increased IL-13 expression might have contributed in part to the increased MCM, type 2 inflammatory markers, MUC5B expression, and mucus obstruction in mice with airway epithelial cell-specific EGFR deficiency.

Airway inflammation, indicated by increased immune cell recruitment and elevated proinflammatory mediators, is a consistent feature of CF and Tg+ airways (26, 27, 31, 32, 39, 40, 48, 57–60). In the current study, the airway epithelial cell-specific EGFR deficiency resulted in increased neutrophil and macrophage infiltration into the airspaces of Tg+ mice. These findings are consistent with the studies where inhibition of EGFR signaling increased neutrophil and macrophage recruitment, and increased mRNA expression of chemokines involved in their recruitment to the inflamed tissues (61–65). Consistent with these reports, the Cre^+/Tg+ mice had increased levels of BALF neutrophil- and macrophage-specific chemokines. Of note, neutrophil elastase (NE), a serine proteinase secreted by neutrophils, has been implicated in the induction of MCM and mucin expression (66, 67). The ablation of NE in Tg+ mice resulted in a significant decrease in MCM, and expression levels of genes associated with mucous cells and mucins secretion, i.e., *Clca1/Gob5*, *Muc5ac*, and *Muc5b* (68). Therefore, it is likely that the neutrophil-derived NE contributed to the increased MCM in Cre^+/Tg+ mice. Macrophages are reported to secrete IL-13 in response to stimulation with IL-33, an alarmin that is increased in Tg+ mice (39, 69). Since Cre^+/Tg+ mice have increased macrophage recruitment, it is possible that increased IL-13 levels in Cre^+/Tg+ mice is attributable to increased IL-13 production by macrophages.

The airway epithelial cell-specific EGFR deficient Tg+ mice, as compared with the EGFR sufficient Tg+ mice, exhibited

10.3389/fimmu.2025.1493950

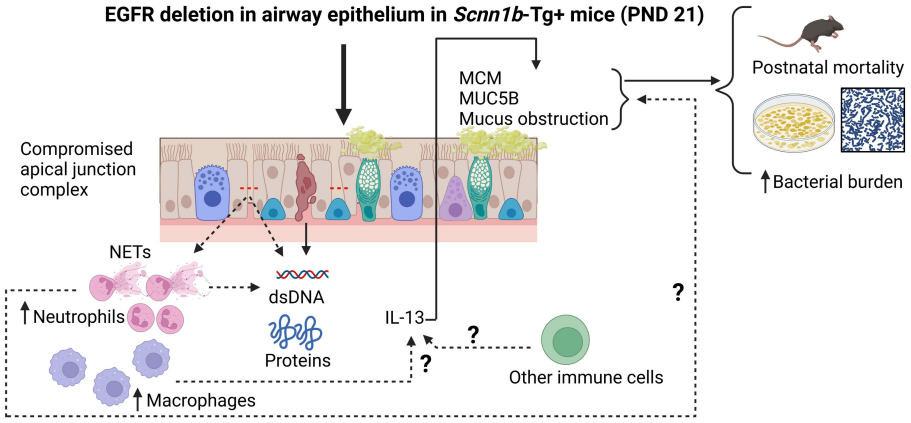

FIGURE 8
Conceptual model illustrating the potential mechanism by which the absence of EGFR in the airway epithelium increases the mucoinflammatory response in Tg+ mice. The deletion of EGFR in the airway epithelial cells in Tg+ mice triggers a series of events that lead to MCM, MUC5B overproduction and mucus obstruction leading to increased postnatal mortality and increased bacterial burden in these mice. The deletion of EGFR in the airway epithelial cells in Tg+ mice compromises apical junction complex integrity which causes increased recruitment of neutrophils and macrophages in the airway. The compromised epithelial barrier integrity, the NETs and the dying cells contribute to the increased BALF total protein and dsDNA contents. Neutrophil-derived NE, macrophage-derived IL-13 or other immune cell-derived IL-13 may contribute to the MCM, MUC5B overproduction and mucus obstruction leading to postnatal mortality and increased bacterial burden in these mice.

significantly increased levels of BALF proteins and dsDNA, which suggests the detrimental effect of EGFR deletion on the epithelial integrity in Tg+ mice. Tight junction, adherens junction, and gap junction proteins are essential for maintaining airway epithelial barrier integrity (70, 71). In the current study, the Cre^{+}/Tg+ mice exhibited relatively reduced mRNA levels of genes encoding junction proteins. Additionally, the immunohistochemical staining for E-Cadherin showed reduced staining intensity in Cre^{+}/Tg+ mice. This finding is consistent with a study that demonstrated decreased cadherin-based cell adhesion upon downregulation of the EGFR pathway (72). However, the role of EGFR in regulating these junction proteins is unclear, with some studies suggesting positive regulation (72), while others suggesting negative regulation (73–76).

The Tg+ mice are prone to spontaneous bacterial infections arising from the aspiration of bacteria of oropharyngeal origin (29). These bacterial infections are usually resolved by 3–4 weeks of age, likely due to the maturation of the immune system in Tg+ juveniles (29). In the current study, the airway epithelial cell-specific deficiency of EGFR resulted in significantly compromised bacterial clearance in Tg+ mice. Since airway epithelial cell-specific EGFR deficiency in Tg+ mice exaggerated the mucus obstruction, the delayed bacterial clearance in these mice was likely caused by the exaggerated mucus obstruction.

A limitation of this study is that it did not investigate how the EGFR deletion in airway epithelial cells in Tg+ juveniles affects the expression of EGFR in other cell types. Additionally, the effect of EGFR deletion in airway epithelial cells on the recruitment of immune cells were only investigated for 4 immune cell populations i.e., macrophages, eosinophils, neutrophils, and lymphocytes. Given the wide repertoire of immune and non-immune cell population, single cell sequencing experiments in the future to investigate the effect of EGFR deletion in airway epithelial cells in Tg+ juvenile on various cell populations are important.

Based on our findings, we propose a conceptual model (Figure 8) wherein the deletion of EGFR in the airway epithelial cells in Tg+ mice triggers a series of events that lead to MCM, MUC5B overproduction and mucus obstruction leading to increased postnatal mortality and increased bacterial burden in these mice. The deletion of EGFR in the airway epithelial cells in Tg + mice compromises apical junction complex integrity, which causes increased recruitment of neutrophils and macrophages in the airway. The compromised epithelial barrier integrity, the NETs and the dying cells contribute to the increased BALF total protein and dsDNA contents. Neutrophil-derived NE, macrophage-derived IL-13 or other immune cell-derived IL-13 may contribute to the MCM, MUC5B overproduction and mucus obstruction leading to postnatal mortality and increased bacterial burden in these mice.

In conclusion, this study demonstrated that the airway epithelial cell-specific deletion of EGFR significantly worsens the mucoinflammatory responses in Tg+ mice lungs, including increased degree of mucus obstruction, MCM, MUC5B production, increased inflammatory cell recruitment, elevated levels of inflammatory mediators and type 2 inflammation-associated markers, compromised postnatal survival, and delayed

bacterial clearance. These data highlight the cell-specific role of the EGFR signaling pathway and suggest that the pan-cellular inhibition of this pathway, using pharmacological inhibitors, may worsen mucoinflammatory lung disease.

Data availability statement

The datasets presented in this study can be found in online repositories. The names of the repository/repositories and accession number(s) can be found in the article/Supplementary Material.

Ethics statement

The animal study was approved by Institutional Animal Care and Use Committee (IACUC) of Louisiana State University. The study was conducted in accordance with the local legislation and institutional requirements.

Author contributions

IC: Data curation, Formal Analysis, Investigation, Methodology, Validation, Writing – original draft, Writing – review & editing. KP: Investigation, Writing – original draft, Writing – review & editing. RK: Formal Analysis, Investigation, Writing – original draft, Writing – review & editing. SP: Formal Analysis, Writing – original draft, Writing – review & editing. AS: Methodology, Writing – review & editing. YS: Conceptualization, Data curation, Formal Analysis, Funding acquisition, Investigation, Methodology, Project administration, Resources, Supervision, Validation, Visualization, Writing – original draft, Writing – review & editing.

Funding

The author(s) declare that financial support was received for the research and/or publication of this article. The work was supported by NIH R01 (R01ES030125) and R21 (R21ES034509) grants.

Acknowledgments

We thank Sherry Ring for histological tissue processing and Thaya Stoufflet for assistance with multiplex cytokine assays.

Conflict of interest

The authors declare that the research was conducted in the absence of any commercial or financial relationships that could be construed as a potential conflict of interest.

The author(s) declared that they were an editorial board member of Frontiers, at the time of submission. This had no impact on the peer review process and the final decision.

Publisher's note

Supplementary material

The Supplementary Material for this article can be found online at: https://www.frontiersin.org/articles/10.3389/fimmu.2025.1493950/full#supplementary-material

SUPPLEMENTARY FIGURE 1
Representative photomicrographs of AB-PAS-stained **(A)**, MUC5B-immunostained **(B)**, and MUC5AC-immunostained **(C)** whole left lung lobe sections from Cre^-/Tg+, and Cre^+/Tg+ mice. All photomicrographs for each stain across both the groups were taken at the same magnification. (Cre^-/Tg+ [blue solid border] and Cre^+/Tg+ [red solid border] mice).

SUPPLEMENTARY FIGURE 2
Absolute quantification of *Cdh1* mRNA **(A)**, *Cldn5* mRNA **(B)**, *Ctnnb1* mRNA **(C)**, *Ocln* mRNA **(D),** *Tjp1* mRNA **(E)**, and *Cx43* mRNA **(F)** in the lungs from WT mice (with Cre^- or Cre^+ status) and Tg+ mice (with Cre^- or Cre^+ status). Sample size (n=5-7/group). **(G)** Representative photomicrographs of E-Cadherin-immunostained left lung lobe sections from Cre^-/Tg+ and Cre^+/Tg+ mice. The photomicrographs across both the groups were taken at the same magnification. (Cre^-/Tg+ [blue solid border] and Cre^+/Tg+ [red solid border] mice). Blue solid arrows indicate strong E-Cadherin staining in airway epithelial cells while dotted blue arrows indicate reduced staining intensity of E-Cadherin in airway epithelial cells. Error bars represent Mean ± SEM. One-way ANOVA followed by Tukey's *post hoc* test was used for the statistical analysis. $*p < 0.05$. To minimize the number of horizontal lines in various panels (e.g., Figure 2A), single horizontal line with small vertical ticks were used to indicate statistically significant differences. The positioning of small vertical ticks indicates the group that is significantly different from the reference group (with no vertical line). In Figure 2A, single horizontal significance line with three vertical ticks suggests significant difference for three comparisons, i.e., Cre^+/Tg+ vs Cre^-/Tg+, Cre^+/Tg+ vs Cre^+/WT, and Cre^+/Tg+ vs Cre^-/WT.

References

1. Ratjen F, Bell SC, Rowe SM, Goss CH, Quittner AL, Bush A. Cystic fibrosis. *Nat Rev Dis Primers.* (2015) 1:15010. doi: 10.1038/nrdp.2015.10

2. Fahy JV, Dickey BF. Airway mucus function and dysfunction. *N Engl J Med.* (2010) 363:2233–47. doi: 10.1056/NEJMra0910061

3. Boucher RC. Airway surface dehydration in cystic fibrosis: pathogenesis and therapy. *Annu Rev Med.* (2007) 58:157–70. doi: 10.1146/annurev.med.58.071905.105316

4. Symmes BA, Stefanski AL, Magin CM, Evans CM. Role of mucins in lung homeostasis: regulated expression and biosynthesis in health and disease. *Biochem Soc Trans.* (2018) 46:707–19. doi: 10.1042/BST20170455

5. Burgel PR, Nadel JA. Roles of epidermal growth factor receptor activation in epithelial cell repair and mucin production in airway epithelium. *Thorax.* (2004) 59:992–6. doi: 10.1136/thx.2003.018879

6. Takeyama K, Dabbagh K, Lee HM, Agusti C, Lausier JA, Ueki IF, et al. Epidermal growth factor system regulates mucin production in airways. *Proc Natl Acad Sci U S A*. (1999) 96:3081–6. doi: 10.1073/pnas.96.6.3081

7. Perrais M, Pigny P, Copin MC, Aubert JP, Van Seuningen I. Induction of MUC2 and MUC5AC mucins by factors of the epidermal growth factor (EGF) family is mediated by EGF receptor/Ras/Raf/extracellular signal-regulated kinase cascade and Sp1. *J Biol Chem*. (2002) 277:32258–67. doi: 10.1074/jbc.M204862200

8. Choudhary I, Vo T, Singamsetty D, Paudel K, Mao Y, Lamichhane R, et al. Myeloid cell-specific IL4Rα deletion protects against mixed allergen-induced lung injury in mice. *J Immunol*. (2022) 208:109.22–.22. doi: 10.4049/jimmunol.208.Supp.109.22

9. Le Floc'h A, Allinne J, Nagashima K, Scott G, Birchard D, Asrat S, et al. Dual blockade of IL-4 and IL-13 with dupilumab, an IL-4Ralpha antibody, is required to broadly inhibit type 2 inflammation. *Allergy*. (2020) 75:1188–204. doi: 10.1111/all.14151

10. Gour N, Wills-Karp M. IL-4 and IL-13 signaling in allergic airway disease. *Cytokine*. (2015) 75:68–78. doi: 10.1016/j.cyto.2015.05.014

11. Livraghi A, Grubb BR, Hudson EJ, Wilkinson KJ, Sheehan JK, Mall MA, et al. Airway and lung pathology due to mucosal surface dehydration in beta-epithelial Na+ channel-overexpressing mice: role of TNF-alpha and IL-4Ralpha signaling, influence of neonatal development, and limited efficacy of glucocorticoid treatment. *J Immunol*. (2009) 182:4357–67. doi: 10.4049/jimmunol.0802557

12. Vallath S, Hynds RE, Succony L, Janes SM, Giangreco A. Targeting EGFR signaling in chronic lung disease: therapeutic challenges and opportunities. *Eur Respir J*. (2014) 44:513–22. doi: 10.1183/09031936.00146413

13. Singh B, Carpenter G, Coffey RJ. EGF receptor ligands: recent advances. *F1000Res*. (2016) 5:F1000 Faculty Rev-2270. doi: 10.12688/f1000research

14. Threadgill DW, Dlugosz AA, Hansen LA, Tennenbaum T, Lichti U, Yee D, et al. Targeted disruption of mouse EGF receptor: effect of genetic background on mutant phenotype. *Science*. (1995) 269:230–4. doi: 10.1126/science.7618084

15. Miettinen PJ, Berger JE, Meneses J, Phung Y, Pedersen RA, Werb Z, et al. Epithelial immaturity and multiorgan failure in mice lacking epidermal growth factor receptor. *Nature*. (1995) 376:337–41. doi: 10.1038/376337a0

16. Sibilia M, Wagner EF. Strain-dependent epithelial defects in mice lacking the EGF receptor. *Science*. (1995) 269:234–8. doi: 10.1126/science.7618085

17. Plopper CG, St George JA, Read LC, Nishio SJ, Weir AJ, Edwards L, et al. Acceleration of alveolar type II cell differentiation in fetal rhesus monkey lung by administration of EGF. *Am J Physiol*. (1992) 262:L313–21. doi: 10.1152/ajplung.1992.262.3.L313

18. Miettinen PJ, Warburton D, Bu D, Zhao JS, Berger JE, Minoo P, et al. Impaired lung branching morphogenesis in the absence of functional EGF receptor. *Dev Biol*. (1997) 186:224–36. doi: 10.1006/dbio.1997.8593

19. Le Cras TD, Hardie WD, Fagan K, Whitsett JA, Korfhagen TR. Disrupted pulmonary vascular development and pulmonary hypertension in transgenic mice overexpressing transforming growth factor-alpha. *Am J Physiol Lung Cell Mol Physiol*. (2003) 285:L1046–54. doi: 10.1152/ajplung.00045.2003

20. Yasui S, Nagai A, Oohira A, Iwashita M, Konno K. Effects of anti-mouse EGF antiserum on prenatal lung development in fetal mice. *Pediatr Pulmonol*. (1993) 15:251–6. doi: 10.1002/ppul.1950150412

21. Tyner JW, Kim EY, Ide K, Pelletier MR, Roswit WT, Morton JD, et al. Blocking airway mucous cell metaplasia by inhibiting EGFR antiapoptosis and IL-13 transdifferentiation signals. *J Clin Invest*. (2006) 116:309–21. doi: 10.1172/JCI25167

22. Takeyama K, Jung B, Shim JJ, Burgel PR, Dao-Pick T, Ueki IF, et al. Activation of epidermal growth factor receptors is responsible for mucin synthesis induced by cigarette smoke. *Am J Physiol Lung Cell Mol Physiol*. (2001) 280:L165–72. doi: 10.1152/ajplung.2001.280.1.L165

23. Burgel PR, Lazarus SC, Tam DC, Ueki IF, Atabai K, Birch M, et al. Human eosinophils induce mucin production in airway epithelial cells via epidermal growth factor receptor activation. *J Immunol*. (2001) 167:5948–54. doi: 10.4049/jimmunol.167.10.5948

24. Shim JJ, Dabbagh K, Ueki IF, Dao-Pick T, Burgel PR, Takeyama K, et al. IL-13 induces mucin production by stimulating epidermal growth factor receptors and by activating neutrophils. *Am J Physiol Lung Cell Mol Physiol*. (2001) 280:L134–40. doi: 10.1152/ajplung.2001.280.1.L134

25. Burgel PR, Montani D, Danel C, Dusser DJ, Nadel JA. A morphometric study of mucins and small airway plugging in cystic fibrosis. *Thorax*. (2007) 62:153–61. doi: 10.1136/thx.2006.062190

26. Mall M, Grubb BR, Harkema JR, O'Neal WK, Boucher RC. Increased airway epithelial Na+ absorption produces cystic fibrosis-like lung disease in mice. *Nat Med*. (2004) 10:487–93. doi: 10.1038/nm1028

27. Mall MA, Harkema JR, Trojanek JB, Treis D, Livraghi A, Schubert S, et al. Development of chronic bronchitis and emphysema in beta-epithelial Na+ channel-overexpressing mice. *Am J Respir Crit Care Med*. (2008) 177:730–42. doi: 10.1164/rccm.200708-1233OC

28. Saini Y, Wilkinson KJ, Terrell KA, Burns KA, Livraghi-Butrico A, Doerschuk CM, et al. Neonatal pulmonary macrophage depletion coupled to defective mucus clearance increases susceptibility to pneumonia and alters pulmonary immune responses. *Am J Respir Cell Mol Biol*. (2016) 54:210–21. doi: 10.1165/rcmb.2014-0111OC

29. Livraghi-Butrico A, Kelly EJ, Klem ER, Dang H, Wolfgang MC, Boucher RC, et al. Mucus clearance, MyD88-dependent and MyD88-independent immunity modulate lung susceptibility to spontaneous bacterial infection and inflammation. *Mucosal Immunol*. (2012) 5:397–408. doi: 10.1038/mi.2012.17

30. Saini Y, Dang H, Livraghi-Butrico A, Kelly EJ, Jones LC, O'Neal WK, et al. Gene expression in whole lung and pulmonary macrophages reflects the dynamic pathology associated with airway surface dehydration. *BMC Genomics*. (2014) 15:726. doi: 10.1186/1471-2164-15-726

31. Mao Y, Patial S, Saini Y. Airway epithelial cell-specific deletion of HMGB1 exaggerates inflammatory responses in mice with muco-obstructive airway disease. *Front Immunol*. (2022) 13:944772. doi: 10.3389/fimmu.2022.944772

32. Choudhary I, Vo T, Paudel K, Yadav R, Mao Y, Patial S, et al. Postnatal ozone exposure disrupts alveolar development, exaggerates mucoinflammatory responses, and suppresses bacterial clearance in developing scnn1b-tg(+) mice lungs. *J Immunol*. (2021) 207:1165–79. doi: 10.4049/jimmunol.2001286

33. Choudhary I, Vo T, Bathula CS, Lamichhane R, Lewis BW, Looper J, et al. Tristetraprolin overexpression in non-hematopoietic cells protects against acute lung injury in mice. *Front Immunol*. (2020) 11:2164. doi: 10.3389/fimmu.2020.02164

34. Patial S, Lewis BW, Vo T, Choudhary I, Paudel K, Mao Y, et al. Myeloid-IL4Ralpha is an indispensable link in IL-33-ILCs-IL-13-IL4Ralpha axis of eosinophil recruitment in murine lungs. *Sci Rep*. (2021) 11:15465. doi: 10.1038/s41598-021-94843-9

35. Schindelin J, Arganda-Carreras I, Frise E, Kaynig V, Longair M, Pietzsch T, et al. Fiji: an open-source platform for biological-image analysis. *Nat Methods*. (2012) 9:676–82. doi: 10.1038/nmeth.2019

36. Choudhary I, Vo T, Paudel K, Patial S, Saini Y. Compartment-specific transcriptomics of ozone-exposed murine lungs reveals sex- and cell type-associated perturbations relevant to mucoinflammatory lung diseases. *Am J Physiol Lung Cell Mol Physiol*. (2021) 320:L99–L125. doi: 10.1152/ajplung.00381.2020

37. Choudhary I, Vo T, Paudel K, Wen X, Gupta R, Kesimer M, et al. Vesicular and extravesicular protein analyses from the airspaces of ozone-exposed mice revealed signatures associated with mucoinflammatory lung disease. *Sci Rep*. (2021) 11:23203. doi: 10.1038/s41598-021-02256-5

38. Vo T, Paudel K, Choudhary I, Patial S, Saini Y. Ozone exposure upregulates the expression of host susceptibility protein TMPRSS2 to SARS-CoV-2. *Sci Rep*. (2022) 12:1357. doi: 10.1038/s41598-022-04906-8

39. Lewis BW, Vo T, Choudhary I, Kidder A, Bathula C, Ehre C, et al. Ablation of IL-33 suppresses th2 responses but is accompanied by sustained mucus obstruction in the scnn1b transgenic mouse model. *J Immunol*. (2020) 204:1650–60. doi: 10.4049/jimmunol.1900234

40. Lewis BW, Choudhary I, Paudel K, Mao Y, Sharma R, Wang Y, et al. The innate lymphoid system is a critical player in the manifestation of mucoinflammatory airway disease in mice. *J Immunol*. (2020) 205:1695–708. doi: 10.4049/jimmunol.2000530

41. Joyner BL, Jones SW, Cairns BA, Harris BD, Coverstone AM, Abode KA, et al. DNA and inflammatory mediators in bronchoalveolar lavage fluid from children with acute inhalational injuries. *J Burn Care Res*. (2013) 34:326–33. doi: 10.1097/BCR.0b013e31825d5126

42. Kirchner KK, Wagener JS, Khan TZ, Copenhaver SC, Accurso FJ. Increased DNA levels in bronchoalveolar lavage fluid obtained from infants with cystic fibrosis. *Am J Respir Crit Care Med*. (1996) 154:1426–9. doi: 10.1164/ajrccm.154.5.8912759

43. Kwong K, Vaishnav RA, Liu Y, Subhedar N, Stromberg AJ, Getchell ML, et al. Target ablation-induced regulation of macrophage recruitment into the olfactory epithelium of Mip-1alpha-/- mice and restoration of function by exogenous MIP-1alpha. *Physiol Genomics*. (2004) 20:73–86. doi: 10.1152/physiolgenomics.00187.2004

44. Nath A, Chattopadhya S, Chattopadhyay U, Sharma NK. Macrophage inflammatory protein (MIP)1alpha and MIP1beta differentially regulate release of inflammatory cytokines and generation of tumoricidal monocytes in Malignancy. *Cancer Immunol Immunother*. (2006) 55:1534–41. doi: 10.1007/s00262-006-0149-3

45. Driscoll KE. Macrophage inflammatory proteins: biology and role in pulmonary inflammation. *Exp Lung Res*. (1994) 20:473–90. doi: 10.3109/01902149409031733

46. Sitkauskiene B, Johansson AK, Sergejeva S, Lundin S, Sjostrand M, Lotvall J. Regulation of bone marrow and airway CD34+ eosinophils by interleukin-5. *Am J Respir Cell Mol Biol*. (2004) 30:367–78. doi: 10.1165/rcmb.2002-0311OC

47. Rosenberg HF, Phipps S, Foster PS. Eosinophil trafficking in allergy and asthma. *J Allergy Clin Immunol*. (2007) 119:1303–10; quiz 11-2. doi: 10.1016/j.jaci.2007.03.048

48. Lewis BW, Sultana R, Sharma R, Noel A, Langohr I, Patial S, et al. Early postnatal secondhand smoke exposure disrupts bacterial clearance and abolishes immune responses in muco-obstructive lung disease. *J Immunol*. (2017) 199:1170–83. doi: 10.4049/jimmunol.1700144

49. Inoue H, Akimoto K, Homma T, Tanaka A, Sagara H. Airway epithelial dysfunction in asthma: relevant to epidermal growth factor receptors and airway epithelial cells. *J Clin Med*. (2020) 9(11):3698. doi: 10.3390/jcm9113698

50. Adib-Conquy M, Pedron T, Petit-Bertron AF, Tabary O, Corvol H, Jacquot J, et al. Neutrophils in cystic fibrosis display a distinct gene expression pattern. *Mol Med*. (2008) 14:36–44. doi: 10.2119/2007-00081.Adib-Conquy

51. Birchenough GM, Johansson ME, Gustafsson JK, Bergstrom JH, Hansson GC. New developments in goblet cell mucus secretion and function. *Mucosal Immunol*. (2015) 8:712–9. doi: 10.1038/mi.2015.32

52. Livraghi-Butrico A, Grubb BR, Wilkinson KJ, Volmer AS, Burns KA, Evans CM, et al. Contribution of mucus concentration and secreted mucins Muc5ac and Muc5b to the pathogenesis of muco-obstructive lung disease. *Mucosal Immunol.* (2017) 10:395–407. doi: 10.1038/mi.2016.63

53. Hur GY, Lee SY, Lee SH, Kim SJ, Lee KJ, Jung JY, et al. Potential use of an anticancer drug gefinitib, an EGFR inhibitor, on allergic airway inflammation. *Exp Mol Med.* (2007) 39:367–75. doi: 10.1038/emm.2007.41

54. Tamaoka M, Hassan M, McGovern T, Ramos-Barbon D, Jo T, Yoshizawa Y, et al. The epidermal growth factor receptor mediates allergic airway remodeling in the rat. *Eur Respir J.* (2008) 32:1213–23. doi: 10.1183/09031936.00166907

55. Le Cras TD, Acciani TH, Mushaben EM, Kramer EL, Pastura PA, Hardie WD, et al. Epithelial EGF receptor signaling mediates airway hyperreactivity and remodeling in a mouse model of chronic asthma. *Am J Physiol Lung Cell Mol Physiol.* (2011) 300: L414–21. doi: 10.1152/ajplung.00346.2010

56. Choudhary I, Lamichhane R, Singamsetty D, Vo T, Brombacher F, Patial S, et al. Cell-specific contribution of IL4 receptor α signaling shapes the overall manifestation of allergic airway disease. *Am J Respir Cell Mol Biol (accepted publication).* (2024) 71 (6):702-17. doi: 10.1165/rcmb.2024-0208OC

57. Bruscia EM, Bonfield TL. Innate and adaptive immunity in cystic fibrosis. *Clin Chest Med.* (2016) 37:17–29. doi: 10.1016/j.ccm.2015.11.010

58. Sagel SD, Kapsner R, Osberg I, Sontag MK, Accurso FJ. Airway inflammation in children with cystic fibrosis and healthy children assessed by sputum induction. *Am J Respir Crit Care Med.* (2001) 164:1425–31. doi: 10.1164/ajrccm.164.8.2104075

59. Elizur A, Cannon CL, Ferkol TW. Airway inflammation in cystic fibrosis. *Chest.* (2008) 133:489–95. doi: 10.1378/chest.07-1631

60. Saini Y, Lewis BW, Yu D, Dang H, Livraghi-Butrico A, Del Piero F, et al. Effect of LysM+ macrophage depletion on lung pathology in mice with chronic bronchitis. *Physiol Rep.* (2018) 6:e13677. doi: 10.14814/phy2.13677

61. Harada C, Kawaguchi T, Ogata-Suetsugu S, Yamada M, Hamada N, Maeyama T, et al. EGFR tyrosine kinase inhibition worsens acute lung injury in mice with repairing airway epithelium. *Am J Respir Crit Care Med.* (2011) 183:743–51. doi: 10.1164/rccm.201002-0188OC

62. Mascia F, Lam G, Keith C, Garber C, Steinberg SM, Kohn E, et al. Genetic ablation of epidermal EGFR reveals the dynamic origin of adverse effects of anti-EGFR therapy. *Sci Transl Med.* (2013) 5:199ra10. doi: 10.1126/scitranslmed.3005773

63. Wang Y, Cheng S, Zhang H, Zhang Y, Ding C, Peng T, et al. Adverse effects of gefitinib on skin and colon in a lung cancer mouse model. *Recent Pat Anticancer Drug Discov.* (2024) 19:308–15. doi: 10.2174/1574892818666230727143750

64. Bangsgaard N, Houtkamp M, Schuurhuis DH, Parren PW, Baadsgaard O, Niessen HW, et al. Neutralization of IL-8 prevents the induction of dermatologic adverse events associated with the inhibition of epidermal growth factor receptor. *PloS One.* (2012) 7:e39706. doi: 10.1371/journal.pone.0039706

65. Dube PE, Liu CY, Girish N, Washington MK, Polk DB. Pharmacological activation of epidermal growth factor receptor signaling inhibits colitis-associated cancer in mice. *Sci Rep.* (2018) 8:9119. doi: 10.1038/s41598-018-27353-w

66. Voynow JA, Young LR, Wang Y, Horger T, Rose MC, Fischer BM. Neutrophil elastase increases MUC5AC mRNA and protein expression in respiratory epithelial cells. *Am J Physiol.* (1999) 276:L835–43. doi: 10.1152/ajplung.1999.276.5.L835

67. Voynow JA, Fischer BM, Malarkey DE, Burch LH, Wong T, Longphre M, et al. Neutrophil elastase induces mucus cell metaplasia in mouse lung. *Am J Physiol Lung Cell Mol Physiol.* (2004) 287:L1293–302. doi: 10.1152/ajplung.00140.2004

68. Gehrig S, Duerr J, Weitnauer M, Wagner CJ, Graeber SY, Schatterny J, et al. Lack of neutrophil elastase reduces inflammation, mucus hypersecretion, and emphysema, but not mucus obstruction, in mice with cystic fibrosis-like lung disease. *Am J Respir Crit Care Med.* (2014) 189:1082–92. doi: 10.1164/rccm.201311-1932OC

69. Yang Z, Grinchuk V, Urban JF Jr., Bohl J, Sun R, Notari L, et al. Macrophages as IL-25/IL-33-responsive cells play an important role in the induction of type 2 immunity. *PLoS One.* (2013) 8:e59441. doi: 10.1371/journal.pone.0059441

70. Yuksel H, Ocalan M, Yilmaz O. E-cadherin: an important functional molecule at respiratory barrier between defense and dysfunction. *Front Physiol.* (2021) 12:720227. doi: 10.3389/fphys.2021.720227

71. Freund-Michel V, Muller B, Marthan R, Savineau JP, Guibert C. Expression and role of connexin-based gap junctions in pulmonary inflammatory diseases. *Pharmacol Ther.* (2016) 164:105–19. doi: 10.1016/j.pharmthera.2016.04.004

72. Cela C, Llimargas M. Egfr is essential for maintaining epithelial integrity during tracheal remodeling in Drosophila. *Development.* (2006) 133:3115–25. doi: 10.1242/dev.02482

73. Petecchia L, Sabatini F, Usai C, Caci E, Varesio L, Rossi GA. Cytokines induce tight junction disassembly in airway cells via an EGFR-dependent MAPK/ERK1/2-pathway. *Lab Invest.* (2012) 92:1140–8. doi: 10.1038/labinvest.2012.67

74. Gavard J, Gutkind JS. A molecular crosstalk between E-cadherin and EGFR signaling networks. In: Haley JD, Gullick WJ, editors. *EGFR Signaling Networks in Cancer Therapy*, vol. p . Humana Press, Totowa, NJ (2008). p. 131–46.

75. Lo HW, Hsu SC, Xia W, Cao X, Shih JY, Wei Y, et al. Epidermal growth factor receptor cooperates with signal transducer and activator of transcription 3 to induce epithelial-mesenchymal transition in cancer cells via up-regulation of TWIST gene expression. *Cancer Res.* (2007) 67:9066–76. doi: 10.1158/0008-5472.CAN-07-0575

76. Ramirez Moreno M, Bulgakova NA. The cross-talk between EGFR and E-cadherin. *Front Cell Dev Biol.* (2021) 9:828673. doi: 10.3389/fcell.2021.828673

Frontiers in Immunology

Explores novel approaches and diagnoses to treat immune disorders.

The official journal of the International Union of Immunological Societies (IUIS) and the most cited in its field, leading the way for research across basic, translational and clinical immunology.

Discover the latest Research Topics

See more →

Frontiers

Avenue du Tribunal-Fédéral 34
1005 Lausanne, Switzerland
frontiersin.org

Contact us

+41 (0)21 510 17 00
frontiersin.org/about/contact